

AFTT/GA/ENG/93D-02

AD-A274 039



①

**CONTROL OF A LARGE SPACE STRUCTURE USING  
MULTIPLE MODEL ADAPTIVE ESTIMATION AND  
CONTROL TECHNIQUES**

THESIS

**DTIC**  
**S** **ELECTE**  
**DEC 23 1993**  
**A**

Presented to the Faculty of the Graduate School of Engineering  
of the Air Force Institute of Technology  
Air University  
In Partial Fulfillment of the  
Requirements for the Degree of  
Master of Science in Astronautical Engineering

Gregory John Schiller, B.S.A.E  
Captain, USAF

December 1993

**93-30985**



**93 12 22 098**

## ***Preface***

The purpose of this thesis is to apply moving-bank multiple model adaptive estimation and control (MMAE/MMAC) algorithms to an actual space structure (SPICE) being examined at Phillips Laboratory at Kirtland AFB, NM. This research follows the work of Captain John Gustafson who began his research with the SPICE-2 model. The primary design tools utilize Kalman filtering and LQG control. When uncertainties exist in the system model, a bank of filters increases the robustness of the LQG control. The moving bank decreases the computational load when the bank of filters is excessively large as a result of numerous discretized points in the uncertain parameter space. Many techniques are investigated for moving the bank as well as for providing the control input determination. Results of this thesis indicate that the MMAE/MMAC algorithms are highly effective in quelling unwanted vibrations in the SPICE structure in the face of parameter variations.

The research accomplished here would not have been possible without the guidance, patience, motivation, and judicious use of the red pen that Dr. Peter Maybeck provided. I wish to thank him for this and for always finding time to aid me in this effort. I wish to thank Lt Colonel Riggins and Dr. Liebst for their time and suggestions. I also wish to thank the individuals at Lockheed (Ross Blankenship and Rick Baldwin), Honeywell (James Chow), and Phillips Lab (Rory Ninnerman) for aiding me in the development of the SPICE system model and controller design. I wish to thank my wife, Robin, for her patience throughout this seemingly endless eighteen months. I love you, and yes, I owe you one (or even a couple). Finally, I'd like to thank my son, Nicholas (2), and daughter, Macie (2 months), for always having a hug ready when I walk in the door.

DTIC QUALITY INSPECTED 3

<input checked="checked" type="checkbox"/>	
<input type="checkbox"/>	
<input type="checkbox"/>	
Library Codes	
Dist	Avail and/or Special
A-1	

## *Table of Contents*

	<b>page</b>
Preface .....	ii
Table of Contents .....	iii
List of Figures .....	viii
List of Tables .....	xviii
Abstract .....	xix
<b>I. Introduction.....</b>	<b>1-1</b>
1.1 Notation.....	1-5
1.2 Background .....	1-6
1.2.1 System Model .....	1-7
1.2.2 Multiple Model Adaptive Estimation .....	1-8
1.2.3 Moving-Bank MMAE .....	1-10
1.2.4 Moving-Bank MMAC .....	1-13
1.3 Past Research.....	1-14
1.4 Problem Statement.....	1-17
1.5 Scope.....	1-18
1.6 Approach .....	1-18
1.7 Summary.....	1-22
<b>II. Background.....</b>	<b>2-1</b>
2.1 Introduction .....	2-1
2.2 Kalman Filter .....	2-1
2.3 MMAE .....	2-5
2.3.1 Bayesian Formulation .....	2-6
2.3.2 Performance Evaluation and Enhancements .....	2-9
2.4 Moving-Bank MMAE Development.....	2-12

	<b>page</b>
2.4.1 Moving the Bank .....	2-12
2.4.2 Expanding the Bank .....	2-15
2.4.3 Contracting the Bank .....	2-16
2.4.4 Initialization of New Elemental Filters .....	2-17
2.5 Stochastic Controller Development .....	2-18
2.6 MMAC .....	2-21
2.6.1 MMAC Control .....	2-21
2.6.2 "Modified" MMAC Control .....	2-22
2.6.3 MAP versus Bayesian MMAC Control .....	2-22
2.6.4 Single Fixed-Gain Control .....	2-22
2.6.5 Single Changeable-Gain Control .....	2-23
2.6.6 "Modified" Single Changeable-Gain Control .....	2-24
2.7 Mathematical Modeling Methods .....	2-25
2.7.1 Physical Coordinate Form .....	2-26
2.7.2 Modal Coordinate Form .....	2-28
2.7.3 Modal Reduction Technique .....	2-30
2.7.4 Internally Balanced Reduction Technique .....	2-34
2.7.5 Component Cost Modal Reduction Technique .....	2-36
2.8 Summary .....	2-38
III. System Development .....	3-1
3.1 Introduction .....	3-1
3.2 SPICE Structure .....	3-1
3.2.1 Physical Structure Description .....	3-1
3.2.2 Actuators and Sensors .....	3-4
3.2.2 Disturbances .....	3-5
3.3 Full Order System Model Description .....	3-5



	<b>page</b>
3.3.1 Disturbances.....	3-7
3.3.2 Structure .....	3-8
3.3.3 Measurement Devices.....	3-11
3.3.4 Feedback Loops and Control Inputs .....	3-16
3.4 Truth Model Selection.....	3-19
3.4.1 Truth Model Simplifications .....	3-19
3.4.2 Truth Model.....	3-22
3.5 Reduced Order Filter Models .....	3-28
3.5.1 Modal Reduction.....	3-28
3.5.2 Modal Cost Reduction.....	3-31
3.6 Physical System Parameter Uncertainty .....	3-32
3.7 Summary.....	3-33
IV. Simulation .....	4-1
4.1 Introduction .....	4-1
4.2 Monte Carlo Analysis.....	4-1
4.2.1 Error Vector Formulation.....	4-2
4.2.2 Error Vector Statistics.....	4-4
4.3 Simulation Software.....	4-5
4.3.1 Preprocessor .....	4-5
4.3.2 Processor .....	4-6
4.3.3 Post Processor.....	4-7
4.4 Analysis Plan.....	4-7
4.4.1 Dynamics Noise Strength and Measurement Noise Covariance Determination.....	4-8
4.4.2 Controller Weighting Matrices.....	4-9
4.4.3 Model Analysis.....	4-10

	<b>page</b>
4.4.4 Sensitivity Analysis.....	4-11
4.4.5 Parameter Identification and Control .....	4-12
4.5 Summary.....	4-14
<b>V Results.....</b>	<b>5-1</b>
5.1 Introduction .....	5-1
5.2 Tuning Procedures .....	5-1
5.2.1 Filter Tuning.....	5-1
5.2.2 Controller Tuning.....	5-3
5.3 Model Analysis .....	5-3
5.3.1 Truth Filter Model.....	5-4
5.3.2 12-, 18-, and 26-Modal Models .....	5-5
5.3.3 10-, 15-, 20-, and 26-Modal-Cost Models.....	5-6
5.3.4 Additional Filter/Controller Design Models.....	5-8
5.3.5 Section Review.....	5-8
5.4 Discretization of Parameter Space .....	5-8
5.5 MMAE Performance .....	5-11
5.5.1 ME/I Performance .....	5-14
5.5.2 Bayesian Form Performance .....	5-16
5.5.3 Section Review.....	5-21
5.6 MMAC Performance.....	5-22
5.7 Summary.....	5-24
<b>VI Conclusions and Recommendations.....</b>	<b>6-1</b>
6.1 Introduction .....	6-1
6.2 Conclusions.....	6-1
6.3 Recommendations .....	6-4

	<b>page</b>
Appendix A: Spice-4 Structure Truth Model .....	A-1
Appendix B: 26-Modal Model.....	B-1
Appendix C: Spice-4 Structure Truth and Modal Models: Open Loop Bode Response .....	C-1
Appendix D: 26-Modal-Cost Model .....	D-1
Appendix E: Modal-Cost filter Models: Open Loop Bode Response.....	E-1
Appendix F: Single Filter Model Analysis.....	F-1
Appendix G: MMAE Design Performance Results.....	G-1
Appendix H: MMAC Design Performance Results.....	H-1
Bibliography .....	BIB-1
Vita.....	VITA-1

## *List of Figures*

	<b>page</b>
Figure 1-1. Multiple Model Adaptive Estimator .....	1-3
Figure 1-2. Multiple Model Adaptive Controller.....	1-4
Figure 1-3. SPICE Space Structure.....	1-6
Figure 1-4. Rotating Two-Bay Truss Model.....	1-8
Figure 1-5. Full-Bank MMAE.....	1-11
Figure 1-6. Moving Bank MMAE Fine Discretization .....	1-12
Figure 1-7. Moving Bank MMAE Coarse Discretization .....	1-12
Figure 1-8. One dimensional Moving Bank MMAE.....	1-13
Figure 2-1. Single Fixed-Gain Controller.....	2-23
Figure 2-2. Single Changeable-Gain Controller .....	2-24
Figure 2-3. Modified Single Changeable-Gain Controller.....	2-25
Figure 3-1. SPICE Structure .....	3-2
Figure 3-2. Flexible SPICE Structure .....	3-3
Figure 3-3. System Model High Level Block Diagram.....	3-6
Figure 3-4. System Model Disturbance Block .....	3-8
Figure 3-5. Wilcoxin Accelerometer Model.....	3-12
Figure 3-6. Sundstrand Accelerometer Model.....	3-13
Figure 3-7. LVDT Model.....	3-15
Figure 3-8. OSS Model.....	3-16
Figure 3-9. Feedback Loops and Control Inputs Model.....	3-18
Figure 3-10. Sundstrand and Wilcoxin Accelerometer Bode Plot.....	3-21
Figure 3-11. Sundstrand and Wilcoxin Noise Bode Plot.....	3-21
Figure 3-12. OSS Noise Bode Plot.....	3-22
Figure 3-13. Truth model block Diagram .....	3-23
Figure 4-1. (a) Estimator Simulation, and (b) Controller Simulation .....	4-3

	page
Figure 4-2. Parameter Discretization Procedure .....	4-12
Figure C-1. Truth vs. 12-mode Modal Reduced (Disturbance 1, X LOS) .....	C-2
Figure C-2. Truth vs. 12-mode Modal Reduced (Disturbance 2, X LOS) .....	C-2
Figure C-3. Truth vs. 12-mode Modal Reduced (Disturbance 3, X LOS) .....	C-2
Figure C-4. Truth vs. 12-mode Modal Reduced (Disturbance 4, X LOS) .....	C-3
Figure C-5. Truth vs. 12-mode Modal Reduced (Disturbance 5, X LOS) .....	C-3
Figure C-6. Truth vs. 12-mode Modal Reduced (Disturbance 6, X LOS) .....	C-3
Figure C-7. Truth vs. 12-mode Modal Reduced (Disturbance 7, X LOS) .....	C-4
Figure C-8. Truth vs. 12-mode Modal Reduced (Disturbance 8, X LOS) .....	C-4
Figure C-9. Truth vs. 12-mode Modal Reduced (Disturbance 9, X LOS) .....	C-4
Figure C-10. Truth vs. 12-mode Modal Reduced (Disturbance 1, Y LOS) .....	C-5
Figure C-11. Truth vs. 12-mode Modal Reduced (Disturbance 2, Y LOS) .....	C-5
Figure C-12. Truth vs. 12-mode Modal Reduced (Disturbance 3, Y LOS) .....	C-5
Figure C-13. Truth vs. 12-mode Modal Reduced (Disturbance 4, Y LOS) .....	C-6
Figure C-14. Truth vs. 12-mode Modal Reduced (Disturbance 5, Y LOS) .....	C-6
Figure C-15. Truth vs. 12-mode Modal Reduced (Disturbance 6, Y LOS) .....	C-6
Figure C-16. Truth vs. 12-mode Modal Reduced (Disturbance 7, Y LOS) .....	C-7
Figure C-17. Truth vs. 12-mode Modal Reduced (Disturbance 8, Y LOS) .....	C-7
Figure C-18. Truth vs. 12-mode Modal Reduced (Disturbance 9, Y LOS) .....	C-7
Figure C-19. Truth vs. 18-mode Modal Reduced (Disturbance 1, X LOS) .....	C-8
Figure C-20. Truth vs. 18-mode Modal Reduced (Disturbance 2, X LOS) .....	C-8
Figure C-21. Truth vs. 18-mode Modal Reduced (Disturbance 3, X LOS) .....	C-8
Figure C-22. Truth vs. 18-mode Modal Reduced (Disturbance 4, X LOS) .....	C-9
Figure C-23. Truth vs. 18-mode Modal Reduced (Disturbance 5, X LOS) .....	C-9
Figure C-24. Truth vs. 18-mode Modal Reduced (Disturbance 6, X LOS) .....	C-9
Figure C-25. Truth vs. 18-mode Modal Reduced (Disturbance 7, X LOS) .....	C-10

	page
Figure C-26. Truth vs. 18-mode Modal Reduced (Disturbance 8, X LOS) .....	C-10
Figure C-27. Truth vs. 18-mode Modal Reduced (Disturbance 9, X LOS) .....	C-10
Figure C-28. Truth vs. 18-mode Modal Reduced (Disturbance 1, Y LOS) .....	C-11
Figure C-29. Truth vs. 18-mode Modal Reduced (Disturbance 2, Y LOS) .....	C-11
Figure C-30. Truth vs. 18-mode Modal Reduced (Disturbance 3, Y LOS) .....	C-11
Figure C-31. Truth vs. 18-mode Modal Reduced (Disturbance 4, Y LOS) .....	C-12
Figure C-32. Truth vs. 18-mode Modal Reduced (Disturbance 5, Y LOS) .....	C-12
Figure C-33. Truth vs. 18-mode Modal Reduced (Disturbance 6, Y LOS) .....	C-12
Figure C-34. Truth vs. 18-mode Modal Reduced (Disturbance 7, Y LOS) .....	C-13
Figure C-35. Truth vs. 18-mode Modal Reduced (Disturbance 8, Y LOS) .....	C-13
Figure C-36. Truth vs. 18-mode Modal Reduced (Disturbance 9, Y LOS) .....	C-13
Figure C-37. Truth vs. 26-mode Modal Reduced (Disturbance 1, X LOS) .....	C-14
Figure C-38. Truth vs. 26-mode Modal Reduced (Disturbance 2, X LOS) .....	C-14
Figure C-39. Truth vs. 26-mode Modal Reduced (Disturbance 3, X LOS) .....	C-14
Figure C-40. Truth vs. 26-mode Modal Reduced (Disturbance 4, X LOS) .....	C-15
Figure C-41. Truth vs. 26-mode Modal Reduced (Disturbance 5, X LOS) .....	C-15
Figure C-42. Truth vs. 26-mode Modal Reduced (Disturbance 6, X LOS) .....	C-15
Figure C-43. Truth vs. 26-mode Modal Reduced (Disturbance 7, X LOS) .....	C-16
Figure C-44. Truth vs. 26-mode Modal Reduced (Disturbance 8, X LOS) .....	C-16
Figure C-45. Truth vs. 26-mode Modal Reduced (Disturbance 9, X LOS) .....	C-16
Figure C-46. Truth vs. 26-mode Modal Reduced (Disturbance 1, Y LOS) .....	C-17
Figure C-47. Truth vs. 26-mode Modal Reduced (Disturbance 2, Y LOS) .....	C-17
Figure C-48. Truth vs. 26-mode Modal Reduced (Disturbance 3, Y LOS) .....	C-17
Figure C-49. Truth vs. 26-mode Modal Reduced (Disturbance 4, Y LOS) .....	C-18
Figure C-50. Truth vs. 26-mode Modal Reduced (Disturbance 5, Y LOS) .....	C-18
Figure C-51. Truth vs. 26-mode Modal Reduced (Disturbance 6, Y LOS) .....	C-18

	<b>page</b>
Figure C-52. Truth vs. 26-mode Modal Reduced (Disturbance 7, Y LOS) .....	C-19
Figure C-53. Truth vs. 26-mode Modal Reduced (Disturbance 8, Y LOS) .....	C-19
Figure C-54. Truth vs. 26-mode Modal Reduced (Disturbance 9, Y LOS) .....	C-19
Figure E-1. Truth vs.10-mode Modal-Cost Reduced (Disturbance 1, X LOS).....	E-2
Figure E-2. Truth vs.10-mode Modal-Cost Reduced (Disturbance 2, X LOS).....	E-2
Figure E-3. Truth vs.10-mode Modal-Cost Reduced (Disturbance 3, X LOS).....	E-2
Figure E-4. Truth vs.10-mode Modal-Cost Reduced (Disturbance 4, X LOS).....	E-3
Figure E-5. Truth vs.10-mode Modal-Cost Reduced (Disturbance 5, X LOS).....	E-3
Figure E-6. Truth vs.10-mode Modal-Cost Reduced (Disturbance 6, X LOS).....	E-3
Figure E-7. Truth vs.10-mode Modal-Cost Reduced (Disturbance 7, X LOS).....	E-4
Figure E-8. Truth vs.10-mode Modal-Cost Reduced (Disturbance 8, X LOS).....	E-4
Figure E-9. Truth vs.10-mode Modal-Cost Reduced (Disturbance 9, X LOS).....	E-4
Figure E-10. Truth vs.10-mode Modal-Cost Reduced (Disturbance 1, Y LOS).....	E-5
Figure E-11. Truth vs.10-mode Modal-Cost Reduced (Disturbance 2, Y LOS).....	E-5
Figure E-12. Truth vs.10-mode Modal-Cost Reduced (Disturbance 3, Y LOS).....	E-5
Figure E-13. Truth vs.10-mode Modal-Cost Reduced (Disturbance 4, Y LOS).....	E-6
Figure E-14. Truth vs.10-mode Modal-Cost Reduced (Disturbance 5, Y LOS).....	E-6
Figure E-15. Truth vs.10-mode Modal-Cost Reduced (Disturbance 6, Y LOS).....	E-6
Figure E-16. Truth vs.10-mode Modal-Cost Reduced (Disturbance 7, Y LOS).....	E-7
Figure E-17. Truth vs.10-mode Modal-Cost Reduced (Disturbance 8, Y LOS).....	E-7
Figure E-18. Truth vs.10-mode Modal-Cost Reduced (Disturbance 9, Y LOS).....	E-7
Figure E-19. Truth vs.15-mode Modal-Cost Reduced (Disturbance 1, X LOS).....	E-8
Figure E-20. Truth vs.15-mode Modal-Cost Reduced (Disturbance 2, X LOS).....	E-8
Figure E-21. Truth vs.15-mode Modal-Cost Reduced (Disturbance 3, X LOS).....	E-8
Figure E-22. Truth vs.15-mode Modal-Cost Reduced (Disturbance 4, X LOS).....	E-9
Figure E-23. Truth vs.15-mode Modal-Cost Reduced (Disturbance 5, X LOS).....	E-9

	<b>page</b>
Figure E-24. Truth vs.15-mode Modal-Cost Reduced (Disturbance 6, X LOS).....	E-9
Figure E-25. Truth vs.15-mode Modal-Cost Reduced (Disturbance 7, X LOS).....	E-10
Figure E-26. Truth vs.15-mode Modal-Cost Reduced (Disturbance 8, X LOS).....	E-10
Figure E-27. Truth vs.15-mode Modal-Cost Reduced (Disturbance 9, X LOS).....	E-10
Figure E-28. Truth vs.15-mode Modal-Cost Reduced (Disturbance 1, Y LOS).....	E-11
Figure E-29. Truth vs.15-mode Modal-Cost Reduced (Disturbance 2, Y LOS).....	E-11
Figure E-30. Truth vs.15-mode Modal-Cost Reduced (Disturbance 3, Y LOS).....	E-11
Figure E-31. Truth vs.15-mode Modal-Cost Reduced (Disturbance 4, Y LOS).....	E-12
Figure E-32. Truth vs.15-mode Modal-Cost Reduced (Disturbance 5, Y LOS).....	E-12
Figure E-33. Truth vs.15-mode Modal-Cost Reduced (Disturbance 6, Y LOS).....	E-12
Figure E-34. Truth vs.15-mode Modal-Cost Reduced (Disturbance 7, Y LOS).....	E-13
Figure E-35. Truth vs.15-mode Modal-Cost Reduced (Disturbance 8, Y LOS).....	E-13
Figure E-36. Truth vs.15-mode Modal-Cost Reduced (Disturbance 9, Y LOS).....	E-13
Figure E-37. Truth vs. 20-mode Modal-Cost Reduced (Disturbance 1, X LOS).....	E-14
Figure E-38. Truth vs. 20-mode Modal-Cost Reduced (Disturbance 2, X LOS).....	E-14
Figure E-39. Truth vs. 20-mode Modal-Cost Reduced (Disturbance 3, X LOS).....	E-14
Figure E-40. Truth vs. 20-mode Modal-Cost Reduced (Disturbance 4, X LOS).....	E-15
Figure E-41. Truth vs. 20-mode Modal-Cost Reduced (Disturbance 5, X LOS).....	E-15
Figure E-42. Truth vs. 20-mode Modal-Cost Reduced (Disturbance 6, X LOS).....	E-15
Figure E-43. Truth vs. 20-mode Modal-Cost Reduced (Disturbance 7, X LOS).....	E-16
Figure E-44. Truth vs. 20-mode Modal-Cost Reduced (Disturbance 8, X LOS).....	E-16
Figure E-45. Truth vs. 20-mode Modal-Cost Reduced (Disturbance 9, X LOS).....	E-16
Figure E-46. Truth vs. 20-mode Modal-Cost Reduced (Disturbance 1, Y LOS).....	E-17
Figure E-47. Truth vs. 20-mode Modal-Cost Reduced (Disturbance 2, Y LOS).....	E-17
Figure E-48. Truth vs. 20-mode Modal-Cost Reduced (Disturbance 3, Y LOS).....	E-17
Figure E-49. Truth vs. 20-mode Modal-Cost Reduced (Disturbance 4, Y LOS).....	E-18



	page
Figure E-50. Truth vs. 20-mode Modal-Cost Reduced (Disturbance 5, Y LOS).....	E-18
Figure E-51. Truth vs. 20-mode Modal-Cost Reduced (Disturbance 6, Y LOS).....	E-18
Figure E-52. Truth vs. 20-mode Modal-Cost Reduced (Disturbance 7, Y LOS).....	E-19
Figure E-53. Truth vs. 20-mode Modal-Cost Reduced (Disturbance 8, Y LOS).....	E-19
Figure E-54. Truth vs. 20-mode Modal-Cost Reduced (Disturbance 9, Y LOS).....	E-19
Figure F-1. Truth Model X-Axis LOS Error - with No Control Applied .....	F-2
Figure F-2. Truth Model Y-Axis LOS Error - with No Control Applied .....	F-2
Figure F-3. Truth Filter Model X-Axis Estimation Error.....	F-3
Figure F-4. Truth Filter Model Y-Axis Estimation Error.....	F-3
Figure F-5. Truth Filter Model X-Axis LOS Error - With Control Applied .....	F-4
Figure F-6. Truth Filter Model Y-Axis LOS Error - With Control Applied .....	F-4
Figure F-7. 12 Modal Filter Model X-Axis Estimation Error .....	F-5
Figure F-8. 12 Modal Filter Model Y-Axis Estimation Error .....	F-5
Figure F-9. 12 Modal Filter Model X-Axis LOS Error - With Control Applied .....	F-6
Figure F-10. 12 Modal Filter Model Y-Axis LOS Error - With Control Applied .....	F-6
Figure F-11. 18 Modal Filter Model X-Axis Estimation Error .....	F-7
Figure F-12. 18 Modal Filter Model Y-Axis Estimation Error .....	F-7
Figure F-13. 18 Modal Filter Model X-Axis LOS Error - With Control Applied .....	F-8
Figure F-14. 18 Modal Filter Model Y-Axis LOS Error - With Control Applied .....	F-8
Figure F-15. 26 Modal Filter Model X-Axis Estimation Error .....	F-9
Figure F-16. 26 Modal Filter Model Y-Axis Estimation Error .....	F-9
Figure F-17. 26 Modal Filter Model X-Axis LOS Error - With Control Applied .....	F-10
Figure F-18. 26 Modal Filter Model Y-Axis LOS Error - With Control Applied .....	F-10
Figure F-19. 10 Modal-Cost Filter Model X-Axis Estimation Error.....	F-11
Figure F-20. 10 Modal-Cost Filter Model Y-Axis Estimation Error.....	F-11
Figure F-21. 10 Modal-Cost Filter Model X-Axis LOS Error-W/ Control Applied ....	F-12

	page
Figure F-22. 10 Modal-Cost Filter Model Y-Axis LOS Error-W/ Control Applied ....	F-12
Figure F-23. 15 Modal-Cost Filter Model X-Axis Estimation Error .....	F-13
Figure F-24. 15 Modal-Cost Filter Model Y-Axis Estimation Error .....	F-13
Figure F-25. 15 Modal-Cost Filter Model X-Axis LOS Error-W/ Control Applied ....	F-14
Figure F-26. 15 Modal-Cost Filter Model Y-Axis LOS Error-W/ Control Applied ....	F-14
Figure F-27. 20 Modal-Cost Filter Model X-Axis Estimation Error .....	F-15
Figure F-28. 20 Modal-Cost Filter Model Y-Axis Estimation Error .....	F-15
Figure F-29. 20 Modal-Cost Filter Model X-Axis LOS Error-W/ Control Applied ....	F-16
Figure F-30. 20 Modal-Cost Filter Model Y-Axis LOS Error-W/ Control Applied ....	F-16
Figure F-31. 26 Modal-Cost Filter Model X-Axis Estimation Error .....	F-17
Figure F-32. 26 Modal-Cost Filter Model Y-Axis Estimation Error .....	F-17
Figure F-33. 26 Modal-Cost Filter Model X-Axis LOS Error-W/ Control Applied ....	F-18
Figure F-34. 26 Modal-Cost Filter Model Y-Axis LOS Error-W/ Control Applied ....	F-18
Figure F-35. 26 Truncated Modal Filter Model X-Axis Estimation Error .....	F-19
Figure F-36. 26 Truncated Modal Filter Model Y-Axis Estimation Error .....	F-19
Figure F-37. 26 Trunc. Modal Filter Model X-Axis LOS Error-W/ Control App .....	F-20
Figure F-38. 26 Trunc. Modal Filter Model Y-Axis LOS Error-W/ Control App .....	F-20
Figure G-1. Parameter Position Monitoring with Parameter Match (MEI) .....	G-2
Figure G-2. Parameter Position Monitoring with Parameter Jump Up (MEI) .....	G-2
Figure G-3. Parameter Position Monitoring with Parameter Jump Down (MEI) .....	G-2
Figure G-4. Parameter Position Monitoring with Parameter Move Up (MEI) .....	G-3
Figure G-5. Parameter Position Monitoring with Parameter Move Down (MEI) .....	G-3
Figure G-6. Residual Monitoring with Parameter Match .....	G-4
Figure G-7. Probability Monitoring with Parameter Match .....	G-4
Figure G-8. Parameter Position Monitoring with Parameter Match .....	G-4
Figure G-9. Residual Monitoring with Parameter Offset Up .....	G-5

	<b>page</b>
Figure G-10. Probability Monitoring with Parameter Offset Up.....	G-5
Figure G-11. Parameter Position Monitoring with Parameter Offset Up .....	G-5
Figure G-12. Residual Monitoring with Parameter Offset Down .....	G-6
Figure G-13. Probability Monitoring with Parameter Offset Down .....	G-6
Figure G-14. Parameter Position Monitoring with Parameter Offset Down.....	G-6
Figure G-15. Residual Monitoring with Parameter Jump Up .....	G-7
Figure G-16. Probability Monitoring with Parameter Jump Up.....	G-7
Figure G-17. Parameter Position Monitoring with Parameter Jump Up .....	G-7
Figure G-18. Residual Monitoring with Parameter Jump Down.....	G-8
Figure G-19. Probability Monitoring with Parameter Jump Down .....	G-8
Figure G-20. Parameter Position Monitoring with Parameter Jump Down.....	G-8
Figure G-21. Residual Monitoring with Parameter Move Up.....	G-9
Figure G-22. Probability Monitoring with Parameter Move Up .....	G-9
Figure G-23. Parameter Position Monitoring with Parameter Move Up.....	G-9
Figure G-24. Residual Monitoring with Parameter Move Down.....	G-10
Figure G-25. Probability Monitoring with Parameter Move Down .....	G-10
Figure G-26. Parameter Position Monitoring with Parameter Move Down.....	G-10
Figure G-27. Parameter Pos. Mon. with Parameter Offset Up (Move Only) .....	G-11
Figure G-28. Parameter Pos. Mon. with Parameter Offset Down (Move Only).....	G-11
Figure G-29. Parameter Pos. Mon. with Parameter Jump Up (Move Only).....	G-12
Figure G-30. Parameter Pos. Mon. with Parameter Jump Down (Move Only).....	G-12
Figure H-1. X-axis LOS Error with Res. Mon., Mod MMAC control, Par. Jump .....	H-2
Figure H-2. Y-axis LOS Error with Res. Mon., Mod MMAC control, Par. Jump .....	H-2
Figure H-3. Residual Monitoring w/MMAC and Parameter Match.....	H-3
Figure H-4. Probability Monitoring w/MMAC and Parameter Match .....	H-3
Figure H-5. Parameter Position Monitoring w/MMAC and Parameter Match.....	H-3

	page
Figure H-6. Residual Monitoring w/Mod MMAC and Parameter Match.....	H-4
Figure H-7. Probability Monitoring w/Mod MMAC and Parameter Match .....	H-4
Figure H-8. Parameter Pos. Monitoring w/Mod MMAC and Parameter Match .....	H-4
Figure H-9. Residual Monitoring w/MAP and Parameter Match.....	H-5
Figure H-10. Probability Monitoring w/MAP and Parameter Match .....	H-5
Figure H-11. Parameter Position Monitoring w/MAP and Parameter Match.....	H-5
Figure H-12. Residual Monitoring w/Changeable Gain and Parameter Match .....	H-6
Figure H-13. Probability Monitoring w/Changeable Gain and Parameter Match .....	H-6
Figure H-14. Parameter Pos. Mon. w/Changeable Gain and Parameter Match.....	H-6
Figure H-15. Residual Monitoring w/MMAC and Parameter Jump .....	H-7
Figure H-16. Probability Monitoring w/MMAC and Parameter Jump .....	H-7
Figure H-17. Parameter Position Monitoring w/MMAC and Parameter Jump.....	H-7
Figure H-18. Residual Monitoring w/Mod MMAC and Parameter Jump .....	H-8
Figure H-19. Probability Monitoring w/Mod MMAC and Parameter Jump.....	H-8
Figure H-20. Parameter Position Monitoring w/Mod MMAC and Parameter Jump .....	H-8
Figure H-21. Residual Monitoring w/MAP and Parameter Jump .....	H-9
Figure H-22. Probability Monitoring w/MAP and Parameter Jump.....	H-9
Figure H-23. Parameter Position Monitoring w/MAP and Parameter Jump .....	H-9
Figure H-24. Residual Monitoring w/Changeable Gain and Parameter Jump.....	H-10
Figure H-25. Probability Monitoring w/Changeable Gain and Parameter Jump .....	H-10
Figure H-26. Parameter Pos. Monitoring w/Changeable Gain and Parameter Jump ...	H-10
Figure H-27. Residual Monitoring w/MMAC and Parameter Move.....	H-11
Figure H-28. Probability Monitoring w/MMAC and Parameter Move .....	H-11
Figure H-29. Parameter Position Monitoring w/MMAC and Parameter Move.....	H-11
Figure H-30. Residual Monitoring w/Mod MMAC and Parameter Move .....	H-12
Figure H-31. Probability Monitoring w/Mod MMAC and Parameter Move .....	H-12

	page
Figure H-32. Parameter Position Mon. w/Mod MMAC and Parameter Move.....	H-12
Figure H-33. Residual Monitoring w/MAP and Parameter Move .....	H-13
Figure H-34. Probability Monitoring w/MAP and Parameter Move .....	H-13
Figure H-35. Parameter Position Monitoring w/MAP and Parameter Move.....	H-13
Figure H-36. Residual Monitoring w/Changeable Gain and Parameter Move.....	H-14
Figure H-37. Probability Monitoring w/Changeable Gain and Parameter Move .....	H-14
Figure H-38. Parameter Pos. Monitoring w/Changeable Gain and Parameter Move...	H-14

### ***List of Tables***

	<b>page</b>
Table 3-1. Modal eigenvalues and natural frequencies for the first 30 modes .....	3-30
Table 3-2. Top 30 Component Cost values and associated modes .....	3-32
Table 5-1. Filter/Controller Model Performance Results.....	5-9
Table 5-2. MMAC Control Performance Results.....	5-24
Table F-1. Filter Model Tuning Parameters .....	F-1

*Abstract*

The purpose of this thesis is to apply moving-bank multiple model adaptive estimation and control (MMAE/MMAC) algorithms to an actual space structure (SPICE) being examined at Phillips Laboratory at Kirtland AFB, NM. The structure consists of a large platform and a smaller platform connected by three legs in a tripod fashion. Kalman filtering and LQG control techniques are utilized as the primary design tool. Implementing a bank of filters increases the robustness of the LQG controller when uncertainties exist in the system model, whereas the moving bank is utilized to reduce the computational load. Several reduced-order models are developed from the truth model using modal analysis and modal cost analysis. The MMAE/MMAC design with a dramatically reduced-order filter model provides an excellent method to estimate a wide range of parameter variations and to quell oscillations in the structure.

# **CONTROL OF A LARGE SPACE STRUCTURE USING MULTIPLE MODEL ADAPTIVE ESTIMATION AND CONTROL TECHNIQUES**

## ***I. Introduction***

In systems in which the dynamic responses are not deterministic but stochastic in nature, Kalman filters have been proven effective at estimating the system states. However, this assumes the system model is comprised of known parameters and that these parameters vary within the robustness range of the Kalman filter as determined by a performance analysis with proper tuning. An example of a typical parameter might be the time constant of a first order lag model, or the damping ratio of a second order model. If these parameters are not known exactly or are not within the range mentioned previously, they may severely degrade the performance of the Kalman filter based on the assumed system model. In actual systems, these parameters may be constant, vary daily (temperature variations), vary over time (possibly due to aging), or make large discrete jumps (as in a structural fatigue or a break). It would be difficult to develop a single non-adaptive Kalman filter to be completely robust in this arena. Multiple Model Adaptive Estimation (MMAE) has been presented as a technique that may prove effective in these situations [25:129]. In principle, each value that the uncertain parameter may take is incorporated into the system model of a single Kalman filter. Many such filters are generated and arrayed in a parallel "bank", each based on a different system model. The output (state estimate) of each filter is probabilistically weighted relative to the others,



using the probability that each hypothesized parameter value is in fact the best value (based on evidence gathered through the history of measurements) at the current time, as determined by a scheme in which the filter based on the correct parameter obtains the highest probability. The sum of the individual probabilities will be equal to the value 1. The weighted outputs are summed to generate the overall adaptive state estimate. A diagram of the MMAE is presented in Figure 1-1. As illustrated, the output of the system,  $z$ , is fed into each Kalman filter (each based on the assumed parameter,  $a_k$  for  $k=1,2,\dots,K$ ) which then outputs a state estimate,  $\hat{x}_k$ , and residual,  $r_k$ . The residual  $r_k$  is the difference between the actual measurement,  $z$ , and the best prediction of its value produced by the Kalman filter based on the assumption that the correct value of the parameter vector is  $a_k$ . A probability weighting factor is generated for each filter state estimate as determined by a hypothesis conditional probability computation [25:130] applied to its residual. The probability weighting factors are multiplied by the appropriate state estimates. The MMAE state estimate is the resulting sum of all these products, which is a probability weighted average.

Unfortunately, there are problems inherent in this technique. If the range of the possible parameters is continuous, the number of Kalman filters required would be infinite. A substantial number of filters might still be required for a discretized parameter space, and this would still be computationally burdensome.

By utilizing a "moving bank" of Kalman filters, the computational load will be lessened. The concept of the moving bank involves using filters defined for a subset of the full parameter space. Thus at any one time only a small portion of the total number of filters will be on-line and actively estimating the system states. The assumed parameters of this subset would attempt to surround the current parameter estimate in the parameter space, and be able to move should the parameter drift or jump. This will be illustrated later

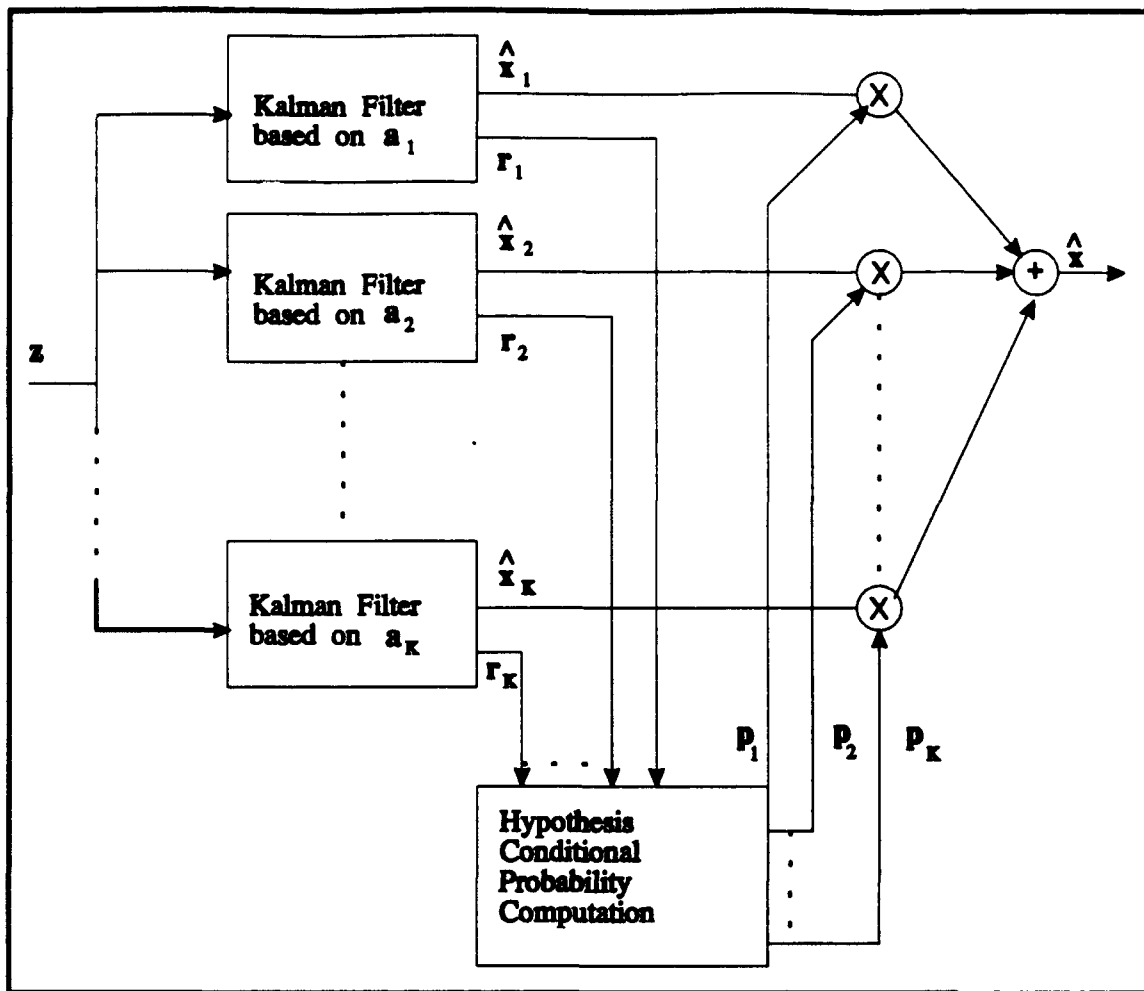


Figure 1-1. Multiple Model Adaptive Estimator [25:132]

in Section 1.2.3. By so doing, the sum of the probabilities of the active filters should be predominant, and the sum of the probabilities of the inactive filters should be negligible. Moving the bank is accomplished by dynamically redeclaring which set of filters will be active. In this manner, the moving bank should be able to track the parameter estimate and thus maintain its validity.

Since this research is being applied to a linearized system model, an obvious choice for the controller is one based on the Linear system model with a Quadratic cost control criterion driven by white Gaussian noises (LQG). Other controllers might suit the needs

of this system, but this thesis will focus strictly on the LQG controller. The Multiple Model Adaptive Controller (MMAC) design is depicted in Figure 1-2. The LQG controller gain  $-G_c^*$  associated with each parameter value  $a_k$  is cascaded with the output state estimate from each associated filter and appropriately weighted (as discussed previously). The sum of all the weighted controls  $u_k$  from each individual LQG controller forms the final control for the system. Additionally, each of the individual filters is provided knowledge of the final control as fed to the real world system (although this is not explicitly shown in Figure 1-2 in order to keep the diagram from becoming unnecessarily complicated).

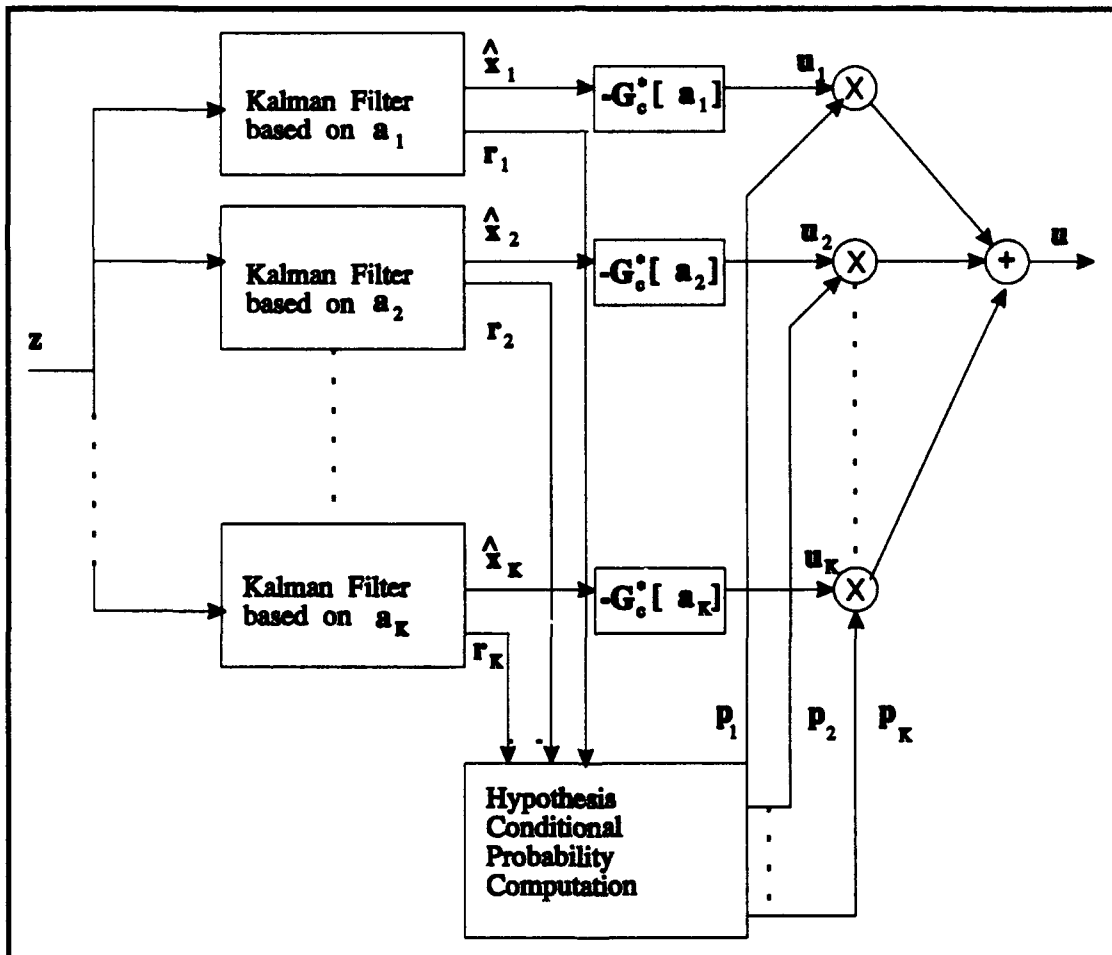


Figure 1-2. Multiple Model Adaptive Controller

Due to the large size of system states involved in this thesis, it will be desirable to attempt to reduce the order of the controller design model. This will further decrease the computational burden, while possibly making the controller physically realizable for the actual system. However, care must be taken not to eliminate states that would adversely affect the performance of the Kalman filters or LQG controllers. There may exist a lower bound on the number of states necessary for good performance (when tested against a *full-order* simulation of the real world system) which may still result in excessive computational loading. It will be necessary to analyze the tradeoff between the two concerns. Additional care must be taken when tuning the filters. Proper tuning by adding pseudonoise to compensate for system model order reduction or other deficiencies may also cloud the filter differences from the parameter discretization and incapacitate the "Hypothesis Conditional Probability Computation" blocks of Figures 1-1 and 1-2. Determination of additional pseudonoise and parameter discretization must be accomplished concurrently.

This thesis will utilize a moving-bank MMAE and LQG-based MMAC controller to control a large flexible space structure (SPace Integrated Controls Experiment, or SPICE), with the primary goal being to quell unwanted vibrations induced in the structure. Figure 1-3 displays a simple rendering of the physical structure located at Phillips Laboratories, Kirtland AFB, NM. This work follows directly from work accomplished by Gustafson [11], but using an updated version of the system model (Version 4 or SPICE-4).

### **1.1 Notation**

Notation used in this thesis will attempt to maintain consistency with [24]. Deterministic and stochastic processes alike will be indicated by the roman typeface. Vectors will be displayed in bold-faced type,  $\mathbf{x}$ , whereas scalars will be normal type,  $x$ .

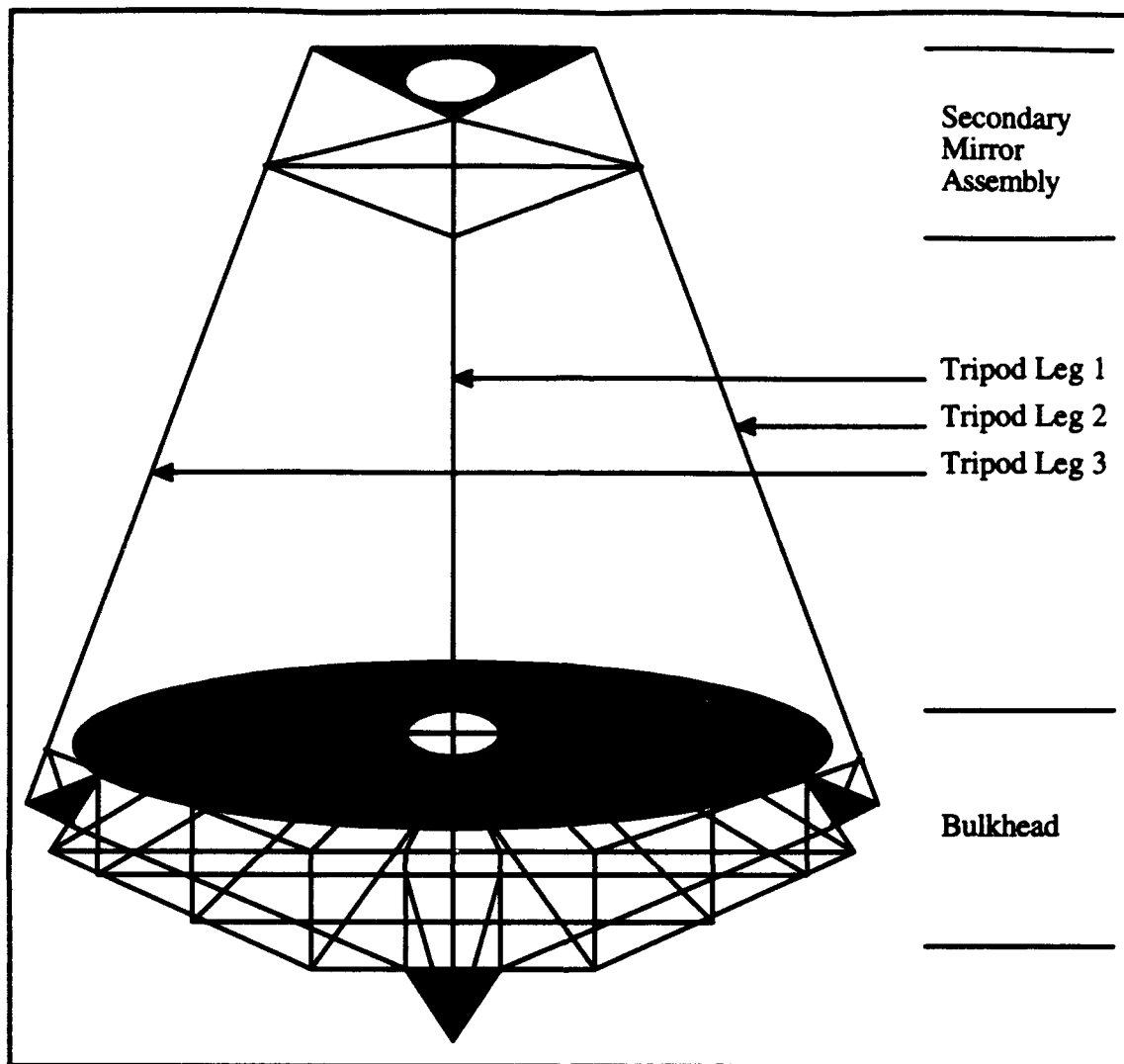


Figure 1-3: SPICE Space Structure

Matrices will be displayed in upper case, **X**. A particular realization of a variable will be displayed in italics, *x*.

## 1.2 Background

The purpose of this section is to explore the four main areas of concern involved with this research. These four include: (1) the system model, (2) Multiple Model Adaptive Estimation (MMAE), (3) Moving-Bank MMAE, and (4) Moving-Bank Multiple Model

Adaptive Controller (MMAC). This discussion will not address the specific problem for which this research is being accomplished, but will present the ideas in a more general sense.

### ***1.2.1 System Model***

The actual system model will be presented in Chapter 3. As stated previously, this model is just an updated version of the true-to-life full system model of 194 states first used in Gustafson's research [11]. Although the physical shapes are different, the development of the models will be very similar. For the purposes of this discussion, a simpler model will be better suited towards an introduction of the concepts. Research accomplished prior to Gustafson employed much more simplistic system models [15,18,33,37,42], of which the latest will be presented here.

The physical shape of the simpler model was that of the two-bay truss structure illustrated in Figure 1-4. This shape was originally devised to emulate an appendage that required adaptive control, which would then exist attached to a much larger space structure. The rectangular structure shown would be attached to a much larger structure (not shown) at the hub. The entire truss structure in the figure can be rotated about the hub in planar motion. The hub can be thought to be fixed with respect to inertial space. Physically slewing the truss structure about the hub (for purposes of pointing or achieving a new angular orientation) results in undesired vibrations which must be quelled. There are accelerometer pairs co-located with actuator pairs (thrusters) at the two positions indicated on the figure. The accelerometers are assumed to measure position and velocity, and the actuators are used to generate control inputs to quell the physical vibrations of the structure. Additionally, there are two gyros located at the hub which measure angular position and velocity.

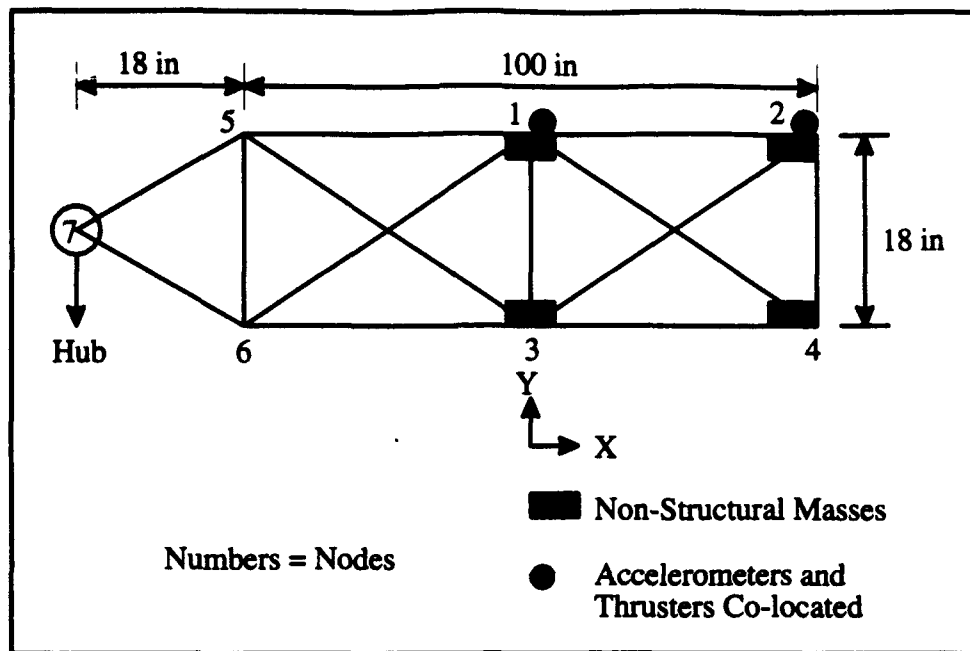


Figure 1-4. Rotating Two-Bay Truss Model

Initially, only a 6-state truth model was developed for the example system [15,18], but was later expanded to 24 states [42]. The 24-state model enhanced the accuracy of the truth model by reducing the number of unmodeled states. These models were developed by applying a finite element analysis in the determination of the mass and stiffness matrices [44]. Chapter 3 will provide a discussion relating the mass and stiffness matrices to the damping ratios ( $\zeta$ ) and natural frequencies ( $\omega_n$ ) of all modeled bending modes. These last two parameters were considered to be unknown and formed the basis for the uncertain system model requiring numerous Kalman filters.

### 1.2.2 Multiple Model Adaptive Estimation

The need for any type of adaptive algorithm arises from uncertainties in the system under scrutiny. MMAE is one method of dealing with these uncertainties. If there are uncertain parameters,  $\mathbf{a}$  (a vector composed of scalar parameters such as  $\zeta$  and  $\omega_n$ ), the state model cannot be determined exactly. These parameters can be thought to fill a space

defined by all the possible values a particular parameter may take ( $\mathbf{a}_k$  for  $k = 1, 2 \dots K$ ). Kalman filters have a subjective level of robustness inherent in their development (able to address relatively small uncertainties in the system model), but in this situation, the possible range of uncertainty is too large. A filter must be generated for each specified parameter value in the space. The parameter space may be already discretized by the physical attributes of the system, but more likely, it is a continuous range. A continuous space must be purposefully discretized to keep the number of filters realizable. Since one filter is necessary for each discretized value, the total number of filters corresponds directly to the number of chosen values in the space. For the example system used in initial research [15,18,33,37,42], there were 2 uncertain parameters  $\mathbf{a} = (\zeta, \omega_n)^T$  that were allowed to vary, each with 10 possible discrete values. The resulting parameter space was a two-dimensional  $10 \times 10$  space, requiring 100 filters ( $K=100$ ). If each parameter had 100 values instead, the number of filters jumps to 10,000. It is easy to see the number of filters can become computationally unbearable quickly as the parameter space grows in size and as more uncertain parameters are added.

The output state estimate,  $\hat{\mathbf{x}}_k$ , from each Kalman filter is based on the parameter value,  $\mathbf{a}_k$ , used in its system model. The state estimate from the filter using the parameter value closest to the true value should be determined to be the most correct. Thus, the magnitude of the output residual,  $\mathbf{r}_k$ , should be the smallest for this filter, whereas the magnitudes from other filters should be relatively larger [25:133]. The residuals are used in conjunction with a hypothesis conditional probability to determine a weighting factor for the corresponding state estimate. This hypothesis probability is the probability that the discrete parameter value used in the filter's system model is closest to the true parameter, conditioned on the history of measurements observed until the current time. Consequently, the highest conditional probability should be assigned to the most correct filter (smallest residual), and lower relative conditional probabilities assigned to the other



filters [25:133]. There are four different methods for determining the final state estimate: (1) the Bayesian form (alluded to in Figure 1-1), (2) Maximum A Posteriori (MAP), (3) the Bayesian form based upon the Maximum Entropy with Identity Covariance (ME/I) density computation, and (4) the MAP form with the ME/I density computation. These methods will be presented in Section 2.3.2.

### ***1.2.3 Moving-Bank MMAE***

The concept of the moving-bank MMAE arose from the need to reduce the computational burden created by a full bank of Kalman filters. In the previous section, a 2-dimensional type bank of 100 filters was introduced and is illustrated in Figure 1-5. On this figure, "Active Filter" designates a discrete parameter value upon which an active filter is based. Currently, it would be computationally infeasible to consider having all these filters active at once. Therefore, it becomes necessary to maintain a minimum possible number of filters active at any time. For the introduced system, the variable parameters ( $\zeta$  and  $\omega_n$ ) can assume only one point or position in the two-dimensional parameter space upon which the bank of filters is based. It is reasonable to assume the filters based on parameter values nearest this point would have the smallest residuals (best state estimates) and those based on values farther away would have larger residuals (relatively poorer state estimates). The filters based on parameter values that are farther away can be "deactivated" without impact on the final state estimate, since their probability  $p_k$  values would be very small. Only the filters based upon closer point values would be active, which would result in the reduction of the computational load. In a 2-space such as this, an immediate choice of the number of filters would be 9 (3x3 block) so that the point defined by the actual parameters would be surrounded. As the parameters vary, this point would drift (or jump) and the bank would have to be made to move. The filters on the side(s) farthest from the drifting point would be deactivated and ones nearest

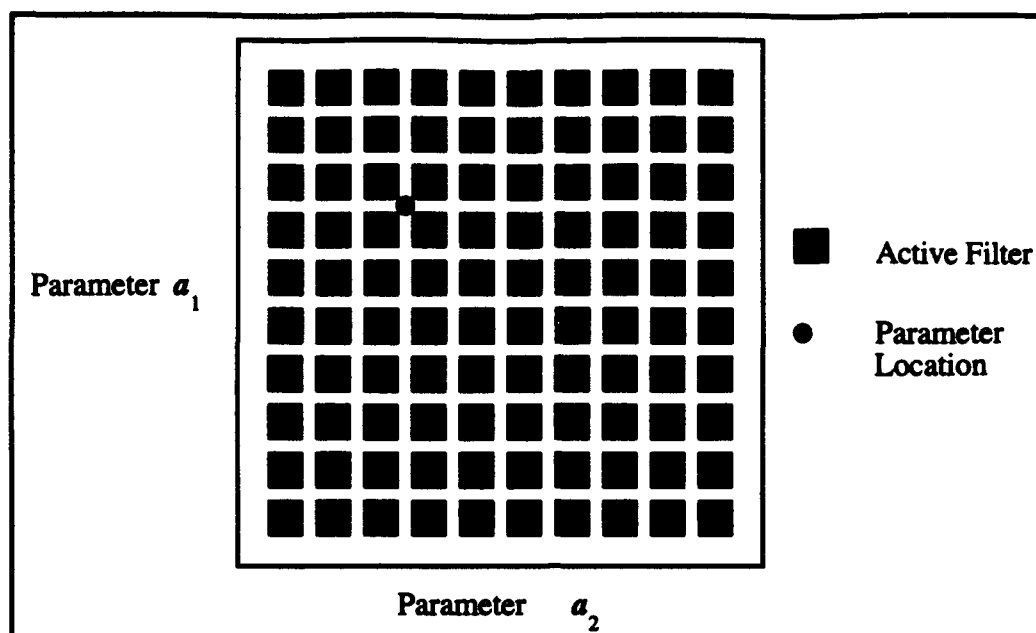


Figure 1-5. Full-Bank MMAE

the new position would be activated. This smaller bank would then "move" by dynamic redeclaration of the active filters, attempting to maintain itself centered within a threshold about the true parameter point. This concept is depicted in Figure 1-6. In this case, the parameter position drifted diagonally, requiring that two sides be deactivated and redeclared. This figure also illustrates what will be referred to as a fine discretization, where the active filters' parameter points are adjacent to each other.

A coarse discretization might be required should the parameter position be totally unknown, as in an initial acquisition phase or in the instance of the true parameter value jumping by a large discrete amount. This is illustrated in Figure 1-7. Here the active Kalman filters' parameter point values are expanded to the widest positions while maintaining consistent relative spacing.

In this research, only one uncertain parameter will be addressed, where the resulting parameter space will be one-dimensional, as illustrated in Figure 1-8 (page 1-13). The full bank (all filters active concurrently), Figure 1-8(1), still would be computationally

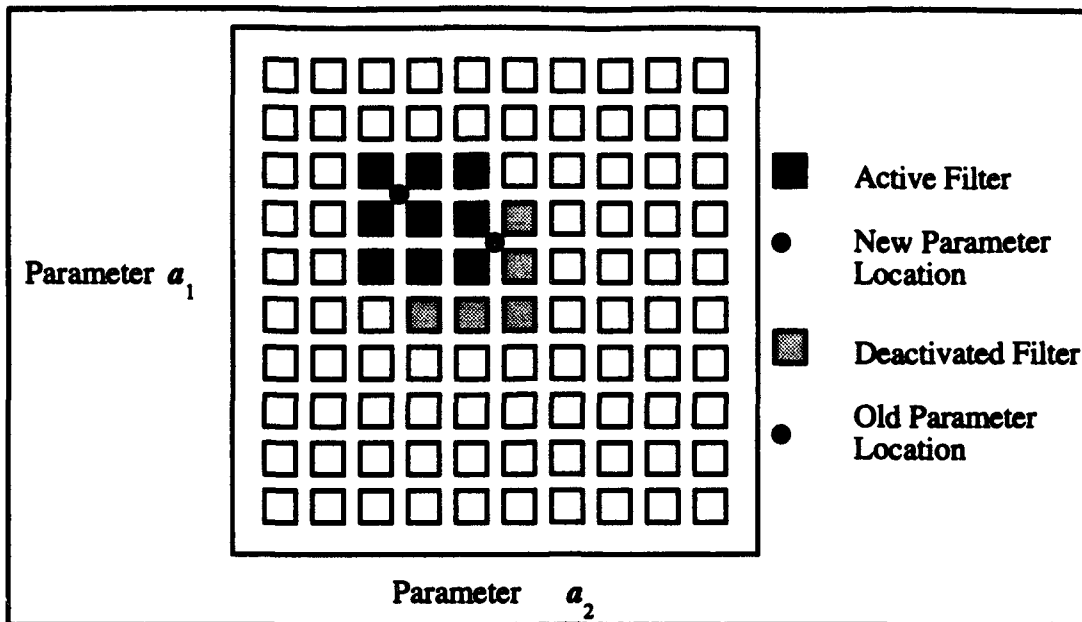


Figure 1-6. Moving Bank MMAE Fine Discretization

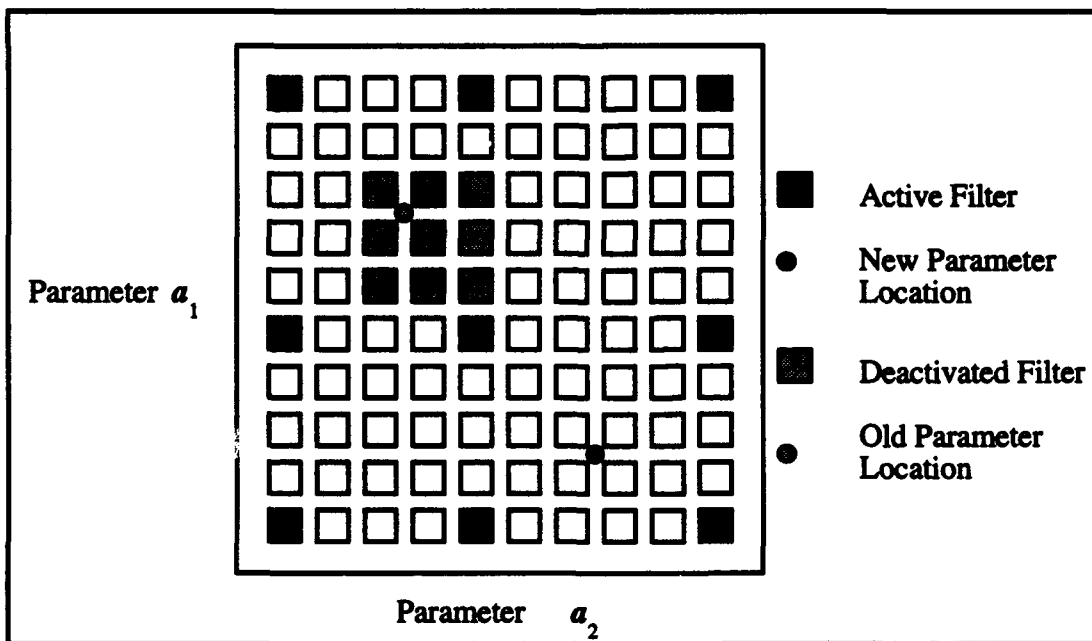


Figure 1-7. Moving Bank MMAE Coarse Discretization

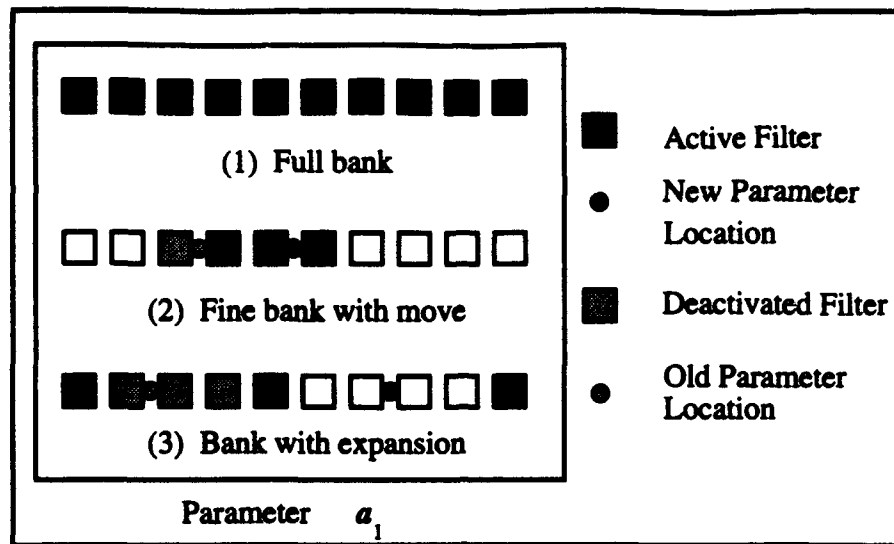


Figure 1-8. One dimensional Moving Bank MMAE

infeasible. The moving bank approach is presented in Figure 1-8 (2), where the move logic is implemented for a small jump in the parameter value. A bank expansion for a large jump is presented in Figure 1-8 (3).

There are 5 methods for deciding to expand, contract, move, or not move the bank. These decision making techniques are: (1) Residual Monitoring, (2) Parameter Position Estimate Monitoring, (3) Parameter Position and "Velocity" Estimate Monitoring, (4) Probability Monitoring, and (5) Parameter Estimation Error Covariance Monitoring [30]. These techniques will be presented in Section 2.4.

#### 1.2.4 Moving-Bank MMAC

As previously mentioned, this thesis will utilize the LQG controller. For this type of controller, the assumptions are that the system is adequately modeled as Linear, the cost is of a Quadratic form, and the noise inputs are Gaussian. Since the desire is to quell the vibration in the structure, which is equivalent to driving all the states to zero (except rigid body states which are ignored), a Regulator form of the LQG controller will be used [26:19]. It is shown in the development of the non-adaptive LQG controller that the

optimal stochastic controller is just the optimal deterministic full-state feedback LQ controller with the actual system states replaced with the conditional state estimate obtained from the Kalman filter. This is referred to as the "certainty equivalence property" [26:17]. This property is readily adaptable to the MMAC application for each assumed parameter value  $\mathbf{a}_k$ , since the state estimates are available from each filter as discussed in the previous section. Using such a structure for a controller when there are uncertain parameter values is a form of "assumed certainty equivalence" [14,26:253]. Thus, each LQG controller is based on one discretized parameter position, as in the MMAE filters. In the general sense, the resulting controller gains are cascaded from each of the state estimates from the MMAE and combined in some manner (discussed later) to form the final controller output. A steady state constant-gain control law can be obtained if the initial transients in the Kalman filter and the final transients in the deterministic optimal controller gain are assumed to be negligible. In order for this to be valid, the control application interval must be long compared to the two transient time periods.

There are six methods for combining the MMAE and LQG controller. These are: (1) MMAC Control, (2) "Modified" MMAC Control, (3) MAP versus Bayesian MMAC Control, (4) Single Fixed-Gain Control, (5) Single Changeable-Gain Control, and (6) "Modified" Single Changeable-Gain Control. These methods will be presented in Section 2.6.1.

### **1.3 Past Research**

Research on this topic was initiated by Hentz and Maybeck in 1984 [14,30]. Hentz was able to show that a moving-bank MMAE performed as well as a full-bank MMAE, but with a resulting order of magnitude less computational load [14]. Hentz began development of the algorithms and appropriate thresholds to move, expand and

contract the bank. Hentz also explored many of the controller design approaches discussed in the previous section.

Filios' major contributions were the insights provided by the use of ambiguity function analysis applied to performance evaluation and appropriate threshold levels for moving and contracting the bank [7]. Unfortunately, the simple application he chose to use did not result in a need for adaptive control [7:93].

The first to utilize the physical structure displayed in Figure 1-4 was Karnick [15,16]. He used a 6-state truth model and 6-state filter model. Karnick's results were not very promising since they indicated that the moving-bank MMAE was never able to identify the uncertain parameters, even though it was sometimes able to provide accurate state estimates [15:93]. Karnick found that the moving bank wandered randomly throughout the parameter space and never provided a consistent parameter estimate. Consequently, the final results indicated that a coarsely discretized full-bank MMAE could perform as well as a finely discretized moving-bank MMAE [15:92].

Lashlee [18,19] examined the difficulties encountered by Karnick. He focused on the tuning aspects of Karnick's design, which includes the dynamics noise strength and measurement noise covariance, the state weighting and control matrices in the deterministic optimal controller synthesis, and the parameter space discretization process. Lashlee demonstrated that it is essential to distinguish strongly between a good and a bad model in order to move the bank effectively. Also, there is a lower bound on the measurement precision that, if exceeded, will severely hamper the moving-bank adaptation process. As a result, Lashlee was able to show a greater performance potential for the moving-bank MMAE with more precise measurements, a properly tuned bank of filters, and an appropriately discretized parameter space [18:199].

Van Der Werken [42] expanded the truth model to 24 states and examined the performance degradation between this and the 6-state filter design models used by Karnick and Lashlee [42:14]. Van Der Werken's results indicated that the moving-bank MMAE could not adapt and provide good estimates of state and parameter position if initially offset from the true parameter position. Thus, he concluded that the unmodeled states had a significant impact on the moving-bank MMAE's ability to provide accurate estimates [42:14]

Schore [31,37] followed Van Der Werken but focused on the appropriate dimension for the reduced order model, initially assuming Van Der Werken's conclusion about the unmodeled states was correct. Schore developed a physically motivated approach to evaluate filter performance which investigated the reduced order filter's estimate of the true total shape of the truss rather than its estimate of individual bending mode generalized coordinates [37]. After correcting some software problems, Schore was able to demonstrate that the performance degradation using the original 6-state filter model and 24-state truth model was negligible [37].

Moyle concentrated on improving the moving-bank MMAE and control algorithms [33]. Software improvements resulted in substantial improvements in the baseline performance. Likewise, improved tuning of the Kalman filters' measurement noises and LQG controllers' weighting matrices resulted in better state estimates and actuator performance, respectively [33]. Moyle had the best success with the ME/I, parameter position monitoring, and modified MMAC combination (see the last paragraphs in Sections 1.2.2 and 1.2.4), achieving performance comparable to the non-adaptive artificially informed benchmark [33]. Moyle also demonstrated that packing the assumed parameter discrete values more densely at higher frequencies for the parameter

discretization had no effect in improving controller performance [33]. This was contrary to the results obtained by Sheldon in his research on this topic [38,39].

Gustafson was the first to implement the entire 194-state SPICE version 2 (SPICE-2) system model as the truth model [11,12]. Gustafson investigated full-order controllers and reduced-order controllers obtained by two methods, internally balanced reduction and modal reduction. Both types of reduced-order based filter/controllers fared poorly, such that no definite choice between the two reduction methods could be determined [11]. Gustafson did have success with a full-order controller, which led to the conclusion that the moving-bank MMAE/MMAC algorithm can provide stabilizing control over all possible values of the uncertain parameters, yet this still did not meet RMS specifications levied by Phillips Laboratories (the sponsor of the research). He felt that the failure lay in the physical structure and not in the MMAE process, and that in order to meet specifications, better actuators and more precise measurement devices would be necessary [11]. Gustafson's parameter discretization method resulted in a  $3 \times 7$  ( $\zeta$  and  $\omega_n$ , respectively) nonlinearly discretized optimal parameter space. It was determined that the controller was insensitive to the damping ratio to the degree that this parameter could possibly be deleted as an uncertain parameter without loss of performance. The best results were obtained using the ME/I technique with parameter position monitoring. Since the parameter space was so small, Gustafson did not use an algorithm to expand or contract the bank. The best results were gained by using a single nominal value for  $\zeta$  and allowing the bank to be one-dimensional in the  $\omega_n$  direction.

#### **1.4 Problem Statement**

This thesis concentrates on applying a moving-bank MMAE/MMAC to the SPICE-4 space structure. Previous work indicated that possible physical, actuator and measurement deficiencies in the SPICE-2 model led to unacceptable controller



performance for controllers based on reduced-order designs [11]. Full-order controllers had more acceptable performances, yet still failed to meet specifications. The updated version 4 is anticipated to have dealt with these deficiencies such that even reduced-order controller designs will meet specification. A physical description of the system will be presented in Chapter 3. It will be vital to have acceptable performance from reduced-order controllers due to the extreme computational burden imposed by the large number of system state encountered in this problem.

### **1.5 Scope**

The focus of this research will be to suppress unwanted vibrations quickly in the SPICE-4 space structure. Unlike the example system used in initial research and the previous version [11,15,18,33,37,42], only one unknown parameter is to be estimated, namely, the undamped natural frequency (the same scalar multiplier is applied to all modes' frequencies [45]). Research will begin with the development of the new system model as the truth model and then to reduced-order models for implementation in the Kalman filters, LQG controllers, and MMAE/MMAC algorithms. Designs and performance analyses will be developed for this structure using the software developed for the previous version as a guide.

### **1.6 Approach**

The development and testing of the MMAE/MMAC for the total structure will encompass 8 steps as follows: (1) development of the system model for the truth model, (2) development of reduced-order models for implementation, (3) generation of Kalman filters for the truth and reduced-order models, (4) discretization of the parameter space, (5) Bayesian MMAE development, (6) development of the moving-bank algorithm, (7) development of the stochastic controller, and (8) performance evaluation.

*Develop the system model for the truth model.* As in the case of the Gustafson's models from the Phillips Lab, the system model was supplied in modal form. Decoupled modes are inherent in this form and will allow easier access to the states than would other forms. The SPICE-4 is at least as complicated as SPICE-2, and thus requires the same large order of truth model state dimension for adequate system representation. Consequently, a reduced-order truth model will have to be developed and validated in order to make it computationally feasible. Gustafson showed this can be accomplished by simply throwing out the higher frequency modes (subject to physical insight) [11]. This concept is presumed still to be applicable. It will also be necessary to check the reasonableness of the truth model via computer simulation.

*Develop reduced-order models for implementation.* Further state reduction will have to be achieved to be considered for actual implementation of controller algorithms. The modal reduction and the internally balanced reduction methods used in previous research will be utilized in attaining the desired order reduction. Additionally Skelton's Component Cost Analysis technique applied to order reduction will also be investigated [40]. The internally balanced reduction was not very successful in the previous work [11]. However, this is inconsistent with similar work done on related projects [6], so this method will be researched further. If the same type of eigenvalue groupings is seen as in previous work, this will make the modal reduction technique more appealing. This is anticipated, since the low frequency bending modes of the tripod structure ought to dominate other higher frequency modes of the two stiffer platform structures. Several models of varying order reduction may have to be developed.

*Generation of Kalman filters for the truth and reduced-order models.* A Kalman filter will be developed for the truth model. The performance of all other reduced-order-model filters will be judged against the performance of the filter based on the truth model.

It will be important to "tune" the truth model properly. The values selected for  $Q_d$  (discrete time dynamics noise covariance) and  $R$  (measurement noise covariance) will be important. Increasing  $Q_d$  for robustness may eliminate the ability of the adaptation process within the multiple model filter to distinguish between the discrete parameter values that characterize the bending modes. There was an apparent lower bound on the measurement precision which severely hampered adaptation in the SPICE-2 [11], but hopefully the SPICE-4 will yield better results. Reduced order filters will then be developed and tuned, using the truth model as the basis and maintaining the same  $a_k$  parameter values. Each filter will be tuned by the Minimum Variable Reduced Order (MVRO) technique [25:25]. Performance analysis will then be performed, comparing the reduced-order filters and controllers against the truth model.

*Discretization of the parameter space.* In SPICE-2, the parameter space was initially 3 X 7 (3 scalar multipliers of the damping ratio  $\zeta$  vs. 7 for natural frequency  $\omega_n$ ). Gustafson showed that there was low sensitivity to the damping ratio [11]. The natural frequency appeared to have the most impact. As such, the damping ratio as a variable parameter will be deleted while the scalar multiplier on the natural frequency will be maintained. Additionally, this multiplier is applied to all of the flexible bending modes' frequencies [45]. Subsequently, it will be necessary to determine the size of the resulting one dimensional parameter space. To accomplish this, the one parameter (scalar multiplier) is varied by discrete step sizes in one direction and successive Monte Carlo runs made until the Kalman filter becomes unstable (or until performance degrades unacceptably in some other respect). A new parameter (scalar multiplier) is then declared at this point (or at a point prior to the onset of instability). This procedure is repeated using the new parameter as the nominal until the parameter space is complete. The actual size or "completeness" is arbitrary but based on physical insight and a need to keep the size reasonable subject to the goals of this research.

*Bayesian MMAE Development.* The Kalman filters for the truth and reduced-order models will be developed for each discretized parameter value in the parameter space. Gustafson implemented the maximum entropy with identity covariance matrix (ME/I) approach to determine the proper probability weighting factors,  $p_k(t_i)$  [11]. This method will be re-examined as well as other possibilities, including the original unaltered residual covariance MMAE method. These methods will be presented in Section 2.3.2. Artificially lower bounding the  $p_k(t_i)$ 's will resolve the "lock-out" condition, also described in Section 2.3.2..

*Development of the moving-bank algorithm.* Previous work indicates that the best method for the moving-bank algorithm is the parameter position method [11]. Other methods (residual monitoring, and probability monitoring) will be re-examined. Methods for contracting and expanding the bank will be examined. Gustafson did not actually use contraction and expansion due to the size of his parameter space [11]. This possibility will be re-addressed subject to the resulting parameter space for this research. Performance analysis will be conducted for the cases of constant, slowly varying, and jump parameter changes.

*Development of the stochastic controller.* LQG techniques will be implemented in the design of the controller. Past research indicated the cross weighting matrix between states and controls could be set to zero with no appreciable impact [11]. Tuning was accomplished by alternately holding the control weighting matrix or state weighting matrix constant and increasing the other until the rms values of the appropriate states (or controls) stopped decreasing drastically (see Section 2.5 for a better understanding of these matrices). The tuning objectives are to achieve tight control of the bending modes without consistently saturating the actuators. Possible controller implementation

techniques will be re-examined. These include MMAC, modified MMAC, MAP, and others, as discussed in Section 2.6.

*Performance evaluation.* Two aspects will be evaluated via computer simulation in determining the effectiveness of the overall design approach used in this research. The primary objective is for the tracking error to meet the specification of less than one  $\mu$ -radian rms. The secondary objective is determining the accuracy of the state estimate,  $\hat{\mathbf{x}}$ , and the uncertain parameter estimate,  $\hat{\mathbf{a}}$ .

### **1.7 Summary**

This chapter has given a brief overview of the concepts of MMAE, moving-bank MMAE, and MMAC. The simple two-bay truss structure was introduced to facilitate a basic understanding of the concept, with the note that this research will examine a much more complex system. Next, the basic operating approaches for the moving-bank MMAE and MMAC were discussed. A brief synopsis of past research results on this topic was then provided. This chapter ended with a statement of the problem, following by the scope that this research will examine, and finally the general approach to the solution. Chapter 2 will discuss the Kalman filter and LQG controller algorithms as well as the moving-bank decision making algorithms. Chapter 3 will introduce and develop the system model for the actual total structure. Chapter 4 will discuss the software required and subsequent simulations necessary to investigate the system performance. Chapter 5 will present the results from this research, after which Chapter 6 will provide conclusions and recommendations for future research.

## ***II. Background***

### ***2.1 Introduction***

This chapter presents the development of the Kalman filter, the MMAE, the moving-bank MMAE, and the LQG controller algorithms. Also, a basic discussion of the mathematical modeling techniques, coordinate forms, and order reduction used in this thesis will be given. This presentation will continue to use the simplified truss model of Section 1.2.1 as an example system when needed. The basic structure of the algorithms will not change when applied to the actual system. A more rigorous development of many of the subjects discussed in this chapter can be found [24,25,26]. A quick review of notation usage in Section 1.1 may be advantageous before reading this chapter.

### ***2.2 Kalman Filter***

A Kalman filter is an "optimal recursive data processing algorithm" that can be shown to be optimal by essentially any standard, given the appropriateness of several underlying assumptions [24]. These assumptions are that the system in question can be adequately modeled as linear with white, Gaussian system and measurement noises. Additionally, the system is assumed to be continuous with linear sample-data measurements. The linear stochastic differential system model upon which the Kalman filter is based is formally written as:

$$\dot{\mathbf{x}}(t) = \mathbf{F}(t)\mathbf{x}(t) + \mathbf{B}(t)\mathbf{u}(t) + \mathbf{G}(t)\mathbf{w}(t) \quad (2.1)$$

where  $\mathbf{x}(\cdot)$  represents an  $n$ -dimensional state vector,  $\mathbf{u}(\cdot)$  is an  $r$ -dimensional deterministic control input vector,  $\mathbf{w}(\cdot)$  is an  $s$ -dimensional white Gaussian noise vector.  $\mathbf{F}(\cdot)$  is an  $n$ -by- $n$  dimensional system dynamics matrix,  $\mathbf{B}(\cdot)$  is an  $n$ -by- $r$  dimensional deterministic input matrix, and  $\mathbf{G}(\cdot)$  is an  $n$ -by- $s$  dimensional noise input matrix

The statistics of the white Gaussian noise are given by:

$$E\{\mathbf{w}(t)\} = \mathbf{0} \quad (2.2)$$

$$E\{\mathbf{w}(t)\mathbf{w}(t')^T\} = \mathbf{Q}(t)\delta(t-t') \quad (2.3)$$

where  $\mathbf{Q}(t)$  is an  $s$ -by- $s$  dimensional positive, semi-definite matrix, and indicates the strength of the dynamics driving noise.  $\delta(\cdot)$  is the Dirac delta function.

Based on the assumptions stated previously, the state vector,  $\mathbf{x}(\cdot)$ , is a Gaussian random vector and can be completely described by its mean and covariance. Since the system model is defined as a differential equation, it is necessary to determine the initial conditions for both the mean and covariance. The initial mean,  $\hat{\mathbf{x}}_0$ , or best guess of the state's initial conditions is given by:

$$E\{\mathbf{x}(t_0)\} = \hat{\mathbf{x}}_0 \quad (2.4)$$

The initial covariance matrix,  $\mathbf{P}_0$ , describes the level of confidence in the initial state estimate. This matrix is given by:

$$E\{[\mathbf{x}(t_0) - \hat{\mathbf{x}}_0][\mathbf{x}(t_0) - \hat{\mathbf{x}}_0]^T\} = \mathbf{P}_0 \quad (2.5)$$

Although the physical system is described by a continuous model, it is desirable to discretize the Kalman filter dynamics model so that it can be implemented on a digital computer. It is inherently better first to discretize the continuous-time system model and then develop the discrete filter, as opposed to discretizing a previously developed continuous-time filter. This procedure involves no approximations and no Riccati differential equation integrations [24:261]. The discretized system model upon which the Kalman filter is based is given by:

$$\mathbf{x}(t_i) = \Phi(t_i, t_{i-1})\mathbf{x}(t_{i-1}) + \mathbf{B}_d(t_{i-1})\mathbf{u}(t_{i-1}) + \mathbf{G}_d(t_{i-1})\mathbf{w}_d(t_{i-1}) \quad (2.6)$$

where  $\Phi(\cdot)$  is the solution to:

$$\dot{\Phi}(t, t_{i-1}) = \mathbf{F}(t)\Phi(t, t_{i-1}) \quad (2.7)$$

with the initial condition:

$$\Phi(t_{i-1}, t_{i-1}) = \mathbf{I} \quad (2.8)$$

This can be simplified further by assuming a time invariant  $\mathbf{F}$ -matrix and using Laplace transform techniques to generate the solution as follows:

$$\Phi(t_i, t_{i-1}) = \Phi(t_i - t_{i-1}) = \mathcal{L}^{-1} \left\{ [s\mathbf{I} - \mathbf{F}]^{-1} \right\} \Big|_{(t_i - t_{i-1})} \quad (2.9)$$

Similar , if  $\mathbf{u}(\cdot)$  is held constant over one sample period, the deterministic matrix  $\mathbf{B}_d(t_{i-1})$  of Equation (2.6) is given by:

$$\mathbf{B}_d(t_{i-1}) = \int_{t_{i-1}}^{t_i} \Phi(t_i, \tau) \mathbf{B}(\tau) d\tau \quad (2.10)$$

The statistics of the discrete-time white Gaussian system dynamics driving noise are given by:

$$E\{\mathbf{w}_d(t_{i-1})\} = \mathbf{0} \quad (2.11)$$

$$E\{\mathbf{w}_d(t_{i-1})\mathbf{w}_d(t_j)^T\} = \mathbf{Q}_d(t_{i-1})\delta_{(i-1)j} \quad (2.12)$$

where  $\delta_{(i-1)j}$  is now the Kronecker delta function.  $\mathbf{Q}_d(\cdot)$  is given by:

$$\mathbf{Q}_d(t_{i-1}) = \int_{t_{i-1}}^{t_i} \Phi(t_i, \tau) \mathbf{G}(\tau) \mathbf{Q}(\tau) \mathbf{G}^T(\tau) \Phi^T(t_i, \tau) d\tau \quad (2.13)$$

where Equation (2.6) is modified such that  $\mathbf{G}_d = \mathbf{I}$  if Equation (2.13) is used to evaluate  $\mathbf{Q}_d$ . The discrete-time measurement update model is defined as:

$$\mathbf{z}(t_i) = \mathbf{H}(t_i)\mathbf{x}(t_i) + \mathbf{v}(t_i) \quad (2.14)$$

where  $\mathbf{z}(\cdot)$  is an  $m$ -dimensional discrete-time measurement vector,  $\mathbf{H}(\cdot)$ , is an  $m$ -by- $n$  dimensional output matrix, and  $\mathbf{v}(\cdot)$  is an  $m$ -dimensional noise vector representing the uncertainty inherent in the measurement device. This noise vector is modeled by white,



Gaussian noise with statistics given by:

$$E\{\mathbf{v}(t_i)\} = \mathbf{0} \quad (2.15)$$

$$E\{\mathbf{v}(t_i)\mathbf{v}(t_j)^T\} = \mathbf{R}(t_i)\delta_{ij} \quad (2.16)$$

where  $\mathbf{R}(t_i)$  is an  $m$ -by- $m$  dimensional, positive definite symmetric matrix and  $\delta_{ij}$  is the Kronecker delta function. Additionally, this model generation assumes that the noise  $\mathbf{w}(\cdot)$  and  $\mathbf{v}(\cdot)$  are uncorrelated [24:205].

One complete cycle of the Kalman filter sequence proceeds first with a propagation segment, then an update segment. In the propagation segment, the state estimate after the most recent measurement update at time,  $t_{i-1}^+$ , is propagated forward to just prior to the next measurement update time,  $t_i^-$ . The superscript '-' denotes the state just prior to a measurement update whereas a '+' denotes the state after a measurement is incorporated. The propagation equations are given by:

$$\hat{\mathbf{x}}(t_i^-) = \Phi(t_i, t_{i-1})\hat{\mathbf{x}}(t_{i-1}^+) + \mathbf{B}_d(t_{i-1})\mathbf{u}(t_{i-1}) \quad (2.17)$$

$$\mathbf{P}(t_i^-) = \Phi(t_i, t_{i-1})\mathbf{P}(t_{i-1}^+)\Phi^T(t_i, t_{i-1}) + \mathbf{Q}_d(t_{i-1}) \quad (2.18)$$

where  $\mathbf{G}_d = \mathbf{I}$ , as explained below Equation (2.13). At the end of the propagation segment, the update segment consists of incorporating the sample data measurement to form the best state estimate at time,  $t_i^+$ . The update equations are given by:

$$\mathbf{K}(t_i) = \mathbf{P}(t_i^-)\mathbf{H}^T(t_i)[\mathbf{H}(t_i)\mathbf{P}(t_i^-)\mathbf{H}^T(t_i) + \mathbf{R}(t_i)]^{-1} \quad (2.19)$$

$$\hat{\mathbf{x}}(t_i^+) = \hat{\mathbf{x}}(t_i^-) + \mathbf{K}(t_i)[\mathbf{z}(t_i) - \mathbf{H}(t_i)\hat{\mathbf{x}}(t_i^-)] \quad (2.20)$$

$$\mathbf{P}(t_i^+) = \mathbf{P}(t_i^-) - \mathbf{K}(t_i)\mathbf{H}(t_i)\mathbf{P}(t_i^-) \quad (2.21)$$

where  $\mathbf{z}(\cdot)$  is the measurement to be incorporated at time  $t_i$ . The residual equation is given by:

$$\mathbf{r}(t_i) = \mathbf{z}(t_i) - \mathbf{H}(t_i)\hat{\mathbf{x}}(t_i^-) \quad (2.22)$$

where  $\mathbf{r}(\cdot)$  is termed the residual (or innovation) and can be seen to equal the term between the brackets in Equation (2.20) [24:228]. This residual is defined as the difference between the current sample data measurement and the best estimate of that measurement based on all the past measurements. This last statement may not be easily seen, yet through the residual process, the state estimate incorporates or "remembers" the entire past history of measurements. This concept is one of the Bayesian fundamentals from which the Kalman filter is developed.

Given that the described system is time invariant with stationary noises, the typical Kalman filter response goes through an initial transient stage, followed by a steady-state stage [24:224]. If the initial transient stage is short enough or if ignoring that transient yields a negligible performance degradation, then a steady-state constant-gain approximation is justified. In this case, the values for  $\mathbf{K}(t_i)$ ,  $\mathbf{P}(t_i^-)$ , and  $\mathbf{P}(t_i^+)$  in the previous equations can be taken to steady state and precomputed for all time. With the stationary noise assumption and a fixed sample rate, constant values for the  $\mathbf{B}_d(t_i)$ , and  $\mathbf{Q}_d(t_i)$  matrices respectively need only be precomputed once. Additionally, the measurement noise covariance matrix,  $\mathbf{R}(t_i)$ , will be assumed constant.

The development of the system model matrices and vectors (as appropriate),  $\mathbf{x}(\cdot)$ ,  $\mathbf{F}(\cdot)$ ,  $\Phi(\cdot, \cdot)$ ,  $\mathbf{B}_d(\cdot)$ ,  $\mathbf{u}(\cdot)$ ,  $\mathbf{Q}_d(\cdot)$ ,  $\mathbf{G}_d(\cdot)$ ,  $\mathbf{z}(\cdot)$ ,  $\mathbf{H}(\cdot)$ , and  $\mathbf{v}(\cdot)$  will be discussed in Chapter 3. In all of the previous equations, the only variables left undetermined by the system model, measurement inputs, or computations are  $\hat{\mathbf{x}}_0$ ,  $\mathbf{P}_0$ ,  $\mathbf{R}(\cdot)$ , and  $\mathbf{Q}_d(\cdot)$ . The iterative proper selection of values to fill these matrices is referred to as "tuning" and will be discussed in Chapter 4.

### 2.3 MMAE

The basic concept of the MMAE was introduced in Chapter 1. The actual MMAE algorithm is based on the properties of conditional probability densities, from a Bayesian

viewpoint. This concept will be presented in this section. A more rigorous discussion of the subject can be found [25:129-139].

### 2.3.1 Bayesian Formulation

A Kalman filter is most precise when the system model matrices described in the previous section are known exactly. However, an uncertain parameter,  $\mathbf{a}$ , with scalar components that affect one or more of the matrices, may cause a subsequent loss of precision in the state estimation. As discussed in Chapter 1,  $\mathbf{a}$  may be defined over a continuous range; thus an infinite number of Kalman filters would be required, each based on a specific realization  $\mathbf{a} = \alpha$  in this range. The infeasibility of this result dictates that the continuous range be discretized such that the parameter  $\mathbf{a}$  will take on a reasonable set of values  $\mathbf{a}_1, \mathbf{a}_2, \dots, \mathbf{a}_K$ , where  $K$  is the total number of Kalman filters. For the example system described in Chapter 1, the parameter space was 2-dimensional, with 10 discrete values for each scalar parameter, resulting in 100 Kalman filters. The actual discretization process will be discussed in Chapter 4.

Since the basic Kalman filter is developed from the Bayesian conditional probability density of the state,  $\mathbf{x}$ , conditioned on the measurement history,  $\mathbf{Z}$  (where  $\mathbf{Z}(t_i) = [\mathbf{z}^T(t_1); \mathbf{z}^T(t_2); \dots; \mathbf{z}^T(t_i)]^T$  from Equation (2.14)), a logical choice for a Bayesian estimator in the case of uncertain parameters would be to add  $\mathbf{a}$  to the left of the conditioning argument and develop the conditional density of all quantities to be estimated, conditioned on all measurements up to and including time  $t_i$ , as follows:

$$f_{\mathbf{x}(t_i), \mathbf{a} | \mathbf{Z}(t_i)}(\xi, \alpha | \mathbf{Z}_i) = f_{\mathbf{x}(t_i) | \mathbf{a}, \mathbf{Z}(t_i)}(\xi | \alpha, \mathbf{Z}_i) f_{\mathbf{a} | \mathbf{Z}(t_i)}(\alpha | \mathbf{Z}_i) \quad (2.23)$$

The first term on the right is nothing more than the Gaussian density function totally defined by the outputs  $\hat{\mathbf{x}}(t_i^+)$  and  $\mathbf{P}(t_i^+)$  of the Kalman filter generated where  $\mathbf{a}$  assumes a specific realization  $\alpha$  (i.e.  $\mathbf{a} = \alpha$ ). The second term can be described by the following

equation:

$$f_{\mathbf{a}|\mathbf{Z}(t_i)}(\alpha|\mathbf{Z}_i) = \sum_{k=1}^K p_k(t_i) \delta(\alpha - \mathbf{a}_k) \quad (2.24)$$

where  $p_k(t_i)$  is the hypothesis conditional probability (sometimes referred to as a weighting factor) that was introduced in Chapter 1, where  $p_k(t_i) = \text{prob}(\mathbf{a} = \mathbf{a}_k | \mathbf{Z}(t_i) = \mathbf{Z}_i)$ . This probability is determined by:

$$p_k(t_i) = \frac{f_{\mathbf{z}(t_i)|\mathbf{a}, \mathbf{Z}(t_{i-1})}(\mathbf{z}_i | \mathbf{a}_k, \mathbf{Z}_{i-1}) p_k(t_{i-1})}{\sum_{j=1}^K f_{\mathbf{z}(t_i)|\mathbf{a}, \mathbf{Z}(t_{i-1})}(\mathbf{z}_i | \mathbf{a}_j, \mathbf{Z}_{i-1}) p_j(t_{i-1})} \quad (2.25)$$

where the first term in the numerator is the probability density function of the current measurement, conditioned on the particular assumed parameter value and the observed past measurement history. This density function is determined by:

$$f_{\mathbf{z}(t_i)|\mathbf{a}, \mathbf{Z}(t_{i-1})}(\mathbf{z}_i | \mathbf{a}_k, \mathbf{Z}_{i-1}) = \frac{1}{(2\pi)^{\frac{m}{2}} |\mathbf{A}_k(t_i)|^{\frac{1}{2}}} \exp\{\cdot\}$$

$$\{\cdot\} = \{-\frac{1}{2} \mathbf{r}_k^T(t_i) \mathbf{A}_k^{-1}(t_i) \mathbf{r}_k(t_i)\} \quad (2.26)$$

where

$$\mathbf{r}_k(t_i) = [\mathbf{z}(t_i) - \mathbf{H}_k(t_i) \hat{\mathbf{x}}_k(t_i^-)]$$

and

$$\mathbf{A}_k(t_i) = [\mathbf{H}_k(t_i) \mathbf{P}_k(t_i^-) \mathbf{H}_k^T(t_i) + \mathbf{R}_k(t_i)]$$

and  $\hat{\mathbf{x}}_k(t_i^-)$ ,  $\mathbf{P}_k(t_i^-)$ ,  $\mathbf{H}_k(t_i)$ ,  $\mathbf{R}_k(t_i)$  are quantities in the  $k$ -th Kalman filter, which is based on the assumption that  $\mathbf{a} = \mathbf{a}_k$ . Since the second term in Equation (2.25) is the previous value of the hypothesis conditional probability, this equation constitutes an iterative solution. The denominator is the sum of the numerator terms from all  $K$  filters at

time  $t_i$ . This can be considered a scaling factor that ensures the sum of all the individual conditional probabilities will equal one.

The resulting conditional mean state estimate from the preceding development is given by:

$$\begin{aligned}\hat{\mathbf{x}}(t_i^+) &= E\{\mathbf{x}(t_i) | \mathbf{Z}(t_i) = \mathbf{Z}_i\} \\ &= \int_{-\infty}^{\infty} \xi \left[ \sum_{k=1}^K f_{\mathbf{x}(t_i) | \mathbf{a}_k, \mathbf{Z}(t_i)}(\xi | \mathbf{a}_k, \mathbf{Z}_i) p_k(t_i) \right] d\xi \\ &= \sum_{k=1}^K \hat{\mathbf{x}}_k(t_i^+) p_k(t_i)\end{aligned}\quad (2.27)$$

where each of the Kalman filter state estimates,  $\hat{\mathbf{x}}_k(t_i^+)$ , based on the parameter  $\mathbf{a}_k$ , is multiplied by its computed weighting factor (the hypothesis conditional probability,  $p_k(t_i)$ ) and summed to create a weighted average final state estimate. The filter structure based on this development has already been depicted in Figure 1-1.

The resulting conditional covariance is similar in structure to Equation (2.27) as seen by the following equation:

$$\begin{aligned}\mathbf{P}(t_i^+) &= E\left\{ \left[ \mathbf{x}(t_i) - \hat{\mathbf{x}}(t_i^+) \right] \left[ \mathbf{x}(t_i) - \hat{\mathbf{x}}(t_i^+) \right]^T | \mathbf{Z}(t_i) = \mathbf{Z}_i \right\} \\ &= \sum_{k=1}^K p_k(t_i) \left\{ \mathbf{P}_k(t_i^+) + \left[ \hat{\mathbf{x}}_k(t_i^+) - \hat{\mathbf{x}}(t_i^+) \right] \left[ \hat{\mathbf{x}}_k(t_i^+) - \hat{\mathbf{x}}(t_i^+) \right]^T \right\}\end{aligned}\quad (2.28)$$

where  $\mathbf{P}_k(t_i^+)$  is the state error covariance from the Kalman filter based on the parameter value,  $\mathbf{a}_k$ . Unlike the individual  $\mathbf{P}_k(t_i^+)$  values, the  $\mathbf{P}(t_i^+)$  can't be precomputed due to its dependency on the measurement history through  $\hat{\mathbf{x}}_k(t_i^+)$ ,  $\hat{\mathbf{x}}(t_i^+)$ , and  $p_k(t_i)$ . Fortunately, this computation is not necessary for on-line use.

It will be useful to compute the conditional mean value for the parameter  $\mathbf{a}$  at any

given time, and this is given by the following:

$$\begin{aligned}
 \hat{\mathbf{a}}(t_i) &= E\{\mathbf{a}(t_i) | \mathbf{Z}(t_i) = \mathbf{Z}_i\} \\
 &= \int_{-\infty}^{\infty} \alpha f_{\mathbf{a}|\mathbf{Z}(t_i)}(\alpha | \mathbf{Z}_i) d\alpha \\
 &= \sum_{k=1}^K \mathbf{a}_k p_k(t_i)
 \end{aligned} \tag{2.29}$$

The corresponding covariance indicates the level of precision in the estimate of the parameter:

$$\begin{aligned}
 \mathbf{P}_i &= E\{[\mathbf{a} - \hat{\mathbf{a}}(t_i)][\mathbf{a} - \hat{\mathbf{a}}(t_i)]^T | \mathbf{Z}(t_i) = \mathbf{Z}_i\} \\
 &= \sum_{k=1}^K [\mathbf{a}_k - \hat{\mathbf{a}}(t_i)][\mathbf{a}_k - \hat{\mathbf{a}}(t_i)]^T p_k(t_i)
 \end{aligned} \tag{2.30}$$

It may be useful to calculate the parameter estimate and covariance, but this is not necessary in determining the state estimate.

### 2.3.2 Performance Evaluation and Enhancements

There are a few inherent problems in the preceding Bayesian formulation. This section will address these specifically and offer potential solutions. Additionally, alternate methods for computing the final state estimate will be addressed.

The residuals of each of the elemental filters provide an indication of filter performance. The filter based on the most correct parameter value,  $\mathbf{a}_k$ , should output the smallest residual magnitude (scaled relative to the filter computed residual covariance,  $\mathbf{A}_k$ ). In this case, Equation (2.26) would provide the corresponding highest conditional density value and Equation (2.25) would subsequently provide the largest probability value for this "best" filter. However, if all the quadratic terms in the exponential portion of Equation (2.26) from each of the active filters are of the same relative magnitude, then

the filter with the smallest  $|\mathbf{A}_k(t_i)|$  term will have the largest probability assigned to it. This can be seen by recognizing the inverse relationship of  $|\mathbf{A}_k(t_i)|$  in the pre-multiplier of the exponent in Equation (2.26). This particular filter may or may not be appropriately weighted. If this filter has an erroneously high probability attached to it, the resulting final state estimate will be degraded.

Four methods can be applied in the evaluation of the final state estimate. The first method is the *Bayesian MMAE form* described in the preceding developments which has the potential problem noted in the previous paragraph.

The second method, *Maximum A Posteriori*, (MAP), makes the assumption that the filter state estimate with the highest probability  $p_k$  will be declared the final state estimate. This method does not provide for a "blending" of estimates from each of the elemental filters, as would the probability-weighted average estimate computations of Equations (2.27) and (2.29). Additionally, this method still suffers from the same problem as the first method.

The third method, *Maximum Entropy with Identity Covariance* (ME/I) density computation, assumes that the residuals are Gaussian with a covariance equal to the identity matrix and follow a "maximally non-committed residual distribution" [38:24]. This method attempts to account for the possibly erroneous affects of the  $|\mathbf{A}_k(t_i)|$  term in the pre-multiplier and the exponentiated quadratic, as well as for an incorrectly evaluated  $\mathbf{A}_k$  value due to model uncertainties, by setting  $\mathbf{A}_k(t_i)$  equal to the identity matrix in both locations. This results in the following equation replacing Equation (2.26) in the Bayesian method above:

$$f_{\mathbf{z}(t_i)|\mathbf{a}, \mathbf{z}(t_{i-1})}(\mathbf{z}_i|\mathbf{a}_k, \mathbf{Z}_{i-1}) = \frac{1}{(2\pi)^{\frac{m}{2}} |\mathbf{I}|^{\frac{1}{2}}} \exp\{\cdot\}$$

$$\{\cdot\} = \{-\frac{1}{2} \mathbf{r}_k^T(t_i) \mathbf{I} \mathbf{r}_k(t_i)\} \quad (2.31)$$

This method insures that the filter with the residual with the lowest (absolute vs. relative) magnitude is correctly given the highest probability.

The fourth technique, *MAP with MEI*, incorporates the MAP form with the MEI density computation.

There is a subtle problem with Equation (2.25). Since this is an iterative equation (the new value is multiplied by the old value in the numerator), should the conditional probability,  $p_k(t_i)$ , become zero at any time, it will remain at zero from that time forth. This condition is termed "lockout". Thus, even if the elemental filter based parameter value,  $a_k$ , were to match the real value closely, which would also imply a precise state estimate, its contribution to the weighted average would be zero. The filter-computed  $p_k$  for the "correct" elemental filter would continue "blithely" at zero unaffected by the real world.

There are two proposed solutions to this problem. An *ad hoc* method for resolving this situation is to add a lower bound artificially to the probability calculation, which would eliminate the possibility of it ever going to zero. A threshold,  $p_{min}$ , is determined such that if the computed hypothesis conditional probability,  $p_k(t_i)$ , should fall below this lower bound, then  $p_k(t_i)$  is set to a minimum value and the remaining probabilities are rescaled to maintain the summation equal to one. The second method would be to add more process pseudonoise to the system dynamics models, but this may contribute to masking the parameter discretization that sets each filter apart from each other, incapacitating the adaptive process. Using this method would require that filter tuning would have to proceed in conjunction with parameter discretization with the possibility of not attaining a viable solution. In any case, the solution process would be difficult and time consuming. The first technique has been the method of choice for past research and will be continued in this research [11,14,15,18,33,37,42]. A third proposed solution, that of defining a Markov process model for transitioning  $p_k$  values from one



sample time to the next will similarly not be pursued, in preference of artificial lower bounds [36].

## **2.4 *Moving-Bank MMAE Development***

In the preceding developments, a full-bank algorithm was alluded to, whereby one Kalman filter is required for every discrete parameter value. However, as stated in Chapter 1, even with a discretized parameter space, the resulting load from the elemental filters may well be computationally burdensome in a full-bank algorithm. The solution proposed is to implement a moving bank of filters. Only a subset of the full bank,  $J$  filters (where  $J < K$ ), is active at any one time. In the example problem,  $J$  was equal to nine filters. Given the one-dimensional bank in this research,  $J$  is equal to three. This technique was originally investigated by Maybeck and Hentz [30]. This section will discuss techniques for moving the bank, expanding the bank, contracting the bank, and initializing new filters.

### **2.4.1 *Moving the Bank***

The moving-bank MMAE allows for dynamic redeclaration of the subset of  $J$  filters, in order to surround the best estimate of the uncertain parameter,  $\hat{a}$ , with the filters based on the closest parameter values. However, the parameter value may not be known a priori or may arbitrarily change for reasons discussed in Chapter 1. If the parameter estimate is determined to be outside the bounds of the current bank by a pre-determined threshold condition (to be discussed later in this section), then the bank is moved in the direction of the parameter estimate. This move can be accomplished in a finely discretized manner should the parameter drift slightly (as depicted previously in Figure 1-6) or in a coarsely discretized manner should the parameter make a large discrete jump (as depicted previously in Figure 1-7). There are 4 methods proposed for implementing the move logic. These methods are: (1) Residual Monitoring, (2) Parameter Position Estimate

Monitoring, (3) Parameter Position and "Velocity" Estimate Monitoring, and (4) Probability Monitoring [30]. In any case, it will be necessary to determine the specific threshold values empirically which is analogous to filter "tuning".

#### **2.4.1.1 Residual Monitoring**

This method is formed on the basis of the likelihood quotient,  $L_j(t_i)$ . This calculation is defined as:

$$L_j(t_i) = \mathbf{r}_j^T(t_i) \mathbf{A}_j(t_i)^{-1} \mathbf{r}_j(t_i) \quad (2.32)$$

and can be seen to be the major contributor to the exponential term in Equation (2.26). The decision to move the bank is based on the value of this scalar quadratic function. The smaller the value (assumed as the result of smaller residuals), the closer the filter-based parameter value is to the actual parameter position. Likewise, the larger the value (assumed as the result of larger residuals), the further the filter based parameter value is from the actual parameter. The threshold for the likelihood quotient is determined such that, if all the filters quotients are above this value, then this is an indication that the true parameter has moved from within the confines of the smaller bank. The decision to move the bank in the direction of the filter with the smallest likelihood value is then made. Past research has shown that determining this threshold is crucial to desired performance [14:61]. Setting the threshold value too high will result in move logic that is too slow in responding to parameter changes. Setting the threshold too low will result in move logic that drives the moving bank erratically throughout the parameter space and fails to maintain a precise state or parameter estimation. An inherent problem in this technique is that it is susceptible to single large measurement noise samples which may cause unnecessary movement [30:1876]. This can be seen since  $L_j(t_i)$  is a function of only the one most recent sample of measurement residual  $\mathbf{r}_j(t_i)$ , rather than a history of recent residuals.

#### ***2.4.1.2 Parameter Position Estimate Monitoring***

The method operates by keeping the moving bank centered over the estimate of the true parameter position determined by Equation (2.29). This position estimate is compared with the location of the center of the moving bank. If the difference is above a set threshold, then the decision is made to move the bank in an attempt to re-center the bank over the estimated position. Unlike the previous method, this technique is based on the entire measurement history and not just the current one. As a result, it is less susceptible to erroneous decisions from single large measurement noise samples [30:1879]. The decision process must be altered slightly to account for the possibility of the parameter estimate to be located at the edge of the Kalman filter based parameter space. The bank would not be able to surround the estimate as desired and so the best that can be accomplished is to center the side of the bank.

#### ***2.4.1.3 Parameter Position and "Velocity" Estimate Monitoring***

An extension of the previous technique, this method attempts to track the "velocity" of the drifting parameter. It may then be possible to predict the location of the parameter position at the next measurement sample time.. The velocity is determined by comparing the history of parameter position estimates over one sample period or several and dividing by the appropriate time increment. The decision to move is made if the predicted position exceeds a threshold as compared to the current center of the moving bank. The bank is then moved in the direction of the estimated parameter velocity vector. Hentz found that, in his work, this technique resulted in no improvement in the speed to acquire the proper estimate while exhibiting a destabilizing affect on the bank's position [14:62].

#### **2.4.1.4 Probability Monitoring**

Similar in nature to the first method, this technique attempts to center the bank over the estimated position based on the conditional probabilities as determined in Equation (2.25). The  $p_k(t_i)$  with the highest value is assumed to correspond to the filter based on the parameter value closest to the true parameter value. If this probability is larger than a pre-determined threshold, the bank will move in the direction of the filter with the highest probability. As in position monitoring, this technique is dependent on the history of measurements and is not as susceptible to single large measurement samples as is the residual monitoring technique.

#### **2.4.2 Expanding the Bank**

Normally the moving bank of filters would move in a fine discretization of the parameter space, but expanding the bank to a coarse discretization may be required in two situations. The first occurs when the true parameter makes a discrete jump to a new location. The second is during initial acquisition. In both situations, the true parameter position may exist far from within the bounds of a small bank based on a fine discretization, such that the bank would not be able to determine the direction to move. (Recall Figures 1-6 and 1-7.) Utilizing a coarse discretization configuration that encompassed the entire parameter space ensures that the parameter position lies within the bounds of the bank, although the parameter and state estimate resolution may suffer due to coarse discretization.

The bank may be originally configured in a coarse discretization for the initial acquisition or expanded from a fine to a coarse discretization for a jump change. By using this coarse configuration for initialization of the bank, Maybeck and Hentz determined that there was substantial improvement in parameter estimation [30]. Expanding the bank requires the use of the *residual monitoring technique* since the other techniques don't

provide the necessary information to make this determination (these other techniques rely on  $\hat{a}$ , which, due to its very computation via Equation (2-29), is confined within the finely discretized bank). Similar to the residual monitoring move logic discussed in Section 2.4.1.1, a higher threshold can be determined such that, if this value is exceeded by all the filters, then this indicates the parameter position has made a much larger jump, hence an expansion to a coarse level of discretization is appropriate.

There are some drawbacks with this method. As before, the same problem with erroneous expansion due to a single large sample of measurement noise exists due to its dependence on single sample periods. Additionally, Hentz found that if the expansion threshold was set too high, the response time was too slow. Likewise, if the threshold was set too low, the bank would expand unnecessarily [14:69].

### **2.4.3 Contracting the Bank**

Contracting the coarsely configured bank will be necessary following either initial acquisition or previous expansion due to a jump parameter change. In both cases, the bank is contracted to surround the true parameter with a fine configuration based on a set criteria for determining the "goodness" of the parameter estimate,  $\hat{a}$ . This decision is determined using the *Parameter Estimation Error Covariance Monitoring* technique. When the covariance of the parameter estimate (as determined in Equation (2.30)) falls below a set threshold, the bank can be contracted down to a fine configuration about the parameter estimate. This contraction can occur in one large step or multiple steps, dependent on the size of the parameter space and the level of coarse discretization. It is desirable to have the contraction occur quickly to enhance the parameter estimation. However, Hentz found that if the threshold was set too high, contraction would occur before a good parameter estimate was obtained. Likewise, setting the threshold too low delayed proper contraction [14:69]. Gustafson found that expansion and contraction in general was unnecessary due to the small relative size of his resulting parameter space

[11]. However, his parameter space was merely a subset of a possibly much larger physically realistic set.

If the parameter space is higher dimensional, a problem occurs with the above procedure. (Since this research will only have a one-dimensional bank, the following is not directly applicable, but is included for completeness.) In the example problem, having a two-by-two covariance matrix caused problems in comparing  $\mathbf{P}_k$  with a single scalar threshold. Hentz compared the largest diagonal element in the matrix with the threshold, whereas Filios had better results by requiring both diagonal elements to be below the threshold [7,14]. Unfortunately, this method has tradeoffs since the appropriate threshold for each diagonal element might be different. Better performance may be gained by allowing separate decisions in each of the parameter space directions, which may lead to rectangular bank shapes as well as square.

Karnick proposed a different method. His technique monitored the probability of an entire side of the bank as defined in the following equation:

$$p_{side}(t_i) = \frac{\sum_{side} f_{z(t_i)|a, Z(t_{i-1})}(z_i | a_j, Z_{i-1})}{\sum_{4sides} f_{z(t_i)|a, Z(t_{i-1})}(z_i | a_j, Z_{i-1})} \quad (2.33)$$

If this probability fell below the threshold, that particular side was contracted towards the parameter estimate. Likewise, if the probability of a side should rise above another threshold, then the other sides were contracted towards the parameter estimate [15:29]. Another variation monitored all four sides such that if the sum of these probabilities fell below a threshold, the bank was contracted.

#### 2.4.4 Initialization of New Elemental Filters

In order to redeclare new elemental filters dynamically as a result of bank movement, many changes must occur. First,  $\Phi$ ,  $\mathbf{B}_d$ ,  $\mathbf{G}_d$ ,  $\mathbf{H}$ ,  $\mathbf{A}$ ,  $\mathbf{D}$ ,  $\mathbf{K}$ ,  $\mathbf{P}(t_i^-)$  and  $\mathbf{P}(t_i^+)$  for the filter and  $\bar{\mathbf{G}}_c^*$  for the controller (to be discussed in the next section) must

be modified to correspond to the new parameter value. These matrices are updated from information stored in memory that corresponds to the new parameter value. The matrix,  $\mathbf{D}$ , is a direct feedthrough matrix that results from the reduced order model development and will be discussed in Chapter 3. Second, an appropriate state estimate,  $\hat{\mathbf{x}}_j(t_i)$ , and probability weight,  $p_j(t_i)$ , must be initialized in the new filter. The state estimate,  $\hat{\mathbf{x}}_j(t_i)$ , is set equal to the current adaptive state estimate,  $\hat{\mathbf{x}}(t_i)$ . There are several methods proposed to initialize  $p_j(t_i)$ .

The first and most used method involves redistributing the values last obtained from the deactivated filters equally among the newly activated filters. The second method reinitializes all the current filters (changed and unchanged) to an equivalent probability weighting (all  $p_j$  values =  $1/K$ ). This proved to converge to a parameter estimate too slowly [14:30]. Hentz attempted to implement a more involved method. His algorithm reassigned the probabilities of the deactivated filters based on the "correctness" of the new filters [14:29]. This method proved to be computationally intensive with no improved performance over the first method and was discarded. If the bank expands or contracts, setting all values equal as in the second method above may be the most appropriate despite the slowness, since the old values may no longer be valid. Additionally, the sum of the new probability weights in all cases must add to one.

Hentz investigated "filter warm-up": allowing the initial transients to dissipate before incorporating the resulting state estimates into the MMAE output. His results showed no improvements in using this procedure over immediate incorporation [14:100].

## 2.5 *Stochastic Controller Development*

It was stated in Chapter 1 that this thesis will use an LQG controller. For this type

of controller, the quadratic cost function to be minimized is defined as:

$$J = E \left\{ \sum_{i=0}^N \frac{1}{2} [\mathbf{x}^T(t_i) \mathbf{X}(t_i) \mathbf{x}(t_i) + \mathbf{u}^T(t_i) \mathbf{U}(t_i) \mathbf{u}(t_i) + 2 \mathbf{x}^T(t_i) \mathbf{S}(t_i) \mathbf{u}(t_i)] \right. \\ \left. + \frac{1}{2} \mathbf{x}^T(t_{N+1}) \mathbf{X}_f \mathbf{x}(t_{N+1}) \right\} \quad (2.34)$$

where the resulting output of the controller is the optimal control function,  $\mathbf{u}^*$  [26:73].

This equation can be restated as:

$$J = E \left\{ \sum_{i=0}^N \frac{1}{2} \begin{bmatrix} \mathbf{x}(t_i) \\ \mathbf{u}(t_i) \end{bmatrix}^T \begin{bmatrix} \mathbf{X}(t_i) & \mathbf{S}(t_i) \\ \mathbf{S}^T(t_i) & \mathbf{U}(t_i) \end{bmatrix} \begin{bmatrix} \mathbf{x}(t_i) \\ \mathbf{u}(t_i) \end{bmatrix} + \frac{1}{2} \mathbf{x}^T(t_{N+1}) \mathbf{X}_f \mathbf{x}(t_{N+1}) \right\} \quad (2.35)$$

where:

- $J$  = scalar cost to be minimized
- $\mathbf{x}(t_i)$  =  $n$ -dimensional state vector
- $\mathbf{X}(t_i)$  =  $n \times n$ -dimensional state weighting matrix
- $\mathbf{X}_f$  =  $n \times n$ -dimensional final state weighting matrix
- $\mathbf{u}(t_i)$  =  $r$ -dimensional control input vector
- $\mathbf{U}(t_i)$  =  $r \times r$ -dimensional control weighting matrix
- $\mathbf{S}(t_i)$  =  $n \times r$ -dimensional cross-weighting matrix
- $t_N$  = last time a control is applied (held constant to next sample period)
- $t_{N+1}$  = final time

The basic form of  $\mathbf{X}(t_i)$  and  $\mathbf{X}_f$  are matrices that are real, symmetric and positive semi-definite. This last property (as opposed to positive definiteness) allows for a zero cost to be placed on states that have negligible impact on desired performance. The basic form of  $\mathbf{U}(t_i)$  is real, symmetric and positive definite. Here, the last property ensures that there are no zero eigenvalues, which relates to allowing infinite power to be commanded through any of the actuators. The cross weighting matrix  $\mathbf{S}(t_i)$  is chosen so that the augmented matrix in Equation (2.35) is positive semi-definite, which ensures a cost-



minimizing controller solution exists (provided that certain stabilizability and detectability conditions in the system design model are met).

For the purposes of this discussion, the weighting matrices are assumed to be diagonal. The diagonal terms of the cost weighting matrices,  $\mathbf{X}(t_i)$  and  $\mathbf{X}_f$ , are selected to reflect the relative importance of maintaining the components of respective state estimates near zero. Larger terms indicate higher emphasis on minimizing the corresponding state. Similarly, the diagonal terms of the control weighting matrix,  $\mathbf{U}(t_i)$ , reflect the level of control energy or power that is to be used. Larger terms indicate smaller levels of control power are to be commanded through the actuators.

The optimal discrete linear feedback control law that adheres to the quadratic cost function in Equation (2.35) and the certainty equivalence concept discussed in Chapter 1 is [26:16]:

$$\mathbf{u}^*(t_i) = -\mathbf{G}_c^*(t_i)\hat{\mathbf{x}}(t_i^+) \quad (2.36)$$

where  $\mathbf{G}_c^*(t_i)$  is determined by solving a backward Riccati difference equation and  $\hat{\mathbf{x}}(t_i^+)$  is the state estimate from the Kalman filter.

A steady state constant-gain control law can be obtained if the initial transients in the Kalman filter and the final transients in the controller gain are assumed to be negligible. In order for this to be valid, the control application interval must be long compared to the transient time period. In this case, the optimal discrete linear feedback control law is [26:243]:

$$\mathbf{u}^*(t_i) = -\overline{\mathbf{G}}_c^*\hat{\mathbf{x}}(t_i^+) \quad (2.37)$$

where  $\hat{\mathbf{x}}(t_i^+)$  is now the state estimate from the constant-gain, steady state Kalman filter.

Tying all the assumptions together, namely a time invariant, linear system driven by white Gaussian noise with a quadratic cost function described above, and the additional

assumption of constant weighting matrices, then the constant-gain steady state control law is as given by Equation (2.37), with [26:242]:

$$\bar{\mathbf{G}}_c^* = [\mathbf{U} + \mathbf{B}_d^T \bar{\mathbf{K}}_c \mathbf{B}_d]^{-1} [\mathbf{B}_d^T \bar{\mathbf{K}}_c \Phi + \mathbf{S}^T] \quad (2.38)$$

where  $\bar{\mathbf{K}}_c^*$  is determined by solving the steady-state Riccati equation:

$$\bar{\mathbf{K}}_c = \mathbf{X} + \Phi^T \bar{\mathbf{K}}_c \Phi - [\mathbf{B}_d^T \bar{\mathbf{K}}_c \Phi + \mathbf{S}^T]^T [\mathbf{U} + \mathbf{B}_d^T \bar{\mathbf{K}}_c \mathbf{B}_d]^{-1} [\mathbf{B}_d^T \bar{\mathbf{K}}_c \Phi + \mathbf{S}^T] \quad (2.39)$$

These assumptions reduce the quadratic cost function to:

$$J = E \left\{ \sum_{i=0}^{\infty} \frac{1}{2} [\mathbf{x}^T(t_i) \mathbf{X} \mathbf{x}(t_i) + \mathbf{u}^T(t_i) \mathbf{U} \mathbf{u}(t_i) + 2 \mathbf{x}^T(t_i) \mathbf{S} \mathbf{u}(t_i)] \right\} \quad (2.40)$$

Previous research results indicated that the cross weighting matrix,  $\mathbf{S}$ , had a negligible magnitude, and it was neglected with no appreciable performance impact [18]. This is the form of control law to be used in this thesis.

## 2.6 MMAC

The general design of the MMAC was depicted in Figure 1-2. One LQG controller as described in the previous section will be developed for each parameter value,  $\mathbf{a}_k$ . As introduced in Chapter 1, there are six methods for combining the MMAE and LQG controller. These are: (1) MMAC Control, (2) "Modified" MMAC Control, (3) MAP verses Bayesian MMAC Control, (4) Single Fixed-Gain Control, (5) Single Changeable-Gain Control, and (6) "Modified" Single Changeable-Gain Control.

### 2.6.1 MMAC Control

This method is of the form depicted in Figure 1-2. The final optimal control output is determined in much the same manner as is the Bayesian form of the optimal state estimate. Each controller output is appropriately weighted based on the filter conditional

probability,  $p_k(t_i)$ , and summed with the others to create a weighted average final controller output.

### **2.6.2 "Modified" MMAC Control**

This *ad hoc* method ignores inputs from filter/controllers assumed to have relatively poor state estimates. It was mentioned in Section 2.3.2 that an artificial lower bound may be added to the conditional probabilities to keep them from ever going to zero. However, this implies these filters have poor estimates (assuming they reached the lower bound for a valid reason) and should not be included in the final controller gain calculation, no matter how small their contribution may be. By applying another threshold on the conditional probabilities higher than the previously mentioned lower bound, filters at the lower bound or in the gap between the two bounds will be effectively eliminated from the MMAC control calculation.

### **2.6.3 MAP versus Bayesian MMAC Control**

Similar in nature to the MAP estimation described in Section 2.3.2, this method states that the elemental LQG controller with the largest computed conditional probability will be declared the controller to be used at the current time. Again, this method doesn't allow for "blending" of the controllers.

### **2.6.4 Single Fixed-Gain Control**

This method assumes that designing the controller based on a nominal parameter position value is appropriate, due to the fact that full-state feedback controllers are inherently robust [14:40]. Figure 2-1 illustrates this design. In this figure, ZOH refers to zero-order-hold, where the control input is held constant over the entire sample period until a new control input is determined. Likewise, T refers to the discrete time sampler

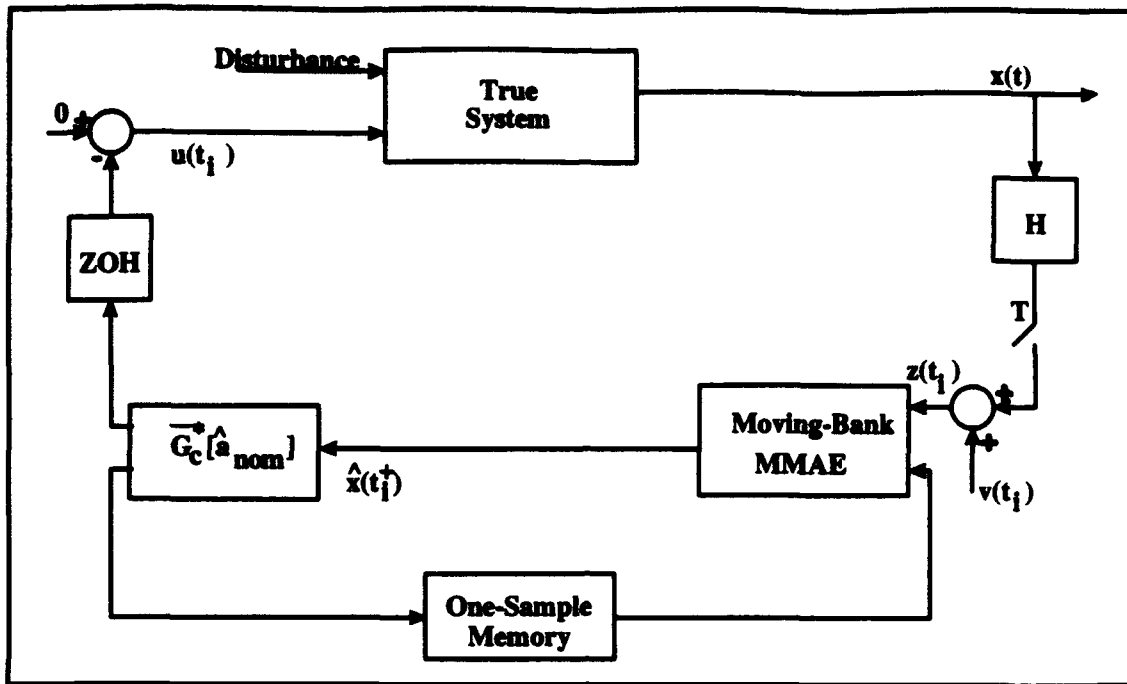


Figure 2-1. Single Fixed-Gain Controller

period. The control law is as follows:

$$u^*(t_i) = -\bar{G}_c^*[a_{nom}]\hat{x}(t_i^+) \quad (2.41)$$

where the state estimate is the only input and the gain is pre-computed. The controller parameters are selected such that the controller provides adequate regulation for any true system parameter value [14:40]. However, it may be extremely difficult to determine  $a_{nom}$ .

### 2.6.5 Single Changeable-Gain Control

This method allows for a changing value for  $\hat{a}(t_i)$  and is illustrated in Figure 2-2

The governing control law is as follows:

$$u^*(t_i) = -\bar{G}_c^*[\hat{a}(t_i)]\hat{x}(t_i^+) \quad (2.42)$$

where the gain is determined as a function of the parameter position estimates. This function is composed in part of a lookup table that is pre-computed based on the discretized parameter space. In the system example given, this would constitute a 10x10

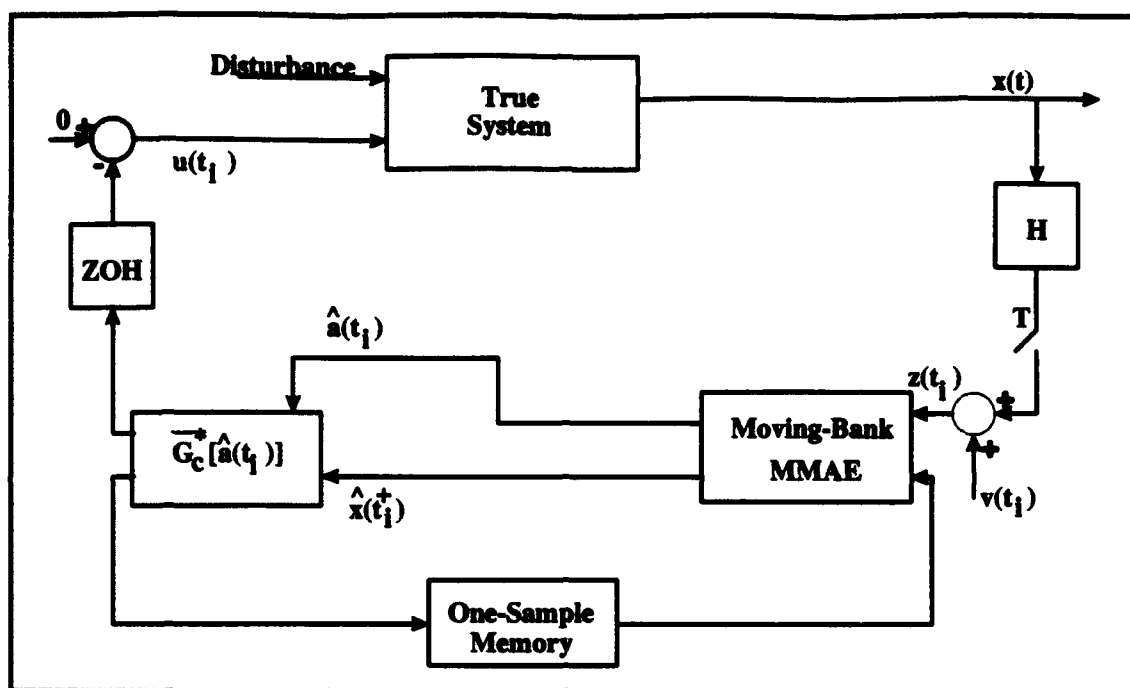


Figure 2-2. Single Changeable-Gain Controller

table. The one gain to be used is interpolated from this table, once  $\hat{a}(t_i)$  is generated by the MMAE algorithm [14:38].

#### 2.6.6 "Modified" Single Changeable-Gain Control

Although very similar in nature to the previous technique, this method states that the MMAE is only necessary to provide an estimate of the uncertain parameter,  $\hat{a}(t_i)$ , whereas its state estimate is not used.  $\hat{a}(t_i)$  is provided to a single separate (not part of the original MMAE) Kalman filter/controller in which the system model and controller gain is based on the estimated parameter position. Figure 2-3 illustrates this technique. If  $\hat{a}(t_i)$  lies between discretized values  $a_k$ , then the  $\hat{x}(t_i^+)$  in Figure 2-2 will be produced by weighted-average blending of a number of elemental filter outputs  $\hat{x}_k(t_i^+)$ , none of which are based on the "correct" parameter value, whereas  $\hat{x}(t_i^+)$  of Figure 2-3 would be produced by a single Kalman filter explicitly based on that correct parameter value. Thus, discretization effects should cause less state estimation degradation in this type of controller than in the form depicted in Figure 2-2. This combination should reduce the

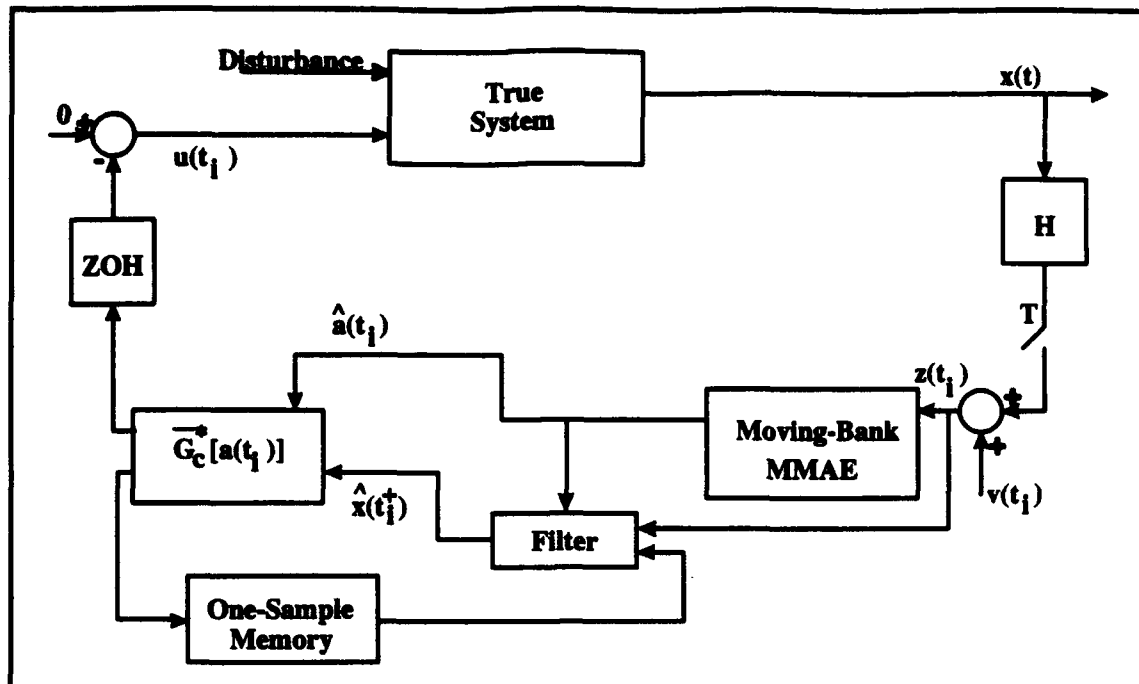


Figure 2-3. Modified Single Changeable-Gain Controller

probability that the control input is generated from filters and/or controllers that assume too small a value for the undamped natural frequency of the system [11:1.17]. Past research has shown that underestimating this value for the important bending modes will lead to system instabilities [39].

## 2.7 Mathematical Modeling Methods

This thesis will utilize various mathematical tools to manipulate the system model under investigation into a format that is more conducive to simulations as well as state order reduction. This section will provide a brief presentation of the physical coordinate form and then discuss the transformation into a more desirable modal form. Due to the excessive computational burden imposed by high dimensioned systems, state order reduction is typically desired, especially for on-line filter/controller implementations. Consequently, three techniques for accomplishing state order reduction will be presented.

### 2.7.1 Physical Coordinate Form

The dynamics of a structure's flexible body modes are described by the following standard second order differential equation [15:40,21:4]:

$$\mathbf{M}\ddot{\mathbf{r}}(t) + \mathbf{C}\dot{\mathbf{r}}(t) + \mathbf{K}\mathbf{r}(t) = \mathbf{F}_1(\mathbf{u}, t) + \mathbf{F}_2(t) \quad (2.43)$$

where:

- $\mathbf{r}(t)$  =  $n$ -dimensional vector representing the structure's physical position
- $\mathbf{M}$  =  $n$ -by- $n$  constant mass matrix
- $\mathbf{C}$  =  $n$ -by- $n$  constant damping matrix
- $\mathbf{K}$  =  $n$ -by- $n$  constant stiffness matrix
- $\mathbf{F}_1(t)$  =  $r$ -dimensional deterministic control inputs
- $\mathbf{F}_2(t)$  =  $r$ -dimensional disturbances and unmodeled control inputs

If the assumptions are made that the inputs enter linearly through time-invariant matrices and that the external disturbances,  $\mathbf{F}_2(t)$ , can be modeled as white Gaussian noises, then Equation (2.43) becomes [15:40,21:4]:

$$\mathbf{M}\ddot{\mathbf{r}}(t) + \mathbf{C}\dot{\mathbf{r}}(t) + \mathbf{K}\mathbf{r}(t) = -\mathbf{b}\mathbf{u}(t) - \mathbf{g}\mathbf{w}(t) \quad (2.44)$$

where:

- $\mathbf{u}(t)$  =  $r$ -dimensional vector actuator inputs
- $\mathbf{b}$  =  $n$ -by- $r$  control input matrix identifying position and relationships between actuators and controlled variables
- $\mathbf{w}(t)$  =  $s$ -dimensional vector of white Gaussian noises representing the dynamics driving noise
- $\mathbf{g}$  =  $n$ -by- $s$  noise input matrix identifying position and relationship between the dynamics driving noise and the controlled variables

Equation (2.44) can be transformed into the following state space form [15:40,21:4]:

$$\dot{\mathbf{x}}(t) = \mathbf{F}\mathbf{x}(t) + \mathbf{B}\mathbf{u}(t) + \mathbf{G}\mathbf{w}(t) \quad (2.45)$$

which is the same form as the system described by Equation (2.1) in Section 2.2 with the exception of constant matrices. Thus, the state vector representation from Equation (2.44) of a general structure is given by:

$$\mathbf{x}(t) = \begin{bmatrix} \dot{\mathbf{r}}(t) \\ \mathbf{r}(t) \end{bmatrix}_{2nx1} \quad (2.46)$$

and the form of the constant system matrices is [11:3-20,15:41]:

$$\mathbf{F} = \begin{bmatrix} -\mathbf{M}^{-1}\mathbf{C}_{n \times n} & -\mathbf{M}^{-1}\mathbf{K}_{n \times n} \\ \mathbf{I}_{n \times n} & \mathbf{0}_{n \times n} \end{bmatrix}_{2n \times 2n} \quad (2.47)$$

$$\mathbf{B} = \begin{bmatrix} -\mathbf{M}^{-1}\mathbf{b}_{n \times r} \\ \mathbf{0}_{n \times r} \end{bmatrix}_{2n \times r} \quad (2.48)$$

$$\mathbf{G} = \begin{bmatrix} -\mathbf{M}^{-1}\mathbf{g}_{n \times s} \\ \mathbf{0}_{n \times s} \end{bmatrix}_{2n \times r} \quad (2.49)$$

For the state vector described in Equation (2.46), the discrete-time measurement description of position and velocity is given by [11:3-20,15:41]:

$$\mathbf{z}(t_i) = \left\{ \begin{bmatrix} \mathbf{H}_v & \mathbf{0} \\ \mathbf{0} & \mathbf{H}_p \end{bmatrix}_{m \times 2n} \mathbf{x}(t_i) \right\} + \mathbf{v}(t_i) \quad (2.50)$$

where:

- $m$  = number of measurements
- $\mathbf{v}(t_i)$  =  $m$ -dimensional measurement uncertainty modeled as a discrete-time white Gaussian noise of covariance  $\mathbf{R}(t_i)$
- $\mathbf{H}_p$  =  $(m/2)$ -by- $n$  position measurement matrix in physical coordinates
- $\mathbf{H}_v$  =  $(m/2)$ -by- $n$  velocity measurement matrix in physical coordinates



For simplicity, an equal number of position and velocity measurements is assumed. The actual measurement matrix may vary as a function of the measurements available, but it does not affect the structure of the system matrices of Equations (2.47) through (2.49).

The disadvantage of the physical coordinate form is that the system equations are highly coupled. This makes it difficult to identify important characteristics of the system.

### 2.7.2 Modal Coordinate Form

Transforming the equations to modal form decouples the modes and makes the identification process simpler. In this research, the damping matrix,  $C$ , is assumed to be a linear combination of the mass and stiffness matrices [21:4]:

$$C = \alpha M + \beta K \quad (2.51)$$

However, the calculation of  $\alpha$  and  $\beta$  is not necessary when transforming to the modal coordinate form, as will be seen. Given the new modal coordinate vector  $\tilde{r}$ , the relationship between the modal and physical forms is described by [21:5]:

$$r = T\tilde{r} \quad (2.52)$$

where  $T$  is a  $n$ -by- $n$  transformation matrix determined from the system eigenvectors calculated from [21:5]:

$$\omega^2 M T = K T \quad (2.53)$$

where the values for  $\omega$  that satisfy this equation are referred to as the natural or modal frequencies. Since the damping matrix  $C$  does not appear in this equation, the previous statement that the parameters in Equation (2.51) are not required is shown to be true.

Now, using the transformation Equation (2.52) to operate on the original system Equation (2.45), the resulting state space equation is given by [21:5]:

$$\dot{\tilde{x}}(t) = \tilde{F}\tilde{x}(t) + \tilde{B}u(t) + \tilde{G}w(t) \quad (2.54)$$

where the transformed state vector from Equation (2.46) is now defined as [21:5]:

$$\tilde{\mathbf{x}}(t) = \begin{bmatrix} \dot{\tilde{\mathbf{r}}}(t) \\ \tilde{\mathbf{r}}(t) \end{bmatrix}_{2nx1} \quad (2.55)$$

and the transformed matrices from Equation (2.45) as applied to Equation (2.44) are defined as [11,21:5]:

$$\tilde{\mathbf{F}} = \begin{bmatrix} -T^{-1}\mathbf{M}^{-1}\mathbf{C}T & -T^{-1}\mathbf{M}^{-1}\mathbf{K}T \\ \mathbf{I} & \mathbf{0} \end{bmatrix}_{2nx2n} \quad (2.56)$$

$$\tilde{\mathbf{B}} = \begin{bmatrix} -T^{-1}\mathbf{M}^{-1}\mathbf{b} \\ \mathbf{0} \end{bmatrix}_{2n \times r} = \tilde{\mathbf{G}} \quad (2.57)$$

$$\tilde{\mathbf{G}} = \begin{bmatrix} -T^{-1}\mathbf{M}^{-1}\mathbf{g} \\ \mathbf{0} \end{bmatrix}_{2n \times r} \quad (2.58)$$

Since the modal form provides for independent equations, the resulting modal vectors are orthogonal (e.g., the transformation matrix is developed from the system eigenvectors which are orthogonal). This fact plus the following relationships:

$$-T^{-1}\mathbf{M}^{-1}\mathbf{C}T = [-2\zeta_i\omega_i] \quad (2.59)$$

$$-T^{-1}\mathbf{M}^{-1}\mathbf{K}T = [-\omega_i^2] \quad (2.60)$$

allows the dynamics matrix to be written as follows:

$$\tilde{\mathbf{F}} = \begin{bmatrix} [-2\zeta_i\omega_i] & [-\omega_i^2] \\ \mathbf{I} & \mathbf{0} \end{bmatrix}_{2nx2n} \quad (2.61)$$

where the upper partitions are now block diagonal in terms of the undamped natural frequency and the damping ratio of the  $i$ -th mode. The transformed measurement

equation from Equation (2.50) may be written as [11]:

$$\tilde{\mathbf{z}}(t_i) = \left\{ \begin{bmatrix} \mathbf{H}_v \mathbf{T} & \mathbf{0} \\ \mathbf{0} & \mathbf{H}_p \mathbf{T} \end{bmatrix}_{m \times 2n} \tilde{\mathbf{x}}(t_i) \right\} + \mathbf{v}(t_i) \quad (2.62)$$

As can be seen from this development, the modal form, unlike the physical form, allows ready access to the individual modes of the system (in terms of the natural frequency and damping ratio). Thus the modal form provides more insight to the physical structure in applicable large order systems such as in this research.

### 2.7.3 Modal Reduction Technique

In modal reduction, the higher frequency modes are eliminated from the system model. This statement is based on the premise that, at the higher frequencies, the structure reaches steady state in a negligibly small amount of time. Moreover, the effects of low frequency modes should dominate because of the physical nature of the structure being two stiff bodies attached by tripod legs. This section will discuss this procedure specifically.

From Equation (2.45), the continuous system model can be partitioned as follows [15:52,17:123]:

$$\dot{\mathbf{x}}(t) = \begin{bmatrix} \dot{\mathbf{x}}_1(t) \\ \dot{\mathbf{x}}_2(t) \end{bmatrix} = \begin{bmatrix} \mathbf{F}_{11} & \mathbf{F}_{12} \\ \mathbf{F}_{21} & \mathbf{F}_{22} \end{bmatrix} \begin{bmatrix} \mathbf{x}_1(t) \\ \mathbf{x}_2(t) \end{bmatrix} + \begin{bmatrix} \mathbf{B}_1 \\ \mathbf{B}_2 \end{bmatrix} \mathbf{u}(t) + \begin{bmatrix} \mathbf{G}_1 \\ \mathbf{G}_2 \end{bmatrix} \mathbf{w}(t) \quad (2.63)$$

where the system is driven by deterministic controls,  $\mathbf{u}(t)$ , and zero-mean, white Gaussian noise  $\mathbf{w}(t)$  of strength  $\mathbf{Q}(t)$  (defined in Equation (2.3), Section 2.2). The upper partition,  $\mathbf{x}_1(t)$ , corresponds to the low frequency modes to be maintained, and the lower partition,  $\mathbf{x}_2(t)$ , corresponds to the high frequency modes to be removed.

Assuming instantaneous steady state ( $\dot{\mathbf{x}}_2(t) = \mathbf{0}$ ), the  $\mathbf{x}_2(t)$  modes can be eliminated with negligible impact to the overall performance of the system. The lower

partition differential equation is set to zero as follows [15:52,17:123]:

$$\dot{\mathbf{x}}_2(t) = \mathbf{F}_{21}\mathbf{x}_1(t) + \mathbf{F}_{22}\mathbf{x}_2(t) + \mathbf{B}_2\mathbf{u}(t) + \mathbf{G}_2\mathbf{w}(t) = \mathbf{0} \quad (2.64)$$

Since  $\mathbf{F}_{21}$  and  $\mathbf{F}_{22}$  are square matrices and  $\mathbf{F}_{22}^{-1}$  is assumed to exist,  $\mathbf{x}_2(t)$  can now be written in terms of  $\mathbf{x}_1(t)$  and system inputs [15:52,17:123]:

$$\mathbf{x}_2(t) = -\mathbf{F}_{22}^{-1}[\mathbf{F}_{21}\mathbf{x}_1(t) + \mathbf{B}_2\mathbf{u}(t) + \mathbf{G}_2\mathbf{w}(t)] \quad (2.65)$$

Substituting Equations (2.64) and (2.65) into Equation (2.63) results in [15:52, 17:123]:

$$\begin{aligned} \dot{\mathbf{x}}_1(t) = & [\mathbf{F}_{11} - \mathbf{F}_{12}\mathbf{F}_{22}^{-1}\mathbf{F}_{21}]\mathbf{x}_1(t) + [\mathbf{B}_1 - \mathbf{F}_{12}\mathbf{F}_{22}^{-1}\mathbf{B}_2]\mathbf{u}(t) \\ & + [\mathbf{G}_1 - \mathbf{F}_{12}\mathbf{F}_{22}^{-1}\mathbf{G}_2]\mathbf{w}(t) \end{aligned} \quad (2.66)$$

Since this research will use a digital implementation, the analogous development is given for the discrete-time case [11:3-24]. The equivalent discrete-time model of Equation (2.63) is as follows:

$$\mathbf{x}(t_{i+1}) = \begin{bmatrix} \mathbf{x}_1(t_{i+1}) \\ \mathbf{x}_2(t_{i+1}) \end{bmatrix} = \begin{bmatrix} \Phi_{11} & \Phi_{12} \\ \Phi_{21} & \Phi_{22} \end{bmatrix} \begin{bmatrix} \mathbf{x}_1(t_i) \\ \mathbf{x}_2(t_i) \end{bmatrix} + \begin{bmatrix} \mathbf{B}_{d1} \\ \mathbf{B}_{d2} \end{bmatrix} \mathbf{u}(t_i) + \begin{bmatrix} \mathbf{G}_{d1} \\ \mathbf{G}_{d2} \end{bmatrix} \mathbf{w}_d(t_i) \quad (2.67)$$

With the same steady state assumption as applied to the discrete time case, ( $\mathbf{x}_2(t_{i+1}) = \mathbf{x}_2(t_i)$ ), the resulting representation of the higher order modes is given as follows:

$$\Phi_{21}\mathbf{x}_1(t_i) + [\Phi_{22} - \mathbf{I}]\mathbf{x}_2(t_i) + \mathbf{B}_{d2}\mathbf{u}(t_i) + \mathbf{G}_{d2}\mathbf{w}_d(t_i) = \mathbf{0} \quad (2.68)$$

$$\mathbf{x}_2(t_i) = -[\Phi_{22} - \mathbf{I}]^{-1}[\Phi_{21}\mathbf{x}_1(t_i) + \mathbf{B}_{d2}\mathbf{u}(t_i) + \mathbf{G}_{d2}\mathbf{w}_d(t_i)] \quad (2.69)$$

The continuous state-space equation can be discretized easily by assuming a first order approximation as follows:

$$\Phi_{22} \cong \mathbf{I} + \mathbf{F}_{22}\Delta t \quad (2.70)$$

$$\Phi_{21} \cong \mathbf{F}_{21}\Delta t \quad (2.71)$$

$$\mathbf{B}_{d2} \equiv \mathbf{B}_2 \Delta t \quad (2.72)$$

$$\mathbf{G}_{d2} \equiv \mathbf{G}_2 \Delta t \quad (2.73)$$

$$\mathbf{Q}_d \equiv \mathbf{Q} / \Delta t \quad (2.74)$$

This last equation is appropriate, since, to first order,  $\mathbf{G}_{d2} \mathbf{Q}_d \mathbf{G}_{d2}^T \equiv \mathbf{G}_2 \mathbf{Q}_2 \mathbf{G}_2^T \Delta t$  and  $\mathbf{G}_{d2} = \mathbf{G}_2 \Delta t$ .

Substituting the Equations (2.70) through (2.74) into Equation (2.69) results in:

$$\mathbf{x}_2(t_i) = -[\mathbf{F}_{22} \Delta t]^{-1} [\mathbf{F}_{21} \Delta t \mathbf{x}_1(t_i) + \mathbf{B}_2 \Delta t \mathbf{u}(t_i) + \mathbf{G}_2 \Delta t \mathbf{w}_d(t_i)] \quad (2.75)$$

where  $\mathbf{w}_d(t_i)$  has covariance  $\mathbf{Q}_d = \mathbf{Q}_2 / \Delta t$ . Simplifying the previous equation results in:

$$\mathbf{x}_2(t_i) = -\mathbf{F}_{22}^{-1} [\mathbf{F}_{21} \mathbf{x}_1(t_i) + \mathbf{B}_2 \mathbf{u}(t_i) + \mathbf{G}_2 \mathbf{w}_d(t_i)] \quad (2.76)$$

This equation is similar to the previous continuous time version, Equation (2.65), except  $\mathbf{w}$  is replaced with  $\mathbf{w}_d$ , a discrete-time white Gaussian noise. Then, substituting Equation (2.76) into the discrete time measurement equation:

$$\mathbf{z}(t_i) = [\mathbf{H}_1 \quad \mathbf{H}_2] \begin{bmatrix} \mathbf{x}_1(t_i) \\ \mathbf{x}_2(t_i) \end{bmatrix} + \mathbf{v}(t_i) \quad (2.77)$$

and expanding, yields:

$$\mathbf{z}(t_i) = [\mathbf{H}_1 - \mathbf{H}_2 \mathbf{F}_{22}^{-1} \mathbf{F}_{21}] \mathbf{x}_1(t_i) - \mathbf{H}_2 \mathbf{F}_{22}^{-1} [\mathbf{B}_2 \mathbf{u}(t_i) + \mathbf{G}_2 \mathbf{w}_d(t_i)] + \mathbf{v}(t_i) \quad (2.78)$$

which results in a direct feedthrough term (the second term) created by the order reduction [15:52,17:123].

Still left to be determined is the cutoff frequency between the desired low frequency modes and the unwanted high frequency modes. This can be accomplished by examining an ascending ordered list of the modal frequencies and determining the natural breaks (subject to physical insight and computational concerns). The preserved low

frequency modes form the basis of the resulting reduced-order model which still retains some information from the eliminated higher frequency modes .

This procedure could be somewhat tedious to accomplish in the physical form of the system equations, but is rather straightforward in the modal form (Equations (2.54) through (2.62)). The system dynamics matrix presented in Equation (2.61) is expanded to the next level as follows to illustrate the modal form further [11:3-26,15:53,17:123]:

$$\tilde{\mathbf{F}} = \left[ \begin{array}{cc|cc} [-2\zeta_1\omega_1] & [-\omega_1^2] & 0 & 0 \\ \mathbf{I} & 0 & 0 & 0 \\ \hline 0 & 0 & [-2\zeta_2\omega_2] & [-\omega_2^2] \\ 0 & 0 & \mathbf{I} & 0 \end{array} \right] \quad (2.79)$$

The low frequency modes to be maintained are represented in the upper left quadrant, and the higher frequency modes to be eliminated are represented in the lower right quadrant. These two quadrants correspond to the  $\mathbf{F}_{11}$  and  $\mathbf{F}_{22}$  partitions in Equation (2.63). The off-diagonal blocks,  $\mathbf{F}_{12}$  and  $\mathbf{F}_{21}$ , are zero. Substituting this information into Equations (2.66) and (2.78) yields [15:53,17:123]:

$$\dot{\tilde{\mathbf{x}}}_r(t) = \tilde{\mathbf{F}}_{11}\tilde{\mathbf{x}}_r(t) + \tilde{\mathbf{B}}_r\mathbf{u}(t) + \tilde{\mathbf{G}}_r\mathbf{w}_r(t) = \tilde{\mathbf{F}}_r\tilde{\mathbf{x}}_r(t) + \tilde{\mathbf{B}}_r\mathbf{u}(t) + \tilde{\mathbf{G}}_r\mathbf{w}_r(t) \quad (2.80)$$

$$\begin{aligned} \mathbf{z}(t_i) &= \tilde{\mathbf{H}}_1\tilde{\mathbf{x}}_r(t_i) - \tilde{\mathbf{H}}_2\tilde{\mathbf{F}}_{22}^{-1}[\tilde{\mathbf{B}}_2\mathbf{u}(t_i) + \tilde{\mathbf{G}}_2\mathbf{w}_d(t_i)] + \mathbf{v}_r(t_i) \\ &= \tilde{\mathbf{H}}_r\tilde{\mathbf{x}}_r(t_i) - \tilde{\mathbf{D}}_u\mathbf{u}(t_i) + \tilde{\mathbf{D}}_w\mathbf{w}_d(t_i) + \mathbf{v}_r(t_i) \end{aligned} \quad (2.81)$$

where the subscript  $r$  denotes "reduced-order." As can be seen through this development and Equation (2.81), the only remaining terms accounting for the high frequency modes eliminated are the direct feedthrough terms,  $\tilde{\mathbf{D}}_u$  and  $\tilde{\mathbf{D}}_w$ . These two terms allow direct measurement of the effects of control inputs,  $\mathbf{u}(t_i)$ , and system dynamics driving noise,  $\mathbf{w}_d(t_i)$ .

#### 2.7.4 Internally Balanced Reduction Technique [5:31]

The internally balanced technique attempts to "balance" a system's input/output relationship and apply a relative performance or level of importance index on the resulting states [22]. This index provides insight to accomplishing order reduction, while distributing the error of the reduction over the entire bandwidth of interest [11:3-27]. This technique is different from the modal reduction in that no distinction is placed on either high or low frequency modes, and thus the assumption of high frequency modes reaching steady-state instantaneously is no longer maintained. Instead, those modes which are least observable and/or controllable are removed, since they would have the least impact on the input/output relationship for the system.

In this technique, the controllability gramian,  $W_c$ , and observability gramian,  $W_o$ , change, but the actual input-output transfer function is not altered. These gramians are determined from the solutions to the following matrix Lyapunov equations:

$$FW_c + W_c F^T + BB^T = 0 \quad (2.82)$$

$$F^T W_o + W_o F + H^T H = 0 \quad (2.83)$$

where internal balancing results when the gramians,  $W_c$  and  $W_o$ , are determined to be equal. Thus, a transformed set of system matrices,  $\tilde{F}$ ,  $\tilde{B}$ , and  $\tilde{H}$ , is desired such that Equations ( 2.82) and ( 2.83) are satisfied and  $\tilde{W}_c = \tilde{W}_o$ .

For efficiency, a diagonal form of the gramian matrix is desired. Once the gramian is calculated, the similarity transformation matrix,  $T_b$ , is determined that will transform the gramian into diagonal form. First, the Cholesky square roots of  $W_c$  and  $W_o$  are determined such that the following is true:

$$W_c = S_c S_c^T \quad (2.84)$$

$$W_o = S_o S_o^T \quad (2.85)$$

Next, the singular value decomposition of  $S_o^T S_c$  is computed:

$$S_o^T S_c = U \Delta V^T \quad (2.86)$$

where  $U^T U = V^T V = I$  and the diagonal matrix,  $\Delta$ , is referred to as the balanced gramian.

Now the desired similarity transformation is calculated:

$$T_b = S_c V \Delta^{-1/2} \quad (2.87)$$

$$T_b^{-1} = \Delta^{-1/2} U^T S_o^T \quad (2.88)$$

and used to form the internally balanced system matrices:

$$\tilde{F} = T_b^{-1} F T_b \quad (2.89)$$

$$\tilde{B} = T_b^{-1} B \quad (2.90)$$

$$\tilde{G} = T_b^{-1} G \quad (2.91)$$

$$\tilde{H} = H T_b \quad (2.92)$$

and the diagonal gramian matrices:

$$\tilde{W}_c = T_b^{-1} W_c T_b^{-T} \quad (2.93)$$

$$\tilde{W}_o = T_b^T W_o T_b \quad (2.94)$$

and  $\tilde{W}_c = \tilde{W}_o = \Delta$ .

Finally, the balanced state vector can be computed:

$$\tilde{x} = T_b^{-1} x \quad (2.95)$$

To accomplish the desired order reduction, the gramian is examined (the diagonal terms, *i.e.*, eigenvalues, form natural groupings and natural breaks) to determine which of



the first  $m$  states are to be maintained. Thus, the resulting reduced-order state vector is simply the first  $m$ -states of the full-order internally-balanced state vector. Subsequently, the system matrices must be modified by extracting the upper left  $m$ -by- $m$  partition of the matrix  $\tilde{\mathbf{F}}$ , along with the corresponding portions of  $\tilde{\mathbf{B}}$ ,  $\tilde{\mathbf{G}}$  and  $\tilde{\mathbf{H}}$ . This results in the following system equation:

$$\dot{\tilde{\mathbf{x}}}_r(t) = \tilde{\mathbf{F}}_r \tilde{\mathbf{x}}_r(t) + \tilde{\mathbf{B}}_r \mathbf{u}(t) + \tilde{\mathbf{G}}_r \mathbf{w}(t) \quad (2.96)$$

where the subscript  $r$  represents reduced order. Finally, the measurement equation becomes:

$$\mathbf{z}_r(t_i) = \tilde{\mathbf{H}}_r \tilde{\mathbf{x}}_r(t_i) + \mathbf{v}_r(t_i) \quad (2.97)$$

where there are no resultant feedthrough terms (unlike the modal reduction method where the terms  $\tilde{\mathbf{D}}_u$  and  $\tilde{\mathbf{D}}_w$  arose mathematically as a result of the reduction technique).

### 2.7.5 Component Cost Modal Reduction Technique [40]

In their Component Cost Analysis (CCA) technique, Skelton and Yousuff propose that the performance of a dynamic system subject to white noise disturbances can be evaluated in terms of a *performance metric*,  $\mathcal{V}$ . This scalar value could represent the total system energy. The underlying question is: "What fraction of the overall system performance metric  $\mathcal{V}$  is due to each component of the system?". By identifying the individual cost associated with each component, or more precisely, each state, it is then possible to consider order reduction based on eliminating those states that have the least impact to the overall cost. The following brief description will illustrate this method.

Assuming a linear time invariant dynamic system as described by Equation (2.45) having  $n$ -states and zero-mean white Gaussian dynamics driving noise (repeated here without the deterministic input and sensor noise to be consistent with the authors' original

presentation):

$$\dot{\mathbf{x}}(t) = \mathbf{F}\mathbf{x}(t) + \mathbf{G}\mathbf{w}(t) \quad (2.98)$$

$$\mathbf{z}(t) = \mathbf{H}\mathbf{x}(t) \quad (2.99)$$

The system performance metric  $\mathcal{V}$  is defined as:

$$\mathcal{V} = \lim_{t \rightarrow \infty} E[\mathbf{z}(t)^T \mathbf{z}(t)] \quad (2.100)$$

where the sum of contributions  $\mathcal{V}_i$  associated with each component state  $x_i$  satisfies the *cost-decomposition property*:

$$\mathcal{V} = \sum_{i=1}^n \mathcal{V}_i \quad (2.101)$$

The individual component costs are determined as follows:

$$\mathcal{V}_i = \text{trace}[\mathbf{X}\mathbf{H}^T \mathbf{H}]_{ii} \quad (2.102)$$

where  $\mathbf{X}$  satisfies the matrix Lyapunov equation:

$$\mathbf{0} = \mathbf{X}\mathbf{F}^T + \mathbf{F}\mathbf{X} + \mathbf{G}\mathbf{G}^T \quad (2.103)$$

The individual components costs may be positive or negative. If  $\mathcal{V}_i < 0$ , then that component's dynamics are said to interact with other components so as to help reduce the overall cost, and thus are "beneficial" to the system. If  $\mathcal{V}_i > 0$ , then that component's dynamics are said to add to the magnitude of the overall cost, and thus are "costly" to the system. The sum of all component costs is nonnegative.

In order to perform order reduction, it is necessary to re-order the system equations such that the states appear in descending order according to the magnitude of their component costs ( $|\mathcal{V}_1| \geq |\mathcal{V}_2| \geq |\mathcal{V}_3| \geq \dots \geq |\mathcal{V}_n|$ ). Then, by examining the rank ordered component costs for natural breaks, state order reduction is accomplished by truncating the partitions of the system equations (as was done in the internally balanced method)

corresponding to the states determined to be least costly . The resultant system equations are as follows:

$$\dot{\mathbf{x}}_r(t) = \mathbf{F}_r \mathbf{x}_r(t) + \mathbf{G}_r \mathbf{w}(t) \quad (2.104)$$

$$\mathbf{z}_r(t) = \mathbf{H}_r \mathbf{x}_r(t) \quad (2.105)$$

This technique can be expanded to apply to the more general system which includes the effects of deterministic inputs and measurement noise. However, the algorithm as described above is not modified (*i.e.*, the terms  $\mathbf{B}$ ,  $\mathbf{u}(t)$ , and  $\mathbf{v}(t_i)$  will still not appear in the CCA algorithm)

## 2.8 *Summary*

This chapter highlighted the concepts that form the foundations of this research. The Kalman filter algorithms and their applications in the Bayesian MMAE development were discussed first. The moving-bank MMAE discussion included methods for moving, expanding and contracting the bank. Next, the stochastic controller development was provided with the subsequent application to the MMAC. Finally, two coordinate forms were discussed as well as three methods for state order reduction. It is important to remember the simplifying assumptions opted in this research. The system for this thesis will be assumed adequately described by linear, time invariant models driven by stationary noises. A constant state weighting matrix and control weighing matrix will be used in the quadratic cost definition for the LQG controller synthesis. The steady state Kalman filter and LQG controller gains will be implemented. Chapter 3 will proceed with the actual system structure model development to be investigated by this research.

### ***III. System Development***

#### ***3.1 Introduction***

This chapter presents a more thorough description of the system under investigation than was given in Chapter 1. First, a brief description of the actual physical structure is provided. Second, the overall system model is broken into its components parts and analyzed. Last, the resulting truth model selection and subsequent reduced order models are discussed.

#### ***3.2 SPICE Structure***

The original SPICE structure was envisioned to be mounted on a larger space platform with the capability of precision pointing along the line of sight (LOS) axis (Reference Figure 3-1). As such, the SPICE structure must be able to be rotated or slewed perpendicular to the LOS axis by an active rigid body control system. Once slewed, the flexible body modes must be quelled to within a predetermined specification along the LOS axis to obtain the desired precision pointing. This thesis will focus strictly on quelling the flexible body vibrations and will ignore the rigid body motion or any residual rigid body effects.

Version 4 of the constantly evolving SPICE structure is investigated in this research. The updated version has many changes from the version 2 examined in Gustafson's research [11]. Most of the updates are due to the addition of actual hardware (sensors and actuators) not physically present in the previous versions. In addition, actual test data taken after these additions was incorporated into the system model. This section will present the new version as well as point out some of the basic changes from version 2.

##### ***3.2.1 Physical Structure Description***

The SPICE structure is divided into three major structural sections as depicted in Figure 3-1. The hexagonal base referred to as the Bulkhead forms the support for the

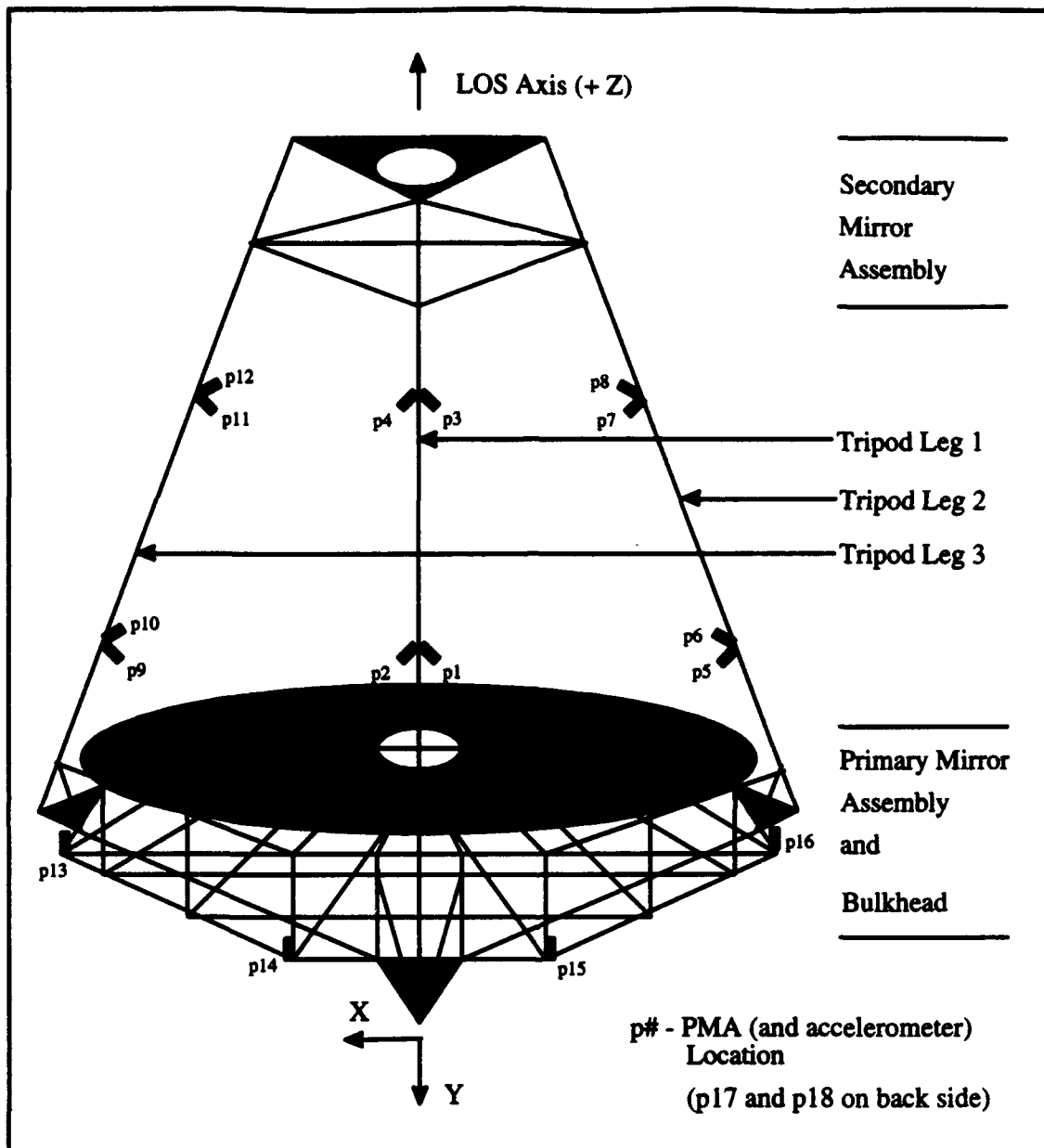


Figure 3-1. SPICE Structure [20:III-14]

entire structure and is 6.19 meters in diameter. The Primary Mirror (PM) Assembly is mounted on top of the bulkhead. Three legs (tripod) connect the bulkhead to the Secondary Mirror (SM) Assembly. The SM Assembly is 1.32 meters in diameter. The overall height of the structure is 8.14 meters. The Z-axis corresponds to the LOS axis and the Y axis points out the tripod leg number one. Each of the PMAs has its own local coordinate frame.

Maintaining the alignment of the SM Assembly and the Bulkhead is the primary concern of this research. An exaggerated example of the SPICE structure exhibiting this misalignment due to its flexible bending modes is illustrated in Figure 3-2. Note that (for the purposes of this research) the alignment is not altered by a pure torsion force about the line of sight axis.

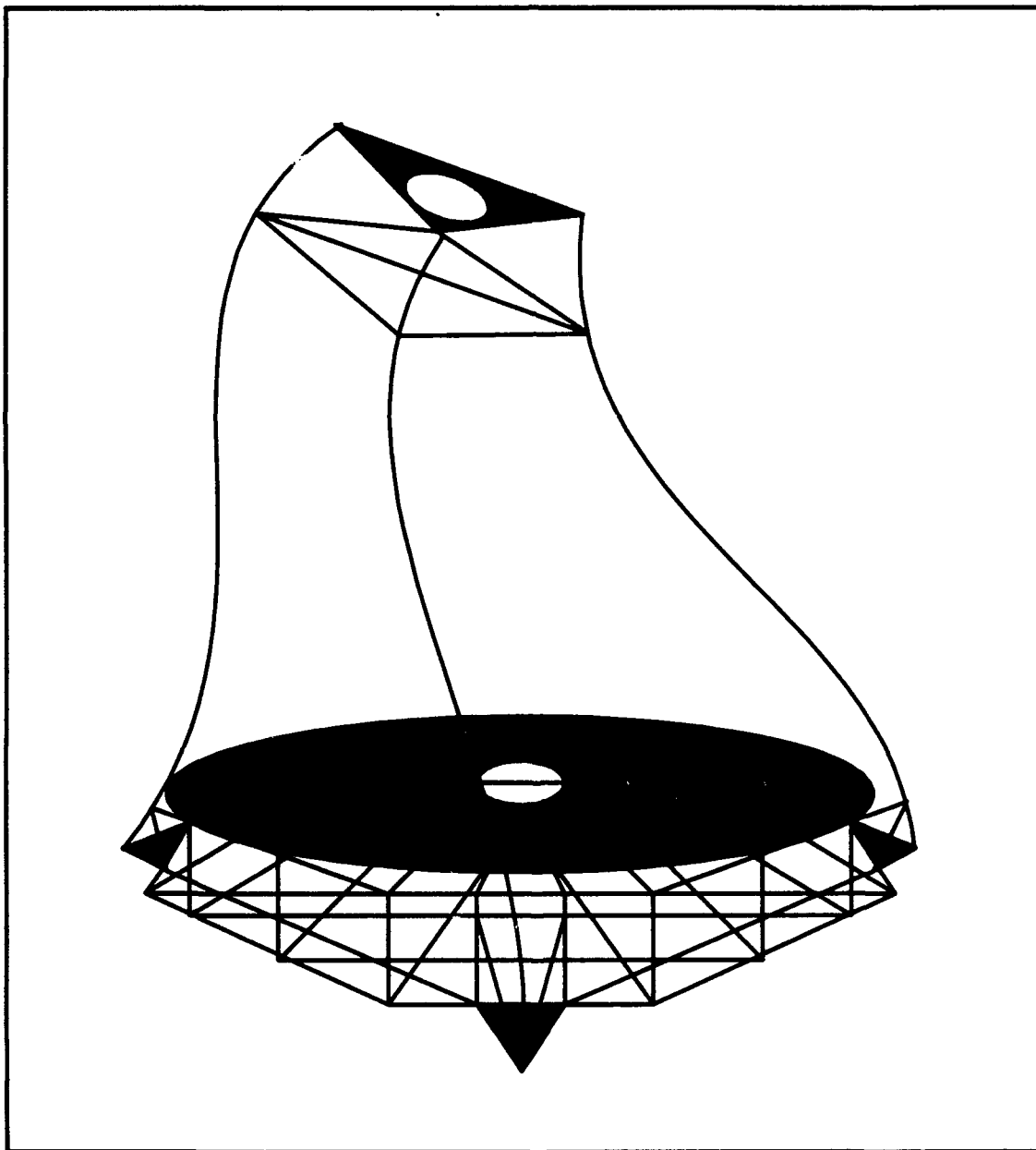


Figure 3-2. Flexible SPICE Structure

### **3.2.2 *Actuators and Sensors***

Actuators provide the control force necessary to quell the structural vibrations. The specific actuator utilized is referred to as a proof mass actuator (PMA). The PMA uses a proof mass that is electro-magnetically moved to counteract the bending motion of the structure at the location of the PMA. (The dynamics of the PMA can be thought of as a simple spring-mass system.) A total of 18 PMAs are mounted on the structure. There are 6 PMAs located such that there is one on the vertical spar at each of the hexagonal corners of the bulkhead pointing in the Z direction. The tripod legs house the remaining 12 PMAs. Each leg has two sets of PMAs mounted along the local orthogonal coordinate axis and optimally located approximately one third and two thirds up the length of the leg respectively. The PMAs were not physically mounted on the structure for version 2 but were included as mathematical models.

Various sensors provide the necessary measurement information to generate the controlling force inputs and to indicate the pointing accuracy. Specifically, three different types of sensors are being used. First, there are a total of 54 accelerometers separated into 18 essentially co-located sets of 3 (one set per PMA) which measure the bending motion of the structure. Each set contains 2 Wilcoxon high frequency accelerometers and 1 Sundstrand low frequency accelerometer. One Wilcoxon accelerometer is physically mounted on each PMA proof mass. The remaining two are co-located on the physical structure at the point of attachment and along the reference axis of each PMA. This is different from version 2, which had modeled only one accelerometer located at each PMA position. The second type of sensor is the Linear Variable Differential Transformer (LVDT), which provides a differential position measurement of the PMA proof mass with respect to the structure. This sensor was not available physically or in model form in version 2. The third type of sensors are the elements of the Optical Scoring System (OSS) which provide line of sight (LOS) measurements between the two mirror assemblies. This

system uses 42 precisely placed laser and sensor pairs to determine a change in position of a laser with respect to the corresponding sensor. Essentially, this gives an indication of the relative displacement between the primary and secondary mirror assemblies. These sensors were modeled but not physically present for version 2.

### **3.2.2 Disturbances**

There are two different types of disturbances entering the physical structure. The first type enters at the base of each tripod leg at the attachment to the bulkhead. There are actually two highly correlated disturbances entering each tripod leg. This adds to a total of 6 input disturbances of this type. These disturbances are imparted to the physical structure during on-ground testing using pairs of magnetic actuators at the base of each tripod leg. In version 2, there was only one modeled disturbance entering each leg. The addition of the second disturbance to each leg is more physically correct with the actual structure. The second type of disturbance enters each tripod leg at the SM Assembly. Here there is only one input per leg, for a total of three.

### **3.3 Full Order System Model Description**

The overall system model is illustrated in Figure 3-3 in a much simplified block diagram format. The actual full system model was provided by Honeywell Inc, Phoenix AZ, in MATRIXx System-Build format [3]. This model is an accurate representation of the actual physical structure and is composed of an extremely high number of states (~1000). The complete model is presented to provide insight and understanding of the actual physical system. In Figure 3-3, the PMA fcmd (force command) refers to the control inputs to the PMAs from the combined feedback loops. In the feedback loop portion, the PMA LAC (low authority control) damping refers to simple rate feedback for the structure, whereas the PMA local damping refers to localized damping for the PMAs. In the subsequent subsections, the individual parts of the overall system model will be separated and analyzed, thus providing a clearer understanding of the



system components illustrated in Figure 3-3. The complexity and excessive size of this model would prohibit its use as a "truth" model. In Section 3.4, the actual truth system model (reduced order) will be presented with all the underlying assumptions and justifications.

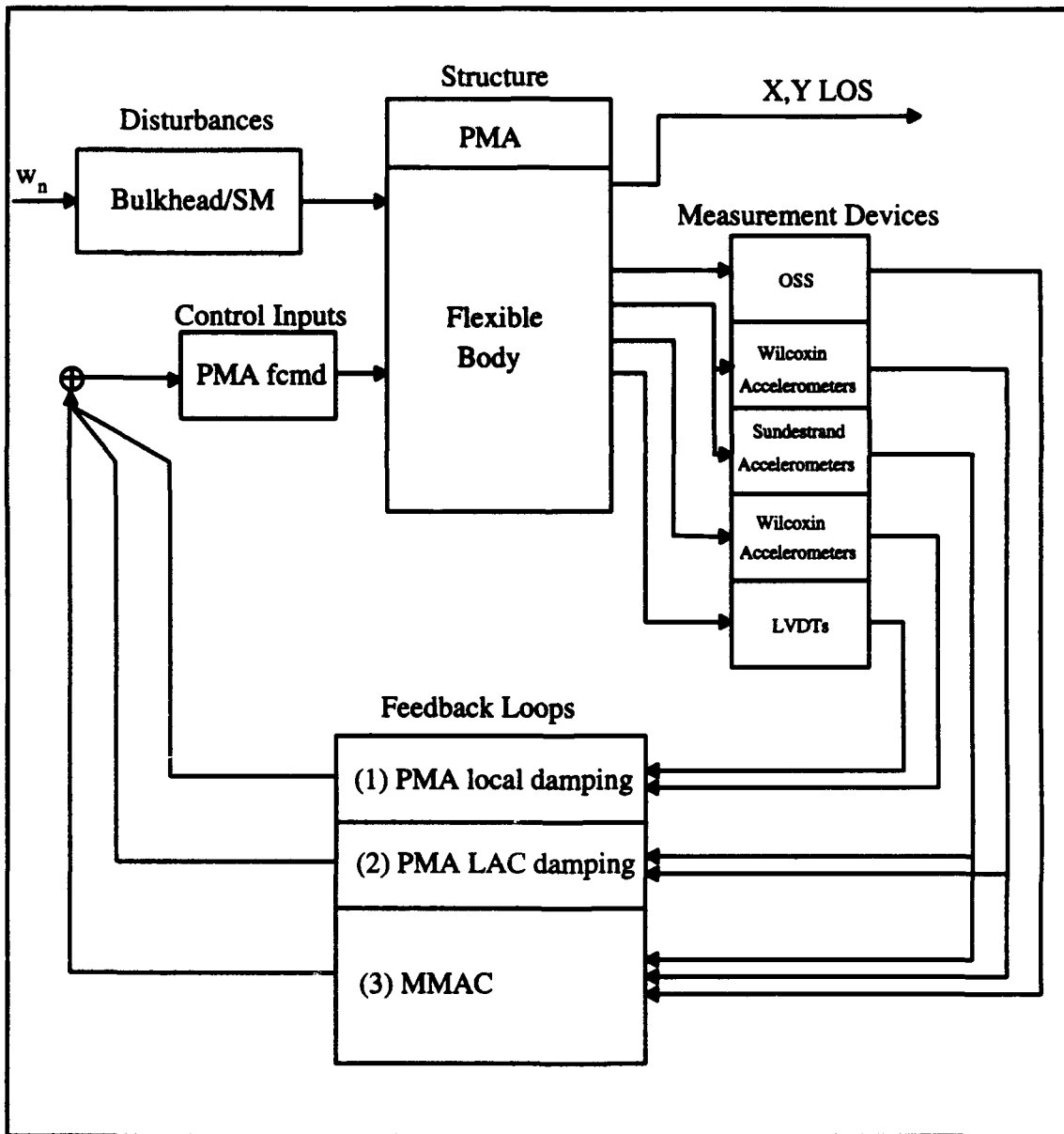


Figure 3-3. System Model High Level Block Diagram

### 3.3.1 Disturbances

The shaping filters that form the disturbance inputs are the same for both types of disturbances, with the only difference being minor gain changes. The fourth order bandpass filter model is depicted in Figure 3-4 (in this figure and subsequent figures, the numbers under the arrows specify the dimensions of the vector quantity). This filter passes six scalar white noise inputs with equivalent statistics (denoted as the vector  $\mathbf{w}_n$  in Figure 3-4) over the 5-10 Hz frequency band. The noise strengths are such that the structure achieves a 100 micro-radian open loop LOS error (this assumes clamping of the proof masses in the PMAs). As stated earlier, the two disturbances entering each tripod leg at the bulkhead are highly correlated, so the three colored noise inputs for this type of disturbance are split at the output of the appropriate gain block. Thus each split signal forms the disturbance inputs of one leg. The form of the state equation is given by:

$$\dot{\mathbf{x}}_n(t) = \mathbf{F}_n \mathbf{x}_n(t) + \mathbf{G}_n \mathbf{w}_n(t) \quad (3.1)$$

where:

- $\mathbf{x}_n(t)$  = 24-state vector representing the disturbance states
- $\mathbf{F}_n$  = 24-by-24 constant fundamental dynamics matrix
- $\mathbf{G}_n$  = 24-by-6 constant noise input matrix
- $\mathbf{w}_n(t)$  = 6-by-1 unit-strength white Gaussian noise vector

and the corresponding output equation is:

$$\mathbf{n}(t) = \mathbf{C}_n \mathbf{x}_n(t) \quad (3.2)$$

where:

- $\mathbf{n}(t)$  = 9-by-1 output colored noise vector
- $\mathbf{C}_n$  = 9-by-24 constant matrix

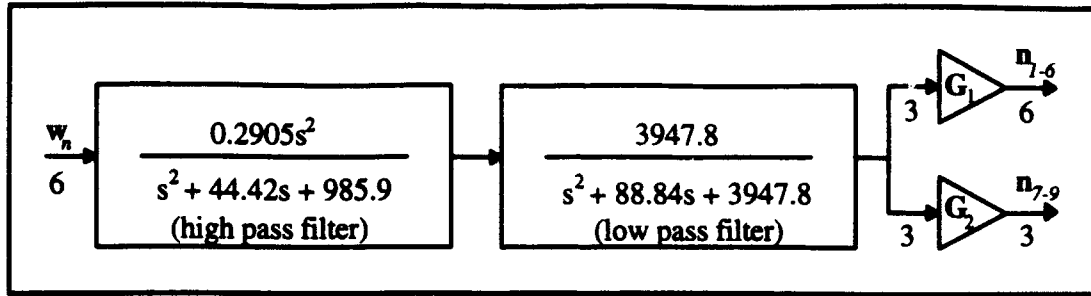


Figure 3-4. System Model Disturbance Block

The output vector is defined as:

$$\mathbf{n} = \begin{bmatrix} n_1 \\ n_2 \\ n_3 \\ n_4 \\ n_5 \\ n_6 \\ n_7 \\ n_8 \\ n_9 \end{bmatrix} = \begin{bmatrix} \text{SMA disturbance Leg 1} \\ \text{SMA disturbance Leg 1} \\ \text{SMA disturbance Leg 1} \\ \text{Bulkhead Z1 disturbance Leg 1} \\ \text{Bulkhead Z2 disturbance Leg 1} \\ \text{Bulkhead Z1 disturbance Leg 2} \\ \text{Bulkhead Z2 disturbance Leg 2} \\ \text{Bulkhead Z1 disturbance Leg 3} \\ \text{Bulkhead Z2 disturbance Leg 3} \end{bmatrix} \quad (3.3)$$

where the Z1 and Z2 indicate the two disturbances are predominantly in the Z direction. (The two magnetic actuators per leg are mounted ~12 degrees off the Z axis). As a result, this filter contributes 24 states to the overall system model.

### 3.3.2 Structure

The structure model of Figure 3-3 refers to the dynamic response of the passive flexible bending modes of the system and of the active control imparted by the PMAs. The flexible body portion of the structure model was developed from finite element analysis and modal test data [1,3]. The full-order flexible body portion is composed of over 180 modes ( $n \sim 180$ ), with natural frequencies that range from 7 to 150 Hz. This adds over 360 states to the overall system model. In previous versions, the PMAs were modeled separately from the structure block since the PMAs had not been physically

added to the structure [11]. Now that the PMAs are physically attached, their system models are incorporated into the structure block in an augmented fashion. (The modal frequencies of the structure portion were adjusted accordingly via subsequent modal tests.) Since the PMAs are essentially spring-mass systems, they are appropriately modeled as second-order systems, each with a damping ratio of  $\sim 0.01$  and natural frequency of  $\sim 5$  Hz. This adds 36 states to the overall system model.

Having been delivered in the desirable modal coordinate form, no transformation from a physical representation was necessary (as discussed in Section 2.7.2). The form of the state equation for the structure is as follows:

$$\dot{\mathbf{x}}_s(t) = \mathbf{F}_s \mathbf{x}_s(t) + \mathbf{B}_s \mathbf{u}_{fcmd}(t) + \mathbf{G}_s \mathbf{n}(t) \quad (3.4)$$

where:

- $\mathbf{x}_s(t) = (36 + 2n)$ -state vector representing the flexible body and PMA modes
- $\mathbf{F}_s = (36 + 2n)$ -by- $(36 + 2n)$  constant structure plant matrix
- $\mathbf{B}_s = (36 + 2n)$ -by-36 constant control input matrix
- $\mathbf{G}_s = (36 + 2n)$ -by-9 constant noise input matrix
- $\mathbf{n}(t) =$  defined in Equations (3.2) and (3.3)
- $\mathbf{u}_{fcmd} = 36$ -by-1 PMA force cmds vector
- $n =$  number of modes representing the structure

The actual structure of the dynamics matrix  $\mathbf{F}_s$  is of the block diagonal form illustrated in Equation (2.79), where the corresponding state vector has the velocity states ordered first and the position states second as shown on the following page:

$$\mathbf{x}_s(t) = \begin{bmatrix} \mathbf{x}_1 \\ \vdots \\ \mathbf{x}_{18} \\ \mathbf{x}_{18+1} \\ \vdots \\ \mathbf{x}_{18+n} \\ \mathbf{x}_{18+n+1} \\ \vdots \\ \mathbf{x}_{18+n+18} \\ \mathbf{x}_{36+n+1} \\ \vdots \\ \mathbf{x}_{36+2n} \end{bmatrix} = \begin{bmatrix} \text{PMA 1 velocity} \\ \vdots \\ \text{PMA 18 velocity} \\ \text{First bending mode velocity} \\ \vdots \\ \text{nth bending mode velocity} \\ \text{PMA 1 position} \\ \vdots \\ \text{PMA 18 position} \\ \text{First bending mode position} \\ \vdots \\ \text{nth bending mode position} \end{bmatrix} \quad (3.5)$$

The associated output equation is as follows:

$$\mathbf{y}_{struct}(t) = \mathbf{C}_s \mathbf{x}_s(t) + \mathbf{D}_{su} \mathbf{u}_{fcmd}(t) + \mathbf{D}_{sn} \mathbf{n}(t) \quad (3.6)$$

where:

- $\mathbf{y}_{struct}(t)$  = 98-by-1 structure output response vector
- $\mathbf{C}_s$  = 98-by-(36+2n) constant matrix
- $\mathbf{D}_{su}$  = 98-by-36 deterministic control input direct feedthrough matrix
- $\mathbf{D}_{sn}$  = 98-by-9 noise direct feedthrough matrix

The output vector is defined as:

$$\mathbf{y} = \begin{bmatrix} y_1 \\ y_2 \\ y_3 \\ \vdots \\ y_{44} \\ y_{45} \\ \vdots \\ y_{62} \\ y_{63} \\ \vdots \\ y_{80} \\ y_{81} \\ \vdots \\ y_{98} \end{bmatrix} = \begin{bmatrix} \text{X Line of Sight} \\ \text{Y Line of Sight} \\ \text{LOS sensor 1 (OSS1)} \\ \vdots \\ \text{LOS sensor 42 (OSS42)} \\ \text{Structure acceleration 1} \\ \vdots \\ \text{Structure acceleration 18} \\ \text{PMA acceleration 1} \\ \vdots \\ \text{PMA acceleration 18} \\ \text{Differential position 1 (PM1 wrt structure)} \\ \vdots \\ \text{Differential position 18 (PM18 wrt structure)} \end{bmatrix} \quad (3.7)$$

The X and Y LOS outputs result from a transformation of the outputs of the LOS optical elements (which reflect the alignment of a particular laser/sensor pair). These LOS sensor outputs (referred to as optical scoring sensor or OSS outputs) are position measurements of the displacement of the primary mirror assembly with respect to the secondary mirror assembly. The structural acceleration outputs relate the acceleration of the structure at the point of attachment of the respective PMAs, along the PMA sensitive axis direction. The PMA acceleration outputs relate the acceleration of the actual proof mass within each PMA, again along the PMA sensitive axis direction. The differential position outputs relate the position of the proof mass relative to the structure at the point of attachment.

### 3.3.3 *Measurement Devices*

The first of the different measurement devices to be discussed is the high frequency Wilcoxin accelerometer. Since this particular type of accelerometer is more effective at higher frequencies, it is appropriately modeled by a second-order high-pass filter as illustrated in Figure 3-5. This effectively eliminates the lower frequencies attributed to rigid body effects (less than 2 Hz). The colored sensor noise is modeled with a high-pass third-order shaping filter. The state space representation is given by:

$$\dot{\mathbf{x}}_{Wacc}(t) = \begin{bmatrix} \dot{\mathbf{x}}_{wa}(t) \\ \dot{\mathbf{x}}_{nwa}(t) \end{bmatrix} = \begin{bmatrix} \mathbf{F}_{wa} & \mathbf{0} \\ \mathbf{0} & \mathbf{F}_{nwa} \end{bmatrix} \begin{bmatrix} \mathbf{x}_{wa}(t) \\ \mathbf{x}_{nwa}(t) \end{bmatrix} + \begin{bmatrix} \mathbf{B}_{wa} \\ \mathbf{0} \end{bmatrix} \mathbf{y}_{acc}(t) + \begin{bmatrix} \mathbf{0} \\ \mathbf{G}_{nwa} \end{bmatrix} \mathbf{w}_{Wacc}(t) \quad (3.8)$$

where:

- $\mathbf{x}_{wa}(t)$  = 36-state vector representing the accelerometer response
- $\mathbf{x}_{nwa}(t)$  = 54-state vector representing the time-correlated accelerometer noise
- $\mathbf{F}_{wa}$  = 36-by-36 constant accelerometer plant matrix
- $\mathbf{F}_{nwa}$  = 54-by-54 constant accelerometer noise shaping filter system matrix
- $\mathbf{B}_{wa}$  = 36-by-18 constant matrix

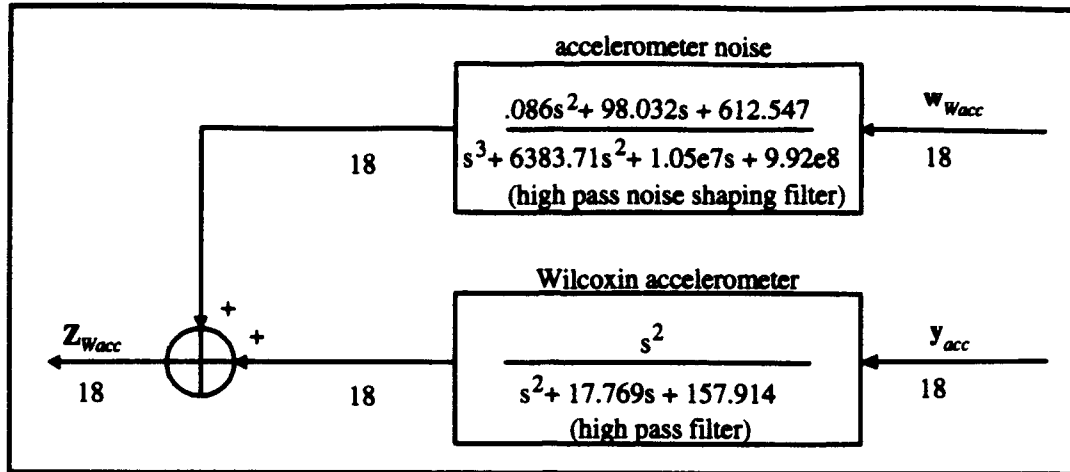


Figure 3-5. Wilcoxin Accelerometer Model

- $G_{nwa} = 54\text{-by-}18$  constant matrix
- $y_{acc}$  = defined by Equation (3.7), (see statement below)
- $w_{wacc} = 18\text{-by-}1$  unit-strength white Gaussian noise vector

The corresponding measurement equation is given as:

$$z_{wacc}(t_i) = \begin{bmatrix} H_{wa} & H_{nwa} \end{bmatrix} \begin{bmatrix} x_{wa}(t_i) \\ x_{nwa}(t_i) \end{bmatrix} + [D_{ywa}] y_{acc}(t_i) \quad (3.9)$$

where:

- $H_{wa} = 18\text{-by-}36$  constant accelerometer measurement matrix
- $H_{nwa} = 18\text{-by-}54$  constant accelerometer noise measurement matrix
- $D_{ywa} = 18\text{-by-}18$  constant feedthrough matrix
- $y_{acc}$  = defined by Equation (3.7), (see following statement)

Since there are actually two sets of Wilcoxin accelerometers (located on the PMA and structure respectively), each represented by Equations (3.8) and (3.9), the separate accelerometer input terms for the 18-dimensional  $y_{acc}$  vector are gained by extracting the appropriate set of components from Equation (3.7) (terms  $y_{63}$  through  $y_{80}$  for the PMA accelerometers and terms  $y_{45}$  through  $y_{62}$  for the structure accelerometers, respectively).

The second sensor type, Sundstrand accelerometer, is more effective at lower frequencies, so it is appropriately modeled by a second-order low-pass filter as illustrated in Figure 3-6. The colored sensor noise is modeled with a second-order low-pass shaping filter. The state space representation is given by:

$$\dot{\mathbf{x}}_{Sacc}(t) = \begin{bmatrix} \dot{\mathbf{x}}_{sa}(t) \\ \dot{\mathbf{x}}_{nsa}(t) \end{bmatrix} = \begin{bmatrix} \mathbf{F}_{sa} & \mathbf{0} \\ \mathbf{0} & \mathbf{F}_{nsa} \end{bmatrix} \begin{bmatrix} \mathbf{x}_{sa}(t) \\ \mathbf{x}_{nsa}(t) \end{bmatrix} + \begin{bmatrix} \mathbf{B}_{sa} \\ \mathbf{0} \end{bmatrix} \mathbf{y}_{acc}(t) + \begin{bmatrix} \mathbf{0} \\ \mathbf{G}_{nsa} \end{bmatrix} \mathbf{w}_{Sacc}(t) \quad (3.10)$$

where:

- $\mathbf{x}_{sa}(t)$  = 36-state vector representing the accelerometer response
- $\mathbf{x}_{nsa}(t)$  = 36-state vector representing the time-correlated accelerometer noise
- $\mathbf{F}_{sa}$  = 36-by-36 constant accelerometer plant matrix
- $\mathbf{F}_{nsa}$  = 36-by-36 constant accelerometer noise shaping filter system matrix
- $\mathbf{B}_{sa}$  = 36-by-18 constant matrix
- $\mathbf{G}_{nsa}$  = 36-by-18 constant matrix
- $\mathbf{y}_{acc}$  = defined by Equation (3.7)
- $\mathbf{w}_{Sacc}$  = 18-by-1 unit-strength white Gaussian noise vector

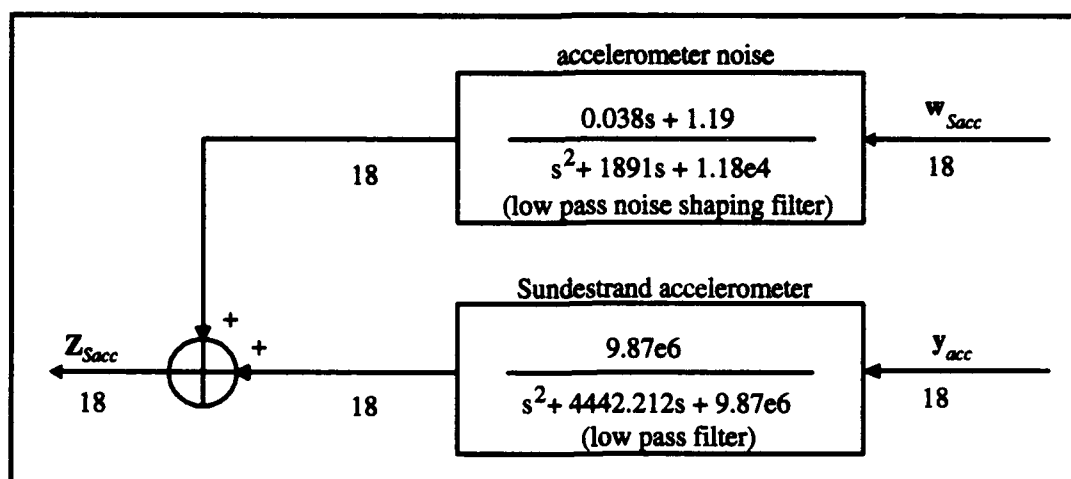


Figure 3-6. Sundstrand Accelerometer Model



The corresponding measurement equation is given as:

$$\mathbf{z}_{Sacc}(t_i) = \begin{bmatrix} \mathbf{H}_{sa} & \mathbf{H}_{nsa} \end{bmatrix} \begin{bmatrix} \mathbf{x}_{sa}(t_i) \\ \mathbf{x}_{nsa}(t_i) \end{bmatrix} \quad (3.11)$$

where:

- $\mathbf{H}_{sa}$  = 18-by-36 constant accelerometer measurement matrix
- $\mathbf{H}_{nsa}$  = 18-by-36 constant accelerometer noise measurement matrix

The accelerometer input vector terms for  $\mathbf{y}_{acc}$  are gained by extracting the appropriate components from Equation (3.7) (terms  $\mathbf{y}_{45}$  through  $\mathbf{y}_{62}$ ).

The third sensor type, LVDT, is modeled by a second-order low-pass filter as illustrated in Figure 3-7. The colored sensor noise is modeled with a second-order low-pass shaping filter. The state space representation is given by:

$$\dot{\mathbf{x}}_{LVDT}(t) = \begin{bmatrix} \mathbf{F}_{LVDT} & \mathbf{0} \\ \mathbf{0} & \mathbf{F}_{nLVDT} \end{bmatrix} \begin{bmatrix} \mathbf{x}_{LVDT}(t) \\ \mathbf{x}_{nLVDT}(t) \end{bmatrix} + \begin{bmatrix} \mathbf{B}_{LVDT} \\ \mathbf{0} \end{bmatrix} \mathbf{y}_{diff}(t) + \begin{bmatrix} \mathbf{0} \\ \mathbf{G}_{nLVDT} \end{bmatrix} \mathbf{w}_{LVDT}(t) \quad (3.12)$$

where:

- $\mathbf{x}_{LVDT}(t)$  = 36-state vector representing the LVDT response
- $\mathbf{x}_{nLVDT}(t)$  = 36-state vector representing the time-correlated LVDT noise
- $\mathbf{F}_{LVDT}$  = 36-by-36 constant LVDT plant matrix
- $\mathbf{F}_{nLVDT}$  = 36-by-36 constant LVDT noise shaping filter system matrix
- $\mathbf{B}_{LVDT}$  = 36-by-18 constant matrix
- $\mathbf{G}_{nLVDT}$  = 36-by-18 constant matrix
- $\mathbf{y}_{diff}$  = defined by Equation (3.7)
- $\mathbf{w}_{LVDT}$  = 18-by-1 unit-strength white Gaussian noise vector

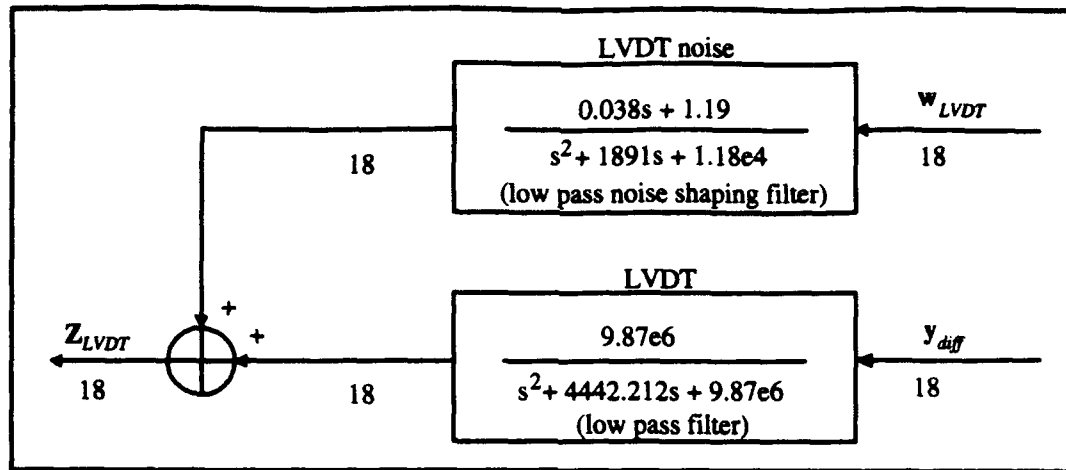


Figure 3-7. LVDT Model

The corresponding measurement equation is given as:

$$\mathbf{z}_{LVDT}(t_i) = [\mathbf{H}_{LVDT} \quad \mathbf{H}_{nLVDT}] \begin{bmatrix} \mathbf{x}_{LVDT}(t_i) \\ \mathbf{x}_{nLVDT}(t_i) \end{bmatrix} \quad (3.13)$$

where:

- $\mathbf{H}_{LVDT}$  = 18-by-36 constant LVDT measurement matrix
- $\mathbf{H}_{nLVDT}$  = 18-by-36 constant LVDT noise measurement matrix

The LVDT input vector terms for  $\mathbf{y}_{diff}$  are gained by extracting the appropriate components from Equation (3.7) (terms  $\mathbf{y}_{81}$  through  $\mathbf{y}_{98}$ ).

The final sensor type, OSS, only requires state space modeling for the colored sensor noise which is modeled with a fourth-order band-pass shaping filter. The state space representation for the model depicted in Figure 3-8 is given by:

$$\dot{\mathbf{x}}_{nOSS}(t) = [\mathbf{F}_{nOSS}] \mathbf{x}_{nOSS}(t) + [\mathbf{G}_{nOSS}] \mathbf{w}_{OSS}(t) \quad (3.14)$$

where:

- $\mathbf{x}_{nOSS}(t)$  = 72-state vector representing the time correlated OSS noise
- $\mathbf{F}_{nOSS}$  = 72-by-72 constant OSS noise plant matrix
- $\mathbf{G}_{nOSS}$  = 72-by-18 constant matrix
- $\mathbf{w}_{OSS}$  = 18-by-1 unit-strength white Gaussian noise vector

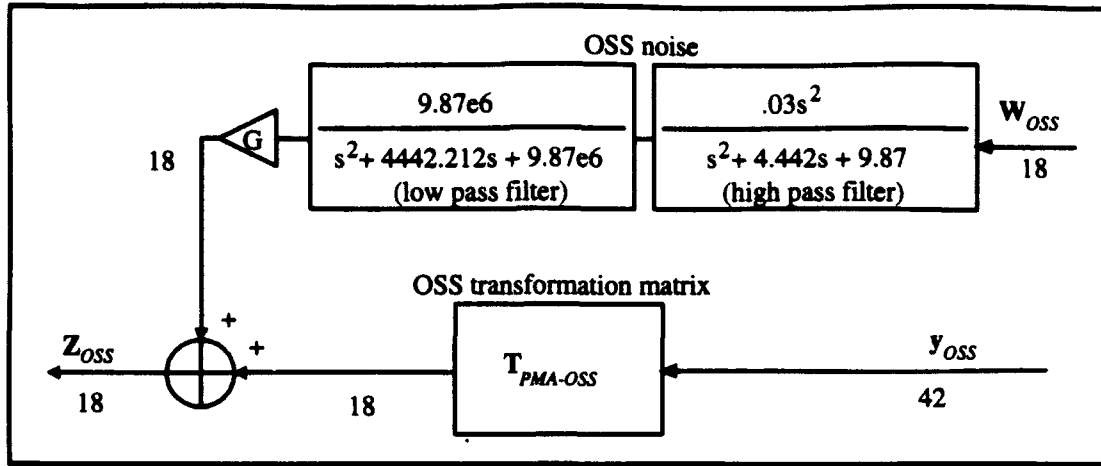


Figure 3-8. OSS Model

The 42 sensor outputs must be coordinatized to correspond to the 18 PMA nodes via a coordinate frame transformation [3]. Thus the form of the measurement equation is as follows:

$$\mathbf{z}_{OSS}(t_i) = [\mathbf{H}_{OSS}] \mathbf{x}_{nOSS} + [\mathbf{T}_{LOS-PMA}] \mathbf{y}_{OSS} \quad (3.15)$$

where:

- $\mathbf{H}_{OSS}$  = 18-by-72 constant matrix
- $\mathbf{T}_{OSS-PMA}$  = 18-by-42 constant OSS Transformation matrix

The OSS input vector terms for  $\mathbf{y}_{OSS}$  are gained by extracting the appropriate components from Equation (3.7) (terms  $\mathbf{y}_3$  through  $\mathbf{y}_{44}$ ).

### 3.3.4 Feedback Loops and Control Inputs

The feedback loop structure is composed of a 3-tiered approach and was illustrated in Figure 3-3. This is the design approach adopted by Lockheed LMSC (the primary controls contractor on the SPICE project) with the exception of a single robust Kalman filter estimator/controller in place of the MMAC block [1,3]. The first and second tiers are maintained in this research based on the advice from Lockheed [1]. The first tier, PMA local damping force, provides for localized damping feedback for the PMAs. The second tier, PMA Low Authority Control (LAC) damping force, provides simple rate

feedback for the entire structure. The final tier is the MMAC design which provides feedback for attaining the desired performance specifications. A more complete illustration with all the appropriate models is provided in Figure 3-9.

In attaining the PMA local damping force (which is essentially a rate differential), the output (differential position) from the LVDT model is low-pass filtered and differentiated. In addition, the output from the Wilcoxin (PMA) accelerometer model is subtracted from that of the Wilcoxin (structure) accelerometer model to form a differential acceleration, which is then high-pass filtered and integrated. The high and low pass filters form a crossover network such that, when summed, there is no interference in the overlapping frequency ranges of the two sensor types. The 18 outputs are gain adjusted and fed to the PMA force commands summing junction.

The second tier, PMA LAC damping force, is formed by feeding the output of the Wilcoxin (structure) accelerometer model and Sundstrand (structure) accelerometer model through a crossover network composed of a high and low pass filters respectively. Again, this eliminates interference in the overlapping frequency ranges from the respective accelerometers. The resulting output is integrated, gain adjusted, and fed to the PMA force commands' summing junction.

The final tier is the MMAC design implemented in this research. This design approach is based on the assumption that there exist uncertain parameters in the structure dynamics such that instabilities arise beyond the robustness range of a single Kalman filter state estimator with LQG control. Thus, an adaptive approach is required as discussed in Chapter 1. Of special note is that only the outputs of the structure accelerometers and OSS are utilized by the MMAC loop. (This is based on the actual system design.)

The control inputs block is composed of two sequential second order filters with additive colored noise that model the dynamics and noise characteristics of the electronics

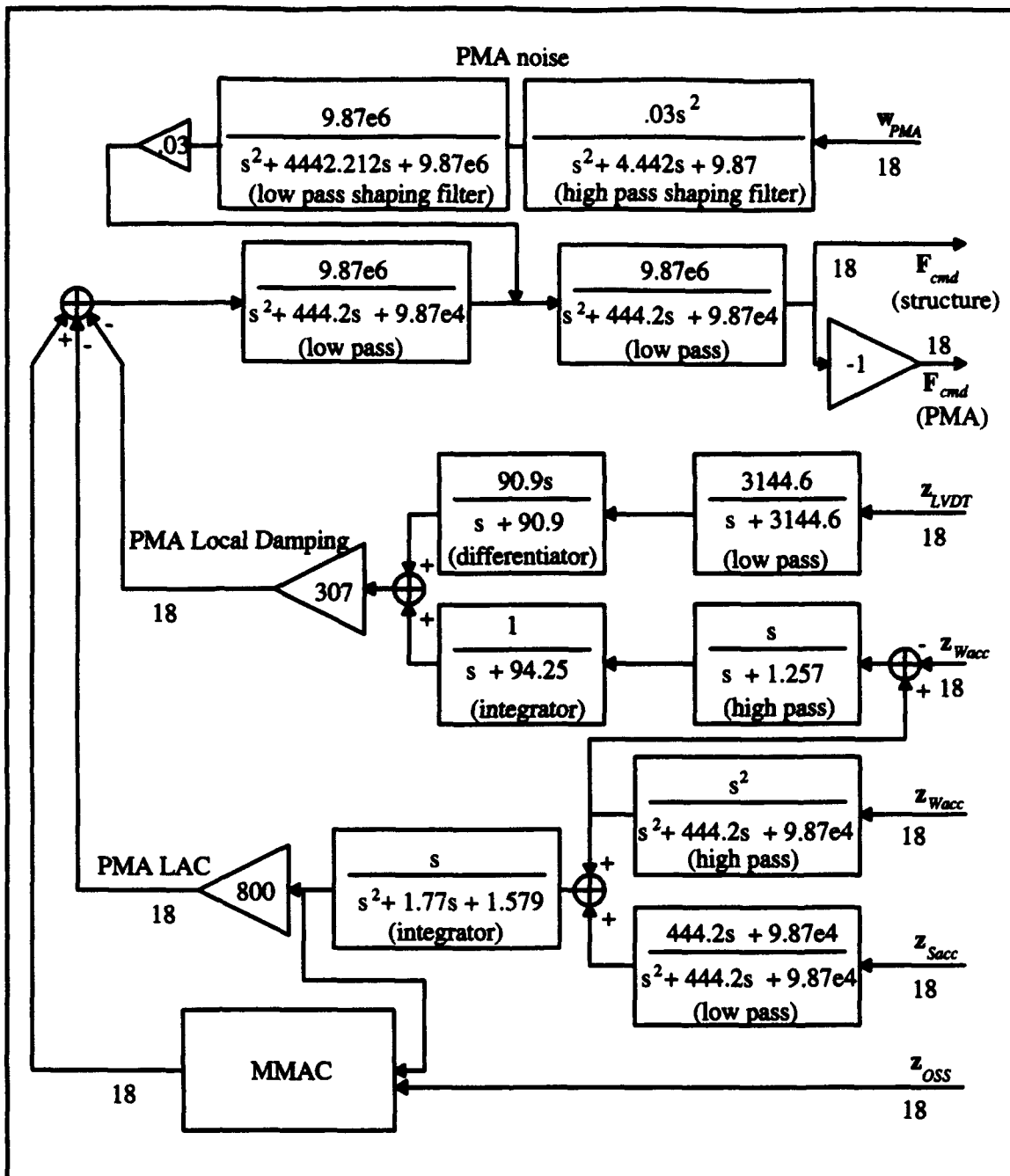


Figure 3-9. Feedback Loops and Control Inputs Model

that generate the PMA force command inputs. Since the PMAs were integrated into the structure, the negative gain block indicates that the 18 PMA force commands act oppositely on the flexible body than the PMAs. Thus, there are 18 PMA inputs and 18 structure inputs, for a total of 36.

### **3.4 Truth Model Selection**

It is easy to see that the number of states ( $690+2n$ ) involved with the system model as presented in Section 3.3 constitutes an extreme computational burden in terms of total simulation time and for use in controller development. Thus, reducing the total number of states becomes a necessity. Yet, the dominant structure modes and system components that will still qualify the truth model as a "true" representation of the physical structure must be maintained. With the previous statements in mind, several assumptions and justifications are made based on the advice of Lockheed controls engineers [1]. First, the structure's flexible bending modes will be truncated at natural frequencies greater than 100 Hz. Second, the measurement devices utilized by the MMAC will be modeled as providing perfect measurements with additive white sensor noise. Third, any low-pass filter with a break frequency beyond the range of frequencies from the structure portion of the system model will be eliminated. Finally, noise inputs on the first two feedback loops and on the PMA control inputs will be eliminated. Each of these statements will be addressed individually in the following section.

#### **3.4.1 Truth Model Simplifications**

Currently, the flexible body portion of the structure block contains 194 modes ranging up to 150 Hz. Truncating this portion of the system model to 100 Hz will eliminate 86 flexible body modes, resulting in 216 states. The underlying assumption is that any modes at higher frequencies will be passively quelled instantaneously and essentially have no effect on the overall system. This is consistent with assumptions made in Gustafson's research and at Lockheed [1,11]. The resulting frequency range (5 - 100 Hz) forms the total frequency range of interest to be considered in this research.

A large proportionate number of overall system states are contributed by the sensor, noise, and feedback loop models. Elimination of these models based on the assumption of measurements with additive *white* noise would decrease the state order

magnitude drastically. This may seem inappropriate at first but will be proven to make sense, given the nature of the mathematical representation of the physical structure used in this research.

First to be addressed is the MMAC feedback loop which utilizes three sensors: the Sundstrand accelerometer, the Wilcoxin accelerometer, and the OSS. In Figure 3-10, Bode plots are shown depicting the frequency response from each of these sensor models. The Sundstrand model is essentially a low-pass filter with a break frequency well above the frequency range of interest ( $>>100$  Hz). The Wilcoxin accelerometer model is essentially a high pass filter with a break frequency below the frequency range of interest ( $<5$  Hz). Viewed together, the combination of their outputs can be treated as a unity gain bandpass encompassing the entire frequency range of interest, where the attenuation outside of this range is ignored. Thus, they can be thought of as providing "perfect" measurements in the sense that there is no attenuation in the frequency range of interest. This same situation loosely applies for the colored noise added to each of these respective sensors. As seen in Figure 3-11, the Sundstrand noise is shaped by a low-pass filter and the Wilcoxin noise is shaped by a high-pass filter. Thus their replacement by white noise is justified for the same reasons as above, where the strength of the white noise is based on an averaged gain. The need for further filtering in this loop is now somewhat superfluous and thus they are eliminated. The OSS requires no states and is not a concern. The colored OSS sensor noise is formed by a band-pass filter where the high and low break frequencies are outside the frequency range of interest (reference Figure 3-12, page 3-22) and thus can be treated as white.

The next issue is to address the integrator and differentiator models. In the physical system, acceleration and position measurements are taken, which must be integrated and differentiated respectively to gain the required rate feedback. However, in the mathematical representation, direct "velocity measurements" are possible for each of

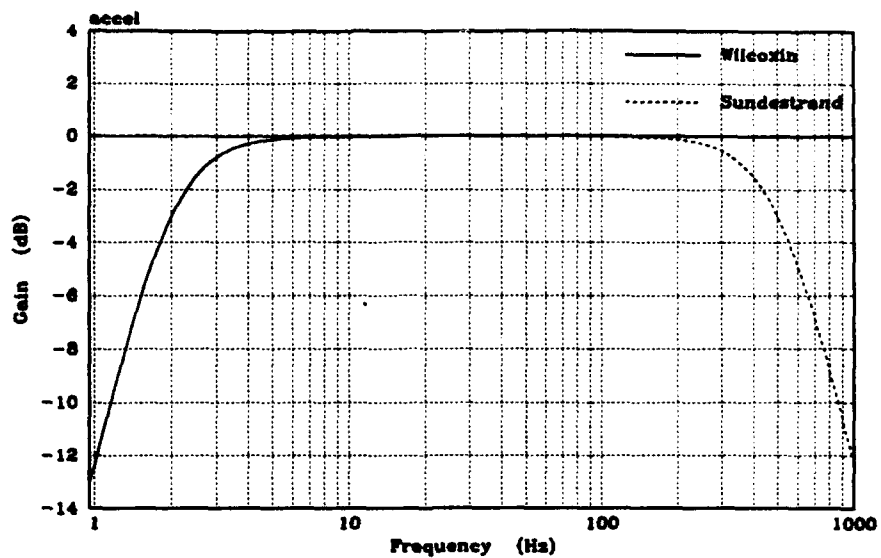


Figure 3-10. Sundestrand and Wilcoxin Accelerometer Bode Plot

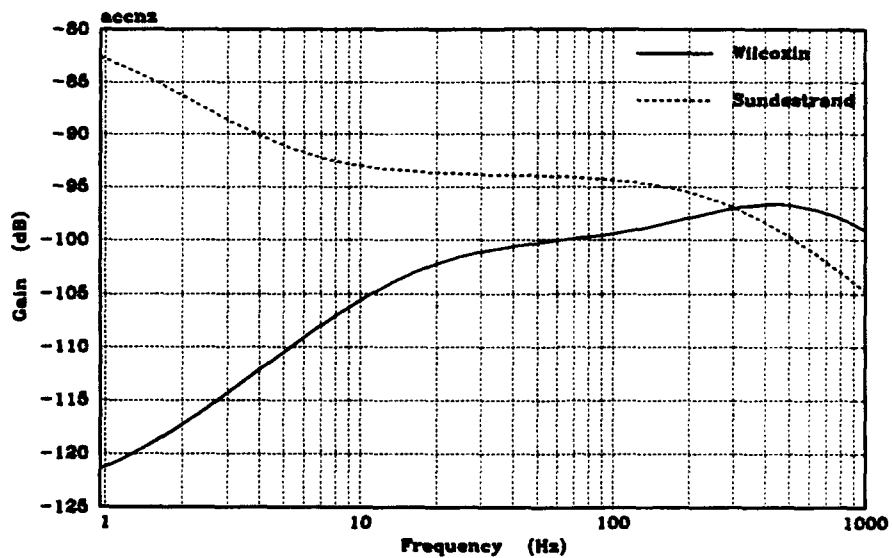


Figure 3-11. Sundestrand and Wilcoxin Noise Bode Plot



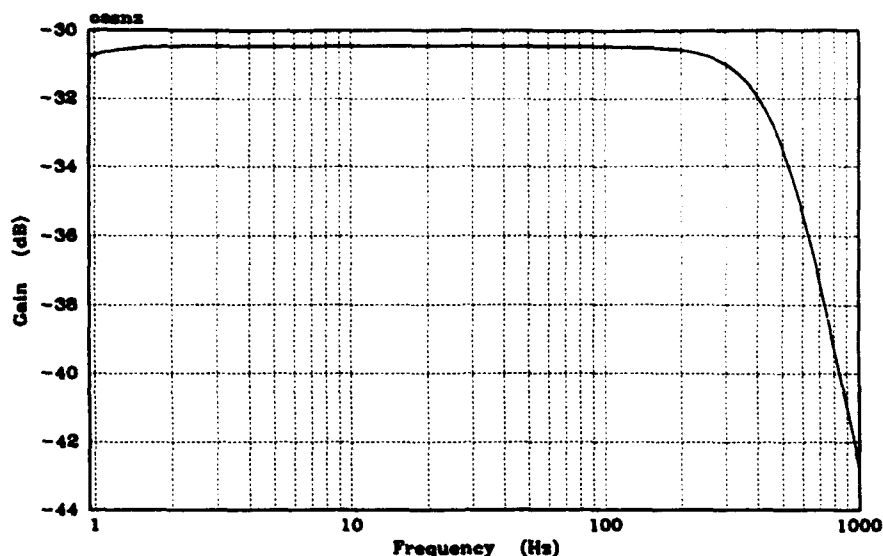


Figure 3-12. OSS Noise Bode Plot

the sensor outputs, thereby eliminating the need for integrators or differentiators in the system model.

The two sequential low-pass filters on the input of the PMA force commands both have break frequencies well beyond the frequency range of interest. Thus, they are unneeded and are removed from the system model.

Finally, the noise inputs on the first two feedback loops and the PMA force commands (not including the disturbance noise inputs and the sensor noise on the inputs to the MMAC) are assumed to have negligible impact on the system performance. The disturbance noise essentially "drowns" out any of these additional noises, so these are eliminated for simplicity.

### 3.4.2 Truth Model

The final version of the truth model with 294 total states is shown in Figure 3-13. The disturbance portion has not been altered, so its state space representation remains as given by Equations (3.1) through (3.3). The structure state equation is still represented by Equations (3.4) and (3.5) with the exception that the number of flexible bending modes is

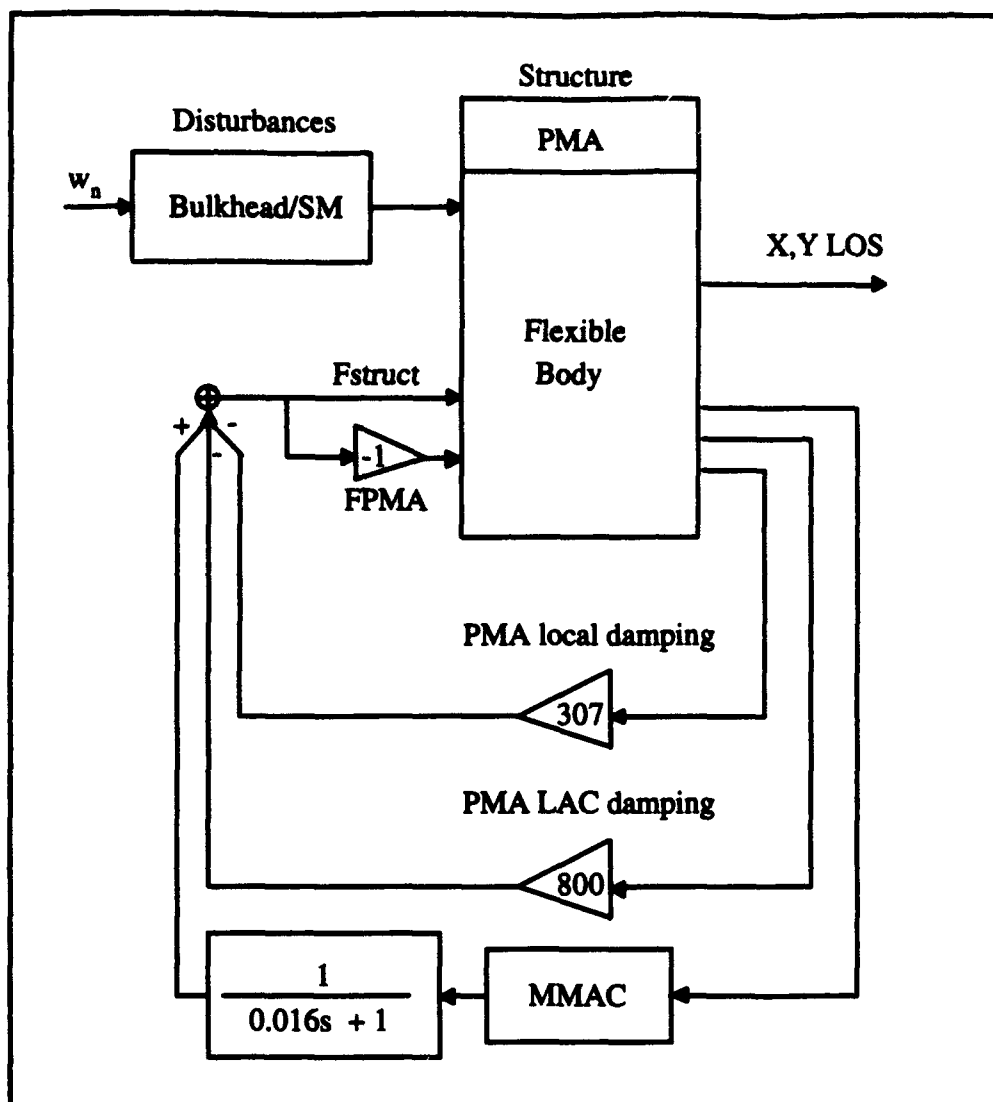


Figure 3-13. Truth Model Block Diagram

now 108 ( $n=108$ ) due to the elimination of the unwanted higher frequency bending modes.

The new associated output equation is given by:

$$\mathbf{y}_{struct}(t) = \mathbf{C}_s \mathbf{x}_s(t) \quad (3.16)$$

where:

- $\mathbf{y}_{struct}(t)$  = 56-by-1 structure output response vector
- $\mathbf{C}_s$  = 56-by-(36+2n) constant matrix

The  $D_{su}$  and  $D_{sn}$  terms from Equation (3.6) have been eliminated since the "velocity measurements" do not involve feedthrough terms. The output vector is now defined as:

$$\mathbf{y} = \begin{bmatrix} y_1 \\ y_2 \\ y_3 \\ \vdots \\ y_{20} \\ y_{21} \\ \vdots \\ y_{38} \\ y_{39} \\ \vdots \\ y_{56} \end{bmatrix} = \begin{bmatrix} \text{X Line of Sight} \\ \text{Y Line of Sight} \\ \text{Transformed OSS 1} \\ \vdots \\ \text{Transformed OSS 18} \\ \text{Structure velocity 1} \\ \vdots \\ \text{Structure velocity 18} \\ \text{PMA velocity 1} \\ \vdots \\ \text{PMA velocity 18} \end{bmatrix} \quad (3.17)$$

where outputs  $y_{63-80}$  from Equation (3.7) have been eliminated. The new differential velocity measurement for the PMA local damping loop is obtained by subtracting outputs  $y_{39-56}$  from outputs  $y_{20-38}$  respectively. Also, the transformation matrix for the OSS LOS sensors was incorporated into the output portion of the structure block, thus reducing the 42 individual sensor outputs to the 18 outputs to the MMAC block.

The addition of the first-order low-pass filter on the control inputs from the MMAC block is based on the advice of Lockheed [1]. This filter provides for a 10 Hz rolloff on the MMAC loop which is needed for stability [1]. The state equation is given by:

$$\dot{\mathbf{x}}_f(t) = \mathbf{F}_f \mathbf{x}_f(t) + \mathbf{B}_f \mathbf{u}_{MMAC}(t) \quad (3.18)$$

where:

- $\mathbf{x}_f(t)$  = 18-state vector representing the filter states
- $\mathbf{F}_f$  = 18-by-18 constant filter plant matrix
- $\mathbf{B}_f$  = 18-by-18 constant matrix
- $\mathbf{u}_{MMAC}(t)$  = 18-by-1 MMAC control vector

There is no dynamics driving noise as this filter is implemented digitally for the physical structure and the states are known exactly. The corresponding output equation is:

$$\mathbf{f}_{MMAC}(t) = \mathbf{C}_f \mathbf{x}_f(t) \quad (3.19)$$

where:

- $\mathbf{f}_{MMAC}(t)$  = 18-by-1 output control vector
- $\mathbf{C}_f$  = 18-by-18 constant matrix

The output vector is defined as:

$$\mathbf{f}_{MMAC} = \begin{bmatrix} f_1 \\ \vdots \\ f_{18} \end{bmatrix} = \begin{bmatrix} \text{Filtered MMAC control to PMA1} \\ \vdots \\ \text{Filtered MMAC control to PMA18} \end{bmatrix} \quad (3.20)$$

where  $\mathbf{f}_{MMAC}$  is then combined with the other feedback loop inputs to form the total input  $\mathbf{f}_{cmd}$  to the structure block.

The final open loop system model can be developed by augmenting all the individual components together. The augmented state equation is given by:

$$\dot{\mathbf{x}}_{as}(t) = \mathbf{F}_{as} \mathbf{x}_{as}(t) + \mathbf{B}_{as} \mathbf{u}_{fcmd}(t) + \mathbf{G}_{as} \mathbf{w}(t) \quad (3.21)$$

where the augmented system matrices are given by:

$$\mathbf{F}_{as} = \begin{bmatrix} \mathbf{F}_{n(24 \times 24)} & \mathbf{0}_{(24 \times 18)} & \mathbf{0}_{(24 \times 36+2n)} \\ \mathbf{0}_{(18 \times 24)} & \mathbf{F}_{f(18 \times 18)} & \mathbf{0}_{(18 \times 36+2n)} \\ \mathbf{G}_s \mathbf{C}_{n(36+2n \times 24)} & \mathbf{B}_s \mathbf{C}_{f(36+2n \times 18)} & \mathbf{F}_{s(36+2n \times 36+2n)} \end{bmatrix}_{78+2n \times 78+2n} \quad (3.22)$$

$$\mathbf{B}_{as} = \begin{bmatrix} \mathbf{0}_{(24 \times 18)} \\ \mathbf{B}_{f(18 \times 18)} \\ \mathbf{0}_{(36+2n \times 18)} \end{bmatrix}_{78+2n \times 18} \quad (3.23)$$

$$\mathbf{G}_{as} = \begin{bmatrix} \mathbf{G}_{n(24 \times 6)} \\ \mathbf{0}_{(18 \times 6)} \\ \mathbf{0}_{(36+2n \times 6)} \end{bmatrix}_{78+2n \times 6} \quad (3.24)$$

and  $\mathbf{w}(t)$  is still a white Gaussian noise vector with  $\mathbf{Q}_t =$  the identity matrix. The augmented state vector is given by:

$$\mathbf{x}_{as}(t) = \begin{bmatrix} \mathbf{x}_1 \\ \vdots \\ \mathbf{x}_{24} \\ \mathbf{x}_{25} \\ \vdots \\ \mathbf{x}_{42} \\ \mathbf{x}_{43} \\ \vdots \\ \mathbf{x}_{60} \\ \mathbf{x}_{61} \\ \vdots \\ \mathbf{x}_{168} \\ \mathbf{x}_{169} \\ \vdots \\ \mathbf{x}_{186} \\ \mathbf{x}_{187} \\ \vdots \\ \mathbf{x}_{294} \end{bmatrix} = \begin{bmatrix} \text{1st disturbance state} \\ \vdots \\ \text{24th disturbance state} \\ \text{1st MMAC filter state} \\ \vdots \\ \text{18th MMAC filter state} \\ \text{PMA 1 velocity} \\ \vdots \\ \text{PMA 18 velocity} \\ \text{1st bending mode velocity} \\ \vdots \\ \text{nth bending mode velocity} \\ \text{PMA 1 position} \\ \vdots \\ \text{PMA 18 position} \\ \text{1st bending mode position} \\ \vdots \\ \text{nth bending mode position} \end{bmatrix} \quad (3.25)$$

The associated augmented output equation is given by:

$$\mathbf{y}_{as}(t) = \mathbf{C}_{as} \mathbf{x}_{as}(t) \quad (3.26)$$

where the augmented output matrix is given by:

$$\mathbf{C}_{as} = \begin{bmatrix} \mathbf{0}_{(56 \times 24)} & \mathbf{0}_{(56 \times 18)} & \mathbf{C}_{s(56 \times 36+2n)} \end{bmatrix} \quad (3.27)$$

and the output vector is still defined by Equation (3.17).

The PMA local damping loop is formed by feeding back the measurements defined by the following:

$$\mathbf{z}_{PMAldamp}(t_i) = \begin{bmatrix} \mathbf{I}_{(18 \times 18)} & -\mathbf{I}_{(18 \times 18)} \end{bmatrix} \mathbf{y}_{as(21-38,39-56)}(t_i) \quad (3.28)$$

where the subscripted numbers for  $\mathbf{y}_{as}$  (here and in subsequent equations) refer to the appropriate partitions from Equation (3.17).

The LAC loop is formed in a similar fashion by feeding back the measurements defined by the following:

$$\mathbf{z}_{LAC}(t_i) = \begin{bmatrix} \mathbf{I}_{(18 \times 18)} \end{bmatrix} \mathbf{y}_{as(21-38)}(t_i) \quad (3.29)$$

As mentioned in Section 3.4.1, no additional noise is added to these loops. The values for the feedback gains on these two feedback loops are based on advice from Lockheed [1].

The measurements input to the MMAC design are defined by the following equation:

$$\mathbf{z}_{MMACinput}(t_i) = \begin{bmatrix} \mathbf{z}_{OSS}(t_i) \\ \mathbf{z}_{Svel}(t_i) \end{bmatrix} = \begin{bmatrix} \mathbf{I}_{(18 \times 18)} & \mathbf{0} \\ \mathbf{0} & \mathbf{I}_{(18 \times 18)} \end{bmatrix} \mathbf{y}_{as(3-38)}(t_i) + \mathbf{v}(t_i)_{(36 \times 1)} \quad (3.30)$$

Substituting the appropriate partitions of Equation (3.27) into Equation (3.30) results in the format consistent with the Kalman filter measurement presentation given in Chapter 2:

$$\mathbf{z}_{MMACinput}(t_i) = \begin{bmatrix} \mathbf{z}_{OSS}(t_i) \\ \mathbf{z}_{Svel}(t_i) \end{bmatrix} = \begin{bmatrix} \mathbf{H}_{Cas(3-20)} \\ \mathbf{H}_{Cas(21-38)} \end{bmatrix} \mathbf{x}_{as}(t_i) + \mathbf{v}(t_i)_{(36 \times 1)} \quad (3.31)$$

where:

- $\mathbf{z}_{MMACinput}$  = 36-by-1 measurement output vector
- $\mathbf{H}_{Cas(3-44)}$  = 18-by-36+2n constant measurement matrix
- $\mathbf{H}_{Cas(45-62)}$  = 18-by-36+2n constant measurement matrix
- $\mathbf{v}(t_i)$  = 36-by-1 white measurement noise vector of covariance  $\mathbf{R}_t$  (the values for  $\mathbf{R}_t$  will be discussed in Chapter 4)

Finally, all the individual matrices for the complete truth model are given in Appendix A.

### **3.5 *Reduced Order Filter Models***

Since the state order magnitude is dominated by the number of flexible body modes, this will be the primary focus of order reduction efforts. In Gustafson's research, the largest number of structure modes maintained in the reduced order models was seven for the internally balanced method and six for the modally reduced method. However, very little success was obtained at this level of reduction [11]. This may have resulted from not maintaining enough of the dominant modes [1]. For this research, a wider range of mode selections will be accomplished in the order reduction. The disturbance states are maintained since the output colored noise is shaped mainly in the frequency range of the lowest (considered dominant) flexible bending modes. Replacement of the colored noise with white noise is anticipated to cause severe performance degradation in the MMAC performance [1].

In Chapter 2, three methods were proposed to accomplish the desired order reduction on the structure portion of the truth model. The immediate goal is to reduce the total number of states, thus alleviating the computational burden. The secondary goal is to find the technique that is the most successful for this application. Numerical instabilities arose when attempting to determine the controllability and observability gramians for the Internally Balanced Technique, possibly due to the large-dimensioned matrices involved. However, very little success was obtained by using this method during previous research [11]. This technique was subsequently abandoned. The results from the Modal Reduction Technique and the Modal Cost Technique are presented in the following two sections.

#### **3.5.1 *Modal Reduction***

Table 3-1 contains information for the first 30 modes of the flexible body portion of the structure model. Several groupings were observed in the natural frequencies

(indicated by relatively large gaps in the sequence). These gaps provide the ideal locations to perform the modal reduction process. Three reduced-order models were developed where the resulting number of flexible body modes was 12, 18, and 26, respectively. Due to the extreme size of all the design models, only the system matrices for the 26-mode model are given in Appendix B.

For purposes of comparison, Bode amplitude ratio plots for the truth model and the three individual filter models are given in Appendix C. These plots indicate the open loop frequency response of the structure portion of each model for each of the 9 disturbance inputs observed at the two LOS outputs. Each plot shows a specific input/output response for each respective filter model, with the corresponding truth model plot superimposed for ease of comparison. As can be seen, there is a very good correspondence between all the filter plots and the truth plots at the lower frequencies. Predictably, the similarities lessen at the higher frequencies. There are some high frequency inconsistencies (large dips in the plots) for Figures C-1, C-2, C-3, C-10, C-11, C-12, C-13, C-20, C-21, C-28, C-29, C-30, C-31, C-39, C-43, C-44, C-48, and C-51. This may be caused by the modal reduction process, where the information maintained from the (eliminated) higher frequency modes somehow adversely impacts the frequency response at the higher frequencies.

Of special note, since the damping ratios are very small, the undamped,  $\omega_n$ , and damped natural frequency,  $\omega_d$  are very close to the same, ( $\omega_n \approx \omega_d$ ).



Mode	Eigenvalue	Damping Ratio	Natural Frequency (Hz)
1	-0.22 ± 43.29j	0.0102	6.889
2	-0.10 ± 49.00j	0.0045	7.800
3	-0.11 ± 49.40j	0.0047	7.8622
4	-0.31 ± 98.03j	0.0064	15.601
5	-0.33 ± 101.60j	0.0066	16.172
6	-0.47 ± 106.85j	0.0088	17.007
7	-0.35 ± 121.52j	0.0058	19.342
8	-0.91 ± 124.65j	0.0146	19.840
9	-0.56 ± 130.94j	0.0086	20.839
10	-0.37 ± 138.53j	0.0054	22.047
11	-1.24 ± 151.69j	0.0164	24.144
12	-0.57 ± 152.13j	0.0076	24.214
13	-1.39 ± 199.83j	0.0140	31.805
14	-1.45 ± 207.39j	0.0140	33.008
15	-1.49 ± 213.79j	0.0140	34.027
16	-1.53 ± 219.70j	0.0140	34.967
17	-1.55 ± 222.66j	0.0140	35.439
18	-1.58 ± 225.63j	0.0140	36.071
19	-1.92 ± 275.24j	0.0140	43.807
20	-1.99 ± 285.58j	0.0140	45.453
21	-2.01 ± 288.01j	0.0140	45.840
22	-2.09 ± 298.92j	0.0140	47.576
23	-2.16 ± 309.46j	0.0140	49.254
24	-2.18 ± 312.05j	0.0140	49.666
25	-2.19 ± 313.34j	0.0140	49.871
26	-2.21 ± 316.51j	0.0140	50.376
27	-2.25 ± 322.17j	0.0140	51.276
28	-2.28 ± 326.76j	0.0140	52.007
29	-2.31 ± 331.21j	0.0140	52.714
30	-2.56 ± 366.25j	0.0140	58.292

Table 3-1. Modal Eigenvalues and Natural Frequencies of the First 30 Modes

### **3.5.2 Modal Cost Reduction**

Table 3-2 contains the first largest 30 component cost values with the corresponding mode numbers. This table lends credibility to the assumption that the lowest frequency modes are dominant in the structure's dynamic response, since many of the lowest frequencies appear near the top of the table (1-13). Once again, several natural groupings were observed (separated by relatively large gaps in the sequence). Three reduced-order models were developed, where the resulting number of flexible body modes was 10, 15, and 20, respectively. Additionally, a 26-mode model was subsequently created to allow direct comparison with the 26-mode model using the modal reduction technique. Due to the extreme size of all the design models, and since the 26-mode model is of most interest because of its performance potential, only the system matrices for this model are given in Appendix D.

Bode amplitude ratio plots for the original three individual filter models are given in Appendix E (along with those of the truth model). Similar to the modal case, there is a very good correspondence between the reduced-order system model plots and the truth model plots at the lower frequencies (but not as good as in the modal reduction technique). Again, the similarities lessen at the higher frequencies. However, the unexplained inconsistencies mentioned in Section 3.5.1 appear less frequently (Figures E-3, E-7, E-9, E-21, E-25, E-26, E-35, and E-53). Recall that, for this modal cost reduction technique, the modes to be eliminated are simply truncated from the model, so there is no residual information from these modes. Therein lies another subtle difference from the modal reduced models, since, for the modally reduced technique, the higher frequency modes are assumed to be quelled instantaneously. The remaining system equations incorporate information from these modes as illustrated in Section 2.7.3. For the modal cost technique, no such assumption is made, and the unwanted modes are eliminated as having negligible impact on performance.

Component Cost ( $\times 10^{-8}$ )	Mode	Component Cost ( $\times 10^{-8}$ )	Mode	Component Cost ( $\times 10^{-8}$ )	Mode
0.348758	3	0.004097	7	0.001411	22
0.344947	2	0.003547	26	0.001166	35
0.031164	1	0.003536	24	0.001089	39
0.027831	4	0.003502	28	0.000880	34
0.012824	12	0.003343	23	0.000485	29
0.008589	8	0.002837	21	0.000434	30
0.006154	5	0.002753	6	0.000266	74
0.005481	9	0.002652	11	0.000264	70
0.005147	20	0.002610	25	0.000262	13
0.004712	27	0.002578	10	0.000256	99

Table 3-2. Top 30 Component Cost Values and Associated Modes

### 3.6 *Physical System Parameter Uncertainty*

In Gustafson's research, the system sensitivity to the damping ratio of each of the flexible bending modes was determined to be negligible [11]. Likewise, the same result is assumed for the present system. This assumption is supported by the additional damping effects of the rate feedback (LAC) [1]. As such, this research will investigate only the effects of uncertainty inherent in the natural frequencies of the structural bending modes. This parameter uncertainty may arise for several reasons. First and possibly foremost, a space structure is subject to severe variations in day and night temperatures [45]. In colder temperatures, the natural frequencies of the flexible bending modes (as a group) will tend to increase. In contrast, in times of solar heating, the natural frequencies will decrease. Other minor effects result from physical aging and fatigue. The combined effects are assumed to cause uncertainties well beyond the level of robustness inherent in a single Kalman filter/LQG controller. For the purposes of this research, the natural frequencies are assumed to vary initially by approximately  $\pm$  ten percent. This implies that the natural frequencies will be varied as one group based on a percentage scalar multiplier of the nominal. The discretization of this parameter space will be determined by sensitivity

analyses, which will be discussed in detail in Chapter 4. The resulting discretized parameter space will require only a one-dimensional bank of filter/controllers in the moving-bank MMAC design.

### **3.7 Summary**

This chapter presented the SPICE-4 structure currently being tested at the Phillips Laboratory. A brief description of the physical structure was provided, along with a more in-depth look at the full system model. Several assumptions and justifications were presented, which led to the resulting truth model selection for this research. The chapter continued with a discussion of the seven reduced-order filter models that were generated using the two model reduction methods. The chapter concluded with the introduction of the uncertain parameter and the size of the resulting parameter space.

The following chapter will discuss the procedures necessary to develop and implement a MMAC for the SPICE Structure.

## ***IV. Simulation***

### ***4.1 Introduction***

This chapter will present the "tools" necessary to analyze the effectiveness of the MMAE and MMAC technique as applied to a computer simulation of the SPICE-4 structure developed in Chapter 3. These tools are: (1) Monte Carlo analysis, (2) simulation software, and (3) the analysis plan.

### ***4.2 Monte Carlo Analysis***

The Monte Carlo Analysis is required to obtain statistical descriptions of the MMAE and MMAC's performance. Through sequential Monte Carlo runs via the simulation software (to be discussed in Section 4.3), many samples of the process are obtained and sample statistics are subsequently evaluated. A covariance analysis might be considered and would provide useful information, but analytically derivable covariance analysis requires that the system under investigation be fully linear (and of lesser order for computational reasons) [24:329]. However, due to the adaptive nature of the MMAE technique, analytical derivations are not viable and the covariance analysis is not available for this application.

As presented in Chapter 3, this research will simulate and analyze a 294-state truth model against seven different reduced-order filter models. Initially, the truth model will be compared against a full-order filter model to provide a benchmark of performance. This full-order filter model will utilize a "full-order" structure model (all 108 flexible bending modes) and will be referred to as the truth filter model. Each reduced-order filter model will have the same basic composition as the truth model with the exception of the flexible bending mode states. The first three reduced-order filter models were developed using the modal reduction method and will be referred to as the 12-modal filter, 18-modal filter, and 26-modal filter, respectively, to indicate the number of flexible bending modes maintained

in the structure block. The last four reduced-order filter models were developed using the modal cost reduction method and will be referred to as the 10-modal-cost filter, 15-modal-cost filter, 20-modal-cost filter, and 26-modal-cost filter, respectively, to indicate the number of flexible bending modes maintained in the structure block. No filter based on the internally balanced method is being evaluated due to the problems encountered, as discussed in Section 3.5.

Two types of simulations will be conducted, as depicted in Figure 4-1, where one analyzes the estimator and the other analyzes the controller. The variables shown in Figure 4-1 are as follows:

- $\mathbf{x}_t(t_i)$  = the truth model states
- $\hat{\mathbf{x}}_f(t_i)$  = filter estimates of the system states
- $\mathbf{a}_t(t_i)$  = the uncertain parameter vector implemented in the truth model
- $\hat{\mathbf{a}}_f(t_i)$  = filter estimates of the uncertain parameter vector
- $\mathbf{e}_a(t_i)$  = the error in the parameter estimate defined as:  $\mathbf{e}_a(t_i) = \mathbf{a}_t(t_i) - \hat{\mathbf{a}}_f(t_i)$
- $\mathbf{e}_x(t_i)$  = the error in the system estimate

The following sections will present the error vector formulation and the error vector statistics.

#### 4.2.1 Error Vector Formulation

In this research, evaluation of the X and Y line of sight (LOS) deviations will indicate the performance capability of the reduced-order filter models. A general error vector is determined by subtracting the estimated X and Y-axis values from the true X and Y-axis values, respectively, and results in a measure of the accuracy of the reduced-order filter's estimate (Figure 4-1(a)). The equation to determine this error vector is given by:

$$\mathbf{e}_x(t_i) = \mathbf{C}_t \mathbf{x}_t(t_i) - \sum_{j=1}^K \mathbf{C}_{f_j} \hat{\mathbf{x}}_{f_j}(t_i) \cdot p_j(t_i) \quad (4.1)$$

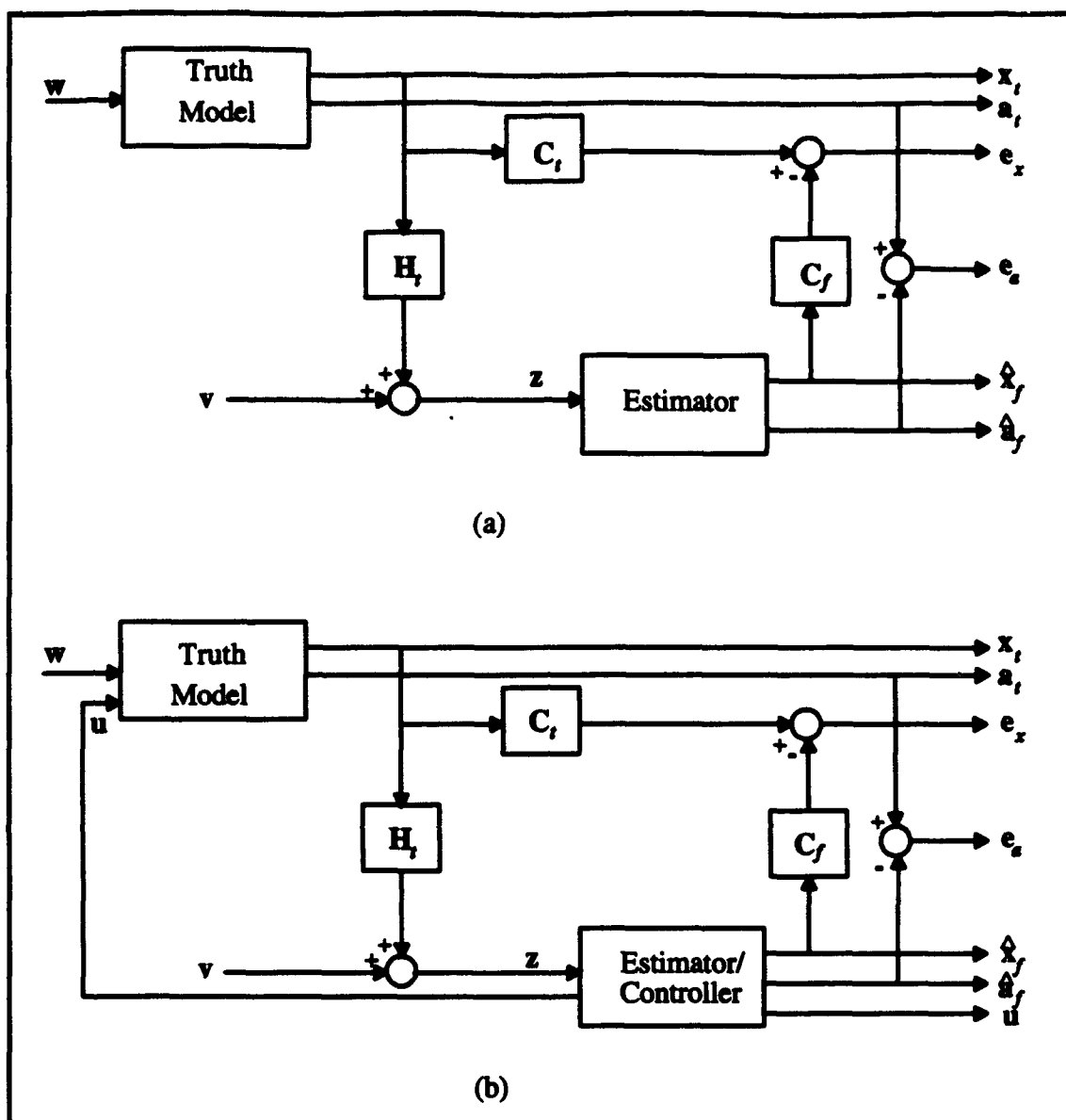


Figure 4-1. (a) Estimator Simulation, and (b) Controller Simulation [36]

where  $C_i$  and  $C_{fj}$  are the output matrices used to determine the X and Y LOS deviations for the truth model and filter model respectively. The summation in Equation (4.1) is appropriate for the MMAE implementation as presented in Chapter 2, where the subscript  $f$  represents filter and the index  $j$  indicates which of the  $K$  bank filter's weighted estimates are being summed. The specific form of the error vector is given by:

$$e_x(t_i) = \begin{bmatrix} e_{x_1}(t_i) \\ e_{x_2}(t_i) \end{bmatrix} = \begin{bmatrix} \text{X - axis LOS position error} \\ \text{Y - axis LOS position error} \end{bmatrix} \quad (4.2)$$

In Figure 4-1(b), a closed-loop estimation and control simulation is desired, where the controller is designed to regulate the position deviations, thus attempting to drive the vibrations of the structure to zero. The same type of statistical analysis can be performed in this case as was done for the estimator simulation. In addition, the performance indicator of the controller capability can be obtained from analysis of just the actual X and Y-axis LOS deviations. This error vector is given by:

$$\mathbf{e}'_x(t_i) = \mathbf{C}_x \mathbf{x}_t(t_i) \quad (4.3)$$

where  $\mathbf{e}'_x(t_i)$  is the vector of LOS deviations from the truth model.

#### 4.2.2 Error Vector Statistics

The statistics of primary concern are the sample mean and covariance of the estimation error and control processes. The mean is calculated by [18:74,42:67]:

$$E\{\mathbf{e}_x(t_i)\} \approx \mathbf{M}_{e_x}(t_i) = \frac{1}{L} \sum_{i=1}^L \mathbf{e}_{x_i}(t_i) \quad (4.4)$$

where  $L$  is the number of Monte Carlo runs made and  $\mathbf{e}_{x_i}(t_i)$  is the value of the error signal during the  $i^{\text{th}}$  simulation at run time  $t_i$ . The covariance of the mean error signal is calculated by [24:130]:

$$\begin{aligned} \mathbf{P}_{e_x}(t_i) &= E\left\{\left[\mathbf{e}_x(t_i) - E\{\mathbf{e}_x(t_i)\}\right]\left[\mathbf{e}_x(t_i) - E\{\mathbf{e}_x(t_i)\}\right]^T\right\} \\ &\approx \frac{1}{L-1} \sum_{i=1}^L \left\{\mathbf{e}_{x_i}(t_i) \mathbf{e}_{x_i}^T(t_i)\right\} - \frac{L}{L-1} \mathbf{M}_{e_x}(t_i) \mathbf{M}_{e_x}^T(t_i) \end{aligned} \quad (4.5)$$

Through a similar development, the statistics for the parameter estimation errors,  $\mathbf{e}_a(t_i)$ , and the LOS deviations,  $\mathbf{e}'_x(t_i)$ , are obtained by substituting the appropriate variables into Equations (4.4) and (4.5). The sample statistics calculated in this research will be based on ten Monte Carlo runs, in which each run will have a ten-second duration.



Additionally, a second statistic is calculated for compact tabular presentation and referred to as the temporal average of the RMS value. This value is calculated by the following:

$$e_{tp} = \frac{1}{N} \sum_{j=i-N+1}^i \sqrt{[M_{e_x}(t_j)M_{e_x}^T(t_j) + P_{e_x}(t_j)]_{pp}} \quad \text{for } p = 1 \text{ and } 2 \quad (4.6)$$

where  $e_{tp}$  is the temporal average of the  $p^{\text{th}}$  component of  $e_x$  or  $e'_x$  and  $N$  is the number of sample periods. For this research, the temporal average will be calculated based on the last five seconds of the run duration.

### 4.3 *Simulation Software*

In the previous thesis research, [11], the software from the long line of related topics [14,15,18,33,37,42] was modified to suit the SPICE application. This software (resident on Sun workstations) is broken into three separate program groups: (1) preprocessor, (2) processor, and (3) post processor. Each of these program groups will be discussed individually in the following sections.

#### 4.3.1 *Preprocessor*

**Inherited Preprocessor.** The previous preprocessor was separated into two separate routines which implemented a MATRIXx portion [22] and a FORTRAN portion [10]. The MATRIXx code first discretized the truth and filter models, then calculated the steady-state Kalman filter gains and the steady-state LQG regulator gains. The resulting information was stored and read by the FORTRAN code, which then determined the filter-computed state covariance and the residual covariance and stored the information in a form compatible with the processor code.

**Current Preprocessor.** A coworker, James Fitch, investigating a related research topic with the older SPICE-2 model, discovered several minor discrepancies with

the MATRIXx algorithms that produced the filter and controller gains [8,9]. This led to his decision to convert the MATRIXx code to MATLAB [23] code where there was more confidence in these particular calculations. He created a separate program to read the state space matrices generated and stored in the MATRIXx SystemBuild format and store them in a form compatible with MATLAB. Additionally, the calculation of the filter state covariance and residual covariance was incorporated into the MATLAB code and removed from the FORTRAN code. Finally, the MATLAB code stored the information in a form compatible with the FORTRAN code. The remaining FORTRAN code was left with the task of reading the information from the MATLAB output and storing it in a form compatible with the processor code.

The resulting MATLAB code still needed to be modified to accommodate the new SPICE-4 version. Mostly this involved changing the input model declarations and the input/output relationships for the Kalman filter state equations.

#### **4.3.2 Processor**

**Inherited Processor:** The previous processor code (FORTRAN) was designed to simulate a moving-bank estimator/controller for the SPICE-2 structure via Monte Carlo analysis. The FORTRAN code first read in information from a data file which contained variables for the specific models used and eliminated the need to change the actual processor code for different model selections. The data from the preprocessor was read into the respective truth and filter bank matrices. Then the processor began the Monte Carlo loops by propagating the truth model and then the bank of filters. Measurements were taken from the truth model to be used in the update portion of the filter models. The respective filter probabilities were calculated and the decisions to move, contract, or expand the bank were made. The processor code had subroutines to implement the residual monitoring, probability monitoring, and the parameter position estimate monitoring methods for dictating the bank movement, as discussed in Section 2.4.

Likewise, there were subroutines to implement MMAC, modified MMAC, MAP, and single changeable-gain control, as discussed in Section 2.5. The code was written to accommodate bank expansion and contraction. The white Gaussian noise vectors used in both the dynamics driving noise and measurement noise generation were produced by a random number generator.

**Current Processor:** The present processor operates much the same as the previous version, as very few changes were made and no major discrepancies were noted. However, Fitch [8,9] modified this program to suit the needs of his research, but the changes were transparent with respect to this research.

#### **4.3.3 *Post Processor***

**Inherited Post Processor:** The previous version of the post processor read data from the processor and generated the statistical analysis parameters discussed in Section 4.2. The specific parameters of greatest interest are the mean and covariance of the estimation position errors, the true LOS deviations with control applied, and the uncertain parameter estimation errors. The output generated by the post processor was compatible with a separate plotting routine.

**Current Post Processor:** Few changes were made to the previous post processor code and no major discrepancies were noted. The output generated was compatible with MATLAB plotting routines and was used for all the plots generated in the remaining chapters.

#### **4.4 *Analysis Plan***

Part of the goal of this research is to determine which of the reduced-order methods, modal reduction or modal cost reduction, is more conducive in the filter/controller design for error estimation and regulation control of the true LOS deviations. Proper tuning of the dynamics driving noise and measurement noise values

will be the first step in this determination. Adjustment of the controller weighting matrices will be the next step in accomplishing the best controller design. After selection of the most effective reduced-order design, the sensitivity to parameter changes for this filter will then be determined. This will generate the parameter space discretization to be used in the moving-bank MMAC parameter identification performance analysis. The following sections will address each of these tasks individually.

#### **4.4.1 Dynamics Noise Strength and Measurement Noise Covariance Determination**

The first step is to determine the specific noise levels for the truth model dynamics driving noise strength and measurement noise covariance,  $Q_t$  and  $R_t$ , respectively. Since the disturbance shaping filters in the SPICE-4 MATRIXx system build model were designed with a unit strength white noise generator for the inputs,  $Q_t$  was set equal to the identity matrix. The equivalent discretized dynamics driving noise,  $Q_{dt}$ , is now approximated by Equation (2.74). The measurement noise shaping filters were removed for the truth model and replaced with an equivalent white noise of covariance  $R_t$ . However, the replacement white noise for the accelerometer measurements is now in terms of velocity rather than the original acceleration so no direct comparison could be made based on the eliminated shaping filters. As a result, it was necessary to obtain an equivalent value for the velocity noise from Lockheed [1]. (The noise values for the OSS measurements were also obtained from Lockheed.) These values are:

$$R_t^* = \begin{bmatrix} R_{1-12}^* \\ R_{13-14}^* \\ R_{15-18}^* \\ R_{19-36}^* \end{bmatrix} = \begin{bmatrix} 0.05 \text{ } \mu\text{radians} / \text{sqrt(Hz)} \\ 0.6 \text{ } \mu\text{radians} / \text{sqrt(Hz)} \\ 1.7 \text{ microns} / \text{sqrt(Hz)} \\ 2 \text{ microns} / \text{sec} / \text{sqrt(Hz)} \end{bmatrix} \quad (4.7)$$

where the superscript \* indicates these are not true variance values but actually indicate the square root of the height of the equivalent continuous-time white noise power spectral density (PSD) plot. In order to determine the correct discrete-time covariance,  $R_{dt}$ , these

values must be squared and multiplied by the frequency bandwidth of interest (~1-100 Hz).

Filter equivalent values for  $Q_d$  and  $R_d$  can now be determined by tuning the filter-predicted standard deviations (from the filter error covariance) to the true error mean plus and minus true error standard deviations resulting from the Monte Carlo runs. It will be important not to mask the performance of elemental filters in the MMAC design by adding too much dynamics driving pseudonoise to the filter designs. This will make the parameter identification process very difficult. The actual tuning procedure will be discussed in more detail in Chapter 5.

#### 4.4.2 Controller Weighting Matrices

The state weighting matrix,  $X$ , and the control weighting matrix,  $U$ , from Equation (2.40) are determined by the following equation:

$$X = p_x C^T C \quad (4.8)$$

$$U = p_u I \quad (4.9)$$

where

- $C$  = the filter LOS output matrix defined in Equation (3.40)
- $I$  = 18-by-18 identity matrix
- $p_x$  = scalar state weighting value
- $p_u$  = scalar control weighting value

The initial values for  $p_x$  and  $p_u$  were obtained from Lockheed and are given as follows [1]:

$$p_x = \frac{1}{[5.62 \text{ } \mu\text{radians}]^2} \quad (4.10)$$

$$p_u = \frac{1}{[85.0 \text{ Newtons}]^2} \quad (4.11)$$

Lockheed specifies the quadratic cost in integral form versus summation form, but for sample times as small as utilized in this research, the differences are assumed to be negligible. The weighting coefficients given in Equations (4.10) and (4.11) are treated initially as the typical (first-cut) form of  $[1/(\text{maximum allowable value})^2]$ . However, the  $p_u$  value shown in Equation (4.11) is considered to be associated with a maximum allowable value imposed by the physical limits of the PMAs, so this value will not be adjusted in controller tuning. As a result, only  $p_x$  will be adjusted to affect the state weighting matrix. Decreasing the value of the denominator in  $p_x$  will increase the "tightness" of control expended on maintaining the state value near zero. The actual controller tuning procedure will be discussed in more detail in Chapter 5

#### **4.4.3 Model Analysis**

Initially the truth filter model (filter based on the truth model) will be investigated against the truth model to provide a benchmark of performance. As such the truth filter model should provide the best possible controller performance on which to base the evaluation of reduced-order models. Very little filter tuning should be required since there is no order reduction between the truth model and truth filter model. Each of the reduced-order models will be examined in turn to determine which will provide the best possible controller performance. If the performances were determined to be similar, then the computation differences between the different models will be considered.

The reduced-order filter models will be examined in the following order: (1) 12-modal filter (102 total states), (2) 18-modal filter (114 total states), (3) 26-modal filter (130 total states), (4) 10-modal-cost filter (98 total states), (5) 15-modal-cost filter (108 total states), (6) 20-modal-cost filter (118 total states), and (7) 26-modal-cost filter (130 total states). To reiterate, the number in each filter refers to the number of flexible body modes maintained in the model. The other states are the same for the truth model and the filter models and are composed of the following: 36 PMA states, 18 controller output

filter states, and 24 disturbance input states. The reason for so many filter models is to generate filters with a wide range of flexible body states, which may have been a contributing factor to the limited success for reduced-order filters used in Gustafson's research [11]. The filter/controllers will be evaluated on the basis of their ability to represent the truth model accurately and their capability to quell the structure to within the required specification. This specification is the one micro-radian allowable X and Y axis LOS deviation [1]. Plots depicting the state estimation error will provide the necessary information to evaluate the estimation accuracy condition. Likewise, plots depicting the LOS deviations and the temporal average RMS calculation will provide the necessary information to evaluate the control condition. After the completion of the model analysis, the single most effective reduced-order model design will be selected to be utilized in the sensitivity analysis and in the subsequent MMAC design.

#### **4.4.4 Sensitivity Analysis**

As discussed in Section 3.6, the natural frequencies of the flexible bending modes of the structure form the basis of the uncertain parameter space. Initially, it was envisioned that the actual discrete parameter points in the space would be determined by performing a sensitivity analysis. This would be accomplished by varying the percentage scalar multiplier of all the natural frequencies within the flexible bending modes in the truth model in one direction at a time until the closed loop system with the single filter/controller (based on the nominal value) in the loop becomes unstable. A discrete parameter value is declared just prior to this point (10 % rollback), where the difference from the nominal value is denoted as  $\delta\omega_1$ . The filter is then updated or re-nominalized to this point (e.g., multiplied by the same percentage change). Now the filter model and the truth model reside at the same "new nominal" point. Again, the truth model is modified in the same direction until the closed loop system with filter/controller in the loop becomes unstable, which results in  $\delta\omega_2$  and a new parameter point. This procedure is repeated

until the ten percent boundary is reached. The opposite direction is then accomplished until the full  $\pm$  ten percent parameter space is completed. Figure 4.2 illustrates this procedure, where the size of the space and number of points is arbitrary and based on the results of the sensitivity analysis. In using this method, it is important to note that increasing the parameter from the nominal (plus 0-10%) results in a space determined where the filter is underestimating the natural frequencies. Similarly, decreasing the parameter from the nominal (minus 0-10%) results in a space determined where the filter is overestimating the natural frequencies.

However, unanticipated problems occurred (to be discussed in Chapter 5) that led to the decision to modify this approach. The resulting parameter space was determined simply by discretizing every 0.5 percent between the range of minus 2 to plus 10 percent. This results in a 21-point one-dimensional parameter space.

#### 4.4.5 Parameter Identification and Control

The ability of the moving bank of filters to identify the true parameter will be of the utmost importance prior to applying LQG control. In order to determine this

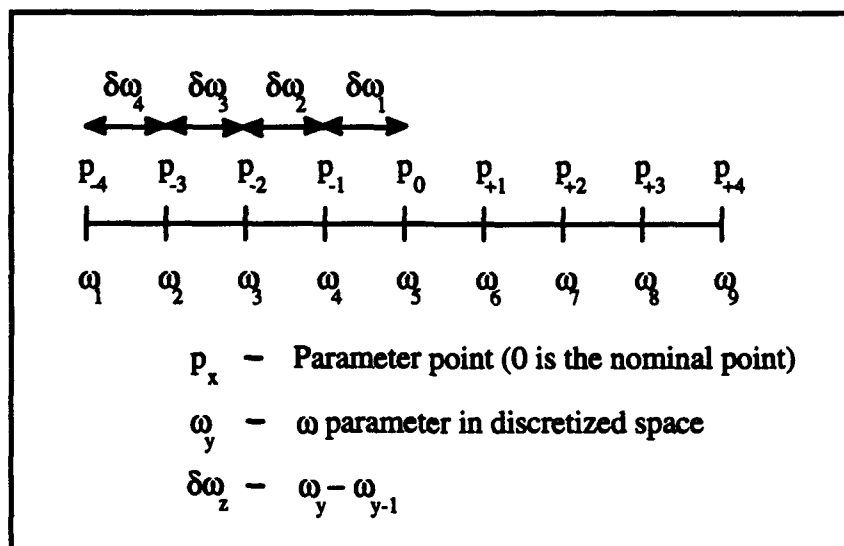


Figure 4-2. Parameter Discretization procedure



capability, many simulations will be run in which the true parameter value will be positioned or moved in various fashions. First, in order to set a baseline of performance, the true parameter (the truth-model-based parameter value) will be set at the nominal value (the original model parameter value prior to parameter variations in the discretized space, i.e.,  $\omega_j$ ). Additionally, the moving bank of filters will be centered at this nominal value. Hence, the moving bank will be artificially informed initially of the true parameter value. This situation might arise in an actual implementation if the filter model were to be based on an accurate depiction of the real world system, where no temperature variations, fatigue, or aging have occurred. Next, the true parameter value will be offset from the initial location of the center of the filter bank. This situation might arise if the estimation and control system were inactive for a period of time and suddenly turned on. During the dormancy period, the real world system might have been subjected to a temperature variation that caused the true parameter to change. The third type simulation will center the filter bank on the true parameter initially, then allow the true parameter to make a discrete jump to a new location. This attempts to simulate a sudden temperature variation or, possibly, damage to the real world system. Finally, the true parameter will be allowed to vary slowly over a period of time, which would simulate the possible temperature variations arising from a transition into- and out-of-sunlight.

Once the parameter estimation analysis is complete, simulations can be run in which LQG control is applied. The optimal situation would be to estimate the true parameter accurately prior to applying LQG control. The first type simulation makes this assumption, such that the filter/controller bank is initially centered on the stationary true parameter value. Although it might be desirable *not* to apply control during periods of parameter variations, this may be unavoidable. The second and third type simulations allow control to be applied while the true parameter either jumps and moves slowly, respectively.

#### **4.5    *Summary***

This chapter has presented the details involved with accomplishing the desired performance analyses through actual simulations. The Monte Carlo analysis method was introduced, as well as the performance evaluation criteria. A brief discussion of the simulation software was then provided. The chapter concluded with a discussion of the simulation analysis plan for accomplishing the desired objectives.

Chapter 5 will present results obtained from the single filter performance analysis, parameter discretization efforts, and the moving-bank MMAE/MMAC performance analysis.

## ***V Results***

### ***5.1 Introduction***

The primary purpose of this thesis is to quell the vibrations induced in the SPICE-4 structure under the assumption that uncertain parameters are present in the dynamics of the flexible body modes. The further assumption is made that non-adaptive controllers do not have enough inherent robustness to design parameter variations to be utilized in the actual physical implementation. As a result, the concept of the multiple model adaptive controller (MMAC) composed of a bank of LQG controllers (each involving a Kalman filter, cascaded with an LQ regulator controller) is proposed to provide the required adaptation process to quell the structure despite the uncertainties.

This chapter begins with a discussion of the tuning procedures used in the filter and controller development. This is followed by an analysis of which of the proposed reduced-order filters is the most effective at meeting the tracking requirements levied by the Phillips Laboratory. The issue of the parameter discretization space is addressed next. Finally, the resulting performance of the MMAE/MMAC designs are presented.

### ***5.2 Tuning Procedures***

This section discusses the specific method by which the filters and controllers are tuned. In this application, the tuning process is accomplished by trial and error, guided by engineering insight, rather than more sophisticated methods. The individual tuning parameters are presented in Table F-1 of Appendix F.

#### ***5.2.1 Filter Tuning***

Tuning the filters is accomplished by visually examining the plots of the mean estimation error and mean estimation error  $\pm$  one standard deviation ( $\pm\sigma_e$ ) calculated from the Monte Carlo runs (Equations (4.4) and (4.5)) versus the filter-predicted mean error (namely, zero)  $\pm$  one standard deviation ( $\pm\sigma_f$ ). The objective is to have the filter-

predicted  $\pm\sigma_f$  match the mean estimation error  $\pm\sigma_e$ , which will result in an optimally tuned filter. The filter-predicted  $\pm\sigma_f$  bounds are modified by alternately adjusting (tuning) the dynamics driving noise of the filter,  $Q_f$ , and the measurement noise covariance,  $R_f$ . *Raising  $Q_f$  implies less confidence in the filter's system model and will result in expansion of the filter-predicted  $\pm\sigma_f$  bounds. Lowering  $Q_f$  implies more confidence in the filter's system model and will result in the opposite affect on the predicted  $\pm\sigma_f$  bounds. Likewise, raising  $R_f$  implies less confidence in the filter's measurement update (noisier measurements) and will result in expansion of the filter-predicted  $\pm\sigma_f$  bounds. The opposite is also true.*

Since there were no changes made between the truth model and filter models for dynamics driving noise or the measurement noise inputs, the primary method of tuning  $Q_f$  and  $R_f$  was by adjusting each of the respective values by a scalar multiplier. This procedure worked well, although there is a noticeable difference in the X and Y axis' tuning, respectively, due to the differences in the two axes on the actual SPICE tripod structure (reference Figure 3-1). In the truth model prior to being discretized, the value for  $Q_t$  is the identity matrix. The parameter variations for  $Q_f$  displayed in Table F-1 are scalar multipliers of  $Q_t$  (e.g., 1). Similarly, the scalar multipliers for  $R_f$  operate on the values (considered to be  $R_t$ ) presented in Equation (4.7). However, during implementation, the scalar multiplier was applied to the standard deviation of the values resulting from Equation (4.7). This is why the multiplier decreases rather than increases, as would be the typical case if operating on the variance values instead of the standard deviations. This unconventional procedure resulted in a rescaling of the diagonal terms relative to each other. (The relative differences were smaller than if the scalar multiplier was applied to  $R_t$ .) The results will show that this method did not appear to cause any appreciable degradation in the MMAE/MMAC performance. As will be seen, changing  $R_f$  had the greatest impact on the filter-predicted  $\pm\sigma_f$  bounds, whereas changing  $Q_f$

**AFTT/GA/ENG/93D-02**

**CONTROL OF A LARGE SPACE STRUCTURE USING  
MULTIPLE MODEL ADAPTIVE ESTIMATION AND  
CONTROL TECHNIQUES**

**THESIS**

**Gregory John Schiller  
Captain, USAF**

**AFTT/GA/ENG/93D-02**

**Approved for public release; distribution unlimited**

had very little impact and was kept very small in view of the desire of not masking parameter changes. It should be noted that the scalar multiplier for  $R_f$  of the truth filter model (filter based on the truth model with no purposeful order reduction) does not result in the expected individual variances for each of the respective measurement devices. The unconventional manner in which  $R_f$  was obtained may have been partly responsible for this result. However, the resulting values are dramatically larger than should have been necessary (i.e.,  $0.007 \times \sigma \gg \sigma^2$ ). Initially, the tuning parameters attained for the filter based on the nominal  $\omega_n$  parameter values were maintained for each of the filters in the discretized space, since the impact of the  $\omega_n$  parameter variations was anticipated to be negligible. Later in this report, this assumption will be shown to be in error.

### **5.2.2 Controller Tuning**

As briefly mentioned in Chapter 4, only the scalar weight affecting the state weighting matrix was adjusted for controller tuning, since the value for the control weighting matrix was assumed to be at its limiting admissible value. Tuning the controller was a simple matter of adjusting the scalar state weighting value until the point of closed loop system instability was reached (determined visually by a divergence in the error estimation plots or the LOS plots). This point implies the "tightest" possible state values will be obtained with slightly smaller state weightings. The weighting value was then tuned back 10 percent. Once again, this value was used initially for all of the controllers in the discretized parameter space. The 10 percent rollback still maintained effective control, yet diminished sensitivity to tuning and parameter variations in the final parameter space.

### **5.3 Model Analysis**

This section presents the results of the tuned truth-model-based and reduced-order filters and steady-state LQG controllers. The results are summarized at the end of this section. For this analysis, a single filter/controller combination based on the nominal truth

model is being utilized. The respective plot results for filters and controllers based on the truth and all reduced-order models are given in Appendix F.

### **5.3.1 Truth Filter Model**

This subsection will present the performance results of the truth-model-based filter and controller. These results will provide a benchmark of performance to which to compare the subsequent reduced-order models.

Figures F-1 and F-2 display the truth model's LOS deviations with no LQG control applied. Recall from Chapter 3, that there is closed loop control in the form of simple rate feedback (LAC) applied to the structure. When references are made to control or no control, this is strictly referring to the application of LQG control since the LAC feedback loop is active in all simulations. For no control, the temporal average RMS values for the truth model X and Y axis LOS deviations are 9.3248 micro-radians 15.7468 and micro-radians respectively. (From this point on, references to the term RMS will imply a temporal average.) This clearly indicates the need for an additional type of control to quell the structure's vibrations to within the one micro-radian specification.

Figures F-3 and F-4 illustrate the error in the Kalman filter estimate of the LOS deviations. The horizontal solid lines indicate the filter-predicted standard deviation of the error of the estimate. Recall that this value results from the assumption of a zero-mean error and is a steady state value. The other lines indicate the mean and mean  $\pm$  one standard deviation of the true error in the estimate resulting from the ten Monte Carlo runs.

Figures F-5 and F-6 illustrate the dramatic reduction in the LOS deviations when LQG control is applied at the one second mark. The resulting RMS values are 0.4711 micro-radians for the X-axis LOS and 0.6632 micro-radians for the Y-axis LOS. Thus the controller based on the truth model indicates the capability to control the structure to

well within the one micro-radian specification. Again, the discrepancy between the X and Y axis values are due to the differences inherent in the geometry of the tripod structure. Of course, implementing a full-order filter/controller such as this would be computationally infeasible. The underlying anticipation is to have a much reduced-order filter/controller performance closely compare with this full-order filter/controller performance.

### **5.3.2 12-, 18-, and 26-Modal Models**

This subsection presents the performance results of the modally reduced filter/controllers. Recall from Chapter 3, that the design model name includes the number of flexible bending modes,  $n$ , maintained in the model and that the total number of states is  $78 + 2n$ . Figures F-7 through F-18 apply to this subsection.

**12-Modal Model.** Figures F-7 and F-8 illustrate the filter tuning and Figures F-9 and F-10 illustrate the results when LQG control is applied. The resulting RMS values are 3.6082 micro-radians for the X-axis LOS and 5.3114 micro-radians for the Y-axis LOS. The controller does have an effect on the LOS deviations, yet does not meet the specification. No doubt, this is attributed to not maintaining enough of the dominant flexible bending modes in the filter/controller. Comparing the magnitudes of the estimation error plots (F-7,8) with those of the truth-model-based filter (F-3,4), this result was predictable as the average error is roughly double that of the truth-model-based filter.

**18-Modal Model.** Figures F-11 and F-12 illustrate the filter tuning and Figures F-13 and F-14 illustrate the results when control is applied. The resulting RMS values are 3.1139 micro-radians for the X-axis LOS and 4.582 micro-radians for the Y-axis LOS. These results are very interesting since the estimation errors are actually lesser in magnitude than for the case of the truth-model-based filter/controller, yet the resulting control is only slightly better than the 12-modal model. It is possible that these additional modes are highly observable, thus having a large impact on reducing the estimation error,



but they are not equally as controllable, thus accounting for the slight decrease in the RMS LOS values from that of the 12-modal model. Or, there may be additional modes that must be included in the controller before the LOS deviations can be effectively reduced to specifications.

**26-Modal Model.** Figures F-15 and F-16 illustrate the filter tuning and Figures F-17 and F-18 illustrate the results when control is applied. The resulting RMS values are 0.6824 micro-radians for the X-axis LOS and 1.012 micro-radians for the Y-axis LOS. This design model is effective in terms of both the estimation error and the control of LOS deviations. It should be noted that, due to the relatively large difference in the performance results between the two axes, each axis' performance will be addressed separately. The one micro-radian specification is met to within an acceptable margin (+.02 micro-radians) for the X axis, while the Y axis is well within the specification. There is some relative control degradation (as compared to the truth-model-based filter/controller) of 45 percent and 53 percent in the X and Y LOS axes, respectively. This level of degradation is still highly encouraging, considering the dramatic level of order reduction involved.

### **5.3.3 10-, 15-, 20-, and 26-Modal Cost Models**

This subsection presents the performance results of the modal-cost-reduced filter/controllers. Figures F-19 through F-34 apply to this subsection.

**10-Modal-Cost Model.** Figures F-19 and F-20 illustrate the filter tuning and Figures F-21 and F-22 illustrate the results when control is applied. The resulting RMS values are 2.0847 micro-radians for the X-axis LOS and 2.6027 micro-radians for the Y-axis LOS. Here is another interesting result. The estimation errors are worse than for any of the previous filter models, but the resulting RMS LOS values are actually better than either the 12- or 18-modal filter/controllers. This result supports the hypothesis upon which this form of reduced order model was based: the modes which have the greatest

effect on the LOS output should be maintained in the design model. This does not necessarily imply that these modes are highly observable, hence the poor estimation performance. However, although the controller performance is superior to that of the 12- and 18-modal filter/controllers, the one micro-radian specification is not met.

**15-Modal-Cost Model.** Figures F-23 and F-24 illustrate the filter tuning and Figures F-25 and F-26 illustrate the results when control is applied. The resulting RMS values are 2.0656 micro-radians for the X-axis LOS and 2.6213 micro-radians for the Y-axis LOS. Somewhat disturbing, these results are not easily explained. Although the estimation errors are less than for the 10-modal-cost filter/controller, the resulting RMS values are practically the same. It is possible that the additional modes are more observable, yet do not provide additional controllability to the system, which is contrary to the modal cost hypothesis.

**20-Modal-Cost Model.** Figures F-27 and F-28 illustrate the filter tuning and Figures F-29 and F-30 illustrate the results when control is applied. The resulting RMS values are 1.6152 micro-radians for the X-axis LOS and 2.3145 micro-radians for the Y-axis LOS. In this case, the RMS values are more encouraging than for the 15-modal-cost filter/controller, yet still do not meet the one micro-radian specification. Although the number of modes is close to the number included in the 18-modal filter/controller, the level of control capability is roughly twice as good. At least for the lower number of modes, the modal cost method appears to out-perform the modal method dramatically.

**26-Modal-Cost Model.** Figures F-31 and F-32 illustrate the filter tuning and Figures F-33 and F-34 illustrate the results when control is applied. The resulting RMS values are 0.6646 micro-radians for the X-axis LOS and 1.0032 micro-radians for the Y-axis LOS. These results show that the modal cost method is still more effective than the modal method as the number of modes is increased, but not as dramatic as in the lower

order filters. Likewise, the one micro-radian specification is met once 26 modes are included in the design model.

#### **5.3.4 Additional Filter/Controller Design Models**

**26-Modal Truncated Model.** This model was developed as a result of problems encountered in the parameter discretization analysis (to be discussed in Section 5.4). Figures F-35 and F-36 illustrate the filter tuning and Figures F-37 and F-38 illustrate the results when control is applied. The resulting RMS values are 0.6465 micro-radians for the X-axis LOS and 0.9825 micro-radians for the Y-axis LOS. This design model proved to be the most effective of all the models, as seen by its ability to meet the one micro-radian specification with a greater margin.

#### **5.3.5 Section Review**

Table 5-1 reviews the relative performance of each of the individual filter/controller design models. Since the 26-modal-cost filter/controller indicated the best performance of reduced-order controllers based on the original two order reduction methods, this model was utilized in the initial parameter discretization analysis. However, problems encountered (to be discussed in Section 5.4) led to other filter model utilizations.

#### **5.4 Discretization of Parameter Space**

Discretizing the parameter space using the initial method described in Section 4.7 resulted in several problems. The first appeared when performing the sensitivity analysis on the 26-modal-cost filter/controller. After determining the first new discretized point at approximately a one percent change in parameter value, and before the second new point was attempted, a "check run" was made. After re-nominalizing the filter/controller model at the first point and leaving the truth model at the same point, a simulation was run to re-test the performance at this "new nominal" value. The resulting filter/controller performance was unstable, and only through re-tuning of the filter and "loosening" of the scalar state weighting value  $p_x$ , was the filter/controller made stable. Still, the best

Design Model	X-Axis Deviation	Y-Axis Deviation
Truth	0.4711 $\mu$ rads	0.6632 $\mu$ rads
12-Modal	3.6082 $\mu$ rads	5.3114 $\mu$ rads
18-modal	3.1139 $\mu$ rads	4.582 $\mu$ rads
26-Modal	0.6824 $\mu$ rads	1.012 $\mu$ rads
10-Modal-Cost	2.0847 $\mu$ rads	2.6027 $\mu$ rads
15-Modal-Cost	2.0656 $\mu$ rads	2.6213 $\mu$ rads
20-Modal-Cost	1.6152 $\mu$ rads	2.3145 $\mu$ rads
26-Modal-Cost	0.6646 $\mu$ rads	1.0032 $\mu$ rads
26-Modal-Truncated	0.6465 $\mu$ rads	0.9825 $\mu$ rads

Table 5-1. Filter/Controller Model Performance Results

possible controller performance was degraded by ~50 percent from that obtained at the original nominal. It is possible that, at the new nominalized value, the modal cost technique would determine a new set of desirable modes to be maintained that are different from the original model.

The 26-modal filter/controller also had severe problems. The MatrixX algorithm (MREDUCE) [22] which accomplished the desired order reduction was unable to provide a reduced order model for parameter values less than 95 percent of the nominal (e.g., a five percent reduction in the nominal values for the natural frequencies). This was due to a near singular matrix present in the truth model that exceeded the computational accuracy of the computer. Additionally, for parameter changes corresponding to lowered undamped natural frequencies, the controller performance became severely degraded. Filter re-tuning did not resolve the problem. At a 2 percent reduction in the nominal

parameter, the best possible controller performance was already degraded by ~20 percent. It is speculated that, due to ill-conditioned matrices, the MATLAB algorithms for the steady-state Kalman filter gain (DLQE) and steady-state LQG control gain (DLQR) [23] had numerical problems, which resulted in the poor performance.

With these problems in mind, the 26-modal truncated model was created, in which the higher frequency modes were simply truncated from the system model. This is similar to the modal-cost reduction method in that the unwanted modes are removed from the system model in the same manner. However, this is different from the modally reduced method, where the system model is still a function of the eliminated higher frequency modes in the form of the direct feedthrough terms, as presented in Section 2.7.3.

A sensitivity analysis was performed for the filter/controller based on this design model, but the same problem as for the 26-modal reduced model was encountered. Again, the controller performance became degraded with a reduction in the nominal parameter value (to about the same degree as the 26-modal model).

In testing these models, several statements can be made about the performance of each model about the nominal parameter value. Every model had *more* difficulty when the design model *underestimated* the natural frequencies than when the design model *overestimated* the natural frequencies. Each closed-loop system with activated filter/controller became unstable at a one percent increase (approximate) in the actual system parameter value, whereas, it was not until a two percent decrease (approximate) that the closed-loop systems became unstable. The 26-modal reduced model appeared to be the most robust in this range, whereas the truncated model appeared to be the least robust.

With all these issues in mind, it was decided to modify the parameter space size. Limiting the parameter reduction to two percent alleviated the problem with poor controller performance past this range. The underlying factor is that this type of

filter/controller design is ineffective beyond this range and other techniques should be pursued. Next, since using the controller stability criterion resulted in only 10 parameter points in the range of -2 to +10 percent parameter change, the parameter space was limited to -2 and +8 percent and discretized at every 0.5 percent change (21 points). This allowed for a full demonstration of the moving-bank MMAE design method, which would have been limited with a smaller space. Finally, the 26-modal reduced-order filter/controller was deemed the most appropriate to be used in the subsequent analyses due to its level of robustness relative to both the 26-modal truncated model and the 26-modal-cost model.

### **5.5 MMAE Performance**

This section presents the results obtained from simulations implementing the MMAE design method utilizing many of the specific techniques discussed in Sections 2.3 and 2.4. However, several techniques were not investigated, based on the results of past research, favorable results of initial simulations in this research, and program coding limitations. Each of the simulations attempt to emulate situations possible in a real world system as discussed in Subsection 4.4.5. The plots addressed in this section are presented in Appendix G. Although there is no legend on each of the plots, it should be readily apparent that the true parameter position is indicated by the straight lines and the parameter position estimate (mean value obtained from a ten run Monte Carlo analysis) is indicated by the wavering lines.

Previous research obtained the best results using the ME/I density computation (recall Subsection 2.3.2) in determination of the final state estimate [11]. Consequently, this approach was implemented initially in this research. Due to the relatively poor performance of this method (to be discussed in Subsection 5.5.1), the original method, using the full Bayesian MMAE form, was adopted. As will be shown, excellent results were obtained using this method. Based on these results and the poor performance in past

research [11] associated with the other modifications, MAP and MAP with ME/I (recall Subsection 2.3.2) were not investigated.

Of the four methods for moving the filter bank (recall Subsection 2.4.1), only three methods were investigated. The parameter position and velocity estimate monitoring method was not attempted as the inherited program was not coded for this method and the extra time to accomplish this was not warranted, based upon performance results of earlier applications of this method [14,30]. Comparisons of the remaining three methods: residual monitoring, probability monitoring, and parameter position estimate monitoring, were carried throughout the rest of the MMAE and MMAC analyses.

Many different parameter position variation combinations were simulated under the general guidelines discussed in Subsection 4.4.5. Only a small subset of these will be presented in Appendix G. It was desired to determine worst case simulations for the types of variations discussed, which are then carried throughout the rest of the research. Each of the simulations were based on 10 Monte Carlo runs of 10 second duration (except where noted).

For the case of an initially artificially informed filter bank (bank center model-based parameter value initially matches the truth-model-based parameter value) and unmoving true parameter, several points were simulated; namely,  $\omega_5$  (nominal),  $\omega_{10}$ ,  $\omega_{15}$ , and  $\omega_{20}$ . Since there was a negligible difference between the results at any of the points, only the results from  $\omega_5$  are presented in Appendix G. In the respective figures of Appendix G, this simulation is referred to as "parameter match".

For the case of an initial offset between the truth-model-based parameter value and the filter bank center model-based parameter value, the following combinations were simulated with a five second duration: (1) bank center initially at  $\omega_5$  and true parameter position at  $\omega_{13}$ , (2) bank center initially at  $\omega_5$  and true parameter position at  $\omega_{17}$ , (3) bank center initially at  $\omega_5$  and true parameter position at  $\omega_{20}$ , (4) bank center initially at

$\omega_{17}$  and true parameter position at  $\omega_5$ , and (5) bank center initially at  $\omega_{17}$  and true parameter position at  $\omega_8$ . Although there were differences noted (to be discussed in Subsection 5.5.2), only combinations (2) and (4) are presented in Appendix G. In the respective figures of Appendix G, these simulations are referred to as parameter offsets either up or down, as appropriate.

The case of discrete parameter position jumps (at the five second mark) was simulated with the following combinations: (1) initial bank center and true parameter position at  $\omega_5$  with a jump in the true parameter position to  $\omega_{13}$ , (2) initial bank center and true parameter position at  $\omega_5$  with a jump in the true parameter position to  $\omega_{17}$ , (3) initial bank center and true parameter position at  $\omega_5$  with a jump in the true parameter position to  $\omega_{20}$ , (4) initial bank center and true parameter position at  $\omega_5$  with a jump in the true parameter position to  $\omega_{16}$ , (5) initial bank center and true parameter position at  $\omega_{17}$  with a jump in the true parameter position to  $\omega_5$ , and (6) initial bank center and true parameter position at  $\omega_{17}$  with a jump in the true parameter position to  $\omega_8$ . Only combinations (2) and (5) are presented in Appendix G, where the differences are discussed in Subsection 5.5.2. In the respective figures of Appendix G, these simulations are referred to as parameter jumps either up or down, as appropriate.

Finally, for the case of slowly moving parameter position values, only two simulations were accomplished: (1) initial bank center and true parameter position at  $\omega_2$  with small discrete positive jumps in the true parameter position every 2 seconds for 30 seconds, (2) initial bank center and true parameter position at  $\omega_{18}$  with small discrete negative jumps in the true parameter position every 2 seconds for 30 seconds. Both of these examples are presented in Appendix G. In the respective figures of Appendix G, these simulations are referred to as parameter moves either up or down, as appropriate.

In any of the situations simulated for this section, the resulting X and Y LOS estimation error plots are essentially identical. As such, only Figures G-1 and G-2 are



presented as single representative examples. Additionally, these plots are indistinguishable from those of the single filter analysis (compare with Figures F-15 and F-16). For reference, these two plots were obtained from the simulation resulting in Figure G-17 (presented out-of-order for purposes of this discussion).

### 5.5.1 ME/I Performance

This subsection discusses the performance results of the parameter position estimation simulations in which the final state estimate is determined by utilizing the ME/I method as a modification to the original Bayesian form. Additionally, the parameter position estimate monitoring method was utilized, since the best results in previous research were obtained with this method [11]. Recall that this modification replaces the residual covariance matrix  $A_k$  in the probability density function (Equation (2.26)) with the identity matrix (Equation (2.31)). The assumption is that this modification will account for possible erroneous effects of the  $A_k$  term. However, in this application, the initial replacement with the identity matrix resulted in the inability of the moving bank to estimate either a matching or moving true parameter value. The problem was found in the density calculation. The absolute magnitude of the likelihood quotient,  $L$  (recall the quadratic term  $[r_k^T I r_k]$  in Equation (2.31)), was so small that the resulting exponent calculation approached "1" for each of the individual filters in the bank (e.g.,  $e^{-0.00001} = 0.99999$ ). The differences in the resulting density calculation among the three filters was still negligible even in the coarsest discretization of the bank. The resulting scaled probability for each of the filters equaled one third, thus the parameter position estimate never changed as determined by Equation (2.29).

An *ad hoc* attempt to alleviate this problem led to artificially scaling  $L$  in each filter by the same scalar value, which allowed for a greater variation in the density calculation. This scaling factor also indirectly affected the determination of the move threshold (recall Subsection 2.4.1), which resulted in a tradeoff between the two. For the parameter

position estimate monitoring method, the move threshold is based on the difference between the parameter position estimate and center of the moving bank. It was decided to set the move threshold to 0.01 and allow the scaling factor to vary. The best result of 500 was determined simply by trial and error.

Figures G-3 through G-7 present the results of the subsequent simulations. For the case of initial parameter match in Figure G-3, the parameter position estimate is quite erratic. This same behavior is exhibited in each of the remaining four figures. The parameter position estimate does track the true parameter, yet never truly "latches on" tightly. In the parameter jump simulations (Figures G-4 and G-5), the parameter position estimate moves slowly in the correct direction. It should be noted that the expansion/contraction logic is inhibited in these simulations. The expansion/contraction thresholds were never determined for the ME/I implementation, since the decision to discontinue its use was made soon after viewing the dramatic improvements displayed by the original Bayesian form (to be discussed in Section 5.5.2).

The reason for the relatively poor result of the ME/I implementation is attributed to the lack of proper scaling of the residuals. Since there are essentially two different types of measurements (position and velocity), each with a varying order of magnitude of accuracy, the resulting residuals have varying orders of magnitude. The information from the relatively more accurate position measurement (smaller individual residual values) is obscured in the equally scaled quadratic by the higher magnitude velocity residuals. It is predictable that better results can be obtained from the original Bayesian form, in which the residuals are properly scaled by the full residual covariance matrix  $A$ . Artificially scaling the individual residuals based on knowledge of their relative accuracy might have some success, yet this was attempted in the previous research with little success [11]. It is conceivable, that given an application using only similar measurement devices or similar relative accuracy, better results might be gained by the ME/I implementation.

### **5.5.2 Bayesian Form Performance**

This subsection discusses the performance results of the parameter position estimation simulations in which the final state estimate is determined by utilizing the original Bayesian form of Equation (2.26). As can be seen, a dramatic level of improvement over the ME/I was obtained with the implementation of the Bayesian form (compare Figures G-3 through G-7 with Figures G-10, G-19, G-22, G-25, G-28, respectively). This was somewhat unexpected, since the residual covariance matrix appeared to be ill-conditioned (the determinant was on the order of  $10^{-248}$ ). However, the inverse was able to be calculated. Additionally, no modifications were made to the pre-multiplier. In this application, using the proper scaling afforded by the true  $A^{-1}$  in the quadratic term of the probability density function resulted in much better performance without any discernible erroneous errors as suggested in Subsection 2.3.2.

The expansion/contraction thresholds were determined while using the parameter position estimate monitoring method. Recall from Subsection 2.4.2 that the expansion threshold is based on the likelihood quotient,  $L$ . If this value is exceeded for all three filters, then the bank is expanded under the assumption that the true parameter position is no longer in the vicinity of the filter bank. When expanded, the three filters were re-located at the widest possible locations in the discretized space;  $\omega_1$ ,  $\omega_{11}$ , and  $\omega_{21}$ , respectively. The threshold determination was obtained by trial and error. A tradeoff had to be made between setting the value low for proper expansion when required, but not too low, which would result in unnecessary expansion. Of course, too high a threshold would not allow for the proper expansion of the bank. The final value of 60 was set, which allowed for expansion given a jump change greater than approximately 4.5 percent (e.g., a jump from  $\omega_5$  to  $\omega_{14}$ ).

Recall from Subsection 2.4.3 that contraction takes place when the variance of the parameter position estimate falls below a set threshold. In determining the contraction

threshold, it was found that two different levels of contraction, medium and fine, resulted in better performance. The medium bank discretization placed the outer two elemental filters at  $\pm 5$  points from the center filter (e.g.,  $\omega_1$ ,  $\omega_6$ , and  $\omega_{11}$ , respectively). The specific thresholds for medium and fine contraction were set at 5.0 and 2.0 respectively. These values were set relatively high, which resulted in very quick contraction of the bank (typically within five sample periods). The reasons for this will be discussed in the subsequent paragraphs.

The anticipated response of the filter bank subject to this expansion and contraction design was to have the bank expand to the widest position (given a large jump change in the true parameter) in order to locate the true parameter position in the proper half of the parameter space. The medium contraction would then locate the true parameter position within the resulting half of the parameter space and a fine contraction would subsequently take place. The contraction logic for determining the center filter for each of the contraction levels was based on the best estimate of the true parameter. In making this determination, it was anticipated that the contraction design would locate the center filter somewhere in between the discrete parameter points of the expanded filter bank. However, after a bank expansion, the contraction logic consistently placed the center filter at one of the expanded filter bank discrete parameter locations. This occurred for both the medium and fine contraction levels. For example, if the true parameter position jumped from  $\omega_5$  to  $\omega_{17}$  (reference Figures G-15 through G-17), the bank would first attempt to contract and center the medium level discretized filter bank at either location  $\omega_{11}$  or  $\omega_{21}$ , i.e., at one of the three parameter values of the coarsest discretization. If the decision were  $\omega_{11}$ , then the resulting bank of filters would be located at  $\omega_6$ ,  $\omega_{11}$ , and  $\omega_{16}$ , respectively. The next contraction would place the finely discretized space at  $\omega_{10}$ ,  $\omega_{11}$ , and  $\omega_{12}$ , or  $\omega_{15}$ ,  $\omega_{16}$ , and  $\omega_{17}$ , depending on which decision was made. The finely discretized bank of filters would then "move" to the correct

location based on the move logic. It should be noted that, if the first contraction decision is to locate the center filter at  $\omega_{21}$ , additional logic will prohibit centering the filter bank at the edge of the discretized space. Instead the logic will place the outer filter at the edge, resulting in the medium-contraction filter bank located at positions  $\omega_{11}$ ,  $\omega_{16}$ , and  $\omega_{21}$ .

No errors could be found in the program coding that would directly cause this situation to occur. In order to compensate for this, the contraction thresholds were set relatively high. Allowing the bank to contract faster to a fine discretization and then move according to the move logic resulted in a faster overall response. It should be noted that the contraction logic usually made the correct decision to center the bank on the filter closest to the true parameter. Occasionally, with the thresholds set high, the contraction logic made a wrong decision but the bank invariably expanded again until the correct decision was made. For the example given in the previous paragraph, the correct decision was to attempt to center the bank on  $\omega_{21}$ , which resulted in the bank located at positions  $\omega_{11}$ ,  $\omega_{16}$  and  $\omega_{21}$ .

Another expansion design was attempted, in which the bank was allowed to expand only to a medium level of discretization at positions  $\omega_6$ ,  $\omega_{11}$ , and  $\omega_{17}$ , i.e., disallowing the coarsest discretization of  $\omega_1$ ,  $\omega_{11}$ , and  $\omega_{21}$ . It was anticipated that this design would allow faster contraction in the correct third of the parameter space, once that was identified correctly at the medium discretization level. This method resulted in a poorer performance for the first few simulations and was subsequently abandoned.

Several examples are shown which inhibit bank expansion and contraction in order to show the relative response time allowing only the move logic to be active (compare Figures G-29 through G-32 with G-13, G-16, G-19, and G-22, respectively). This comparison was only accomplished using the parameter position estimate monitoring method. The move threshold was set at 0.15 for each of these simulations (to be discussed later in this section). In all cases, the expansion/contraction simulations appear

much like underdamped responses, whereas the move-only simulations appear as overdamped responses. For this application, it is more desirable to have the parameter position estimate approach the true parameter position rapidly as with expansion/contraction (better overall state estimates during the transition time), than slowly with move-only (poorer overall state estimates during the transition time).

Once the Bayesian form was selected and expansion/contraction thresholds determined, simulations could be run comparing the relative responses utilizing each of the three parameter position estimation techniques. Move thresholds had to be determined for each of the three techniques, since they are each based on a different hypothesis for the move logic. For the parameter position estimate monitoring method, the move threshold is based on the difference between the parameter position estimate and center of the moving bank. If this value is exceeded, then a decision is made to move the bank in the direction of the parameter estimate. For the residual monitoring technique, the move threshold is based on the likelihood quotient,  $L$  (same as the expansion logic). If this value is exceeded for all three filters, then a decision is made to move the bank in the direction of the filter with the smallest  $L$ . For the probability monitoring technique, the move threshold is based on the conditional probability. If the conditional probability of the filter with the highest value exceeds the threshold, then a decision is made to move the bank in the direction of this filter. In each case, there was a tradeoff between consistency (less variation of the parameter position estimate around the true parameter position value during a "tracking" phase) and response time (how quickly the parameter position estimate approaches the true parameter in an "acquisition" or "re-acquisition" phase). Setting the threshold too low resulted in unnecessary move decisions, whereas setting the threshold too high resulted in slow responses to actual parameter position changes. The move thresholds for the remaining two techniques, residual and probability monitoring, were 10 and 0.9, respectively. It should be noted that neither the residual nor the probability

monitoring method requires that the bank be centered on the current parameter position estimate.

Figures G-8 through G-28 present a small sampling of all the runs accomplished as discussed previously in this section. Each simulation is presented with each of the techniques on the same page for ease of comparison. No one particular technique can be said to be the most effective. The residual monitoring technique appears to give the quickest response time. The probability monitoring appears to give the most consistent response. Despite its success in previous research [11], the parameter position estimate monitoring technique appears to give the poorest relative response, both in terms of consistency and response time. The overall response is still excellent, especially in comparison to previous research [11]. The reasons for the differences can be found in the hypothesis conditions for which each technique is based. (Additionally, the sensitivity of the individual techniques to their respective threshold values affects the outcome to a minor degree.)

In the residual monitoring technique, the decision to move is based on the single most recent sample of the residuals (no past history), which accounts for this method having the fastest response time. However, this method is supposed to be plagued by single large disturbance input samples, which may cause unnecessary move decisions. However, it is possible that the simple rate feedback active in all simulations reduces the effect of large disturbance samples, resulting in better conditioned residuals. This may account for the relatively good consistency. Even during short periods of excursions from the nominal, the actual magnitudes of these variations are relatively small. (This concern can be limited to a minor degree by a judicious choice of the threshold value.)

The probability monitoring method is based on not only the current measurement sample, but also on the past history of measurements. This acts as a "smoothing agent", which results in better overall consistency. In fact, once the parameter position estimate

"latched" tightly onto the true parameter, no variations were seen until the true parameter position moved again. Additionally, the response time is not much worse than for the residual monitoring technique.

The parameter position estimate monitoring technique is similar to the probability monitoring in that it is based on the current and past history of individual measurements (or residuals) for each of the filters in the bank. This technique would be expected to display a level of consistency at least better than that of the residual technique. Yet, in each of the plots, this technique is clearly more erratic than the other techniques. Again, the choice of threshold value affects the results to a minor degree, but does not account for the overall poorer performance. It is speculated that the fact that this is the only technique that requires the bank to be centered on the parameter position estimate might somehow account for the relative performance degradation. The speed of response is similar to those of the other methods if the criterion is based simply on the desire to have the parameter position estimate in the close vicinity of the true parameter. If the additional transient variations are taken into account, then the performance can be said to be poorer.

### **5.5.3 Section Review**

In this section, it was shown that the original Bayesian formulation of the probably density function for measurements (residuals) in Equation (2.26) resulted in dramatically better performance than that achieved by the ME/I method. In terms of parameter position estimation, all three move logic techniques resulted in excellent parameter position estimation responses. However, none of the techniques can be said to be the best. Each had positive and negative attributes. The residual monitoring method was shown to have the fastest response time, yet suffered to a minor degree in terms of consistency. Utilizing the probability monitoring technique resulted in much better consistency, yet the response time was relatively slower. The parameter position



monitoring technique was slightly worse in both respects. The state estimation error results for all the simulations conducted were practically identical to those of the single filter analysis.

### **5.6 MMAC Performance**

This section presents the results obtained from simulations implementing the MMAC design method utilizing many of the specific techniques discussed in Section 2.6. These control methods include: MMAC, modified MMAC, MAP, and "modified" MAP (to be discussed below). The MMAC utilizes the unconditional "blending" of the control inputs from each of the active filter/controllers. Modified MMAC institutes a lower bound of 0.25 on the probability of each filter/controller in the probability-weighted average computation to form the MMAC control output, which precludes the blending of those under this threshold. The MAP method declares the filter/controller with the highest probability as the one to provide the final control. The fixed-gain, single-changeable-gain, and modified single-changeable-gain control methods were not investigated. The inherited program code did not implement any of these methods as presented in Section 2.6, and the additional time to investigate these methods was not warranted, due to the outstanding performance of the MMAC. The inherited code implemented what was referred to as the modified single-changeable-gain control but in actuality this was not so. What the code implemented was similar to the MAP method. Instead of the single filter/controller with the highest probability, this method allowed the filter/controller based on the parameter value closest to the parameter position estimate to generate the control inputs. This method is closest in concept to MAP control and will be referred to "modified" MAP control for the remainder of this research. Additionally, the three different move logic techniques presented in the previous section are carried through in this section to show the possible effects of control on parameter position estimation. Appendix H presents all the plots associated with this section.

Applying control in the face of true parameter position variations did not dramatically degrade the LOS deviations for any of the four methods investigated. In fact, only during the short period of time in which the filter bank was expanding, contracting or moving in response to a parameter position variation did the actual LOS deviation degrade from that of single controller performances presented in Section 5.3. In any of the situations simulated for this section, the resulting X and Y LOS error plots are essentially identical. As such, only Figures H-1 and H-2 are presented as single representative examples. These figures are shown in an expanded view in an attempt to determine a difference visually in the LOS deviations during a parameter change as discussed in Section 5.6. If presented with a normal scale, these plots would be indistinguishable from those of the single filter analysis (Figures F-17 and F-18). For reference, these two plots were obtained from the simulation resulting in Figure H-18 (presented out-of-order for purposes of this discussion). Note the lack of any visible change after the true parameter position jumps from  $\omega_5$  to  $\omega_{17}$  at the five second mark. In an attempt to discern any differences between any of the combinations, the temporal RMS average calculation was limited to a short period of time (5 to 5.75 seconds) during the parameter jump simulations, just after the true parameter jump occurred (reference Figures H-3 through H-14). Table 5-2 presents the results of these calculations. The differences between any of the combinations are so small as to be considered negligible. However, the modified MMAC is consistently worst by a small percentage. The performance degradation during this time frame places the Y LOS deviations outside the one micro-radian specification. Again, the difference between the X and Y LOS performance is due to the geometry of the tripod legs relative to the X and Y axes. Yet, given the short period of time and the drastic change in the true parameter, this result is still highly encouraging.

In terms of parameter position estimation, Figures H-3 through H-38 show a small representative sample of all the simulations that were run, yet no consistent trends or even

	MMAC	Mod MMAC	MAP	Mod MAP
Residual Monitoring	X LOS = 0.93603 $\mu$ rad	X LOS = 0.95019 $\mu$ rad	X LOS = 0.93031 $\mu$ rad	X LOS = 0.93417 $\mu$ rad
	Y LOS = 0.12406 $\mu$ rad	Y LOS = 0.12758 $\mu$ rad	Y LOS = 0.12387 $\mu$ rad	Y LOS = 0.12387 $\mu$ rad
Probability Monitoring	X LOS = 0.92396 $\mu$ rad	X LOS = 0.93859 $\mu$ rad	X LOS = 0.92428 $\mu$ rad	X LOS = 0.92282 $\mu$ rad
	Y LOS = 0.12485 $\mu$ rad	Y LOS = 0.12769 $\mu$ rad	Y LOS = 0.12479 $\mu$ rad	Y LOS = 0.12467 $\mu$ rad
Parameter Position Monitoring	X LOS = 0.91759 $\mu$ rad	X LOS = 0.94510 $\mu$ rad	X LOS = 0.92132 $\mu$ rad	X LOS = 0.91624 $\mu$ rad
	Y LOS = 0.12260 $\mu$ rad	Y LOS = 0.12765 $\mu$ rad	Y LOS = 0.12231 $\mu$ rad	Y LOS = 0.12211 $\mu$ rad

Table 5-2. MMAC Control Performance Results

major differences were visible between the effects any of the four methods. The modified MMAC control (with an intermediate threshold on the probabilities of 0.25 for control computation as in Section 2.6.2) appeared to improve the results of the MMAC control slightly. The results from the MAP and modified MAP control methods appear to be practically indistinguishable. The same characteristics of the move logic techniques presented in Section 5.5 can be applied here also. The effect of control does appear to cause more variations (less consistency) in the parameter position estimates for all techniques and simulations.

## 5.7 Summary

This chapter presented the results from all the analyses performed in this research. The chapter began with a discussion of single filter and controller tuning procedures. Each of the individual filter/controller performances was then examined. The best results were obtained with the 26-modal-based model and the 26-modal-cost-based model. In both models, the LOS deviation specification of one micro-radian was met. Due to

unforeseen difficulties, the original parameter discretization determination method had to be abandoned. The final parameter space resulted in 21 evenly spaced points between a 2 percent reduction and an 8 percent increase in the nominal parameter value.

In the MMAE analysis section, the original Bayesian form of residual probability density calculation was shown to result in much better performance than the ME/I formulation. All three move logic techniques displayed very good parameter position tracking characteristics. The residual monitoring technique had a faster response time, whereas the probability monitoring technique had better consistency. Allowing filter bank expansion and medium/fine contraction resulted in slightly better performance than by allowing just move logic. All control design methods investigated had essentially the same performance abilities in the MMAC analysis section. When the parameter position estimate was allowed to settle following a true parameter move, the MMAC controller performance was identical to that of the single controller. The X-axis LOS errors were well within the one micro-radian specification, whereas the Y-axis LOS errors resided on the specification. Of special note, even when the true parameter was allowed to vary, only the Y-axis exceeded the specification.

## **VI    *Conclusions and Recommendations***

### **6.1    *Introduction***

The focus of this research has been to apply moving-bank multiple model adaptive estimation and control (MMAE/MMAC) algorithms to quell undesirable vibrations in the SPICE-4 space structure. The necessity for adaptive control was based on concerns that unadaptive controller designs do not demonstrate enough inherent robustness to be effective in the presence of uncertain parameters in the system model. In this application, the uncertain parameter was assumed to be a scalar multiplier of the undamped natural frequencies in the flexible body modes of the physical structure. The design procedure began with the development of the new system model as the truth model and then to reduced-order models for implementation in the Kalman filters, LQG controllers, and moving-bank MMAE/MMAC algorithms. Inherited simulation software was modified slightly to accommodate system models changes from the previous version, and then performance analyses were conducted to test the capabilities of the resulting various design-model-based single filter/controllers. The parameter space was then discretized to allow for parameter variations. Finally, the ability of a moving bank of filter/controllers to estimate the uncertain parameter accurately and apply control effectively was examined.

The final conclusion of the research indicates that the moving-bank MMAE/MMAC design method is extremely effective in quelling unwanted vibrations in the SPICE-4 structure even during periods of large parameter variations. This conclusion is substantiated in the following section.

### **6.2    *Conclusions***

In Chapter 4, it was shown that the dramatic order reduction required in the original system model supplied by the Phillips Laboratory resulted in a truth system model selection that was still a very good representation of the real world system. Many

reduced-order models were generated, in which the only order reduction took place in the flexible body portion of the truth system model. Of the three original order reduction methods presented in Chapter 2, the internally-balanced method had to be abandoned due to numerical problems. This does not imply that this was necessarily a poor modeling method, just that it was impossible to utilize in this application given the ill-conditioned matrices inherent in the system model. Much better success was obtained with the modally-reduced design models and the modal-cost-reduced design models. In each case, it was necessary to include 26 modes in the design model in order for the resulting single Kalman filter/LQG controller performance to meet the LOS RMS specification of one micro-radian levied by Phillips Laboratory. Even though not originally presented, the 26-mode truncated-model-based filter/controller was also very effective at meeting the specification, although its use was discontinued after the single filter analysis. It should be noted that, in each case, the X LOS deviations were always well within the specification, whereas the Y LOS deviations essentially resided on the specification. Of the filter/controllers based on lesser numbers of modes in the design models, the modal-cost method was clearly more effective than the modal method, even though the design specification was not met.

During the original parameter discretization procedure, it was discovered that the modal-cost-based filter/controller performance became degraded when the design model was based on a new parameter value (i.e., an increase or decrease in the scalar multiplier of the undamped natural frequencies). At the new parameter values, the controller performance was not able to meet the LOS specification. It was speculated that, at the new parameter value, the modal-cost method would have determined a new set of appropriate modes to be maintained in the design model, different from the modes based on the nominal parameter value. The use of the modal-cost order reduction method was discontinued at this point.

The original discretization procedure also had to be abandoned. The problem occurred with a reduction in the parameter value. Both the 26-mode modal- and truncated-based filter/controllers experienced an unacceptable performance degradation past a 2 percent reduction in the nominal parameter value. If the discretized space were cut off at this point, the resulting space would not have allowed for a good test of the moving-bank MMAE/MMAC algorithms. The discretized parameter space was modified to be evenly spaced at 0.5 percent increments from a 2 percent reduction to an 8 percent increase in the nominal parameter value. This resulted in a 21-point parameter space that allowed for a full analysis of the moving-bank method, with expansion and contraction as well as motion of the filter bank. The 26-mode modal-based-model was finally chosen to continue the moving-bank analysis, due to its relative robustness as compared to the 26-mode truncated model.

Of the two formulations in the residual probability density function used for computation of the hypothesis probabilities within the multiple model methodology, the use of the original Bayesian form resulted in much better parameter position estimation ability than the use of the Maximum Entropy with Identity residual covariance modification (ME/I). Allowing expansion and contraction of the filter bank consistently resulted in a faster overall response time than allowing move logic only. Although all of the three move logic techniques investigated were very effective at parameter identification, there was no clear winner. The residual monitoring technique reacted to parameter changes more quickly, whereas the probability monitoring technique reacted with less estimation error variance. The parameter position estimate monitoring technique was the poorest performer. Residual monitoring was expected to have the quickest response, since the move logic was based only on the most recent measurement sample. Probability monitoring was more consistent, since the move logic incorporated the past history of measurement samples. The results for the parameter position estimate method

were unexpected and somewhat difficult to explain. Possible threshold effects in combination with the actual move logic may have contributed to the poorer performance.

After applying LQG-based control with *any* of the methods investigated, the resulting performance was indistinguishable from that of the single controller analysis utilizing the same model-based filter/controller. Only by examining the LOS RMS average for a short period of time around a large parameter jump was a difference detectable. Even then, the one micro-radian specification was exceeded only in the Y LOS direction. The X-axis LOS errors were still within the specification. Once the short transition period after a parameter move was expired, the Y-axis LOS error once again resided on the specification. There were no major trends noted between any of the different MMAC control methods investigated. All worked equally well. The only visible effect of control on parameter estimates was a slight increase in the parameter position estimation variation for all the simulations.

These results indicate that the MMAE/MMAC algorithms will provide highly effective control for the SPICE-4 structure, even with large parameter variations. The following section will present areas of future research.

### **6.3 Recommendations**

This research proved the effectiveness of the moving-bank MMAE/MMAC algorithms as applied to the SPICE-4 structure. Future recommendations are:

1. Explore the effects of dither inputs to the system model to enhance parameter identification above what was achieved in this research [8].
2. Investigate possible alternative modal-cost-based models determined for each of the discretized parameter points in an attempt to overcome the difficulties discovered in the research.



3. Apply the reduced-order filter/controllers developed in this research against the original full-order (large) system model first presented in Chapter 3 and determine if the same performance is achieved.
4. Investigate possible methods to apply effective control to the system model in the region that caused difficulties in this research (parameter reduction beyond two percent).
5. Apply the methods investigated in this research to the large space structure residing in the Astronautical Laboratory at AFIT. Current research is attempting to determine an accurate system model for the structure prior to any control considerations [6]. This structure is similar to the tripod construction in the SPICE structure.
6. Investigate the effect of utilizing the more appropriately scaled  $R_f$  values for the filter models.
7. Explore a possible dual parameter space in which the different parameters are based on independent multipliers of groupings of natural frequencies vice the single scalar multiplier utilized in this research.
8. Investigate the possibility of implementing a simple windowing procedure for the residual monitoring technique in which the most recent  $n$  measurement samples are utilized in the move logic vice the single most recent measurement sample. This may decrease parameter estimation variation without a large increase in the response time.

### **Appendix A: Spice-4 Structure Truth Model**

This appendix presents the various matrices associated with the truth model as described in Chapter 3. This is representative of the open loop system. The individual matrices are briefly described below. Additionally, several matrices below ( $B_s$ ,  $G_s$ , and  $C_s$ ) contain large blocks of zeros which are not presented. The specific format of these matrices is shown below (e.g., the last 126 rows of  $B_s$  are zeros).

Structure (reference Equations (3.4) and (3.16)):

- $F_s = (36+2n)$ -by- $(36+2n)$  constant structure plant matrix
- $B_s = (36+2n)$ -by-36 constant control input matrix

$$= \begin{bmatrix} B_{s1((18+n) \times 36)} \\ \mathbf{0}_{((18+n) \times 36)} \end{bmatrix}_{((36+2n) \times 36)}$$

- $G_s = (36+2n)$ -by-9 constant noise input matrix

$$= \begin{bmatrix} G_{s1((18+n) \times 9)} \\ \mathbf{0}_{((18+n) \times 9)} \end{bmatrix}_{((36+2n) \times 9)}$$

- $C_s = 56$ -by- $(36+2n)$  constant output matrix

$$= \begin{bmatrix} C_{s1(36 \times (18+n))} & \mathbf{0}_{(36 \times (18+n))} \\ \mathbf{0}_{(20 \times (18+n))} & C_{s2(20 \times (18+n))} \end{bmatrix}_{(56 \times (36+2n))}$$

Disturbance (reference Equations (3.1) and (3.2)):

- $F_n = 24$ -by-24 constant fundamental noise dynamics matrix
- $G_n = 24$ -by-6 constant noise input matrix
- $C_n = 9$ -by-24 constant output matrix

Controller output filter (reference Equations (3.18) and (3.19)):

- $F_f = 18$ -by-18 constant filter plant matrix
- $B_f = 18$ -by-18 constant matrix
- $C_f = 18$ -by-18 constant output matrix

$F_s =$

Mode	$-2\zeta\omega_n$	$-\omega_n^2$	Mode	$-2\zeta\omega_n$	$-\omega_n^2$
1	-5.8448D-01	-8.5404D+02	46	-4.5748D+00	-1.0678D+05
2	-6.0874D-01	-9.2642D+02	47	-4.6371D+00	-1.0971D+05
3	-6.0937D-01	-9.2834D+02	48	-5.1277D+00	-1.3415D+05
4	-6.2216D-01	-9.6770D+02	49	-5.2953D+00	-1.4306D+05
5	-6.2234D-01	-9.6826D+02	50	-5.3940D+00	-1.4845D+05
6	-6.2304D-01	-9.7046D+02	51	-5.4261D+00	-1.5022D+05
7	-6.2581D-01	-9.7908D+02	52	-5.5915D+00	-1.5951D+05
8	-6.2589D-01	-9.7935D+02	53	-5.5938D+00	-1.5964D+05
9	-6.2603D-01	-9.7977D+02	54	-5.7666D+00	-1.6966D+05
10	-6.2624D-01	-9.8043D+02	55	-5.8039D+00	-1.7186D+05
11	-6.2633D-01	-9.8073D+02	56	-5.9139D+00	-1.7844D+05
12	-6.2699D-01	-9.8278D+02	57	-6.3054D+00	-2.0285D+05
13	-6.2700D-01	-9.8283D+02	58	-6.3338D+00	-2.0468D+05
14	-6.2706D-01	-9.8300D+02	59	-6.3824D+00	-2.0783D+05
15	-6.2741D-01	-9.8411D+02	60	-6.4090D+00	-2.0957D+05
16	-6.3197D-01	-9.9847D+02	61	-6.6175D+00	-2.2343D+05
17	-6.3382D-01	-1.0043D+03	62	-6.6563D+00	-2.2605D+05
18	-6.3383D-01	-1.0043D+03	63	-6.6668D+00	-2.2676D+05
19	-4.4330D-01	-1.8741D+03	64	-6.7008D+00	-2.2909D+05
20	-2.1955D-01	-2.4016D+03	65	-6.7131D+00	-2.2993D+05
21	-2.3220D-01	-2.4408D+03	66	-6.7383D+00	-2.3166D+05
22	-6.2740D-01	-9.6101D+03	67	-6.7578D+00	-2.3300D+05
23	-6.7063D-01	-1.0325D+04	68	-6.7734D+00	-2.3407D+05
24	-9.4034D-01	-1.1418D+04	69	-6.8587D+00	-2.4001D+05
25	-7.0486D-01	-1.4769D+04	70	-6.8977D+00	-2.4275D+05
26	-1.8200D+00	-1.5540D+04	71	-6.9206D+00	-2.4436D+05
27	-1.1261D+00	-1.7147D+04	72	-6.9587D+00	-2.4706D+05
28	-7.4808D-01	-1.9192D+04	73	-6.9673D+00	-2.4767D+05
29	-2.4879D+00	-2.3012D+04	74	-6.9858D+00	-2.4898D+05
30	-1.1562D+00	-2.3146D+04	75	-6.9963D+00	-2.4974D+05
31	-2.7978D+00	-3.9936D+04	76	-6.9965D+00	-2.4975D+05
32	-2.9036D+00	-4.3015D+04	77	-6.9999D+00	-2.4999D+05
33	-2.9932D+00	-4.5710D+04	78	-7.0010D+00	-2.5007D+05
34	-3.0759D+00	-4.8272D+04	79	-7.0156D+00	-2.5112D+05
35	-3.1174D+00	-4.9583D+04	80	-7.0438D+00	-2.5314D+05
36	-3.1730D+00	-5.1366D+04	81	-7.0550D+00	-2.5394D+05
37	-3.8535D+00	-7.5762D+04	82	-7.1901D+00	-2.6376D+05
38	-3.9983D+00	-8.1561D+04	83	-7.2130D+00	-2.6545D+05
39	-4.0323D+00	-8.2954D+04	84	-7.2876D+00	-2.7097D+05
40	-4.1851D+00	-8.9361D+04	85	-7.3081D+00	-2.7249D+05
41	-4.3326D+00	-9.5773D+04	86	-7.3724D+00	-2.7730D+05
42	-4.3689D+00	-9.7383D+04	87	-7.4833D+00	-2.8571D+05
43	-4.3869D+00	-9.8187D+04	88	-7.5471D+00	-2.9060D+05
44	-4.4313D+00	-1.0019D+05	89	-7.5838D+00	-2.9344D+05
45	-4.5106D+00	-1.0380D+05	90	-7.6050D+00	-2.9508D+05

91	-7.6149D+00	-2.9585D+05	109	-7.8379D+00	-3.1343D+05
92	-7.6651D+00	-2.9977D+05	110	-7.8379D+00	-3.1343D+05
93	-7.6677D+00	-2.9996D+05	111	-7.8380D+00	-3.1344D+05
94	-7.6923D+00	-3.0190D+05	112	-7.8383D+00	-3.1347D+05
95	-7.7635D+00	-3.0751D+05	113	-7.8385D+00	-3.1348D+05
96	-7.7923D+00	-3.0979D+05	114	-7.8385D+00	-3.1348D+05
97	-7.8026D+00	-3.1062D+05	115	-7.8711D+00	-3.1609D+05
98	-7.8070D+00	-3.1096D+05	116	-8.0121D+00	-3.2752D+05
99	-7.8076D+00	-3.1101D+05	117	-8.1561D+00	-3.3939D+05
100	-7.8080D+00	-3.1104D+05	118	-8.2089D+00	-3.4381D+05
101	-7.8081D+00	-3.1105D+05	119	-8.2604D+00	-3.4813D+05
102	-7.8082D+00	-3.1106D+05	120	-8.2790D+00	-3.4970D+05
103	-7.8084D+00	-3.1107D+05	121	-8.3080D+00	-3.5216D+05
104	-7.8084D+00	-3.1108D+05	122	-8.4075D+00	-3.6064D+05
105	-7.8090D+00	-3.1113D+05	123	-8.4110D+00	-3.6094D+05
106	-7.8159D+00	-3.1167D+05	124	-8.6216D+00	-3.7924D+05
107	-7.8167D+00	-3.1174D+05	125	-8.6242D+00	-3.7948D+05
108	-7.8330D+00	-3.1304D+05	126	-8.6611D+00	-3.8273D+05

$B_s =$

Columns 1 thru 6

2.0825D-02	-1.9380D-02	5.4088D-03	-4.8615D-03	1.7901D-02	-1.5062D-02
-7.9624D-03	-9.4290D-03	-3.7621D-03	-4.0896D-03	9.2551D-03	-5.5808D-04
4.8065D-03	-4.1117D-03	6.7170D-04	-3.5865D-04	2.5588D-03	1.0726D-02
2.4055D-03	-5.3274D-04	3.9175D-03	-9.8286D-04	-8.8023D-04	-5.8466D-04
-6.2029D-04	-2.1723D-03	-9.8336D-04	-3.7525D-03	-2.4147D-03	1.0503D-03
-5.5048D-04	-6.8749D-04	-7.8423D-04	-1.2311D-03	-9.4900D-04	-2.0401D-03
-8.2665D-04	7.1069D-04	1.1465D-03	-1.0145D-03	6.0654D-04	-2.0616D-05
2.5584D-04	3.3590D-04	-9.1416D-04	-8.5733D-04	-1.0135D-04	4.5536D-04
1.0181D-03	1.0139D-03	-6.7856D-04	-7.9555D-04	6.2180D-04	-3.4855D-04
-2.8130D-04	3.2280D-04	-6.8399D-05	-7.9516D-05	3.8447D-04	-3.9670D-04
-1.4195D-04	2.8107D-04	6.7669D-05	7.1693D-05	7.5526D-04	9.1037D-04
-6.9834D-05	6.8963D-05	1.7653D-04	-1.6981D-04	-1.1638D-05	-6.3135D-06
-2.1815D-06	2.1249D-06	-3.6374D-05	-2.9386D-05	-4.3108D-05	3.1560D-05
3.2105D-05	-2.9890D-05	-1.2043D-04	1.3778D-04	8.1165D-05	-8.4986D-05
3.8729D-05	-3.8316D-05	-1.4322D-04	1.4951D-04	5.4485D-05	-5.5825D-05
-2.6955D-04	-2.7634D-04	-1.6335D-04	-1.6301D-04	-2.6080D-04	-2.8837D-04
-2.0228D-03	4.2964D-04	-1.5711D-04	1.4685D-04	1.2849D-03	-2.1148D-03
-2.1939D-04	2.0062D-03	-1.3831D-04	1.5386D-04	-1.8034D-03	-7.2034D-04
-5.7383D-02	5.1451D-02	-1.7732D-02	1.5406D-02	-4.6813D-02	3.5042D-02
3.5596D-02	5.4591D-02	1.6685D-02	2.2033D-02	-5.7328D-02	-1.8325D-03
-3.3235D-02	1.5275D-02	-9.8121D-03	2.0525D-03	1.0854D-03	-6.6632D-02
-4.8382D-02	3.6968D-02	-8.0728D-02	6.4903D-02	2.7353D-02	-1.9310D-03
2.1924D-02	3.3992D-02	3.5100D-02	5.9481D-02	4.0128D-02	-3.5271D-02
-3.1502D-02	-3.1249D-02	-5.0113D-02	-5.2441D-02	-1.9097D-02	-3.4792D-02
4.8542D-03	3.9360D-03	4.9479D-02	-3.7048D-02	1.5019D-02	-1.4405D-02

-3.4610D-02	-3.7056D-02	-4.4808D-02	-5.1492D-02	5.1877D-03	2.0672D-02
2.4742D-02	-7.0010D-03	-2.9458D-03	1.5510D-02	-3.8896D-02	-2.6679D-02
1.9822D-02	2.5229D-02	-3.7735D-04	1.7194D-03	3.9881D-02	4.2077D-02
3.0427D-02	3.4769D-02	-3.1504D-02	-4.9741D-02	-9.8180D-03	-1.8154D-02
1.1445D-02	3.7294D-03	-4.1495D-02	2.3546D-02	1.5148D-02	1.2447D-02
-9.6273D-02	6.3869D-02	7.3746D-02	-4.5165D-02	1.9921D-02	-3.4638D-04
5.8787D-02	9.2329D-02	-4.7043D-02	-7.3714D-02	2.4178D-02	-1.7379D-02
1.8144D-02	1.1304D-02	-1.1937D-02	-2.9254D-03	-2.9355D-02	3.2665D-02
-3.5474D-03	-7.3836D-03	1.0236D-02	4.6998D-03	2.9615D-03	1.9463D-02
-8.7285D-03	4.3026D-03	1.5077D-02	-5.5001D-03	-9.8789D-02	2.8955D-02
-3.6844D-03	-1.3203D-02	7.3814D-04	1.5691D-02	-3.8148D-02	-1.0140D-01
-7.7808D-03	-7.7766D-03	8.7264D-03	9.8636D-03	-1.8169D-03	-7.7932D-03
-1.9869D-02	7.9912D-03	-5.8518D-03	1.8994D-02	5.4274D-03	-1.7367D-02
1.5954D-03	1.6713D-02	-1.4592D-02	-4.5709D-03	-2.4081D-02	-8.4755D-03
2.1872D-02	-2.1572D-02	4.8236D-02	-4.9775D-02	5.1002D-04	-8.1887D-03
-1.0603D-02	-1.3239D-02	1.8710D-02	7.3679D-03	1.0252D-02	-3.2205D-03
-1.0172D-03	7.7044D-03	-9.0440D-04	-6.6180D-03	-1.9426D-02	-1.3994D-02
3.7932D-03	7.4290D-04	-8.7199D-03	2.6735D-03	2.1788D-03	-2.7823D-03
-3.5114D-04	1.1647D-03	-4.0010D-04	-2.4351D-03	-1.6183D-02	2.3512D-02
-1.2400D-03	2.2107D-03	-2.1272D-02	2.0394D-02	6.5539D-03	1.1191D-03
2.7054D-03	2.2760D-03	-4.1960D-03	-1.9248D-03	-2.2450D-03	-9.0702D-03
-1.7086D-03	-4.1469D-03	5.0255D-04	5.6121D-03	-1.7250D-02	2.0818D-02
5.4021D-03	5.2195D-03	-6.5151D-03	-6.1392D-03	5.9618D-03	5.8832D-03
-1.0032D-03	1.2887D-03	3.8591D-04	-7.1603D-04	-8.6593D-04	1.2228D-03
1.7936D-03	-1.1577D-03	-4.9838D-03	4.3096D-03	-1.9034D-03	-1.5044D-03
-1.1601D-03	-1.5347D-03	8.0074D-04	2.1875D-03	4.0587D-04	5.7296D-04
-1.0518D-03	7.2521D-04	3.7595D-04	5.1326D-05	5.6412D-04	-3.5734D-04
3.8115D-05	-4.7317D-04	4.0708D-04	5.2616D-04	5.5933D-04	-3.0414D-04
-6.0625D-03	-5.6384D-03	5.6847D-03	4.1021D-03	2.9092D-03	1.6036D-03
-1.2056D-03	-1.1615D-03	-9.9944D-04	2.9848D-03	6.4703D-03	6.8772D-03
-1.0846D-03	-1.2504D-03	8.0984D-04	6.2275D-04	-2.1386D-03	-2.0653D-03
-7.5946D-04	-1.1258D-03	-8.6159D-05	8.0319D-04	-1.0427D-03	-7.4150D-04
2.4198D-03	-2.3518D-03	-1.1715D-02	1.1566D-02	-6.7564D-05	9.1450D-05
4.2594D-04	5.3651D-04	1.5550D-03	2.1459D-04	7.5117D-04	-1.1073D-03
1.4394D-03	-1.1139D-03	-3.8335D-03	4.1774D-03	2.5202D-03	-2.4905D-03
-8.4999D-03	-6.6327D-03	-6.8309D-03	-6.8943D-03	1.4195D-03	-1.2182D-03
-2.0763D-03	1.9482D-03	9.8527D-03	-1.0054D-02	-1.1771D-04	-1.3759D-03
1.3089D-03	8.1946D-04	1.9108D-03	1.4724D-03	7.0170D-04	-1.0828D-04
2.5979D-03	-2.9024D-03	-9.5893D-03	9.4118D-03	6.3393D-04	-4.6676D-05
1.4434D-03	-2.2485D-03	-1.3528D-03	7.9854D-04	-6.1488D-04	2.3866D-03
2.6168D-03	-6.5113D-05	-4.6589D-03	6.3059D-03	2.6524D-03	1.1308D-03
5.6079D-04	5.6776D-04	6.1443D-03	-5.2007D-03	1.8479D-03	-8.3863D-04
-1.7950D-04	1.4847D-04	-4.9672D-03	5.1583D-03	-4.0083D-03	-3.2352D-03
2.5277D-04	-1.2439D-04	-2.3195D-02	2.3249D-02	-2.7906D-04	1.8576D-04
2.0377D-04	-9.8351D-05	-8.8070D-03	8.9256D-03	-4.4307D-04	4.0222D-05
9.3627D-04	-4.3278D-04	2.7429D-03	-2.0618D-03	-2.8611D-04	5.6349D-05
6.5940D-05	7.6462D-05	1.4200D-04	6.2906D-07	1.0840D-04	3.8109D-05
-3.5894D-03	3.7368D-03	-1.1923D-02	1.2028D-02	-4.0410D-04	9.1945D-04
5.5132D-05	3.3519D-04	1.0987D-03	-6.6144D-04	7.5711D-05	-4.7428D-04

2.2625D-05	-1.1758D-06	-7.9057D-04	7.3789D-04	-2.7957D-03	2.9600D-03
8.2355D-05	1.2036D-04	9.8019D-04	-8.2288D-04	2.8104D-03	-2.7880D-03
-3.6493D-05	-2.3055D-04	-7.5068D-04	4.4651D-04	-4.4294D-04	7.3286D-04
-5.6044D-04	3.9982D-04	-7.3090D-05	-1.0508D-04	-2.8428D-03	2.6773D-03
-4.1420D-03	4.1014D-03	4.6069D-03	-4.6244D-03	-5.4643D-04	5.0071D-04
-3.3344D-04	4.1331D-04	8.4227D-04	-8.2176D-04	4.0411D-04	-4.6991D-04
5.2655D-04	-5.9097D-04	1.0770D-04	-1.2178D-04	-6.5649D-04	6.8507D-04
3.2260D-02	-3.2245D-02	-1.6374D-02	1.6372D-02	-3.3464D-03	3.4032D-03
1.3081D-03	-1.4323D-03	-8.0259D-04	5.7476D-04	7.3799D-03	-7.3128D-03
-5.2366D-02	5.2322D-02	3.8076D-02	-3.7963D-02	-6.9018D-03	6.8051D-03
-7.5112D-05	-7.7593D-05	1.7647D-04	1.6311D-04	4.4750D-04	-5.5768D-04
2.2435D-02	-2.2474D-02	-1.7750D-02	1.7653D-02	-1.0663D-02	1.0822D-02
-5.2096D-04	2.4987D-04	1.2442D-03	2.3040D-04	5.7021D-03	-5.1572D-03
6.7384D-03	-3.3627D-03	-1.4121D-03	6.3201D-03	4.6151D-02	-4.5670D-02
1.0904D-02	1.4637D-02	1.2872D-02	9.9837D-03	-6.1811D-03	8.5140D-03
-1.0228D-02	6.5049D-03	5.5893D-03	-8.2090D-03	1.8502D-02	-1.8748D-02
-8.3630D-04	1.4016D-03	1.1699D-03	-4.7696D-04	-2.0084D-02	2.0138D-02
-6.5308D-03	6.3502D-03	7.1028D-03	-4.5138D-03	2.5413D-03	-4.1990D-03
3.8733D-03	-2.2051D-03	3.1124D-04	6.3054D-03	-1.9568D-02	1.6239D-02
-6.7843D-03	-6.3143D-03	-6.8738D-03	-8.3141D-03	-3.7281D-03	1.2072D-02
1.6356D-03	8.0302D-04	1.8498D-03	3.6134D-03	-5.5747D-03	-4.9842D-03
1.5159D-04	6.7821D-04	1.6374D-03	1.4302D-03	1.0111D-02	9.7530D-03
-1.2173D-02	1.1646D-02	2.9125D-03	-3.3428D-03	-1.1193D-03	4.7067D-04
7.4819D-04	-9.4626D-04	-3.3694D-04	2.6639D-04	-1.2229D-03	1.6384D-03
9.1789D-04	-9.1710D-04	6.4327D-04	-5.8727D-04	9.9837D-04	-8.5760D-04
2.0398D-04	-1.7623D-04	-8.3100D-05	3.2247D-05	2.9414D-03	-2.7496D-03
4.6342D-04	-3.8835D-04	-7.7462D-05	1.1782D-04	-3.0636D-03	3.0485D-03
4.4372D-04	-1.8744D-04	-5.9377D-05	6.1468D-05	-4.3239D-03	4.2048D-03
7.2307D-04	-4.2559D-04	-2.9408D-04	2.6303D-04	-4.2842D-03	4.1992D-03
3.2658D-04	1.0758D-04	6.1178D-05	6.9437D-06	-4.8374D-03	4.5016D-03
2.1957D-04	-5.8115D-05	3.0020D-04	3.4339D-04	1.6137D-03	-1.3108D-03
-4.1675D-03	-5.2231D-03	-5.1865D-03	-4.3768D-03	8.4888D-04	-5.0505D-04
-4.2530D-03	2.1091D-03	1.2151D-03	-3.5789D-03	-4.4858D-03	4.7442D-03
-5.9299D-04	-1.5685D-04	-7.5207D-04	-1.5391D-03	1.6116D-03	1.7077D-03
6.1288D-04	-5.9005D-04	-3.9834D-04	4.1155D-04	-3.1858D-04	3.8925D-04
4.0789D-05	-2.7143D-05	2.4982D-05	9.3759D-05	-7.2509D-04	5.3640D-04
-2.1237D-04	-1.2412D-04	-2.7831D-04	-4.4067D-04	6.2056D-04	8.7015D-04
-8.5243D-04	8.2332D-04	5.0478D-04	-5.4148D-04	-5.7194D-04	5.7286D-04
1.2835D-04	-5.2106D-05	-6.0592D-05	6.4220D-05	3.7394D-04	-3.8847D-04
3.5145D-04	-3.2562D-04	-2.2288D-04	2.7555D-04	-5.3416D-04	5.2481D-04
-8.5534D-04	5.1054D-04	-1.3396D-03	-1.5964D-03	-2.4530D-02	-2.3651D-02
5.0715D-02	-4.8791D-02	-2.0398D-02	2.1464D-02	-3.1082D-03	5.5398D-03
6.8124D-03	3.8103D-03	-3.8574D-03	-4.3801D-03	-1.7990D-02	1.2270D-02
1.0531D-02	-1.3477D-02	-2.7712D-03	6.7726D-03	1.7512D-02	-2.4146D-02
9.2247D-03	-2.4173D-03	-8.5951D-03	1.5832D-03	-1.2632D-02	3.9105D-03
-9.9648D-04	2.9828D-03	-1.3602D-03	-1.8724D-03	5.6663D-03	-6.2398D-03
2.0674D-03	7.3424D-04	-9.2828D-04	-5.8939D-03	4.9088D-02	-4.6893D-02
6.9696D-03	-3.7385D-04	-5.3382D-04	-8.9007D-03	3.4285D-03	1.2758D-02
1.0742D-02	1.1636D-02	-1.7181D-02	-1.4364D-02	-1.4564D-02	-2.5592D-03

2.7282D-02	2.8231D-02	-3.5396D-02	-3.9854D-02	5.1117D-03	-1.3688D-02
1.3465D-02	4.9978D-03	-1.6803D-02	-6.9514D-03	-2.7899D-02	-2.2140D-02
-7.6428D-03	-8.0982D-03	1.4669D-02	1.6974D-02	-1.2869D-02	-1.6169D-02

Columns 7 thru 12

4.9201D-03	-3.8118D-03	1.5341D-02	-1.9922D-02	3.7168D-03	-5.5175D-03
2.6861D-03	1.1287D-03	-8.8118D-04	8.3928D-03	9.8314D-04	2.3411D-03
2.2043D-03	3.6813D-03	-1.0794D-02	-3.4214D-03	-3.8192D-03	-2.5098D-03
-1.2176D-03	-7.5855D-04	-3.1609D-04	2.6599D-03	-4.6071D-04	3.4083D-03
-2.8657D-03	1.3455D-03	1.1557D-03	-4.0799D-04	1.6316D-03	-3.1526D-04
-1.1559D-03	-2.8596D-03	-1.9489D-03	-7.2251D-04	-3.0709D-03	-8.5277D-04
1.1768D-04	8.6878D-04	1.1875D-04	-6.3526D-04	-8.2110D-04	-9.2793D-05
1.0808D-03	-4.0698D-04	4.2411D-04	-2.7676D-04	-4.1586D-04	1.2428D-03
-3.5522D-04	3.0468D-04	-2.8550D-04	7.1359D-04	1.2431D-04	-5.5212D-04
-3.7277D-04	-1.3131D-04	-9.2781D-04	-7.8434D-04	9.9283D-04	8.2761D-04
-8.6180D-04	-9.1350D-04	5.2437D-04	-7.8544D-05	-8.0722D-05	1.2027D-05
8.7743D-05	-2.6812D-05	-1.1060D-05	2.1460D-05	4.8146D-05	-1.0835D-04
9.3909D-05	-2.4455D-05	6.2668D-05	-5.9120D-05	-1.1855D-04	1.4133D-04
-2.3772D-04	2.7665D-04	6.4987D-05	-5.6053D-05	-2.3274D-04	1.7358D-04
-1.9699D-04	2.1238D-04	5.1867D-05	-4.6325D-05	-1.9484D-04	1.7199D-04
-1.9282D-04	-1.9296D-04	-2.9253D-04	-2.5300D-04	-1.8382D-04	-1.8425D-04
2.6394D-04	-2.7531D-04	8.9817D-04	1.6178D-03	-1.9306D-05	5.1470D-05
-9.2309D-05	5.5113D-05	1.9833D-03	-1.4359D-03	2.5834D-04	-2.5279D-04
-1.5479D-02	1.0920D-02	-3.6183D-02	5.4460D-02	-1.0708D-02	1.8088D-02
-2.0904D-02	-4.7952D-03	1.8468D-02	-4.6623D-02	3.0121D-03	-1.5209D-02
-4.0749D-03	-2.4557D-02	6.3126D-02	2.0232D-02	2.4629D-02	1.1589D-02
3.5939D-02	-7.0070D-04	9.8047D-03	-3.9005D-02	1.1815D-02	-5.2862D-02
5.3015D-02	-4.9947D-02	-3.5264D-02	3.0894D-02	-5.5205D-02	4.4546D-02
-2.6130D-02	-5.7174D-02	-3.9809D-02	-1.9007D-02	-7.0204D-02	-2.2761D-02
5.4638D-02	-5.1953D-02	4.6154D-03	-1.2825D-02	3.6461D-02	-6.7366D-02
4.6766D-02	5.8877D-03	3.2776D-02	1.4001D-02	3.7584D-02	4.9023D-02
-4.9868D-02	-5.8560D-02	2.7890D-02	4.4393D-02	5.0325D-02	4.0695D-02
3.1240D-02	3.2968D-02	3.3092D-02	2.3553D-02	1.2023D-02	1.8842D-02
5.8053D-02	-5.3442D-04	-8.9602D-03	-5.0732D-03	-2.5531D-02	4.8057D-02
-1.9617D-03	-6.4951D-02	-2.5194D-02	-2.2010D-02	5.4046D-02	2.5852D-02
-1.8918D-02	-1.0358D-02	6.7605D-03	-3.0982D-02	5.5822D-03	2.7860D-02
-2.8023D-02	1.3286D-02	-2.5435D-02	1.6848D-02	2.2923D-02	-1.9283D-02
9.4076D-03	-2.5384D-02	9.0341D-02	-5.1484D-02	-6.8434D-02	3.1722D-02
-3.3749D-03	-6.3617D-03	-5.8418D-02	-8.7342D-02	4.0589D-02	6.4889D-02
7.6189D-02	-2.1322D-02	-2.5844D-02	2.6148D-02	2.3307D-02	-2.6088D-02
2.5878D-02	7.6359D-02	-1.7667D-02	-2.9915D-02	1.9321D-02	2.5662D-02
5.3870D-03	7.7372D-03	-7.7305D-03	-1.8524D-03	7.7975D-03	5.4077D-03
2.3636D-03	8.5026D-03	1.3410D-02	1.6100D-02	-1.2703D-02	-1.7926D-02
1.6640D-02	1.6639D-02	1.2057D-02	-1.5039D-02	1.9314D-03	4.9999D-04
-3.1811D-05	6.7767D-03	6.1005D-03	-3.4448D-04	-2.9321D-03	-8.5054D-04
-7.7113D-03	4.7632D-04	1.3566D-02	1.0552D-02	-2.1809D-03	-2.3599D-02
1.0716D-02	2.4738D-02	1.4024D-02	6.5963D-03	-1.0523D-02	-1.1844D-02
1.2601D-03	2.0376D-03	2.1235D-02	-2.6720D-02	3.8753D-02	-3.4446D-02

-2.5801D-02	1.9450D-02	-5.4075D-03	-1.4896D-03	9.3353D-03	-1.6482D-04
-3.9184D-03	-6.0208D-03	-2.9935D-03	-5.0448D-03	6.6600D-05	9.7224D-03
6.7680D-03	5.3640D-03	-9.4342D-03	1.3848D-02	-4.2610D-02	3.8245D-02
-5.2154D-02	4.9477D-02	1.1755D-03	3.1170D-03	-5.5203D-03	4.7052D-04
-9.2103D-03	-8.3751D-03	5.6647D-03	5.5019D-03	-7.3972D-03	-8.4551D-03
-9.0665D-04	3.6040D-04	-8.8067D-04	1.1051D-03	-4.5634D-04	1.9160D-04
6.3767D-03	-1.4119D-03	5.4227D-04	1.5048D-03	4.3021D-03	-7.2031D-03
8.9182D-03	-1.0572D-02	1.7044D-03	7.5990D-04	-8.1451D-03	4.7729D-03
-6.0769D-04	1.5969D-03	2.8370D-04	-5.5777D-05	-7.2205D-04	-8.3767D-04
-1.8699D-03	3.3272D-04	-5.9762D-04	8.2594D-04	7.9599D-04	-1.4161D-03
-4.3665D-03	-6.3939D-04	4.0895D-03	4.7844D-03	-3.5589D-03	-5.6596D-03
-7.2863D-03	-7.2308D-03	-5.3124D-03	-4.5966D-03	6.6309D-03	3.4979D-03
2.4388D-03	1.9707D-03	-1.5150D-03	-1.6273D-03	1.4163D-03	1.5566D-03
1.3273D-03	1.1594D-03	-4.3420D-04	-1.1894D-03	4.6274D-04	1.5820D-03
-2.0528D-04	-3.4746D-04	2.1892D-04	4.1004D-05	2.4286D-04	2.2413D-04
-6.8164D-04	7.1315D-04	-2.1407D-03	1.7146D-03	3.8008D-03	-3.7548D-03
-2.1569D-03	2.3097D-03	1.5076D-03	-1.7443D-03	-3.2867D-03	2.7302D-03
-9.8611D-04	1.6677D-03	-1.0753D-03	1.5860D-03	1.9951D-03	-9.7735D-04
-1.1733D-03	1.3242D-03	1.6511D-03	5.2548D-04	-1.4699D-03	2.1452D-03
-2.0453D-03	1.5078D-03	-8.8312D-05	7.7353D-04	2.5784D-03	-3.1161D-03
-9.5451D-04	2.3688D-03	-8.0554D-04	-1.7756D-03	-4.3863D-03	1.3386D-03
3.7850D-03	-1.2772D-03	-4.9271D-03	-1.8195D-03	-1.3993D-04	-6.3229D-03
8.7261D-04	2.5708D-03	1.1594D-03	4.0941D-03	6.8467D-03	-2.6619D-03
-3.7435D-03	4.6453D-03	-3.1886D-03	-1.2958D-03	3.2198D-04	-3.9294D-03
-3.2187D-03	-2.6622D-03	-4.7193D-04	-4.1613D-04	2.7233D-03	-3.2103D-03
-1.1204D-03	1.0515D-03	6.3207D-05	7.1236D-05	-2.0108D-03	2.1294D-03
4.9175D-03	-5.3076D-03	4.6310D-04	-3.5544D-04	1.2932D-02	-1.2749D-02
-1.1219D-02	1.0951D-02	1.0937D-04	-5.4600D-04	9.9860D-03	-1.0433D-02
2.6231D-04	-1.3960D-04	3.5834D-06	1.4882D-04	-2.4894D-04	3.8452D-04
-3.0952D-03	3.6162D-03	-1.5392D-03	1.0099D-03	-5.4366D-03	4.8445D-03
8.4824D-04	-1.2761D-03	-4.3672D-03	4.4252D-03	-1.4391D-02	1.4405D-02
-9.3695D-03	9.3937D-03	-5.3244D-04	7.0229D-04	-1.1512D-03	1.2644D-03
9.1751D-03	-9.1938D-03	7.7699D-04	-7.4819D-04	1.5809D-03	-1.6560D-03
-1.9880D-03	2.2171D-03	4.1241D-04	-3.2781D-04	1.5762D-03	-1.5085D-03
-8.8142D-03	8.6296D-03	-8.4299D-04	1.2303D-03	-2.2901D-03	2.6643D-03
-2.2027D-03	2.2195D-03	-5.7769D-04	6.3890D-04	-9.4642D-04	9.4314D-04
5.4041D-04	-5.4563D-04	1.0676D-04	-8.5472D-05	-4.0010D-03	3.9938D-03
-4.0206D-03	4.0168D-03	2.1505D-05	4.9373D-05	7.0178D-04	-5.8416D-04
-5.4589D-04	6.1702D-04	-3.1832D-03	3.1142D-03	-8.3111D-05	7.5929D-06
-6.0248D-04	6.8897D-04	-1.0957D-02	1.0998D-02	2.6456D-03	-2.5469D-03
3.5635D-03	-3.2695D-03	-8.9308D-03	8.9969D-03	4.9661D-03	-5.3212D-03
2.6556D-05	4.0789D-04	-9.5854D-04	8.3781D-04	6.9331D-04	-2.8258D-04
5.6825D-03	-6.0038D-03	-1.3149D-02	1.2962D-02	8.6793D-03	-8.2594D-03
-4.0050D-03	2.8708D-03	-5.4569D-02	5.4497D-02	4.1703D-02	-4.1665D-02
-3.4578D-02	3.4620D-02	1.0745D-02	-9.6338D-03	-9.2532D-03	7.7063D-03
5.6827D-03	-5.1785D-03	1.7642D-03	1.3228D-03	9.9541D-04	1.0239D-03
-1.5358D-02	1.3742D-02	6.0410D-03	-6.2949D-03	-5.0329D-03	5.6078D-03
1.5702D-02	-1.6174D-02	1.1376D-02	-1.1503D-02	-9.3788D-03	9.3905D-03
-5.1484D-03	1.9637D-04	8.2724D-03	-1.0139D-02	-7.4973D-03	8.9546D-03



1.4220D-02	-1.5441D-02	3.8237D-03	-1.1294D-02	-1.0740D-02	2.4125D-03
8.3476D-03	-5.5179D-03	1.1401D-02	4.5768D-03	2.0104D-03	7.9084D-03
-3.0262D-03	-3.6332D-03	1.5869D-02	1.5399D-02	1.5812D-02	1.6591D-02
1.0116D-02	1.0701D-02	1.6311D-03	1.7400D-03	2.4214D-03	2.9477D-03
4.0814D-04	-6.2438D-04	-1.0671D-03	1.6463D-03	4.8394D-04	-7.5851D-04
5.1244D-04	-5.9267D-04	-8.6781D-03	8.2823D-03	3.1354D-03	-3.3722D-03
-2.8274D-04	3.0130D-04	-1.0408D-03	9.5233D-04	5.8764D-04	-5.9220D-04
-9.9563D-04	1.3095D-03	-5.3999D-04	5.7062D-04	-5.9071D-05	3.5831D-04
1.1510D-03	-1.2451D-03	-6.1176D-04	4.5936D-04	-5.4159D-04	4.2704D-04
2.5579D-03	-2.5359D-03	6.1687D-04	-7.1997D-04	-1.2383D-04	2.4925D-04
1.4895D-03	-1.6764D-03	3.2446D-04	-5.9732D-04	-1.0676D-04	2.6888D-04
1.9136D-03	-1.6727D-03	2.0995D-03	-2.0821D-03	-7.2694D-04	8.6237D-04
-2.6939D-04	9.6400D-04	5.2058D-04	-2.1531D-04	2.2931D-04	4.3812D-04
-6.0023D-04	4.6838D-04	1.0454D-03	-5.8920D-04	-6.7736D-04	6.6762D-04
3.6761D-03	-3.6402D-03	-3.5685D-03	4.0126D-03	3.1379D-03	-3.0392D-03
7.4913D-04	7.8337D-04	-1.4777D-02	-1.4048D-02	-1.4226D-02	-1.4853D-02
3.3503D-04	-2.2964D-04	-3.8112D-04	3.8374D-04	2.9727D-04	-3.2228D-04
4.4889D-04	-5.8155D-04	8.0565D-04	-1.6186D-04	-7.3475D-05	7.0710D-04
6.0354D-04	4.0467D-04	-1.7668D-03	-1.6665D-03	-1.7960D-03	-1.8880D-03
4.5904D-04	-4.6726D-04	-5.9504D-04	4.8687D-04	3.6722D-04	-4.7665D-04
-2.9616D-04	3.3749D-04	-5.0514D-04	4.1715D-04	3.5791D-04	-3.9698D-04
4.6928D-04	-3.8844D-04	-1.1719D-04	4.7874D-04	3.9932D-04	-8.1982D-05
-2.3816D-02	-2.4555D-02	-1.4585D-03	-1.1654D-03	-2.1105D-03	-2.9626D-03
1.2366D-03	-5.3080D-03	-5.6227D-03	1.2599D-03	4.1113D-03	-1.7654D-03
1.2851D-02	-7.8285D-03	3.7494D-02	-4.0877D-02	-2.0502D-02	2.6488D-02
-8.9822D-03	1.7003D-02	2.6166D-02	-1.5429D-02	-1.7212D-02	6.0901D-03
1.0561D-02	1.0138D-03	-3.0134D-02	3.1103D-02	1.7786D-02	-2.1647D-02
-3.8234D-03	5.4312D-03	-1.1555D-02	9.8426D-03	7.4017D-03	-6.0509D-03
-3.2807D-02	3.3622D-02	-3.6630D-03	-4.5794D-04	5.6868D-03	4.2302D-04
-1.0128D-02	-1.1902D-02	-1.4839D-02	-7.6984D-03	1.6525D-02	1.4595D-02
1.3386D-02	9.7869D-03	1.2432D-03	-6.8769D-03	5.2273D-03	2.6041D-03
-2.0025D-03	1.3714D-02	-2.3545D-02	-1.2038D-02	2.6718D-02	1.7462D-02
3.2772D-02	2.8919D-02	1.4373D-02	2.5066D-02	-2.0998D-02	-3.0824D-02
2.0242D-02	2.3704D-02	-1.2735D-02	-1.0947D-02	1.9762D-02	1.9124D-02

Columns 13 thru 18

-1.7012D-03	-9.3260D-05	1.0002D-03	1.7186D-03	4.3424D-05	-9.5038D-04
-3.8429D-04	-5.5845D-03	-5.2358D-03	3.2831D-04	5.6523D-03	5.3340D-03
-6.1782D-03	-2.9594D-03	3.4337D-03	6.1818D-03	2.8427D-03	-3.2773D-03
-5.5292D-04	-5.1681D-04	-3.1398D-04	4.5266D-04	5.0638D-04	-2.7944D-04
-2.5868D-04	6.7995D-04	7.9327D-04	3.1171D-04	-9.1301D-05	-5.3576D-04
4.1930D-04	1.0557D-04	7.1248D-05	4.2165D-04	4.8722D-04	4.4675D-04
1.6346D-04	3.2379D-04	-3.2964D-04	-1.7693D-04	1.0339D-04	-1.0672D-04
2.4226D-04	-2.1807D-05	-9.6626D-06	2.3124D-04	-2.9392D-04	-3.0520D-04
-1.3176D-04	-2.1414D-05	-6.9406D-05	-1.5084D-04	8.9133D-05	8.5253D-05
-4.0261D-05	-1.9072D-05	6.0886D-05	1.7865D-05	4.8771D-05	6.2876D-05
-5.9409D-05	-7.2264D-05	1.2593D-05	2.2427D-07	-2.6634D-05	-8.2893D-06
-1.6550D-05	-4.3894D-04	3.4886D-04	2.0442D-04	-6.3242D-04	5.3487D-04

-5.5168D-04	1.5326D-04	4.0531D-04	-6.0181D-04	2.2397D-04	3.6730D-04
3.8851D-04	-4.9281D-04	4.1770D-04	-2.3769D-04	1.3320D-04	-2.0966D-04
-1.2550D-04	1.1386D-04	-1.2055D-04	1.3840D-04	-1.5012D-04	1.4322D-04
-1.9485D-03	-1.9305D-03	-1.9310D-03	-1.9501D-03	-1.9653D-03	-1.9647D-03
-2.6466D-03	8.9418D-04	3.2011D-03	2.4237D-03	-5.0838D-04	-3.2828D-03
-2.1601D-03	-3.3199D-03	-1.2433D-03	2.4035D-03	3.3576D-03	8.6619D-04
4.9675D-03	4.1142D-04	-3.2624D-03	-5.0311D-03	-1.8783D-04	3.0714D-03
5.3365D-03	2.2522D-02	1.7317D-02	-4.7915D-03	-2.2660D-02	-1.7881D-02
2.2858D-02	8.0833D-03	-1.6079D-02	-2.2940D-02	-7.3308D-03	1.5294D-02
-1.3726D-02	-1.5007D-02	1.3411D-02	1.1380D-02	6.8362D-04	2.4165D-03
7.6959D-03	4.0665D-03	8.3214D-03	1.0959D-02	-1.3555D-02	-1.3353D-02
3.2595D-03	2.8205D-03	4.3776D-04	3.2862D-04	-1.1777D-02	-1.1901D-02
-6.6266D-03	-2.3430D-03	3.5147D-05	5.4491D-03	-3.4526D-03	3.2830D-03
9.8636D-03	1.1290D-02	1.7904D-02	1.7890D-02	-2.2044D-02	-2.1434D-02
-2.4487D-02	-2.5193D-02	1.8937D-02	1.8385D-02	4.0536D-05	1.1628D-03
4.5715D-04	-2.2726D-04	-9.5629D-03	-8.3652D-03	-1.2097D-02	-1.3244D-02
-2.1008D-02	-1.6700D-02	-4.0795D-03	-1.0332D-02	2.4935D-02	2.7186D-02
1.6401D-02	2.2081D-02	-2.7369D-02	-2.3954D-02	9.8421D-03	3.3597D-03
-8.5691D-03	6.2674D-03	-5.3483D-03	2.1074D-03	8.7746D-03	-3.2001D-03
1.4736D-02	-3.0377D-03	-4.3959D-03	1.7463D-02	-1.2852D-02	-1.3684D-02
1.5797D-02	-5.5109D-03	-1.3977D-02	1.2264D-02	2.2581D-03	-1.3276D-02
1.1012D-02	-2.5225D-02	1.5387D-02	1.3801D-02	-2.2462D-02	1.2375D-02
8.4619D-03	2.8993D-03	-1.3866D-02	1.3702D-02	-6.5487D-03	-1.3103D-03
1.2139D-02	1.0361D-02	-1.3144D-02	8.3976D-03	1.2395D-02	-1.9241D-02
-2.6684D-02	-3.3698D-02	-3.4513D-02	-2.6621D-02	-3.6749D-02	-3.8477D-02
1.5669D-02	-2.3007D-02	2.1295D-02	2.4860D-02	-1.9935D-02	5.8940D-03
-3.2900D-02	-1.4509D-02	1.5507D-02	-2.5540D-02	-7.9550D-04	1.9731D-02
-1.2863D-02	2.0993D-03	5.0104D-03	1.0298D-02	-9.1220D-03	5.4007D-03
2.1983D-02	-2.7378D-02	-2.7878D-02	1.3120D-02	-2.2741D-03	2.1467D-02
1.9545D-02	9.3887D-04	1.7005D-02	-3.0371D-02	-2.7171D-02	1.8647D-02
-1.8161D-02	2.4834D-02	-4.4263D-03	7.6056D-03	-2.0355D-02	1.4732D-02
4.7143D-03	-4.2384D-03	1.8724D-02	-1.7029D-02	2.6571D-02	-2.2161D-02
-2.6158D-02	3.0840D-02	-3.0629D-02	2.4043D-02	-6.5227D-03	8.2216D-03
-2.2580D-02	1.6228D-02	-5.3793D-03	5.0253D-03	-2.2296D-02	2.9862D-02
-8.3785D-03	7.1815D-03	-1.5479D-02	2.3383D-02	-2.0225D-02	1.2444D-02
-6.2874D-03	-1.1546D-02	-9.7670D-03	-7.4707D-03	-6.8103D-03	-1.0963D-02
-2.2051D-02	2.3572D-02	-2.4047D-02	2.1719D-02	-2.4722D-02	2.4268D-02
-1.5522D-02	-3.2133D-03	-4.4252D-03	2.0553D-02	1.8656D-02	-1.5240D-02
-1.6247D-02	2.2615D-02	2.1246D-02	-9.9678D-03	-5.1798D-03	-1.3687D-02
-5.8000D-03	2.3293D-02	-1.8599D-02	-6.6058D-03	2.4297D-02	-1.6536D-02
-2.3395D-02	4.6713D-03	1.6299D-02	-2.3074D-02	6.7683D-03	1.8804D-02
3.3424D-03	-4.1734D-03	-2.4809D-03	3.6064D-03	-1.8758D-03	-8.2339D-04
-1.7768D-03	2.4528D-03	-3.7478D-03	2.5191D-03	3.6271D-03	-5.3051D-03
-5.8727D-03	-6.0903D-03	-5.7937D-03	-6.0529D-03	-6.2057D-03	-5.5296D-03
-4.9849D-03	4.3860D-03	6.2581D-03	-6.3385D-03	-4.6669D-03	-5.4971D-03
-1.6757D-02	-7.8301D-03	9.2053D-03	1.6060D-02	2.2384D-02	-2.2144D-02
2.4165D-03	-2.1870D-02	-2.8184D-02	1.5598D-02	1.4866D-02	1.5917D-02
2.9786D-02	-2.1329D-02	6.6616D-03	-2.2823D-02	9.6209D-03	-8.7374D-04
-1.1055D-02	8.8916D-03	8.9088D-03	-1.1660D-02	1.5542D-03	2.3684D-03

-1.8868D-02	2.0037D-02	-2.5524D-02	2.4175D-02	6.9070D-02	-6.8697D-02
-5.5537D-02	5.3996D-02	5.4427D-02	-5.7110D-02	7.4736D-03	-2.8512D-03
-4.3557D-02	4.7100D-02	-4.4980D-02	4.1054D-02	-1.4616D-02	1.4604D-02
1.6721D-02	-1.6701D-02	1.4338D-02	-1.4358D-02	2.9112D-02	-3.0717D-02
6.1856D-03	-7.2650D-04	-2.2651D-03	9.2658D-04	6.4710D-03	-7.2626D-03
-6.8161D-03	3.1994D-03	1.0746D-03	4.3684D-03	-7.7067D-03	4.1334D-03
3.0046D-03	1.7691D-03	3.7888D-04	-4.9117D-03	-9.6345D-04	-4.2102D-03
8.9719D-04	6.1932D-03	-5.7517D-03	-1.3477D-03	1.5720D-02	-1.5631D-02
1.0339D-04	7.0610D-03	-1.3721D-02	8.3858D-03	4.9361D-03	-7.9248D-03
1.4049D-02	-1.2620D-02	-6.7164D-03	1.1403D-02	-4.4888D-03	-2.4160D-03
-8.6199D-03	-8.4593D-03	-8.3789D-03	-8.4727D-03	-7.9477D-03	-8.0418D-03
2.1579D-03	-1.1024D-03	-2.0239D-03	-1.9377D-03	-8.9320D-03	1.0863D-02
-4.4142D-04	-1.2670D-03	-9.0362D-03	4.2766D-03	9.7600D-04	-4.2214D-04
-1.5536D-02	-9.1640D-03	-2.6118D-02	-2.4511D-02	-8.3415D-03	-7.3561D-03
-2.0717D-02	-2.7010D-02	-7.2202D-03	-9.6211D-03	-1.6258D-02	-1.7506D-02
1.7359D-02	1.8365D-02	1.4978D-03	2.6994D-04	-3.0304D-02	-2.9707D-02
-1.9957D-02	-1.3318D-02	2.2817D-02	2.6241D-02	-9.1192D-03	-8.2002D-03
1.8405D-03	4.0764D-03	-3.4896D-03	-1.5261D-03	-2.5891D-03	1.4794D-03
2.1524D-03	8.7663D-04	1.1213D-03	-1.3940D-03	-7.8323D-04	-2.0386D-03
1.2134D-03	-8.8666D-04	-7.1098D-04	-1.7431D-03	1.5981D-03	6.5913D-04
1.2164D-02	1.1293D-03	-3.3839D-03	-1.1162D-02	-1.1421D-02	1.2685D-02
-7.7709D-03	1.7618D-02	1.7200D-02	-8.9695D-03	-9.8323D-03	-7.2791D-03
1.1358D-02	-4.6959D-03	2.7270D-03	-9.9054D-03	-9.5788D-03	1.0191D-02
-4.2936D-03	-3.0340D-03	-2.6500D-03	-4.6615D-03	-3.5588D-03	-3.9565D-03
-8.2248D-03	4.3107D-03	-9.3702D-03	1.3263D-02	-6.3624D-03	6.5120D-03
3.5513D-03	-8.2254D-03	2.6059D-03	-4.2479D-03	1.4037D-02	-7.9483D-03
-1.7089D-02	1.7521D-02	-8.1044D-03	5.2027D-04	-5.3497D-05	5.9396D-03
4.9785D-03	-7.1357D-03	3.9647D-03	-1.8077D-03	-7.4948D-03	3.6023D-03
1.9496D-02	-3.0939D-02	2.6315D-02	-1.5477D-02	-5.0602D-02	5.1641D-02
-4.6489D-02	3.8470D-02	4.5115D-02	-5.0524D-02	3.5522D-03	8.2804D-03
2.9715D-04	7.3269D-03	-8.4062D-03	5.0651D-03	6.7906D-03	-8.2575D-03
2.1973D-03	-1.0396D-04	7.6047D-03	-2.1742D-04	-4.1482D-03	1.2013D-04
4.8315D-04	-3.7234D-03	-2.0365D-03	-8.7524D-04	-3.2064D-03	-3.5063D-03
1.6252D-03	1.6411D-03	2.8681D-03	-4.3421D-05	1.7706D-04	2.6293D-03
1.2713D-03	7.2314D-04	1.1110D-03	9.2401D-04	1.5900D-03	5.9320D-04
-1.3455D-03	-9.6960D-05	2.1141D-04	9.3717D-04	4.3709D-03	-4.5710D-03
2.7424D-04	1.6808D-05	1.0080D-03	-1.1516D-03	-2.9743D-04	-6.8597D-05
1.0732D-05	-1.2672D-04	4.0906D-04	-1.7872D-04	9.0706D-04	-9.6268D-04
2.3073D-04	-2.1122D-04	-3.7550D-04	4.5307D-04	1.2319D-04	2.2993D-04
-3.1894D-04	1.7517D-04	-5.6744D-04	5.7638D-04	-1.4228D-05	4.1111D-05
4.9310D-04	-4.5152D-04	5.8989D-05	-1.5051D-04	1.2955D-04	4.5434D-05
-2.3987D-04	3.3630D-04	-5.4325D-05	-3.4585D-05	-4.1005D-04	3.5252D-04
-3.6585D-04	3.9294D-04	1.6710D-04	7.5989D-05	2.0459D-04	-9.5737D-05
7.1864D-04	-3.8828D-05	7.5375D-04	-1.2161D-04	6.4361D-04	4.1089D-05
-2.5035D-03	2.1735D-03	-2.8373D-03	2.3216D-03	-2.9651D-03	2.6112D-03
1.1588D-02	-1.2287D-02	1.2736D-02	-1.2461D-02	1.3590D-02	-1.4169D-02
-3.9875D-04	-1.2122D-03	-7.0324D-04	-6.2787D-04	2.0913D-04	-1.5515D-03
-2.9954D-05	-3.0787D-04	3.9528D-04	-3.7448D-05	2.5098D-04	-2.5307D-04
-1.3866D-04	4.2203D-04	5.5006D-04	-2.0706D-04	-1.1474D-04	-3.3904D-04

-9.8391D-05	-3.0869D-04	-2.6535D-04	-1.3978D-04	-3.3885D-05	-4.9637D-04
-2.4740D-05	-1.6135D-04	1.5483D-04	5.2737D-06	-6.4991D-05	2.2181D-05
1.2756D-03	-1.0536D-03	-1.3908D-03	1.4920D-03	1.4343D-04	-4.0940D-04
-6.4577D-04	9.5513D-04	-3.8251D-04	9.6907D-05	1.5093D-03	-1.4482D-03
-1.1750D-03	-1.1882D-03	-7.7058D-04	-1.2337D-03	-7.7437D-04	-1.5456D-03
3.0910D-02	-1.2578D-02	1.2519D-02	-3.0444D-02	-2.0484D-02	2.0151D-02
3.2768D-02	-5.3247D-02	-4.7692D-02	3.4288D-02	2.2343D-02	1.0084D-02
-4.4708D-02	2.8673D-02	2.1326D-03	2.1597D-02	4.4485D-02	-5.1481D-02
1.9651D-02	-2.6545D-02	-2.8486D-02	2.8022D-02	3.7566D-02	-3.1550D-02
-5.8219D-02	5.8635D-02	-7.5559D-02	7.4781D-02	-7.1456D-02	7.1402D-02
3.3736D-02	-3.3568D-02	2.0556D-02	-1.3472D-02	6.6478D-03	-1.4031D-02
-3.6954D-02	4.8068D-02	-2.5108D-02	8.0015D-03	5.5024D-02	-4.9502D-02
-4.6993D-02	3.3483D-02	5.0399D-02	-5.6526D-02	-4.7046D-03	2.4650D-02
3.4819D-03	1.1558D-02	1.9679D-02	1.2380D-02	-1.6800D-02	-1.9201D-02
2.1574D-02	1.8354D-02	-9.0896D-03	-1.6526D-02	-9.0334D-03	4.3063D-03
-1.9951D-02	-1.7580D-02	-1.8934D-02	-2.2693D-02	-2.4467D-02	-2.3136D-02

Columns 19 thru 24

1.5603D-01	-1.4520D-01	4.0524D-02	-3.6424D-02	1.3412D-01	-1.1285D-01
-1.3264D-01	-1.5707D-01	-6.2669D-02	-6.8125D-02	1.5417D-01	-9.2965D-03
8.2740D-02	-7.0780D-02	1.1563D-02	-6.1740D-03	4.4048D-02	1.8464D-01
1.3249D-01	-2.9342D-02	2.1577D-01	-5.4134D-02	-4.8481D-02	-3.2202D-02
-3.5286D-02	-1.2357D-01	-5.5939D-02	-2.1346D-01	-1.3736D-01	5.9746D-02
-3.5855D-02	-4.4779D-02	-5.1081D-02	-8.0190D-02	-6.1813D-02	-1.3288D-01
-1.2513D-01	1.0758D-01	1.7354D-01	-1.5356D-01	9.1813D-02	-3.1206D-03
4.0396D-02	5.3038D-02	-1.4434D-01	-1.3537D-01	-1.6003D-02	7.1901D-02
1.7239D-01	1.7169D-01	-1.1490D-01	-1.3471D-01	1.0529D-01	-5.9018D-02
-5.3726D-02	6.1652D-02	-1.3064D-02	-1.5187D-02	7.3432D-02	-7.5768D-02
-2.8792D-02	5.7011D-02	1.3726D-02	1.4542D-02	1.5319D-01	1.8466D-01
-2.4451D-02	2.4146D-02	6.1809D-02	-5.9457D-02	-4.0747D-03	-2.2106D-03
-7.7783D-04	7.5763D-04	-1.2970D-02	-1.0478D-02	-1.5371D-02	1.1253D-02
1.2212D-02	-1.1369D-02	-4.5808D-02	5.2406D-02	3.0873D-02	-3.2326D-02
2.5733D-02	-2.5458D-02	-9.5160D-02	9.9337D-02	3.6202D-02	-3.7092D-02
2.0625D-02	2.1145D-02	1.2499D-02	1.2473D-02	1.9955D-02	2.2065D-02
1.0641D-01	-2.2602D-02	8.2650D-03	-7.7256D-03	-6.7594D-02	1.1125D-01
1.1532D-02	-1.0546D-01	7.2703D-03	-8.0877D-03	9.4793D-02	3.7864D-02
6.3653D-02	-5.7073D-02	1.9669D-02	-1.7089D-02	5.1373D-02	-3.8870D-02
-2.4776D-02	-3.7998D-02	-1.1614D-02	-1.5336D-02	3.9903D-02	1.2755D-03
2.2509D-02	-1.0345D-02	6.6454D-03	-1.3901D-03	-7.3510D-04	4.5128D-02
5.5290D-03	-4.2246D-03	9.2255D-03	-7.4170D-03	-3.1258D-03	2.2068D-04
-2.3137D-03	-3.5873D-03	-3.7042D-03	-6.2773D-03	-4.2349D-03	3.7223D-03
2.9761D-03	2.9522D-03	4.7343D-03	4.9542D-03	1.8041D-03	3.2869D-03
-3.4710D-04	-2.8144D-04	-3.5380D-03	2.6491D-03	-1.0739D-03	1.0300D-03
2.3437D-03	2.5094D-03	3.0343D-03	3.4870D-03	-3.5130D-04	-1.3999D-03
-1.5089D-03	4.2695D-04	1.7965D-04	-9.4585D-04	2.3721D-03	1.6270D-03
-1.0731D-03	-1.3657D-03	2.0428D-05	-9.3083D-05	-2.1590D-03	-2.2779D-03
-1.3614D-03	-1.5557D-03	1.4096D-03	2.2257D-03	4.3930D-04	8.1229D-04
-5.0904D-04	-1.6587D-04	1.8455D-03	-1.0472D-03	-6.7372D-04	-5.5359D-04

2.4361D-03	-1.6161D-03	-1.8660D-03	1.1429D-03	-5.0407D-04	8.7649D-06
-1.3786D-03	-2.1651D-03	1.1032D-03	1.7286D-03	-5.6699D-04	4.0754D-04
-3.9985D-04	-2.4910D-04	2.6305D-04	6.4466D-05	6.4689D-04	-7.1984D-04
7.3939D-05	1.5390D-04	-2.1335D-04	-9.7958D-05	-6.1726D-05	-4.0567D-04
1.7702D-04	-8.7259D-05	-3.0576D-04	1.1155D-04	2.0035D-03	-5.8722D-04
7.2078D-05	2.5829D-04	-1.4440D-05	-3.0696D-04	7.4629D-04	1.9838D-03
1.0255D-04	1.0250D-04	-1.1502D-04	-1.3001D-04	2.3948D-05	1.0272D-04
2.4303D-04	-9.7747D-05	7.1578D-05	-2.3233D-04	-6.6387D-05	2.1243D-04
-1.9183D-05	-2.0096D-04	1.7546D-04	5.4961D-05	2.8955D-04	1.0191D-04
-2.4392D-04	2.4058D-04	-5.3794D-04	5.5510D-04	-5.6879D-06	9.1322D-05
1.1025D-04	1.3766D-04	-1.9454D-04	-7.6610D-05	-1.0660D-04	3.3486D-05
1.0400D-05	-7.8772D-05	9.2468D-06	6.7664D-05	1.9862D-04	1.4308D-04
-3.8461D-05	-7.5327D-06	8.8416D-05	-2.7108D-05	-2.2092D-05	2.8211D-05
3.4887D-06	-1.1572D-05	3.9752D-06	2.4194D-05	1.6079D-04	-2.3360D-04
1.1886D-05	-2.1191D-05	2.0391D-04	-1.9550D-04	-6.2824D-05	-1.0727D-05
-2.5203D-05	-2.1204D-05	3.9090D-05	1.7932D-05	2.0915D-05	8.4498D-05
1.5489D-05	3.7594D-05	-4.5558D-06	-5.0876D-05	1.5638D-04	-1.8872D-04
-3.9983D-05	-3.8632D-05	4.8221D-05	4.5439D-05	-4.4126D-05	-4.3544D-05
6.9593D-06	-8.9399D-06	-2.6771D-06	4.9672D-06	6.0071D-06	-8.4830D-06
-1.1988D-05	7.7375D-06	3.3310D-05	-2.8804D-05	1.2722D-05	1.0055D-05
7.6616D-06	1.0136D-05	-5.2885D-06	-1.4447D-05	-2.6806D-06	-3.7840D-06
6.5394D-06	-4.5087D-06	-2.3374D-06	-3.1912D-07	-3.5072D-06	2.2218D-06
-2.3677D-07	2.9394D-06	-2.5288D-06	-3.2685D-06	-3.4746D-06	1.8894D-06
3.5424D-05	3.2946D-05	-3.3216D-05	-2.3969D-05	-1.6999D-05	-9.3701D-06
6.9535D-06	6.6991D-06	5.7646D-06	-1.7216D-05	-3.7319D-05	-3.9666D-05
6.0236D-06	6.9448D-06	-4.4978D-06	-3.4587D-06	1.1878D-05	1.1471D-05
3.7081D-06	5.4969D-06	4.2067D-07	-3.9216D-06	5.0907D-06	3.6203D-06
-1.1709D-05	1.1380D-05	5.6685D-05	-5.5965D-05	3.2698D-07	-4.4232D-07
-2.0295D-06	-2.5564D-06	-7.4094D-06	-1.0225D-06	-3.5793D-06	5.2759D-06
-6.8014D-06	5.2632D-06	1.8114D-05	-1.9739D-05	-1.1908D-05	1.1768D-05
3.7661D-05	2.9388D-05	3.0266D-05	3.0547D-05	-6.2898D-06	5.3975D-06
9.0926D-06	-8.5316D-06	-4.3146D-05	4.4026D-05	5.1547D-07	6.0251D-06
-5.7140D-06	-3.5772D-06	-8.3410D-06	-6.4274D-06	-3.0632D-06	4.7251D-07
-1.1225D-05	1.2541D-05	4.1434D-05	-4.0667D-05	-2.7391D-06	2.0176D-07
-6.2139D-06	9.6797D-06	5.8236D-06	-3.4377D-06	2.6471D-06	-1.0275D-05
-1.1181D-05	2.7821D-07	1.9906D-05	-2.6943D-05	-1.1333D-05	-4.8316D-06
-2.3823D-06	-2.4118D-06	-2.6101D-05	2.2093D-05	-7.8500D-06	3.5625D-06
7.5902D-07	-6.2779D-07	2.1003D-05	-2.1811D-05	1.6949D-05	1.3680D-05
-1.0423D-06	5.1289D-07	9.5641D-05	-9.5867D-05	1.1506D-06	-7.6598D-07
-8.3072D-07	4.0094D-07	3.5903D-05	-3.6387D-05	1.8062D-06	-1.6403D-07
-3.7916D-06	1.7526D-06	-1.1108D-05	8.3495D-06	1.1587D-06	-2.2814D-07
-2.6411D-07	-3.0625D-07	-5.6874D-07	-2.5229D-09	-4.3416D-07	-1.5262D-07
1.4341D-05	-1.4930D-05	4.7635D-05	-4.8057D-05	1.6145D-06	-3.6734D-06
-2.1911D-07	-1.3321D-06	-4.3662D-06	2.6287D-06	-3.0090D-07	1.8848D-06
-8.9643D-08	4.6565D-09	3.1323D-06	-2.9236D-06	1.1077D-05	-1.1728D-05
-3.2629D-07	-4.7685D-07	-3.8835D-06	3.2602D-06	-1.1135D-05	1.1046D-05
1.4446D-07	9.1256D-07	2.9713D-06	-1.7673D-06	1.7533D-06	-2.9006D-06
2.2176D-06	-1.5820D-06	2.8921D-07	4.1576D-07	1.1249D-05	-1.0594D-05
1.6321D-05	-1.6161D-05	-1.8153D-05	1.8221D-05	2.1531D-06	-1.9730D-06

1.3033D-06	-1.6155D-06	-3.2921D-06	3.2120D-06	-1.5796D-06	1.8365D-06
-2.0516D-06	2.3026D-06	-4.1961D-07	4.7449D-07	2.5579D-06	-2.6692D-06
-1.2100D-04	1.2094D-04	6.1413D-05	-6.1408D-05	1.2551D-05	-1.2764D-05
-4.8750D-06	5.3377D-06	2.9910D-06	-2.1420D-06	-2.7503D-05	2.7253D-05
1.9117D-04	-1.9101D-04	-1.3900D-04	1.3859D-04	2.5195D-05	-2.4843D-05
2.7271D-07	2.8169D-07	-6.4066D-07	-5.9210D-07	-1.6243D-06	2.0245D-06
-8.0022D-05	8.0162D-05	6.3311D-05	-6.2965D-05	3.8030D-05	-3.8600D-05
1.8033D-06	-8.6493D-07	-4.3068D-06	-7.9754D-07	-1.9738D-05	1.7852D-05
-2.2931D-05	1.1444D-05	4.8056D-06	-2.1508D-05	-1.5706D-04	1.5542D-04
-3.6747D-05	-4.9328D-05	-4.3379D-05	-3.3646D-05	2.0831D-05	-2.8693D-05
3.4277D-05	-2.1799D-05	-1.8731D-05	2.7510D-05	-6.2004D-05	6.2830D-05
2.7954D-06	-4.6851D-06	-3.9105D-06	1.5943D-06	6.7131D-05	-6.7313D-05
2.1543D-05	-2.0947D-05	-2.3430D-05	1.4890D-05	-8.3831D-06	1.3851D-05
-1.2768D-05	7.2693D-06	-1.0260D-06	-2.0786D-05	6.4506D-05	-5.3533D-05
2.2221D-05	2.0681D-05	2.2514D-05	2.7232D-05	1.2211D-05	-3.9540D-05
-5.2592D-06	-2.5820D-06	-5.9477D-06	-1.1618D-05	1.7925D-05	1.6026D-05
-4.8382D-07	-2.1646D-06	-5.2258D-06	-4.5646D-06	-3.2271D-05	-3.1128D-05
3.8749D-05	-3.7071D-05	-9.2710D-06	1.0641D-05	3.5629D-06	-1.4983D-06
-2.3789D-06	3.0086D-06	1.0713D-06	-8.4709D-07	3.8883D-06	-5.2093D-06
-2.9180D-06	2.9151D-06	-2.0452D-06	1.8668D-06	-3.1738D-06	2.7260D-06
-6.4850D-07	5.6140D-07	2.6474D-07	-1.0181D-07	-9.3500D-06	8.7413D-06
-1.4730D-06	1.2344D-06	2.4621D-07	-3.7454D-07	9.7380D-06	-9.6901D-06
-1.4104D-06	5.9610D-07	1.8894D-07	-1.9516D-07	1.3744D-05	-1.3365D-05
-2.2984D-06	1.3538D-06	9.3521D-07	-8.3544D-07	1.3617D-05	-1.3346D-05
-1.0379D-06	-3.4264D-07	-1.9431D-07	-2.2440D-08	1.5375D-05	-1.4308D-05
-6.9781D-07	1.8510D-07	-9.5377D-07	-1.0910D-06	-5.1283D-06	4.1659D-06
1.3221D-05	1.6569D-05	1.6453D-05	1.3885D-05	-2.6929D-06	1.6022D-06
1.3489D-05	-6.6893D-06	-3.8541D-06	1.1351D-05	1.4227D-05	-1.5047D-05
1.8729D-06	4.9537D-07	2.3753D-06	4.8610D-06	-5.0899D-06	-5.3936D-06
-1.9333D-06	1.8613D-06	1.2566D-06	-1.2982D-06	1.0050D-06	-1.2279D-06
-1.2870D-07	8.5635D-08	-7.8768D-08	-2.9579D-07	2.2873D-06	-1.6921D-06
6.6989D-07	3.9152D-07	8.7791D-07	1.3900D-06	-1.9575D-06	-2.7448D-06
2.6886D-06	-2.5968D-06	-1.5921D-06	1.7078D-06	1.8040D-06	-1.8068D-06
-4.0477D-07	1.6427D-07	1.9107D-07	-2.0255D-07	-1.1794D-06	1.2252D-06
-1.1084D-06	1.0269D-06	7.0294D-07	-8.6908D-07	1.6847D-06	-1.6553D-06
2.6753D-06	-1.5968D-06	4.1901D-06	4.9932D-06	7.6723D-05	7.3977D-05
-1.5307D-04	1.4727D-04	6.1567D-05	-6.4785D-05	9.3817D-06	-1.6721D-05
-1.9841D-05	-1.1097D-05	1.1234D-05	1.2757D-05	5.2396D-05	-3.5735D-05
-3.0277D-05	3.8744D-05	7.9669D-06	-1.9471D-05	-5.0344D-05	6.9418D-05
-2.6190D-05	6.8629D-06	2.4403D-05	-4.4948D-06	3.5865D-05	-1.1102D-05
2.8164D-06	-8.4304D-06	3.8445D-06	5.2921D-06	-1.6015D-05	1.7636D-05
-5.8024D-06	-2.0607D-06	2.6053D-06	1.6542D-05	-1.3777D-04	1.3161D-04
-1.9099D-05	1.0245D-06	1.4629D-06	2.4391D-05	-9.3954D-06	-3.4962D-05
-2.9413D-05	-3.1861D-05	4.7045D-05	3.9329D-05	3.9878D-05	7.0074D-06
-7.1085D-05	-7.3560D-05	9.2228D-05	1.0384D-04	-1.3319D-05	3.5665D-05
-3.5063D-05	-1.3014D-05	4.3754D-05	1.8101D-05	7.2650D-05	5.7654D-05
1.9733D-05	2.0908D-05	-3.7873D-05	-4.3824D-05	3.3227D-05	4.1746D-05

Columns 25 thru 30

3.6863D-02	-2.8560D-02	1.1494D-01	-1.4926D-01	2.7847D-02	-4.1339D-02
4.4745D-02	1.8802D-02	-1.4679D-02	1.3981D-01	1.6377D-02	3.8998D-02
3.7945D-02	6.3370D-02	-1.8582D-01	-5.8897D-02	-6.5745D-02	-4.3205D-02
-6.7065D-02	-4.1779D-02	-1.7409D-02	1.4650D-01	-2.5375D-02	1.8772D-01
-1.6302D-01	7.6542D-02	6.5745D-02	-2.3209D-02	9.2813D-02	-1.7934D-02
-7.5288D-02	-1.8626D-01	-1.2694D-01	-4.7061D-02	-2.0002D-01	-5.5545D-02
1.7813D-02	1.3151D-01	1.7976D-02	-9.6160D-02	-1.2429D-01	-1.4046D-02
1.7065D-01	-6.4261D-02	6.6966D-02	-4.3699D-02	-6.5664D-02	1.9623D-01
-6.0147D-02	5.1590D-02	-4.8343D-02	1.2083D-01	2.1049D-02	-9.3488D-02
-7.1196D-02	-2.5080D-02	-1.7721D-01	-1.4980D-01	1.8962D-01	1.5807D-01
-1.7481D-01	-1.8529D-01	1.0636D-01	-1.5932D-02	-1.6373D-02	2.4394D-03
3.0722D-02	-9.3877D-03	-3.8726D-03	7.5139D-03	1.6857D-02	-3.7937D-02
3.3484D-02	-8.7194D-03	2.2345D-02	-2.1080D-02	-4.2271D-02	5.0390D-02
-9.0421D-02	1.0523D-01	2.4719D-02	-2.1321D-02	-8.8529D-02	6.6023D-02
-1.3089D-01	1.4111D-01	3.4462D-02	-3.0780D-02	-1.2945D-01	1.1428D-01
1.4754D-02	1.4765D-02	2.2383D-02	1.9359D-02	1.4065D-02	1.4098D-02
-1.3885D-02	1.4483D-02	-4.7250D-02	-8.5107D-02	1.0156D-03	-2.7077D-03
4.8522D-03	-2.8970D-03	-1.0425D-01	7.5478D-02	-1.3579D-02	1.3288D-02
1.7170D-02	-1.2113D-02	4.0136D-02	-6.0410D-02	1.1878D-02	-2.0064D-02
1.4550D-02	3.3377D-03	-1.2855D-02	3.2452D-02	-2.0966D-03	1.0586D-02
2.7598D-03	1.6632D-02	-4.2753D-02	-1.3703D-02	-1.6680D-02	-7.8489D-03
-4.1071D-03	8.0075D-05	-1.1205D-03	4.4574D-03	-1.3503D-03	6.0410D-03
-5.5948D-03	5.2711D-03	3.7216D-03	-3.2603D-03	5.8260D-03	-4.7012D-03
2.4686D-03	5.4013D-03	3.7608D-03	1.7956D-03	6.6323D-03	2.1503D-03
-3.9069D-03	3.7149D-03	-3.3002D-04	9.1706D-04	-2.6071D-03	4.8170D-03
-3.1669D-03	-3.9870D-04	-2.2196D-03	-9.4813D-04	-2.5451D-03	-3.3197D-03
3.0411D-03	3.5713D-03	-1.7008D-03	-2.7073D-03	-3.0691D-03	-2.4818D-03
-1.6912D-03	-1.7848D-03	-1.7915D-03	-1.2751D-03	-6.5087D-04	-1.0200D-03
-2.5976D-03	2.3913D-05	4.0093D-04	2.2700D-04	1.1424D-03	-2.1503D-03
8.7247D-05	2.8888D-03	1.1205D-03	9.7893D-04	-2.4038D-03	-1.1498D-03
4.7870D-04	2.6209D-04	-1.7107D-04	7.8397D-04	-1.4125D-04	-7.0498D-04
6.5714D-04	-3.1156D-04	5.9646D-04	-3.9510D-04	-5.3756D-04	4.5219D-04
-2.0731D-04	5.5939D-04	-1.9908D-03	1.1346D-03	1.5081D-03	-6.9906D-04
7.0342D-05	1.3260D-04	1.2176D-03	1.8205D-03	-8.4599D-04	-1.3525D-03
-1.5451D-03	4.3242D-04	5.2413D-04	-5.3030D-04	-4.7268D-04	5.2907D-04
-5.0625D-04	-1.4938D-03	3.4563D-04	5.8523D-04	-3.7799D-04	-5.0202D-04
-7.1004D-05	-1.0198D-04	1.0189D-04	2.4415D-05	-1.0278D-04	-7.1276D-05
-2.8911D-05	-1.0400D-04	-1.6403D-04	-1.9693D-04	1.5538D-04	2.1927D-04
-2.0007D-04	-2.0007D-04	-1.4498D-04	1.8083D-04	-2.3223D-05	-6.0118D-06
3.5479D-07	-7.5576D-05	-6.8034D-05	3.8417D-06	3.2700D-05	9.4854D-06
8.0180D-05	-4.9527D-06	-1.4106D-04	-1.0972D-04	2.2677D-05	2.4538D-04
-1.0956D-04	-2.5293D-04	-1.4338D-04	-6.7442D-05	1.0759D-04	1.2109D-04
-1.2777D-05	-2.0660D-05	-2.1532D-04	2.7093D-04	-3.9294D-04	3.4927D-04
2.5634D-04	-1.9324D-04	5.3726D-05	1.4800D-05	-9.2750D-05	1.6375D-06
3.7561D-05	5.7714D-05	2.8695D-05	4.8359D-05	-6.3846D-07	-9.3197D-05
-6.3051D-05	-4.9971D-05	8.7889D-05	-1.2901D-04	3.9695D-04	-3.5629D-04
4.7280D-04	-4.4853D-04	-1.0656D-05	-2.8257D-05	5.0044D-05	-4.2654D-06

6.8169D-05	6.1987D-05	-4.1927D-05	-4.0722D-05	5.4750D-05	6.2580D-05
6.2895D-06	-2.5002D-06	6.1093D-06	-7.6663D-06	3.1657D-06	-1.3292D-06
-4.2620D-05	9.4368D-06	-3.6244D-06	-1.0058D-05	-2.8754D-05	4.8144D-05
-5.8900D-05	6.9824D-05	-1.1256D-05	-5.0187D-06	5.3794D-05	-3.1522D-05
3.7781D-06	-9.9282D-06	-1.7638D-06	3.4681D-07	4.4890D-06	5.2079D-06
1.1616D-05	-2.0669D-06	3.7124D-06	-5.1307D-06	-4.9447D-06	8.7966D-06
2.5514D-05	3.7360D-06	-2.3895D-05	-2.7955D-05	2.0795D-05	3.3070D-05
4.2027D-05	4.1706D-05	3.0641D-05	2.6512D-05	-3.8246D-05	-2.0175D-05
-1.3545D-05	-1.0945D-05	8.4141D-06	9.0382D-06	-7.8662D-06	-8.6454D-06
-6.4806D-06	-5.6608D-06	2.1200D-06	5.8073D-06	-2.2593D-06	-7.7241D-06
9.9323D-07	1.6811D-06	-1.0592D-06	-1.9834D-07	-1.1752D-06	-1.0845D-06
3.2479D-06	-3.3979D-06	1.0200D-05	-8.1699D-06	-1.8110D-05	1.7891D-05
1.0192D-05	-1.0914D-05	-7.1238D-06	8.2422D-06	1.5530D-05	-1.2901D-05
4.3693D-06	-7.3892D-06	4.7643D-06	-7.0273D-06	-8.8401D-06	4.3305D-06
5.1380D-06	-5.7986D-06	-7.2304D-06	-2.3011D-06	6.4368D-06	-9.3940D-06
8.9285D-06	-6.5819D-06	3.8548D-07	-3.3767D-06	-1.1256D-05	1.3603D-05
4.1242D-06	-1.0235D-05	3.4806D-06	7.6722D-06	1.8952D-05	-5.7839D-06
-1.6294D-05	5.4985D-06	2.1211D-05	7.8330D-06	6.0239D-07	2.7220D-05
-3.7283D-06	-1.0984D-05	-4.9538D-06	-1.7493D-05	-2.9254D-05	1.1373D-05
1.5902D-05	-1.9733D-05	1.3545D-05	5.5046D-06	-1.3677D-06	1.6692D-05
1.3610D-05	1.1257D-05	1.9955D-06	1.7596D-06	-1.1515D-05	1.3574D-05
4.6197D-06	-4.3358D-06	-2.6063D-07	-2.9376D-07	8.2912D-06	-8.7804D-06
-2.0047D-05	2.1638D-05	-1.8879D-06	1.4490D-06	-5.2718D-05	5.1974D-05
4.5434D-05	-4.4348D-05	-4.4291D-07	2.2111D-06	-4.0440D-05	4.2251D-05
-1.0506D-06	5.5913D-07	-1.4352D-08	-5.9604D-07	9.9705D-07	-1.5401D-06
1.2366D-05	-1.4448D-05	6.1495D-06	-4.0351D-06	2.1721D-05	-1.9355D-05
-3.3710D-06	5.0715D-06	1.7356D-05	-1.7586D-05	5.7194D-05	-5.7249D-05
3.7123D-05	-3.7219D-05	2.1096D-06	-2.7826D-06	4.5611D-06	-5.0096D-06
-3.6352D-05	3.6426D-05	-3.0784D-06	2.9643D-06	-6.2634D-06	6.5612D-06
7.8687D-06	-8.7755D-06	-1.6323D-06	1.2975D-06	-6.2387D-06	5.9710D-06
3.4876D-05	-3.4146D-05	3.3356D-06	-4.8679D-06	9.0614D-06	-1.0542D-05
8.6791D-06	-8.7454D-06	2.2763D-06	-2.5174D-06	3.7292D-06	-3.7163D-06
-2.1122D-06	2.1329D-06	-4.1732D-07	3.3398D-07	1.5639D-05	-1.5610D-05
1.5665D-05	-1.5651D-05	-8.3772D-08	-1.9235D-07	-2.7344D-06	2.6656D-06
2.0477D-06	-2.3141D-06	1.1939D-05	-1.1680D-05	3.1177D-07	-2.8641D-08
2.2453D-06	-2.5676D-06	4.0835D-05	-4.0986D-05	-9.8598D-06	9.4917D-06
-1.3009D-05	1.1935D-05	3.2603D-05	-3.2843D-05	-1.8129D-05	1.9425D-05
-9.6534D-08	-1.4807D-06	3.4794D-06	-3.0414D-06	-2.5167D-06	1.0259D-06
-2.0267D-05	2.1415D-05	4.6899D-05	-4.6230D-05	-3.0958D-05	2.9459D-05
1.3864D-05	-9.9375D-06	1.8889D-04	-1.8864D-04	-1.4436D-04	1.4423D-04
1.1767D-04	-1.1782D-04	-3.6566D-05	3.2785D-05	3.1490D-05	-2.6225D-05
-1.9151D-05	1.7452D-05	-5.9457D-06	-4.4580D-06	-3.3546D-06	-3.4508D-06
5.1468D-05	-4.6051D-05	-2.0245D-05	2.1096D-05	1.6866D-05	-1.8793D-05
-5.2484D-05	5.4062D-05	-3.8025D-05	3.8448D-05	3.1349D-05	-3.1388D-05
1.6983D-05	-6.4777D-07	-2.7288D-05	3.3447D-05	2.4731D-05	-2.9538D-05
-4.6877D-05	5.0902D-05	-1.2605D-05	3.7232D-05	3.5404D-05	-7.5530D-06
-2.7341D-05	1.8073D-05	-3.7342D-05	-1.4991D-05	-6.5849D-06	-2.5903D-05
9.7304D-06	1.1682D-05	-5.1024D-05	-4.9515D-05	-5.0842D-05	-5.3345D-05
-3.2285D-05	-3.4154D-05	-5.2059D-06	-5.5533D-06	-7.7280D-06	-9.4079D-06



-1.2992D-06	1.9874D-06	3.3968D-06	-5.2403D-06	-1.5405D-06	2.4144D-06
-1.6293D-06	1.8844D-06	2.7593D-05	-2.6334D-05	-9.9691D-06	1.0722D-05
8.9888D-07	-9.5813D-07	3.3089D-06	-3.0277D-06	-1.8682D-06	1.8824D-06
3.1647D-06	-4.1618D-06	1.7161D-06	-1.8134D-06	1.8792D-07	-1.1384D-06
-3.6586D-06	3.9580D-06	1.9445D-06	-1.4601D-06	1.7216D-06	-1.3574D-06
-8.1306D-06	8.0606D-06	-1.9608D-06	2.2885D-06	3.9359D-07	-7.9224D-07
-4.7343D-06	5.3290D-06	-1.0316D-06	1.8990D-06	3.3948D-07	-8.5404D-07
-6.0819D-06	5.3161D-06	-6.6729D-06	6.6176D-06	2.3104D-06	-2.7413D-06
8.5601D-07	-3.0633D-06	-1.6544D-06	6.8435D-07	-7.2868D-07	-1.3921D-06
1.9041D-06	-1.4858D-06	-3.3162D-06	1.8691D-06	2.1488D-06	-2.1179D-06
-1.1659D-05	1.1545D-05	1.1318D-05	-1.2727D-05	-9.9523D-06	9.6392D-06
-2.3661D-06	-2.4742D-06	4.6670D-05	4.4369D-05	4.4932D-05	4.6913D-05
-1.0569D-06	7.2436D-07	1.2023D-06	-1.2105D-06	-9.3775D-07	1.0166D-06
-1.4160D-06	1.8344D-06	-2.5413D-06	5.1050D-07	2.3174D-07	-2.2305D-06
-1.9038D-06	-1.2765D-06	5.5732D-06	5.2565D-06	5.6654D-06	5.9554D-06
-1.4478D-06	1.4738D-06	1.8768D-06	-1.5356D-06	-1.1582D-06	1.5034D-06
9.3407D-07	-1.0645D-06	1.5932D-06	-1.3157D-06	-1.1288D-06	1.2520D-06
-1.4801D-06	1.2251D-06	3.6968D-07	-1.5100D-06	-1.2595D-06	2.5849D-07
7.4492D-05	7.6803D-05	4.5619D-06	3.6452D-06	6.6012D-06	9.2662D-06
-3.7323D-06	1.6021D-05	1.6971D-05	-3.8030D-06	-1.2409D-05	5.3285D-06
-3.7426D-05	2.2800D-05	-1.0920D-04	1.1905D-04	5.9711D-05	-7.7145D-05
2.5823D-05	-4.8882D-05	-7.5226D-05	4.4356D-05	4.9484D-05	-1.7508D-05
-2.9983D-05	-2.8784D-06	8.5554D-05	-8.8306D-05	-5.0496D-05	6.1459D-05
1.0806D-05	-1.5351D-05	3.2659D-05	-2.7819D-05	-2.0920D-05	1.7102D-05
9.2076D-05	-9.4364D-05	1.0281D-05	1.2852D-06	-1.5960D-05	-1.1873D-06
2.7755D-05	3.2615D-05	4.0665D-05	2.1096D-05	-4.5283D-05	-3.9996D-05
-3.6653D-05	-2.6797D-05	-3.4040D-06	1.8829D-05	-1.4313D-05	-7.1303D-06
5.2178D-06	-3.5733D-05	6.1349D-05	3.1366D-05	-6.9615D-05	-4.5498D-05
-8.5339D-05	-7.5304D-05	-3.7426D-05	-6.5272D-05	5.4680D-05	8.0266D-05
-5.2262D-05	-6.1200D-05	3.2879D-05	2.8262D-05	-5.1023D-05	-4.9376D-05

Columns 31 thru 36

-1.2746D-02	-6.9874D-04	7.4938D-03	1.2877D-02	3.2535D-04	-7.1205D-03
-6.4015D-03	-9.3027D-02	-8.7218D-02	5.4689D-03	9.4157D-02	8.8854D-02
-1.0635D-01	-5.0943D-02	5.9108D-02	1.0642D-01	4.8936D-02	-5.6416D-02
-3.0454D-02	-2.8465D-02	-1.7293D-02	2.4932D-02	2.7890D-02	-1.5391D-02
-1.4715D-02	3.8679D-02	4.5126D-02	1.7732D-02	-5.1938D-03	-3.0477D-02
2.7311D-02	6.8763D-03	4.6408D-03	2.7464D-02	3.1735D-02	2.9099D-02
2.4743D-02	4.9012D-02	-4.9898D-02	-2.6782D-02	1.5650D-02	-1.6155D-02
3.8253D-02	-3.4432D-03	-1.5257D-03	3.6513D-02	-4.6409D-02	-4.8191D-02
-2.2310D-02	-3.6259D-03	-1.1752D-02	-2.5540D-02	1.5093D-02	1.4436D-02
-7.6896D-03	-3.6426D-03	1.1629D-02	3.4121D-03	9.3149D-03	1.2009D-02
-1.2050D-02	-1.4658D-02	2.5544D-03	4.5490D-05	-5.4024D-03	-1.6814D-03
-5.7948D-03	-1.5369D-01	1.2215D-01	7.1574D-02	-2.2143D-01	1.8727D-01
-1.9670D-01	5.4645D-02	1.4452D-01	-2.1458D-01	7.9858D-02	1.3096D-01
1.4778D-01	-1.8745D-01	1.5888D-01	-9.0411D-02	5.0666D-02	-7.9750D-02
-8.3387D-02	7.5656D-02	-8.0098D-02	9.1961D-02	-9.9745D-02	9.5159D-02
1.4909D-01	1.4771D-01	1.4775D-01	1.4921D-01	1.5037D-01	1.5033D-01

1.3923D-01	-4.7040D-02	-1.6840D-01	-1.2751D-01	2.6744D-02	1.7270D-01
1.1354D-01	1.7451D-01	6.5354D-02	-1.2634D-01	-1.7649D-01	-4.5531D-02
-5.5103D-03	-4.5638D-04	3.6189D-03	5.5808D-03	2.0835D-04	-3.4070D-03
-3.7145D-03	-1.5676D-02	-1.2053D-02	3.3351D-03	1.5772D-02	1.2446D-02
-1.5481D-02	-5.4746D-03	1.0890D-02	1.5537D-02	4.9650D-03	-1.0358D-02
1.5686D-03	1.7150D-03	-1.5326D-03	-1.3005D-03	-7.8124D-05	-2.7616D-04
-8.1218D-04	-4.2915D-04	-8.7818D-04	-1.1565D-03	1.4305D-03	1.4092D-03
-3.0793D-04	-2.6645D-04	-4.1356D-05	-3.1046D-05	1.1126D-03	1.1243D-03
4.7384D-04	1.6753D-04	-2.5132D-06	-3.8964D-04	2.4688D-04	-2.3476D-04
-6.6795D-04	-7.6451D-04	-1.2124D-03	-1.2115D-03	1.4928D-03	1.4515D-03
1.4933D-03	1.5364D-03	-1.1549D-03	-1.1212D-03	-2.4721D-06	-7.0911D-05
-2.4748D-05	1.2303D-05	5.1769D-04	4.5285D-04	6.5489D-04	7.1695D-04
9.4000D-04	7.4724D-04	1.8254D-04	4.6232D-04	-1.1157D-03	-1.2165D-03
-7.2943D-04	-9.8206D-04	1.2173D-03	1.0654D-03	-4.3774D-04	-1.4943D-04
2.1683D-04	-1.5859D-04	1.3533D-04	-5.3326D-05	-2.2203D-04	8.0974D-05
-3.4557D-04	7.1234D-05	1.0308D-04	-4.0950D-04	3.0139D-04	3.2088D-04
-3.4811D-04	1.2144D-04	3.0802D-04	-2.7025D-04	-4.9762D-05	2.9257D-04
-2.2952D-04	5.2577D-04	-3.2070D-04	-2.8766D-04	4.6818D-04	-2.5792D-04
-1.7161D-04	-5.8799D-05	2.8120D-04	-2.7789D-04	1.3281D-04	2.6573D-05
-2.3747D-04	-2.0269D-04	2.5713D-04	-1.6428D-04	-2.4248D-04	3.7642D-04
3.5170D-04	4.4415D-04	4.5490D-04	3.5088D-04	4.8437D-04	5.0714D-04
-1.9166D-04	2.8142D-04	-2.6048D-04	-3.0408D-04	2.4384D-04	-7.2095D-05
3.9559D-04	1.7446D-04	-1.8646D-04	3.0709D-04	9.5650D-06	-2.3724D-04
1.4345D-04	-2.3412D-05	-5.5878D-05	-1.1485D-04	1.0173D-04	-6.0230D-05
-2.2857D-04	2.8468D-04	2.8987D-04	-1.3642D-04	2.3645D-05	-2.2321D-04
-1.9983D-04	-9.5992D-06	-1.7386D-04	3.1053D-04	2.7780D-04	-1.9065D-04
1.8414D-04	-2.5181D-04	4.4881D-05	-7.7118D-05	2.0639D-04	-1.4938D-04
-4.6838D-05	4.2110D-05	-1.8603D-04	1.6919D-04	-2.6399D-04	2.2018D-04
2.5074D-04	-2.9563D-04	2.9361D-04	-2.3048D-04	6.2526D-05	-7.8811D-05
2.1036D-04	-1.5118D-04	5.0114D-05	-4.6816D-05	2.0771D-04	-2.7819D-04
7.5954D-05	-6.5103D-05	1.4032D-04	-2.1197D-04	1.8334D-04	-1.1281D-04
4.6535D-05	8.5456D-05	7.2290D-05	5.5294D-05	5.0406D-05	8.1144D-05
1.5297D-04	-1.6352D-04	1.6682D-04	-1.5067D-04	1.7150D-04	-1.6835D-04
1.0374D-04	2.1477D-05	2.9577D-05	-1.3737D-04	-1.2469D-04	1.0186D-04
1.0730D-04	-1.4936D-04	-1.4032D-04	6.5832D-05	3.4210D-05	9.0397D-05
3.6059D-05	-1.4482D-04	1.1563D-04	4.1069D-05	-1.5106D-04	1.0281D-04
1.4533D-04	-2.9018D-05	-1.0125D-04	1.4333D-04	-4.2045D-05	-1.1681D-04
-1.9530D-05	2.4386D-05	1.4496D-05	-2.1072D-05	1.0960D-05	4.8112D-06
1.0248D-05	-1.4147D-05	2.1617D-05	-1.4530D-05	-2.0921D-05	3.0599D-05
3.2617D-05	3.3826D-05	3.2178D-05	3.3618D-05	3.4466D-05	3.0711D-05
2.4339D-05	-2.1414D-05	-3.0555D-05	3.0948D-05	2.2786D-05	2.6839D-05
8.1081D-05	3.7887D-05	-4.4541D-05	-7.7706D-05	-1.0831D-04	1.0714D-04
-1.1514D-05	1.0421D-04	1.3429D-04	-7.4320D-05	-7.0834D-05	-7.5844D-05
-1.4074D-04	1.0078D-04	-3.1477D-05	1.0784D-04	-4.5461D-05	4.1286D-06
4.8980D-05	-3.9397D-05	-3.9473D-05	5.1662D-05	-6.8864D-06	-1.0494D-05
8.2624D-05	-8.7744D-05	1.1177D-04	-1.0587D-04	-3.0247D-04	3.0083D-04
2.4244D-04	-2.3571D-04	-2.3759D-04	2.4930D-04	-3.2624D-05	1.2446D-05
1.8820D-04	-2.0351D-04	1.9435D-04	-1.7739D-04	6.3154D-05	-6.3102D-05
-7.1983D-05	7.1898D-05	-6.1727D-05	6.1811D-05	-1.2533D-04	1.3224D-04

-2.6429D-05	3.1041D-06	9.6779D-06	-3.9590D-06	-2.7648D-05	3.1031D-05
2.8955D-05	-1.3591D-05	-4.5649D-06	-1.8557D-05	3.2738D-05	-1.7559D-05
-1.2704D-05	-7.4805D-06	-1.6021D-06	2.0768D-05	4.0738D-06	1.7802D-05
-3.6994D-06	-2.5537D-05	2.3716D-05	5.5570D-06	-6.4818D-05	6.4454D-05
-4.2149D-07	-2.8785D-05	5.5936D-05	-3.4186D-05	-2.0123D-05	3.2307D-05
-5.6895D-05	5.1108D-05	2.7199D-05	-4.6177D-05	1.8178D-05	9.7841D-06
3.4525D-05	3.3882D-05	3.3560D-05	3.3936D-05	3.1832D-05	3.2210D-05
-8.6214D-06	4.4045D-06	8.0862D-06	7.7416D-06	3.5686D-05	-4.3401D-05
1.7543D-06	5.0352D-06	3.5911D-05	-1.6996D-05	-3.8788D-06	1.6776D-06
6.1555D-05	3.6309D-05	1.0348D-04	9.7116D-05	3.3050D-05	2.9146D-05
8.2082D-05	1.0701D-04	2.8606D-05	3.8119D-05	6.4413D-05	6.9358D-05
-6.8710D-05	-7.2690D-05	-5.9286D-06	-1.0685D-06	1.1995D-04	1.1758D-04
7.8968D-05	5.2697D-05	-9.0283D-05	-1.0383D-04	3.6083D-05	3.2447D-05
-7.2521D-06	-1.6062D-05	1.3750D-05	6.0133D-06	1.0202D-05	-5.8293D-06
-8.4130D-06	-3.4264D-06	-4.3826D-06	5.4489D-06	3.0614D-06	7.9683D-06
-4.7276D-06	3.4547D-06	2.7702D-06	6.7917D-06	-6.2268D-06	-2.5681D-06
-4.5623D-05	-4.2355D-06	1.2692D-05	4.1866D-05	4.2836D-05	-4.7577D-05
2.8960D-05	-6.5658D-05	-6.4100D-05	3.3427D-05	3.6643D-05	2.7127D-05
-4.1462D-05	1.7143D-05	-9.9552D-06	3.6161D-05	3.4968D-05	-3.7202D-05
1.5586D-05	1.1013D-05	9.6198D-06	1.6922D-05	1.2919D-05	1.4363D-05
2.9336D-05	-1.5375D-05	3.3422D-05	-4.7308D-05	2.2694D-05	-2.3227D-05
-1.2293D-05	2.8473D-05	-9.0206D-06	1.4704D-05	-4.8590D-05	2.7513D-05
5.8155D-05	-5.9624D-05	2.7580D-05	-1.7705D-06	1.8205D-07	-2.0213D-05
-1.6778D-05	2.4048D-05	-1.3361D-05	6.0923D-06	2.5258D-05	-1.2140D-05
-6.5336D-05	1.0368D-04	-8.8186D-05	5.1865D-05	1.6958D-04	-1.7306D-04
1.5539D-04	-1.2859D-04	-1.5080D-04	1.6888D-04	-1.1873D-05	-2.7678D-05
-9.8021D-07	-2.4169D-05	2.7729D-05	-1.6708D-05	-2.2400D-05	2.7239D-05
-7.2433D-06	3.4271D-07	-2.5069D-05	7.1673D-07	1.3675D-05	-3.9599D-07
-1.5825D-06	1.2195D-05	6.6702D-06	2.8667D-06	1.0502D-05	1.1484D-05
-5.2258D-06	-5.2766D-06	-9.2221D-06	1.3961D-07	-5.6933D-07	-8.4544D-06
-4.0574D-06	-2.3080D-06	-3.5457D-06	-2.9491D-06	-5.0745D-06	-1.8933D-06
4.2830D-06	3.0866D-07	-6.7294D-07	-2.9832D-06	-1.3913D-05	1.4550D-05
-8.7192D-07	-5.3426D-08	-3.2051D-06	3.6614D-06	9.4568D-07	2.1817D-07
-3.3814D-08	4.0305D-07	-1.3003D-06	5.6763D-07	-2.8837D-06	3.0608D-06
-7.3415D-07	6.7104D-07	1.1934D-06	-1.4385D-06	-3.9149D-07	-7.3182D-07
1.0137D-06	-5.5695D-07	1.8036D-06	-1.8321D-06	4.5289D-08	-1.3080D-07
-1.5674D-06	1.4353D-06	-1.8747D-07	4.7894D-07	-4.1187D-07	-1.4459D-07
7.6175D-07	-1.0693D-06	1.7251D-07	1.1138D-07	1.3034D-06	-1.1213D-06
1.1632D-06	-1.2487D-06	-5.3104D-07	-2.4248D-07	-6.5033D-07	3.0483D-07
-2.2840D-06	1.2332D-07	-2.3954D-06	3.8702D-07	-2.0453D-06	-1.3087D-07
7.9420D-06	-6.8950D-06	9.0006D-06	-7.3648D-06	9.4062D-06	-8.2836D-06
-3.6752D-05	3.8968D-05	-4.0394D-05	3.9521D-05	-4.3104D-05	4.4938D-05
1.2594D-06	3.8286D-06	2.2211D-06	1.9831D-06	-6.6052D-07	4.9003D-06
9.4542D-08	9.7125D-07	-1.2469D-06	1.1816D-07	-7.9176D-07	7.9831D-07
4.3746D-07	-1.3312D-06	-1.7351D-06	6.5312D-07	3.6193D-07	1.0695D-06
3.1040D-07	9.7376D-07	8.3702D-07	4.4096D-07	1.0685D-07	1.5657D-06
7.8017D-08	5.0887D-07	-4.8835D-07	-1.6685D-08	2.0501D-07	-6.9968D-08
-4.0232D-06	3.3231D-06	4.3864D-06	-4.7056D-06	-4.5240D-07	1.2913D-06
2.0368D-06	-3.0123D-06	1.2065D-06	-3.0570D-07	-4.7602D-06	4.5674D-06

3.6752D-06	3.7165D-06	2.4102D-06	3.8588D-06	2.4221D-06	4.8343D-06
-9.3298D-05	3.7964D-05	-3.7786D-05	9.1891D-05	6.1827D-05	-6.0824D-05
-9.5435D-05	1.5508D-04	1.3890D-04	-9.9862D-05	-6.5072D-05	-2.9370D-05
1.2853D-04	-8.2431D-05	-6.1312D-06	-6.2090D-05	-1.2789D-04	1.4800D-04
-5.5791D-05	7.5365D-05	8.0875D-05	-7.9557D-05	-1.0666D-04	8.9574D-05
1.6455D-04	-1.6572D-04	2.1356D-04	-2.1136D-04	2.0196D-04	-2.0181D-04
-9.4683D-05	9.4212D-05	-5.7692D-05	3.7810D-05	-1.8658D-05	3.9379D-05
1.0127D-04	-1.3172D-04	6.8806D-05	-2.1927D-05	-1.5079D-04	1.3565D-04
1.2867D-04	-9.1681D-05	-1.3800D-04	1.5477D-04	1.2882D-05	-6.7493D-05
-9.0725D-06	-3.0117D-05	-5.1274D-05	-3.2258D-05	4.3774D-05	5.0030D-05
-5.6178D-05	-4.7793D-05	2.3669D-05	4.3034D-05	2.3523D-05	-1.1214D-05
5.1510D-05	4.5388D-05	4.8885D-05	5.8591D-05	6.3171D-05	5.9733D-05

G<sub>r</sub> =

Columns 1 thru 6

-1.8280D-02	-1.5537D-02	-1.1224D-03	1.4389D-03	-5.0311D-04	1.8313D-03
-3.3036D-04	4.3229D-04	1.3378D-03	-5.3114D-03	-5.2584D-03	3.0946D-03
1.8050D-03	9.3150D-04	-3.6901D-03	2.9605D-04	1.9551D-04	4.2035D-03
1.5137D-03	6.1015D-04	-4.4760D-04	-4.1444D-04	-5.1397D-04	6.7384D-04
8.4810D-04	-7.5246D-04	-1.1619D-04	9.3173D-04	6.8291D-04	1.3652D-04
1.3335D-04	6.3630D-04	6.3179D-04	2.7081D-05	-2.7486D-05	6.1166D-04
8.4899D-04	2.4283D-05	-2.8836D-05	2.7510D-04	-2.7479D-04	2.6505D-04
-5.7104D-05	9.6007D-04	-1.5845D-05	-4.5929D-04	-4.5851D-04	3.9169D-04
1.1360D-04	-2.2933D-04	9.4218D-05	1.4193D-04	-7.1689D-06	4.1344D-05
-3.2285D-04	-5.3640D-05	-1.4557D-04	-1.4642D-04	8.4966D-05	-4.4882D-05
-2.6272D-04	-1.2639D-04	6.1544D-05	3.2932D-07	1.8993D-04	-7.4053D-05
-1.3169D-04	1.3235D-04	9.9466D-05	1.4102D-04	-1.7967D-04	8.1487D-06
-6.6143D-05	-2.1002D-04	-2.2381D-05	1.0040D-04	1.2230D-04	-9.0157D-05
-2.2202D-04	-1.9204D-04	2.1722D-05	-2.6375D-04	2.5034D-04	-3.1820D-04
-2.1563D-04	-2.5924D-04	-1.0790D-05	-4.2934D-04	4.3463D-04	-4.6306D-04
-3.5058D-08	-5.6082D-05	-2.4212D-03	-2.1020D-03	-2.0687D-03	-2.1308D-03
5.5851D-03	-5.0089D-03	-1.3024D-03	2.2881D-03	2.3172D-03	1.2434D-03
5.0345D-03	5.5709D-03	-4.8792D-04	-2.7823D-03	-2.3254D-03	3.3225D-03
5.2296D-02	4.1093D-02	3.8289D-03	-2.2949D-03	-3.7316D-04	-3.4666D-03
5.2799D-03	1.7393D-02	-3.2174D-03	1.8195D-02	1.7853D-02	-1.2117D-02
4.8303D-03	-1.2800D-02	1.7510D-02	-3.0833D-03	-4.2590D-03	-1.3429D-02
-2.2675D-02	-6.7205D-03	3.0855D-03	-3.7516D-04	2.0441D-03	-2.4917D-03
-4.7464D-03	9.1332D-03	-1.2044D-03	-6.6510D-03	-2.1659D-03	1.0915D-03
-2.2464D-04	7.2323D-03	1.4954D-02	5.6789D-03	2.4521D-03	6.9536D-03
3.7347D-02	3.1894D-02	5.4341D-03	1.1129D-03	-1.1298D-03	1.0926D-03
1.5943D-03	2.6161D-02	-1.0601D-02	-3.2449D-03	-1.1734D-03	-2.1584D-03
-1.9238D-02	-1.3227D-03	3.6104D-03	1.1313D-03	3.5036D-03	2.9780D-03
2.5891D-03	3.4970D-03	2.1627D-02	1.1031D-02	5.8993D-03	1.2133D-02
1.5934D-03	2.5785D-03	-3.2993D-03	1.2767D-02	7.2188D-03	-1.1110D-02
1.0402D-03	4.5475D-03	-2.0724D-02	4.4089D-03	7.1555D-05	9.8260D-03
-3.2706D-02	-1.2698D-02	-6.0470D-03	2.8925D-03	2.3309D-03	4.7400D-03

-9.1788D-03	-1.3292D-02	-6.9404D-04	-1.2481D-02	-1.5630D-02	3.7917D-03
6.2004D-03	-5.7390D-03	-7.9753D-05	-1.0009D-02	-1.1910D-02	5.9448D-03
1.6723D-02	-7.1773D-03	6.6502D-03	-4.9512D-03	-3.4712D-03	-3.5543D-03
-3.1017D-02	-3.6592D-02	1.7392D-03	-2.7521D-03	-6.2305D-03	5.9703D-03
2.6549D-03	9.4137D-03	-3.5817D-04	-1.0629D-04	-1.7012D-03	1.1862D-02
2.6253D-04	8.9905D-04	6.0812D-03	5.2232D-04	-3.2343D-03	-8.2684D-04
-2.0122D-03	6.9568D-04	-1.1229D-02	4.3506D-03	-2.4326D-03	-4.2653D-04
-2.7503D-03	-4.1351D-03	-6.8443D-04	-1.3813D-03	-3.7212D-04	5.3549D-03
6.8552D-05	1.0005D-02	-1.6930D-03	4.9932D-06	1.7323D-03	2.3870D-03
2.2722D-03	5.9060D-03	-9.6330D-03	-3.7643D-05	-4.5177D-03	5.2239D-03
-4.7519D-03	-2.3217D-04	-1.1224D-02	-6.5433D-03	8.5614D-03	5.1610D-03
1.0617D-02	6.6949D-03	1.0134D-03	4.9744D-03	1.8230D-03	-1.7626D-03
-6.2577D-03	-1.9252D-03	3.5488D-03	1.6494D-03	9.0410D-03	4.4540D-03
4.6578D-03	-1.1673D-03	3.9286D-03	-6.5141D-03	5.7837D-03	7.5515D-03
-5.2549D-03	-4.0025D-03	-2.1910D-03	6.2756D-03	2.7092D-03	1.6285D-03
-6.7076D-03	3.4741D-03	-1.6500D-03	9.4557D-04	-6.9259D-03	-3.9420D-03
2.2969D-04	2.4123D-04	-1.3389D-02	1.4773D-02	2.4752D-02	1.2805D-02
-6.0891D-04	-2.2149D-04	-5.0292D-04	-5.2230D-03	6.4567D-03	-4.9762D-03
2.0465D-03	-2.0257D-04	-5.2210D-04	8.8949D-04	9.0624D-04	-7.5330D-03
3.6146D-04	-1.7483D-03	-8.3698D-04	-7.7648D-03	-1.1783D-02	2.9493D-03
-4.5370D-04	8.3132D-05	1.9366D-03	-4.9530D-03	-1.3090D-03	-3.9408D-03
1.1771D-04	5.0484D-04	-7.9015D-05	-7.1288D-03	-1.2430D-02	8.4792D-03
7.4089D-04	-3.8190D-04	-8.3807D-03	-9.4674D-03	-1.8110D-02	4.0988D-03
-3.9465D-04	-5.8139D-04	1.3164D-02	-1.1608D-03	-4.2952D-03	9.6539D-03
-1.7119D-04	-5.8906D-05	1.4382D-02	9.0366D-04	1.9564D-03	-4.7696D-04
-1.7824D-04	3.1514D-04	7.9339D-03	-6.7542D-03	-9.4412D-03	-6.6900D-03
-3.3882D-03	-5.9370D-04	1.6595D-03	2.3351D-03	1.9071D-03	-8.7123D-04
1.0345D-04	-1.4064D-03	1.1111D-03	-1.8896D-04	1.5820D-03	-2.1721D-03
-8.7423D-04	-2.1023D-03	-1.9156D-03	1.8786D-03	2.6449D-04	3.0988D-03
4.3219D-04	2.4656D-03	-1.4433D-03	3.1637D-03	-2.7716D-04	4.8793D-04
8.1131D-04	1.9553D-04	5.7385D-04	3.9921D-04	-5.8222D-04	-5.4735D-03
-1.8720D-05	-1.0476D-03	-3.5665D-04	-7.8764D-03	-9.9471D-03	3.2195D-03
-3.1282D-04	-8.7872D-04	-3.7294D-03	1.5139D-03	-1.6118D-03	-1.9440D-03
2.4270D-03	3.3304D-04	-6.0377D-03	8.7274D-05	4.7982D-04	-4.3400D-03
-4.6631D-04	6.7393D-04	3.4358D-03	1.5990D-03	1.2824D-03	-2.8622D-03
1.4905D-03	-7.6349D-04	-7.3898D-04	7.1506D-04	1.0083D-03	2.0016D-03
-2.2898D-03	-1.1855D-03	-1.7634D-03	8.3281D-04	4.5013D-04	2.0737D-03
-3.0080D-03	-1.6959D-03	-7.7766D-04	-2.2279D-03	2.1690D-03	-7.0865D-04
1.2564D-05	5.7634D-04	-5.5024D-04	-2.8275D-04	7.3527D-04	3.4052D-04
4.1087D-06	-7.2891D-04	6.0179D-04	1.5654D-04	-1.8280D-03	-2.1705D-04
1.0363D-05	2.5307D-05	-3.6398D-04	3.0908D-04	-6.3853D-05	2.8914D-04
-2.6164D-03	-2.1794D-03	2.3664D-04	-1.6710D-03	1.0298D-03	-7.3384D-04
-1.2516D-03	-7.5832D-04	-1.6120D-04	-3.9786D-04	-1.9951D-03	1.2893D-03
-1.4967D-03	-1.3205D-03	-3.0052D-04	2.5482D-03	2.7966D-03	2.8456D-04
1.5510D-03	1.3660D-03	-3.7094D-04	9.6953D-04	1.3401D-03	2.5097D-03
-2.3358D-04	-2.7496D-04	-9.2188D-05	-2.6628D-04	-1.8121D-05	1.4682D-03
-1.3527D-03	-1.2830D-03	-4.5313D-04	-8.0702D-04	1.3716D-03	-8.5538D-04
2.1438D-03	8.0161D-04	3.2979D-04	-4.4036D-04	8.0599D-04	-3.6208D-04
-1.0663D-03	-7.2998D-04	-1.0447D-04	1.9623D-04	3.5809D-05	-2.2381D-05

-1.5257D-03	-2.0021D-03	5.6303D-05	-2.6160D-05	-1.9479D-04	2.5566D-04
-3.4958D-04	2.8199D-03	7.9562D-04	6.0367D-05	1.4575D-03	-8.8492D-04
-1.7410D-04	-5.9908D-04	-4.0682D-05	6.6705D-04	-1.8244D-03	-3.0975D-04
-1.5271D-03	-4.7816D-03	-3.4774D-04	9.9595D-04	-1.7328D-03	-7.2253D-04
-2.6128D-05	-5.2575D-05	-7.4494D-04	4.8311D-03	8.1239D-03	5.0485D-03
-1.6889D-03	1.3912D-03	-4.9500D-04	-1.1619D-03	1.1224D-03	-4.8832D-04
-3.3448D-03	-2.4864D-03	-1.5516D-04	-1.6641D-03	-7.9904D-05	1.6603D-03
4.1455D-03	7.0196D-04	5.5625D-03	-2.8393D-03	-4.2139D-04	-8.4834D-04
-1.2857D-04	5.3879D-04	1.0593D-02	1.4286D-03	-3.6898D-04	2.5155D-03
1.7953D-03	-5.1350D-04	-2.9728D-03	4.7403D-04	-1.6420D-03	6.9889D-04
-7.8047D-04	6.6035D-04	-2.6850D-04	1.1271D-04	9.6194D-04	2.6185D-03
1.3820D-03	3.6318D-04	-1.0184D-02	-6.4089D-03	-2.3585D-03	1.1626D-02
-1.3685D-03	1.4904D-03	-5.5480D-03	-1.1499D-02	-1.0117D-02	-1.1227D-03
-7.3981D-04	3.7192D-05	2.3201D-02	-2.0899D-03	-3.4960D-03	6.0386D-03
5.3860D-04	-1.8028D-04	-6.1813D-03	-2.2289D-03	-1.0265D-03	-2.8034D-03
-3.5947D-04	-1.2930D-04	-6.2504D-03	-1.4009D-03	-5.6160D-04	-8.8717D-04
-8.8041D-04	-1.3164D-03	7.6246D-04	1.6465D-04	2.0784D-04	6.5149D-05
-8.0936D-04	-4.4409D-04	1.2887D-04	1.6046D-04	-8.2238D-05	9.7358D-05
4.0297D-04	2.7585D-04	4.9172D-05	9.8008D-05	8.9235D-06	-1.1131D-04
2.3549D-04	1.1395D-04	-6.1191D-04	-4.3234D-04	-2.5016D-04	-2.3907D-05
-4.1181D-04	-1.6718D-04	3.8557D-05	1.5870D-04	2.4570D-04	-1.5870D-04
-1.6230D-04	2.0505D-04	-2.4663D-04	-1.7273D-04	-2.2552D-04	-5.0071D-06
-4.9138D-04	-8.7040D-05	-6.0634D-05	-2.2916D-04	-2.1510D-04	-2.9143D-04
-2.3153D-04	-1.8177D-05	-6.2750D-04	-5.5247D-04	-3.9326D-04	2.1354D-04
2.1003D-04	8.7113D-05	-2.6577D-03	-4.8494D-04	-2.6931D-04	-5.2808D-04
7.7567D-05	5.0022D-05	1.1579D-03	-8.9710D-05	5.9674D-04	8.6660D-05
-7.4734D-04	-4.7490D-04	1.1523D-03	1.4458D-03	-2.5898D-03	1.4539D-03
-2.3314D-04	1.0357D-04	1.2298D-03	1.1478D-03	4.2358D-04	1.1261D-03
-4.3921D-05	3.0611D-05	8.9790D-05	8.5014D-05	-2.3371D-04	-1.2639D-04
-1.6684D-05	3.1011D-05	-4.8614D-05	-1.7388D-04	-1.6445D-04	8.4874D-06
-5.5766D-05	7.1951D-06	7.9492D-04	1.9476D-05	-1.7191D-04	4.9735D-05
-1.1241D-04	-1.0320D-04	1.6756D-06	-2.8539D-06	1.0907D-04	8.1364D-06
5.4143D-06	-2.7426D-05	-6.0025D-05	1.9387D-04	1.7720D-04	-1.4611D-04
-6.3944D-05	1.0541D-05	8.1944D-05	-6.1473D-05	-5.5928D-05	-1.0654D-04
3.9423D-04	-9.7721D-06	5.5136D-03	1.5068D-03	6.3377D-04	8.3335D-04
2.4338D-03	4.5603D-03	-3.3075D-03	1.4554D-05	-5.5410D-03	3.6050D-03
1.8557D-03	2.2747D-04	-5.1873D-03	8.3896D-03	6.7234D-03	-3.4934D-03
2.1988D-03	3.4196D-03	1.3134D-02	-3.0276D-03	-5.3824D-03	-7.0407D-03
-3.8946D-03	-2.7070D-03	4.8515D-03	7.0266D-03	7.4403D-03	-1.0065D-02
-2.4569D-04	-1.1323D-03	-1.3485D-03	4.3703D-03	7.4485D-04	1.3589D-04
5.3114D-03	5.6442D-04	-5.4364D-03	5.4148D-03	3.7297D-03	-1.0106D-03
1.7985D-03	-4.6310D-04	-1.3369D-02	1.6236D-03	-6.3434D-03	-3.7252D-03
-8.5687D-04	-2.1799D-03	-1.3814D-03	-3.9029D-03	-7.8544D-03	1.7154D-04
9.9399D-04	-2.1177D-03	-5.9405D-03	-1.3658D-02	-2.0889D-02	2.5174D-03
-3.1643D-03	-6.3148D-04	1.0184D-02	-3.4390D-03	-9.7339D-03	1.0921D-02
-1.6863D-04	-4.2142D-04	-1.0190D-02	1.5294D-02	1.9270D-02	1.8521D-02

Columns 7 thru 9

-9.5681D-05	-3.2239D-04	-2.1956D-03
2.7210D-03	2.3118D-03	2.4773D-03
4.4897D-03	-4.8030D-03	-4.3820D-03
5.9283D-04	-6.1756D-04	-4.4520D-04
1.7956D-04	-5.0532D-04	-4.9778D-04
4.4169D-04	4.6014D-04	4.4833D-04
3.7162D-04	-3.4507D-04	-3.1373D-04
2.0805D-05	-2.5979D-05	4.7634D-04
1.5244D-05	-2.5379D-05	-3.5379D-05
-2.1365D-04	9.6810D-05	1.3298D-04
-1.3968D-04	1.8260D-04	-1.5294D-06
-2.1712D-04	2.7566D-04	-7.6514D-06
-5.8976D-05	-1.1671D-04	3.4812D-05
3.0973D-04	-2.9216D-04	2.7320D-04
4.9531D-04	-5.1685D-04	4.0186D-04
-2.0964D-03	-2.1347D-03	-2.0926D-03
8.7809D-04	-3.5178D-03	-3.1213D-03
3.1234D-03	-6.2041D-04	-8.4161D-04
-1.2554D-03	2.6322D-03	4.6564D-03
-1.2472D-02	-5.9733D-03	-5.2023D-03
-1.3443D-02	1.7296D-02	1.6903D-02
-1.1394D-03	3.4854D-03	5.1447D-05
-1.0495D-03	4.3897D-04	1.7283D-03
1.6882D-03	6.0275D-03	3.2930D-03
-1.6490D-03	4.4095D-03	-2.4967D-04
-3.8635D-03	-4.9765D-03	-6.6584D-04
-1.5028D-04	4.6528D-03	1.4277D-03
7.8880D-03	1.0233D-02	7.4263D-03
-4.6739D-03	-2.5773D-03	-3.3175D-03
6.5625D-03	-1.4220D-02	-7.4552D-03
4.2914D-03	-4.4664D-03	-5.3383D-03
1.9348D-03	7.1419D-04	3.1108D-03
7.0739D-03	-1.3162D-03	3.5202D-05
-7.2523D-03	1.5230D-02	2.0326D-02
6.3865D-03	2.8866D-03	2.7651D-03
1.7349D-02	-2.1233D-03	3.2388D-05
-2.1320D-03	-4.6023D-04	-2.9439D-03
2.6501D-03	-4.5168D-03	4.5302D-04
-4.1506D-04	-2.7127D-03	2.2157D-03
1.4262D-03	-1.8164D-03	-3.8281D-03
-5.5434D-03	-6.5287D-03	7.1117D-03
-4.2874D-03	2.4277D-03	-1.8026D-03
-5.9643D-03	-1.5029D-03	2.4428D-03
-5.5117D-03	-7.4657D-03	-1.3036D-03
1.8921D-03	7.6153D-04	-1.0825D-02
-9.2231D-03	-5.2204D-03	5.7108D-03
3.2181D-03	4.2130D-03	1.2435D-03

2.1824D-02	1.3469D-02	2.2709D-02
6.4057D-03	-5.5868D-03	5.5607D-03
-1.0178D-02	4.6753D-03	9.2733D-03
5.4875D-03	5.3138D-03	8.0250D-03
-1.0696D-02	9.2335D-03	1.2080D-02
8.1365D-03	-4.0710D-04	5.9555D-03
6.0058D-03	6.6111D-03	1.4072D-02
1.9308D-02	-7.9000D-03	-1.3811D-02
-5.7103D-04	3.0330D-04	5.0252D-04
-9.3809D-03	-6.2959D-03	-8.4423D-03
-3.2308D-03	2.1726D-03	2.3613D-03
-3.1519D-03	-3.9387D-03	-4.4997D-03
1.1890D-03	1.0003D-03	-2.1172D-03
9.2281D-04	-2.9009D-04	2.8122D-04
-7.7336D-03	4.8074D-03	8.3401D-03
5.7665D-03	4.1863D-03	4.5882D-03
-3.7353D-03	4.8110D-03	2.5171D-03
-1.1765D-03	2.9139D-03	2.8928D-03
-1.6094D-03	-2.6183D-03	1.1870D-03
-3.3218D-04	-3.0180D-04	-1.1826D-03
-8.0341D-04	-4.9979D-04	8.3013D-04
1.2424D-04	-2.0898D-04	4.5243D-04
1.9451D-04	7.9998D-04	-1.4505D-03
1.4764D-03	5.1292D-04	-1.8512D-04
-1.9399D-05	2.6429D-04	-7.6367D-06
-1.1441D-03	2.2683D-04	2.9354D-03
2.4481D-03	-1.8080D-03	1.8270D-03
3.6417D-03	5.7272D-04	6.2066D-04
1.9253D-04	2.8226D-03	2.8686D-03
3.9455D-04	-2.5470D-04	1.0830D-03
6.2571D-04	3.7085D-04	-2.3661D-04
4.8486D-05	-1.0887D-04	4.4674D-04
-3.3724D-04	3.2999D-04	-5.1850D-04
-4.7937D-04	1.9729D-04	6.5918D-05
7.6047D-04	4.5944D-04	-1.0944D-03
7.4016D-04	-1.2228D-03	-1.9615D-04
6.5037D-04	4.0126D-04	-1.6107D-03
8.2887D-03	4.9198D-03	8.1960D-03
-8.3114D-04	-8.3949D-04	4.7401D-04
-1.7144D-04	1.5820D-03	-3.2785D-03
3.0740D-03	2.8113D-03	1.9245D-03
1.1491D-03	1.3423D-03	6.6810D-04
2.1196D-03	-2.1550D-03	7.7432D-04
-2.4823D-03	-2.1166D-03	9.3365D-04
1.0114D-02	-7.7875D-03	-7.8548D-03
8.3273D-04	8.0249D-03	7.1274D-03
3.7055D-03	6.6212D-03	2.9405D-03
-1.2184D-03	-8.9946D-04	-8.3969D-05
-5.0431D-04	-1.4396D-03	-6.9475D-04



-1.9238D-02	-1.3227D-03	3.6104D-03	1.1313D-03	3.5036D-03	2.9780D-03
2.5891D-03	3.4970D-03	2.1627D-02	1.1031D-02	5.8993D-03	1.2133D-02
1.5934D-03	2.5785D-03	-3.2993D-03	1.2767D-02	7.2188D-03	-1.1110D-02
1.0402D-03	4.5475D-03	-2.0724D-02	4.4089D-03	7.1555D-05	9.8260D-03
-3.2706D-02	-1.2698D-02	-6.0470D-03	2.8925D-03	2.3309D-03	4.7400D-03
-9.1788D-03	-1.3292D-02	-6.9404D-04	-1.2481D-02	-1.5630D-02	3.7917D-03
6.2004D-03	-5.7390D-03	-7.9753D-05	-1.0009D-02	-1.1910D-02	5.9448D-03
1.6723D-02	-7.1773D-03	6.6502D-03	-4.9512D-03	-3.4712D-03	-3.5543D-03
-3.1017D-02	-3.6592D-02	1.7392D-03	-2.7521D-03	-6.2305D-03	5.9703D-03
2.6549D-03	9.4137D-03	-3.5817D-04	-1.0629D-04	-1.7012D-03	1.1862D-02
2.6253D-04	8.9905D-04	6.0812D-03	5.2232D-04	-3.2343D-03	-8.2684D-04
-2.0122D-03	6.9568D-04	-1.1229D-02	4.3506D-03	-2.4326D-03	-4.2653D-04
-2.7503D-03	-4.1351D-03	-6.8443D-04	-1.3813D-03	-3.7212D-04	5.3549D-03
6.8552D-05	1.0005D-02	-1.6930D-03	4.9932D-06	1.7323D-03	2.3870D-03
2.2722D-03	5.9060D-03	-9.6330D-03	-3.7643D-05	-4.5177D-03	5.2239D-03
-4.7519D-03	-2.3217D-04	-1.1224D-02	-6.5433D-03	8.5614D-03	5.1610D-03
1.0617D-02	6.6949D-03	1.0134D-03	4.9744D-03	1.8230D-03	-1.7626D-03
-6.2577D-03	-1.9252D-03	3.5488D-03	1.6494D-03	9.0410D-03	4.4540D-03

Columns 7 thru 9

-9.5681D-05	-3.2239D-04	-2.1956D-03
2.7210D-03	2.3118D-03	2.4773D-03
4.4897D-03	-4.8030D-03	-4.3820D-03
5.9283D-04	-6.1756D-04	-4.4520D-04
1.7956D-04	-5.0532D-04	-4.9778D-04
4.4169D-04	4.6014D-04	4.4833D-04
3.7162D-04	-3.4507D-04	-3.1373D-04
2.0805D-05	-2.5979D-05	4.7634D-04
1.5244D-05	-2.5379D-05	-3.5379D-05
-2.1365D-04	9.6810D-05	1.3298D-04
-1.3968D-04	1.8260D-04	-1.5294D-06
-2.1712D-04	2.7566D-04	-7.6514D-06
-5.8976D-05	-1.1671D-04	3.4812D-05
3.0973D-04	-2.9216D-04	2.7320D-04
4.9531D-04	-5.1685D-04	4.0186D-04
-2.0964D-03	-2.1347D-03	-2.0926D-03
8.7809D-04	-3.5178D-03	-3.1213D-03
3.1234D-03	-6.2041D-04	-8.4161D-04
-1.2554D-03	2.6322D-03	4.6564D-03
-1.2472D-02	-5.9733D-03	-5.2023D-03
-1.3443D-02	1.7296D-02	1.6903D-02
-1.1394D-03	3.4854D-03	5.1447D-05
-1.0495D-03	4.3897D-04	1.7283D-03
1.6882D-03	6.0275D-03	3.2930D-03
-1.6490D-03	4.4095D-03	-2.4967D-04
-3.8635D-03	-4.9765D-03	-6.6584D-04
-1.5028D-04	4.6528D-03	1.4277D-03
7.8880D-03	1.0233D-02	7.4263D-03

-4.6739D-03	-2.5773D-03	-3.3175D-03
6.5625D-03	-1.4220D-02	-7.4552D-03
4.2914D-03	-4.4664D-03	-5.3383D-03
1.9348D-03	7.1419D-04	3.1108D-03
7.0739D-03	-1.3162D-03	3.5202D-05
-7.2523D-03	1.5230D-02	2.0326D-02
6.3865D-03	2.8866D-03	2.7651D-03
1.7349D-02	-2.1233D-03	3.2388D-05
-2.1320D-03	-4.6023D-04	-2.9439D-03
2.6501D-03	-4.5168D-03	4.5302D-04
-4.1506D-04	-2.7127D-03	2.2157D-03
1.4262D-03	-1.8164D-03	-3.8281D-03
-5.5434D-03	-6.5287D-03	7.1117D-03
-4.2874D-03	2.4277D-03	-1.8026D-03
-5.9643D-03	-1.5029D-03	2.4428D-03
-5.5117D-03	-7.4657D-03	-1.3036D-03

CF26 =

Columns 1 thru 6

2.0825D-02	-7.9624D-03	4.8065D-03	2.4055D-03	-6.2029D-04	-5.5048D-04
-1.9380D-02	-9.4290D-03	-4.1117D-03	-5.3274D-04	-2.1723D-03	-6.8749D-04
5.4088D-03	-3.7621D-03	6.7170D-04	3.9175D-03	-9.8336D-04	-7.8423D-04
-4.8615D-03	-4.0896D-03	-3.5865D-04	-9.8286D-04	-3.7525D-03	-1.2311D-03
1.7901D-02	9.2551D-03	2.5588D-03	-8.8023D-04	-2.4147D-03	-9.4900D-04
-1.5062D-02	-5.5808D-04	1.0726D-02	-5.8466D-04	1.0503D-03	-2.0401D-03
4.9201D-03	2.6861D-03	2.2043D-03	-1.2176D-03	-2.8657D-03	-1.1559D-03
-3.8118D-03	1.1287D-03	3.6813D-03	-7.5855D-04	1.3455D-03	-2.8596D-03
1.5341D-02	-8.8118D-04	-1.0794D-02	-3.1609D-04	1.1557D-03	-1.9489D-03
-1.9922D-02	8.3928D-03	-3.4214D-03	2.6599D-03	-4.0799D-04	-7.2251D-04
3.7168D-03	9.8314D-04	-3.8192D-03	-4.6071D-04	1.6316D-03	-3.0709D-03
-5.5175D-03	2.3411D-03	-2.5098D-03	3.4083D-03	-3.1526D-04	-8.5277D-04
-1.7012D-03	-3.8429D-04	-6.1782D-03	-5.5292D-04	-2.5868D-04	4.1930D-04
-9.3260D-05	-5.5845D-03	-2.9594D-03	-5.1681D-04	6.7995D-04	1.0557D-04
1.0002D-03	-5.2358D-03	3.4337D-03	-3.1398D-04	7.9327D-04	7.1248D-05
1.7186D-03	3.2831D-04	6.1818D-03	4.5266D-04	3.1171D-04	4.2165D-04
4.3424D-05	5.6523D-03	2.8427D-03	5.0638D-04	-9.1301D-05	4.8722D-04
-9.5038D-04	5.3340D-03	-3.2773D-03	-2.7944D-04	-5.3576D-04	4.4675D-04
1.5603D-01	-1.3264D-01	8.2740D-02	1.3249D-01	-3.5286D-02	-3.5855D-02
-1.4520D-01	-1.5707D-01	-7.0780D-02	-2.9342D-02	-1.2357D-01	-4.4779D-02
4.0524D-02	-6.2669D-02	1.1563D-02	2.1577D-01	-5.5939D-02	-5.1081D-02
-3.6424D-02	-6.8125D-02	-6.1740D-03	-5.4134D-02	-2.1346D-01	-8.0190D-02
1.3412D-01	1.5417D-01	4.4048D-02	-4.8481D-02	-1.3736D-01	-6.1813D-02
-1.1285D-01	-9.2965D-03	1.8464D-01	-3.2202D-02	5.9746D-02	-1.3288D-01
3.6863D-02	4.4745D-02	3.7945D-02	-6.7065D-02	-1.6302D-01	-7.5288D-02
-2.8560D-02	1.8802D-02	6.3370D-02	-4.1779D-02	7.6542D-02	-1.8626D-01

1.1494D-01	-1.4679D-02	-1.8582D-01	-1.7409D-02	6.5745D-02	-1.2694D-01
-1.4926D-01	1.3981D-01	-5.8897D-02	1.4650D-01	-2.3209D-02	-4.7061D-02
2.7847D-02	1.6377D-02	-6.5745D-02	-2.5375D-02	9.2813D-02	-2.0002D-01
-4.1339D-02	3.8998D-02	-4.3205D-02	1.8772D-01	-1.7934D-02	-5.5545D-02
-1.2746D-02	-6.4015D-03	-1.0635D-01	-3.0454D-02	-1.4715D-02	2.7311D-02
-6.9874D-04	-9.3027D-02	-5.0943D-02	-2.8465D-02	3.8679D-02	6.8763D-03
7.4938D-03	-8.7218D-02	5.9108D-02	-1.7293D-02	4.5126D-02	4.6408D-03
1.2877D-02	5.4689D-03	1.0642D-01	2.4932D-02	1.7732D-02	2.7464D-02
3.2535D-04	9.4157D-02	4.8936D-02	2.7890D-02	-5.1938D-03	3.1735D-02
-7.1205D-03	8.8854D-02	-5.6416D-02	-1.5391D-02	-3.0477D-02	2.9099D-02

Columns 7 thru 12

-8.2665D-04	2.5584D-04	1.0181D-03	-2.8130D-04	-1.4195D-04	-6.9834D-05
7.1069D-04	3.3590D-04	1.0139D-03	3.2280D-04	2.8107D-04	6.8963D-05
1.1465D-03	-9.1416D-04	-6.7856D-04	-6.8399D-05	6.7669D-05	1.7653D-04
-1.0145D-03	-8.5733D-04	-7.9555D-04	-7.9516D-05	7.1693D-05	-1.6981D-04
6.0654D-04	-1.0135D-04	6.2180D-04	3.8447D-04	7.5526D-04	-1.1638D-05
-2.0616D-05	4.5536D-04	-3.4855D-04	-3.9670D-04	9.1037D-04	-6.3135D-06
1.1768D-04	1.0808D-03	-3.5522D-04	-3.7277D-04	-8.6180D-04	8.7743D-05
8.6878D-04	-4.0698D-04	3.0468D-04	-1.3131D-04	-9.1350D-04	-2.6812D-05
1.1875D-04	4.2411D-04	-2.8550D-04	-9.2781D-04	5.2437D-04	-1.1060D-05
-6.3526D-04	-2.7676D-04	7.1359D-04	-7.8434D-04	-7.8544D-05	2.1460D-05
-8.2110D-04	-4.1586D-04	1.2431D-04	9.9283D-04	-8.0722D-05	4.8146D-05
-9.2793D-05	1.2428D-03	-5.5212D-04	8.2761D-04	1.2027D-05	-1.0835D-04
1.6346D-04	2.4226D-04	-1.3176D-04	-4.0261D-05	-5.9409D-05	-1.6550D-05
3.2379D-04	-2.1807D-05	-2.1414D-05	-1.9072D-05	-7.2264D-05	-4.3894D-04
-3.2964D-04	-9.6626D-06	-6.9406D-05	6.0886D-05	1.2593D-05	3.4886D-04
-1.7693D-04	2.3124D-04	-1.5084D-04	1.7865D-05	2.2427D-07	2.0442D-04
1.0339D-04	-2.9392D-04	8.9133D-05	4.8771D-05	-2.6634D-05	-6.3242D-04
-1.0672D-04	-3.0520D-04	8.5253D-05	6.2876D-05	-8.2893D-06	5.3487D-04
-1.2513D-01	4.0396D-02	1.7239D-01	-5.3726D-02	-2.8792D-02	-2.4451D-02
1.0758D-01	5.3038D-02	1.7169D-01	6.1652D-02	5.7011D-02	2.4146D-02
1.7354D-01	-1.4434D-01	-1.1490D-01	-1.3064D-02	1.3726D-02	6.1809D-02
-1.5356D-01	-1.3537D-01	-1.3471D-01	-1.5187D-02	1.4542D-02	-5.9457D-02
9.1813D-02	-1.6003D-02	1.0529D-01	7.3432D-02	1.5319D-01	-4.0747D-03
-3.1206D-03	7.1901D-02	-5.9018D-02	-7.5768D-02	1.8466D-01	-2.2106D-03
1.7813D-02	1.7065D-01	-6.0147D-02	-7.1196D-02	-1.7481D-01	3.0722D-02
1.3151D-01	-6.4261D-02	5.1590D-02	-2.5080D-02	-1.8529D-01	-9.3877D-03
1.7976D-02	6.6966D-02	-4.8343D-02	-1.7721D-01	1.0636D-01	-3.8726D-03
-9.6160D-02	-4.3699D-02	1.2083D-01	-1.4980D-01	-1.5932D-02	7.5139D-03
-1.2429D-01	-6.5664D-02	2.1049D-02	1.8962D-01	-1.6373D-02	1.6857D-02
-1.4046D-02	1.9623D-01	-9.3488D-02	1.5807D-01	2.4394D-03	-3.7937D-02
2.4743D-02	3.8253D-02	-2.2310D-02	-7.6896D-03	-1.2050D-02	-5.7948D-03
4.9012D-02	-3.4432D-03	-3.6259D-03	-3.6426D-03	-1.4658D-02	-1.5369D-01
-4.9898D-02	-1.5257D-03	-1.1752D-02	1.1629D-02	2.5544D-03	1.2215D-01
-2.6782D-02	3.6513D-02	-2.5540D-02	3.4121D-03	4.5490D-05	7.1574D-02
1.5650D-02	-4.6409D-02	1.5093D-02	9.3149D-03	-5.4024D-03	-2.2143D-01
-1.6155D-02	-4.8191D-02	1.4436D-02	1.2009D-02	-1.6814D-03	1.8727D-01

Columns 13 thru 18

-2.1815D-06	3.2105D-05	3.8729D-05	-2.6955D-04	-2.0228D-03	-2.1939D-04
2.1249D-06	-2.9890D-05	-3.8316D-05	-2.7634D-04	4.2964D-04	2.0062D-03
-3.6374D-05	-1.2043D-04	-1.4322D-04	-1.6335D-04	-1.5711D-04	-1.3831D-04
-2.9386D-05	1.3778D-04	1.4951D-04	-1.6301D-04	1.4685D-04	1.5386D-04
-4.3108D-05	8.1165D-05	5.4485D-05	-2.6080D-04	1.2849D-03	-1.8034D-03
3.1560D-05	-8.4986D-05	-5.5825D-05	-2.8837D-04	-2.1148D-03	-7.2034D-04
9.3909D-05	-2.3772D-04	-1.9699D-04	-1.9282D-04	2.6394D-04	-9.2309D-05
-2.4455D-05	2.7665D-04	2.1238D-04	-1.9296D-04	-2.7531D-04	5.5113D-05
6.2668D-05	6.4987D-05	5.1867D-05	-2.9253D-04	8.9817D-04	1.9833D-03
-5.9120D-05	-5.6053D-05	-4.6325D-05	-2.5300D-04	1.6178D-03	-1.4359D-03
-1.1855D-04	-2.3274D-04	-1.9484D-04	-1.8382D-04	-1.9306D-05	2.5834D-04
1.4133D-04	1.7358D-04	1.7199D-04	-1.8425D-04	5.1470D-05	-2.5279D-04
-5.5168D-04	3.8851D-04	-1.2550D-04	-1.9485D-03	-2.6466D-03	-2.1601D-03
1.5326D-04	-4.9281D-04	1.1386D-04	-1.9305D-03	8.9418D-04	-3.3199D-03
4.0531D-04	4.1770D-04	-1.2055D-04	-1.9310D-03	3.2011D-03	-1.2433D-03
-6.0181D-04	-2.3769D-04	1.3840D-04	-1.9501D-03	2.4237D-03	2.4035D-03
2.2397D-04	1.3320D-04	-1.5012D-04	-1.9653D-03	-5.0838D-04	3.3576D-03
3.6730D-04	-2.0966D-04	1.4322D-04	-1.9647D-03	-3.2828D-03	8.6619D-04
-7.7783D-04	1.2212D-02	2.5733D-02	2.0625D-02	1.0641D-01	1.1532D-02
7.5763D-04	-1.1369D-02	-2.5458D-02	2.1145D-02	-2.2602D-02	-1.0546D-01
-1.2970D-02	-4.5808D-02	-9.5160D-02	1.2499D-02	8.2650D-03	7.2703D-03
-1.0478D-02	5.2406D-02	9.9337D-02	1.2473D-02	-7.7256D-03	-8.0877D-03
-1.5371D-02	3.0873D-02	3.6202D-02	1.9955D-02	-6.7594D-02	9.4793D-02
1.1253D-02	-3.2326D-02	-3.7092D-02	2.2065D-02	1.1125D-01	3.7864D-02
3.3484D-02	-9.0421D-02	-1.3089D-01	1.4754D-02	-1.3885D-02	4.8522D-03
-8.7194D-03	1.0523D-01	1.4111D-01	1.4765D-02	1.4483D-02	-2.8970D-03
2.2345D-02	2.4719D-02	3.4462D-02	2.2383D-02	-4.7250D-02	-1.0425D-01
-2.1080D-02	-2.1321D-02	-3.0780D-02	1.9359D-02	-8.5107D-02	7.5478D-02
-4.2271D-02	-8.8529D-02	-1.2945D-01	1.4065D-02	1.0156D-03	-1.3579D-02
5.0390D-02	6.6023D-02	1.1428D-01	1.4098D-02	-2.7077D-03	1.3288D-02
-1.9670D-01	1.4778D-01	-8.3387D-02	1.4909D-01	1.3923D-01	1.1354D-01
5.4645D-02	-1.8745D-01	7.5656D-02	1.4771D-01	-4.7040D-02	1.7451D-01
1.4452D-01	1.5888D-01	-8.0098D-02	1.4775D-01	-1.6840D-01	6.5354D-02
-2.1458D-01	-9.0411D-02	9.1961D-02	1.4921D-01	-1.2751D-01	-1.2634D-01
7.9858D-02	5.0666D-02	-9.9745D-02	1.5037D-01	2.6744D-02	-1.7649D-01
1.3096D-01	-7.9750D-02	9.5159D-02	1.5033D-01	1.7270D-01	-4.5531D-02

Columns 19 thru 24

-5.7383D-02	3.5596D-02	-3.3235D-02	-4.8382D-02	2.1924D-02	-3.1502D-02
5.1451D-02	5.4591D-02	1.5275D-02	3.6968D-02	3.3992D-02	-3.1249D-02
-1.7732D-02	1.6685D-02	-9.8121D-03	-8.0728D-02	3.5100D-02	-5.0113D-02
1.5406D-02	2.2033D-02	2.0525D-03	6.4903D-02	5.9481D-02	-5.2441D-02
-4.6313D-02	-5.7328D-02	1.0854D-03	2.7353D-02	4.0128D-02	-1.9097D-02
3.5042D-02	-1.8325D-03	-6.6632D-02	-1.9310D-03	-3.5271D-02	-3.4792D-02

-1.5479D-02	-2.0904D-02	-4.0749D-03	3.5939D-02	5.3015D-02	-2.6130D-02
1.0920D-02	-4.7952D-03	-2.4557D-02	-7.0070D-04	-4.9947D-02	-5.7174D-02
-3.6183D-02	1.8468D-02	6.3126D-02	9.8047D-03	-3.5264D-02	-3.9809D-02
5.4460D-02	-4.6623D-02	2.0232D-02	-3.9005D-02	3.0894D-02	-1.9007D-02
-1.0708D-02	3.0121D-03	2.4629D-02	1.1815D-02	-5.5205D-02	-7.0204D-02
1.8088D-02	-1.5209D-02	1.1589D-02	-5.2862D-02	4.4546D-02	-2.2761D-02
4.9675D-03	5.3365D-03	2.2858D-02	-1.3726D-02	7.6959D-03	3.2595D-03
4.1142D-04	2.2522D-02	8.0833D-03	-1.5007D-02	4.0665D-03	2.8205D-03
-3.2624D-03	1.7317D-02	-1.6079D-02	1.3411D-02	8.3214D-03	4.3776D-04
-5.0311D-03	-4.7915D-03	-2.2940D-02	1.1380D-02	1.0959D-02	3.2862D-04
-1.8783D-04	-2.2660D-02	-7.3308D-03	6.8362D-04	-1.3555D-02	-1.1777D-02
3.0714D-03	-1.7881D-02	1.5294D-02	2.4165D-03	-1.3353D-02	-1.1901D-02
6.3653D-02	-2.4776D-02	2.2509D-02	5.5290D-03	-2.3137D-03	2.9761D-03
-5.7073D-02	-3.7998D-02	-1.0345D-02	-4.2246D-03	-3.5873D-03	2.9522D-03
1.9669D-02	-1.1614D-02	6.6454D-03	9.2255D-03	-3.7042D-03	4.7343D-03
-1.7089D-02	-1.5336D-02	-1.3901D-03	-7.4170D-03	-6.2773D-03	4.9542D-03
5.1373D-02	3.9903D-02	-7.3510D-04	-3.1258D-03	-4.2349D-03	1.8041D-03
-3.8870D-02	1.2755D-03	4.5128D-02	2.2068D-04	3.7223D-03	3.2869D-03
1.7170D-02	1.4550D-02	2.7598D-03	-4.1071D-03	-5.5948D-03	2.4686D-03
-1.2113D-02	3.3377D-03	1.6632D-02	8.0075D-05	5.2711D-03	5.4013D-03
4.0136D-02	-1.2855D-02	-4.2753D-02	-1.1205D-03	3.7216D-03	3.7608D-03
-6.0410D-02	3.2452D-02	-1.3703D-02	4.4574D-03	-3.2603D-03	1.7956D-03
1.1878D-02	-2.0966D-03	-1.6680D-02	-1.3503D-03	5.8260D-03	6.6323D-03
-2.0064D-02	1.0586D-02	-7.8489D-03	6.0410D-03	-4.7012D-03	2.1503D-03
-5.5103D-03	-3.7145D-03	-1.5481D-02	1.5686D-03	-8.1218D-04	-3.0793D-04
-4.5638D-04	-1.5676D-02	-5.4746D-03	1.7150D-03	-4.2915D-04	-2.6645D-04
3.6189D-03	-1.2053D-02	1.0890D-02	-1.5326D-03	-8.7818D-04	-4.1356D-05
5.5808D-03	3.3351D-03	1.5537D-02	-1.3005D-03	-1.1565D-03	-3.1046D-05
2.0835D-04	1.5772D-02	4.9650D-03	-7.8124D-05	1.4305D-03	1.1126D-03
-3.4070D-03	1.2446D-02	-1.0358D-02	-2.7616D-04	1.4092D-03	1.1243D-03

Columns 25 thru 30

4.8542D-03	-3.4610D-02	2.4742D-02	1.9822D-02	3.0427D-02	1.1445D-02
3.9360D-03	-3.7056D-02	-7.0010D-03	2.5229D-02	3.4769D-02	3.7294D-03
4.9479D-02	-4.4808D-02	-2.9458D-03	-3.7735D-04	-3.1504D-02	-4.1495D-02
-3.7048D-02	-5.1492D-02	1.5510D-02	1.7194D-03	-4.9741D-02	2.3546D-02
1.5019D-02	5.1877D-03	-3.8896D-02	3.9881D-02	-9.8180D-03	1.5148D-02
-1.4405D-02	2.0672D-02	-2.6679D-02	4.2077D-02	-1.8154D-02	1.2447D-02
5.4638D-02	4.6766D-02	-4.9868D-02	3.1240D-02	5.8053D-02	-1.9617D-03
-5.1953D-02	5.8877D-03	-5.8560D-02	3.2968D-02	-5.3442D-04	-6.4951D-02
4.6154D-03	3.2776D-02	2.7890D-02	3.3092D-02	-8.9602D-03	-2.5194D-02
-1.2825D-02	1.4001D-02	4.4393D-02	2.3553D-02	-5.0732D-03	-2.2010D-02
3.6461D-02	3.7584D-02	5.0325D-02	1.2023D-02	-2.5531D-02	5.4046D-02
-6.7366D-02	4.9023D-02	4.0695D-02	1.8842D-02	4.8057D-02	2.5852D-02
-6.6266D-03	9.8636D-03	-2.4487D-02	4.5715D-04	-2.1008D-02	1.6401D-02
-2.3430D-03	1.1290D-02	-2.5193D-02	-2.2726D-04	-1.6700D-02	2.2081D-02
3.5147D-05	1.7904D-02	1.8937D-02	-9.5629D-03	-4.0795D-03	-2.7369D-02
5.4491D-03	1.7890D-02	1.8385D-02	-8.3652D-03	-1.0332D-02	-2.3954D-02

-3.4526D-03	-2.2044D-02	4.0536D-05	-1.2097D-02	2.4935D-02	9.8421D-03
3.2830D-03	-2.1434D-02	1.1628D-03	-1.3244D-02	2.7186D-02	3.3597D-03
-3.4710D-04	2.3437D-03	-1.5089D-03	-1.0731D-03	-1.3614D-03	-5.0904D-04
-2.8144D-04	2.5094D-03	4.2695D-04	-1.3657D-03	-1.5557D-03	-1.6587D-04
-3.5380D-03	3.0343D-03	1.7965D-04	2.0428D-05	1.4096D-03	1.8455D-03
2.6491D-03	3.4870D-03	-9.4585D-04	-9.3083D-05	2.2257D-03	-1.0472D-03
-1.0739D-03	-3.5130D-04	2.3721D-03	-2.1590D-03	4.3930D-04	-6.7372D-04
1.0300D-03	-1.3999D-03	1.6270D-03	-2.2779D-03	8.1229D-04	-5.5359D-04
-3.9069D-03	-3.1669D-03	3.0411D-03	-1.6912D-03	-2.5976D-03	8.7247D-05
3.7149D-03	-3.9870D-04	3.5713D-03	-1.7848D-03	2.3913D-05	2.8888D-03
-3.3002D-04	-2.2196D-03	-1.7008D-03	-1.7915D-03	4.0093D-04	1.1205D-03
9.1706D-04	-9.4813D-04	-2.7073D-03	-1.2751D-03	2.2700D-04	9.7893D-04
-2.6071D-03	-2.5451D-03	-3.0691D-03	-6.5087D-04	1.1424D-03	-2.4038D-03
4.8170D-03	-3.3197D-03	-2.4818D-03	-1.0200D-03	-2.1503D-03	-1.1498D-03
4.7384D-04	-6.6795D-04	1.4933D-03	-2.4748D-05	9.4000D-04	-7.2943D-04
1.6753D-04	-7.6451D-04	1.5364D-03	1.2303D-05	7.4724D-04	-9.8206D-04
-2.5132D-06	-1.2124D-03	-1.1549D-03	5.1769D-04	1.8254D-04	1.2173D-03
-3.8964D-04	-1.2115D-03	-1.1212D-03	4.5285D-04	4.6232D-04	1.0654D-03
2.4688D-04	1.4928D-03	-2.4721D-06	6.5489D-04	-1.1157D-03	-4.3774D-04
-2.3476D-04	1.4515D-03	-7.0911D-05	7.1695D-04	-1.2165D-03	-1.4943D-04

Columns 31 thru 36

-9.6273D-02	5.8787D-02	1.8144D-02	-3.5474D-03	-8.7285D-03	-3.6844D-03
6.3869D-02	9.2329D-02	1.1304D-02	-7.3836D-03	4.3026D-03	-1.3203D-02
7.3746D-02	-4.7043D-02	-1.1937D-02	1.0236D-02	1.5077D-02	7.3814D-04
-4.5165D-02	-7.3714D-02	-2.9254D-03	4.6998D-03	-5.5001D-03	1.5691D-02
1.9921D-02	2.4178D-02	-2.9355D-02	2.9615D-03	-9.8789D-02	-3.8148D-02
-3.4638D-04	-1.7379D-02	3.2665D-02	1.9463D-02	2.8955D-02	-1.0140D-01
-1.8918D-02	-2.8023D-02	9.4076D-03	-3.3749D-03	7.6189D-02	2.5878D-02
-1.0358D-02	1.3286D-02	-2.5384D-02	-6.3617D-03	-2.1322D-02	7.6359D-02
6.7605D-03	-2.5435D-02	9.0341D-02	-5.8418D-02	-2.5844D-02	-1.7667D-02
-3.0982D-02	1.6848D-02	-5.1484D-02	-8.7342D-02	2.6148D-02	-2.9915D-02
5.5822D-03	2.2923D-02	-6.8434D-02	4.0589D-02	2.3307D-02	1.9321D-02
2.7860D-02	-1.9283D-02	3.1722D-02	6.4889D-02	-2.6088D-02	2.5662D-02
-8.5691D-03	1.4736D-02	1.5797D-02	1.1012D-02	8.4619D-03	1.2139D-02
6.2674D-03	-3.0377D-03	-5.5109D-03	-2.5225D-02	2.8993D-03	1.0361D-02
-5.3483D-03	-4.3959D-03	-1.3977D-02	1.5387D-02	-1.3866D-02	-1.3144D-02
2.1074D-03	1.7463D-02	1.2264D-02	1.3801D-02	1.3702D-02	8.3976D-03
8.7746D-03	-1.2852D-02	2.2581D-03	-2.2462D-02	-6.5487D-03	1.2395D-02
-3.2001D-03	-1.3684D-02	-1.3276D-02	1.2375D-02	-1.3103D-03	-1.9241D-02
2.4361D-03	-1.3786D-03	-3.9985D-04	7.3939D-05	1.7702D-04	7.2078D-05
-1.6161D-03	-2.1651D-03	-2.4910D-04	1.5390D-04	-8.7259D-05	2.5829D-04
-1.8660D-03	1.1032D-03	2.6305D-04	-2.1335D-04	-3.0576D-04	-1.4440D-05
1.1429D-03	1.7286D-03	6.4466D-05	-9.7958D-05	1.1155D-04	-3.0696D-04
-5.0407D-04	-5.6699D-04	6.4689D-04	-6.1726D-05	2.0035D-03	7.4629D-04
8.7649D-06	4.0754D-04	-7.1984D-04	-4.0567D-04	-5.8722D-04	1.9838D-03
4.7870D-04	6.5714D-04	-2.0731D-04	7.0342D-05	-1.5451D-03	-5.0625D-04
2.6209D-04	-3.1156D-04	5.5939D-04	1.3260D-04	4.3242D-04	-1.4938D-03

-1.7107D-04	5.9646D-04	-1.9908D-03	1.2176D-03	5.2413D-04	3.4563D-04
7.8397D-04	-3.9510D-04	1.1346D-03	1.8205D-03	-5.3030D-04	5.8523D-04
-1.4125D-04	-5.3756D-04	1.5081D-03	-8.4599D-04	-4.7268D-04	-3.7799D-04
-7.0498D-04	4.5219D-04	-6.9906D-04	-1.3525D-03	5.2907D-04	-5.0202D-04
2.1683D-04	-3.4557D-04	-3.4811D-04	-2.2952D-04	-1.7161D-04	-2.3747D-04
-1.5859D-04	7.1234D-05	1.2144D-04	5.2577D-04	-5.8799D-05	-2.0269D-04
1.3533D-04	1.0308D-04	3.0802D-04	-3.2070D-04	2.8120D-04	2.5713D-04
-5.3326D-05	-4.0950D-04	-2.7025D-04	-2.8766D-04	-2.7789D-04	-1.6428D-04
-2.2203D-04	3.0139D-04	-4.9762D-05	4.6818D-04	1.3281D-04	-2.4248D-04
8.0974D-05	3.2088D-04	2.9257D-04	-2.5792D-04	2.6573D-05	3.7642D-04

Columns 37 thru 42

-7.7808D-03	-1.9869D-02	1.5954D-03	2.1872D-02	-1.0603D-02	-1.0172D-03
-7.7766D-03	7.9912D-03	1.6713D-02	-2.1572D-02	-1.3239D-02	7.7044D-03
8.7264D-03	-5.8518D-03	-1.4592D-02	4.8236D-02	1.8710D-02	-9.0440D-04
9.8636D-03	1.8994D-02	-4.5709D-03	-4.9775D-02	7.3679D-03	-6.6180D-03
-1.8169D-03	5.4274D-03	-2.4081D-02	5.1002D-04	1.0252D-02	-1.9426D-02
-7.7932D-03	-1.7367D-02	-8.4755D-03	-8.1887D-03	-3.2205D-03	-1.3994D-02
5.3870D-03	2.3636D-03	1.6640D-02	-3.1811D-05	-7.7113D-03	1.0716D-02
7.7372D-03	8.5026D-03	1.6639D-02	6.7767D-03	4.7632D-04	2.4738D-02
-7.7305D-03	1.3410D-02	1.2057D-02	6.1005D-03	1.3566D-02	1.4024D-02
-1.8524D-03	1.6100D-02	-1.5039D-02	-3.4448D-04	1.0552D-02	6.5963D-03
7.7975D-03	-1.2703D-02	1.9314D-03	-2.9321D-03	-2.1809D-03	-1.0523D-02
5.4077D-03	-1.7926D-02	4.9999D-04	-8.5054D-04	-2.3599D-02	-1.1844D-02
-2.6684D-02	1.5669D-02	-3.2900D-02	-1.2863D-02	2.1983D-02	1.9545D-02
-3.3698D-02	-2.3007D-02	-1.4509D-02	2.0993D-03	-2.7378D-02	9.3887D-04
-3.4513D-02	2.1295D-02	1.5507D-02	5.0104D-03	-2.7878D-02	1.7005D-02
-2.6621D-02	2.4860D-02	-2.5540D-02	1.0298D-02	1.3120D-02	-3.0371D-02
-3.6749D-02	-1.9935D-02	-7.9550D-04	-9.1220D-03	-2.2741D-03	-2.7171D-02
-3.8477D-02	5.8940D-03	1.9731D-02	5.4007D-03	2.1467D-02	1.8647D-02
1.0255D-04	2.4303D-04	-1.9183D-05	-2.4392D-04	1.1025D-04	1.0400D-05
1.0250D-04	-9.7747D-05	-2.0096D-04	2.4058D-04	1.3766D-04	-7.8772D-05
-1.1502D-04	7.1578D-05	1.7546D-04	-5.3794D-04	-1.9454D-04	9.2468D-06
-1.3001D-04	-2.3233D-04	5.4961D-05	5.5510D-04	-7.6610D-05	6.7664D-05
2.3948D-05	-6.6387D-05	2.8955D-04	-5.6879D-06	-1.0660D-04	1.9862D-04
1.0272D-04	2.1243D-04	1.0191D-04	9.1322D-05	3.3486D-05	1.4308D-04
-7.1004D-05	-2.8911D-05	-2.0007D-04	3.5479D-07	8.0180D-05	-1.0956D-04
-1.0198D-04	-1.0400D-04	-2.0007D-04	-7.5576D-05	-4.9527D-06	-2.5293D-04
1.0189D-04	-1.6403D-04	-1.4498D-04	-6.8034D-05	-1.4106D-04	-1.4338D-04
2.4415D-05	-1.9693D-04	1.8083D-04	3.8417D-06	-1.0972D-04	-6.7442D-05
-1.0278D-04	1.5538D-04	-2.3223D-05	3.2700D-05	2.2677D-05	1.0759D-04
-7.1276D-05	2.1927D-04	-6.0118D-06	9.4854D-06	2.4538D-04	1.2109D-04
3.5170D-04	-1.9166D-04	3.9559D-04	1.4345D-04	-2.2857D-04	-1.9983D-04
4.4415D-04	2.8142D-04	1.7446D-04	-2.3412D-05	2.8468D-04	-9.5992D-06
4.5490D-04	-2.6048D-04	-1.8646D-04	-5.5878D-05	2.8987D-04	-1.7386D-04
3.5088D-04	-3.0408D-04	3.0709D-04	-1.1485D-04	-1.3642D-04	3.1053D-04
4.8437D-04	2.4384D-04	9.5650D-06	1.0173D-04	2.3645D-05	2.7780D-04
5.0714D-04	-7.2095D-05	-2.3724D-04	-6.0230D-05	-2.2321D-04	-1.9065D-04

Columns 43 thru 48

3.7932D-03	-3.5114D-04	0.0000D+00	0.0000D+00	0.0000D+00	0.0000D+00
7.4290D-04	1.1647D-03	0.0000D+00	0.0000D+00	0.0000D+00	0.0000D+00
-8.7199D-03	-4.0010D-04	0.0000D+00	0.0000D+00	0.0000D+00	0.0000D+00
2.6735D-03	-2.4351D-03	0.0000D+00	0.0000D+00	0.0000D+00	0.0000D+00
2.1788D-03	-1.6183D-02	0.0000D+00	0.0000D+00	0.0000D+00	0.0000D+00
-2.7823D-03	2.3512D-02	0.0000D+00	0.0000D+00	0.0000D+00	0.0000D+00
1.2601D-03	-2.5801D-02	0.0000D+00	0.0000D+00	0.0000D+00	0.0000D+00
2.0376D-03	1.9450D-02	0.0000D+00	0.0000D+00	0.0000D+00	0.0000D+00
2.1235D-02	-5.4075D-03	0.0000D+00	0.0000D+00	0.0000D+00	0.0000D+00
-2.6720D-02	-1.4896D-03	0.0000D+00	0.0000D+00	0.0000D+00	0.0000D+00
3.8753D-02	9.3353D-03	0.0000D+00	0.0000D+00	0.0000D+00	0.0000D+00
-3.4446D-02	-1.6482D-04	0.0000D+00	0.0000D+00	0.0000D+00	0.0000D+00
-1.8161D-02	4.7143D-03	0.0000D+00	0.0000D+00	0.0000D+00	0.0000D+00
2.4834D-02	-4.2384D-03	0.0000D+00	0.0000D+00	0.0000D+00	0.0000D+00
-4.4263D-03	1.8724D-02	0.0000D+00	0.0000D+00	0.0000D+00	0.0000D+00
7.6056D-03	-1.7029D-02	0.0000D+00	0.0000D+00	0.0000D+00	0.0000D+00
-2.0355D-02	2.6571D-02	0.0000D+00	0.0000D+00	0.0000D+00	0.0000D+00
1.4732D-02	-2.2161D-02	0.0000D+00	0.0000D+00	0.0000D+00	0.0000D+00
-3.8461D-05	3.4887D-06	0.0000D+00	0.0000D+00	0.0000D+00	0.0000D+00
-7.5327D-06	-1.1572D-05	0.0000D+00	0.0000D+00	0.0000D+00	0.0000D+00
8.8416D-05	3.9752D-06	0.0000D+00	0.0000D+00	0.0000D+00	0.0000D+00
-2.7108D-05	2.4194D-05	0.0000D+00	0.0000D+00	0.0000D+00	0.0000D+00
-2.2092D-05	1.6079D-04	0.0000D+00	0.0000D+00	0.0000D+00	0.0000D+00
2.8211D-05	-2.3360D-04	0.0000D+00	0.0000D+00	0.0000D+00	0.0000D+00
-1.2777D-05	2.5634D-04	0.0000D+00	0.0000D+00	0.0000D+00	0.0000D+00
-2.0660D-05	-1.9324D-04	0.0000D+00	0.0000D+00	0.0000D+00	0.0000D+00
-2.1532D-04	5.3726D-05	0.0000D+00	0.0000D+00	0.0000D+00	0.0000D+00
2.7093D-04	1.4800D-05	0.0000D+00	0.0000D+00	0.0000D+00	0.0000D+00
-3.9294D-04	-9.2750D-05	0.0000D+00	0.0000D+00	0.0000D+00	0.0000D+00
3.4927D-04	1.6375D-06	0.0000D+00	0.0000D+00	0.0000D+00	0.0000D+00
1.8414D-04	-4.6838D-05	0.0000D+00	0.0000D+00	0.0000D+00	0.0000D+00
-2.5181D-04	4.2110D-05	0.0000D+00	0.0000D+00	0.0000D+00	0.0000D+00
4.4881D-05	-1.8603D-04	0.0000D+00	0.0000D+00	0.0000D+00	0.0000D+00
-7.7118D-05	1.6919D-04	0.0000D+00	0.0000D+00	0.0000D+00	0.0000D+00
2.0639D-04	-2.6399D-04	0.0000D+00	0.0000D+00	0.0000D+00	0.0000D+00
-1.4938D-04	2.2018D-04	0.0000D+00	0.0000D+00	0.0000D+00	0.0000D+00
0.0000D+00	0.0000D+00	8.2192D-05	5.2920D-05	-5.8617D-05	1.0954D-05
0.0000D+00	0.0000D+00	5.5167D-06	2.1632D-05	3.7803D-05	-1.5747D-05
0.0000D+00	0.0000D+00	-4.1958D-04	-2.4597D-05	-1.4430D-04	-1.9811D-04
0.0000D+00	0.0000D+00	1.2184D-05	-1.6538D-04	5.2554D-06	2.4765D-05
0.0000D+00	0.0000D+00	9.5835D-05	-6.0167D-05	-4.5796D-05	6.0875D-05
0.0000D+00	0.0000D+00	-6.9668D-06	1.5496D-05	-3.7690D-05	1.9489D-05
0.0000D+00	0.0000D+00	-3.8327D-04	-2.0038D-04	1.6037D-04	2.1030D-05
0.0000D+00	0.0000D+00	2.8833D-05	9.9612D-05	1.6077D-04	-5.7120D-05
0.0000D+00	0.0000D+00	1.2266D-04	1.3896D-05	6.5701D-05	-7.0880D-05
0.0000D+00	0.0000D+00	1.4042D-06	-3.6101D-05	-7.9689D-09	9.0793D-06



0.0000D+00	0.0000D+00	-4.0373D-04	1.8487D-04	1.2150D-04	1.6261D-04
0.0000D+00	0.0000D+00	-4.1726D-05	7.8528D-05	-1.6227D-04	4.3717D-05
0.0000D+00	0.0000D+00	4.4540D-04	-4.6701D-03	2.0807D-04	-3.1230D-04
0.0000D+00	0.0000D+00	1.2589D-03	2.3941D-04	4.5094D-03	4.6061D-04
0.0000D+00	0.0000D+00	-4.3426D-03	-9.1632D-04	-1.6733D-02	-2.1305D-04
0.0000D+00	0.0000D+00	8.5697D-03	-1.6900D-02	2.6374D-04	-4.5974D-04
0.0000D+00	0.0000D+00	4.3404D-03	9.4817D-04	1.6731D-02	2.1000D-04
0.0000D+00	0.0000D+00	5.5133D-03	1.7181D-02	-1.1149D-03	3.3040D-04
0.0000D+00	0.0000D+00	9.6080D-05	-1.0996D-03	3.9042D-05	2.9082D-05
0.0000D+00	0.0000D+00	2.7969D-04	6.1425D-05	1.1001D-03	-1.0529D-04

Columns 49 thru 54

6.6108D-05	-2.8417D-05	5.0482D-05	-7.9112D-05	3.8919D-05	8.8048D-06
-1.1764D-05	-2.3698D-05	-5.9609D-05	-3.4100D-05	1.1042D-05	1.2986D-05
-1.1137D-04	-1.9293D-05	-1.9803D-04	7.7233D-06	-1.6052D-05	3.0246D-05
-4.1106D-05	2.3769D-05	2.2039D-08	7.9453D-05	-5.6550D-05	-6.9648D-06
-2.1984D-05	4.0000D-05	4.8640D-05	7.5367D-05	-3.2005D-05	-1.4000D-05
7.6611D-06	-1.5866D-05	6.1188D-05	-3.4529D-05	1.9655D-05	-1.0389D-05
1.8499D-04	-7.7720D-05	6.9519D-05	-1.5875D-04	4.8851D-05	-2.9862D-06
-1.5285D-05	-3.3186D-05	-7.1969D-05	-4.4682D-05	6.2266D-06	1.6141D-05
-3.9584D-05	-8.0918D-06	-8.2730D-05	-2.9045D-06	-3.5243D-06	4.9097D-06
-1.2767D-05	-1.2746D-06	-4.4528D-07	7.5372D-05	-2.3001D-05	-8.4589D-06
-8.1651D-05	1.0327D-04	6.5240D-05	1.7135D-04	-4.7670D-05	-2.3009D-05
4.1854D-05	-1.8131D-05	7.4065D-05	-4.4196D-05	1.3357D-05	1.5134D-05
5.8445D-04	-2.2213D-04	4.1806D-06	-1.8684D-05	1.1074D-04	7.5120D-05
2.9185D-04	-5.2569D-06	6.9080D-05	1.6229D-05	-2.5413D-05	1.1744D-04
-1.6678D-04	1.2219D-04	2.1238D-04	-1.7714D-05	1.8133D-05	2.4392D-04
7.3246D-04	-8.5384D-06	2.3570D-05	1.1658D-04	-4.6802D-04	-1.5155D-04
1.7118D-04	-1.2781D-04	-2.1266D-04	1.1416D-05	-1.1730D-05	-2.4094D-04
-8.3317D-04	4.5376D-05	-3.0371D-07	-1.1610D-04	4.6451D-04	1.9490D-04
-4.9009D-05	6.2807D-05	-2.6169D-07	5.8120D-05	-8.3494D-05	-3.4204D-05
-5.8020D-05	-1.7716D-05	-7.5245D-05	-8.7945D-07	-5.3068D-08	-4.0391D-05

Columns 55 thru 60

-4.7716D-06	-6.5742D-05	9.7871D-05	-9.1054D-05	-8.7941D-07	-1.4786D-05
1.5699D-05	8.2509D-05	7.1782D-05	1.8257D-05	1.1945D-06	-8.0070D-05
2.6284D-05	5.6070D-05	3.2446D-05	1.4376D-04	6.4666D-05	-9.3161D-06
-8.3047D-06	1.6544D-05	-9.8339D-05	1.1555D-05	-2.7004D-07	-5.3149D-06
-2.5823D-06	-2.7071D-05	-1.3545D-04	-6.2221D-05	-2.1058D-07	-1.2077D-05
-6.7327D-06	-1.0010D-04	3.5340D-05	-3.1865D-05	-2.0430D-06	-8.0216D-05
-2.9078D-06	-1.2026D-04	8.8851D-05	1.1219D-04	8.8752D-05	-7.1563D-06
-1.0399D-05	7.7584D-05	6.6304D-05	1.6399D-05	1.6189D-07	-7.0605D-06
6.6840D-06	1.5466D-04	2.1129D-05	-2.2527D-05	8.3756D-07	-1.1094D-05
-1.9780D-06	1.7614D-05	-1.0660D-04	1.3600D-05	9.6308D-07	-8.4442D-05
-2.0077D-05	-8.9704D-05	-8.2402D-05	1.2561D-04	8.0130D-05	-1.1989D-05
-1.6722D-05	-9.3903D-05	3.2276D-05	-2.8206D-05	-1.9200D-07	-7.4656D-06

-6.9771D-05	-2.9458D-05	1.7203D-04	-1.6404D-05	6.1670D-06	-2.1072D-06
1.0239D-04	-1.8241D-04	-3.2412D-05	-3.9225D-05	1.3274D-05	-4.3440D-08
1.1629D-04	-4.3157D-04	-9.2885D-05	-1.6623D-04	-7.0271D-05	-1.5929D-05
1.5153D-04	1.0804D-04	-4.5602D-04	1.8978D-05	-8.8033D-05	3.2649D-06
-1.1818D-04	4.2939D-04	1.0873D-04	1.6424D-04	7.0041D-05	2.7356D-06
-1.5227D-04	-3.0691D-05	4.4699D-04	-1.2457D-04	-1.3839D-04	-6.6776D-06
2.6276D-05	1.3724D-05	-8.3650D-05	9.7752D-06	5.0930D-08	-2.5393D-06
-2.5096D-05	8.6310D-05	1.7924D-05	2.3623D-05	2.0160D-06	-5.8461D-06

Columns 61 thru 66

7.8357D-05	-3.3035D-05	-1.4227D-04	-3.1451D-04	4.9621D-04	-2.3742D-03
-3.7737D-05	-1.1727D-04	-9.2071D-06	-4.5813D-06	-1.4985D-05	1.9745D-03
-1.1234D-04	-1.0580D-04	1.0315D-03	2.8220D-04	6.8494D-04	6.5891D-03
-8.3438D-05	9.3005D-05	-6.0525D-05	9.7543D-04	-1.9085D-04	-8.3949D-04
-1.4914D-05	8.3255D-05	-2.2003D-04	5.0405D-04	2.1285D-04	-3.0313D-03
1.2124D-04	2.4738D-05	9.0077D-06	1.3986D-05	1.3146D-06	-1.7321D-03
1.5970D-04	-4.7886D-05	8.4447D-04	8.9161D-04	-1.0839D-03	-1.8195D-03
-3.6668D-05	-1.1388D-04	-1.3238D-04	-7.4136D-04	-8.5828D-04	5.2978D-03
-6.5893D-05	-5.3444D-05	-3.4139D-04	-1.8993D-04	-4.5735D-04	4.9668D-03
-8.2637D-05	9.1591D-05	5.1025D-07	-2.0806D-05	1.3601D-05	-2.6781D-04
-3.6157D-05	1.5824D-04	9.4951D-04	-1.0462D-03	-5.1572D-04	-3.4111D-03
1.1842D-04	2.4402D-05	1.9627D-04	-3.1647D-04	1.0382D-03	-4.9525D-03
7.6809D-04	-8.5119D-04	-1.6215D-03	2.1778D-02	-4.4097D-03	1.5486D-03
8.3862D-04	7.4166D-04	-4.3784D-03	-4.5223D-03	-2.1135D-02	-9.7480D-03
-1.2054D-03	-1.0774D-03	1.5799D-02	1.7363D-02	8.0363D-02	-5.0137D-02
1.0663D-03	-1.2286D-03	-2.4192D-02	8.0665D-02	-1.2183D-02	-2.1330D-03
1.2125D-03	1.0687D-03	-1.5788D-02	-1.7546D-02	-8.0321D-02	5.0228D-02
-1.0953D-03	1.2174D-03	-1.2584D-02	-8.1991D-02	2.0120D-02	8.0386D-03
-3.9431D-05	4.0548D-05	-3.6048D-04	5.0655D-03	-9.7753D-04	-8.8494D-04
-3.8740D-05	-3.7140D-05	-1.0124D-03	-1.0960D-03	-5.1004D-03	7.4713D-03

Columns 67 thru 72

-4.6707D-03	-2.6108D-03	2.5388D-04	-6.7757D-03	-4.9226D-03	-2.9016D-03
-7.5899D-04	-9.4838D-04	5.9152D-04	-1.1265D-03	3.6009D-03	-1.8622D-03
1.3094D-03	-3.6980D-04	-3.4147D-03	9.1872D-04	4.2364D-03	-1.9965D-03
6.6293D-03	1.3207D-04	-7.5474D-04	1.2532D-02	-3.5087D-03	-8.2107D-03
4.1361D-03	2.3836D-03	4.0960D-04	7.0391D-03	-5.0368D-03	1.3216D-03
-1.2887D-03	-5.9152D-04	-6.0658D-04	-2.1639D-03	-3.4053D-03	-2.0780D-04
-5.4513D-03	-2.2300D-03	-5.4324D-03	-4.6289D-03	-1.6375D-03	-1.5530D-03
-1.3797D-03	-5.4971D-03	1.0202D-03	-4.8297D-04	7.4364D-03	-1.4909D-02
6.1680D-04	-9.0762D-04	2.8815D-03	1.5111D-03	8.6729D-03	-3.8334D-03
2.1643D-03	9.7129D-04	-9.6275D-05	3.7071D-03	-6.2172D-04	4.1797D-05
4.9875D-03	2.4110D-03	-5.3748D-03	2.8687D-03	-3.3162D-03	3.6841D-05
-2.9309D-03	-4.5898D-03	-2.4562D-03	-3.5418D-03	-1.1701D-02	-1.0549D-02
-1.3557D-02	-2.6401D-03	-2.1386D-03	-1.7003D-03	-4.1834D-04	-5.4014D-04
-2.0443D-03	-1.5559D-06	-5.7891D-03	-1.6217D-04	-4.2026D-03	2.1074D-03

-7.0161D-03	5.1709D-03	-1.0850D-02	-1.6069D-02	-8.6045D-02	1.5931D-02
4.3457D-02	3.2781D-02	-1.6626D-02	8.3893D-02	-7.5135D-03	2.2548D-02
6.2633D-03	-5.8857D-03	1.0783D-02	1.5027D-02	8.5919D-02	-1.7392D-02
-4.1134D-02	-3.1145D-02	-1.0008D-02	-8.7090D-02	9.5176D-03	-2.2076D-02
7.1408D-03	3.7231D-03	9.3395D-05	7.2836D-03	-6.3875D-04	1.4651D-03
1.2179D-03	-6.6101D-04	1.8393D-03	1.7417D-03	7.0052D-03	-2.2853D-03

Columns 73 thru 78

8.2948D-03	9.9507D-03	2.8690D-03	-8.5141D-03	-3.6354D-03	-1.3821D-02
3.4591D-03	-3.4872D-03	-2.2696D-03	-3.4374D-03	-6.4700D-03	6.0305D-03
-3.2708D-04	-1.9469D-03	-1.3311D-02	-1.3307D-03	-2.5827D-03	1.2408D-02
-1.5451D-02	-3.8278D-03	-3.1646D-03	1.4790D-02	3.9522D-03	-3.2717D-04
-1.2429D-02	2.7615D-03	-8.6579D-05	1.1729D-02	6.1775D-03	-2.3486D-03
1.1899D-03	4.5844D-03	3.4420D-03	-2.7229D-03	-2.3027D-04	-1.4323D-02
7.1913D-04	-8.3258D-04	3.5581D-03	-3.5299D-03	-7.3014D-03	-1.3237D-02
1.1595D-02	-1.1594D-02	5.9040D-04	-2.2122D-04	7.1048D-05	1.4653D-03
3.9762D-03	-1.1866D-02	-1.0317D-03	9.8452D-04	-3.6275D-03	1.2049D-02
-4.4812D-03	-1.0423D-03	-1.7346D-03	8.8137D-03	8.6415D-03	4.9243D-03
-5.3539D-04	6.5921D-04	1.1056D-03	4.8196D-03	1.9534D-02	6.0134D-04
4.6154D-03	1.5929D-02	-6.9900D-04	-1.3265D-03	3.7356D-03	-1.3505D-02
4.2727D-02	1.0015D-02	2.0567D-03	-1.1932D-02	-7.1228D-03	-3.1127D-03
-1.1105D-02	4.5251D-02	7.7789D-03	2.9512D-04	3.2854D-03	-7.9555D-03
-1.5841D-02	6.8148D-02	-3.9991D-02	-8.2201D-03	-1.0998D-02	1.7604D-02
-7.2798D-02	-2.3188D-02	3.9902D-03	1.3456D-02	-5.5770D-02	-1.5317D-02
1.8310D-02	-6.7520D-02	4.0088D-02	7.3175D-03	1.1471D-02	-1.8553D-02
7.3660D-02	1.5675D-02	1.0367D-02	-8.8092D-03	4.4579D-02	1.5029D-02
-8.5416D-03	-2.0014D-03	-1.1802D-04	-7.8501D-05	2.2047D-03	4.6120D-04
1.7492D-03	-8.6626D-03	-2.0845D-03	4.3353D-04	-5.4931D-04	-1.6605D-04

Columns 79 thru 84

-6.8666D-04	-4.7513D-03	2.0876D-02	4.7840D-02	1.0645D-03	4.2100D-02
-4.9989D-03	-1.2345D-02	2.6914D-02	2.6909D-02	7.7154D-02	3.2158D-02
-6.0487D-03	-9.7816D-03	5.2740D-03	5.5179D-02	5.7476D-02	2.5994D-02
-5.8274D-04	-1.7190D-03	4.0616D-03	-3.9026D-02	5.6352D-02	-1.0867D-02
7.4179D-03	7.3612D-03	-3.4775D-04	-2.2551D-02	4.5810D-02	-2.0162D-03
-2.3666D-03	3.9764D-03	2.7585D-02	-8.1401D-02	2.1782D-03	-4.2546D-02
-1.6333D-02	5.2766D-03	-4.6870D-03	-7.4048D-02	2.0530D-02	-3.9518D-02
-6.5551D-03	-1.2465D-02	2.7539D-02	-3.1311D-02	-5.5312D-02	-3.0005D-02
-1.3963D-03	-1.1455D-02	1.2343D-02	-3.3424D-02	-3.5716D-02	-2.8013D-02
5.2105D-03	1.9319D-03	5.6022D-02	3.9321D-02	-5.5194D-02	9.8300D-03
2.5274D-04	9.0819D-03	2.7374D-02	2.1651D-02	-7.1909D-02	-8.3425D-03
-3.6103D-04	-5.6001D-03	2.8164D-02	6.3130D-02	9.2468D-03	4.0121D-02
-2.2168D-03	-1.2456D-03	1.4800D-02	3.8678D-02	-5.7802D-02	4.9204D-03
5.0807D-04	1.9803D-03	1.5643D-03	6.2540D-02	4.0262D-02	3.7617D-02
1.3718D-02	-2.6039D-02	5.5036D-03	3.1193D-01	2.0479D-01	2.1965D-01
-1.2166D-02	1.0241D-03	-1.1305D-01	-2.4508D-01	3.2485D-01	-7.9261D-02

-1.4160D-02	2.4208D-02	5.5969D-03	-3.0292D-01	-2.1687D-01	-2.1625D-01
3.6464D-02	-1.1652D-02	1.0926D-01	2.1515D-01	-3.4819D-01	4.7344D-02
9.4057D-04	-8.3335D-04	1.0270D-02	2.5606D-02	-3.7087D-02	8.4054D-03
5.1424D-04	-1.6762D-03	3.8024D-03	3.4599D-02	3.7147D-02	2.7764D-02

Columns 85 thru 88

-7.0163D-02	-2.3618D-02	2.5509D-02	3.9196D-02
7.7281D-03	-2.9521D-02	-3.8655D-02	-4.9560D-03
1.3291D-03	-1.5009D-02	-4.8839D-02	2.3019D-02
3.5341D-02	-1.6063D-02	-4.0172D-02	-4.6710D-02
6.2855D-02	-5.4082D-02	-3.8900D-02	-4.8318D-02
2.4085D-02	1.4739D-02	2.6402D-04	-3.5567D-02
1.7441D-02	1.2220D-02	-2.3421D-02	-1.8168D-02
-6.3952D-03	2.8643D-02	4.0190D-02	2.9815D-03
1.6905D-02	6.6031D-02	4.2930D-02	-3.0817D-02
-3.1076D-02	1.5836D-02	3.4944D-02	3.5118D-02
-2.7477D-02	1.5305D-02	1.5982D-02	5.2152D-02
-2.4861D-02	-1.5294D-02	-3.4398D-03	4.1404D-02
-3.7503D-03	5.3738D-03	2.2217D-02	2.6476D-02
-3.6389D-03	-2.2122D-03	-1.7495D-02	1.3642D-02
-7.5093D-02	-1.7726D-01	-1.2001D-01	1.2350D-01
2.5890D-01	-9.6672D-02	-2.2915D-01	-2.4661D-01
6.1198D-02	1.8234D-01	1.3089D-01	-1.1171D-01
-2.5498D-01	1.2401D-01	2.3735D-01	2.3541D-01
-3.3293D-02	1.3737D-02	2.9427D-02	3.2704D-02
-5.0461D-03	-3.3246D-02	-2.5252D-02	1.0809D-02

$D_{wf} =$

Columns 1 thru 6

-5.9766D-20	-3.1751D-20	2.2291D-19	-1.6460D-20	-6.4228D-20	1.4204D-19
1.6627D-20	4.2943D-20	-8.1367D-20	4.4823D-20	1.0410D-19	-1.5082D-19
6.0561D-20	2.7756D-20	-1.4415D-19	2.3560D-20	5.2554D-20	-1.0305D-19
6.0235D-22	-2.8447D-20	2.3034D-21	2.6514D-20	-3.6496D-21	1.3126D-19
5.7186D-20	6.0395D-20	-2.8966D-19	2.7529D-20	1.1897D-19	-8.9904D-20
-4.1578D-20	-6.9853D-20	2.9366D-19	-5.2002D-20	-1.3391D-19	6.6395D-20
-3.3031D-20	3.0737D-20	-1.1218D-21	-4.5433D-20	-1.9665D-19	1.1571D-19
1.7797D-20	-1.2289D-20	4.0441D-21	1.4662D-20	1.2864D-19	-1.3434D-19
-5.9710D-21	-2.2931D-21	8.0544D-20	3.5862D-20	1.0759D-19	-6.1188D-20
2.0120D-20	1.2156D-20	-4.4792D-20	3.1434D-20	3.9213D-20	2.3539D-20
-6.4481D-21	4.1475D-22	-6.9755D-20	-8.9638D-20	-4.1419D-20	4.7785D-20
4.3000D-21	-3.1548D-21	2.4641D-20	1.0391D-19	3.3013D-20	-9.1041D-21
-4.0477D-20	5.4905D-20	2.3642D-19	-4.0188D-20	2.8029D-19	-1.5541D-19
2.4232D-20	-2.6958D-20	-1.3124D-19	-6.8956D-20	-4.1333D-19	-7.0903D-20
5.6862D-20	1.6410D-20	-2.5780D-19	3.1752D-19	5.1091D-19	-4.6787D-20

-4.9155D-20	2.5312D-20	1.9952D-19	-1.1888D-19	-1.0847D-19	1.9234D-19
-3.1439D-20	-2.7981D-20	9.7143D-20	-3.0637D-19	-5.8664D-19	9.4204D-21
-3.4607D-21	1.6749D-21	1.7102D-20	2.9433D-19	5.1504D-19	-1.2366D-19
1.8598D-22	9.6963D-23	-6.9986D-22	-1.8116D-23	1.6388D-22	-5.2725D-22
-9.4371D-23	-1.7251D-22	4.3146D-22	-1.8347D-22	-3.1386D-22	5.2613D-22
-2.0779D-22	-9.4355D-23	3.6032D-22	6.1338D-23	-1.6675D-22	3.8338D-22
6.1736D-23	1.2352D-22	-1.1199D-22	-1.5035D-22	-4.0128D-23	-3.9981D-22
-1.7812D-22	-2.7538D-22	1.1755D-21	4.5345D-23	-1.3975D-22	1.8265D-22
1.4385D-22	3.6349D-22	-1.2978D-21	1.6010D-22	2.1804D-22	-3.8502D-23
6.8812D-23	-4.2239D-22	8.7697D-22	2.9957D-22	1.1807D-21	-7.3275D-22
-2.9307D-23	3.0438D-22	-7.6221D-22	-2.7706D-22	-9.0026D-22	7.5133D-22
2.1576D-23	6.7598D-24	-3.1686D-22	-1.0911D-22	-5.4506D-22	3.1945D-22
-1.1206D-22	-2.0035D-23	1.4839D-22	-2.2526D-22	-1.4364D-22	-1.7556D-22
8.5611D-23	-5.0540D-23	3.8549D-22	6.6888D-22	1.0783D-22	-8.8190D-23
-2.2572D-23	3.2119D-23	-1.8728D-22	-6.7687D-22	9.5425D-24	-1.0211D-22
6.0077D-23	-2.9308D-22	-6.9159D-22	1.1047D-22	-1.7036D-21	8.2415D-22
-2.9398D-23	2.0605D-22	3.4620D-22	5.1835D-22	2.4495D-21	6.1820D-22
-1.8328D-22	-1.7131D-22	1.0382D-21	-1.3530D-21	-2.2545D-21	-3.3758D-22
1.6106D-22	-3.8642D-23	-7.3804D-22	2.1117D-22	-2.2332D-23	-7.3127D-22
1.4802D-22	4.1667D-23	1.2995D-22	1.9605D-21	3.1815D-21	4.3132D-22
-5.5448D-23	4.6516D-23	-1.8590D-22	-1.7168D-21	-2.2728D-21	-3.8956D-23
1.9170D-09	-1.8700D-09	-1.0221D-09	-7.2757D-09	-2.9356D-09	3.7564D-09
2.6546D-09	7.2958D-10	-5.9358D-10	-2.0146D-09	2.6607D-09	1.7953D-09
3.2351D-09	1.0357D-09	1.2868D-09	-2.9945D-09	1.8099D-09	1.0078D-09
5.9194D-10	1.2995D-09	2.1176D-09	-8.9564D-10	-4.5279D-09	-2.1767D-09
2.4543D-10	1.4067D-09	-6.7364D-10	1.6282D-09	8.9439D-09	-3.4635D-09
-2.0794D-09	7.5570D-10	-2.9022D-09	2.4326D-09	7.8119D-10	-1.5796D-09
-7.7814D-10	7.1272D-10	-2.3020D-09	5.9832D-10	-6.5346D-09	-4.1123D-09
-3.3360D-09	-6.2834D-10	-1.6153D-09	2.4989D-09	-2.8156D-09	-1.3683D-09
-5.1623D-09	-1.2009D-09	1.0701D-09	4.1935D-09	-4.1495D-09	1.8247D-09
-4.4909D-10	-1.2619D-09	-2.5017D-09	1.2806D-09	1.6877D-09	7.1074D-10
3.8093D-10	-4.0137D-10	-1.2562D-09	2.4240D-09	1.2239D-10	-2.4272D-09
2.6387D-09	-7.4894D-10	1.0156D-08	-4.0100D-09	7.3843D-10	1.5873D-09
-1.4680D-10	-1.3633D-09	-2.1618D-09	-4.1292D-10	-3.3258D-09	1.3674D-09
2.6841D-09	6.7232D-11	-3.1978D-09	-2.8086D-09	1.2306D-09	5.8213D-10
1.7030D-08	4.2367D-10	1.2112D-08	-2.2005D-08	1.2742D-08	1.2644D-08
3.7219D-10	7.7450D-09	3.7628D-09	-2.1557D-09	1.2292D-09	-1.0834D-08
-1.7031D-08	-8.4374D-10	-1.2863D-08	2.2482D-08	-1.2655D-08	-1.2297D-08
-3.7927D-09	-8.3285D-09	-4.7158D-09	4.5655D-09	-9.3969D-10	7.8124D-09
-2.8601D-10	-8.6467D-10	1.0179D-09	-7.7272D-10	-5.3846D-10	1.4635D-09
2.5873D-09	3.1975D-10	3.1199D-09	-2.7141D-09	2.1123D-09	7.1290D-10

Columns 7 thru 9

2.1368D-19	1.0123D-20	-2.7514D-20
-1.8350D-19	-6.8909D-20	-1.3713D-19
-1.9357D-19	-1.4071D-20	-1.0867D-20
1.8721D-19	1.2286D-19	2.2601D-19
-1.5727D-19	-1.1851D-19	4.9508D-21

1.2356D-19	1.0925D-19	1.7298D-20
1.1760D-19	-1.7992D-19	-3.2257D-19
-1.5212D-19	1.3965D-19	2.3205D-19
-1.2220D-19	-3.6901D-20	-2.5121D-20
1.3714D-20	4.2826D-20	1.3444D-20
2.2354D-19	2.1674D-20	1.0507D-19
-1.4152D-19	2.1911D-21	-8.1280D-20
-1.6666D-19	-2.6680D-19	-2.9971D-19
-5.2861D-20	6.1889D-20	-5.3056D-20
-3.2801D-19	2.1988D-19	2.4520D-19
2.6959D-19	-1.0884D-19	7.8191D-20
2.4755D-19	-1.0055D-19	-1.7711D-19
-3.7171D-19	1.4410D-19	9.0845D-20
-7.1820D-22	-1.0087D-22	2.2819D-24
6.9065D-22	2.5645D-22	4.7799D-22
7.1318D-22	1.7188D-22	3.3926D-22
-7.0284D-22	-5.0464D-22	-9.9558D-22
3.0993D-22	8.1398D-22	4.3909D-22
-3.5539D-22	-7.4447D-22	-6.1886D-22
-5.2049D-22	1.6375D-21	2.3227D-21
8.3614D-22	-1.5590D-21	-1.9043D-21
4.0528D-22	1.5268D-22	5.7533D-23
6.0600D-23	-2.9452D-22	-6.3725D-23
-1.3303D-21	1.5449D-22	-6.1690D-22
9.4879D-22	-1.1553D-22	5.5031D-22
9.6131D-22	1.2923D-21	1.2548D-21
5.3700D-22	-3.1174D-22	4.1460D-22
7.7521D-22	-7.0986D-22	-7.8856D-22
-8.4820D-22	-7.9596D-23	-1.2950D-21
-1.0354D-21	6.8415D-22	1.0544D-21
1.4567D-21	-1.0312D-21	-8.2400D-22
-3.3341D-09	3.7601D-09	4.0134D-09
2.8699D-09	1.7311D-09	-1.9103D-09
3.4584D-09	5.2376D-10	-6.5552D-09
5.3214D-10	1.7194D-10	-3.3068D-09
-2.2800D-09	2.0016D-09	-7.2088D-09
6.6783D-10	-1.7775D-10	3.6712D-09
1.9622D-09	9.0976D-10	4.1292D-09
-5.6712D-09	-3.0692D-09	3.7625D-09
4.5958D-09	-6.8501D-09	-2.5468D-10
7.2388D-10	-3.6043D-10	2.6109D-09
-4.7246D-09	-1.2656D-09	5.1863D-09
-7.9135D-10	1.0502D-09	-6.9452D-09
8.5443D-10	-2.9727D-10	3.1545D-09
-3.1073D-09	1.8634D-09	9.1878D-11
3.7011D-09	1.1811D-08	-2.1998D-08
1.1136D-08	9.4201D-09	-1.2210D-08
-4.3933D-09	-1.2446D-08	2.2643D-08
-1.0559D-08	-1.2080D-08	1.5793D-08

-1.4201D-09	-6.3227D-10	1.7762D-09
7.1714D-10	2.4461D-09	-4.7097D-09

$D_{uf} =$

Columns 1 thru 6

-2.5605D-19	2.5982D-19	1.0392D-19	-1.5713D-19	-3.0526D-19	-1.1113D-19
2.3110D-19	-4.8285D-19	5.8565D-21	3.7902D-19	-6.0096D-20	4.4877D-19
2.2553D-19	-2.2282D-19	-7.4863D-20	1.8692D-19	2.6552D-19	5.2333D-20
-2.6228D-19	3.6298D-19	1.5125D-19	-2.7995D-19	1.7149D-19	-3.9643D-19
3.2054D-19	-5.8015D-19	5.0926D-22	3.3928D-19	4.0075D-19	3.2515D-19
-3.9143D-19	6.8435D-19	-1.4470D-20	-5.0147D-19	-2.0570D-19	-3.3944D-19
5.6796D-19	-2.2451D-19	-1.3659D-19	4.5089D-20	-5.3610D-19	4.8337D-19
-3.9961D-19	7.3597D-20	4.0294D-20	8.8066D-20	3.4408D-19	-4.1868D-19
-3.3216D-19	1.2202D-19	2.4256D-19	5.9793D-20	2.1071D-19	1.1227D-20
5.7247D-20	-1.2971D-19	1.7302D-20	1.2464D-19	-2.9754D-20	4.6903D-21
1.9523D-19	-3.7414D-20	-1.6617D-19	-7.4381D-20	-1.7252D-19	2.3517D-21
-9.4411D-20	-4.0338D-20	1.2346D-19	4.6252D-20	8.5813D-20	-3.0306D-20
-2.3500D-19	-5.3114D-19	3.1153D-19	7.2619D-19	-3.0458D-19	5.0712D-19
4.8277D-19	2.5685D-19	-3.7240D-19	-4.8183D-19	4.3501D-20	-3.8774D-20
-4.6936D-19	-2.8972D-19	6.0942D-19	5.5613D-19	7.4392D-19	9.8103D-20
-1.1917D-19	1.6231D-19	4.6841D-20	-8.2812D-20	-2.9567D-19	-2.1631D-19
7.0153D-19	4.1391D-19	-6.0896D-19	-6.2064D-19	-2.4866D-19	-1.8131D-19
-6.6782D-19	-2.2748D-19	5.5296D-19	4.7004D-19	-2.3721D-19	4.6502D-19
8.0763D-22	-6.8740D-22	-4.3872D-22	4.1426D-22	7.7087D-22	3.0797D-22
-1.2271D-21	2.0012D-21	8.2329D-23	-1.3457D-21	-1.0377D-23	-1.7674D-21
-7.9278D-22	6.7960D-22	5.6755D-22	-8.6808D-22	-5.0706D-22	-3.3597D-22
1.4847D-21	-1.6357D-21	-9.5795D-22	1.2487D-21	-4.2106D-22	1.6810D-21
-2.2186D-21	2.7286D-21	2.7124D-22	-1.2673D-21	-8.4950D-22	-2.1427D-21
2.9277D-21	-3.5352D-21	-2.0289D-22	2.4535D-21	1.2251D-22	2.3131D-21
-5.5853D-21	3.5027D-21	1.0228D-21	-1.6043D-21	2.7568D-21	-4.6472D-21
4.4258D-21	-2.5714D-21	-5.8825D-22	4.9343D-22	-1.9466D-21	4.2956D-21
1.4419D-21	-5.0628D-22	-1.0105D-21	-3.0506D-22	-8.1504D-22	-1.0453D-22
-3.9271D-23	2.4412D-22	-2.3804D-23	-3.8343D-22	-1.3276D-22	3.0120D-22
-1.1497D-21	4.1004D-22	7.4246D-22	1.5484D-22	1.0441D-21	-5.1372D-22
4.5982D-22	2.0282D-22	-6.5477D-22	-1.4595D-22	-3.3045D-22	3.4168D-22
9.6501D-22	2.9434D-21	-1.6740D-21	-4.0165D-21	2.6151D-22	-2.6514D-21
-2.0361D-21	-2.1225D-21	2.1288D-21	3.4763D-21	3.9572D-22	4.6785D-22
1.0745D-21	1.9994D-21	-2.4127D-21	-3.4221D-21	-2.4693D-21	-2.2071D-22
2.4881D-21	-1.6553D-21	-1.2911D-21	8.8004D-22	3.7001D-22	1.5112D-21
-5.0453D-21	-8.3267D-22	3.7596D-21	2.5254D-21	1.6947D-21	-1.0815D-21
3.1925D-21	5.0418D-22	-2.5050D-21	-1.7011D-21	7.4585D-22	-1.5282D-22
-3.2220D-09	1.4594D-09	-9.5428D-09	1.1696D-08	4.0157D-09	-3.1151D-09
2.0084D-09	1.2983D-09	-1.0400D-08	5.3182D-09	2.4339D-09	3.2030D-09
-1.4044D-09	2.5768D-09	6.4368D-09	-6.3804D-09	4.0930D-09	7.0676D-10
-7.4846D-09	-7.6658D-09	9.1774D-09	9.5278D-09	-3.2787D-09	5.0988D-09

1.4878D-09	8.0942D-10	-6.5082D-09	5.6483D-09	-6.3234D-09	8.5978D-09
1.4054D-09	2.0110D-09	4.8243D-09	-1.0367D-08	3.1321D-10	2.3951D-09
9.3897D-10	-3.1425D-09	1.0748D-08	-8.1933D-09	-4.3806D-09	4.5895D-09
1.0481D-09	-5.7885D-10	8.3156D-09	-8.0531D-09	-9.8733D-09	-1.0487D-08
1.3841D-09	-1.0582D-09	5.2135D-09	-6.2104D-09	-2.9058D-09	2.0362D-11
8.7596D-10	8.6643D-10	-1.0838D-09	-1.5808D-09	2.5000D-09	1.2908D-10
7.8712D-10	7.4249D-10	4.6937D-09	-6.6787D-09	3.5061D-09	-8.7305D-09
-1.1156D-09	1.0059D-09	-7.4696D-09	8.7797D-09	4.5398D-09	-2.6610D-09
2.3143D-09	2.6143D-09	-2.0008D-09	-3.2025D-09	6.0628D-10	-3.8468D-09
-1.2709D-09	8.0085D-10	-4.2558D-09	4.6041D-09	4.4682D-09	1.7508D-09
-7.3316D-09	5.6015D-09	-4.3256D-08	4.6113D-08	2.1375D-08	1.3790D-09
-3.0658D-09	-1.7496D-09	5.1411D-09	3.8331D-09	-1.7051D-08	3.1083D-08
6.9178D-09	-6.0119D-09	4.3614D-08	-4.5819D-08	-2.0003D-08	-3.2386D-09
1.7763D-09	2.8296D-09	6.7214D-10	-9.5633D-09	1.0581D-08	-2.6259D-08
9.5104D-10	1.0040D-09	-1.0939D-09	-1.2622D-09	2.3352D-09	-5.2831D-09
-6.5527D-10	1.0498D-09	-5.1268D-09	5.5434D-09	2.7597D-09	2.2794D-09

Columns 7 thru 12

3.6248D-19	2.0070D-19	-5.3450D-21	3.9869D-19	-1.3829D-19	-3.7345D-19
-4.8632D-20	-4.1605D-19	2.6997D-19	-2.9468D-19	-2.6954D-19	1.3108D-19
-4.3216D-19	-1.8062D-19	-3.0866D-20	-2.7405D-19	1.1563D-19	3.0314D-19
2.2192D-20	3.5559D-19	-2.4166D-19	9.5686D-20	3.2827D-19	1.3141D-20
-2.1015D-19	-1.8301D-19	-2.7074D-20	-2.4990D-19	2.4166D-20	3.0658D-19
5.9039D-20	1.9317D-19	-7.0305D-20	2.6475D-19	1.5776D-19	-2.3056D-19
7.2927D-19	-1.7073D-20	2.2071D-19	6.9021D-20	-3.8017D-19	-1.3555D-19
-5.8979D-19	-3.9788D-20	-6.8580D-20	-6.5784D-20	1.1987D-19	-8.5787D-21
-1.4877D-19	-1.4941D-20	-8.1299D-22	1.5732D-19	-2.9998D-20	-9.2059D-20
-3.1469D-20	-9.7344D-20	2.1619D-20	-1.1323D-19	4.6546D-20	1.3071D-19
8.8472D-20	1.1658D-19	-1.9166D-20	-1.2698D-19	4.3289D-20	7.0357D-20
-5.8144D-20	-1.0285D-19	1.1841D-21	5.8103D-20	-2.9838D-20	-5.6529D-20
-1.1629D-19	-6.4616D-19	6.2366D-19	2.4096D-19	-7.8331D-19	-2.2780D-19
-4.0587D-21	1.0147D-19	-2.2190D-19	-1.1434D-19	4.8637D-19	8.2117D-20
-7.4571D-19	-1.7465D-19	-5.1597D-19	-1.3595D-19	6.2623D-19	6.3377D-19
5.2965D-19	2.2879D-19	2.4550D-19	2.2245D-19	-4.3257D-19	-5.1261D-19
4.0618D-19	5.0350D-19	-9.7714D-20	2.4775D-19	-8.6312D-20	-4.2256D-19
-2.6068D-19	-9.1609D-19	2.0475D-19	-4.0422D-19	-1.8923D-19	2.2733D-19
-1.2440D-21	-7.7680D-22	2.0395D-22	-1.3417D-21	4.6483D-22	1.2032D-21
1.3744D-22	1.4844D-21	-8.3077D-22	1.1972D-21	9.3283D-22	-6.4032D-22
1.7400D-21	7.7705D-22	-1.7032D-22	9.2391D-22	-1.8902D-22	-1.0486D-21
-2.6079D-22	-1.1783D-21	7.4896D-22	-4.5170D-22	-1.2290D-21	2.5313D-22
-3.1632D-22	8.1725D-22	-1.6591D-22	7.5002D-22	3.0618D-22	-1.1173D-21
9.3131D-22	-9.8564D-22	5.3378D-22	-9.6025D-22	-1.2602D-21	8.5059D-22
-4.9075D-21	6.3458D-22	-1.3157D-21	1.7976D-22	2.7608D-21	-1.7441D-23
4.3475D-21	-2.7075D-22	7.6957D-22	1.3477D-23	-1.5121D-21	5.5311D-22
6.8985D-22	-5.5284D-25	-7.8249D-23	-5.4105D-22	5.8744D-23	2.6477D-22
1.4003D-22	2.0218D-22	-2.2639D-23	5.0754D-22	-2.8341D-22	-6.7269D-22
-3.2206D-22	-5.8162D-22	1.4912D-22	3.9987D-22	-1.0022D-22	-2.8147D-23
-3.5539D-24	8.3139D-22	-5.4160D-23	-3.5573D-22	2.5666D-22	3.1055D-22



1.9002D-21	3.0324D-21	-2.2367D-21	-1.1534D-21	2.9702D-21	3.8100D-22
-5.3116D-22	-2.6942D-22	5.1217D-22	8.8158D-22	-2.0732D-21	-1.0235D-24
2.3302D-21	-3.4599D-22	2.2084D-21	-1.6422D-22	-2.3263D-21	-2.4473D-21
-1.3285D-21	-4.7676D-22	-6.9591D-22	-2.2844D-22	1.2350D-21	1.8210D-21
-2.1973D-21	-1.4854D-21	3.3689D-22	-3.9503D-22	6.7849D-22	1.3063D-21
1.4049D-21	3.4266D-21	-4.0762D-22	1.5531D-21	2.6217D-22	-8.2929D-22
3.5878D-09	-5.3968D-09	-9.9288D-11	4.2920D-10	-7.6168D-09	8.5860D-09
-4.7486D-09	-2.5297D-09	2.6136D-09	-1.2687D-09	7.9157D-09	-1.1059D-08
4.7327D-09	-1.0309D-08	4.3295D-09	-8.7920D-09	1.7419D-08	-1.2428D-08
-8.7961D-09	8.3610D-09	2.0795D-09	-4.2278D-09	1.2803D-08	-9.3621D-09
-1.4542D-08	1.2864D-08	1.4908D-09	-4.9554D-09	9.3856D-09	-5.5959D-09
-7.9156D-09	3.6140D-09	1.1050D-09	2.2182D-09	-2.3216D-09	-2.2673D-09
9.1267D-09	-7.8611D-09	3.1248D-09	-1.8592D-10	7.7874D-09	-1.1727D-08
1.2936D-08	1.1394D-08	-2.5811D-09	5.7992D-09	-1.1851D-08	9.2241D-09
-4.6845D-09	8.8579D-09	-6.7587D-09	7.9522D-09	-1.7312D-08	1.6379D-08
3.8508D-09	-8.8083D-09	1.3467D-09	3.8922D-09	-1.2682D-08	5.1623D-09
1.4688D-08	-8.5540D-09	-1.2005D-09	4.7591D-09	6.0282D-09	-9.6079D-09
6.5391D-09	-8.1370D-09	-7.5635D-09	-9.8207D-09	1.0970D-08	1.0075D-08
3.8772D-09	-1.0936D-09	-2.5403D-09	1.1182D-09	-4.1747D-09	5.1624D-09
-1.1122D-09	-5.1119D-09	-7.5360D-10	-4.6223D-09	4.5459D-09	7.9572D-10
5.3069D-10	-3.0198D-08	6.3520D-09	-2.4420D-08	4.2192D-08	-1.8737D-08
-5.0073D-08	3.5235D-08	1.1959D-08	-1.8518D-08	5.3883D-08	-4.8795D-08
1.9317D-09	2.8509D-08	-7.3206D-09	2.6024D-08	-4.4907D-08	2.1123D-08
4.7008D-08	-2.9570D-08	-1.6317D-08	2.4203D-08	-5.9697D-08	5.2359D-08
6.6930D-09	-3.9516D-09	-2.6802D-09	3.0811D-09	-6.9131D-09	6.4190D-09
-2.0128D-09	-3.7018D-09	1.2951D-09	-5.8841D-09	8.8744D-09	-3.8136D-09

Columns 13 thru 18

6.1308D-19	-2.4101D-19	5.7721D-20	-3.4246D-19	5.9978D-19	-8.7748D-19
-3.2279D-19	3.0392D-20	-2.2915D-19	3.0761D-19	-4.2049D-19	1.0254D-18
-4.3029D-19	1.9515D-19	-1.9028D-19	3.9019D-19	-4.7405D-19	6.5531D-19
2.7382D-19	-2.8961D-19	5.7665D-19	-7.2888D-19	5.8881D-19	-1.1174D-18
3.2706D-19	-3.8929D-19	-1.0479D-19	1.7706D-19	-2.1166D-19	3.8536D-19
-4.9430D-19	5.7757D-19	-7.5029D-20	7.8786D-20	-3.7650D-20	-1.5213D-19
8.4279D-19	-3.5350D-19	2.5868D-19	-6.6322D-19	-2.0878D-19	5.9763D-19
-4.9092D-19	1.5164D-19	5.1917D-20	3.8950D-19	6.1414D-19	-8.9747D-19
1.1299D-19	-5.9536D-20	-7.3020D-19	8.6736D-19	-5.1263D-21	-4.7902D-20
7.8880D-20	-2.3660D-19	4.3488D-19	-5.1423D-19	1.7191D-19	-1.3212D-19
-1.2336D-19	4.7329D-20	6.4077D-19	-6.9651D-19	-1.5006D-19	7.2143D-21
1.7724D-19	-2.5162D-19	-6.7637D-20	3.0138D-20	3.7993D-20	1.3600D-19
1.2443D-18	-1.2950D-18	-1.0322D-19	3.1394D-19	3.4503D-19	3.2163D-19
-1.4785D-18	1.7789D-18	7.0452D-19	-9.1901D-19	-2.0321D-19	5.7485D-19
-6.9851D-19	-2.3063D-19	-1.7206D-18	1.7061D-18	-1.6430D-18	1.5107D-18
1.6506D-18	-8.3563D-19	5.8068D-19	-6.1275D-19	1.2981D-18	-2.2077D-18
-5.4269D-19	1.1617D-18	1.1935D-18	-1.1697D-18	6.1386D-19	-1.5439D-19
2.1127D-19	-1.1854D-18	-9.6619D-19	1.2745D-18	-4.0034D-19	4.3101D-19
-2.5840D-21	1.2889D-21	6.5853D-23	9.2132D-22	-2.3240D-21	3.5575D-21
6.4203D-22	2.9332D-22	8.0025D-22	-1.0987D-21	1.5210D-21	-3.5975D-21

2.0562D-21	-1.3641D-21	1.1305D-21	-1.8056D-21	2.0946D-21	-3.1853D-21
-6.0861D-22	9.7142D-22	-2.6577D-21	3.1630D-21	-2.3873D-21	4.2859D-21
-2.0520D-21	1.5677D-21	-1.3022D-22	5.0278D-22	1.6152D-21	-3.0179D-21
3.3096D-21	-2.9763D-21	1.1327D-21	-1.7076D-21	-5.0262D-22	1.9207D-21
-6.9940D-21	3.5240D-21	-1.9669D-21	4.7413D-21	2.7884D-21	-5.7941D-21
5.5285D-21	-2.4643D-21	3.9599D-22	-3.4861D-21	-4.2425D-21	6.8632D-21
-1.7010D-22	1.0025D-22	3.0962D-21	-3.5690D-21	5.0458D-23	6.5799D-23
-3.9203D-22	1.0781D-21	-1.4532D-21	1.6573D-21	-1.1460D-21	1.2628D-21
1.2569D-21	-1.2951D-21	-1.7563D-21	1.9731D-21	2.1514D-21	-1.3229D-21
-1.7408D-21	2.1209D-21	-7.4502D-22	9.8043D-22	-1.0925D-21	7.4284D-23
-5.1308D-21	5.9282D-21	2.4929D-21	-3.6934D-21	-1.4947D-22	-3.1591D-21
6.9331D-21	-8.4399D-21	-5.9789D-21	6.5283D-21	-4.0372D-22	-1.9304D-21
1.1607D-21	1.7854D-21	8.1598D-21	-6.5645D-21	7.2598D-21	-6.2319D-21
-6.7037D-21	4.4302D-21	-2.6853D-21	1.7385D-21	-6.1892D-21	1.1768D-20
4.6698D-21	-6.9965D-21	-7.8579D-21	7.2024D-21	-1.7306D-21	-2.6968D-21
-2.1624D-21	6.1823D-21	4.5736D-21	-5.7145D-21	1.0364D-21	1.2527D-21
9.8106D-10	-4.0074D-10	-2.1472D-08	1.6910D-08	-3.3530D-09	1.7852D-08
-3.8130D-09	3.9876D-09	-1.1571D-08	1.2826D-08	8.2692D-09	-7.4863D-09
5.6027D-09	1.5973D-08	-1.9370D-08	1.5079D-09	6.9419D-09	-1.9461D-09
1.0633D-09	-6.6816D-09	-4.6369D-09	-1.5751D-09	5.6642D-09	-3.6525D-09
-2.6030D-09	1.5082D-08	4.9026D-09	-6.4411D-09	-7.2766D-09	4.8973D-09
1.2452D-08	-1.1177D-08	5.8255D-09	-5.9898D-09	-3.6332D-09	5.3189D-09
1.3282D-08	-8.6031D-09	1.5488D-08	7.4287D-09	-1.1249D-08	-5.6804D-09
5.8018D-09	-4.6960D-09	7.1079D-09	-1.2985D-08	-8.8296D-09	2.1672D-09
-6.2613D-09	3.1057D-09	7.2696D-09	4.6517D-09	6.9290D-09	-6.0426D-09
-6.5944D-09	7.7715D-09	6.4323D-09	-4.7126D-09	-3.1601D-09	2.1824D-09
-1.1217D-08	-5.8921D-09	8.5784D-09	-2.4174D-09	3.9208D-09	1.7084D-08
-1.2653D-08	7.0713D-09	-6.9188D-09	8.4728D-09	-2.9244D-09	-4.2492D-09
-1.3770D-09	-8.7484D-10	-1.8608D-09	-5.1901D-11	-1.3959D-09	3.5577D-09
-2.3438D-09	6.1665D-09	-6.1487D-09	3.4645D-09	-6.9548D-10	1.0911D-09
-2.8659D-08	4.9996D-08	-5.7973D-08	3.8181D-08	1.1125D-08	-1.3177D-08
1.9918D-08	-1.0255D-08	7.8812D-09	8.0041D-09	6.7006D-09	-4.3971D-08
2.8579D-08	-4.9367D-08	5.7876D-08	-3.8118D-08	-1.1105D-08	1.5771D-08
-1.4553D-08	-1.4941D-09	-2.3447D-10	-1.5590D-08	-3.0818D-09	4.2319D-08
-4.3953D-09	2.1623D-09	5.0839D-10	-2.5948D-09	-1.5665D-09	5.2076D-09
-2.1384D-09	9.0708D-09	-1.2207D-08	6.5340D-09	3.1065D-09	3.3161D-10

Columns 19 thru 24

8.9652D-22	-8.4348D-22	-4.0485D-22	5.1949D-22	7.6612D-22	2.6238D-22
-8.6653D-22	1.5225D-21	8.2271D-23	-1.1089D-21	1.8433D-22	-1.1913D-21
-7.4695D-22	6.6789D-22	5.3610D-22	-8.4167D-22	-6.5565D-22	-1.9667D-22
8.8168D-22	-1.1654D-21	-7.4691D-22	1.1062D-21	-4.7563D-22	1.1346D-21
-1.1364D-21	1.8325D-21	5.5318D-23	-9.3778D-22	-1.1021D-21	-8.9965D-22
1.4175D-21	-2.1910D-21	-1.4171D-22	1.5271D-21	6.0656D-22	9.2742D-22
-1.6750D-21	7.0685D-22	2.4948D-22	-1.2725D-22	1.4780D-21	-1.5180D-21
1.1062D-21	-1.6670D-22	1.8892D-22	-4.4504D-22	-9.7833D-22	1.3282D-21
9.8261D-22	-4.3402D-22	-6.5789D-22	-1.6329D-22	-5.5814D-22	-7.6731D-23
-2.1650D-22	3.4440D-22	6.2689D-23	-3.8759D-22	4.9582D-23	8.5063D-23

-5.0544D-22	1.7765D-22	4.0601D-22	1.7072D-22	6.1449D-22	-2.9769D-22
2.1191D-22	1.0941D-22	-4.1939D-22	9.3126D-24	-3.3801D-22	3.4963D-22
5.4131D-22	1.5148D-21	-4.5904D-22	-2.3367D-21	9.0981D-22	-1.5383D-21
-1.3773D-21	-7.0291D-22	6.4067D-22	1.6097D-21	-7.0836D-23	3.0379D-22
1.2612D-21	7.5158D-22	-1.2716D-21	-1.8537D-21	-2.0553D-21	-2.5359D-22
4.1964D-22	-4.9263D-22	-4.4126D-22	4.8811D-22	7.8881D-22	5.5339D-22
-1.8897D-21	-1.1176D-21	1.5117D-21	1.5791D-21	7.0844D-22	1.9296D-22
1.7749D-21	5.9539D-22	-1.4440D-21	-1.1066D-21	7.6030D-22	-1.0370D-21
-2.8147D-24	2.2056D-24	1.5330D-24	-1.3205D-24	-1.7190D-24	-6.8613D-25
4.3445D-24	-6.3953D-24	-3.9832D-25	3.8177D-24	5.9045D-26	4.6635D-24
2.4719D-24	-1.8857D-24	-4.2249D-24	5.0921D-24	1.0253D-24	1.6517D-24
-4.7224D-24	5.2304D-24	5.2281D-24	-6.1657D-24	9.9046D-25	-5.2537D-24
7.2749D-24	-8.5549D-24	-2.6901D-25	2.8997D-24	2.3400D-24	6.0755D-24
-9.9273D-24	1.1255D-23	1.1961D-24	-7.4338D-24	-6.2152D-25	-6.4916D-24
1.7121D-23	-1.1016D-23	-2.2860D-24	4.8459D-24	-7.4843D-24	1.4279D-23
-1.3108D-23	7.7456D-24	-3.9528D-25	-4.8021D-26	5.4560D-24	-1.3216D-23
-4.3439D-24	1.8708D-24	2.5812D-24	1.0020D-24	2.0549D-24	7.0104D-25
3.2908D-25	-4.9354D-25	-8.0269D-25	1.5164D-24	7.6470D-25	-1.5348D-24
2.8961D-24	-1.6263D-24	-1.5511D-24	-1.1941D-25	-4.1640D-24	3.9936D-24
-7.9665D-25	-5.7254D-25	2.5487D-24	-8.6897D-25	1.8486D-24	-3.3410D-24
-2.1433D-24	-8.3495D-24	1.3379D-24	1.4246D-23	-1.2512D-24	9.0027D-24
5.6941D-24	5.8730D-24	-2.3170D-24	-1.2779D-23	-1.3397D-24	-3.3523D-24
-2.6743D-24	-5.4340D-24	3.2157D-24	1.2883D-23	7.0088D-24	1.4122D-24
-7.6694D-24	5.1442D-24	6.1792D-24	-5.2238D-24	-1.1252D-24	-4.6402D-24
1.4298D-23	1.4684D-24	-9.9829D-24	-5.6451D-24	-5.1613D-24	5.2977D-24
-8.5233D-24	-1.0589D-24	6.8690D-24	3.3371D-24	-2.1773D-24	-1.5943D-24
1.8761D-11	-1.0998D-11	1.0100D-10	-1.0944D-10	-4.0846D-11	2.7468D-11
-6.8972D-12	-7.2336D-12	7.9957D-11	-5.9653D-11	-2.4334D-11	-3.0719D-11
1.7899D-11	-1.3188D-11	-3.2173D-11	1.9645D-11	-4.4807D-11	-3.1329D-12
3.6792D-11	3.8434D-11	-4.3280D-11	-4.5336D-11	2.6122D-11	-4.8814D-11
2.5783D-12	3.7960D-13	5.6054D-11	-6.8223D-11	4.1727D-11	-7.4559D-11
-9.0554D-12	-7.8804D-12	-5.3582D-11	7.9530D-11	9.2703D-12	-1.4173D-11
-1.5231D-12	2.5333D-11	-1.1006D-10	8.2563D-11	3.7057D-11	-2.3688D-11
-9.4602D-12	5.1708D-12	-7.5874D-11	7.8804D-11	5.8015D-11	6.1970D-11
-1.2145D-11	6.6979D-12	-5.0429D-11	6.0252D-11	4.2557D-11	8.4768D-12
-1.0272D-11	-1.0390D-11	1.0683D-11	1.5450D-11	-1.6448D-11	9.9536D-12
-1.2118D-11	-5.3511D-12	-5.0599D-11	7.0321D-11	-2.2898D-11	7.3545D-11
8.2695D-12	-9.1200D-12	7.4162D-11	-7.9121D-11	-4.2641D-11	2.2364D-11
-7.1644D-12	-8.6658D-12	4.1430D-12	1.2445D-11	-8.2409D-12	2.5010D-11
7.5441D-12	-5.5880D-12	4.6979D-11	-4.9467D-11	-2.6680D-11	-4.1229D-12
5.5462D-11	-4.2737D-11	4.0929D-10	-4.3321D-10	-2.0462D-10	-3.9966D-11
3.7768D-11	4.3250D-11	-5.5684D-11	-4.9846D-11	1.2897D-10	-2.8121D-10
-5.5110D-11	4.2360D-11	-4.0885D-10	4.3432D-10	1.9628D-10	5.6644D-11
-3.6245D-11	-4.4775D-11	1.0592D-11	9.7182D-11	-8.2929D-11	2.6064D-10
-8.9482D-12	-1.0265D-11	1.0130D-11	1.2002D-11	-1.7997D-11	4.5620D-11
1.0507D-11	-6.4833D-12	5.6366D-11	-6.5326D-11	-3.0085D-11	-1.8070D-11

Columns 25 thru 30

-9.5255D-22	-4.8821D-22	7.3476D-23	-1.1463D-21	3.6435D-22	1.0202D-21
4.9276D-23	1.1238D-21	-7.5800D-22	8.3702D-22	8.0747D-22	-3.7661D-22
1.4290D-21	3.2282D-22	9.5370D-23	8.2330D-22	-2.7321D-22	-9.6934D-22
-2.4805D-22	-8.4729D-22	6.0764D-22	-3.1874D-22	-9.9859D-22	1.5005D-22
4.4683D-22	4.4222D-22	6.6358D-23	6.9225D-22	-3.5061D-23	-8.4298D-22
-2.9358D-23	-5.4161D-22	2.0598D-22	-7.9669D-22	-5.8060D-22	7.5169D-22
-2.1051D-21	7.7699D-23	-5.6420D-22	-9.3852D-23	1.1360D-21	1.5557D-22
1.7150D-21	1.5507D-22	1.4535D-22	1.6851D-22	-2.9982D-22	9.8548D-23
5.0386D-22	-7.8436D-23	1.6919D-23	-4.3130D-22	8.3715D-24	2.6666D-22
1.8526D-23	3.3405D-22	-4.9190D-23	3.2734D-22	-7.4580D-23	-4.5713D-22
9.6384D-23	-4.7533D-22	4.6762D-24	3.3733D-22	-1.7283D-22	-1.8467D-23
-2.2612D-22	5.0914D-22	1.8158D-23	-1.9205D-22	1.5269D-22	9.0565D-23
7.8180D-22	1.5564D-21	-1.6247D-21	-6.4336D-22	2.2103D-21	3.8555D-22
-4.0412D-22	-2.0766D-22	5.4009D-22	3.1865D-22	-1.5466D-21	-1.5324D-23
2.5133D-21	-2.6376D-23	1.4453D-21	3.3584D-22	-1.7324D-21	-1.8764D-21
-1.8355D-21	-2.0605D-22	-7.7285D-22	-5.2773D-22	1.1893D-21	1.5521D-21
-9.3768D-22	-1.4121D-21	2.7826D-22	-6.0144D-22	2.5528D-22	1.1153D-21
3.2547D-22	2.8658D-21	-6.0190D-22	1.0886D-21	7.0233D-22	-5.8368D-22
3.3472D-24	1.8626D-24	-8.1839D-25	3.9470D-24	-1.4101D-24	-3.2080D-24
2.1696D-25	-4.1483D-24	2.3115D-24	-3.2693D-24	-2.9375D-24	1.7797D-24
-7.2565D-24	-7.1443D-25	2.3069D-25	-3.1323D-24	2.9728D-25	4.1647D-24
2.5555D-24	2.2063D-24	-1.5578D-24	1.5574D-24	4.1225D-24	-2.2491D-24
1.8439D-24	-2.1360D-24	3.9664D-25	-1.9786D-24	-9.1987D-25	3.0942D-24
-3.7075D-24	3.1684D-24	-1.3747D-24	2.9813D-24	4.4861D-24	-3.4097D-24
1.4579D-23	-1.8853D-24	3.2001D-24	-1.1838D-24	-8.6713D-24	2.0162D-24
-1.2928D-23	2.7075D-25	-1.7186D-24	7.2810D-26	4.1821D-24	-2.2385D-24
-2.9268D-24	9.8480D-25	1.5851D-25	1.4301D-24	3.5087D-25	-8.8372D-25
2.5250D-25	-1.1461D-24	-6.9954D-26	-1.4922D-24	2.6921D-25	2.7256D-24
-2.3257D-24	3.4283D-24	-1.1285D-26	-1.1365D-24	1.0937D-24	-1.5066D-24
3.7967D-24	-4.6909D-24	-1.5827D-26	1.2669D-24	-1.5195D-24	-1.3662D-25
-9.5207D-24	-6.0643D-24	5.5675D-24	3.0515D-24	-8.5197D-24	5.6792D-25
5.4485D-24	-4.8714D-25	-8.6557D-25	-2.3605D-24	7.1294D-24	-1.8928D-24
-1.0684D-23	4.4808D-24	-6.5710D-24	1.5824D-25	6.3986D-24	8.4848D-24
7.0282D-24	-1.6942D-24	2.8802D-24	4.3767D-25	-3.3951D-24	-6.6882D-24
4.3594D-24	5.0304D-24	-9.0211D-25	5.3906D-25	-2.1681D-24	-3.1757D-24
-5.6031D-25	-1.2641D-23	1.3223D-24	-3.9427D-24	-1.9290D-24	2.1282D-24
-2.9843D-11	5.1550D-11	1.8210D-11	2.0526D-12	6.2168D-11	-9.3901D-11
4.4170D-11	2.4135D-11	-1.8417D-11	2.3929D-11	-7.9279D-11	8.1000D-11
-4.5345D-11	9.9903D-11	-3.2697D-11	7.5823D-11	-1.7180D-10	1.2314D-10
8.4689D-11	-7.0411D-11	-2.0924D-11	3.7976D-11	-1.1481D-10	9.0686D-11
1.4766D-10	-1.1647D-10	-1.4557D-11	4.4413D-11	-8.7287D-11	5.2915D-11
5.0650D-11	-3.9367D-11	-1.1352D-11	-2.3067D-11	2.1509D-11	2.2564D-11
-5.5493D-11	2.9311D-11	-3.4547D-11	3.5097D-12	-7.7472D-11	1.1692D-10

-7.9273D-11	-6.5800D-11	2.0565D-11	-5.4289D-11	1.1381D-10	-8.0781D-11
3.2165D-11	-9.5308D-11	4.8574D-11	-7.3549D-11	1.7567D-10	-1.5017D-10
-3.9923D-11	5.9179D-11	-1.0659D-12	-2.9629D-11	9.7679D-11	-5.5060D-11
-1.4437D-10	8.5269D-11	8.2487D-12	-2.9466D-11	-2.7381D-11	5.0272D-11
-5.5897D-11	7.8097D-11	3.6489D-11	5.7123D-11	-6.0632D-11	-5.3241D-11
-3.3905D-11	1.9376D-11	1.3443D-11	-1.6505D-11	4.8964D-11	-4.3476D-11
-2.0889D-12	3.5604D-11	-5.2134D-13	2.9127D-11	-3.6090D-11	5.3613D-12
8.2683D-12	2.9603D-10	-3.5374D-11	2.3960D-10	-4.0336D-10	1.5699D-10
4.7013D-10	-3.1449D-10	-1.2125D-10	1.5685D-10	-4.8549D-10	4.5968D-10
-3.3752D-11	-2.8046D-10	4.3528D-11	-2.5031D-10	4.2903D-10	-1.8183D-10
-4.3495D-10	2.4573D-10	1.4218D-10	-2.0299D-10	5.5546D-10	-4.9727D-10
-7.0245D-11	4.3260D-11	2.2677D-11	-2.5887D-11	7.2561D-11	-6.9340D-11
1.6540D-11	3.8845D-11	-8.9173D-12	5.1685D-11	-8.8572D-11	3.9792D-11

Columns 31 thru 36

-1.8399D-21	8.1308D-22	-1.6075D-22	8.6229D-22	-1.8421D-21	2.7136D-21
7.6847D-22	-5.3395D-23	6.5056D-22	-8.6709D-22	1.2131D-21	-2.7311D-21
1.7193D-21	-1.1144D-21	1.0143D-21	-1.4320D-21	1.6985D-21	-2.2557D-21
-1.1077D-21	1.2514D-21	-2.1021D-21	2.4566D-21	-1.8778D-21	3.1618D-21
-8.9049D-22	1.0438D-21	1.8657D-22	-3.3232D-22	6.3107D-22	-1.2032D-21
1.4778D-21	-1.6955D-21	3.8814D-22	-3.8967D-22	2.6616D-22	3.2094D-22
-2.6301D-21	1.2858D-21	-6.1116D-22	1.8616D-21	1.4811D-22	-1.4489D-21
1.5603D-21	-6.0519D-22	-3.0651D-22	-1.0942D-21	-1.4839D-21	2.5516D-21
-4.5366D-23	-9.8070D-23	2.3025D-21	-2.6517D-21	1.6980D-22	-6.2080D-23
-3.4032D-22	7.5774D-22	-1.4467D-21	1.6899D-21	-6.6230D-22	4.7869D-22
9.9736D-22	-8.8434D-22	-1.2002D-21	1.2516D-21	1.2130D-21	-5.0459D-22
-1.3783D-21	1.6669D-21	-5.1941D-22	6.5931D-22	-8.8441D-22	2.3042D-22
-2.2510D-21	2.4717D-21	9.8980D-22	-1.6038D-21	-2.4106D-22	-1.3512D-21
2.9386D-21	-3.8778D-21	-2.2449D-21	3.0904D-21	7.0544D-23	-1.3722D-21
2.2399D-21	8.4420D-23	6.0760D-21	-5.6533D-21	4.6773D-21	-4.9854D-21
-4.9243D-21	2.8759D-21	-2.8283D-21	2.5895D-21	-3.7948D-21	6.6301D-21
1.9248D-21	-3.3537D-21	-3.0605D-21	2.8786D-21	-1.5754D-21	2.5384D-22
-1.0575D-21	3.6909D-21	1.8172D-21	-2.7964D-21	8.1018D-22	-4.9206D-22
7.9599D-24	-4.2276D-24	-1.6276D-25	-2.1547D-24	7.3902D-24	-1.1371D-23
-7.1958D-25	-1.3988D-24	-1.9216D-24	2.8124D-24	-3.9949D-24	8.9351D-24
-1.0249D-23	8.6264D-24	-7.7879D-24	8.7098D-24	-8.6842D-24	1.2057D-23
4.7033D-24	-6.4791D-24	1.1564D-23	-1.2430D-23	8.1882D-24	-1.2561D-23
6.0245D-24	-4.6820D-24	1.3407D-24	-2.7065D-24	-4.2907D-24	8.6481D-24
-1.0357D-23	9.5107D-24	-4.7478D-24	6.4010D-24	-5.2108D-25	-3.8480D-24
2.1262D-23	-1.1645D-23	5.0374D-24	-1.3851D-23	-4.5314D-24	1.4556D-23
-1.6653D-23	7.9542D-24	-2.2600D-25	1.0158D-23	1.0250D-23	-1.9347D-23
-1.6377D-24	2.0011D-24	-1.0986D-23	1.2076D-23	-1.8259D-24	1.6296D-24
2.0765D-24	-3.9861D-24	5.8207D-24	-6.5160D-24	5.0598D-24	-4.7932D-24
-9.6762D-24	1.0513D-23	-1.0952D-24	1.1314D-24	-1.3396D-23	8.7734D-24
1.2598D-23	-1.4516D-23	9.2853D-24	-1.0126D-23	1.0398D-23	-6.0555D-24
4.5183D-24	-6.9147D-24	-1.4257D-23	1.7526D-23	-5.7831D-24	1.3604D-23
-9.5168D-24	1.3878D-23	2.1432D-23	-2.4348D-23	5.9564D-24	2.2627D-24
-7.0779D-24	9.3098D-26	-3.2804D-23	2.5933D-23	-2.1382D-23	2.3147D-23

2.2261D-23	-1.6966D-23	1.6653D-23	-1.1791D-23	1.8610D-23	-3.6352D-23
-1.7258D-23	2.2469D-23	1.8428D-23	-1.6137D-23	2.2757D-24	9.9982D-24
1.0892D-23	-2.2024D-23	-4.7390D-24	8.9277D-24	1.0543D-24	-9.5832D-24
1.0687D-10	-1.3866D-10	1.7327D-10	-1.1509D-10	3.5468D-11	-1.1780D-10
5.1506D-11	-2.6702D-11	1.0274D-10	-9.6229D-11	-5.3913D-11	6.1058D-11
-9.3479D-11	-5.1663D-11	6.4400D-11	4.1984D-11	-7.4910D-11	7.5172D-11
-3.8473D-11	2.6403D-11	6.0026D-12	-1.3564D-11	-4.7390D-11	4.0961D-11
2.7988D-11	-1.0272D-10	6.4342D-11	-7.7073D-11	4.1068D-11	8.3758D-12
-9.2923D-11	9.8300D-11	-4.3587D-11	7.1923D-11	2.5437D-11	-2.5131D-11
-1.3529D-10	1.3310D-10	-1.8447D-10	3.3039D-11	-4.8974D-12	1.1055D-10
-5.0742D-11	5.2591D-11	-9.6589D-11	8.3609D-11	4.1667D-11	-4.7840D-11
4.3491D-11	1.2729D-11	-6.6214D-11	-1.0683D-11	5.1143D-11	-8.2090D-11
5.2836D-11	-4.7500D-11	-3.5879D-11	3.5508D-11	4.4143D-11	-8.3045D-12
-6.0930D-12	1.1138D-10	-9.0038D-11	7.4081D-11	-7.2701D-11	-6.0635D-11
8.1722D-11	-9.5803D-11	7.5337D-11	-7.6164D-11	-9.4162D-13	-1.1615D-12
1.8096D-11	3.7607D-13	6.1382D-12	7.1564D-12	1.0605D-11	-3.3511D-11
3.0449D-11	-6.4753D-11	6.9503D-11	-3.8075D-11	8.1735D-13	-3.8828D-12
2.6006D-10	-5.0762D-10	5.8811D-10	-3.4694D-10	-1.0803D-10	1.2289D-10
-2.1382D-10	9.2207D-11	-3.0930D-11	-1.1844D-10	-4.5590D-11	3.7491D-10
-2.5540D-10	5.0474D-10	-5.8392D-10	3.4680D-10	1.0874D-10	-1.4614D-10
2.2076D-10	-4.9348D-11	-1.9853D-12	1.2695D-10	7.5966D-11	-4.1187D-10
4.4072D-11	-2.6325D-11	-1.1016D-11	2.6942D-11	1.7500D-11	-4.7625D-11
3.0152D-11	-8.1659D-11	9.5244D-11	-6.2455D-11	-3.7200D-11	3.4479D-11

***Appendix C: Spice-4 Structure Truth and Modal Models: Open Loop Bode Response***

This appendix contains Bode plots of the responses in the X and Y LOS axis to the nine disturbance inputs for each of the modal reduced filters (12-, 18-, and 26-mode). The truth model response has been added for ease of comparison. Notice the high frequency inconsistencies (large dips in the plots) in Figures C-1, C-2, C-3, C-10, C-11, C-12, C-13, C-20, C-21, C-28, C-29, C-30, C-31, C-39, C-43, C-44, C-48, and C-51.

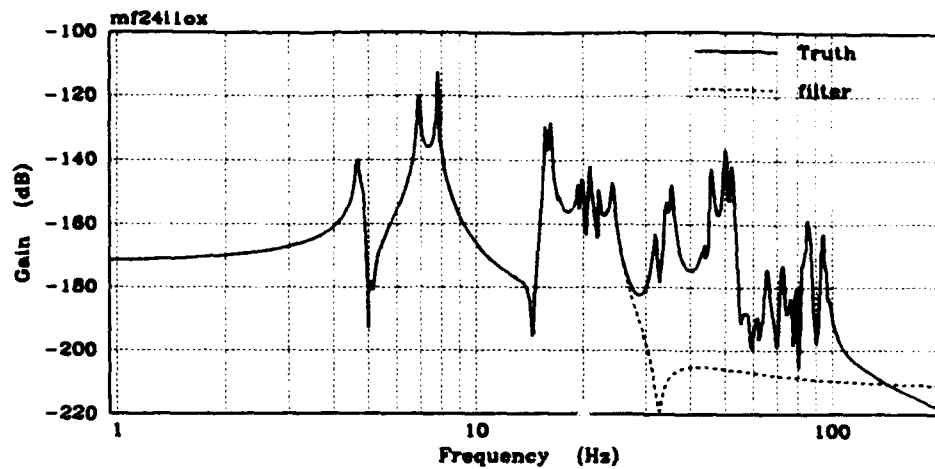


Figure C-1. Truth vs. 12-mode Modal Reduced (Disturbance 1, X LOS)

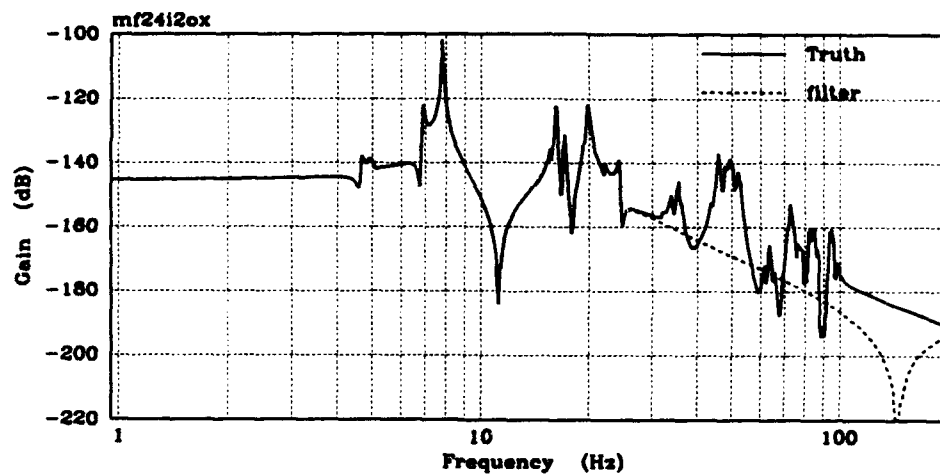


Figure C-2. Truth vs. 12-mode Modal Reduced (Disturbance 2, X LOS)

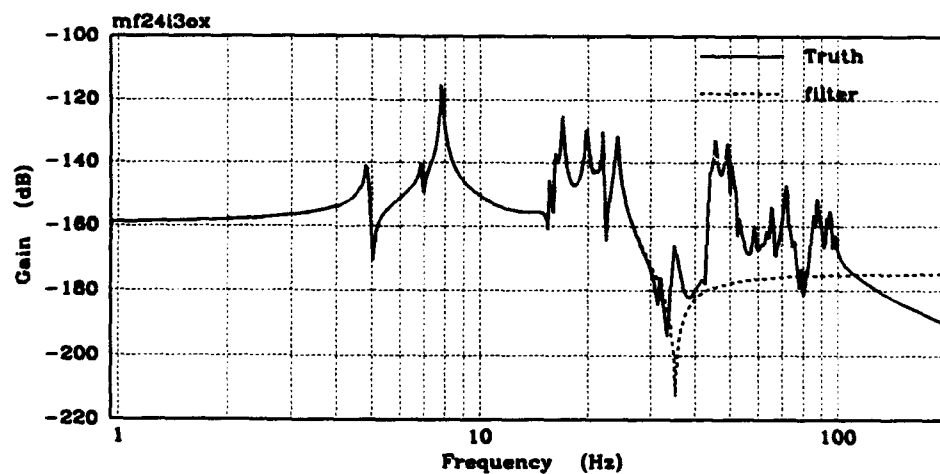


Figure C-3. Truth vs. 12-mode Modal Reduced (Disturbance 3, X LOS)



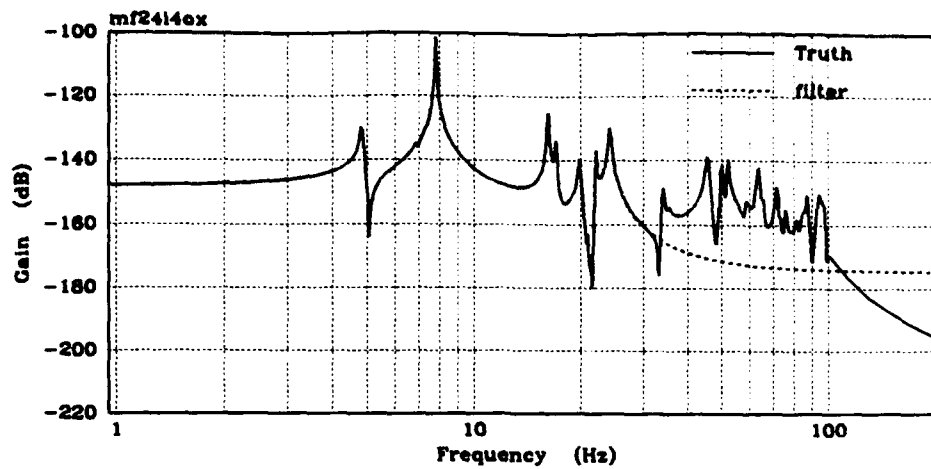


Figure C-4. Truth vs. 12-mode Modal Reduced (Disturbance 4, X LOS)

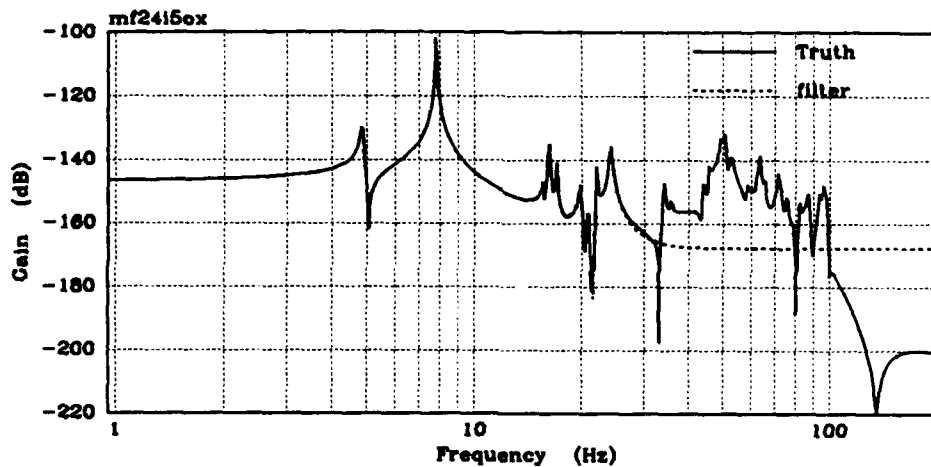


Figure C-5. Truth vs. 12-mode Modal Reduced (Disturbance 5, X LOS)

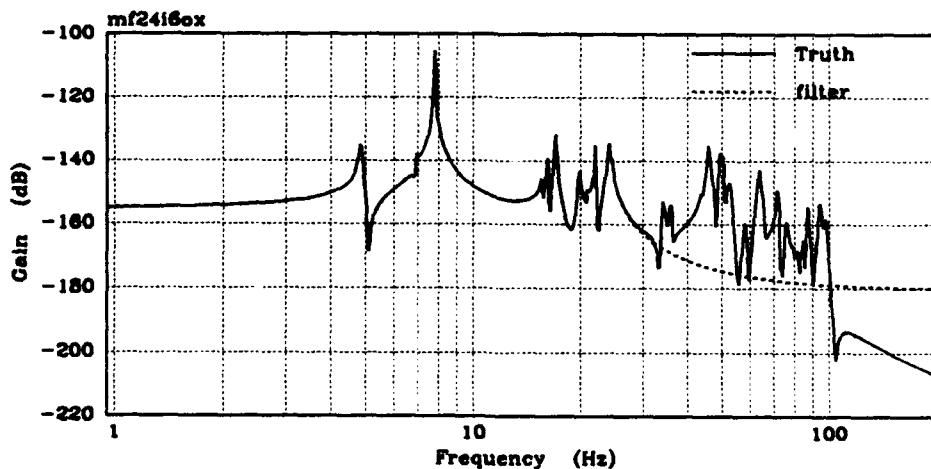


Figure C-6. Truth vs. 12-mode Modal Reduced (Disturbance 6, X LOS)

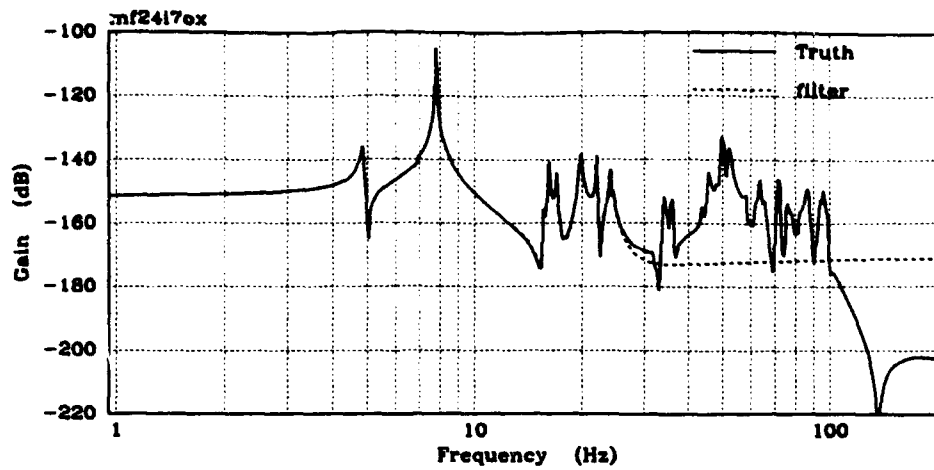


Figure C-7. Truth vs. 12-mode Modal Reduced (Disturbance 7, X LOS)

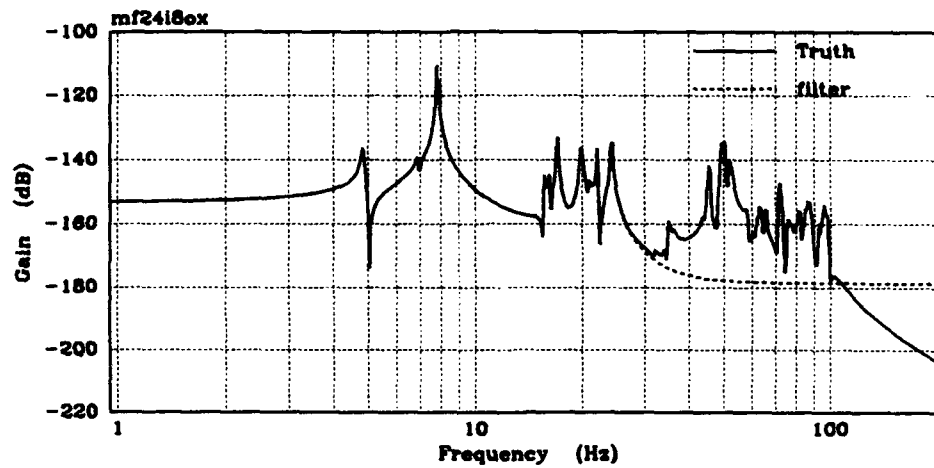


Figure C-8. Truth vs. 12-mode Modal Reduced (Disturbance 8, X LOS)

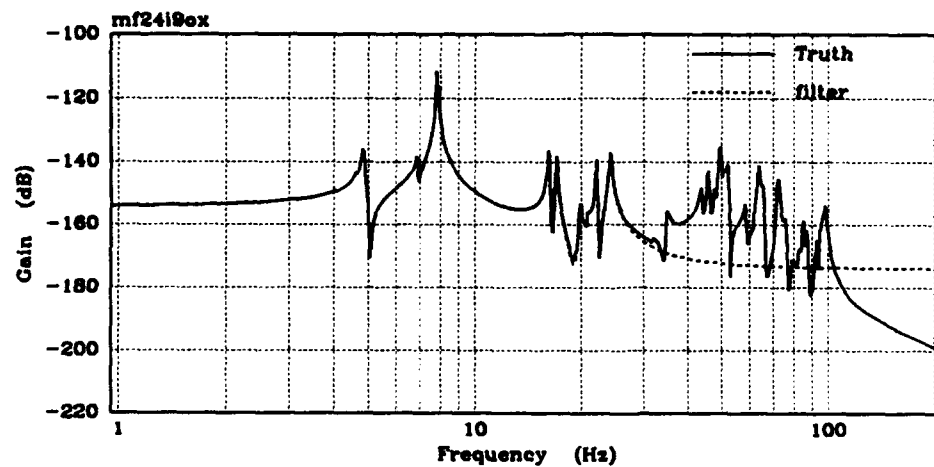


Figure C-9. Truth vs. 12-mode Modal Reduced (Disturbance 9, X LOS)

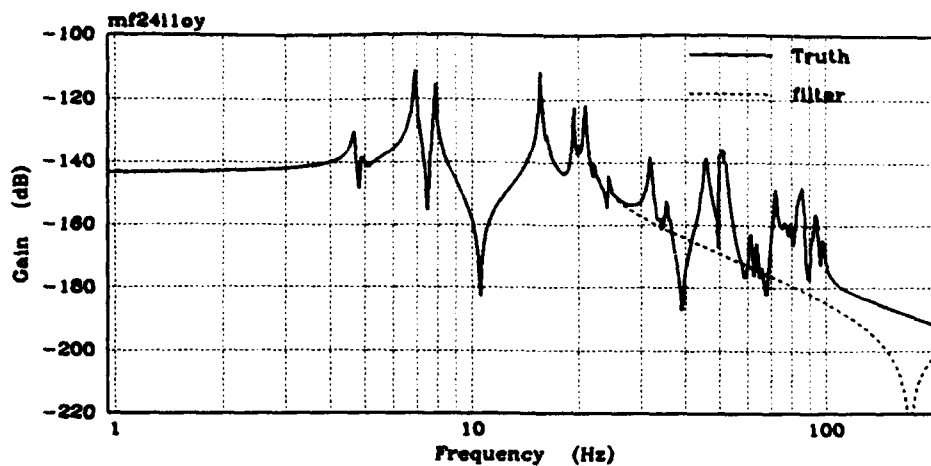


Figure C-10. Truth vs. 12-mode Modal Reduced (Disturbance 1, Y LOS)

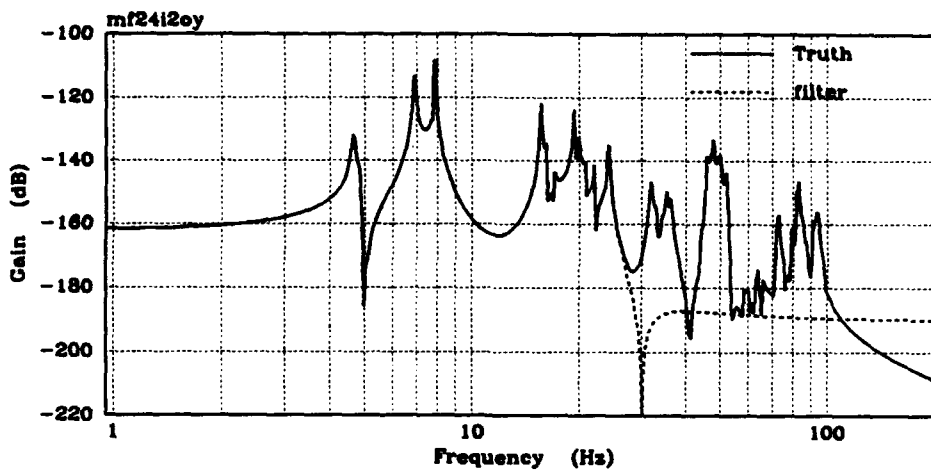


Figure C-11. Truth vs. 12-mode Modal Reduced (Disturbance 2, Y LOS)

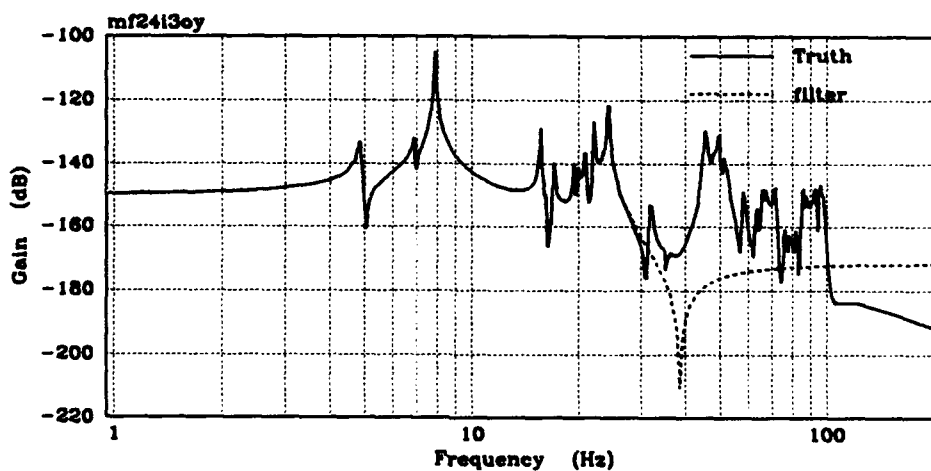


Figure C-12. Truth vs. 12-mode Modal Reduced (Disturbance 3, Y LOS)

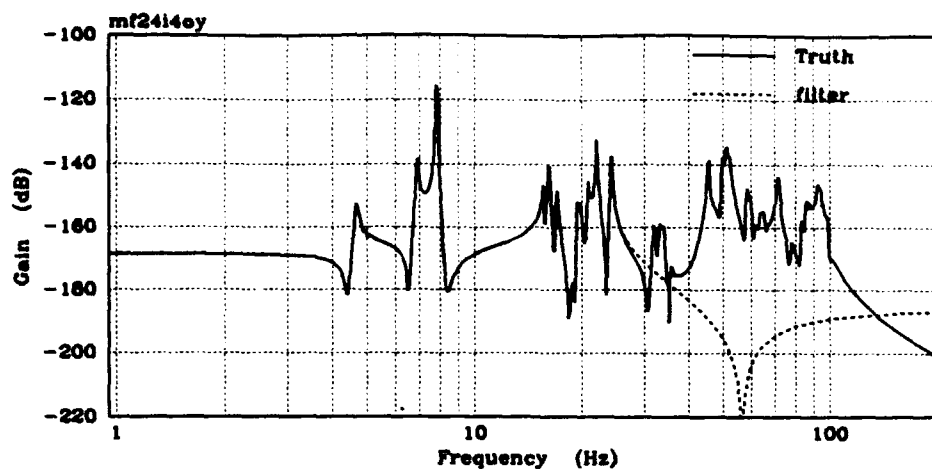


Figure C-13. Truth vs. 12-mode Modal Reduced (Disturbance 4, Y LOS)

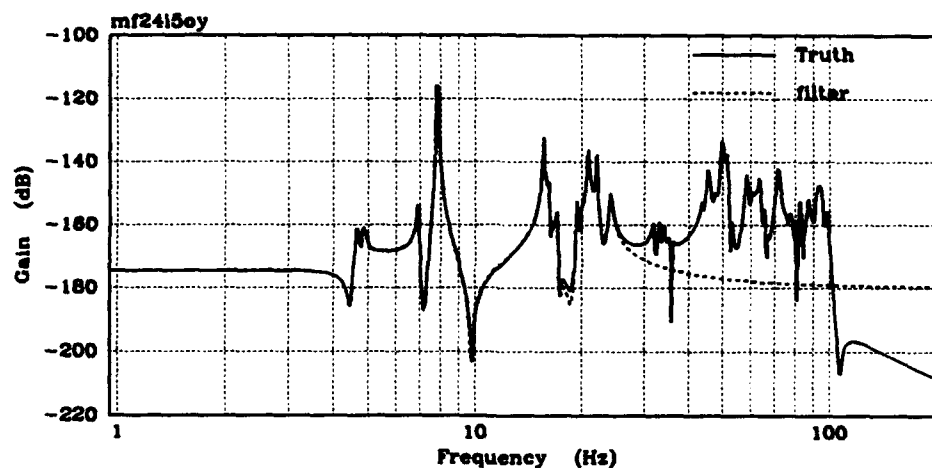


Figure C-14. Truth vs. 12-mode Modal Reduced (Disturbance 5, Y LOS)

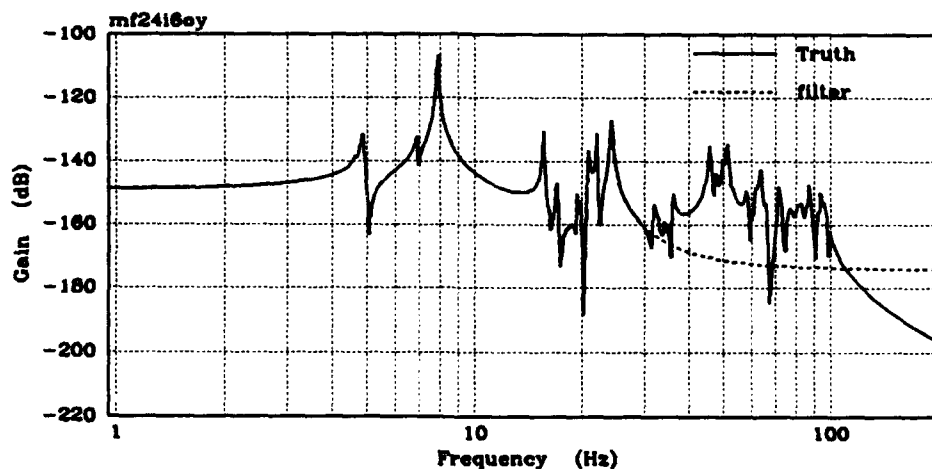


Figure C-15. Truth vs. 12-mode Modal Reduced (Disturbance 6, Y LOS)

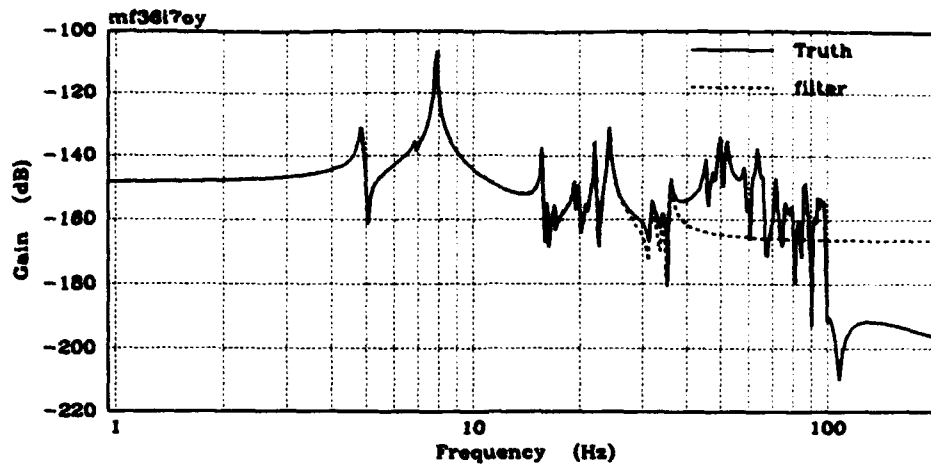


Figure C-16. Truth vs. 12-mode Modal Reduced (Disturbance 7, Y LOS)

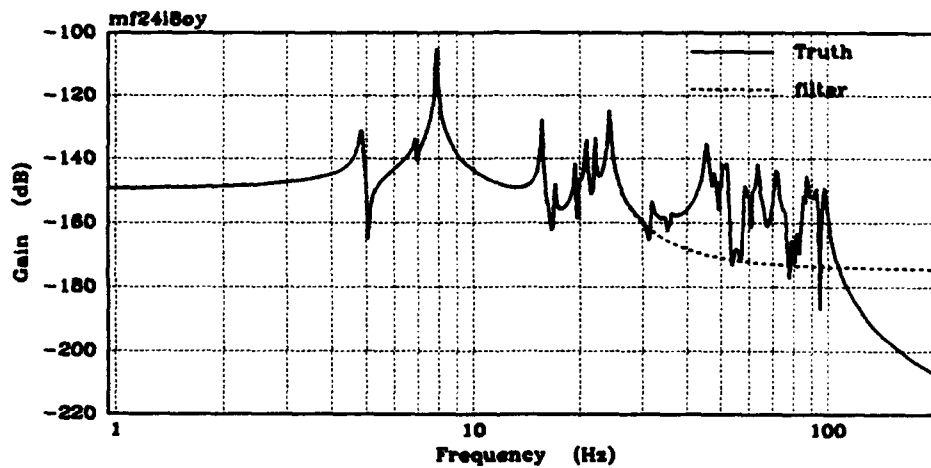


Figure C-17. Truth vs. 12-mode Modal Reduced (Disturbance 8, Y LOS)

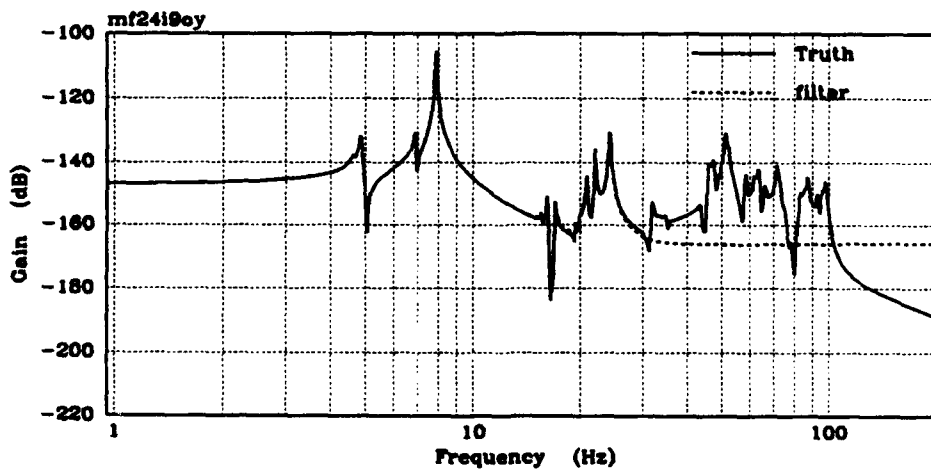


Figure C-18. Truth vs. 12-mode Modal Reduced (Disturbance 9, Y LOS)

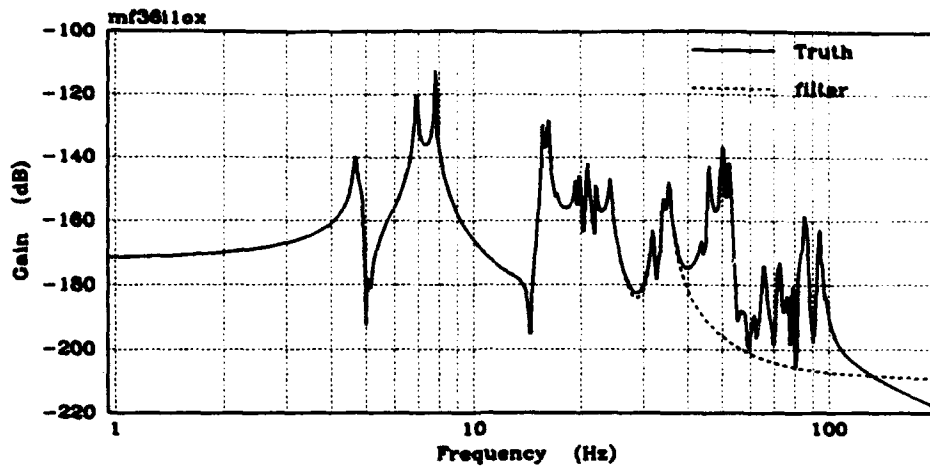


Figure C-19. Truth vs. 18-mode Modal Reduced (Disturbance 1, X LOS)

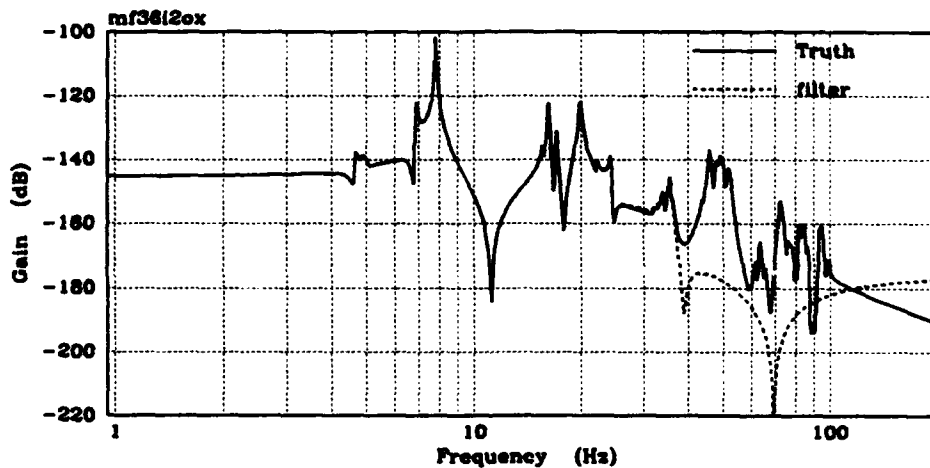


Figure C-20. Truth vs. 18-mode Modal Reduced (Disturbance 2, X LOS)

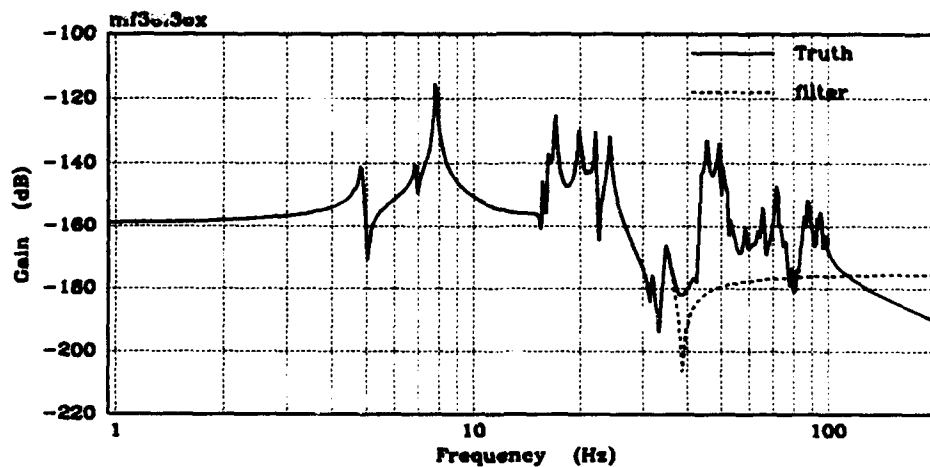


Figure C-21. Truth vs. 18-mode Modal Reduced (Disturbance 3, X LOS)

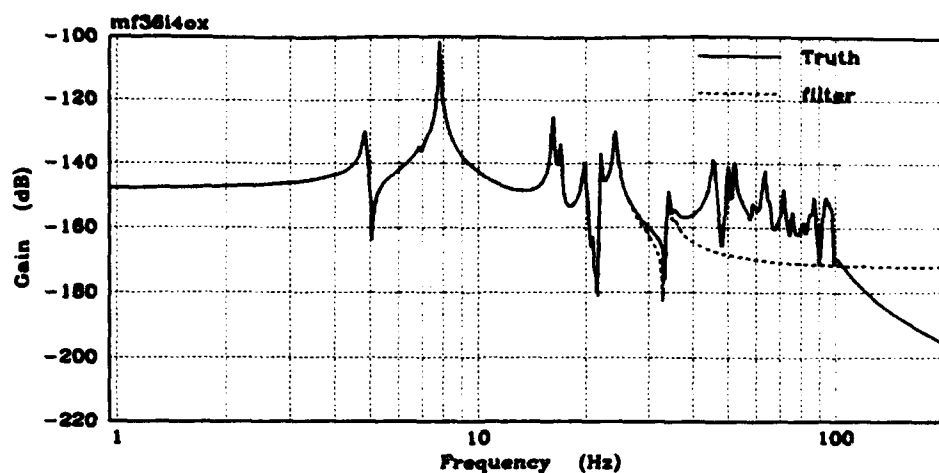


Figure C-22. Truth vs. 18-mode Modal Reduced (Disturbance 4, X LOS)

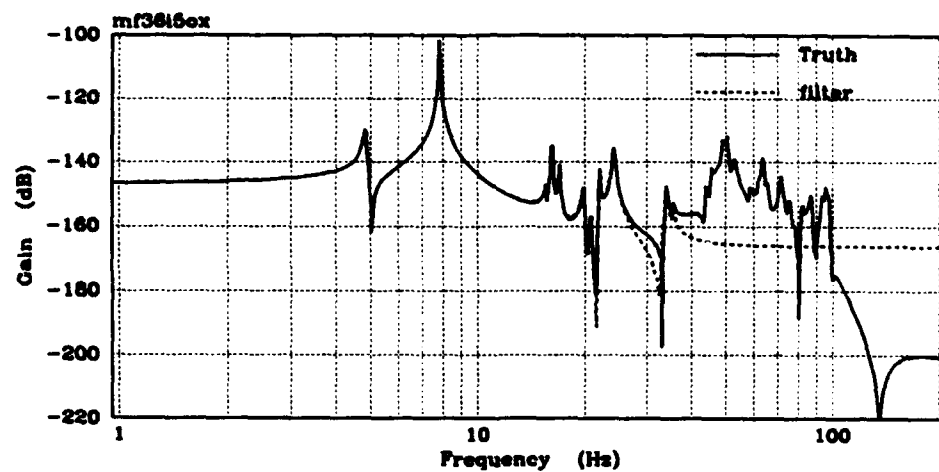


Figure C-23. Truth vs. 18-mode Modal Reduced (Disturbance 5, X LOS)

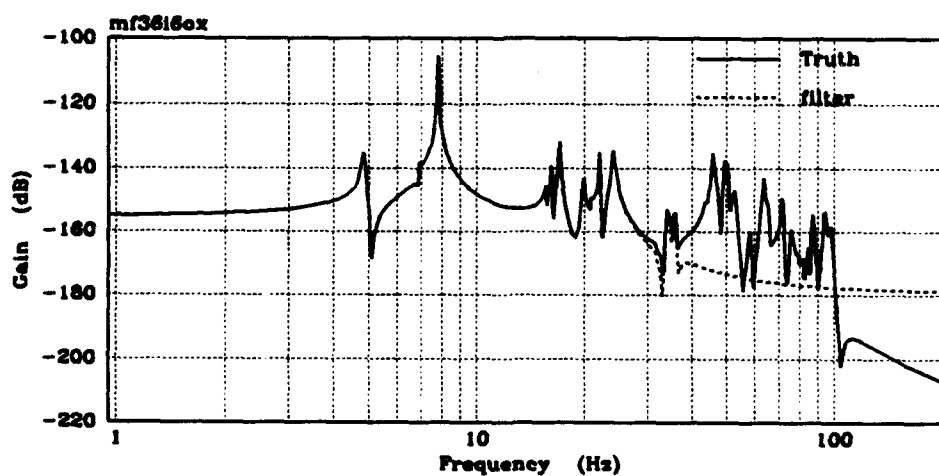


Figure C-24. Truth vs. 18-mode Modal Reduced (Disturbance 6, X LOS)

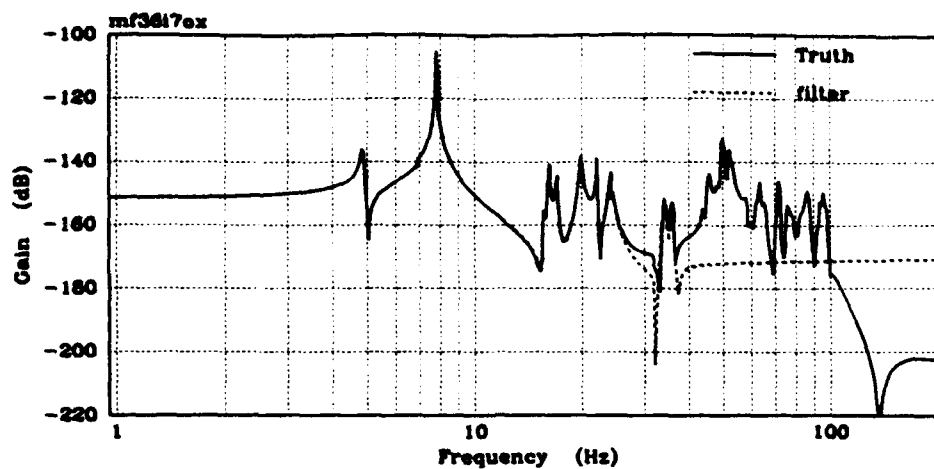


Figure C-25. Truth vs. 18-mode Modal Reduced (Disturbance 7, X LOS)

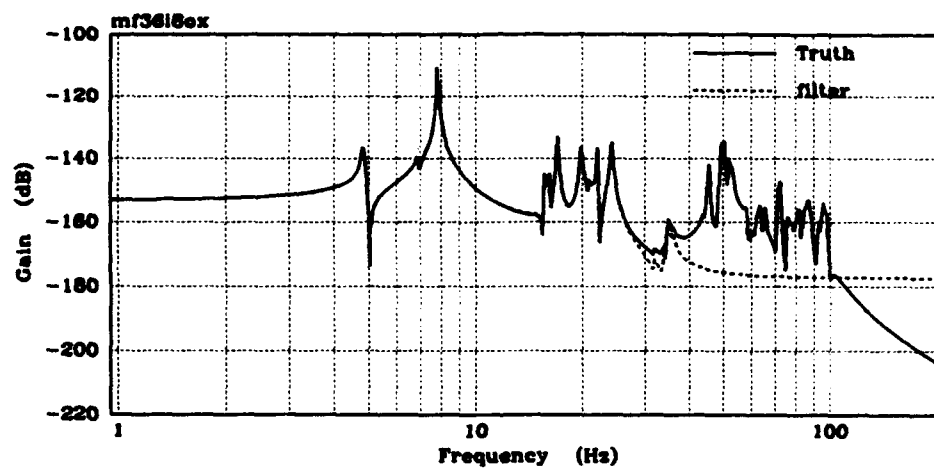


Figure C-26. Truth vs. 18-mode Modal Reduced (Disturbance 8, X LOS)

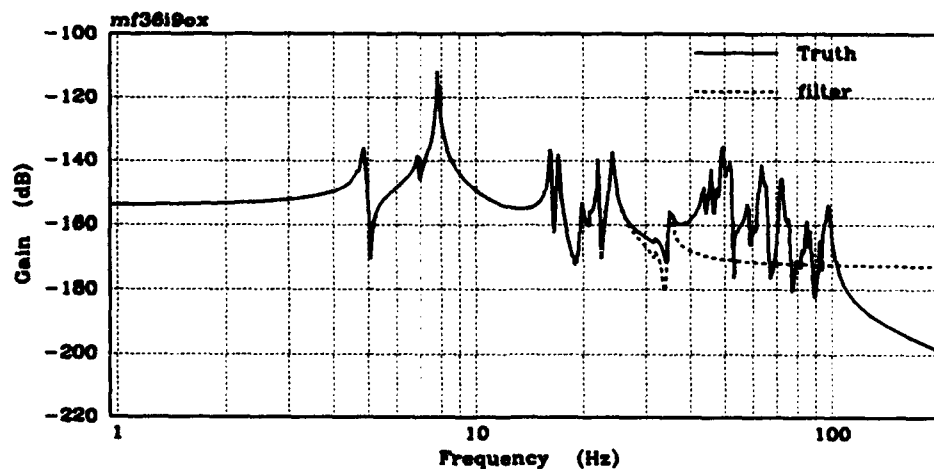


Figure C-27. Truth vs. 18-mode Modal Reduced (Disturbance 9, X LOS)



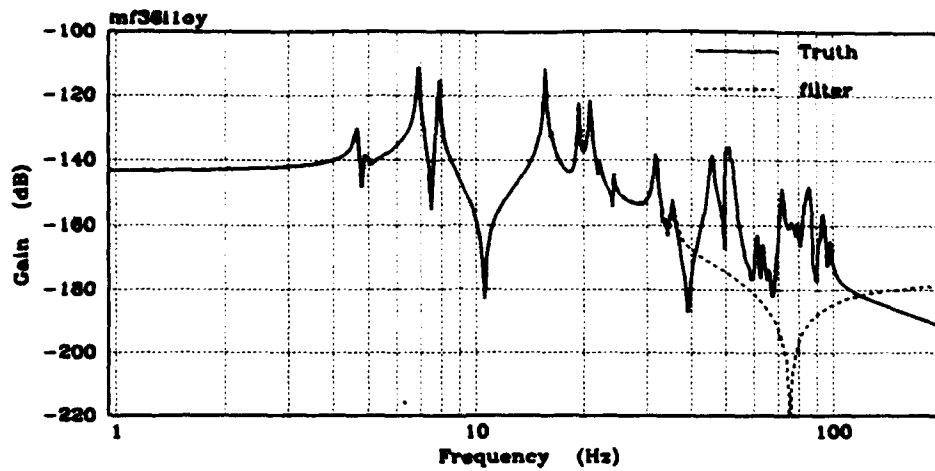


Figure C-28. Truth vs. 18-mode Modal Reduced (Disturbance 1, Y LOS)

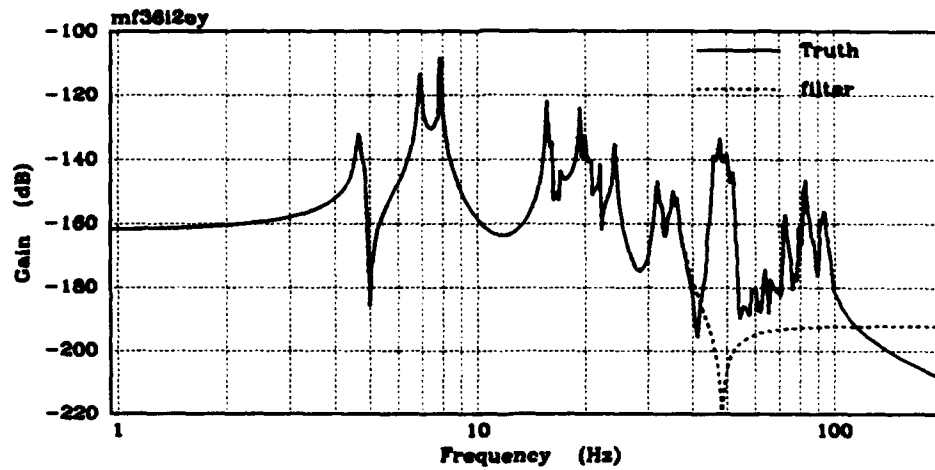


Figure C-29. Truth vs. 18-mode Modal Reduced (Disturbance 2, Y LOS)

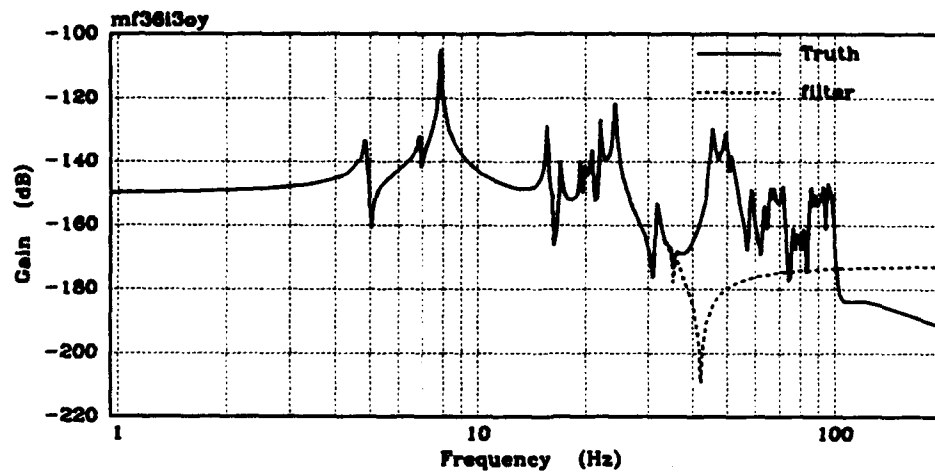


Figure C-30. Truth vs. 18-mode Modal Reduced (Disturbance 3, Y LOS)

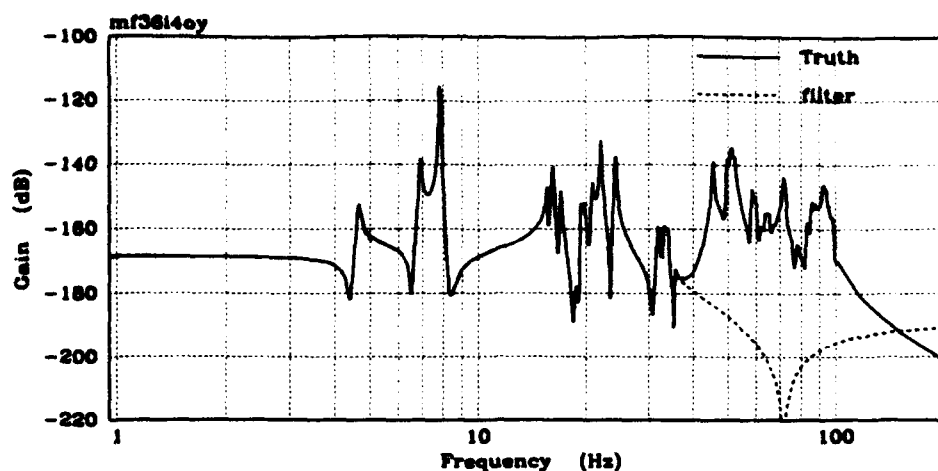


Figure C-31. Truth vs. 18-mode Modal Reduced (Disturbance 4, Y LOS)

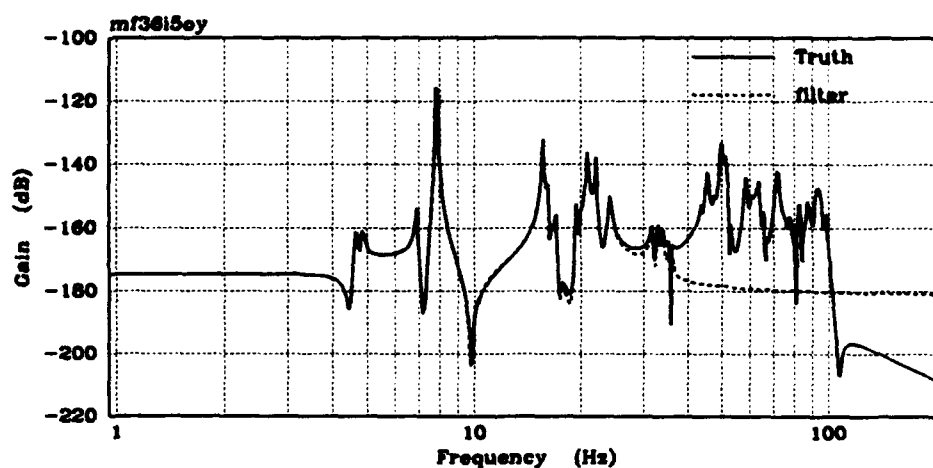


Figure C-32. Truth vs. 18-mode Modal Reduced (Disturbance 5, Y LOS)

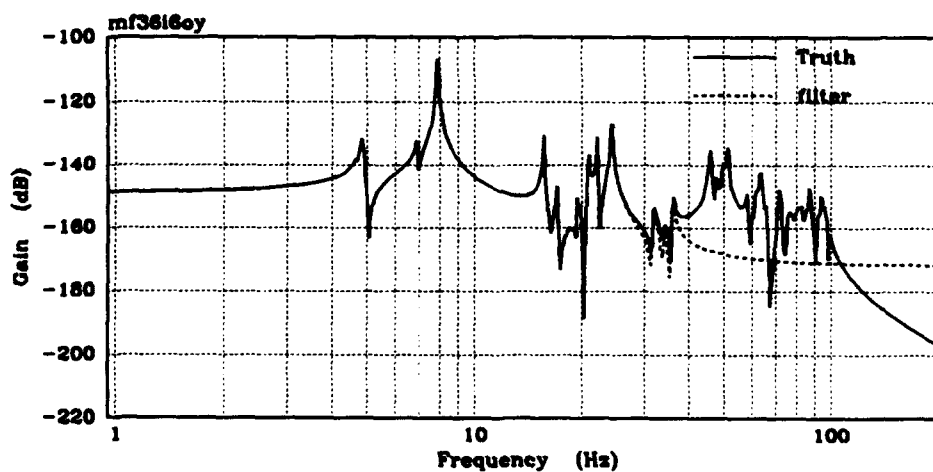


Figure C-33. Truth vs. 18-mode Modal Reduced (Disturbance 6, Y LOS)

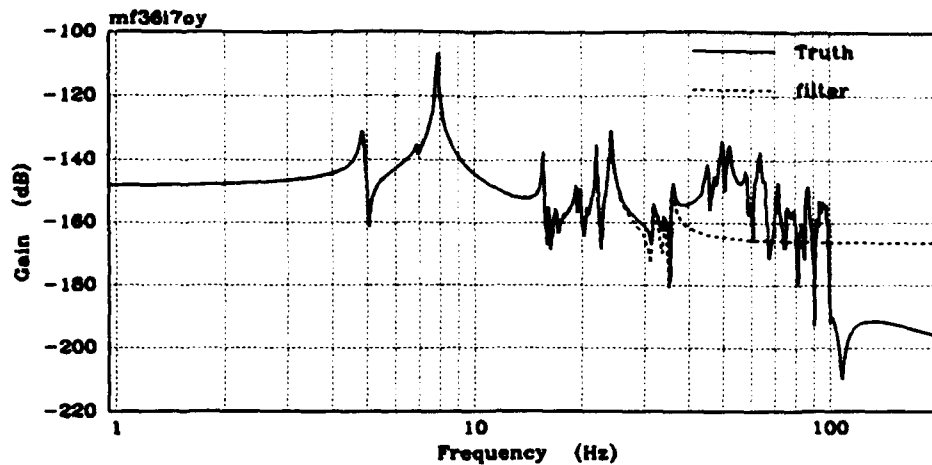


Figure C-34. Truth vs. 18-mode Modal Reduced (Disturbance 7, Y LOS)

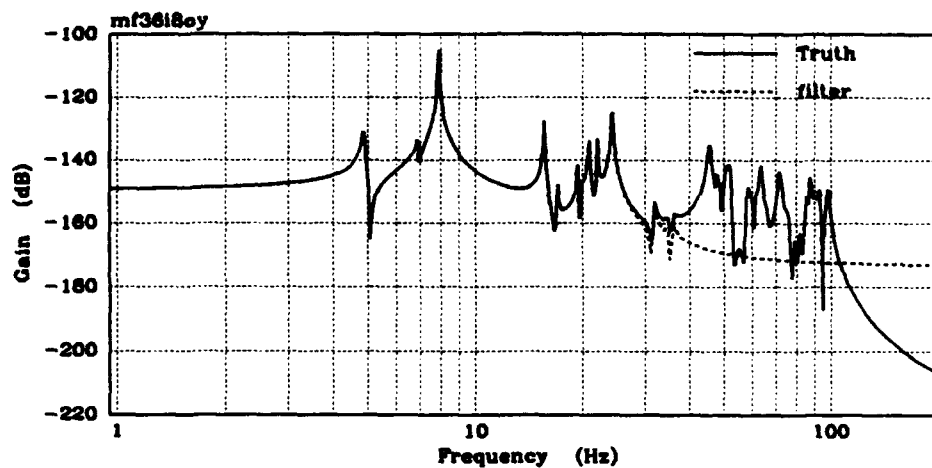


Figure C-35. Truth vs. 18-mode Modal Reduced (Disturbance 8, Y LOS)

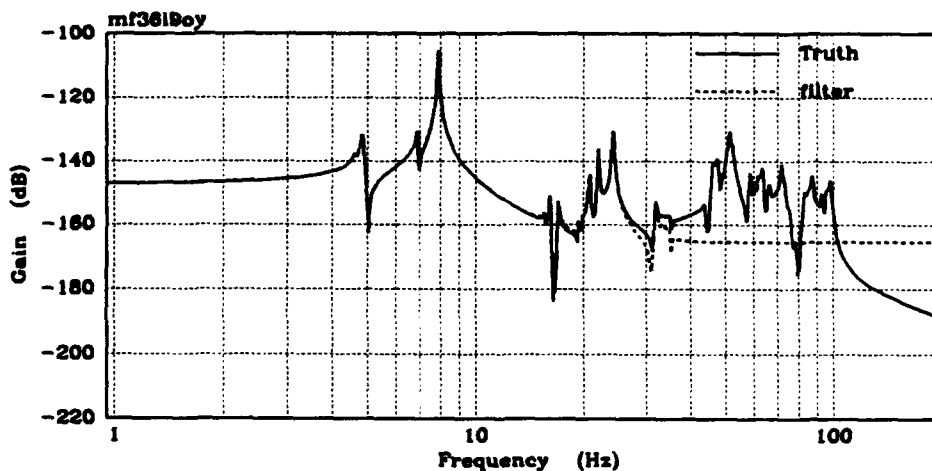


Figure C-36. Truth vs. 18-mode Modal Reduced (Disturbance 9, Y LOS)

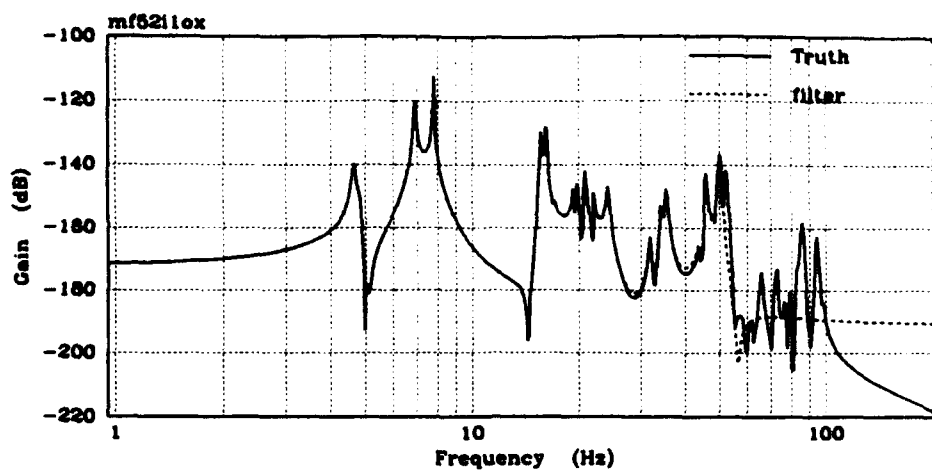


Figure C-37. Truth vs. 26-mode Modal Reduced (Disturbance 1, X LOS)

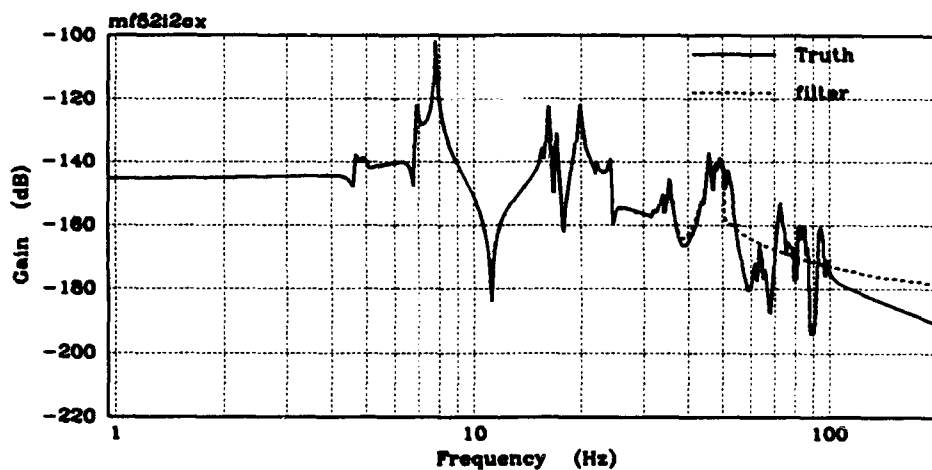


Figure C-38. Truth vs. 26-mode Modal Reduced (Disturbance 2, X LOS)

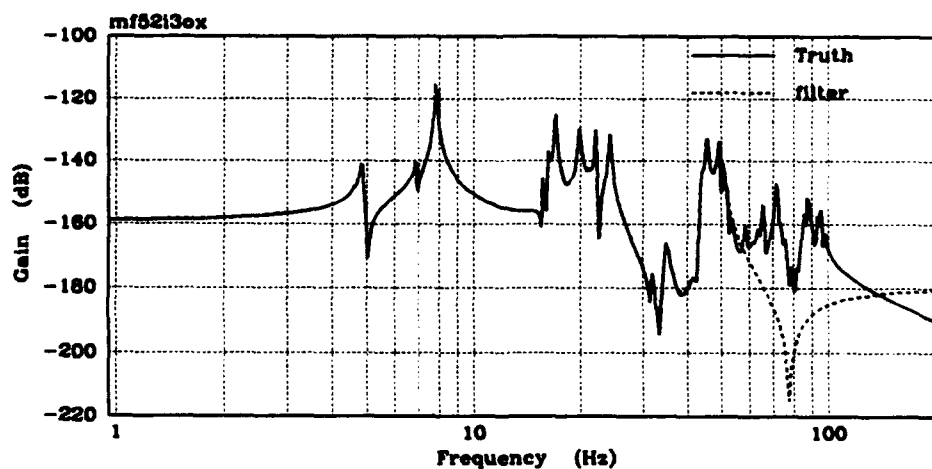


Figure C-39. Truth vs. 26-mode Modal Reduced (Disturbance 3, X LOS)

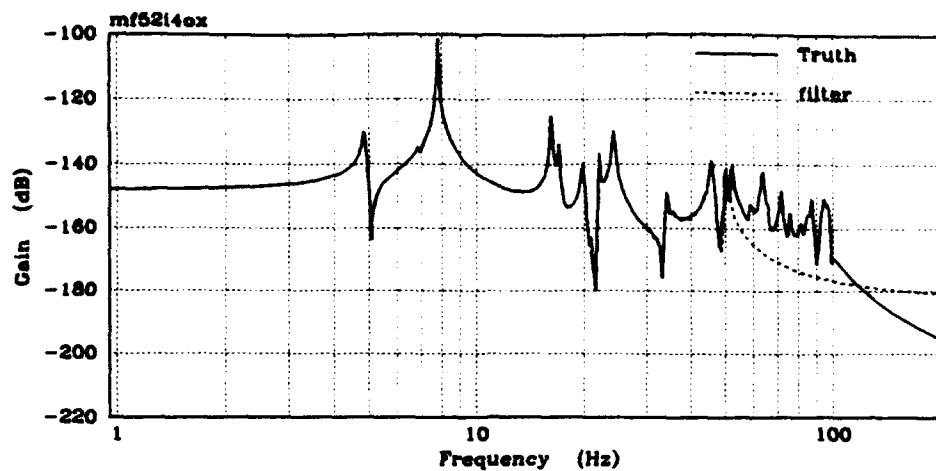


Figure C-40. Truth vs. 26-mode Modal Reduced (Disturbance 4, X LOS)

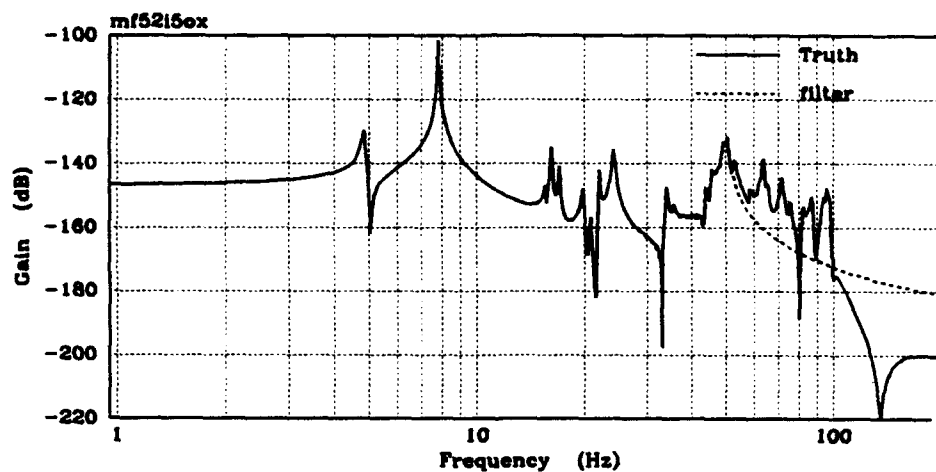


Figure C-41. Truth vs. 26-mode Modal Reduced (Disturbance 5, X LOS)

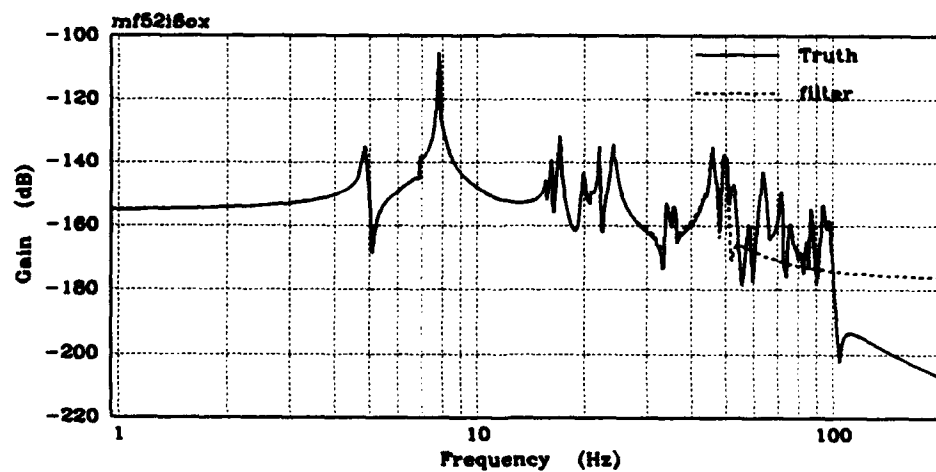


Figure C-42. Truth vs. 26-mode Modal Reduced (Disturbance 6, X LOS)

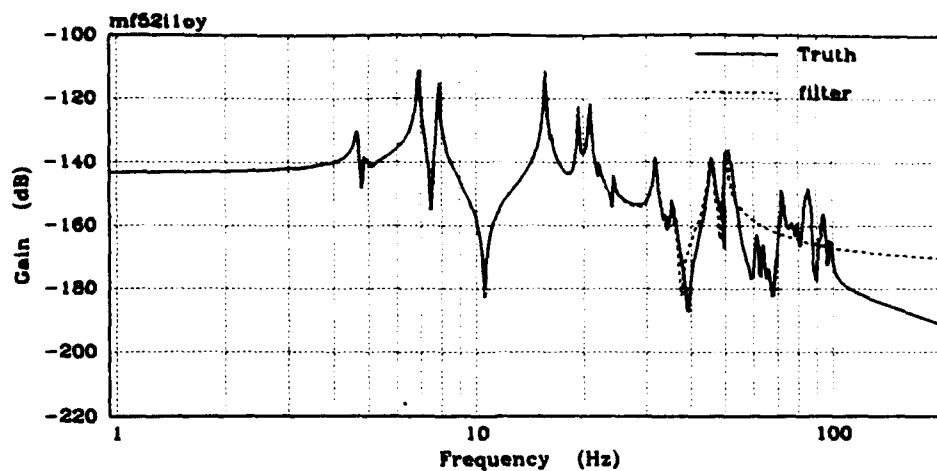


Figure C-46. Truth vs. 26-mode Modal Reduced (Disturbance 1, Y LOS)

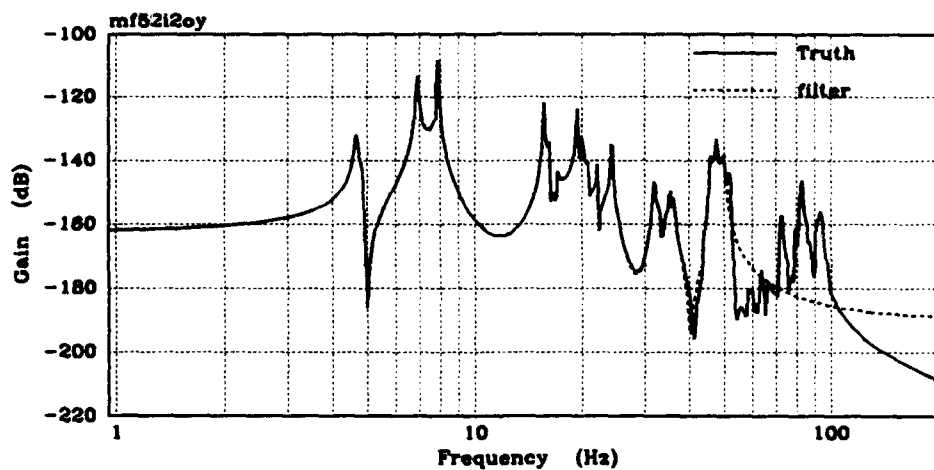


Figure C-47. Truth vs. 26-mode Modal Reduced (Disturbance 2, Y LOS)

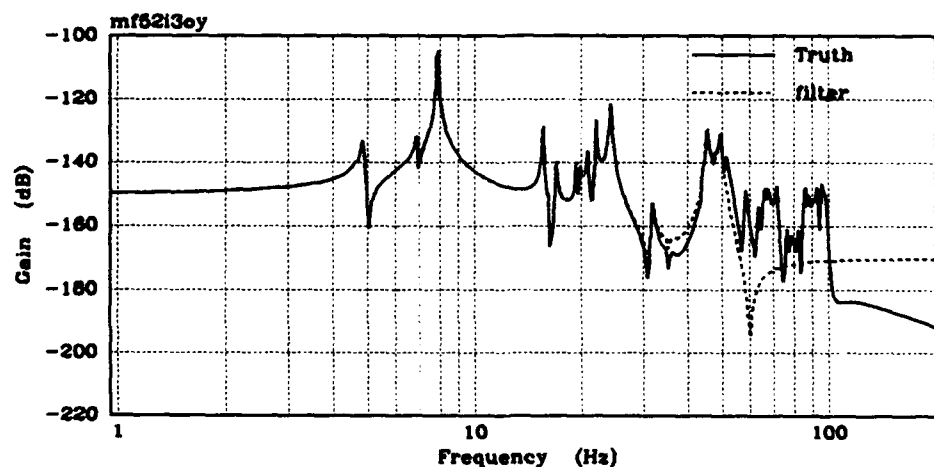


Figure C-48. Truth vs. 26-mode Modal Reduced (Disturbance 3, Y LOS)

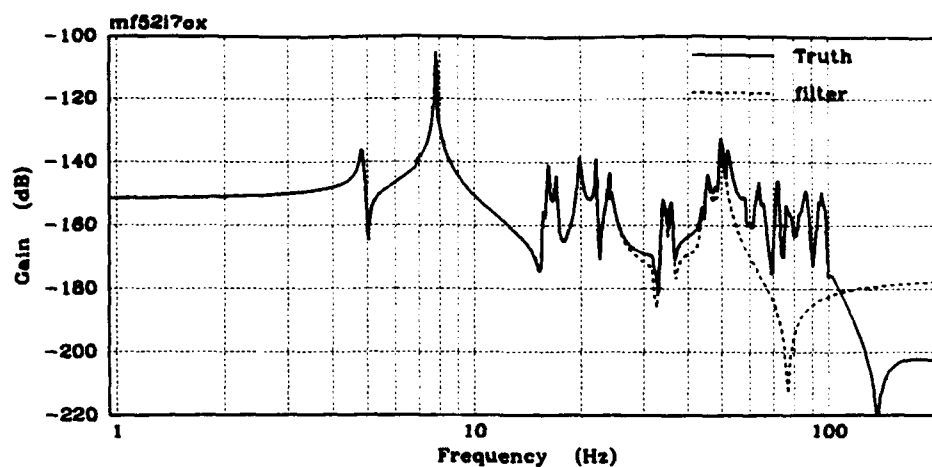


Figure C-43. Truth vs. 26-mode Modal Reduced (Disturbance 7, X LOS)

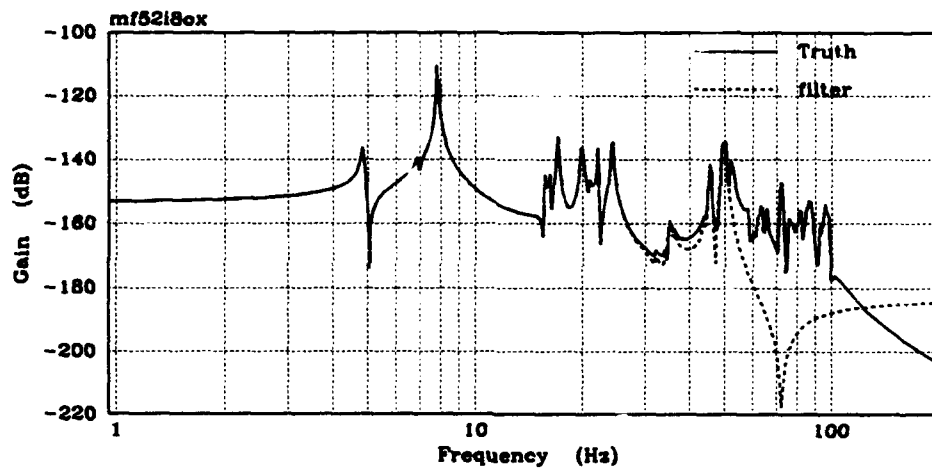


Figure C-44. Truth vs. 26-mode Modal Reduced (Disturbance 8, X LOS)

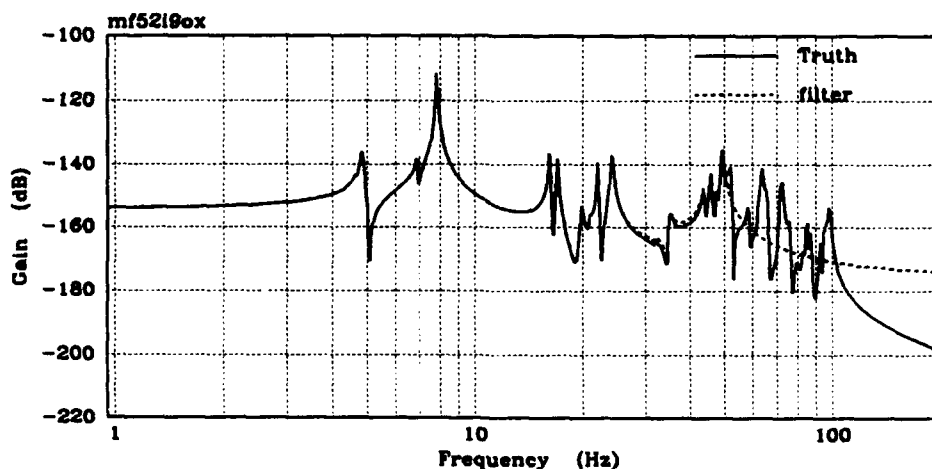


Figure C-45. Truth vs. 26-mode Modal Reduced (Disturbance 9, X LOS)

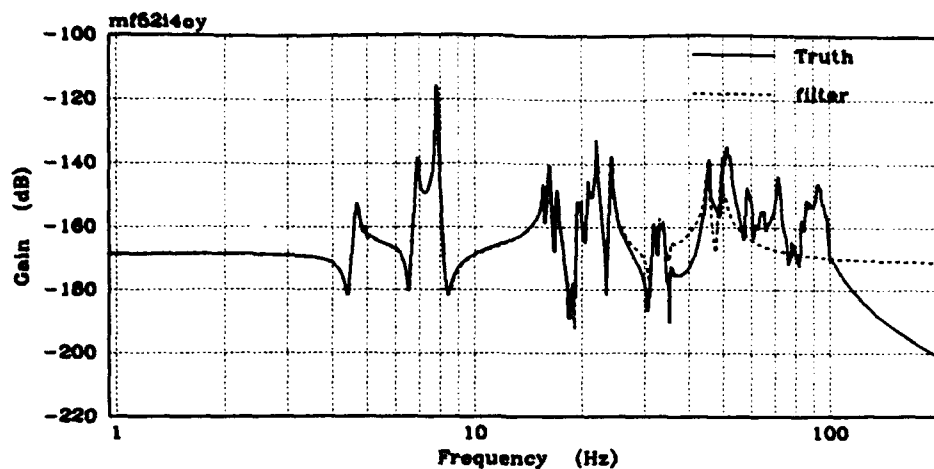


Figure C-49. Truth vs. 26-mode Modal Reduced (Disturbance 4, Y LOS)

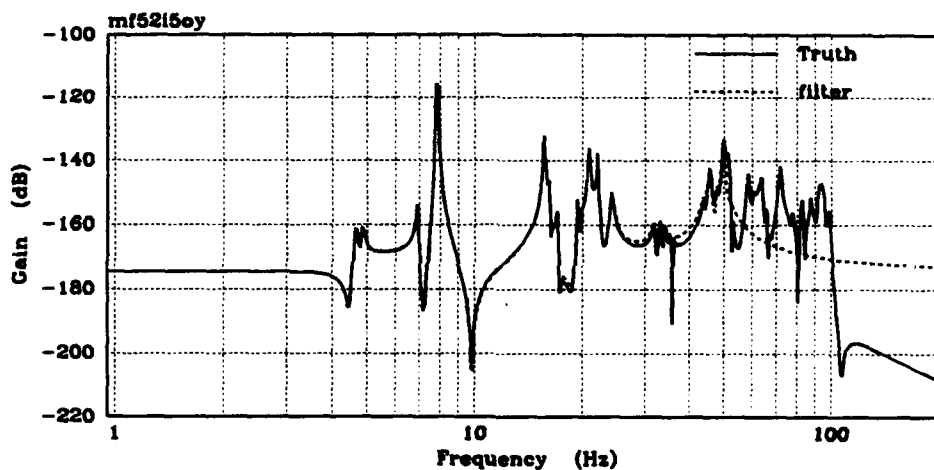


Figure C-50. Truth vs. 26-mode Modal Reduced (Disturbance 5, Y LOS)

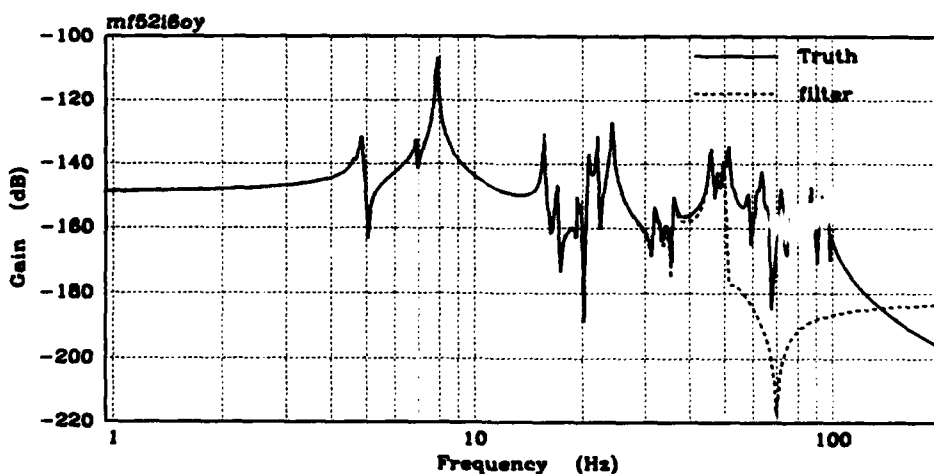


Figure C-51. Truth vs. 26-mode Modal Reduced (Disturbance 6, Y LOS)



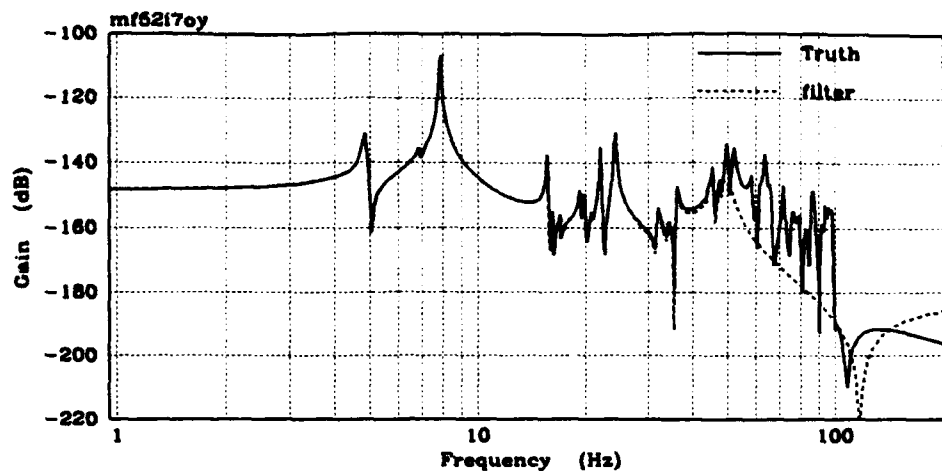


Figure C-52. Truth vs. 26-mode Modal Reduced (Disturbance 7, Y LOS)

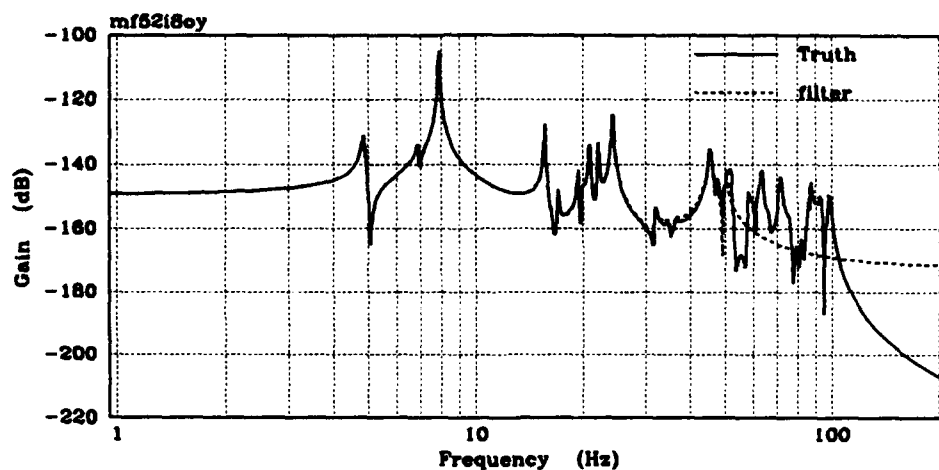


Figure C-53. Truth vs. 26-mode Modal Reduced (Disturbance 8, Y LOS)

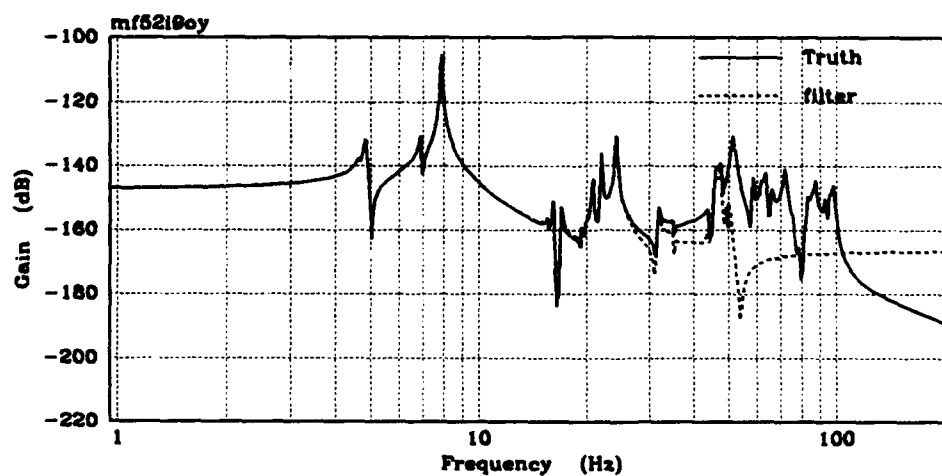


Figure C-54. Truth vs. 26-mode Modal Reduced (Disturbance 9, Y LOS)

#### Appendix D: 26-Modal-Cost Model

This appendix presents the various matrices associated with the 26-Modal-Cost Model as described in Chapter 3. This is representative of the open loop system. Since the only order reduction involves the structure portion of the truth model, the disturbance and control output filter matrices are not repeated. The individual matrices for the reduced-order structure portion are briefly described below (in this model  $n=26$ ). The subscript  $f$  (i.e., *filter*) indicates that these matrices correspond to a reduced-order model. Additionally, several matrices ( $\mathbf{B}_f$ ,  $\mathbf{G}_f$ , and  $\mathbf{C}_f$ ) contain relatively large blocks of zeros which are not presented. The specific format of these matrices is shown below (e.g., the last 44 rows of  $\mathbf{B}_f$  are zeros).

Structure (reference Equations (3.4) and (3.16)):

- $\mathbf{F}_f = (36+2n)$ -by- $(36+2n)$  constant structure plant matrix
- $\mathbf{B}_f = (36+2n)$ -by-36 constant control input matrix

$$= \begin{bmatrix} \mathbf{B}_{f1((18+n) \times 36)} \\ \mathbf{0}_{((18+n) \times 36)} \end{bmatrix}_{((36+2n) \times 36)}$$

- $\mathbf{G}_f = (36+2n)$ -by-9 constant noise input matrix

$$= \begin{bmatrix} \mathbf{G}_{f1((18+n) \times 9)} \\ \mathbf{0}_{((18+n) \times 9)} \end{bmatrix}_{((36+2n) \times 9)}$$

- $\mathbf{C}_f = 56$ -by- $(36+2n)$  constant output matrix

$$= \begin{bmatrix} \mathbf{C}_{f1(36 \times (18+n))} & \mathbf{0}_{(36 \times (18+n))} \\ \mathbf{0}_{(20 \times (18+n))} & \mathbf{C}_{f2(20 \times (18+n))} \end{bmatrix}_{(56 \times (36+2n))}$$

$F_f =$

Mode	$-2\zeta\omega_n$	$-\omega_n^2$	Mode	$-2\zeta\omega_n$	$-\omega_n^2$
1	-5.8448D-01	-8.5404D+02	23	-6.7063D-01	-1.0325D+04
2	-6.0874D-01	-9.2642D+02	24	-9.4034D-01	-1.1418D+04
3	-6.0937D-01	-9.2834D+02	25	-7.0486D-01	-1.4769D+04
4	-6.2216D-01	-9.6770D+02	26	-1.8200D+00	-1.5540D+04
5	-6.2234D-01	-9.6826D+02	27	-1.1261D+00	-1.7147D+04
6	-6.2304D-01	-9.7046D+02	28	-7.4808D-01	-1.9192D+04
7	-6.2581D-01	-9.7908D+02	29	-2.4879D+00	-2.3012D+04
8	-6.2589D-01	-9.7935D+02	30	-1.1562D+00	-2.3146D+04
9	-6.2603D-01	-9.7977D+02	31	-3.9983D+00	-8.1561D+04
10	-6.2624D-01	-9.8043D+02	32	-4.0323D+00	-8.2954D+04
11	-6.2633D-01	-9.8073D+02	33	-4.1851D+00	-8.9361D+04
12	-6.2699D-01	-9.8278D+02	34	-4.3377D+00	-9.5773D+04
13	-6.2700D-01	-9.8283D+02	35	-4.3667D+00	-9.7383D+04
14	-6.2706D-01	-9.8300D+02	36	-4.3869D+00	-9.8187D+04
15	-6.2741D-01	-9.8411D+02	37	-4.4313D+00	-1.0019D+05
16	-6.3197D-01	-9.9847D+02	38	-4.5106D+00	-1.0380D+05
17	-6.3382D-01	-1.0043D+03	39	-4.5748D+00	-1.0678D+05
18	-6.3383D-01	-1.0043D+03	40	-4.6371D+00	-1.0971D+05
19	-4.4330D-01	-1.8741D+03	41	-5.1277D+00	-1.3415D+05
20	-2.1955D-01	-2.4016D+03	42	-5.5915D+00	-1.5951D+05
21	-2.3220D-01	-2.4408D+03	43	-5.5938D+00	-1.5964D+05
22	-6.2740D-01	-9.6101D+03	44	-6.3054D+00	-2.0285D+05

$B_f =$

Columns 1 thru 6

2.0825D-02	-1.9380D-02	5.4088D-03	-4.8615D-03	1.7901D-02	-1.5062D-02
-7.9624D-03	-9.4290D-03	-3.7621D-03	-4.0896D-03	9.2551D-03	-5.5808D-04
4.8065D-03	-4.1117D-03	6.7170D-04	-3.5865D-04	2.5588D-03	1.0726D-02
2.4055D-03	-5.3274D-04	3.9175D-03	-9.8286D-04	-8.8023D-04	-5.8466D-04
-6.2029D-04	-2.1723D-03	-9.8336D-04	-3.7525D-03	-2.4147D-03	1.0503D-03
-5.5048D-04	-6.8749D-04	-7.8423D-04	-1.2311D-03	-9.4900D-04	-2.0401D-03
-8.2665D-04	7.1069D-04	1.1465D-03	-1.0145D-03	6.0654D-04	-2.0616D-05
2.5584D-04	3.3590D-04	-9.1416D-04	-8.5733D-04	-1.0135D-04	4.5536D-04
1.0181D-03	1.0139D-03	-6.7856D-04	-7.9555D-04	6.2180D-04	-3.4855D-04
-2.8130D-04	3.2280D-04	-6.8399D-05	-7.9516D-05	3.8447D-04	-3.9670D-04
-1.4195D-04	2.8107D-04	6.7669D-05	7.1693D-05	7.5526D-04	9.1037D-04
-6.9834D-05	6.8963D-05	1.7653D-04	-1.6981D-04	-1.1638D-05	-6.3135D-06
-2.1815D-06	2.1249D-06	-3.6374D-05	-2.9386D-05	-4.3108D-05	3.1560D-05
3.2105D-05	-2.9890D-05	-1.2043D-04	1.3778D-04	8.1165D-05	-8.4986D-05
3.8729D-05	-3.8316D-05	-1.4322D-04	1.4951D-04	5.4485D-05	-5.5825D-05
-2.6955D-04	-2.7634D-04	-1.6335D-04	-1.6301D-04	-2.6080D-04	-2.8837D-04
-2.0228D-03	4.2964D-04	-1.5711D-04	1.4685D-04	1.2849D-03	-2.1148D-03
-2.1939D-04	2.0062D-03	-1.3831D-04	1.5386D-04	-1.8034D-03	-7.2034D-04

-5.7383D-02	5.1451D-02	-1.7732D-02	1.5406D-02	-4.6313D-02	3.5042D-02
3.5596D-02	5.4591D-02	1.6685D-02	2.2033D-02	-5.7328D-02	-1.8325D-03
-3.3235D-02	1.5275D-02	-9.8121D-03	2.0525D-03	1.0854D-03	-6.6632D-02
-4.8382D-02	3.6968D-02	-8.0728D-02	6.4903D-02	2.7353D-02	-1.9310D-03
2.1924D-02	3.3992D-02	3.5100D-02	5.9481D-02	4.0128D-02	-3.5271D-02
-3.1502D-02	-3.1249D-02	-5.0113D-02	-5.2441D-02	-1.9097D-02	-3.4792D-02
4.8542D-03	3.9360D-03	4.9479D-02	-3.7048D-02	1.5019D-02	-1.4405D-02
-3.4610D-02	-3.7056D-02	-4.4808D-02	-5.1492D-02	5.1877D-03	2.0672D-02
2.4742D-02	-7.0010D-03	-2.9458D-03	1.5510D-02	-3.8896D-02	-2.6679D-02
1.9822D-02	2.5229D-02	-3.7735D-04	1.7194D-03	3.9881D-02	4.2077D-02
3.0427D-02	3.4769D-02	-3.1504D-02	-4.9741D-02	-9.8180D-03	-1.8154D-02
1.1445D-02	3.7294D-03	-4.1495D-02	2.3546D-02	1.5148D-02	1.2447D-02
-1.9869D-02	7.9912D-03	-5.8518D-03	1.8994D-02	5.4274D-03	-1.7367D-02
1.5954D-03	1.6713D-02	-1.4592D-02	-4.5709D-03	-2.4081D-02	-8.4755D-03
2.1872D-02	-2.1572D-02	4.8236D-02	-4.9775D-02	5.1002D-04	-8.1887D-03
-1.0603D-02	-1.3239D-02	1.8710D-02	7.3679D-03	1.0252D-02	-3.2205D-03
-1.0172D-03	7.7044D-03	-9.0440D-04	-6.6180D-03	-1.9426D-02	-1.3994D-02
3.7932D-03	7.4290D-04	-8.7199D-03	2.6735D-03	2.1788D-03	-2.7823D-03
-3.5114D-04	1.1647D-03	-4.0010D-04	-2.4351D-03	-1.6183D-02	2.3512D-02
-1.2400D-03	2.2107D-03	-2.1272D-02	2.0394D-02	6.5539D-03	1.1191D-03
2.7054D-03	2.2760D-03	-4.1960D-03	-1.9248D-03	-2.2450D-03	-9.0702D-03
-1.7086D-03	-4.1469D-03	5.0255D-04	5.6121D-03	-1.7250D-02	2.0818D-02
5.4021D-03	5.2195D-03	-6.5151D-03	-6.1392D-03	5.9618D-03	5.8832D-03
-1.0518D-03	7.2521D-04	3.7595D-04	5.1326D-05	5.6412D-04	-3.5734D-04
3.8115D-05	-4.7317D-04	4.0708D-04	5.2616D-04	5.5933D-04	-3.0414D-04
-7.5946D-04	-1.1258D-03	-8.6159D-05	8.0319D-04	-1.0427D-03	-7.4150D-04

Columns 7 thru 12

4.9201D-03	-3.8118D-03	1.5341D-02	-1.9922D-02	3.7168D-03	-5.5175D-03
2.6861D-03	1.1287D-03	-8.8118D-04	8.3928D-03	9.8314D-04	2.3411D-03
2.2043D-03	3.6813D-03	-1.0794D-02	-3.4214D-03	-3.8192D-03	-2.5098D-03
-1.2176D-03	-7.5855D-04	-3.1609D-04	2.6599D-03	-4.6071D-04	3.4083D-03
-2.8657D-03	1.3455D-03	1.1557D-03	-4.0799D-04	1.6316D-03	-3.1526D-04
-1.1559D-03	-2.8596D-03	-1.9489D-03	-7.2251D-04	-3.0709D-03	-8.5277D-04
1.1768D-04	8.6878D-04	1.1875D-04	-6.3526D-04	-8.2110D-04	-9.2793D-05
1.0808D-03	-4.0698D-04	4.2411D-04	-2.7676D-04	-4.1586D-04	1.2428D-03
-3.5522D-04	3.0468D-04	-2.8550D-04	7.1359D-04	1.2431D-04	-5.5212D-04
-3.7277D-04	-1.3131D-04	-9.2781D-04	-7.8434D-04	9.9283D-04	8.2761D-04
-8.6180D-04	-9.1350D-04	5.2437D-04	-7.8544D-05	-8.0722D-05	1.2027D-05
8.7743D-05	-2.6812D-05	-1.1060D-05	2.1460D-05	4.8146D-05	-1.0835D-04
9.3909D-05	-2.4455D-05	6.2668D-05	-5.9120D-05	-1.1855D-04	1.4133D-04
-2.3772D-04	2.7665D-04	6.4987D-05	-5.6053D-05	-2.3274D-04	1.7358D-04
-1.9699D-04	2.1238D-04	5.1867D-05	-4.6325D-05	-1.9484D-04	1.7199D-04
-1.9282D-04	-1.9296D-04	-2.9253D-04	-2.5300D-04	-1.8382D-04	-1.8425D-04
2.6394D-04	-2.7531D-04	8.9817D-04	1.6178D-03	-1.9306D-05	5.1470D-05
-9.2309D-05	5.5113D-05	1.9833D-03	-1.4359D-03	2.5834D-04	-2.5279D-04
-1.5479D-02	1.0920D-02	-3.6183D-02	5.4460D-02	-1.0708D-02	1.8088D-02

-2.0904D-02	-4.7952D-03	1.8468D-02	-4.6623D-02	3.0121D-03	-1.5209D-02
-4.0749D-03	-2.4557D-02	6.3126D-02	2.0232D-02	2.4629D-02	1.1589D-02
3.5939D-02	-7.0070D-04	9.8047D-03	-3.9005D-02	1.1815D-02	-5.2862D-02
5.3015D-02	-4.9947D-02	-3.5264D-02	3.0894D-02	-5.5205D-02	4.4546D-02
-2.6130D-02	-5.7174D-02	-3.9809D-02	-1.9007D-02	-7.0204D-02	-2.2761D-02
5.4638D-02	-5.1953D-02	4.6154D-03	-1.2825D-02	3.6461D-02	-6.7366D-02
4.6766D-02	5.8877D-03	3.2776D-02	1.4001D-02	3.7584D-02	4.9023D-02
-4.9868D-02	-5.8560D-02	2.7890D-02	4.4393D-02	5.0325D-02	4.0695D-02
3.1240D-02	3.2968D-02	3.3092D-02	2.3553D-02	1.2023D-02	1.8842D-02
5.8053D-02	-5.3442D-04	-8.9602D-03	-5.0732D-03	-2.5531D-02	4.8057D-02
-1.9617D-03	-6.4951D-02	-2.5194D-02	-2.2010D-02	5.4046D-02	2.5852D-02
2.3636D-03	8.5026D-03	1.3410D-02	1.6100D-02	-1.2703D-02	-1.7926D-02
1.6640D-02	1.6639D-02	1.2057D-02	-1.5039D-02	1.9314D-03	4.9999D-04
-3.1811D-05	6.7767D-03	6.1005D-03	-3.4448D-04	-2.9321D-03	-8.5054D-04
-7.7113D-03	4.7632D-04	1.3566D-02	1.0552D-02	-2.1809D-03	-2.3599D-02
1.0716D-02	2.4738D-02	1.4024D-02	6.5963D-03	-1.0523D-02	-1.1844D-02
1.2601D-03	2.0376D-03	2.1235D-02	-2.6720D-02	3.8753D-02	-3.4446D-02
-2.5801D-02	1.9450D-02	-5.4075D-03	-1.4896D-03	9.3353D-03	-1.6482D-04
-3.9184D-03	-6.0208D-03	-2.9935D-03	-5.0448D-03	6.6600D-05	9.7224D-03
6.7680D-03	5.3640D-03	-9.4342D-03	1.3848D-02	-4.2610D-02	3.8245D-02
-5.2154D-02	4.9477D-02	1.1755D-03	3.1170D-03	-5.5203D-03	4.7052D-04
-9.2103D-03	-8.3751D-03	5.6647D-03	5.5019D-03	-7.3972D-03	-8.4551D-03
-6.0769D-04	1.5969D-03	2.8370D-04	-5.5777D-05	-7.2205D-04	-8.3767D-04
-1.8699D-03	3.3272D-04	-5.9762D-04	8.2594D-04	7.9599D-04	-1.4161D-03
1.3273D-03	1.1594D-03	-4.3420D-04	-1.1894D-03	4.6274D-04	1.5820D-03

Columns 13 thru 18

-1.7012D-03	-9.3260D-05	1.0002D-03	1.7186D-03	4.3424D-05	-9.5038D-04
-3.8429D-04	-5.5845D-03	-5.2358D-03	3.2831D-04	5.6523D-03	5.3340D-03
-6.1782D-03	-2.9594D-03	3.4337D-03	6.1818D-03	2.8427D-03	-3.2773D-03
-5.5292D-04	-5.1681D-04	-3.1398D-04	4.5266D-04	5.0638D-04	-2.7944D-04
-2.5868D-04	6.7995D-04	7.9327D-04	3.1171D-04	-9.1301D-05	-5.3576D-04
4.1930D-04	1.0557D-04	7.1248D-05	4.2165D-04	4.8722D-04	4.4675D-04
1.6346D-04	3.2379D-04	-3.2964D-04	-1.7693D-04	1.0339D-04	-1.0672D-04
2.4226D-04	-2.1807D-05	-9.6626D-06	2.3124D-04	-2.9392D-04	-3.0520D-04
-1.3176D-04	-2.1414D-05	-6.9406D-05	-1.5084D-04	8.9133D-05	8.5253D-05
-4.0261D-05	-1.9072D-05	6.0886D-05	1.7865D-05	4.8771D-05	6.2876D-05
-5.9409D-05	-7.2264D-05	1.2593D-05	2.2427D-07	-2.6634D-05	-8.2893D-06
-1.6550D-05	-4.3894D-04	3.4886D-04	2.0442D-04	-6.3242D-04	5.3487D-04
-5.5168D-04	1.5326D-04	4.0531D-04	-6.0181D-04	2.2397D-04	3.6730D-04
3.8851D-04	-4.9281D-04	4.1770D-04	-2.3769D-04	1.3320D-04	-2.0966D-04
-1.2550D-04	1.1386D-04	-1.2055D-04	1.3840D-04	-1.5012D-04	1.4322D-04
-1.9485D-03	-1.9305D-03	-1.9310D-03	-1.9501D-03	-1.9653D-03	-1.9647D-03
-2.6466D-03	8.9418D-04	3.2011D-03	2.4237D-03	-5.0838D-04	-3.2828D-03
-2.1601D-03	-3.3199D-03	-1.2433D-03	2.4035D-03	3.3576D-03	8.6619D-04
4.9675D-03	4.1142D-04	-3.2624D-03	-5.0311D-03	-1.8783D-04	3.0714D-03
5.3365D-03	2.2522D-02	1.7317D-02	-4.7915D-03	-2.2660D-02	-1.7881D-02

2.2858D-02	8.0833D-03	-1.6079D-02	-2.2940D-02	-7.3308D-03	1.5294D-02
-1.3726D-02	-1.5007D-02	1.3411D-02	1.1380D-02	6.8362D-04	2.4165D-03
7.6959D-03	4.0665D-03	8.3214D-03	1.0959D-02	-1.3555D-02	-1.3353D-02
3.2595D-03	2.8205D-03	4.3776D-04	3.2862D-04	-1.1777D-02	-1.1901D-02
-6.6266D-03	-2.3430D-03	3.5147D-05	5.4491D-03	-3.4526D-03	3.2830D-03
9.8636D-03	1.1290D-02	1.7904D-02	1.7890D-02	-2.2044D-02	-2.1434D-02
-2.4487D-02	-2.5193D-02	1.8937D-02	1.8385D-02	4.0536D-05	1.1628D-03
4.5715D-04	-2.2726D-04	-9.5629D-03	-8.3652D-03	-1.2097D-02	-1.3244D-02
-2.1008D-02	-1.6700D-02	-4.0795D-03	-1.0332D-02	2.4935D-02	2.7186D-02
1.6401D-02	2.2081D-02	-2.7369D-02	-2.3954D-02	9.8421D-03	3.3597D-03
1.5669D-02	-2.3007D-02	2.1295D-02	2.4860D-02	-1.9935D-02	5.8940D-03
-3.2900D-02	-1.4509D-02	1.5507D-02	-2.5540D-02	-7.9550D-04	1.9731D-02
-1.2863D-02	2.0993D-03	5.0104D-03	1.0298D-02	-9.1220D-03	5.4007D-03
2.1983D-02	-2.7378D-02	-2.7878D-02	1.3120D-02	-2.2741D-03	2.1467D-02
1.9545D-02	9.3887D-04	1.7005D-02	-3.0371D-02	-2.7171D-02	1.8647D-02
-1.8161D-02	2.4834D-02	-4.4263D-03	7.6056D-03	-2.0355D-02	1.4732D-02
4.7143D-03	-4.2384D-03	1.8724D-02	-1.7029D-02	2.6571D-02	-2.2161D-02
-2.6158D-02	3.0840D-02	-3.0629D-02	2.4043D-02	-6.5227D-03	8.2216D-03
-2.2580D-02	1.6228D-02	-5.3793D-03	5.0253D-03	-2.2296D-02	2.9862D-02
-8.3785D-03	7.1815D-03	-1.5479D-02	2.3383D-02	-2.0225D-02	1.2444D-02
-6.2874D-03	-1.1546D-02	-9.7670D-03	-7.4707D-03	-6.8103D-03	-1.0963D-02
-5.8000D-03	2.3293D-02	-1.8599D-02	-6.6058D-03	2.4297D-02	-1.6536D-02
-2.3395D-02	4.6713D-03	1.6299D-02	-2.3074D-02	6.7683D-03	1.8804D-02
-4.9849D-03	4.3860D-03	6.2581D-03	-6.3385D-03	-4.6669D-03	-5.4971D-03

Columns 19 thru 24

1.5603D-01	-1.4520D-01	4.0524D-02	-3.6424D-02	1.3412D-01	-1.1285D-01
-1.3264D-01	-1.5707D-01	-6.2669D-02	-6.8125D-02	1.5417D-01	-9.2965D-03
8.2740D-02	-7.0780D-02	1.1563D-02	-6.1740D-03	4.4048D-02	1.8464D-01
1.3249D-01	-2.9342D-02	2.1577D-01	-5.4134D-02	-4.8481D-02	-3.2202D-02
-3.5286D-02	-1.2357D-01	-5.5939D-02	-2.1346D-01	-1.3736D-01	5.9746D-02
-3.5855D-02	-4.4779D-02	-5.1081D-02	-8.0190D-02	-6.1813D-02	-1.3288D-01
-1.2513D-01	1.0758D-01	1.7354D-01	-1.5356D-01	9.1813D-02	-3.1206D-03
4.0396D-02	5.3038D-02	-1.4434D-01	-1.3537D-01	-1.6003D-02	7.1901D-02
1.7239D-01	1.7169D-01	-1.1490D-01	-1.3471D-01	1.0529D-01	-5.9018D-02
-5.3726D-02	6.1652D-02	-1.3064D-02	-1.5187D-02	7.3432D-02	-7.5768D-02
-2.8792D-02	5.7011D-02	1.3726D-02	1.4542D-02	1.5319D-01	1.8466D-01
-2.4451D-02	2.4146D-02	6.1809D-02	-5.9457D-02	-4.0747D-03	-2.2106D-03
-7.7783D-04	7.5763D-04	-1.2970D-02	-1.0478D-02	-1.5371D-02	1.1253D-02
1.2212D-02	-1.1369D-02	-4.5808D-02	5.2406D-02	3.0873D-02	-3.2326D-02
2.5733D-02	-2.5458D-02	-9.5160D-02	9.9337D-02	3.6202D-02	-3.7092D-02
2.0625D-02	2.1145D-02	1.2499D-02	1.2473D-02	1.9955D-02	2.2065D-02
1.0641D-01	-2.2602D-02	8.2650D-03	-7.7256D-03	-6.7594D-02	1.1125D-01
1.1532D-02	-1.0546D-01	7.2703D-03	-8.0877D-03	9.4793D-02	3.7864D-02
6.3653D-02	-5.7073D-02	1.9669D-02	-1.7089D-02	5.1373D-02	-3.8870D-02
-2.4776D-02	-3.7998D-02	-1.1614D-02	-1.5336D-02	3.9903D-02	1.2755D-03
2.2509D-02	-1.0345D-02	6.6454D-03	-1.3901D-03	-7.3510D-04	4.5128D-02

5.5290D-03	-4.2246D-03	9.2255D-03	-7.4170D-03	-3.1258D-03	2.2068D-04
-2.3137D-03	-3.5873D-03	-3.7042D-03	-6.2773D-03	-4.2349D-03	3.7223D-03
2.9761D-03	2.9522D-03	4.7343D-03	4.9542D-03	1.8041D-03	3.2869D-03
-3.4710D-04	-2.8144D-04	-3.5380D-03	2.6491D-03	-1.0739D-03	1.0300D-03
2.3437D-03	2.5094D-03	3.0343D-03	3.4870D-03	-3.5130D-04	-1.3999D-03
-1.5089D-03	4.2695D-04	1.7965D-04	-9.4585D-04	2.3721D-03	1.6270D-03
-1.0731D-03	-1.3657D-03	2.0428D-05	-9.3083D-05	-2.1590D-03	-2.2779D-03
-1.3614D-03	-1.5557D-03	1.4096D-03	2.2257D-03	4.3930D-04	8.1229D-04
-5.0904D-04	-1.6587D-04	1.8455D-03	-1.0472D-03	-6.7372D-04	-5.5359D-04
2.4303D-04	-9.7747D-05	7.1578D-05	-2.3233D-04	-6.6387D-05	2.1243D-04
-1.9183D-05	-2.0096D-04	1.7546D-04	5.4961D-05	2.8955D-04	1.0191D-04
-2.4392D-04	2.4058D-04	-5.3794D-04	5.5510D-04	-5.6879D-06	9.1322D-05
1.1025D-04	1.3766D-04	-1.9454D-04	-7.6610D-05	-1.0660D-04	3.3486D-05
1.0400D-05	-7.8772D-05	9.2468D-06	6.7664D-05	1.9862D-04	1.4308D-04
-3.8461D-05	-7.5327D-06	8.8416D-05	-2.7108D-05	-2.2092D-05	2.8211D-05
3.4887D-06	-1.1572D-05	3.9752D-06	2.4194D-05	1.6079D-04	-2.3360D-04
1.1886D-05	-2.1191D-05	2.0391D-04	-1.9550D-04	-6.2824D-05	-1.0727D-05
-2.5203D-05	-2.1204D-05	3.9090D-05	1.7932D-05	2.0915D-05	8.4498D-05
1.5489D-05	3.7594D-05	-4.5558D-06	-5.0876D-05	1.5638D-04	-1.8872D-04
-3.9983D-05	-3.8632D-05	4.8221D-05	4.5439D-05	-4.4126D-05	-4.3544D-05
6.5394D-06	-4.5087D-06	-2.3374D-06	-3.1912D-07	-3.5072D-06	2.2218D-06
-2.3677D-07	2.9394D-06	-2.5288D-06	-3.2685D-06	-3.4746D-06	1.8894D-06
3.7081D-06	5.4969D-06	4.2067D-07	-3.9216D-06	5.0907D-06	3.6203D-06

Columns 25 thru 30

3.6863D-02	-2.8560D-02	1.1494D-01	-1.4926D-01	2.7847D-02	-4.1339D-02
4.4745D-02	1.8802D-02	-1.4679D-02	1.3981D-01	1.6377D-02	3.8998D-02
3.7945D-02	6.3370D-02	-1.8582D-01	-5.8897D-02	-6.5745D-02	-4.3205D-02
-6.7065D-02	-4.1779D-02	-1.7409D-02	1.4650D-01	-2.5375D-02	1.8772D-01
-1.6302D-01	7.6542D-02	6.5745D-02	-2.3209D-02	9.2813D-02	-1.7934D-02
-7.5288D-02	-1.8626D-01	-1.2694D-01	-4.7061D-02	-2.0002D-01	-5.5545D-02
1.7813D-02	1.3151D-01	1.7976D-02	-9.6160D-02	-1.2429D-01	-1.4046D-02
1.7065D-01	-6.4261D-02	6.6966D-02	-4.3699D-02	-6.5664D-02	1.9623D-01
-6.0147D-02	5.1590D-02	-4.8343D-02	1.2083D-01	2.1049D-02	-9.3488D-02
-7.1196D-02	-2.5080D-02	-1.7721D-01	-1.4980D-01	1.8962D-01	1.5807D-01
-1.7481D-01	-1.8529D-01	1.0636D-01	-1.5932D-02	-1.6373D-02	2.4394D-03
3.0722D-02	-9.3877D-03	-3.8726D-03	7.5139D-03	1.6857D-02	-3.7937D-02
3.3484D-02	-8.7194D-03	2.2345D-02	-2.1080D-02	-4.2271D-02	5.0390D-02
-9.0421D-02	1.0523D-01	2.4719D-02	-2.1321D-02	-8.8529D-02	6.6023D-02
-1.3089D-01	1.4111D-01	3.4462D-02	-3.0780D-02	-1.2945D-01	1.1428D-01
1.4754D-02	1.4765D-02	2.2383D-02	1.9359D-02	1.4065D-02	1.4098D-02
-1.3885D-02	1.4483D-02	-4.7250D-02	-8.5107D-02	1.0156D-03	-2.7077D-03
4.8522D-03	-2.8970D-03	-1.0425D-01	7.5478D-02	-1.3579D-02	1.3288D-02
1.7170D-02	-1.2113D-02	4.0136D-02	-6.0410D-02	1.1878D-02	-2.0064D-02
1.4550D-02	3.3377D-03	-1.2855D-02	3.2452D-02	-2.0966D-03	1.0586D-02
2.7598D-03	1.6632D-02	-4.2753D-02	-1.3703D-02	-1.6680D-02	-7.8489D-03
-4.1071D-03	8.0075D-05	-1.1205D-03	4.4574D-03	-1.3503D-03	6.0410D-03

-5.5948D-03	5.2711D-03	3.7216D-03	-3.2603D-03	5.8260D-03	-4.7012D-03
2.4686D-03	5.4013D-03	3.7608D-03	1.7956D-03	6.6323D-03	2.1503D-03
-3.9069D-03	3.7149D-03	-3.3002D-04	9.1706D-04	-2.6071D-03	4.8170D-03
-3.1669D-03	-3.9870D-04	-2.2196D-03	-9.4813D-04	-2.5451D-03	-3.3197D-03
3.0411D-03	3.5713D-03	-1.7008D-03	-2.7073D-03	-3.0691D-03	-2.4818D-03
-1.6912D-03	-1.7848D-03	-1.7915D-03	-1.2751D-03	-6.5087D-04	-1.0200D-03
-2.5976D-03	2.3913D-05	4.0093D-04	2.2700D-04	1.1424D-03	-2.1503D-03
8.7247D-05	2.8888D-03	1.1205D-03	9.7893D-04	-2.4038D-03	-1.1498D-03
-2.8911D-05	-1.0400D-04	-1.6403D-04	-1.9693D-04	1.5538D-04	2.1927D-04
-2.0007D-04	-2.0007D-04	-1.4498D-04	1.8083D-04	-2.3223D-05	-6.0118D-06
3.5479D-07	-7.5576D-05	-6.8034D-05	3.8417D-06	3.2700D-05	9.4854D-06
8.0180D-05	-4.9527D-06	-1.4106D-04	-1.0972D-04	2.2677D-05	2.4538D-04
-1.0956D-04	-2.5293D-04	-1.4338D-04	-6.7442D-05	1.0759D-04	1.2109D-04
-1.2777D-05	-2.0660D-05	-2.1532D-04	2.7093D-04	-3.9294D-04	3.4927D-04
2.5634D-04	-1.9324D-04	5.3726D-05	1.4800D-05	-9.2750D-05	1.6375D-06
3.7561D-05	5.7714D-05	2.8695D-05	4.8359D-05	-6.3846D-07	-9.3197D-05
-6.3051D-05	-4.9971D-05	8.7889D-05	-1.2901D-04	3.9695D-04	-3.5629D-04
4.7280D-04	-4.4853D-04	-1.0656D-05	-2.8257D-05	5.0044D-05	-4.2654D-06
6.8169D-05	6.1987D-05	-4.1927D-05	-4.0722D-05	5.4750D-05	6.2580D-05
3.7781D-06	-9.9282D-06	-1.7638D-06	3.4681D-07	4.4890D-06	5.2079D-06
1.1616D-05	-2.0669D-06	3.7124D-06	-5.1307D-06	-4.9447D-06	8.7966D-06
-6.4806D-06	-5.6608D-06	2.1200D-06	5.8073D-06	-2.2593D-06	-7.7241D-06

Columns 31 thru 36

-1.2746D-02	-6.9874D-04	7.4938D-03	1.2877D-02	3.2535D-04	-7.1205D-03
-6.4015D-03	-9.3027D-02	-8.7218D-02	5.4689D-03	9.4157D-02	8.8854D-02
-1.0635D-01	-5.0943D-02	5.9108D-02	1.0642D-01	4.8936D-02	-5.6416D-02
-3.0454D-02	-2.8465D-02	-1.7293D-02	2.4932D-02	2.7890D-02	-1.5391D-02
-1.4715D-02	3.8679D-02	4.5126D-02	1.7732D-02	-5.1938D-03	-3.0477D-02
2.7311D-02	6.8763D-03	4.6408D-03	2.7464D-02	3.1735D-02	2.9099D-02
2.4743D-02	4.9012D-02	-4.9898D-02	-2.6782D-02	1.5650D-02	-1.6155D-02
3.8253D-02	-3.4432D-03	-1.5257D-03	3.6513D-02	-4.6409D-02	-4.8191D-02
-2.2310D-02	-3.6259D-03	-1.1752D-02	-2.5540D-02	1.5093D-02	1.4436D-02
-7.6896D-03	-3.6426D-03	1.1629D-02	3.4121D-03	9.3149D-03	1.2009D-02
-1.2050D-02	-1.4658D-02	2.5544D-03	4.5490D-05	-5.4024D-03	-1.6814D-03
-5.7948D-03	-1.5369D-01	1.2215D-01	7.1574D-02	-2.2143D-01	1.8727D-01
-1.9670D-01	5.4645D-02	1.4452D-01	-2.1458D-01	7.9858D-02	1.3096D-01
1.4778D-01	-1.8745D-01	1.5888D-01	-9.0411D-02	5.0666D-02	-7.9750D-02
-8.3387D-02	7.5656D-02	-8.0098D-02	9.1961D-02	-9.9745D-02	9.5159D-02
1.4909D-01	1.4771D-01	1.4775D-01	1.4921D-01	1.5037D-01	1.5033D-01
1.3923D-01	-4.7040D-02	-1.6840D-01	-1.2751D-01	2.6744D-02	1.7270D-01
1.1354D-01	1.7451D-01	6.5354D-02	-1.2634D-01	-1.7649D-01	-4.5531D-02
-5.5103D-03	-4.5638D-04	3.6189D-03	5.5808D-03	2.0835D-04	-3.4070D-03
-3.7145D-03	-1.5676D-02	-1.2053D-02	3.3351D-03	1.5772D-02	1.2446D-02
-1.5481D-02	-5.4746D-03	1.0890D-02	1.5537D-02	4.9650D-03	-1.0358D-02
1.5686D-03	1.7150D-03	-1.5326D-03	-1.3005D-03	-7.8124D-05	-2.7616D-04
-8.1218D-04	-4.2915D-04	-8.7818D-04	-1.1565D-03	1.4305D-03	1.4092D-03



-3.0793D-04	-2.6645D-04	-4.1356D-05	-3.1046D-05	1.1126D-03	1.1243D-03
4.7384D-04	1.6753D-04	-2.5132D-06	-3.8964D-04	2.4688D-04	-2.3476D-04
-6.6795D-04	-7.6451D-04	-1.2124D-03	-1.2115D-03	1.4928D-03	1.4515D-03
1.4933D-03	1.5364D-03	-1.1549D-03	-1.1212D-03	-2.4721D-06	-7.0911D-05
-2.4748D-05	1.2303D-05	5.1769D-04	4.5285D-04	6.5489D-04	7.1695D-04
9.4000D-04	7.4724D-04	1.8254D-04	4.6232D-04	-1.1157D-03	-1.2165D-03
-7.2943D-04	-9.8206D-04	1.2173D-03	1.0654D-03	-4.3774D-04	-1.4943D-04
-1.9166D-04	2.8142D-04	-2.6048D-04	-3.0408D-04	2.4384D-04	-7.2095D-05
3.9559D-04	1.7446D-04	-1.8646D-04	3.0709D-04	9.5650D-06	-2.3724D-04
1.4345D-04	-2.3412D-05	-5.5878D-05	-1.1485D-04	1.0173D-04	-6.0230D-05
-2.2857D-04	2.8468D-04	2.8987D-04	-1.3642D-04	2.3645D-05	-2.2321D-04
-1.9983D-04	-9.5992D-06	-1.7386D-04	3.1053D-04	2.7780D-04	-1.9065D-04
1.8414D-04	-2.5181D-04	4.4881D-05	-7.7118D-05	2.0639D-04	-1.4938D-04
-4.6838D-05	4.2110D-05	-1.8603D-04	1.6919D-04	-2.6399D-04	2.2018D-04
2.5074D-04	-2.9563D-04	2.9361D-04	-2.3048D-04	6.2526D-05	-7.8811D-05
2.1036D-04	-1.5118D-04	5.0114D-05	-4.6816D-05	2.0771D-04	-2.7819D-04
7.5954D-05	-6.5103D-05	1.4032D-04	-2.1197D-04	1.8334D-04	-1.1281D-04
4.6535D-05	8.5456D-05	7.2290D-05	5.5294D-05	5.0406D-05	8.1144D-05
3.6059D-05	-1.4482D-04	1.1563D-04	4.1069D-05	-1.5106D-04	1.0281D-04
1.4533D-04	-2.9018D-05	-1.0125D-04	1.4333D-04	-4.2045D-05	-1.1681D-04
2.4339D-05	-2.1414D-05	-3.0555D-05	3.0948D-05	2.2786D-05	2.6839D-05

$G_f =$

Columns 1 thru 6

-1.8280D-02	-1.5537D-02	-1.1224D-03	1.4389D-03	-5.0311D-04	1.8313D-03
-3.3036D-04	4.3229D-04	1.3378D-03	-5.3114D-03	-5.2584D-03	3.0946D-03
1.8050D-03	9.3150D-04	-3.6901D-03	2.9605D-04	1.9551D-04	4.2035D-03
1.5137D-03	6.1015D-04	-4.4760D-04	-4.1444D-04	-5.1397D-04	6.7384D-04
8.4810D-04	-7.5246D-04	-1.1619D-04	9.3173D-04	6.8291D-04	1.3652D-04
1.3335D-04	6.3630D-04	6.3179D-04	2.7081D-05	-2.7486D-05	6.1166D-04
8.4899D-04	2.4283D-05	-2.8836D-05	2.7510D-04	-2.7479D-04	2.6505D-04
-5.7104D-05	9.6007D-04	-1.5845D-05	-4.5929D-04	-4.5851D-04	3.9169D-04
1.1360D-04	-2.2933D-04	9.4218D-05	1.4193D-04	-7.1689D-06	4.1344D-05
-3.2285D-04	-5.3640D-05	-1.4557D-04	-1.4642D-04	8.4966D-05	-4.4882D-05
-2.6272D-04	-1.2639D-04	6.1544D-05	3.2932D-07	1.8993D-04	-7.4053D-05
-1.3169D-04	1.3235D-04	9.9466D-05	1.4102D-04	-1.7967D-04	8.1487D-06
-6.6143D-05	-2.1002D-04	-2.2381D-05	1.0040D-04	1.2230D-04	-9.0157D-05
-2.2202D-04	-1.9204D-04	2.1722D-05	-2.6375D-04	2.5034D-04	-3.1820D-04
-2.1563D-04	-2.5924D-04	-1.0790D-05	-4.2934D-04	4.3463D-04	-4.6306D-04
-3.5058D-08	-5.6082D-05	-2.4212D-03	-2.1020D-03	-2.0687D-03	-2.1308D-03
5.5851D-03	-5.0089D-03	-1.3024D-03	2.2881D-03	2.3172D-03	1.2434D-03
5.0345D-03	5.5709D-03	-4.8792D-04	-2.7823D-03	-2.3254D-03	3.3225D-03
5.2296D-02	4.1093D-02	3.8289D-03	-2.2949D-03	-3.7316D-04	-3.4666D-03
5.2799D-03	1.7393D-02	-3.2174D-03	1.8195D-02	1.7853D-02	-1.2117D-02
4.8303D-03	-1.2800D-02	1.7510D-02	-3.0833D-03	-4.2590D-03	-1.3429D-02
-2.2675D-02	-6.7205D-03	3.0855D-03	-3.7516D-04	2.0441D-03	-2.4917D-03

-4.7464D-03	9.1332D-03	-1.2044D-03	-6.6510D-03	-2.1659D-03	1.0915D-03
-2.2464D-04	7.2323D-03	1.4954D-02	5.6789D-03	2.4521D-03	6.9536D-03
3.7347D-02	3.1894D-02	5.4341D-03	1.1129D-03	-1.1298D-03	1.0926D-03
1.5943D-03	2.6161D-02	-1.0601D-02	-3.2449D-03	-1.1734D-03	-2.1584D-03
-1.9238D-02	-1.3227D-03	3.6104D-03	1.1313D-03	3.5036D-03	2.9780D-03
2.5891D-03	3.4970D-03	2.1627D-02	1.1031D-02	5.8993D-03	1.2133D-02
1.5934D-03	2.5785D-03	-3.2993D-03	1.2767D-02	7.2188D-03	-1.1110D-02
1.0402D-03	4.5475D-03	-2.0724D-02	4.4089D-03	7.1555D-05	9.8260D-03
-2.0122D-03	6.9568D-04	-1.1229D-02	4.3506D-03	-2.4326D-03	-4.2653D-04
-2.7503D-03	-4.1351D-03	-6.8443D-04	-1.3813D-03	-3.7212D-04	5.3549D-03
2.2722D-03	5.9060D-03	-9.6330D-03	-3.7643D-05	-4.5177D-03	5.2239D-03
-1.7519D-03	-2.3217D-04	-1.1224D-02	-6.5433D-03	8.5614D-03	5.1610D-03
1.0617D-02	6.6949D-03	1.0134D-03	4.9744D-03	1.8230D-03	-1.7626D-03
-6.2577D-03	-1.9252D-03	3.5488D-03	1.6494D-03	9.0410D-03	4.4540D-03
4.6578D-03	-1.1673D-03	3.9286D-03	-6.5141D-03	5.7837D-03	7.5515D-03
-5.2549D-03	-4.0025D-03	-2.1910D-03	6.2756D-03	2.7092D-03	1.6285D-03

Columns 7 thru 9

-9.5681D-05	-3.2239D-04	-2.1956D-03
2.7210D-03	2.3118D-03	2.4773D-03
4.4897D-03	-4.8030D-03	-4.3820D-03
5.9283D-04	-6.1756D-04	-4.4520D-04
1.7956D-04	-5.0532D-04	-4.9778D-04
4.4169D-04	4.6014D-04	4.4833D-04
3.7162D-04	-3.4507D-04	-3.1373D-04
2.0805D-05	-2.5979D-05	4.7634D-04
1.5244D-05	-2.5379D-05	-3.5379D-05
-2.1365D-04	9.6810D-05	1.3298D-04
-1.3968D-04	1.8260D-04	-1.5294D-06
-2.1712D-04	2.7566D-04	-7.6514D-06
-5.8976D-05	-1.1671D-04	3.4812D-05
3.0973D-04	-2.9216D-04	2.7320D-04
4.9531D-04	-5.1685D-04	4.0186D-04
-2.0964D-03	-2.1347D-03	-2.0926D-03
8.7809D-04	-3.5178D-03	-3.1213D-03
3.1234D-03	-6.2041D-04	-8.4161D-04
-1.2554D-03	2.6322D-03	4.6564D-03
-1.2472D-02	-5.9733D-03	-5.2023D-03
-1.3443D-02	1.7296D-02	1.6903D-02
-1.1394D-03	3.4854D-03	5.1447D-05
-1.0495D-03	4.3897D-04	1.7283D-03
1.6882D-03	6.0275D-03	3.2930D-03
-1.6490D-03	4.4095D-03	-2.4967D-04
-3.8635D-03	-4.9765D-03	-6.6584D-04
-1.5028D-04	4.6528D-03	1.4277D-03
7.8880D-03	1.0233D-02	7.4263D-03
-4.6739D-03	-2.5773D-03	-3.3175D-03

6.5625D-03	-1.4220D-02	-7.4552D-03
2.6501D-03	-4.5168D-03	4.5302D-04
-4.1506D-04	-2.7127D-03	2.2157D-03
-5.5434D-03	-6.5287D-03	7.1117D-03
-4.2874D-03	2.4277D-03	-1.8026D-03
-5.9643D-03	-1.5029D-03	2.4428D-03
-5.5117D-03	-7.4657D-03	-1.3036D-03
1.8921D-03	7.6153D-04	-1.0825D-02
-9.2231D-03	-5.2204D-03	5.7108D-03

$C_f =$

Columns 1 thru 6

2.0825D-02	-7.9624D-03	4.8065D-03	2.4055D-03	-6.2029D-04	-5.5048D-04
-1.9380D-02	-9.4290D-03	-4.1117D-03	-5.3274D-04	-2.1723D-03	-6.8749D-04
5.4088D-03	-3.7621D-03	6.7170D-04	3.9175D-03	-9.8336D-04	-7.8423D-04
-4.8615D-03	-4.0896D-03	-3.5865D-04	-9.8286D-04	-3.7525D-03	-1.2311D-03
1.7901D-02	9.2551D-03	2.5588D-03	-8.8023D-04	-2.4147D-03	-9.4900D-04
-1.5062D-02	-5.5808D-04	1.0726D-02	-5.8466D-04	1.0503D-03	-2.0401D-03
4.9201D-03	2.6861D-03	2.2043D-03	-1.2176D-03	-2.8657D-03	-1.1559D-03
-3.8118D-03	1.1287D-03	3.6813D-03	-7.5855D-04	1.3455D-03	-2.8596D-03
1.5341D-02	-8.8118D-04	-1.0794D-02	-3.1609D-04	1.1557D-03	-1.9489D-03
-1.9922D-02	8.3928D-03	-3.4214D-03	2.6599D-03	-4.0799D-04	-7.2251D-04
3.7168D-03	9.8314D-04	-3.8192D-03	-4.6071D-04	1.6316D-03	-3.0709D-03
-5.5175D-03	2.3411D-03	-2.5098D-03	3.4083D-03	-3.1526D-04	-8.5277D-04
-1.7012D-03	-3.8429D-04	-6.1782D-03	-5.5292D-04	-2.5868D-04	4.1930D-04
-9.3260D-05	-5.5845D-03	-2.9594D-03	-5.1681D-04	6.7995D-04	1.0557D-04
1.0002D-03	-5.2358D-03	3.4337D-03	-3.1398D-04	7.9327D-04	7.1248D-05
1.7186D-03	3.2831D-04	6.1818D-03	4.5266D-04	3.1171D-04	4.2165D-04
4.3424D-05	5.6523D-03	2.8427D-03	5.0638D-04	-9.1301D-05	4.8722D-04
-9.5038D-04	5.3340D-03	-3.2773D-03	-2.7944D-04	-5.3576D-04	4.4675D-04
1.5603D-01	-1.3264D-01	8.2740D-02	1.3249D-01	-3.5286D-02	-3.5855D-02
-1.4520D-01	-1.5707D-01	-7.0780D-02	-2.9342D-02	-1.2357D-01	-4.4779D-02
4.0524D-02	-6.2669D-02	1.1563D-02	2.1577D-01	-5.5939D-02	-5.1081D-02
-3.6424D-02	-6.8125D-02	-6.1740D-03	-5.4134D-02	-2.1346D-01	-8.0190D-02
1.3412D-01	1.5417D-01	4.4048D-02	-4.8481D-02	-1.3736D-01	-6.1813D-02
-1.1285D-01	-9.2965D-03	1.8464D-01	-3.2202D-02	5.9746D-02	-1.3288D-01
3.6863D-02	4.4745D-02	3.7945D-02	-6.7065D-02	-1.6302D-01	-7.5288D-02
-2.8560D-02	1.8802D-02	6.3370D-02	-4.1779D-02	7.6542D-02	-1.8626D-01
1.1494D-01	-1.4679D-02	-1.8582D-01	-1.7409D-02	6.5745D-02	-1.2694D-01
-1.4926D-01	1.3981D-01	-5.8897D-02	1.4650D-01	-2.3209D-02	-4.7061D-02
2.7847D-02	1.6377D-02	-6.5745D-02	-2.5375D-02	9.2813D-02	-2.0002D-01
-4.1339D-02	3.8998D-02	-4.3205D-02	1.8772D-01	-1.7934D-02	-5.5545D-02
-1.2746D-02	-6.4015D-03	-1.0635D-01	-3.0454D-02	-1.4715D-02	2.7311D-02
-6.9874D-04	-9.3027D-02	-5.0943D-02	-2.8465D-02	3.8679D-02	6.8763D-03
7.4938D-03	-8.7218D-02	5.9108D-02	-1.7293D-02	4.5126D-02	4.6408D-03
1.2877D-02	5.4689D-03	1.0642D-01	2.4932D-02	1.7732D-02	2.7464D-02

3.2535D-04	9.4157D-02	4.8936D-02	2.7890D-02	5.1938D-03	3.1735D-02
-7.1205D-03	8.8854D-02	-5.6416D-02	-1.5391D-02	-3.0477D-02	2.9099D-02

Columns 7 thru 12

-8.2665D-04	2.5584D-04	1.0181D-03	-2.8130D-04	-1.4195D-04	-6.9834D-05
7.1069D-04	3.3590D-04	1.0139D-03	3.2280D-04	2.8107D-04	6.8963D-05
1.1465D-03	-9.1416D-04	-6.7856D-04	-6.8399D-05	6.7669D-05	1.7653D-04
-1.0145D-03	-8.5733D-04	-7.9555D-04	-7.9516D-05	7.1693D-05	-1.6981D-04
6.0654D-04	-1.0135D-04	6.2180D-04	3.8447D-04	7.5526D-04	-1.1638D-05
-2.0616D-05	4.5536D-04	-3.4855D-04	-3.9670D-04	9.1037D-04	-6.3135D-06
1.1768D-04	1.0808D-03	-3.5522D-04	-3.7277D-04	-8.6180D-04	8.7743D-05
8.6878D-04	-4.0698D-04	3.0468D-04	-1.3131D-04	-9.1350D-04	-2.6812D-05
1.1875D-04	4.2411D-04	-2.8550D-04	-9.2781D-04	5.2437D-04	-1.1060D-05
-6.3526D-04	-2.7676D-04	7.1359D-04	-7.8434D-04	-7.8544D-05	2.1460D-05
-8.2110D-04	-4.1586D-04	1.2431D-04	9.9283D-04	-8.0722D-05	4.8146D-05
-9.2793D-05	1.2428D-03	-5.5212D-04	8.2761D-04	1.2027D-05	-1.0835D-04
1.6346D-04	2.4226D-04	-1.3176D-04	-4.0261D-05	-5.9409D-05	-1.6550D-05
3.2379D-04	-2.1807D-05	-2.1414D-05	-1.9072D-05	-7.2264D-05	-4.3894D-04
-3.2964D-04	-9.6626D-06	-6.9406D-05	6.0886D-05	1.2593D-05	3.4886D-04
-1.7693D-04	2.3124D-04	-1.5084D-04	1.7865D-05	2.2427D-07	2.0442D-04
1.0339D-04	-2.9392D-04	8.9133D-05	4.8771D-05	-2.6634D-05	-6.3242D-04
-1.0672D-04	-3.0520D-04	8.5253D-05	6.2876D-05	-8.2893D-06	5.3487D-04
-1.2513D-01	4.0396D-02	1.7239D-01	-5.3726D-02	-2.8792D-02	-2.4451D-02
1.0758D-01	5.3038D-02	1.7169D-01	6.1652D-02	5.7011D-02	2.4146D-02
1.7354D-01	-1.4434D-01	-1.1490D-01	-1.3064D-02	1.3726D-02	6.1809D-02
-1.5356D-01	-1.3537D-01	-1.3471D-01	-1.5187D-02	1.4542D-02	-5.9457D-02
9.1813D-02	-1.6003D-02	1.0529D-01	7.3432D-02	1.5319D-01	-4.0747D-03
-3.1206D-03	7.1901D-02	-5.9018D-02	-7.5768D-02	1.8466D-01	-2.2106D-03
1.7813D-02	1.7065D-01	-6.0147D-02	-7.1196D-02	-1.7481D-01	3.0722D-02
1.3151D-01	-6.4261D-02	5.1590D-02	-2.5080D-02	-1.8529D-01	-9.3877D-03
1.7976D-02	6.6966D-02	-4.8343D-02	-1.7721D-01	1.0636D-01	-3.8726D-03
-9.6160D-02	-4.3699D-02	1.2083D-01	-1.4980D-01	-1.5932D-02	7.5139D-03
-1.2429D-01	-6.5664D-02	2.1049D-02	1.8962D-01	-1.6373D-02	1.6857D-02
-1.4046D-02	1.9623D-01	-9.3488D-02	1.5807D-01	2.4394D-03	-3.7937D-02
2.4743D-02	3.8253D-02	-2.2310D-02	-7.6896D-03	-1.2050D-02	-5.7948D-03
4.9012D-02	-3.4432D-03	-3.6259D-03	-3.6426D-03	-1.4658D-02	-1.5369D-01
-4.9898D-02	-1.5257D-03	-1.1752D-02	1.1629D-02	2.5544D-03	1.2215D-01
-2.6782D-02	3.6513D-02	-2.5540D-02	3.4121D-03	4.5490D-05	7.1574D-02
1.5650D-02	-4.6409D-02	1.5093D-02	9.3149D-03	-5.4024D-03	-2.2143D-01
-1.6155D-02	-4.8191D-02	1.4436D-02	1.2009D-02	-1.6814D-03	1.8727D-01

Columns 13 thru 18

-2.1815D-06	3.2105D-05	3.8729D-05	-2.6955D-04	-2.0228D-03	-2.1939D-04
2.1249D-06	-2.9890D-05	-3.8316D-05	-2.7634D-04	4.2964D-04	2.0062D-03
-3.6374D-05	-1.2043D-04	-1.4322D-04	-1.6335D-04	-1.5711D-04	-1.3831D-04
-2.9386D-05	1.3778D-04	1.4951D-04	-1.6301D-04	1.4685D-04	1.5386D-04

-4.3108D-05	8.1165D-05	5.4485D-05	-2.6080D-04	1.2849D-03	-1.8034D-03
3.1560D-05	-8.4986D-05	-5.5825D-05	-2.8837D-04	-2.1148D-03	-7.2034D-04
9.3909D-05	-2.3772D-04	-1.9699D-04	-1.9282D-04	2.6394D-04	-9.2309D-05
-2.4455D-05	2.7665D-04	2.1238D-04	-1.9296D-04	-2.7531D-04	5.5113D-05
6.2668D-05	6.4987D-05	5.1867D-05	-2.9253D-04	8.9817D-04	1.9833D-03
-5.9120D-05	-5.6053D-05	-4.6325D-05	-2.5300D-04	1.6178D-03	-1.4359D-03
-1.1855D-04	-2.3274D-04	-1.9484D-04	-1.8382D-04	-1.9306D-05	2.5834D-04
1.4133D-04	1.7358D-04	1.7199D-04	-1.8425D-04	5.1470D-05	-2.5279D-04
-5.5168D-04	3.8851D-04	-1.2550D-04	-1.9485D-03	-2.6466D-03	-2.1601D-03
1.5326D-04	-4.9281D-04	1.1386D-04	-1.9305D-03	8.9418D-04	-3.3199D-03
4.0531D-04	4.1770D-04	-1.2055D-04	-1.9310D-03	3.2011D-03	-1.2433D-03
-6.0181D-04	-2.3769D-04	1.3840D-04	-1.9501D-03	2.4237D-03	2.4035D-03
2.2397D-04	1.3320D-04	-1.5012D-04	-1.9653D-03	-5.0838D-04	3.3576D-03
3.6730D-04	-2.0966D-04	1.4322D-04	-1.9647D-03	-3.2828D-03	8.6619D-04
-7.7783D-04	1.2212D-02	2.5733D-02	2.0625D-02	1.0641D-01	1.1532D-02
7.5763D-04	-1.1369D-02	-2.5458D-02	2.1145D-02	-2.2602D-02	-1.0546D-01
-1.2970D-02	-4.5808D-02	-9.5160D-02	1.2499D-02	8.2650D-03	7.2703D-03
-1.0478D-02	5.2406D-02	9.9337D-02	1.2473D-02	-7.7256D-03	-8.0877D-03
-1.5371D-02	3.0873D-02	3.6202D-02	1.9955D-02	-6.7594D-02	9.4793D-02
1.1253D-02	-3.2326D-02	-3.7092D-02	2.2065D-02	1.5D-01	3.7864D-02
3.3484D-02	-9.0421D-02	-1.3089D-01	1.4754D-02	1.5885D-02	4.8522D-03
-8.7194D-03	1.0523D-01	1.4111D-01	1.4765D-02	1.4483D-02	-2.8970D-03
2.2345D-02	2.4719D-02	3.4462D-02	2.2383D-02	-4.7250D-02	-1.0425D-01
-2.1080D-02	-2.1321D-02	-3.0780D-02	1.9359D-02	-8.5107D-02	7.5478D-02
-4.2271D-02	-8.8529D-02	-1.2945D-01	1.4065D-02	1.0156D-03	-1.3579D-02
5.0390D-02	6.6023D-02	1.1428D-01	1.4098D-02	-2.7077D-03	1.3288D-02
-1.9670D-01	1.4778D-01	-8.3387D-02	1.4909D-01	1.3923D-01	1.1354D-01
5.4645D-02	-1.8745D-01	7.5656D-02	1.4771D-01	-4.7040D-02	1.7451D-01
1.4452D-01	1.5888D-01	-8.0098D-02	1.4775D-01	-1.6840D-01	6.5354D-02
-2.1458D-01	-9.0411D-02	9.1961D-02	1.4921D-01	-1.2751D-01	-1.2634D-01
7.9858D-02	5.0666D-02	-9.9745D-02	1.5037D-01	2.6744D-02	-1.7649D-01
1.3096D-01	-7.9750D-02	9.5159D-02	1.5033D-01	1.7270D-01	-4.5531D-02

Columns 19 thru 24

-5.7383D-02	3.5596D-02	-3.3235D-02	-4.8382D-02	2.1924D-02	-3.1502D-02
5.1451D-02	5.4591D-02	1.5275D-02	3.6968D-02	3.3992D-02	-3.1249D-02
-1.7732D-02	1.6685D-02	-9.8121D-03	-8.0728D-02	3.5100D-02	-5.0113D-02
1.5406D-02	2.2033D-02	2.0525D-03	6.4903D-02	5.9481D-02	-5.2441D-02
-4.6313D-02	-5.7328D-02	1.0854D-03	2.7353D-02	4.0128D-02	-1.9097D-02
3.5042D-02	-1.8325D-03	-6.6632D-02	-1.9310D-03	-3.5271D-02	-3.4792D-02
-1.5479D-02	-2.0904D-02	-4.0749D-03	3.5939D-02	5.3015D-02	-2.6130D-02
1.0920D-02	-4.7952D-03	-2.4557D-02	-7.0070D-04	-4.9947D-02	-5.7174D-02
-3.6183D-02	1.8468D-02	6.3126D-02	9.8047D-03	-3.5264D-02	-3.9809D-02
5.4460D-02	-4.6623D-02	2.0232D-02	-3.9005D-02	3.0894D-02	-1.9007D-02
-1.0708D-02	3.0121D-03	2.4629D-02	1.1815D-02	-5.5205D-02	-7.0204D-02
1.8088D-02	-1.5209D-02	1.1589D-02	-5.2862D-02	4.4546D-02	-2.2761D-02
4.9675D-03	5.3365D-03	2.2858D-02	-1.3726D-02	7.6959D-03	3.2595D-03

4.1142D-04	2.2522D-02	8.0833D-03	-1.5007D-02	4.0665D-03	2.8205D-03
-3.2624D-03	1.7317D-02	-1.6079D-02	1.3411D-02	8.3214D-03	4.3776D-04
-5.0311D-03	-4.7915D-03	-2.2940D-02	1.1380D-02	1.0959D-02	3.2862D-04
-1.8783D-04	-2.2660D-02	-7.3308D-03	6.8362D-04	-1.3555D-02	-1.1777D-02
3.0714D-03	-1.7881D-02	1.5294D-02	2.4165D-03	-1.3353D-02	-1.1901D-02
6.3653D-02	-2.4776D-02	2.2509D-02	5.5290D-03	-2.3137D-03	2.9761D-03
-5.7073D-02	-3.7998D-02	-1.0345D-02	-4.2246D-03	-3.5873D-03	2.9522D-03
1.9669D-02	-1.1614D-02	6.6454D-03	9.2255D-03	-3.7042D-03	4.7343D-03
-1.7089D-02	-1.5336D-02	-1.3901D-03	-7.4170D-03	-6.2773D-03	4.9542D-03
5.1373D-02	3.9903D-02	-7.3510D-04	-3.1258D-03	-4.2349D-03	1.8041D-03
-3.8870D-02	1.2755D-03	4.5128D-02	2.2068D-04	3.7223D-03	3.2869D-03
1.7170D-02	1.4550D-02	2.7598D-03	-4.1071D-03	-5.5948D-03	2.4686D-03
-1.2113D-02	3.3377D-03	1.6632D-02	8.0075D-05	5.2711D-03	5.4013D-03
4.0136D-02	-1.2855D-02	-4.2753D-02	-1.1205D-03	3.7216D-03	3.7608D-03
-6.0410D-02	3.2452D-02	-1.3703D-02	4.4574D-03	-3.2603D-03	1.7956D-03
1.1878D-02	-2.0966D-03	-1.6680D-02	-1.3503D-03	5.8260D-03	6.6323D-03
-2.0064D-02	1.0586D-02	-7.8489D-03	6.0410D-03	-4.7012D-03	2.1503D-03
-5.5103D-03	-3.7145D-03	-1.5481D-02	1.5686D-03	-8.1218D-04	-3.0793D-04
-4.5638D-04	-1.5676D-02	-5.4746D-03	1.7150D-03	-4.2915D-04	-2.6645D-04
3.6189D-03	-1.2053D-02	1.0890D-02	-1.5326D-03	-8.7818D-04	-4.1356D-05
5.5808D-03	3.3351D-03	1.5537D-02	-1.3005D-03	-1.1565D-03	-3.1046D-05
2.0835D-04	1.5772D-02	4.9650D-03	-7.8124D-05	1.4305D-03	1.1126D-03
-3.4070D-03	1.2446D-02	-1.0358D-02	-2.7616D-04	1.4092D-03	1.1243D-03

Columns 25 thru 30

4.8542D-03	-3.4610D-02	2.4742D-02	1.9822D-02	3.0427D-02	1.1445D-02
3.9360D-03	-3.7056D-02	-7.0010D-03	2.5229D-02	3.4769D-02	3.7294D-03
4.9479D-02	-4.4808D-02	-2.9458D-03	-3.7735D-04	-3.1504D-02	-4.1495D-02
-3.7048D-02	-5.1492D-02	1.5510D-02	1.7194D-03	-4.9741D-02	2.3546D-02
1.5019D-02	5.1877D-03	-3.8896D-02	3.9881D-02	-9.8180D-03	1.5148D-02
-1.4405D-02	2.0672D-02	-2.6679D-02	4.2077D-02	-1.8154D-02	1.2447D-02
5.4638D-02	4.6766D-02	-4.9868D-02	3.1240D-02	5.8053D-02	-1.9617D-03
-5.1953D-02	5.8877D-03	-5.8560D-02	3.2968D-02	-5.3442D-04	-6.4951D-02
4.6154D-03	3.2776D-02	2.7890D-02	3.3092D-02	-8.9602D-03	-2.5194D-02
-1.2825D-02	1.4001D-02	4.4393D-02	2.3553D-02	-5.0732D-03	-2.2010D-02
3.6461D-02	3.7584D-02	5.0325D-02	1.2023D-02	-2.5531D-02	5.4046D-02
-6.7366D-02	4.9023D-02	4.0695D-02	1.8842D-02	4.8057D-02	2.5852D-02
-6.6266D-03	9.8636D-03	-2.4487D-02	4.5715D-04	-2.1008D-02	1.6401D-02
-2.3430D-03	1.1290D-02	-2.5193D-02	-2.2726D-04	-1.6700D-02	2.2081D-02
3.5147D-05	1.7904D-02	1.8937D-02	-9.5629D-03	-4.0795D-03	-2.7369D-02
5.4491D-03	1.7890D-02	1.8385D-02	-8.3652D-03	-1.0332D-02	-2.3954D-02
-3.4526D-03	-2.2044D-02	4.0536D-05	-1.2097D-02	2.4935D-02	9.8421D-03
3.2830D-03	-2.1434D-02	1.1628D-03	-1.3244D-02	2.7186D-02	3.3597D-03
-3.4710D-04	2.3437D-03	-1.5089D-03	-1.0731D-03	-1.3614D-03	-5.0904D-04
-2.8144D-04	2.5094D-03	4.2695D-04	-1.3657D-03	-1.5557D-03	-1.6587D-04
-3.5380D-03	3.0343D-03	1.7965D-04	2.0428D-05	1.4096D-03	1.8455D-03
2.6491D-03	3.4870D-03	-9.4585D-04	-9.3083D-05	2.2257D-03	-1.0472D-03

-1.0739D-03	-3.5130D-04	2.3721D-03	-2.1590D-03	4.3930D-04	-6.7372D-04
1.0300D-03	-1.3999D-03	1.6270D-03	-2.2779D-03	8.1229D-04	-5.5359D-04
-3.9069D-03	-3.1669D-03	3.0411D-03	-1.6912D-03	-2.5976D-03	8.7247D-05
3.7149D-03	-3.9870D-04	3.5713D-03	-1.7848D-03	2.3913D-05	2.8888D-03
-3.3002D-04	-2.2196D-03	-1.7008D-03	-1.7915D-03	4.0093D-04	1.1205D-03
9.1706D-04	-9.4813D-04	-2.7073D-03	-1.2751D-03	2.2700D-04	9.7893D-04
-2.6071D-03	-2.5451D-03	-3.0691D-03	-6.5087D-04	1.1424D-03	-2.4038D-03
4.8170D-03	-3.3197D-03	-2.4818D-03	-1.0200D-03	-2.1503D-03	-1.1498D-03
4.7384D-04	-6.6795D-04	1.4933D-03	-2.4748D-05	9.4000D-04	-7.2943D-04
1.6753D-04	-7.6451D-04	1.5364D-03	1.2303D-05	7.4724D-04	-9.8206D-04
-2.5132D-06	-1.2124D-03	-1.1549D-03	5.1769D-04	1.8254D-04	1.2173D-03
-3.8964D-04	-1.2115D-03	-1.1212D-03	4.5285D-04	4.6232D-04	1.0654D-03
2.4688D-04	1.4928D-03	-2.4721D-06	6.5489D-04	-1.1157D-03	-4.3774D-04
-2.3476D-04	1.4515D-03	-7.0911D-05	7.1695D-04	-1.2165D-03	-1.4943D-04

Columns 31 thru 36

-1.9869D-02	1.5954D-03	2.1872D-02	-1.0603D-02	-1.0172D-03	3.7932D-03
7.9912D-03	1.6713D-02	-2.1572D-02	-1.3239D-02	7.7044D-03	7.4290D-04
-5.8518D-03	-1.4592D-02	4.8236D-02	1.8710D-02	-9.0440D-04	-8.7199D-03
1.8994D-02	-4.5709D-03	-4.9775D-02	7.3679D-03	-6.6180D-03	2.6735D-03
5.4274D-03	-2.4081D-02	5.1002D-04	1.0252D-02	-1.9426D-02	2.1788D-03
-1.7367D-02	-8.4755D-03	-8.1887D-03	-3.2205D-03	-1.3994D-02	-2.7823D-03
2.3636D-03	1.6640D-02	-3.1811D-05	-7.7113D-03	1.0716D-02	1.2601D-03
8.5026D-03	1.6639D-02	6.7767D-03	4.7632D-04	2.4738D-02	2.0376D-03
1.3410D-02	1.2057D-02	6.1005D-03	1.3566D-02	1.4024D-02	2.1235D-02
1.6100D-02	-1.5039D-02	-3.4448D-04	1.0552D-02	6.5963D-03	-2.6720D-02
-1.2703D-02	1.9314D-03	-2.9321D-03	-2.1809D-03	-1.0523D-02	3.8753D-02
-1.7926D-02	4.9999D-04	-8.5054D-04	-2.3599D-02	-1.1844D-02	-3.4446D-02
1.5669D-02	-3.2900D-02	-1.2863D-02	2.1983D-02	1.9545D-02	-1.8161D-02
-2.3007D-02	-1.4509D-02	2.0993D-03	-2.7378D-02	9.3887D-04	2.4834D-02
2.1295D-02	1.5507D-02	5.0104D-03	-2.7878D-02	1.7005D-02	-4.4263D-03
2.4860D-02	-2.5540D-02	1.0298D-02	1.3120D-02	-3.0371D-02	7.6056D-03
-1.9935D-02	-7.9550D-04	-9.1220D-03	-2.2741D-03	-2.7171D-02	-2.0355D-02
5.8940D-03	1.9731D-02	5.4007D-03	2.1467D-02	1.8647D-02	1.4732D-02
2.4303D-04	-1.9183D-05	-2.4392D-04	1.1025D-04	1.0400D-05	-3.8461D-05
-9.7747D-05	-2.0096D-04	2.4058D-04	1.3766D-04	-7.8772D-05	-7.5327D-06
7.1578D-05	1.7546D-04	-5.3794D-04	-1.9454D-04	9.2468D-06	8.8416D-05
-2.3233D-04	5.4961D-05	5.5510D-04	-7.6610D-05	6.7664D-05	-2.7108D-05
-6.6387D-05	2.8955D-04	-5.6879D-06	-1.0660D-04	1.9862D-04	-2.2092D-05
2.1243D-04	1.0191D-04	9.1322D-05	3.3486D-05	1.4308D-04	2.8211D-05
-2.8911D-05	-2.0007D-04	3.5479D-07	8.0180D-05	-1.0956D-04	-1.2777D-05
-1.0400D-04	-2.0007D-04	-7.5576D-05	-4.9527D-06	-2.5293D-04	-2.0660D-05
-1.6403D-04	-1.4498D-04	-6.8034D-05	-1.4106D-04	-1.4338D-04	-2.1532D-04
-1.9693D-04	1.8083D-04	3.8417D-06	-1.0972D-04	-6.7442D-05	2.7093D-04
1.5538D-04	-2.3223D-05	3.2700D-05	2.2677D-05	1.0759D-04	-3.9294D-04
2.1927D-04	-6.0118D-06	9.4854D-06	2.4538D-04	1.2109D-04	3.4927D-04
-1.9166D-04	3.9559D-04	1.4345D-04	-2.2857D-04	-1.9983D-04	1.8414D-04

2.8142D-04	1.7446D-04	-2.3412D-05	2.8468D-04	-9.5992D-06	-2.5181D-04
-2.6048D-04	-1.8646D-04	-5.5878D-05	2.8987D-04	-1.7386D-04	4.4881D-05
-3.0408D-04	3.0709D-04	-1.1485D-04	-1.3642D-04	3.1053D-04	-7.7118D-05
2.4384D-04	9.5650D-06	1.0173D-04	2.3645D-05	2.7780D-04	2.0639D-04
-7.2095D-05	-2.3724D-04	-6.0230D-05	-2.2321D-04	-1.9065D-04	-1.4938D-04

Columns 37 thru 42

-3.5114D-04	-1.2400D-03	2.7054D-03	-1.7086D-03	5.4021D-03	-1.0518D-03
1.164 D-03	2.2107D-03	2.2760D-03	-4.1469D-03	5.2195D-03	7.2521D-04
-4.0010D-04	-2.1272D-02	-4.1960D-03	5.0255D-04	-6.5151D-03	3.7595D-04
-2.4351D-03	2.0394D-02	-1.9248D-03	5.6121D-03	-6.1392D-03	5.1326D-05
-1.6183D-02	6.5539D-03	-2.2450D-03	-1.7250D-02	5.9618D-03	5.6412D-04
2.3512D-02	1.1191D-03	-9.0702D-03	2.0818D-02	5.8832D-03	-3.5734D-04
-2.5801D-02	-3.9184D-03	6.7680D-03	-5.2154D-02	-9.2103D-03	-6.0769D-04
1.9450D-02	-6.0208D-03	5.3640D-03	4.9477D-02	-8.3751D-03	1.5969D-03
-5.4075D-03	-2.9935D-03	-9.4342D-03	1.1755D-03	5.6647D-03	2.8370D-04
-1.4896D-03	-5.0448D-03	1.3848D-02	3.1170D-03	5.5019D-03	-5.5777D-05
9.3353D-03	6.6600D-05	-4.2610D-02	-5.5203D-03	-7.3972D-03	-7.2205D-04
-1.6482D-04	9.7224D-03	3.8245D-02	4.7052D-04	-8.4551D-03	-8.3767D-04
4.7143D-03	-2.6158D-02	-2.2580D-02	-8.3785D-03	-6.2874D-03	-5.8000D-03
-4.2384D-03	3.0840D-02	1.6228D-02	7.1815D-03	-1.1546D-02	2.3293D-02
1.8724D-02	-3.0629D-02	-5.3793D-03	-1.5479D-02	-9.7670D-03	-1.8599D-02
-1.7029D-02	2.4043D-02	5.0253D-03	2.3383D-02	-7.4707D-03	-6.6058D-03
2.6571D-02	-6.5227D-03	-2.2296D-02	-2.0225D-02	-6.8103D-03	2.4297D-02
-2.2161D-02	8.2216D-03	2.9862D-02	1.2444D-02	-1.0963D-02	-1.6536D-02
3.4887D-06	1.1886D-05	-2.5203D-05	1.5489D-05	-3.9983D-05	6.5394D-06
-1.1572D-05	-2.1191D-05	-2.1204D-05	3.7594D-05	-3.8632D-05	-4.5087D-06
3.9752D-06	2.0391D-04	3.9090D-05	-4.5558D-06	4.8221D-05	-2.3374D-06
2.4194D-05	-1.9550D-04	1.7932D-05	-5.0876D-05	4.5439D-05	-3.1912D-07
1.6079D-04	-6.2824D-05	2.0915D-05	1.5638D-04	-4.4126D-05	-3.5072D-06
-2.3360D-04	-1.0727D-05	8.4498D-05	-1.8872D-04	-4.3544D-05	2.2218D-06
2.5634D-04	3.7561D-05	-6.3051D-05	4.7280D-04	6.8169D-05	3.7781D-06
-1.9324D-04	5.7714D-05	-4.9971D-05	-4.4853D-04	6.1987D-05	-9.9282D-06
5.3726D-05	2.8695D-05	8.7889D-05	-1.0656D-05	-4.1927D-05	-1.7638D-06
1.4800D-05	4.8359D-05	-1.2901D-04	-2.8257D-05	-4.0722D-05	3.4681D-07
-9.2750D-05	-6.3846D-07	3.9695D-04	5.0044D-05	5.4750D-05	4.4890D-06
1.6375D-06	-9.3197D-05	-3.5629D-04	-4.2654D-06	6.2580D-05	5.2079D-06
-4.6838D-05	2.5074D-04	2.1036D-04	7.5954D-05	4.6535D-05	3.6059D-05
4.2110D-05	-2.9563D-04	-1.5118D-04	-6.5103D-05	8.5456D-05	-1.4482D-04
-1.8603D-04	2.9361D-04	5.0114D-05	1.4032D-04	7.2290D-05	1.1563D-04
1.6919D-04	-2.3048D-04	-4.6816D-05	-2.1197D-04	5.5294D-05	4.1069D-05
-2.6399D-04	6.2526D-05	2.0771D-04	1.8334D-04	5.0406D-05	-1.5106D-04
2.2018D-04	-7.8811D-05	-2.7819D-04	-1.1281D-04	8.1144D-05	1.0281D-04



## Columns 43 thru 48

3.8115D-05	-7.5946D-04	0.0000D+00	0.0000D+00	0.0000D+00	0.0000D+00
-4.7317D-04	-1.1258D-03	0.0000D+00	0.0000D+00	0.0000D+00	0.0000D+00
4.0708D-04	-8.6159D-05	0.0000D+00	0.0000D+00	0.0000D+00	0.0000D+00
5.2616D-04	8.0319D-04	0.0000D+00	0.0000D+00	0.0000D+00	0.0000D+00
5.5933D-04	-1.0427D-03	0.0000D+00	0.0000D+00	0.0000D+00	0.0000D+00
-3.0414D-04	-7.4150D-04	0.0000D+00	0.0000D+00	0.0000D+00	0.0000D+00
-1.8699D-03	1.3273D-03	0.0000D+00	0.0000D+00	0.0000D+00	0.0000D+00
3.3272D-04	1.1594D-03	0.0000D+00	0.0000D+00	0.0000D+00	0.0000D+00
-5.9762D-04	-4.3420D-04	0.0000D+00	0.0000D+00	0.0000D+00	0.0000D+00
8.2594D-04	-1.1894D-03	0.0000D+00	0.0000D+00	0.0000D+00	0.0000D+00
7.9599D-04	4.6274D-04	0.0000D+00	0.0000D+00	0.0000D+00	0.0000D+00
-1.4161D-03	1.5820D-03	0.0000D+00	0.0000D+00	0.0000D+00	0.0000D+00
-2.3395D-02	-4.9849D-03	0.0000D+00	0.0000D+00	0.0000D+00	0.0000D+00
4.6713D-03	4.3860D-03	0.0000D+00	0.0000D+00	0.0000D+00	0.0000D+00
1.6299D-02	6.2581D-03	0.0000D+00	0.0000D+00	0.0000D+00	0.0000D+00
-2.3074D-02	-6.3385D-03	0.0000D+00	0.0000D+00	0.0000D+00	0.0000D+00
6.7683D-03	-4.6669D-03	0.0000D+00	0.0000D+00	0.0000D+00	0.0000D+00
1.8804D-02	-5.4971D-03	0.0000D+00	0.0000D+00	0.0000D+00	0.0000D+00
-2.3677D-07	3.7081D-06	0.0000D+00	0.0000D+00	0.0000D+00	0.0000D+00
2.9394D-06	5.4969D-06	0.0000D+00	0.0000D+00	0.0000D+00	0.0000D+00
-2.5288D-06	4.2067D-07	0.0000D+00	0.0000D+00	0.0000D+00	0.0000D+00
-3.2685D-06	-3.9216D-06	0.0000D+00	0.0000D+00	0.0000D+00	0.0000D+00
-3.4746D-06	5.0907D-06	0.0000D+00	0.0000D+00	0.0000D+00	0.0000D+00
1.8894D-06	3.6203D-06	0.0000D+00	0.0000D+00	0.0000D+00	0.0000D+00
1.1616D-05	-6.4806D-06	0.0000D+00	0.0000D+00	0.0000D+00	0.0000D+00
-2.0669D-06	-5.6608D-06	0.0000D+00	0.0000D+00	0.0000D+00	0.0000D+00
3.7124D-06	2.1200D-06	0.0000D+00	0.0000D+00	0.0000D+00	0.0000D+00
-5.1307D-06	5.8073D-06	0.0000D+00	0.0000D+00	0.0000D+00	0.0000D+00
-4.9447D-06	-2.2593D-06	0.0000D+00	0.0000D+00	0.0000D+00	0.0000D+00
8.7966D-06	-7.7241D-06	0.0000D+00	0.0000D+00	0.0000D+00	0.0000D+00
1.4533D-04	2.4339D-05	0.0000D+00	0.0000D+00	0.0000D+00	0.0000D+00
-2.9018D-05	-2.1414D-05	0.0000D+00	0.0000D+00	0.0000D+00	0.0000D+00
-1.0125D-04	-3.0555D-05	0.0000D+00	0.0000D+00	0.0000D+00	0.0000D+00
1.4333D-04	3.0948D-05	0.0000D+00	0.0000D+00	0.0000D+00	0.0000D+00
-4.2045D-05	2.2786D-05	0.0000D+00	0.0000D+00	0.0000D+00	0.0000D+00
-1.1681D-04	2.6839D-05	0.0000D+00	0.0000D+00	0.0000D+00	0.0000D+00
0.0000D+00	0.0000D+00	8.2192D-05	5.2920D-05	-5.8617D-05	1.0954D-05
0.0000D+00	0.0000D+00	5.5167D-06	2.1632D-05	3.7803D-05	-1.5747D-05
0.0000D+00	0.0000D+00	-4.1958D-04	-2.4597D-05	-1.4430D-04	-1.9811D-04
0.0000D+00	0.0000D+00	1.2184D-05	-1.6538D-04	5.2554D-06	2.4765D-05
0.0000D+00	0.0000D+00	9.5835D-05	-6.0167D-05	-4.5796D-05	6.0875D-05
0.0000D+00	0.0000D+00	-6.9668D-06	1.5496D-05	-3.7690D-05	1.9489D-05
0.0000D+00	0.0000D+00	-3.8327D-04	-2.0038D-04	1.6037D-04	2.1030D-05
0.0000D+00	0.0000D+00	2.8833D-05	9.9612D-05	1.6077D-04	-5.7120D-05
0.0000D+00	0.0000D+00	1.2266D-04	1.3896D-05	6.5701D-05	-7.0880D-05
0.0000D+00	0.0000D+00	1.4042D-06	-3.6101D-05	-7.9689D-09	9.0793D-06

0.0000D+00	0.0000D+00	-4.0373D-04	1.8487D-04	1.2150D-04	1.6261D-04
0.0000D+00	0.0000D+00	-4.1726D-05	7.8528D-05	-1.6227D-04	4.3717D-05
0.0000D+00	0.0000D+00	4.4540D-04	-4.6701D-03	2.0807D-04	-3.1230D-04
0.0000D+00	0.0000D+00	1.2589D-03	2.3941D-04	4.5094D-03	4.6061D-04
0.0000D+00	0.0000D+00	-4.3426D-03	-9.1632D-04	-1.6733D-02	-2.1305D-04
0.0000D+00	0.0000D+00	8.5697D-03	-1.6900D-02	2.6374D-04	-4.5974D-04
0.0000D+00	0.0000D+00	4.3404D-03	9.4817D-04	1.6731D-02	2.1000D-04
0.0000D+00	0.0000D+00	5.5133D-03	1.7181D-02	-1.1149D-03	3.3040D-04
0.0000D+00	0.0000D+00	9.6080D-05	-1.0996D-03	3.9042D-05	2.9082D-05
0.0000D+00	0.0000D+00	2.7969D-04	6.1425D-05	1.1001D-03	-1.0529D-04

Columns 49 thru 54

6.6108D-05	-2.8417D-05	5.0482D-05	-7.9112D-05	3.8919D-05	8.8048D-06
-1.1764D-05	-2.3698D-05	-5.9609D-05	-3.4100D-05	1.1042D-05	1.2986D-05
-1.1137D-04	-1.9293D-05	-1.9803D-04	7.7233D-06	-1.6052D-05	3.0246D-05
-4.1106D-05	2.3769D-05	2.2039D-08	7.9453D-05	-5.6550D-05	-6.9648D-06
-2.1984D-05	4.0000D-05	4.8640D-05	7.5367D-05	-3.2005D-05	-1.4000D-05
7.6611D-06	-1.5866D-05	6.1188D-05	-3.4529D-05	1.9655D-05	-1.0389D-05
1.8499D-04	-7.7720D-05	6.9519D-05	-1.5875D-04	4.8851D-05	-2.9862D-06
-1.5285D-05	-3.3186D-05	-7.1969D-05	-4.4682D-05	6.2266D-06	1.6141D-05
-3.9584D-05	-8.0918D-06	-8.2730D-05	-2.9045D-06	-3.5243D-06	4.9097D-06
-1.2767D-05	-1.2746D-06	-4.4528D-07	7.5372D-05	-2.3001D-05	-8.4589D-06
-8.1651D-05	1.0327D-04	6.5240D-05	1.7135D-04	-4.7670D-05	-2.3009D-05
4.1854D-05	-1.8131D-05	7.4065D-05	-4.4196D-05	1.3357D-05	1.5134D-05
5.8445D-04	-2.2213D-04	4.1806D-06	-1.8684D-05	1.1074D-04	7.5120D-05
2.9185D-04	-5.2569D-06	6.9080D-05	1.6229D-05	-2.5413D-05	1.1744D-04
-1.6678D-04	1.2219D-04	2.1238D-04	-1.7714D-05	1.8133D-05	2.4392D-04
7.3246D-04	-8.5384D-06	2.3570D-05	1.1658D-04	-4.6802D-04	-1.5155D-04
1.7118D-04	-1.2781D-04	-2.1266D-04	1.1416D-05	-1.1730D-05	-2.4094D-04
-8.3317D-04	4.5376D-05	-3.0371D-07	-1.1610D-04	4.6451D-04	1.9490D-04
-4.9009D-05	6.2807D-05	-2.6169D-07	5.8120D-05	-8.3494D-05	-3.4204D-05
-5.8020D-05	-1.7716D-05	-7.5245D-05	-8.7945D-07	-5.3068D-08	-4.0391D-05

Columns 55 thru 60

-4.7716D-06	-6.5742D-05	9.7871D-05	-9.1054D-05	-8.7941D-07	-1.4786D-05
1.5699D-05	8.2509D-05	7.1782D-05	1.8257D-05	1.1945D-06	-8.0070D-05
2.6284D-05	5.6070D-05	3.2446D-05	1.4376D-04	6.4666D-05	-9.3161D-06
-8.3047D-06	1.6544D-05	-9.8339D-05	1.1555D-05	-2.7004D-07	-5.3149D-06
-2.5823D-06	-2.7071D-05	-1.3545D-04	-6.2221D-05	-2.1058D-07	-1.2077D-05
-6.7327D-06	-1.0010D-04	3.5340D-05	-3.1865D-05	-2.0430D-06	-8.0216D-05
-2.9078D-06	-1.2026D-04	8.8851D-05	1.1219D-04	8.8752D-05	-7.1563D-06
-1.0399D-05	7.7584D-05	6.6304D-05	1.6399D-05	1.6189D-07	-7.0605D-06
6.6840D-06	1.5466D-04	2.1129D-05	-2.2527D-05	8.3756D-07	-1.1094D-05
-1.9780D-06	1.7614D-05	-1.0660D-04	1.3600D-05	9.6308D-07	-8.4442D-05
-2.0077D-05	-8.9704D-05	-8.2402D-05	1.2561D-04	8.0130D-05	-1.1989D-05
-1.6722D-05	-9.3903D-05	3.2276D-05	-2.8206D-05	-1.9200D-07	-7.4656D-06

-6.9771D-05	-2.9458D-05	1.7203D-04	-1.6404D-05	6.1670D-06	-2.1072D-06
1.0239D-04	-1.8241D-04	-3.2412D-05	-3.9225D-05	1.3274D-05	-4.3440D-08
1.1629D-04	-4.3157D-04	-9.2885D-05	-1.6623D-04	-7.0271D-05	-1.5929D-05
1.5153D-04	1.0804D-04	-4.5602D-04	1.8978D-05	-8.8033D-05	3.2649D-06
-1.1818D-04	4.2939D-04	1.0873D-04	1.6424D-04	7.0041D-05	2.7356D-06
-1.5227D-04	-3.0691D-05	4.4699D-04	-1.2457D-04	-1.3839D-04	-6.6776D-06
2.6276D-05	1.3724D-05	-8.3650D-05	9.7752D-06	5.0930D-08	-2.5393D-06
-2.5096D-05	8.6310D-05	1.7924D-05	2.3623D-05	2.0160D-06	-5.8461D-06

Columns 61 thru 66

7.8357D-05	-3.3035D-05	-1.4227D-04	-3.1451D-04	4.9621D-04	-2.3742D-03
-3.7737D-05	-1.1727D-04	-9.2071D-06	-4.5813D-06	-1.4985D-05	1.9745D-03
-1.1234D-04	-1.0580D-04	1.0315D-03	2.8220D-04	6.8494D-04	6.5891D-03
-8.3438D-05	9.3005D-05	-6.0525D-05	9.7543D-04	-1.9085D-04	-8.3949D-04
-1.4914D-05	8.3255D-05	-2.2003D-04	5.0405D-04	2.1285D-04	-3.0313D-03
1.2124D-04	2.4738D-05	9.0077D-06	1.3986D-05	1.3146D-06	-1.7321D-03
1.5970D-04	-4.7886D-05	8.4447D-04	8.9161D-04	-1.0839D-03	-1.8195D-03
-3.6668D-05	-1.1388D-04	-1.3238D-04	-7.4136D-04	-8.5828D-04	5.2978D-03
-6.5893D-05	-5.3444D-05	-3.4139D-04	-1.8993D-04	-4.5735D-04	4.9668D-03
-8.2637D-05	9.1591D-05	5.1025D-07	-2.0806D-05	1.3601D-05	-2.6781D-04
-3.6157D-05	1.5824D-04	9.4951D-04	-1.0462D-03	-5.1572D-04	-3.4111D-03
1.1842D-04	2.4402D-05	1.9627D-04	-3.1647D-04	1.0382D-03	-4.9525D-03
7.6809D-04	-8.5119D-04	-1.6215D-03	2.1778D-02	-4.4097D-03	1.5486D-03
8.3862D-04	7.4166D-04	-4.3784D-03	-4.5223D-03	-2.1135D-02	-9.7480D-03
-1.2054D-03	-1.0774D-03	1.5799D-02	1.7363D-02	8.0363D-02	-5.0137D-02
1.0663D-03	-1.2286D-03	-2.4192D-02	8.0665D-02	-1.2183D-02	-2.1330D-03
1.2125D-03	1.0687D-03	-1.5788D-02	-1.7546D-02	-8.0321D-02	5.0228D-02
-1.0953D-03	1.2174D-03	-1.2584D-02	-8.1991D-02	2.0120D-02	8.0386D-03
-3.9431D-05	4.0548D-05	-3.6048D-04	5.0655D-03	-9.7753D-04	-8.8494D-04
-3.8740D-05	-3.7140D-05	-1.0124D-03	-1.0960D-03	-5.1004D-03	7.4713D-03

Columns 67 thru 72

-4.6707D-03	-2.6108D-03	2.5388D-04	-6.7757D-03	-4.9226D-03	-2.9016D-03
-7.5899D-04	-9.4838D-04	5.9152D-04	-1.1265D-03	3.6009D-03	-1.8622D-03
1.3094D-03	-3.6980D-04	-3.4147D-03	9.1872D-04	4.2364D-03	-1.9965D-03
6.6293D-03	1.3207D-04	-7.5474D-04	1.2532D-02	-3.5087D-03	-8.2107D-03
4.1361D-03	2.3836D-03	4.0960D-04	7.0391D-03	-5.0368D-03	1.3216D-03
-1.2887D-03	-5.9152D-04	-6.0658D-04	-2.1639D-03	-3.4053D-03	-2.0780D-04
-5.4513D-03	-2.2300D-03	-5.4324D-03	-4.6289D-03	-1.6375D-03	-1.5530D-03
-1.3797D-03	-5.4971D-03	1.0202D-03	-4.8297D-04	7.4364D-03	-1.4909D-02
6.1680D-04	-9.0762D-04	2.8815D-03	1.5111D-03	8.6729D-03	-3.8334D-03
2.1643D-03	9.7129D-04	-9.6275D-05	3.7071D-03	-6.2172D-04	4.1797D-05
4.9875D-03	2.4110D-03	-5.3748D-03	2.8687D-03	-3.3162D-03	3.6841D-05
-2.9309D-03	-4.5898D-03	-2.4562D-03	-3.5418D-03	-1.1701D-02	-1.0549D-02
-1.3557D-02	-2.6401D-03	-2.1386D-03	-1.7003D-03	-4.1834D-04	-5.4014D-04
-2.0443D-03	-1.5559D-06	-5.7891D-03	-1.6217D-04	-4.2026D-03	2.1074D-03

-7.0161D-03	5.1709D-03	-1.0850D-02	-1.6069D-02	-8.6045D-02	1.5931D-02
4.3457D-02	3.2781D-02	-1.6626D-02	8.3893D-02	-7.5135D-03	2.2548D-02
6.2633D-03	-5.8857D-03	1.0783D-02	1.5027D-02	8.5919D-02	-1.7392D-02
-4.1134D-02	-3.1145D-02	-1.0008D-02	-8.7090D-02	9.5176D-03	-2.2076D-02
7.1408D-03	3.7231D-03	9.3395D-05	7.2836D-03	-6.3875D-04	1.4651D-03
1.2179D-03	-6.6101D-04	1.8393D-03	1.7417D-03	7.0052D-03	-2.2853D-03

Columns 73 thru 78

8.2948D-03	9.9507D-03	4.7840D-02	1.0645D-03	4.2100D-02	-7.0163D-02
3.4591D-03	-3.4872D-03	2.6909D-02	7.7154D-02	3.2158D-02	7.7281D-03
-3.2708D-04	-1.9469D-03	5.5179D-02	5.7476D-02	2.5994D-02	1.3291D-03
-1.5451D-02	-3.8278D-03	-3.9026D-02	5.6352D-02	-1.0867D-02	3.5341D-02
-1.2429D-02	2.7615D-03	-2.2551D-02	4.5810D-02	-2.0162D-03	6.2855D-02
1.1899D-03	4.5844D-03	-8.1401D-02	2.1782D-03	-4.2546D-02	2.4085D-02
7.1913D-04	-8.3258D-04	-7.4048D-02	2.0530D-02	-3.9518D-02	1.7441D-02
1.1595D-02	-1.1594D-02	-3.1311D-02	-5.5312D-02	-3.0005D-02	-6.3952D-03
3.9762D-03	-1.1866D-02	-3.3424D-02	-3.5716D-02	-2.8013D-02	1.6905D-02
-4.4812D-03	-1.0423D-03	3.9321D-02	-5.5194D-02	9.8300D-03	-3.1076D-02
-5.3539D-04	6.5921D-04	2.1651D-02	-7.1909D-02	-8.3425D-03	-2.7477D-02
4.6154D-03	1.5929D-02	6.3130D-02	9.2468D-03	4.0121D-02	-2.4861D-02
4.2727D-02	1.0015D-02	3.8678D-02	-5.7802D-02	4.9204D-03	-3.7503D-03
-1.1105D-02	4.5251D-02	6.2540D-02	4.0262D-02	3.7617D-02	-3.6389D-03
-1.5841D-02	6.8148D-02	3.1193D-01	2.0479D-01	2.1965D-01	-7.5093D-02
-7.2798D-02	-2.3188D-02	-2.4508D-01	3.2485D-01	-7.9261D-02	2.5890D-01
1.8310D-02	-6.7520D-02	-3.0292D-01	-2.1687D-01	-2.1625D-01	6.1198D-02
7.3660D-02	1.5675D-02	2.1515D-01	-3.4819D-01	4.7344D-02	-2.5498D-01
-8.5416D-03	-2.0014D-03	2.5606D-02	-3.7087D-02	8.4054D-03	-3.3293D-02
1.7492D-03	-8.6626D-03	3.4599D-02	3.7147D-02	2.7764D-02	-5.0461D-03

Columns 79 thru 84

-2.3618D-02	2.5509D-02	3.9196D-02	5.6526D-02	1.5612D-02	-8.8318D-03
-2.9521D-02	-3.8655D-02	-4.9560D-03	2.9986D-02	-2.0998D-02	2.8181D-03
-1.5009D-02	-4.8839D-02	2.3019D-02	9.7412D-03	-4.6492D-02	-2.1699D-02
-1.6063D-02	-4.0172D-02	-4.6710D-02	4.9894D-04	-3.0939D-02	1.8411D-02
-5.4082D-02	-3.8900D-02	-4.8318D-02	3.0679D-02	-2.7037D-02	3.3424D-02
1.4739D-02	2.6402D-04	-3.5567D-02	-2.8312D-02	2.9735D-03	4.6799D-03
1.2220D-02	-2.3421D-02	-1.8168D-02	-5.4137D-02	-2.4467D-02	2.1552D-04
2.8643D-02	4.0190D-02	2.9815D-03	-4.1399D-02	3.2955D-02	-1.7252D-03
6.6031D-02	4.2930D-02	-3.0817D-02	-3.4511D-02	5.1028D-02	1.5385D-02
1.5836D-02	3.4944D-02	3.5118D-02	-1.4702D-03	1.7224D-02	-6.5128D-03
1.5305D-02	1.5982D-02	5.2152D-02	-3.3692D-02	8.0671D-03	-3.2357D-02
-1.5294D-02	-3.4398D-03	4.1404D-02	4.1361D-02	-5.1551D-03	-1.5417D-02
5.3738D-03	2.2217D-02	2.6476D-02	-1.5643D-03	1.4289D-02	-6.8574D-03
-2.2122D-03	-1.7495D-02	1.3642D-02	2.8253D-02	-9.9827D-03	-4.1547D-03
-1.7726D-01	-1.2001D-01	1.2350D-01	2.2985D-01	-1.0748D-01	-3.2227D-02
-9.6672D-02	-2.2915D-01	-2.4661D-01	-5.0677D-03	-1.4257D-01	9.5940D-02

1.8234D-01	1.3089D-01	-1.1171D-01	-2.2975D-01	1.1575D-01	2.6666D-02
1.2401D-01	2.3735D-01	2.3541D-01	-2.1015D-02	1.6250D-01	-8.2447D-02
1.3737D-02	2.9427D-02	3.2704D-02	-2.1323D-04	2.2925D-02	-1.4775D-02
-3.3246D-02	-2.5252D-02	1.0809D-02	3.6266D-02	-2.3860D-02	-3.0288D-03

Columns 85 thru 88

-1.3633D-02	4.3576D-02	2.8479D-02	-3.7968D-02
2.9132D-02	3.4135D-03	-1.0403D-03	2.9990D-02
-8.2424D-03	3.9537D-02	-2.1850D-02	-3.2416D-02
-3.1623D-02	5.1647D-03	1.6134D-02	2.1516D-02
-8.7381D-03	2.3286D-03	-5.2198D-02	-4.5880D-02
2.7771D-02	-1.5705D-03	5.1158D-04	2.9833D-02
-9.7459D-03	-4.0962D-02	-2.7161D-02	-4.1333D-02
-2.5758D-02	1.2502D-02	-1.4066D-02	3.2645D-02
-1.1555D-02	-4.4871D-02	2.2219D-02	-3.6882D-02
2.9710D-02	-2.0628D-03	4.1891D-05	3.6864D-02
-4.2229D-03	3.9509D-04	4.9979D-02	-3.2248D-02
-2.6773D-02	-1.8361D-02	-6.2403D-03	3.0428D-02
2.1674D-03	2.1158D-03	9.0822D-03	5.2788D-03
-1.6663D-03	9.7216D-03	-2.2537D-03	-3.4893D-03
8.4547D-04	8.6474D-02	-2.5506D-02	-9.0724D-03
2.2429D-03	-3.0234D-02	-1.0210D-01	5.2120D-02
-3.4046D-03	-8.5474D-02	2.7180D-02	-4.9091D-03
-6.9047D-05	2.2947D-02	1.0368D-01	-3.5206D-02
1.4428D-03	5.7221D-03	2.1473D-02	1.6392D-02
-4.7767D-03	2.0150D-02	-1.1579D-02	-2.0008D-02

### ***Appendix E: Modal Cost Models: Open Loop Bode Response***

This appendix contains Bode plots of the responses in the X and Y LOS axis to the nine disturbance inputs for each of the modal-cost reduced filters (10-, 15-, and 20-mode). The truth model response has been added for ease of comparison. Notice the high frequency inconsistencies (large dips in the plots) in Figures E-3, E-7, E-9, E-21, E-25, E-26, E-32, E-35, and E-53.

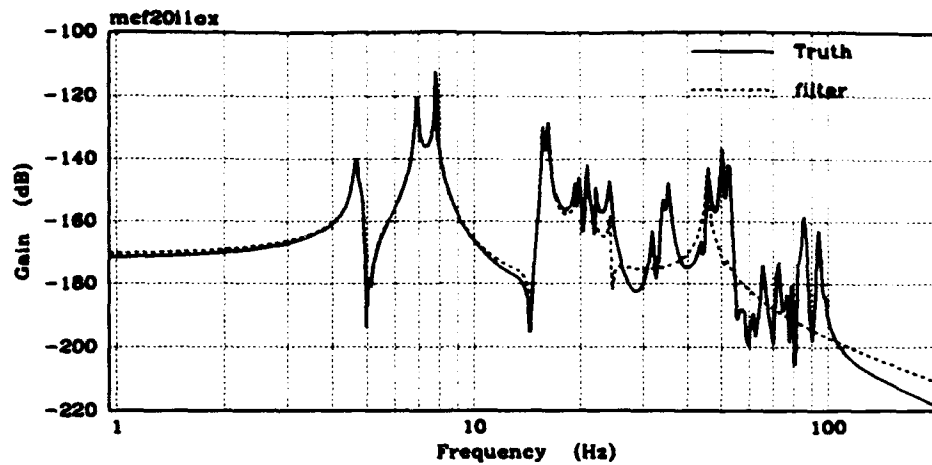


Figure E-1. Truth vs. 10-mode Modal-Cost Reduced (Disturbance 1, X LOS)

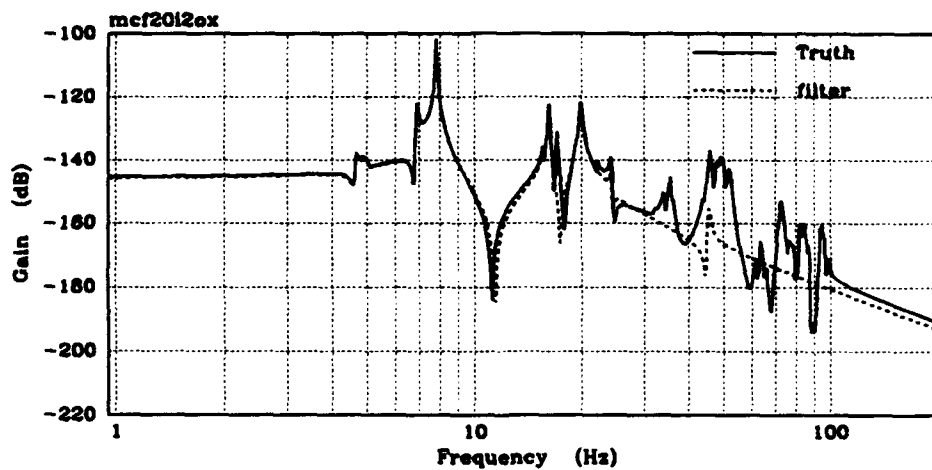


Figure E-2. Truth vs. 10-mode Modal-Cost Reduced (Disturbance 2, X LOS)

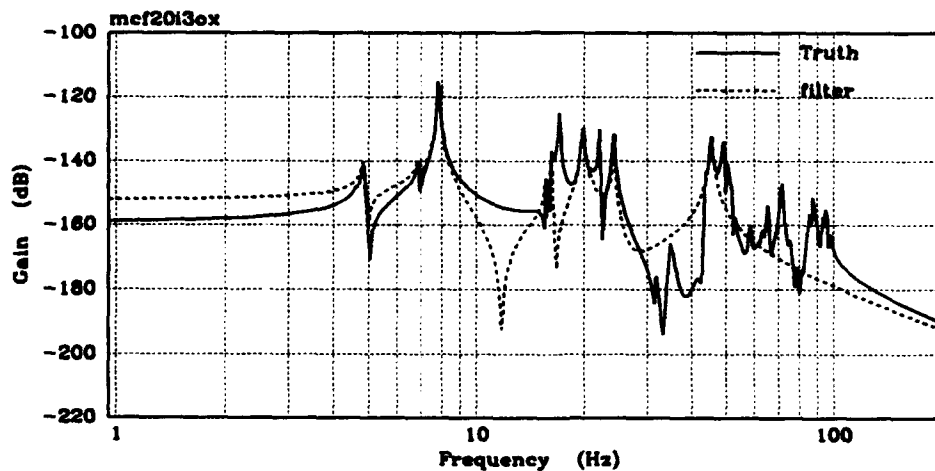


Figure E-3. Truth vs. 10-mode Modal-Cost Reduced (Disturbance 3, X LOS)

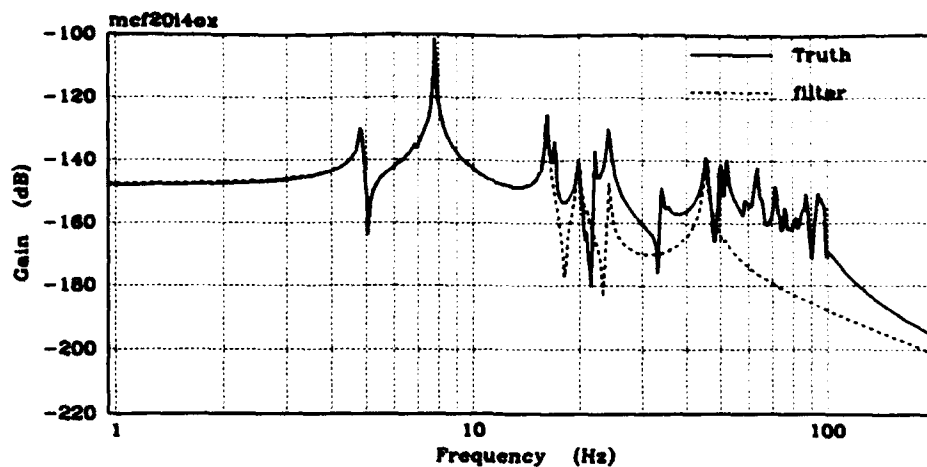


Figure E-4. Truth vs. 10-mode Modal-Cost Reduced (Disturbance 4, X LOS)

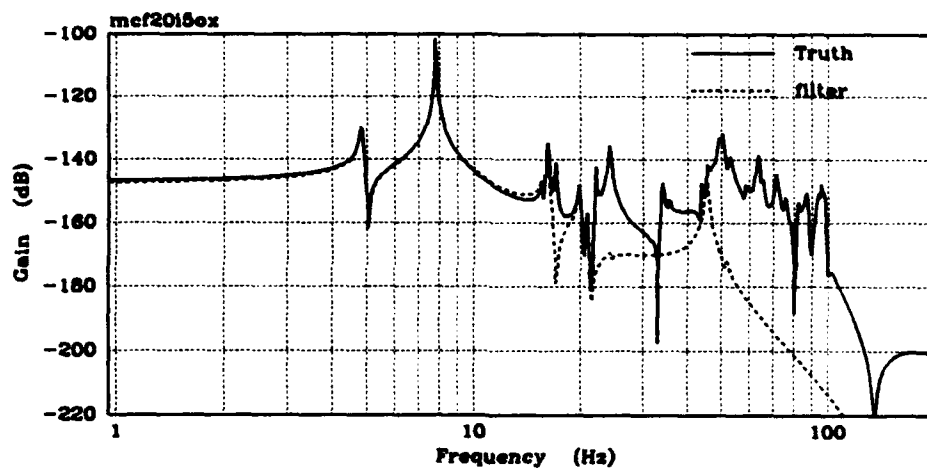


Figure E-5. Truth vs. 10-mode Modal-Cost Reduced (Disturbance 5, X LOS)

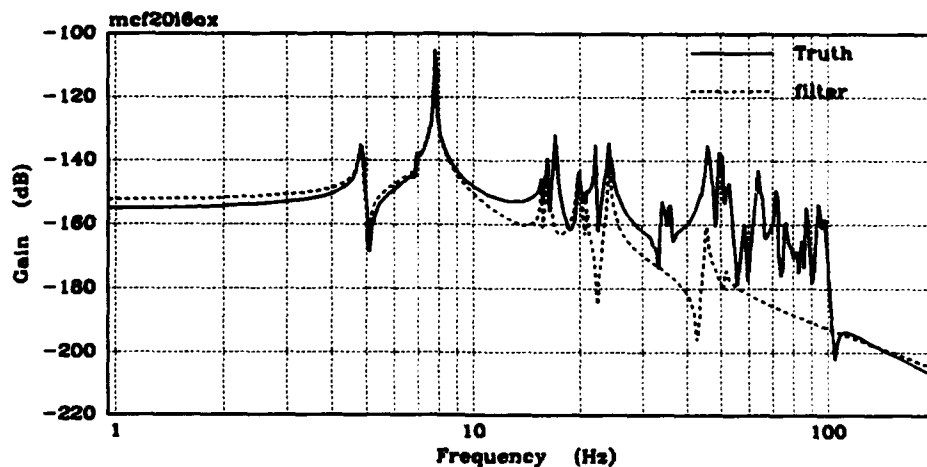


Figure E-6. Truth vs. 10-mode Modal-Cost Reduced (Disturbance 6, X LOS)



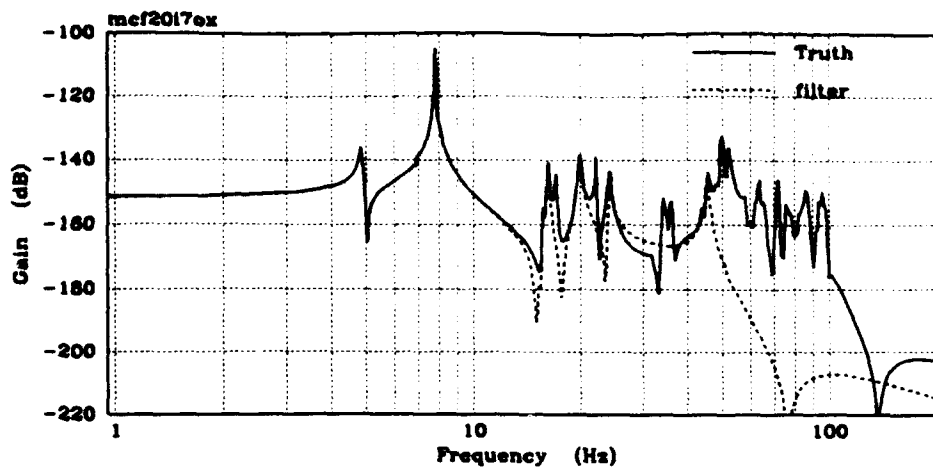


Figure E-7. Truth vs. 10-mode Modal-Cost Reduced (Disturbance 7, X LOS)

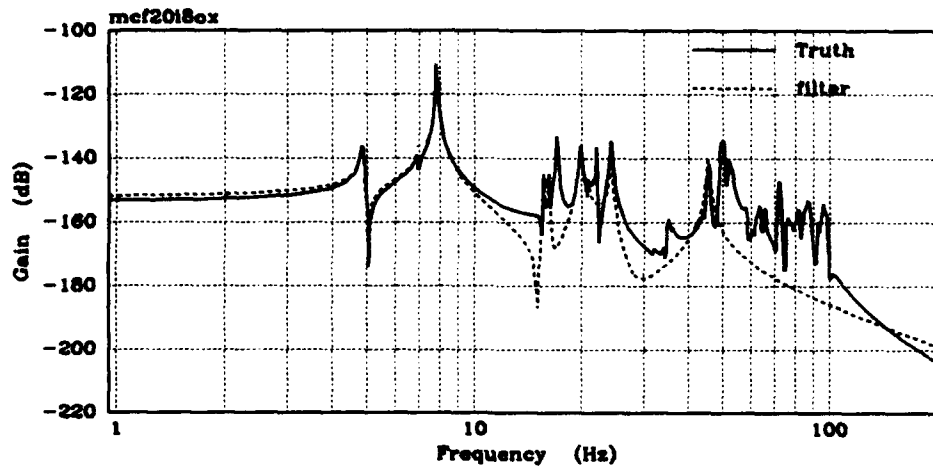


Figure E-8. Truth vs. 10-mode Modal-Cost Reduced (Disturbance 8, X LOS)

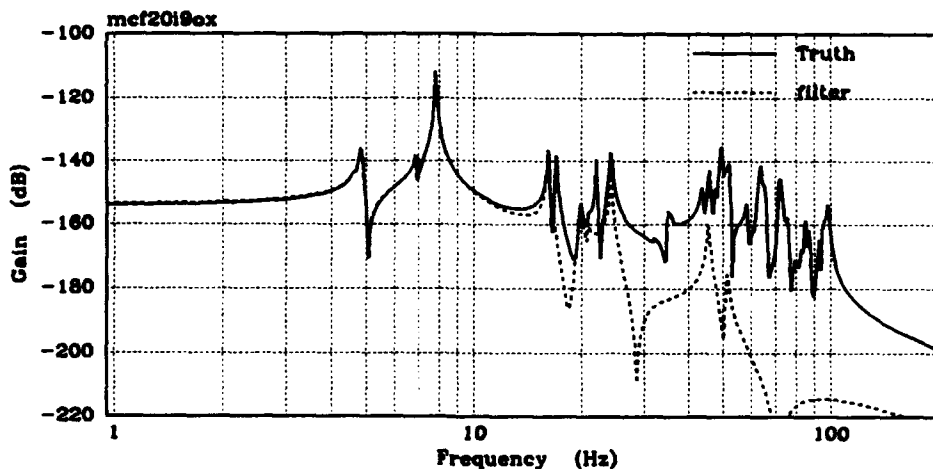


Figure E-9. Truth vs. 10-mode Modal-Cost Reduced (Disturbance 9, X LOS)

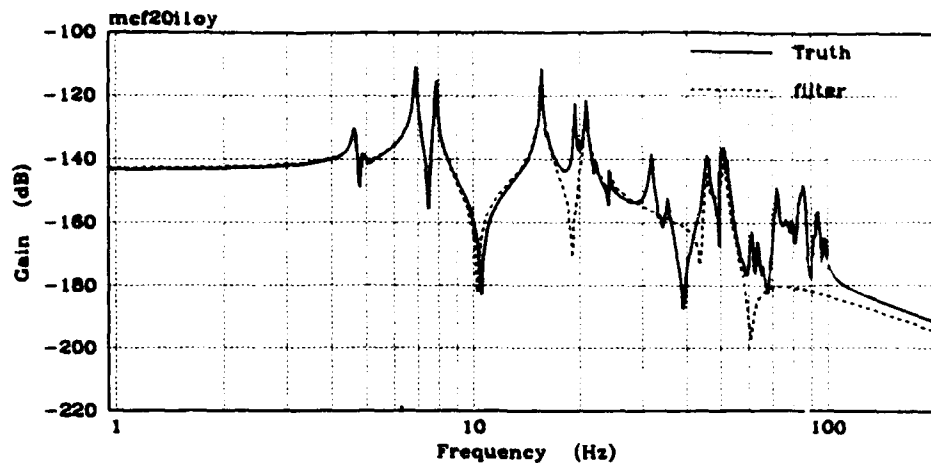


Figure E-10. Truth vs. 10-mode Modal-Cost Reduced (Disturbance 1, Y LOS)

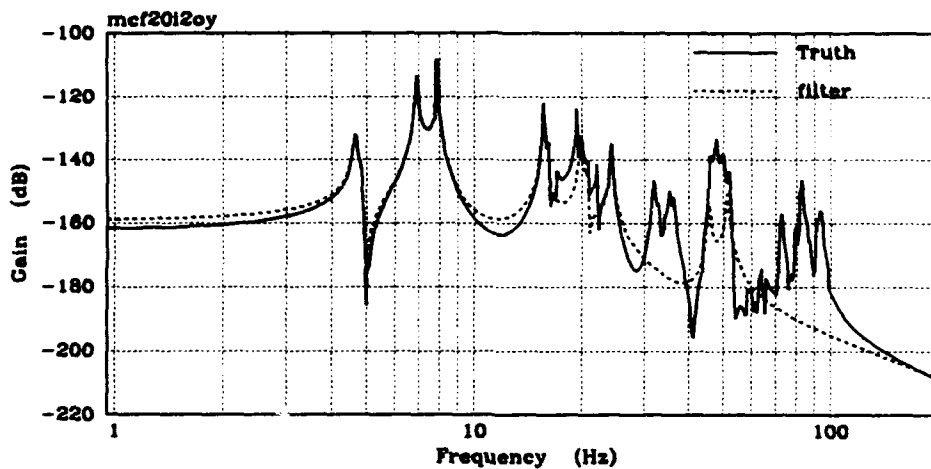


Figure E-11. Truth vs. 10-mode Modal-Cost Reduced (Disturbance 2, Y LOS)

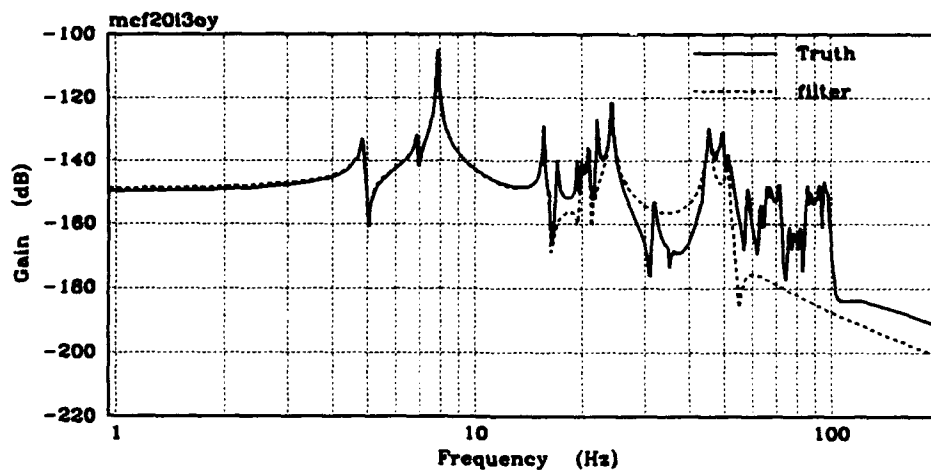


Figure E-12. Truth vs. 10-mode Modal-Cost Reduced (Disturbance 3, Y LOS)

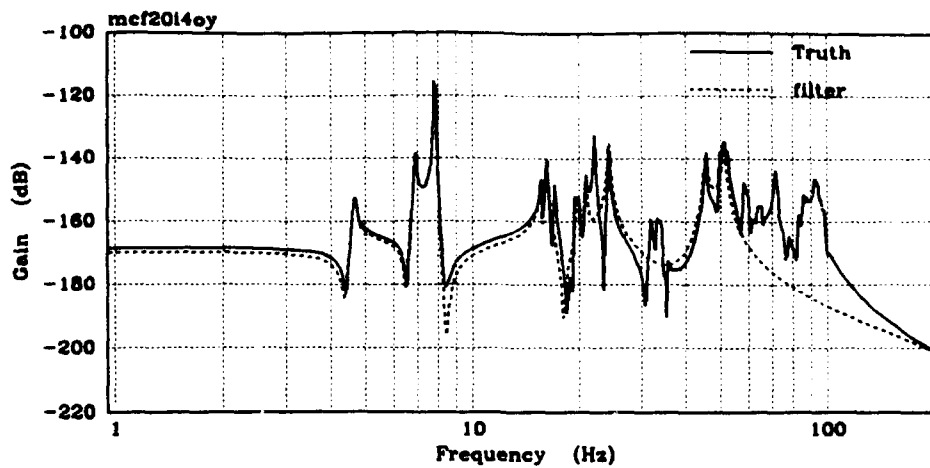


Figure E-13. Truth vs. 10-mode Modal-Cost Reduced (Disturbance 4, Y LOS)

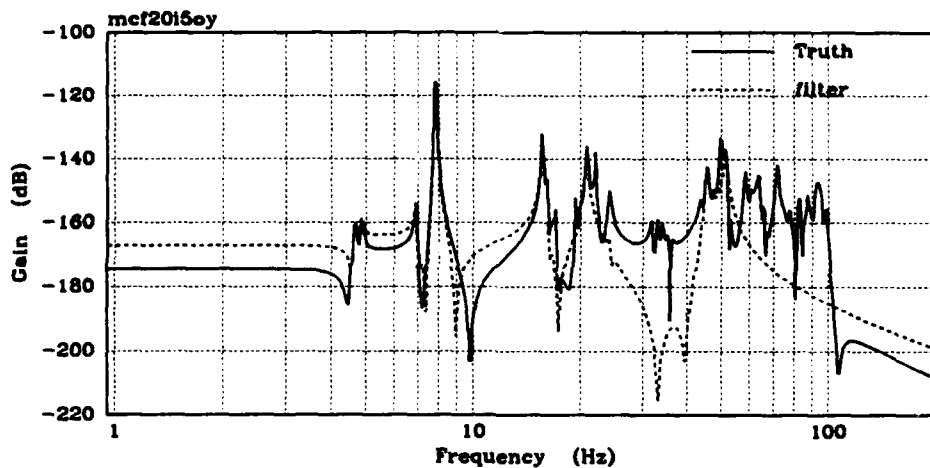


Figure E-14. Truth vs. 10-mode Modal-Cost Reduced (Disturbance 5, Y LOS)

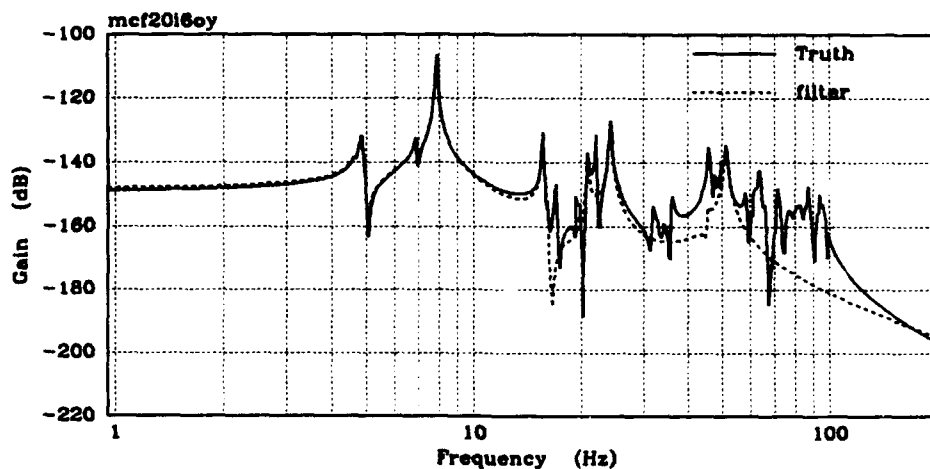


Figure E-15. Truth vs. 10-mode Modal-Cost Reduced (Disturbance 6, Y LOS)

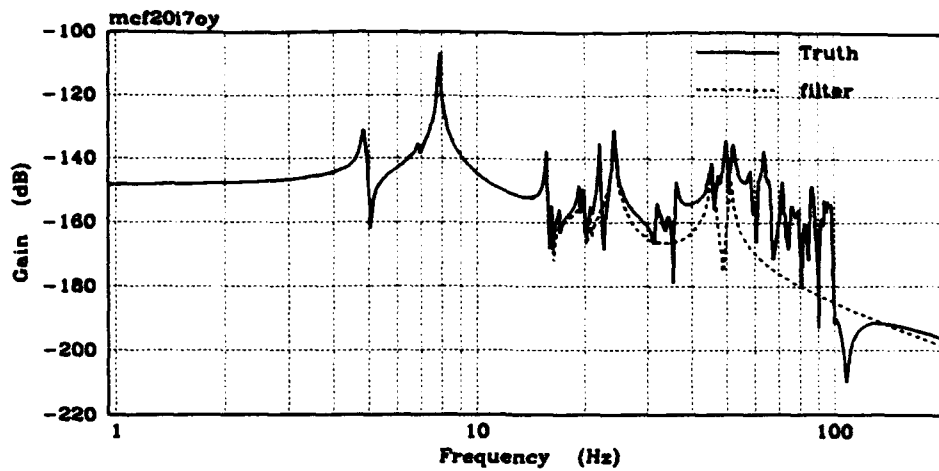


Figure E-16. Truth vs. 10-mode Modal-Cost Reduced (Disturbance 7, Y LOS)

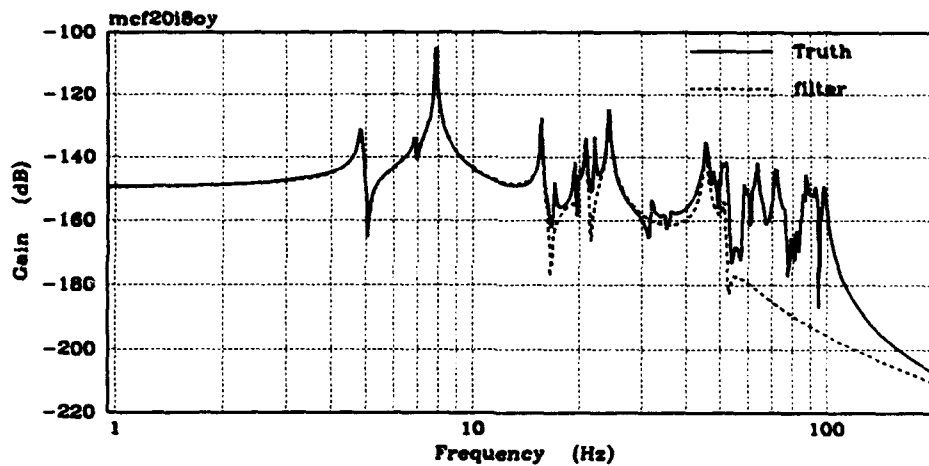


Figure E-17. Truth vs. 10-mode Modal-Cost Reduced (Disturbance 8, Y LOS)

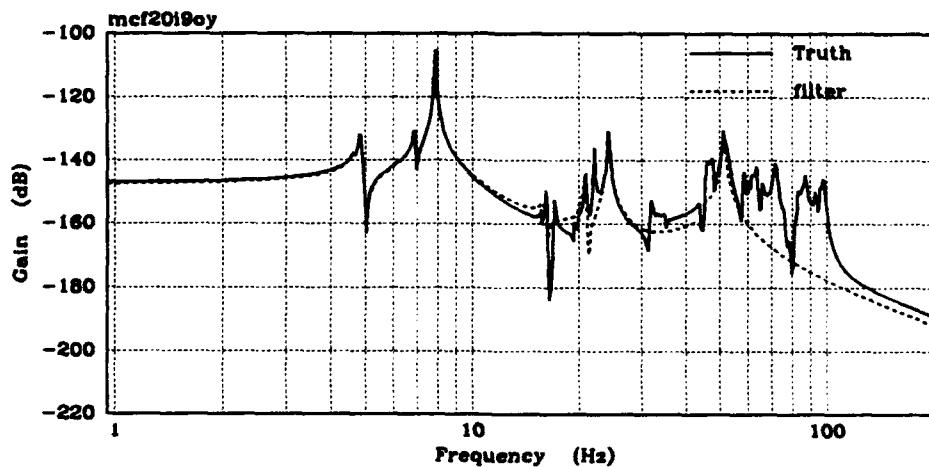


Figure E-18. Truth vs. 10-mode Modal-Cost Reduced (Disturbance 9, Y LOS)

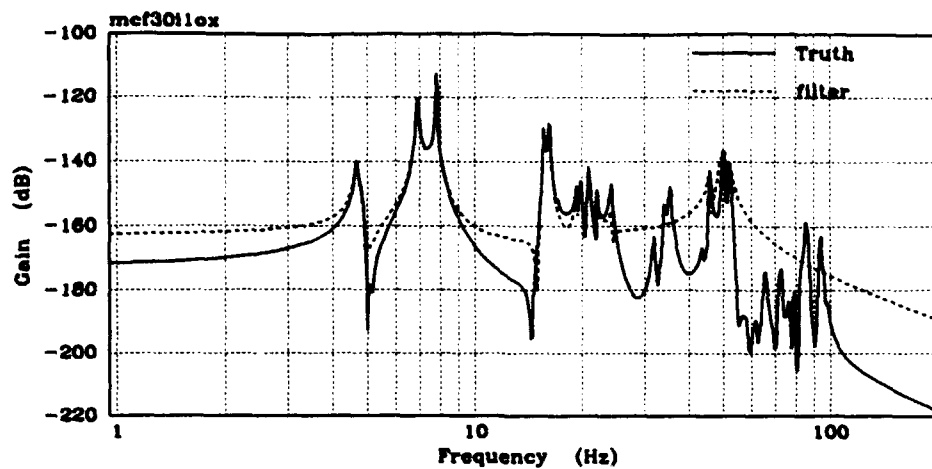


Figure E-19. Truth vs. 15-mode Modal-Cost Reduced (Disturbance 1, X LOS)

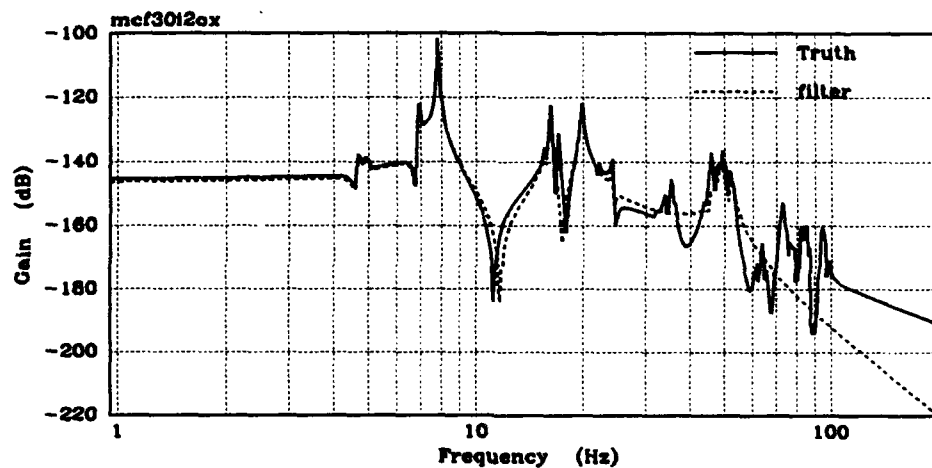


Figure E-20. Truth vs. 15-mode Modal-Cost Reduced (Disturbance 2, X LOS)

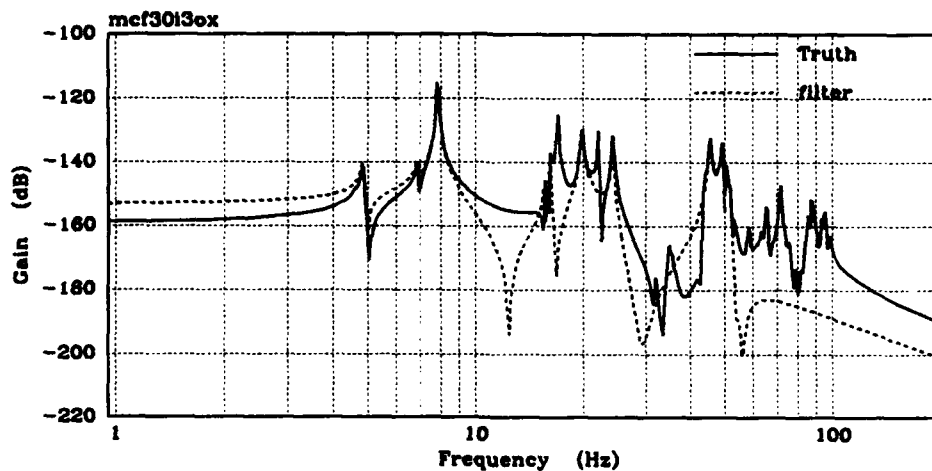


Figure E-21. Truth vs. 15-mode Modal-Cost Reduced (Disturbance 3, X LOS)

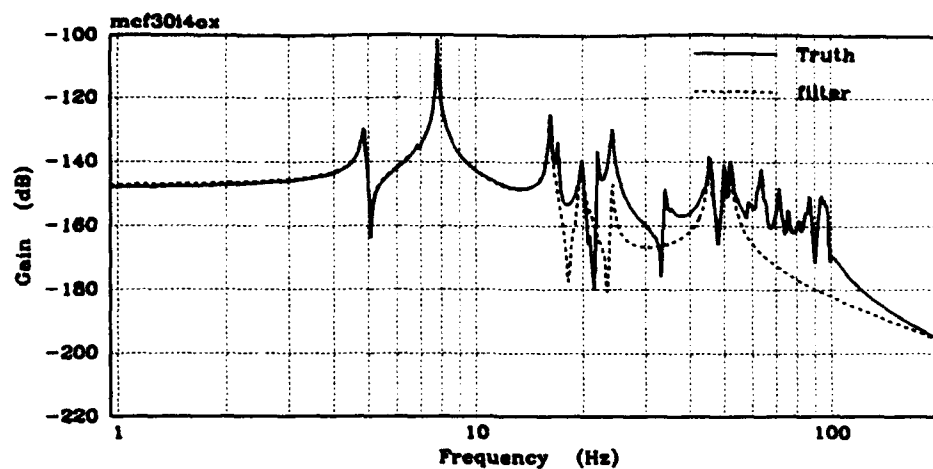


Figure E-22. Truth vs. 15-mode Modal-Cost Reduced (Disturbance 4, X LOS)

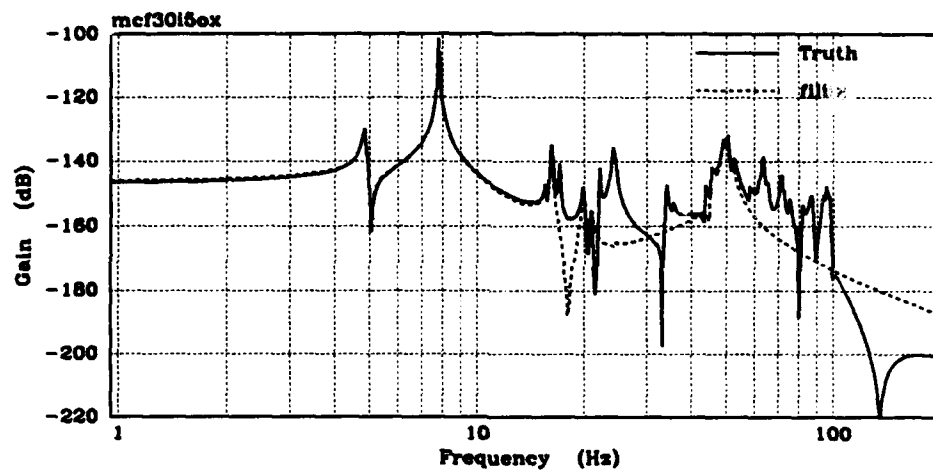


Figure E-23. Truth vs. 15-mode Modal-Cost Reduced (Disturbance 5, X LOS)

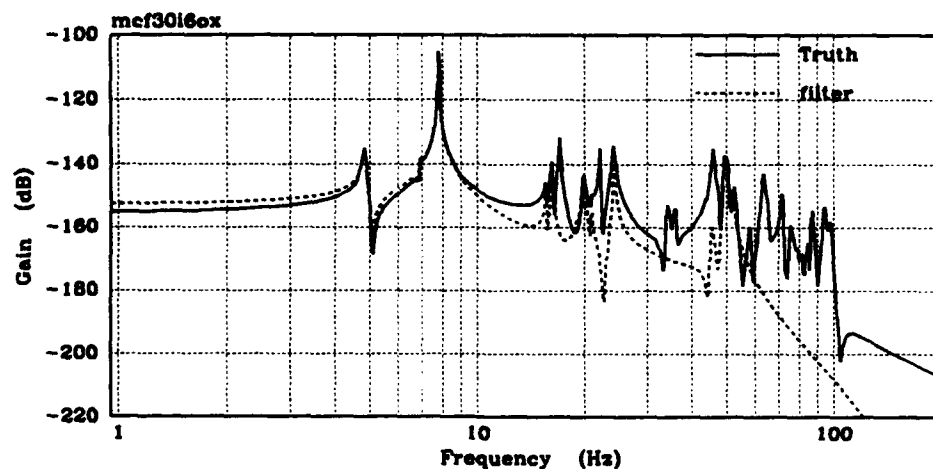


Figure E-24. Truth vs. 15-mode Modal-Cost Reduced (Disturbance 6, X LOS)

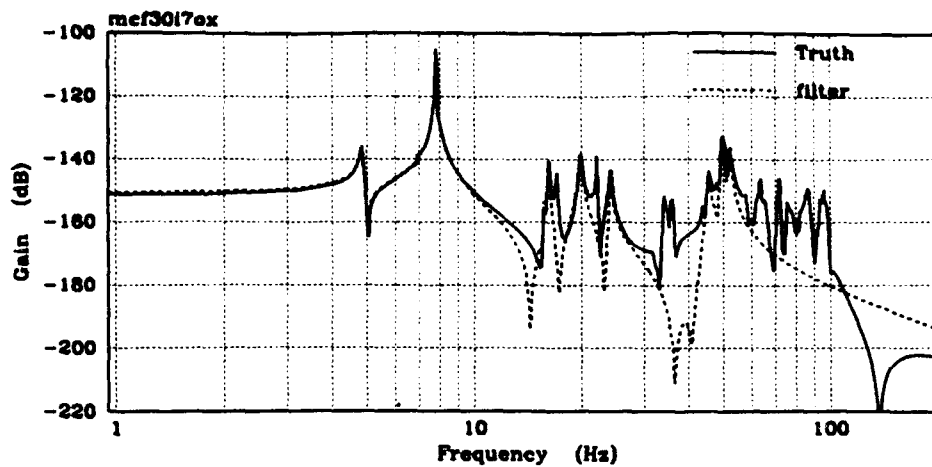


Figure E-25. Truth vs. 15-mode Modal-Cost Reduced (Disturbance 7, X LOS)

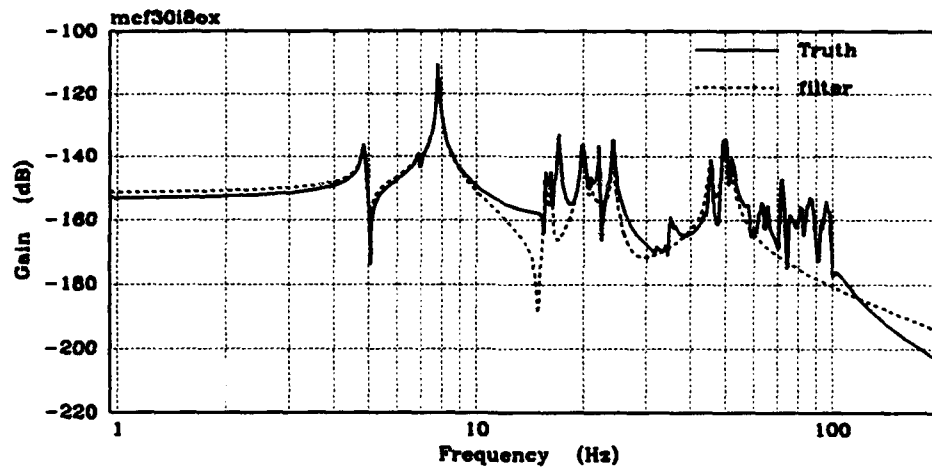


Figure E-26. Truth vs. 15-mode Modal-Cost Reduced (Disturbance 8, X LOS)

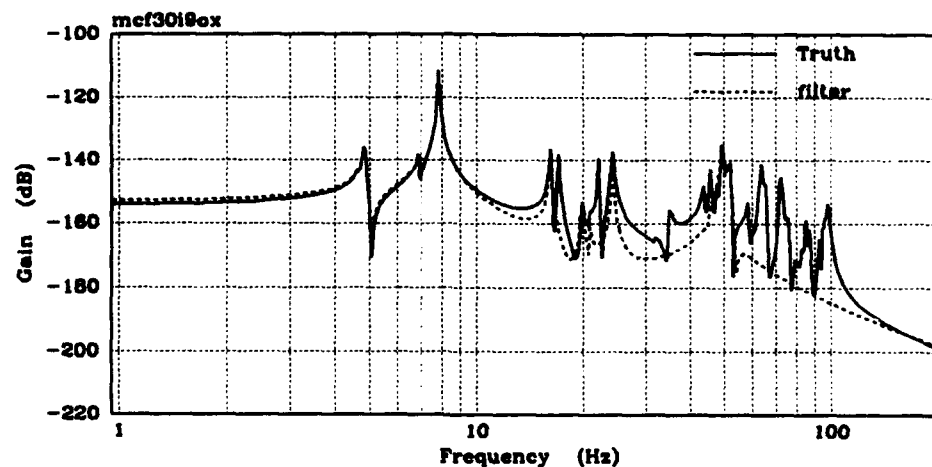


Figure E-27. Truth vs. 15-mode Modal-Cost Reduced (Disturbance 9, X LOS)

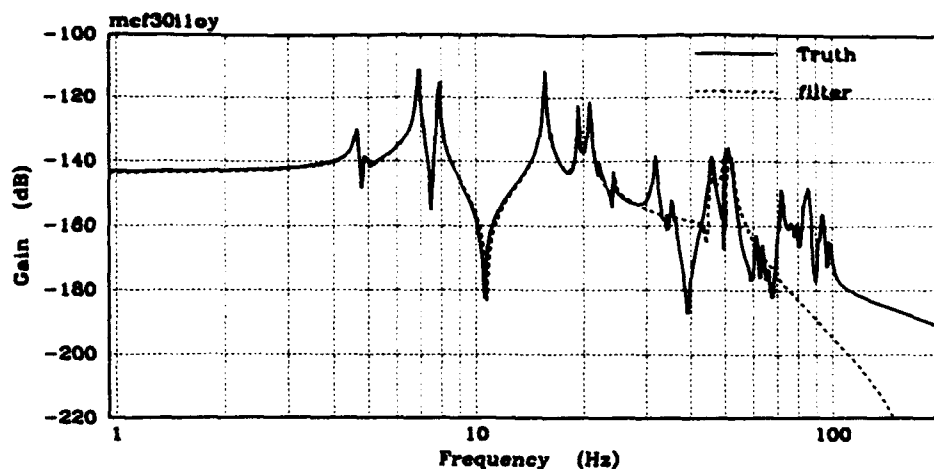


Figure E-28. Truth vs. 15-mode Modal-Cost Reduced (Disturbance 1, Y LOS)

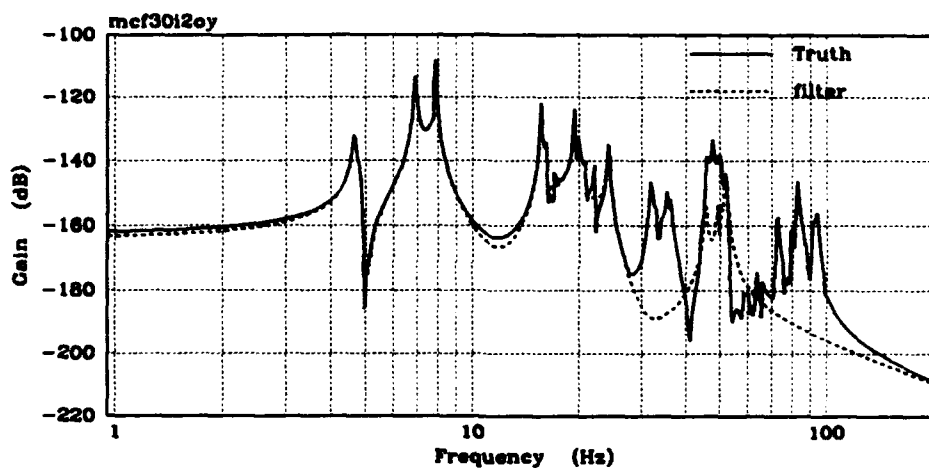


Figure E-29. Truth vs. 15-mode Modal-Cost Reduced (Disturbance 2, Y LOS)

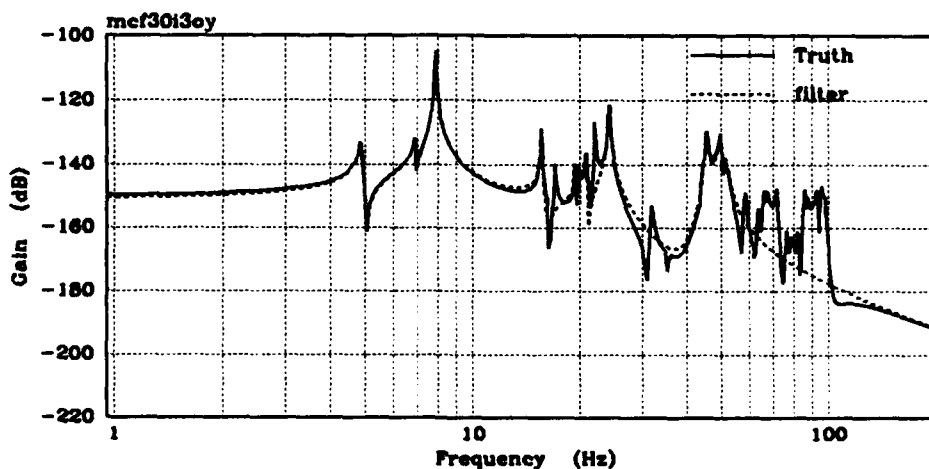


Figure E-30. Truth vs. 15-mode Modal-Cost Reduced (Disturbance 3, Y LOS)



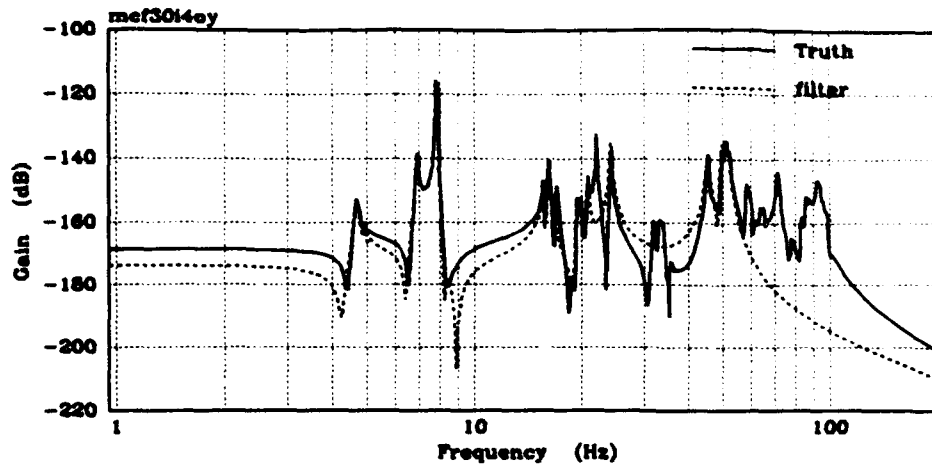


Figure E-31. Truth vs. 15-mode Modal-Cost Reduced (Disturbance 4, Y LOS)

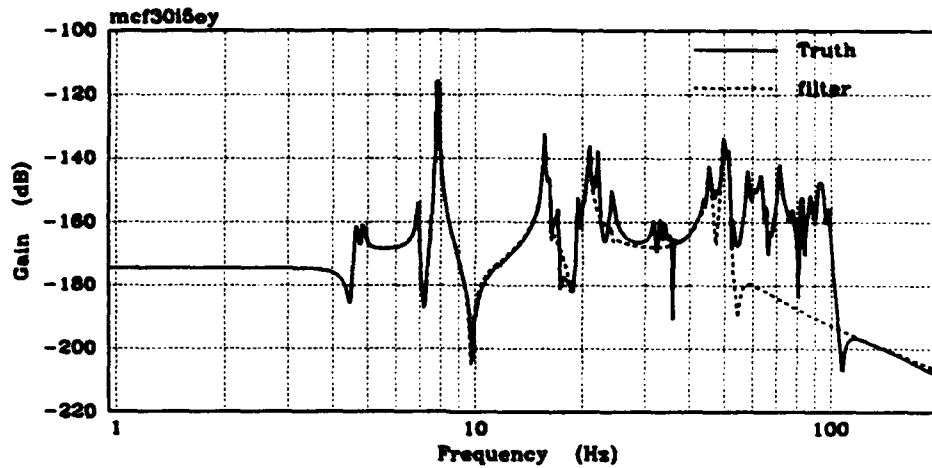


Figure E-32. Truth vs. 15-mode Modal-Cost Reduced (Disturbance 5, Y LOS)

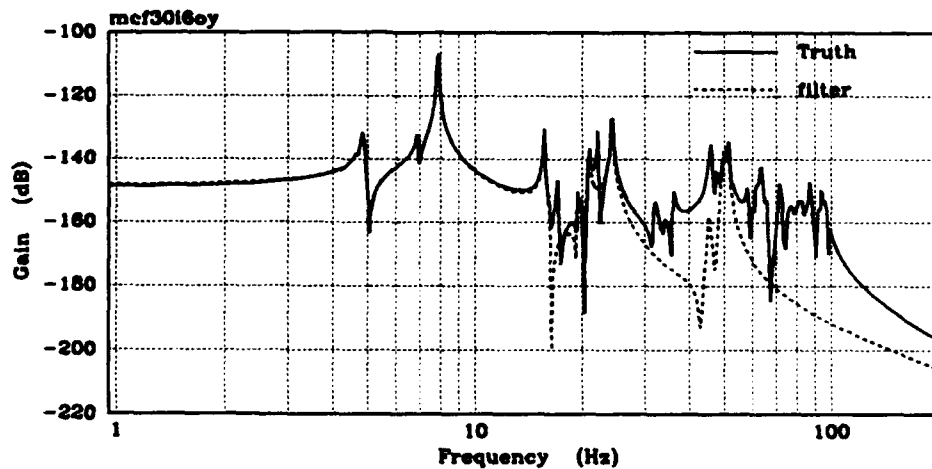


Figure E-33. Truth vs. 15-mode Modal-Cost Reduced (Disturbance 6, Y LOS)

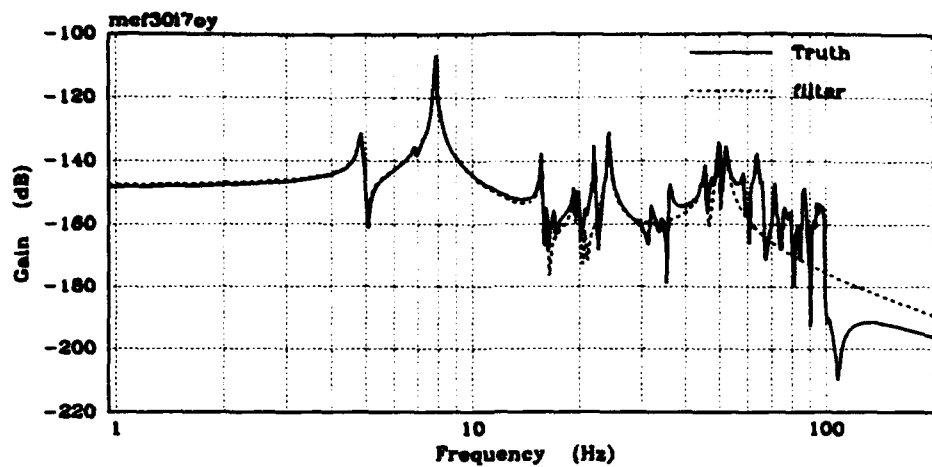


Figure E-34. Truth vs. 15-mode Modal-Cost Reduced (Disturbance 7, Y LOS)

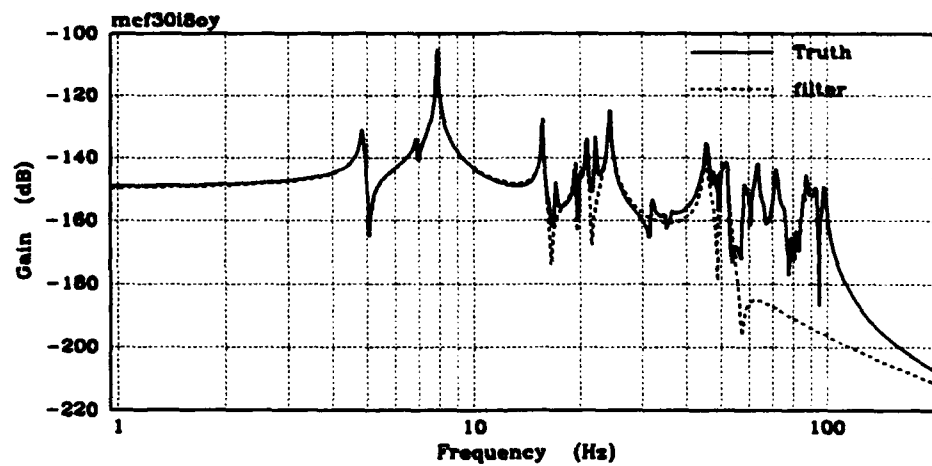


Figure E-35. Truth vs. 15-mode Modal-Cost Reduced (Disturbance 8, Y LOS)

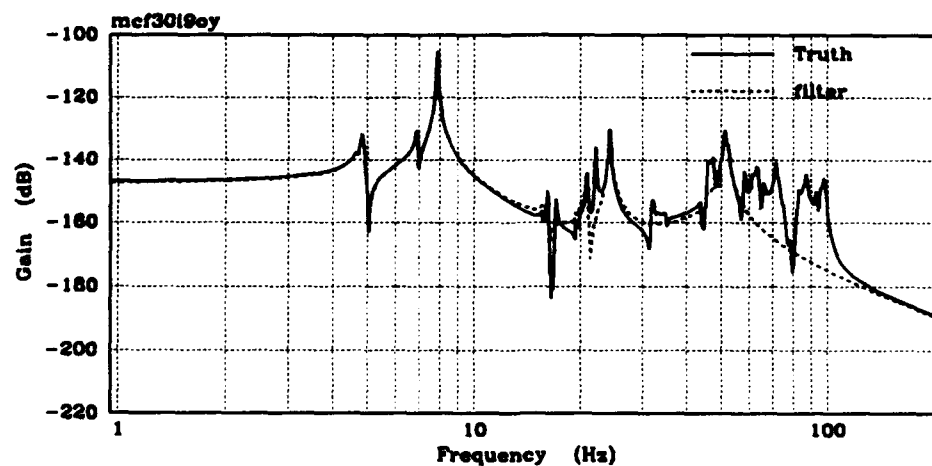


Figure E-36. Truth vs. 15-mode Modal-Cost Reduced (Disturbance 9, Y LOS)

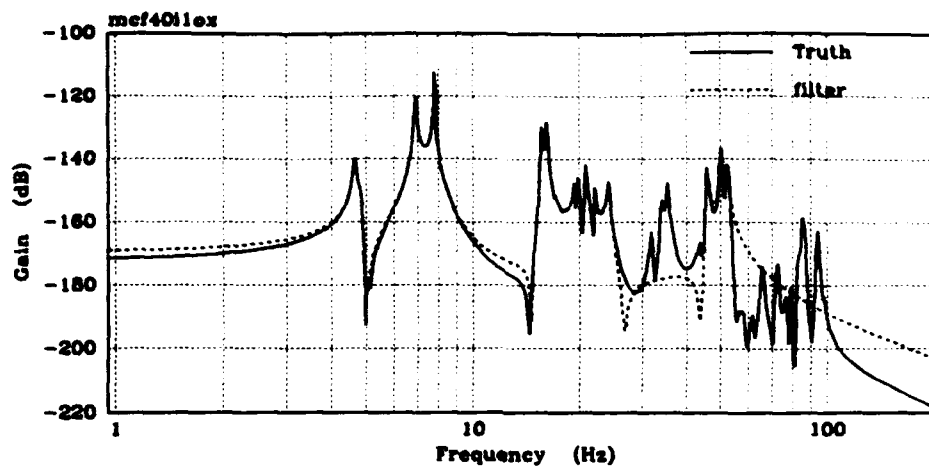


Figure E-37. Truth vs. 20-mode Modal-Cost Reduced (Disturbance 1, X LOS)

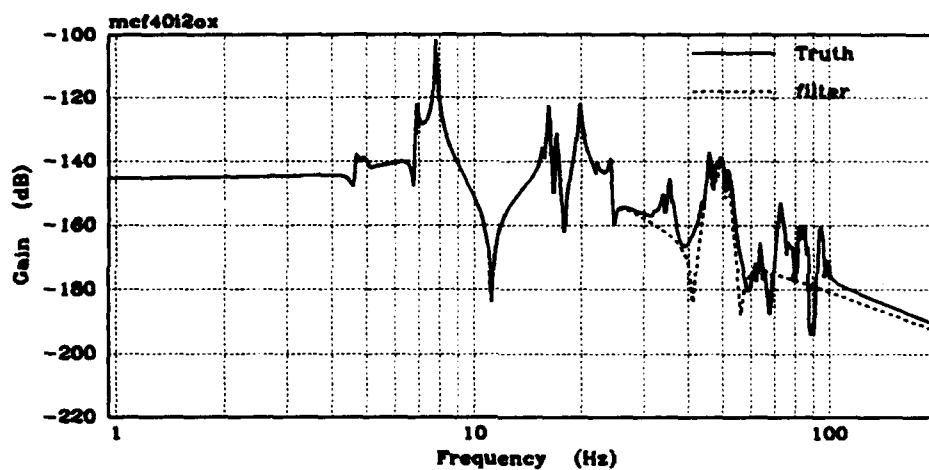


Figure E-38. Truth vs. 20-mode Modal-Cost Reduced (Disturbance 2, X LOS)

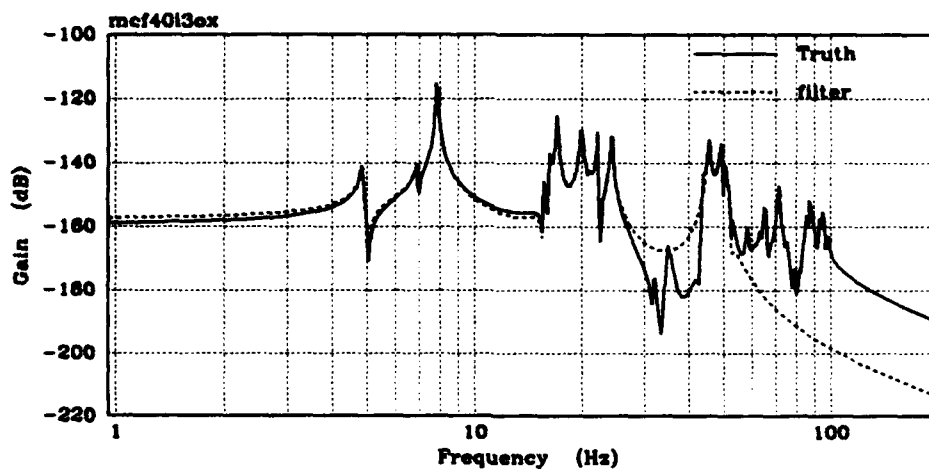


Figure E-39. Truth vs. 20-mode Modal-Cost Reduced (Disturbance 3, X LOS)

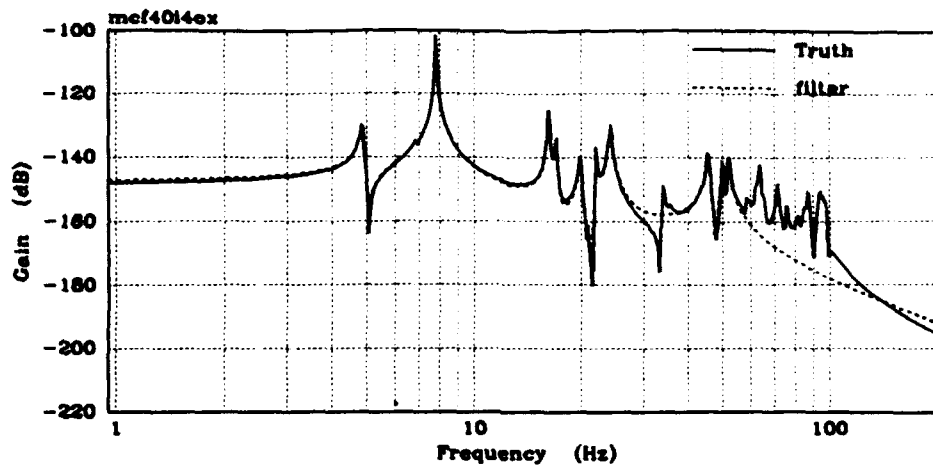


Figure E-40. Truth vs. 20-mode Modal-Cost Reduced (Disturbance 4, X LOS)

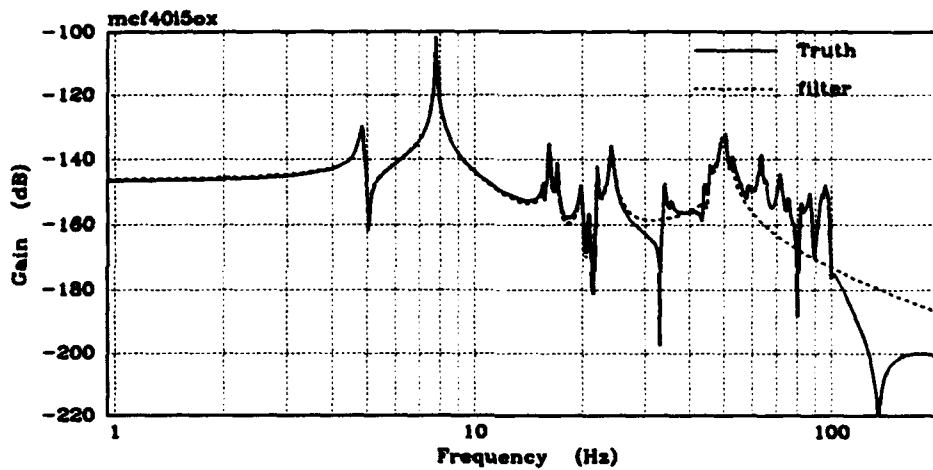


Figure E-41. Truth vs. 20-mode Modal-Cost Reduced (Disturbance 5, X LOS)

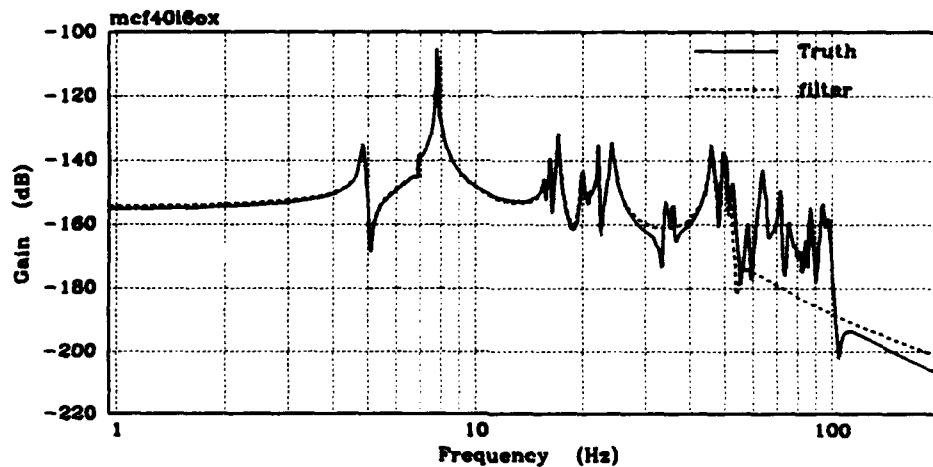


Figure E-42. Truth vs. 20-mode Modal-Cost Reduced (Disturbance 6, X LOS)

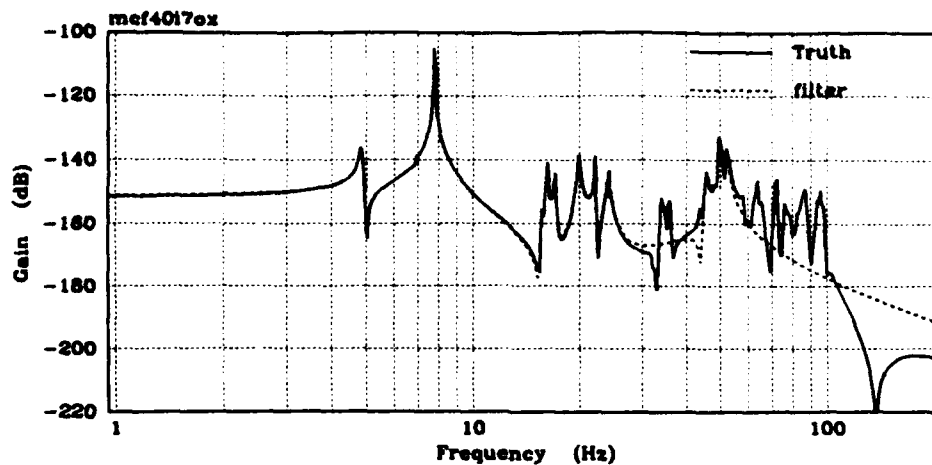


Figure E-43. Truth vs. 20-mode Modal-Cost Reduced (Disturbance 7, X LOS)

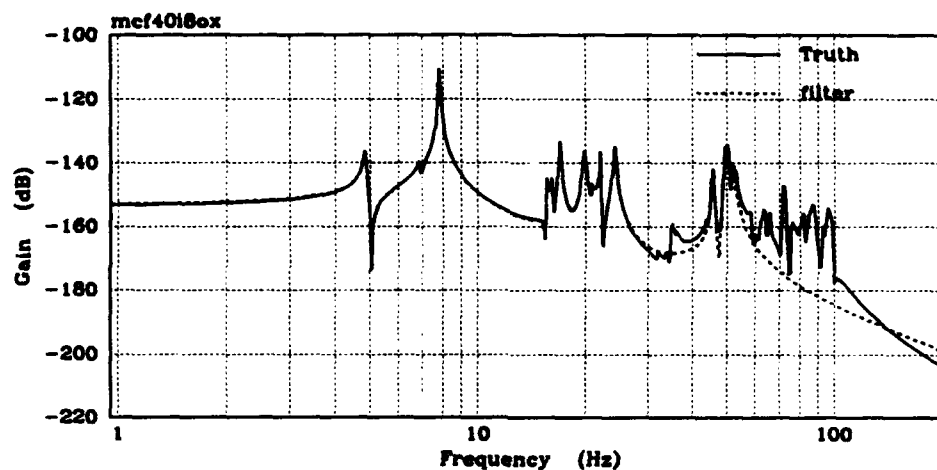


Figure E-44. Truth vs. 20-mode Modal-Cost Reduced (Disturbance 8, X LOS)

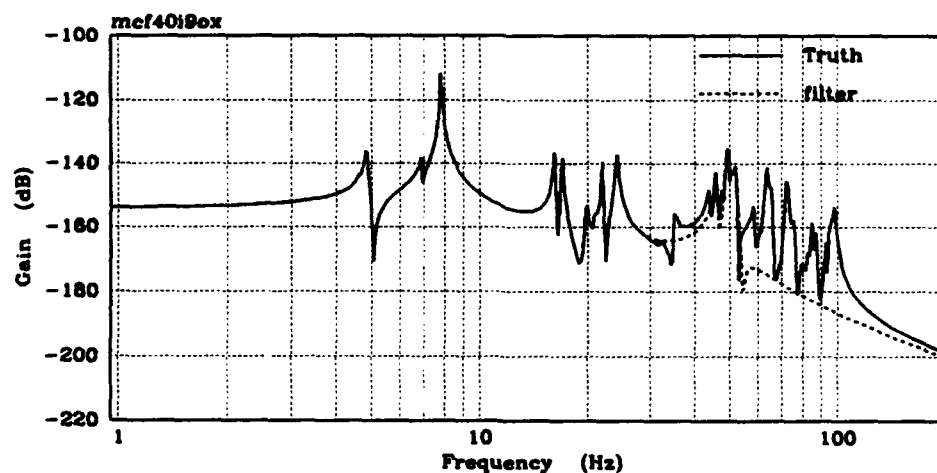


Figure E-45. Truth vs. 20-mode Modal-Cost Reduced (Disturbance 9, X LOS)

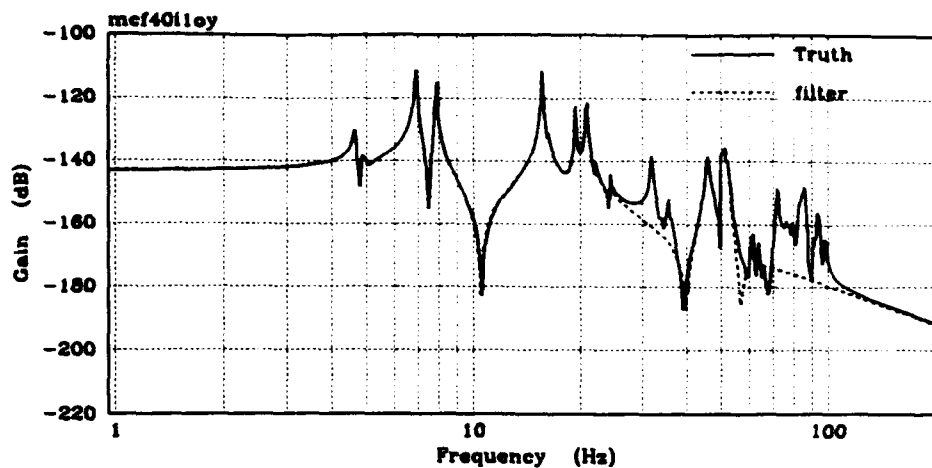


Figure E-46. Truth vs. 20-mode Modal-Cost Reduced (Disturbance 1, Y LOS)

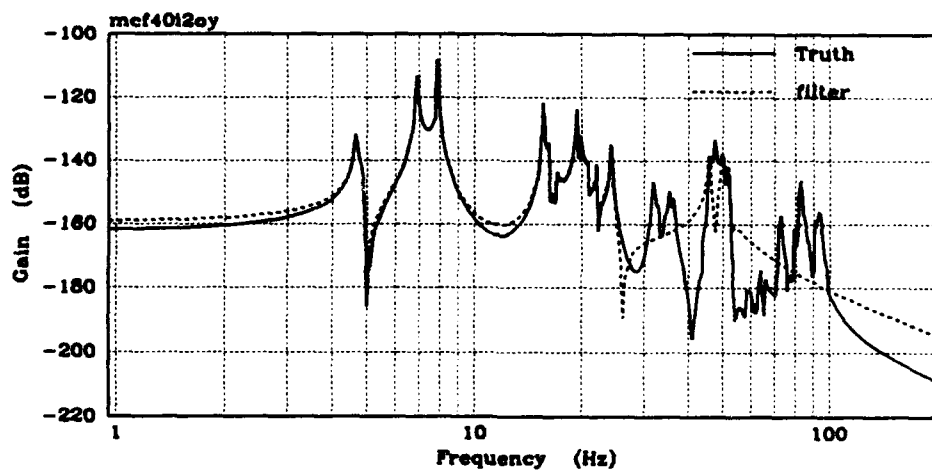


Figure E-47. Truth vs. 20-mode Modal-Cost Reduced (Disturbance 2, Y LOS)

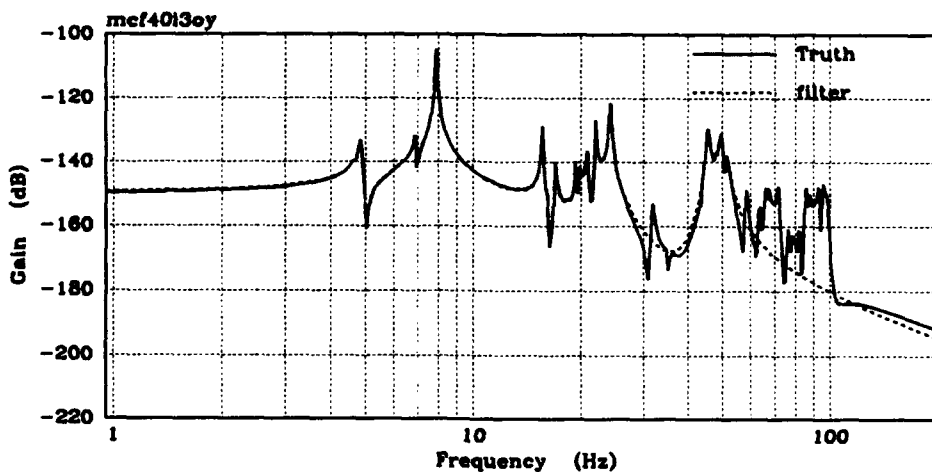


Figure E-48. Truth vs. 20-mode Modal-Cost Reduced (Disturbance 3, Y LOS)

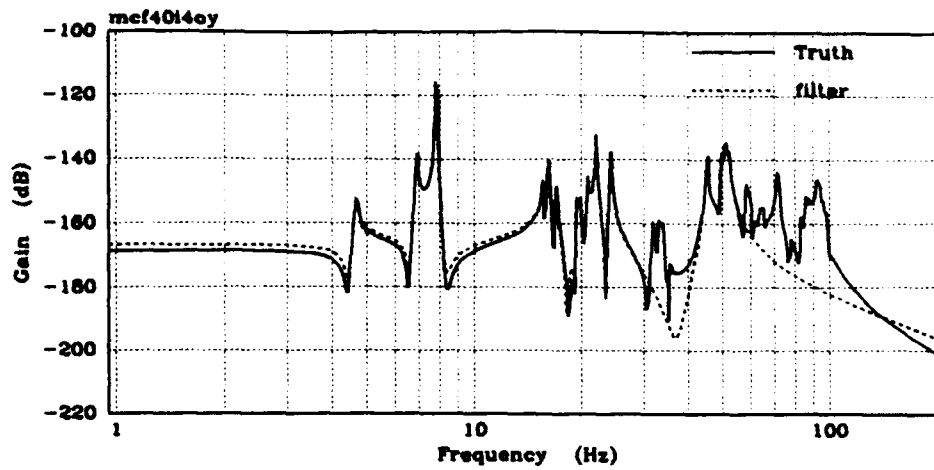


Figure E-49. Truth vs. 20-mode Modal-Cost Reduced (Disturbance 4, Y LOS)

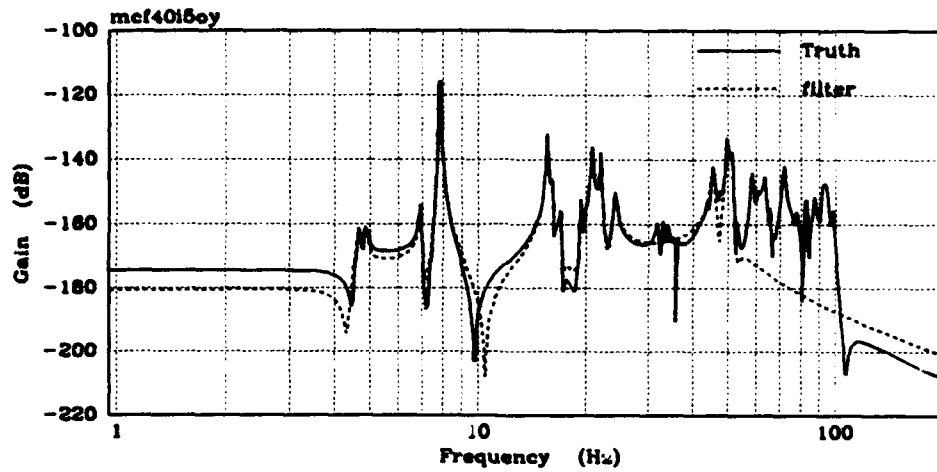


Figure E-50. Truth vs. 20-mode Modal-Cost Reduced (Disturbance 5, Y LOS)

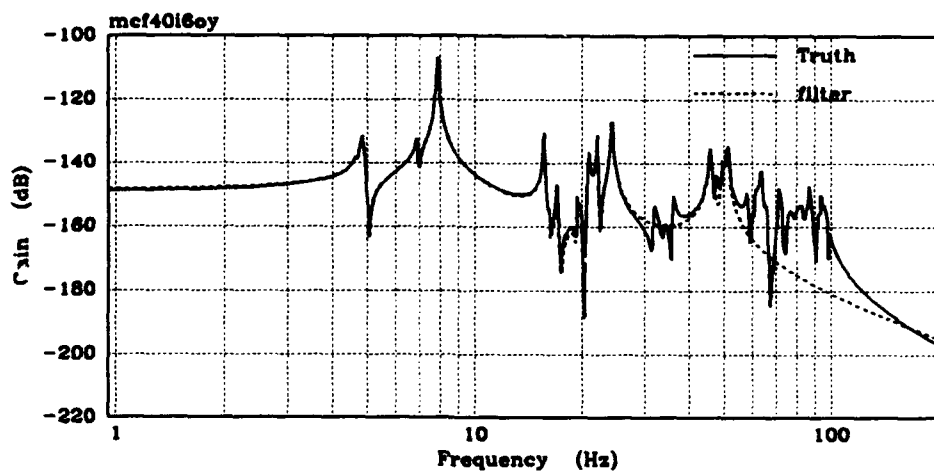


Figure E-51. Truth vs. 20-mode Modal-Cost Reduced (Disturbance 6, Y LOS)

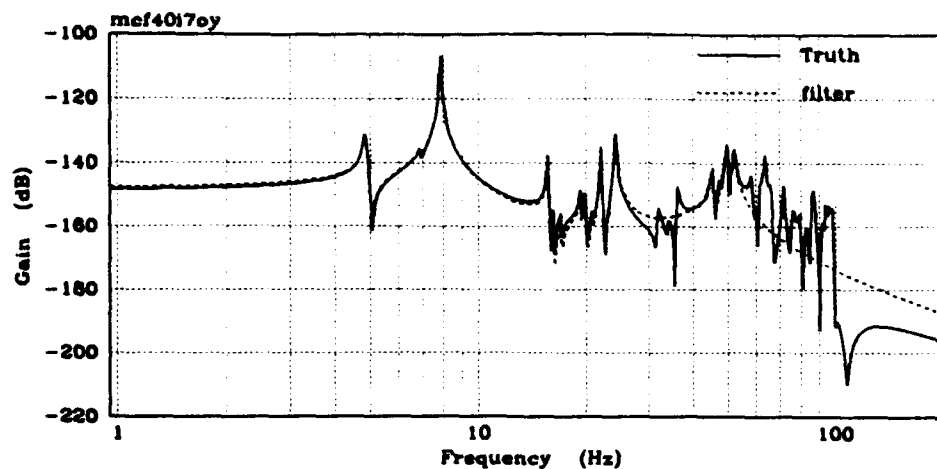


Figure E-52. Truth vs. 20-mode Modal-Cost Reduced (Disturbance 7, Y LOS)

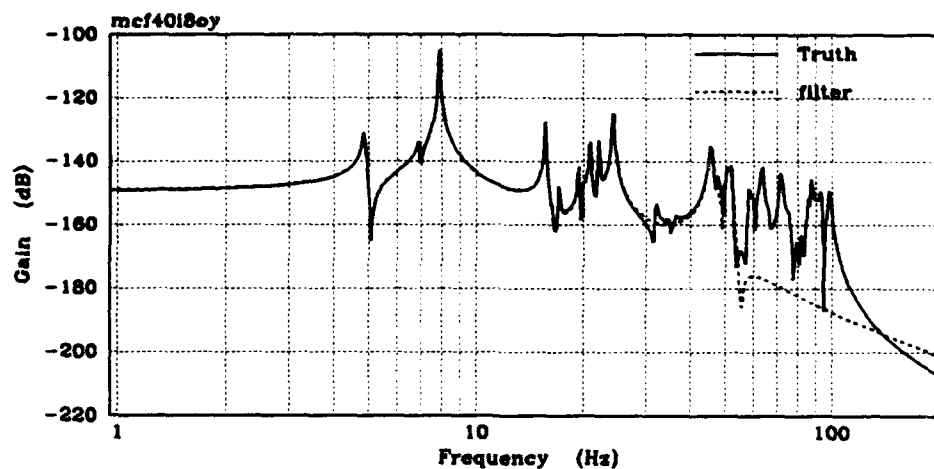


Figure E-53. Truth vs. 20-mode Modal-Cost Reduced (Disturbance 8, Y LOS)

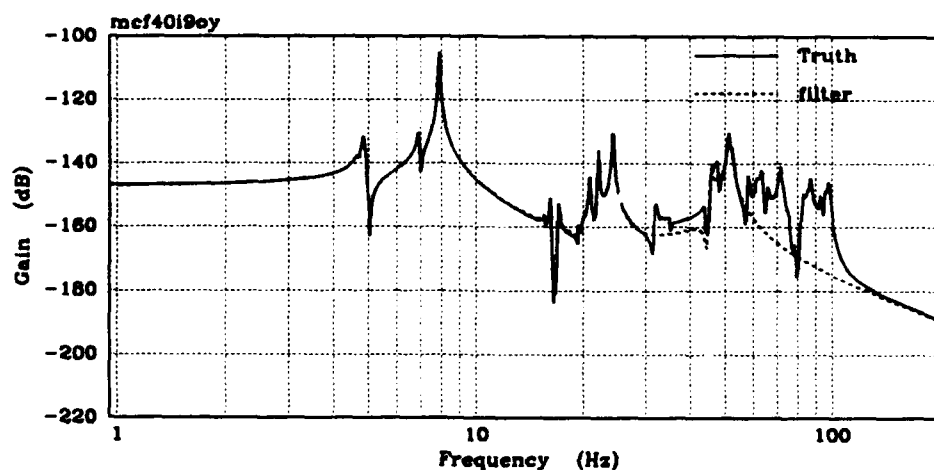


Figure E-54. Truth vs. 20-mode Modal-Cost Reduced (Disturbance 9, Y LOS)



### **Appendix F: Single Filter Model Analysis**

This appendix presents all the individual tuning parameters in Table F-1 and all the plot results for each filter model. Section 5.2.1 discusses the generation of  $Q_f$  and  $R_f$ , respectively. Section 4.4.2 (Equation (4.10)) and Section 5.2.2 discusses the generation of the  $1/p_x$  values. Plots F-1, 2 illustrate the open loop response of the truth model (no LQG control). For each of the filter plots groups, the first two plots illustrate the filter tuning about the X and Y LOS axis, respectively (as discussed in Section 5.2.1). The next two plots illustrate each filter/controller's performance about the X and Y LOS axis, respectively, when closed loop LQG control is applied.

Filter Model	$Q_f$	$R_f$	$1/p_x$
Truth filter	1	.007	1
12-Modal	3	0.08	25
18-Modal	3	.004	21
26-Modal	2	.004	2.5
10-Modal-Cost	4	0.4	6
15-Modal-Cost	3	0.3	5.9
20-Modal-Cost	3	.08	6
26-Modal-Cost	2	.003	2.5
26-Modal-Trunc.	2	.004	2

Table F-1. Filter Model Tuning Parameters

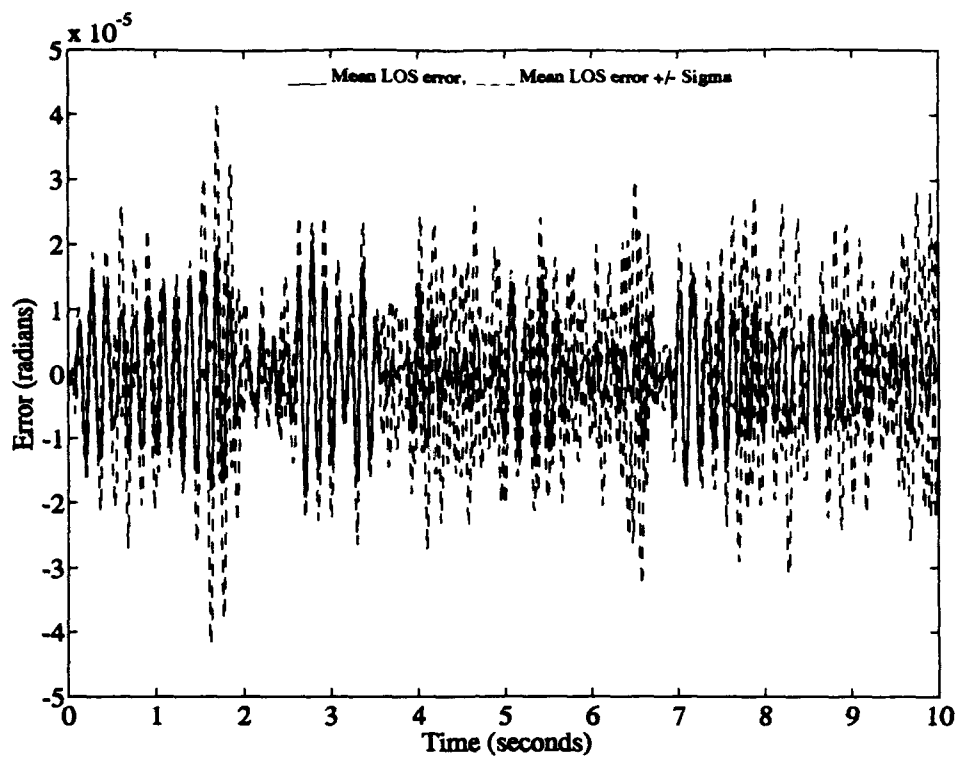


Figure F-1. Truth Model X-Axis LOS Error - with No Control Applied

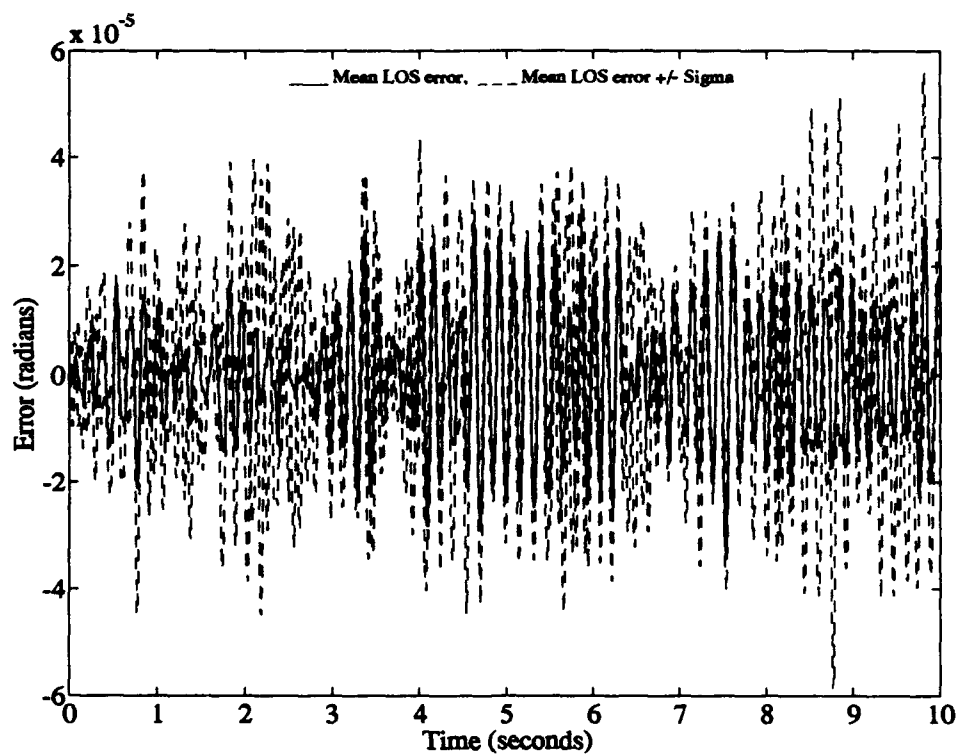


Figure F-2. Truth Model Y-Axis LOS Error - with No Control Applied

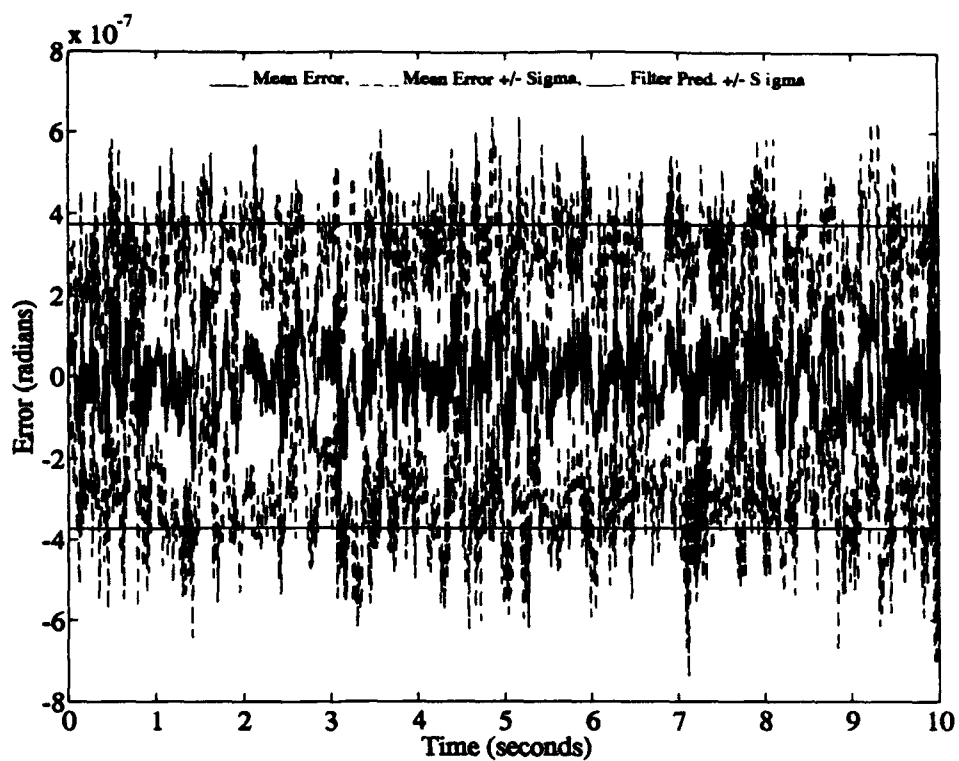


Figure F-3. Truth-Model-Based Filter X-Axis Estimation Error

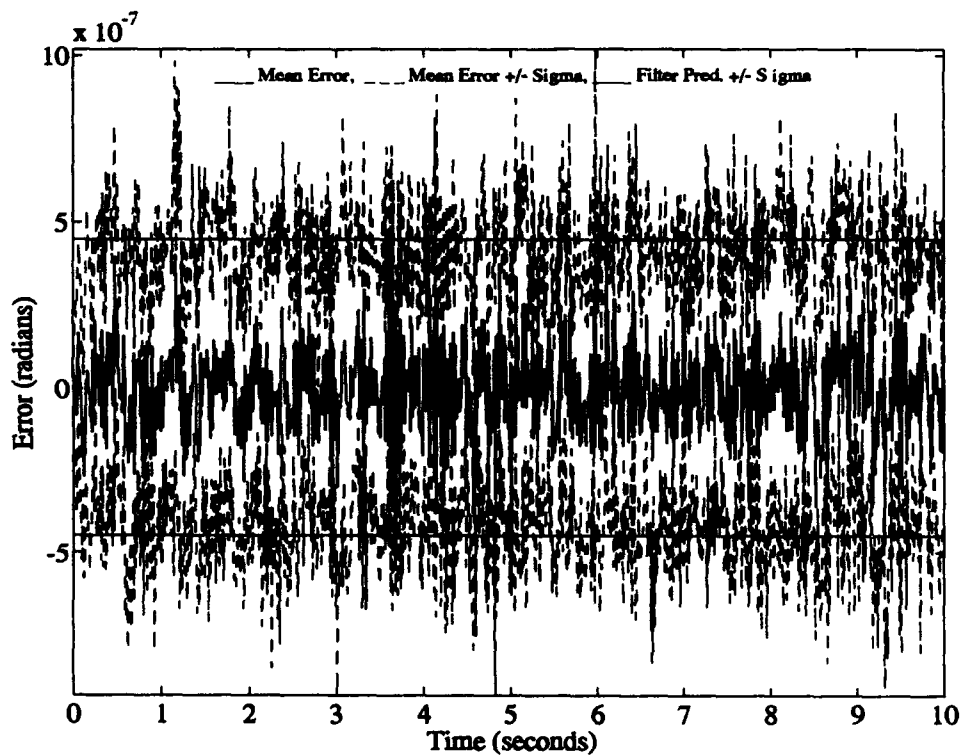


Figure F-4. Truth-Model-Based Filter Y-Axis Estimation Error

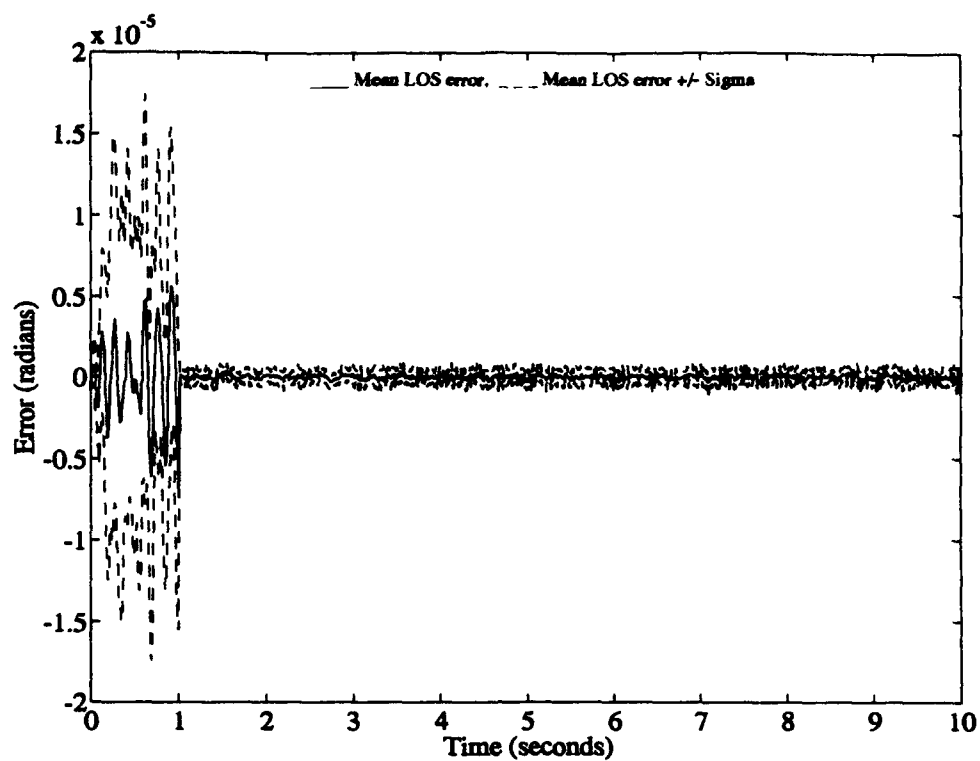


Figure F-5. Truth-Model-Based Controller X-Axis LOS Error - With Control Applied

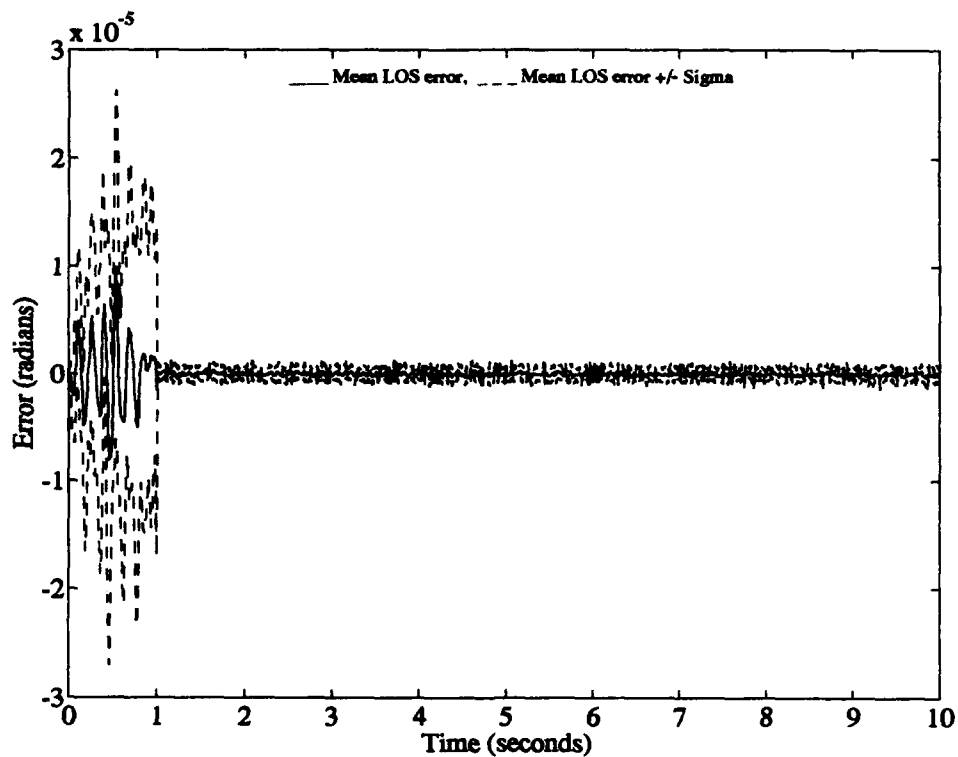


Figure F-6. Truth-Model-Based Controller Y-Axis LOS Error - With Control Applied

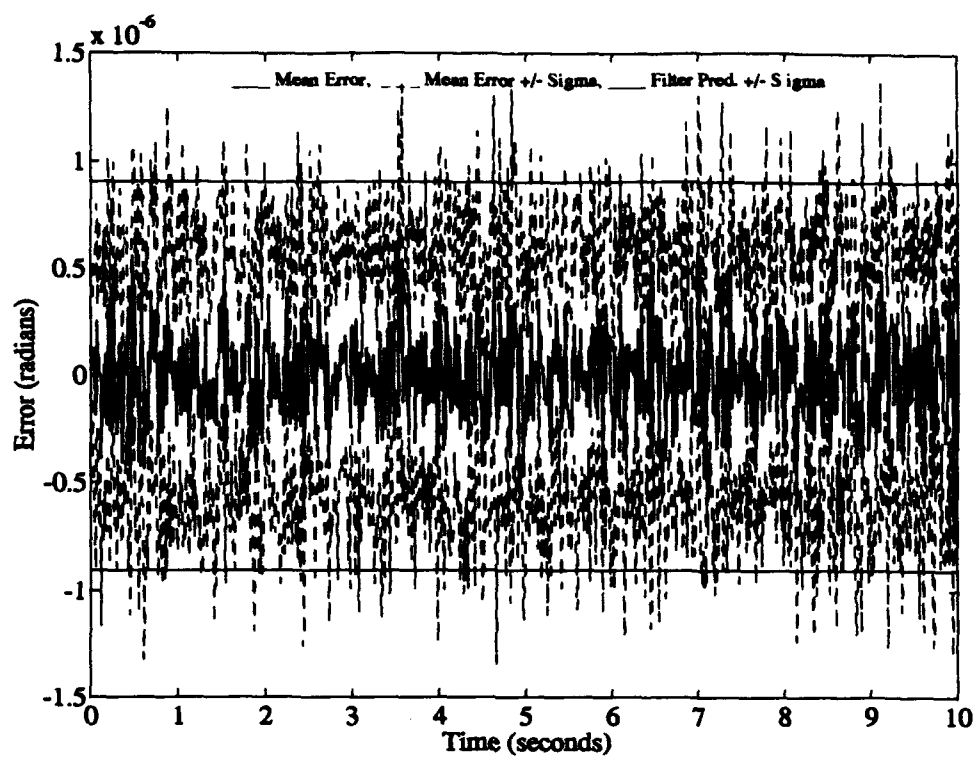


Figure F-7. 12-Modal Model Filter X-Axis Estimation Error

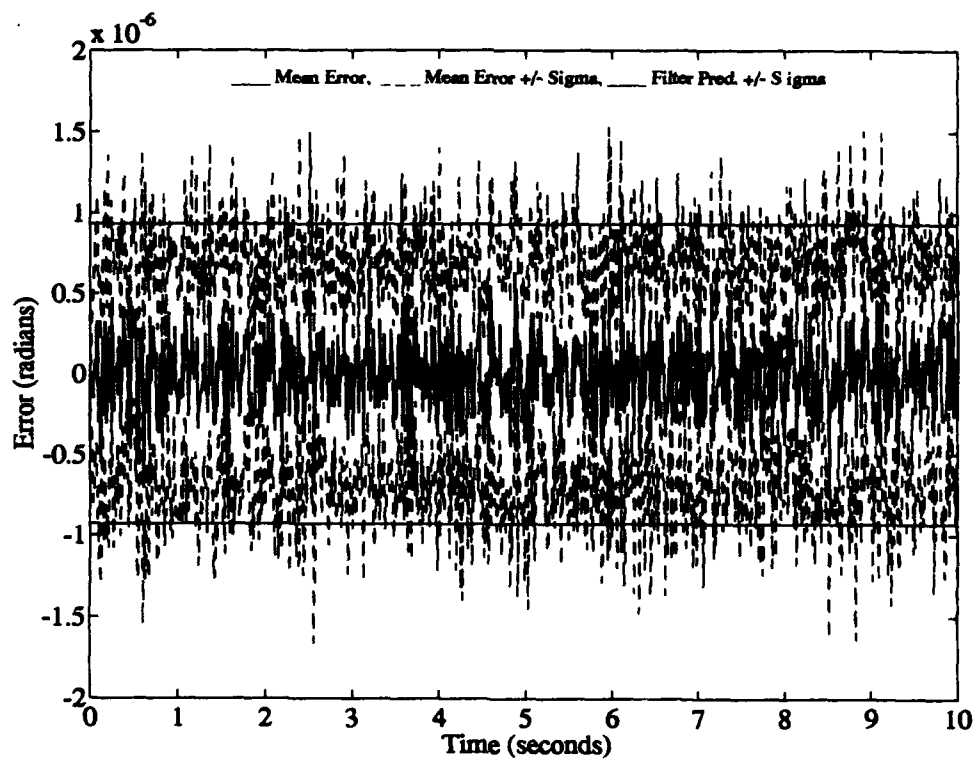


Figure F-8. 12-Modal Model Filter Y-Axis Estimation Error

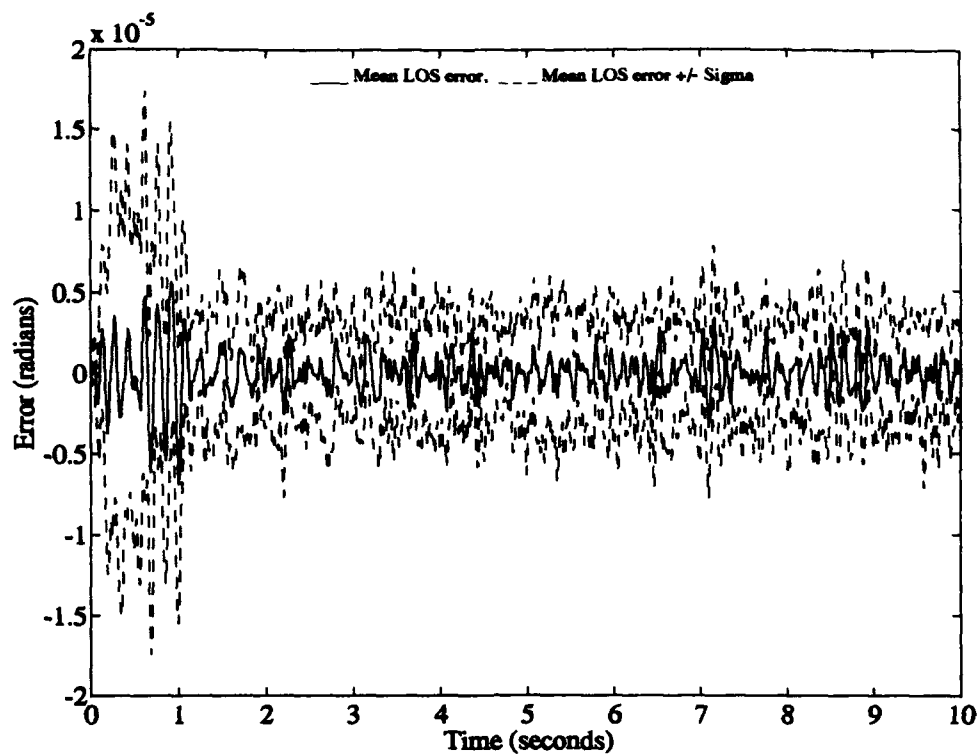


Figure F-9. 12-Modal Model Controller X-Axis LOS Error - With Control Applied

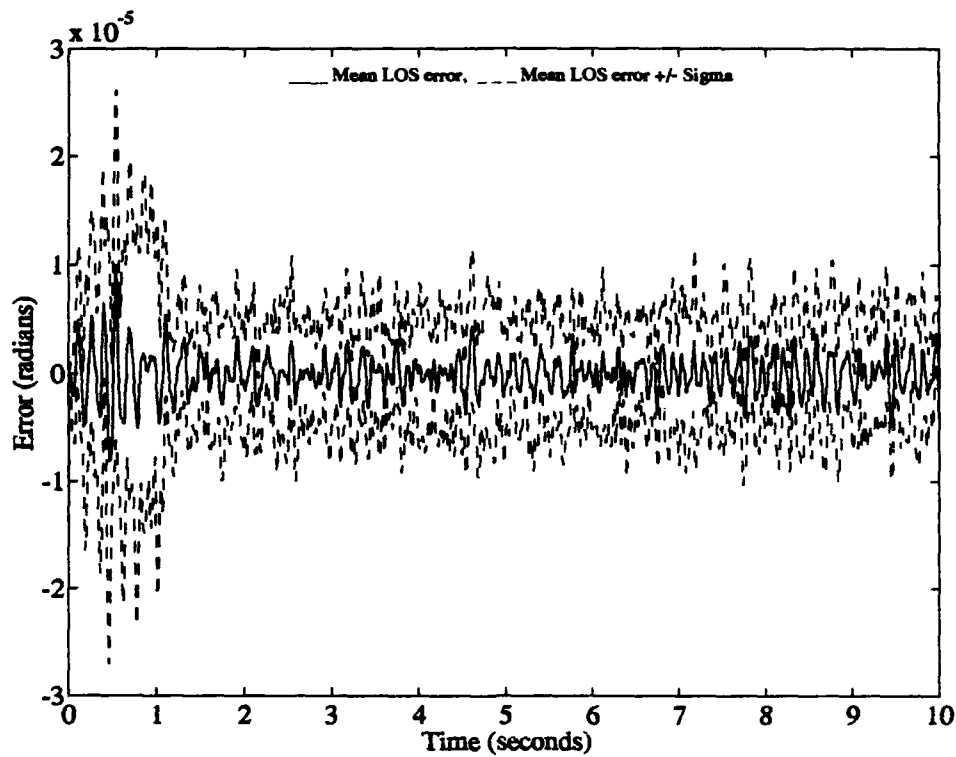


Figure F-10. 12-Modal Model Controller Y-Axis LOS Error - With Control Applied

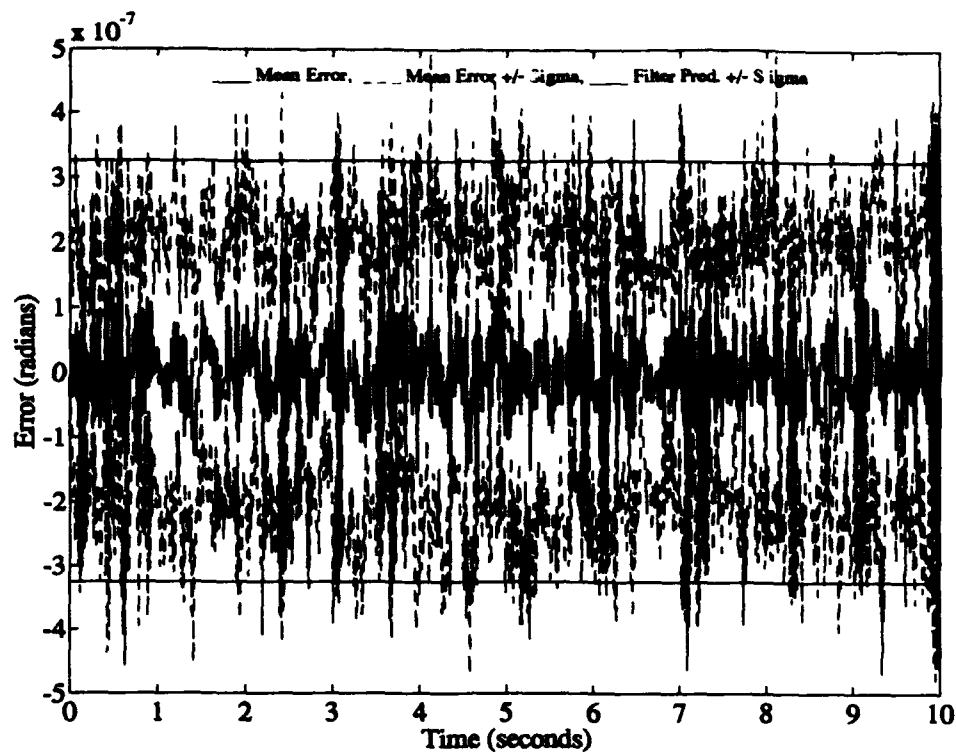


Figure F-11. 18-Modal Model Filter X-Axis Estimation Error

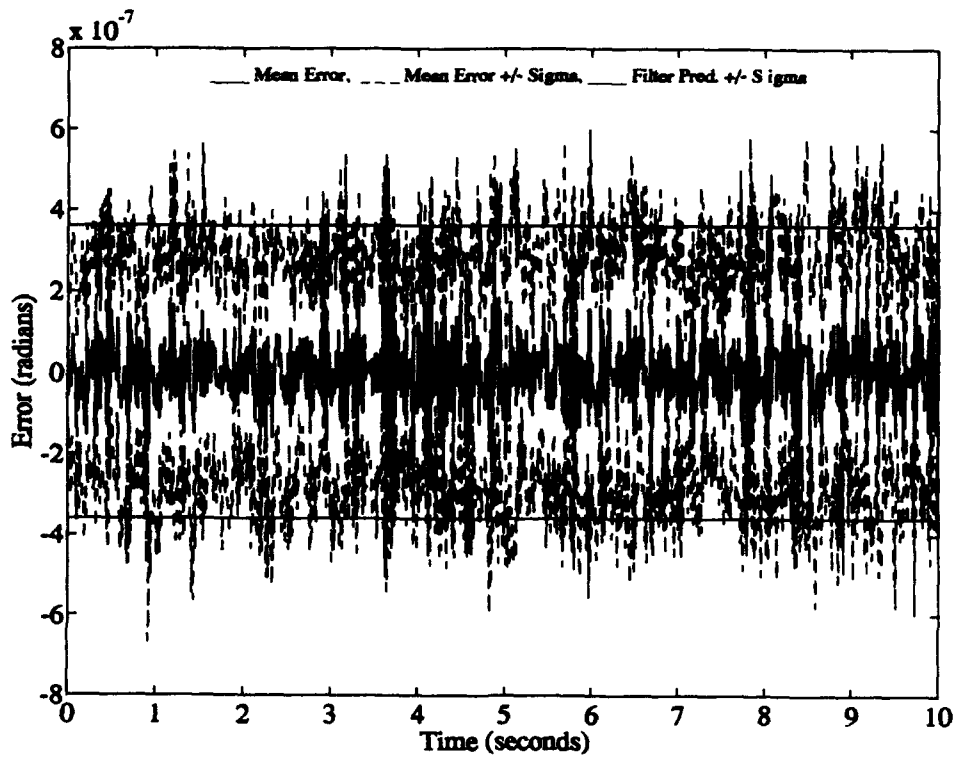


Figure F-12. 18-Modal Model Filter Y-Axis Estimation Error

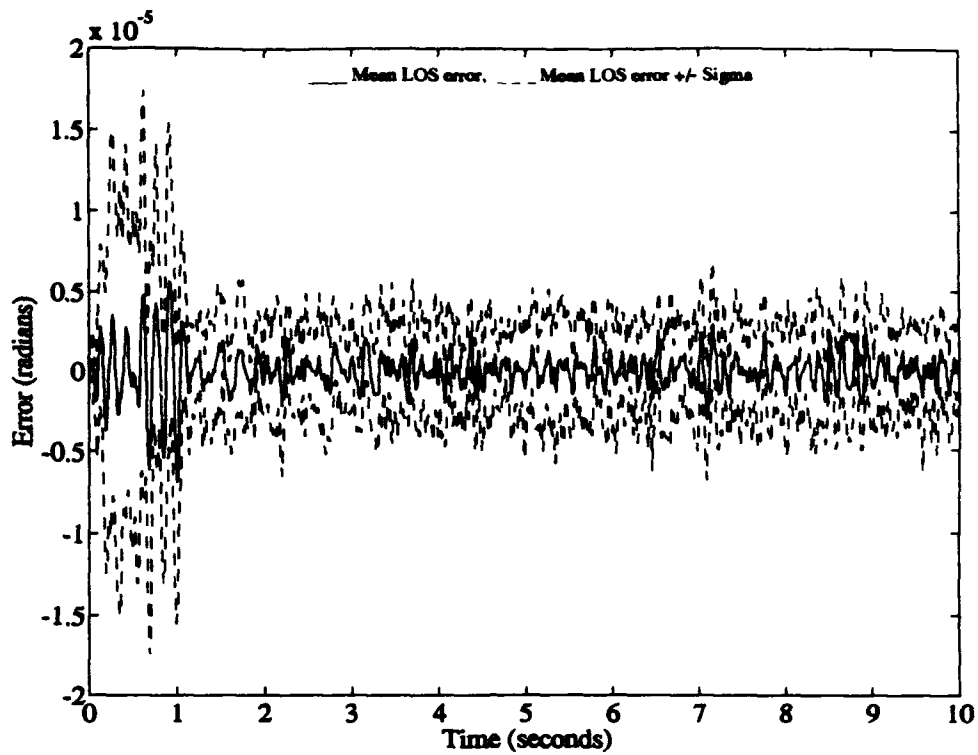


Figure F-13. 18-Modal Model Controller X-Axis LOS Error - With Control Applied

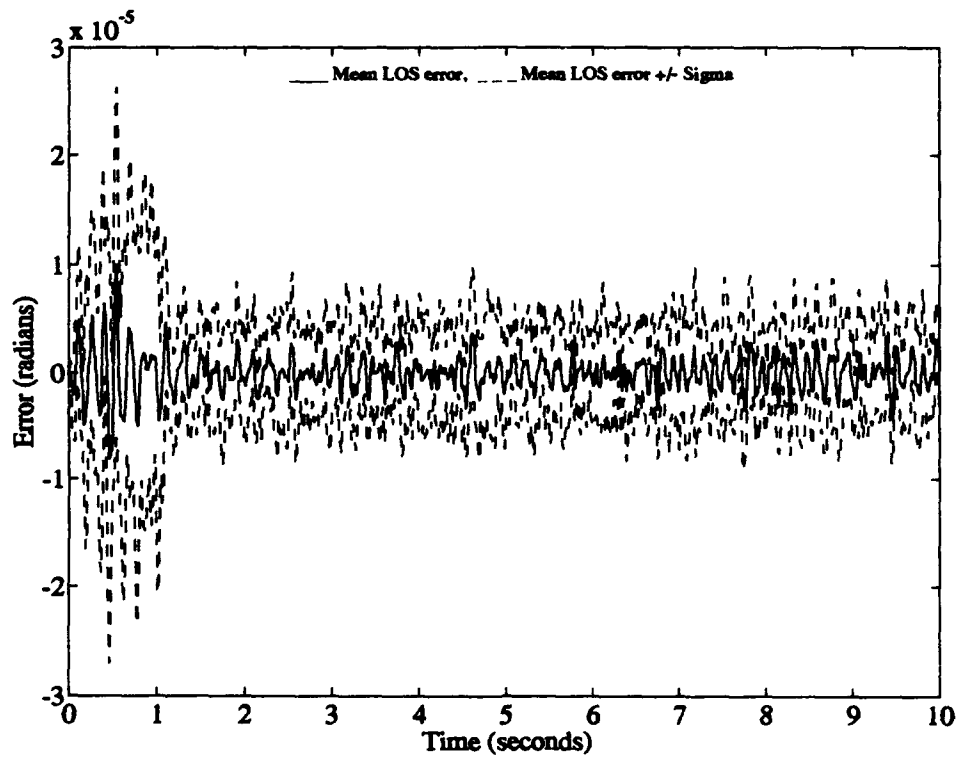


Figure F-14. 18-Modal Model Controller Y-Axis LOS Error - With Control Applied



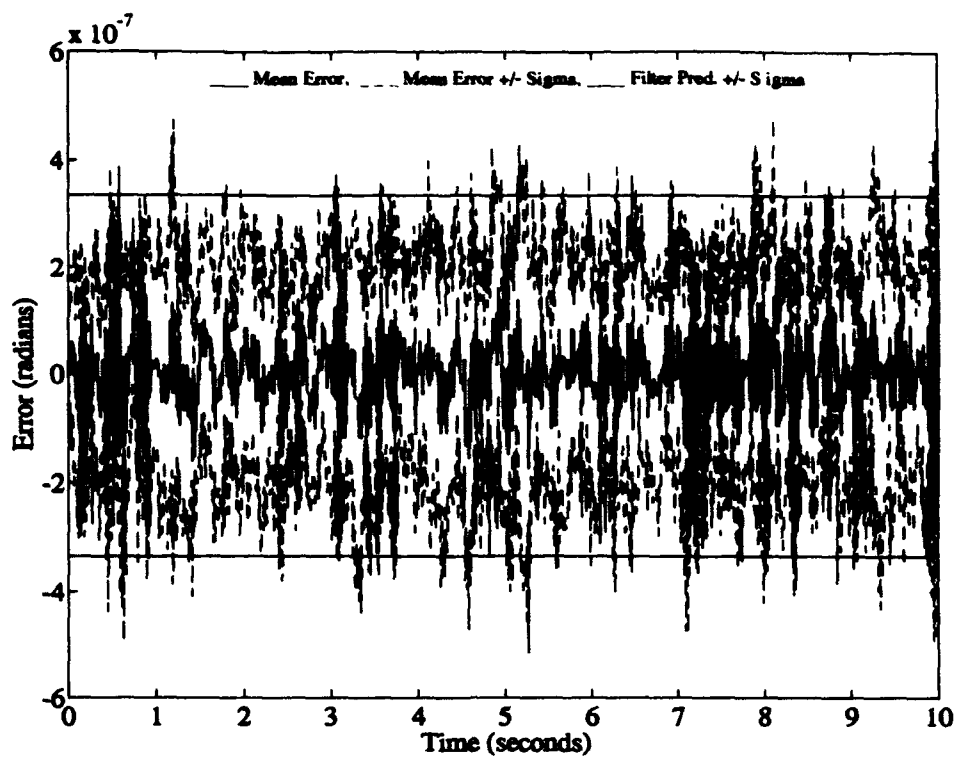


Figure F-15. 26-Modal Model Filter X-Axis Estimation Error

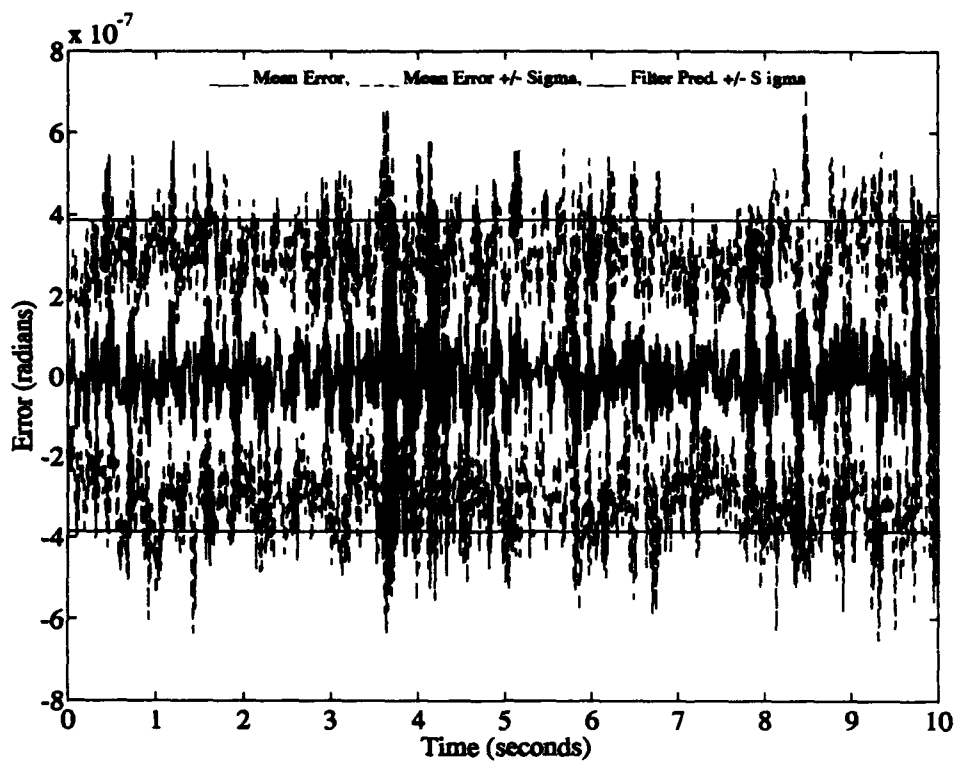


Figure F-16. 26-Modal Model Filter Y-Axis Estimation Error

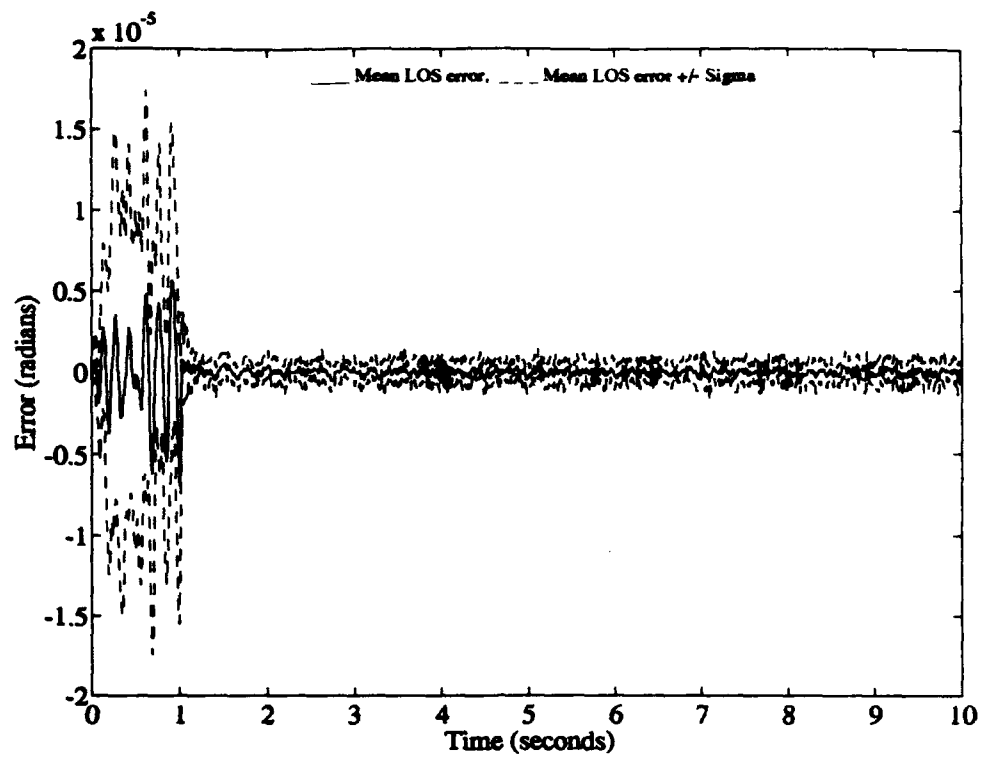


Figure F-17. 26-Modal Model Controller X-Axis LOS Error - With Control Applied

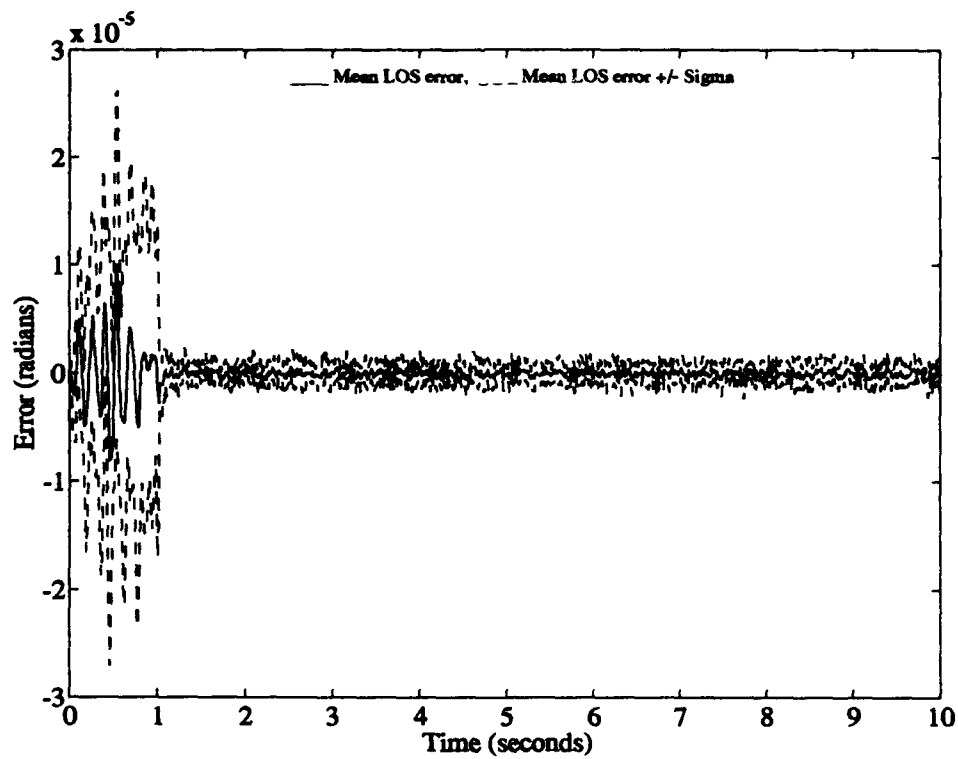


Figure F-18. 26-Modal Model Controller Y-Axis LOS Error - With Control Applied

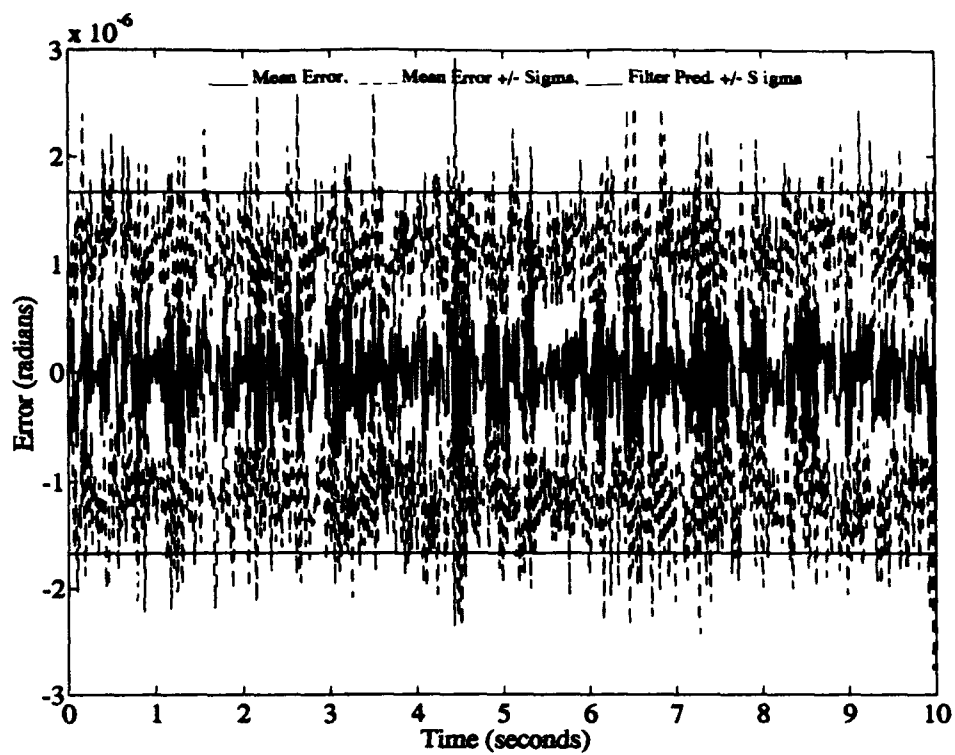


Figure F-19. 10-Modal-Cost Model Filter X-Axis Estimation Error

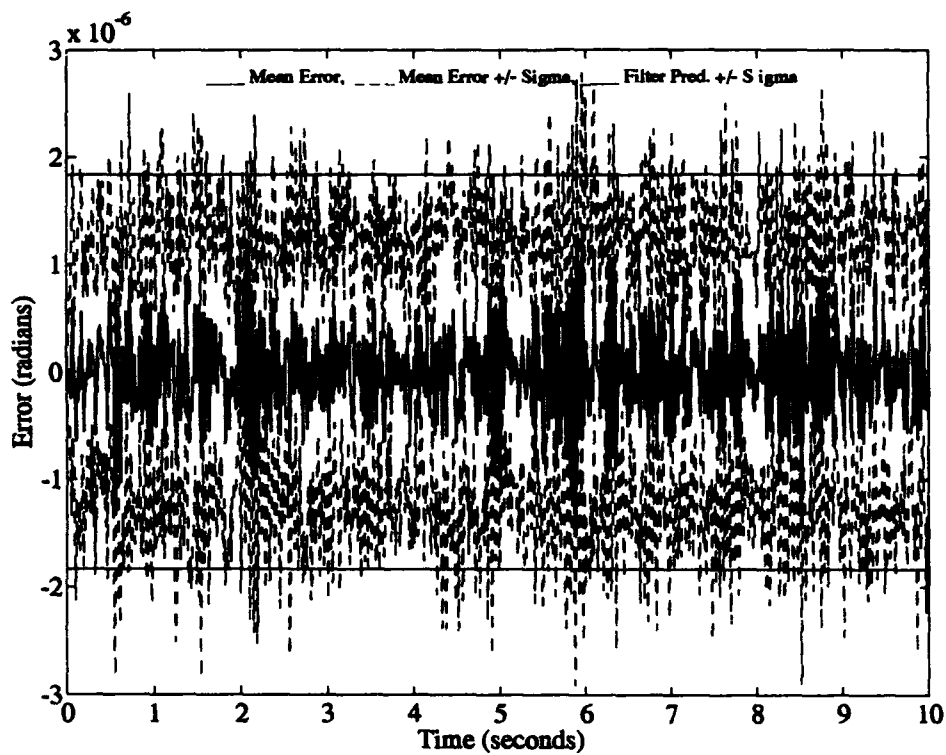


Figure F-20. 10-Modal-Cost Model Filter Y-Axis Estimation Error

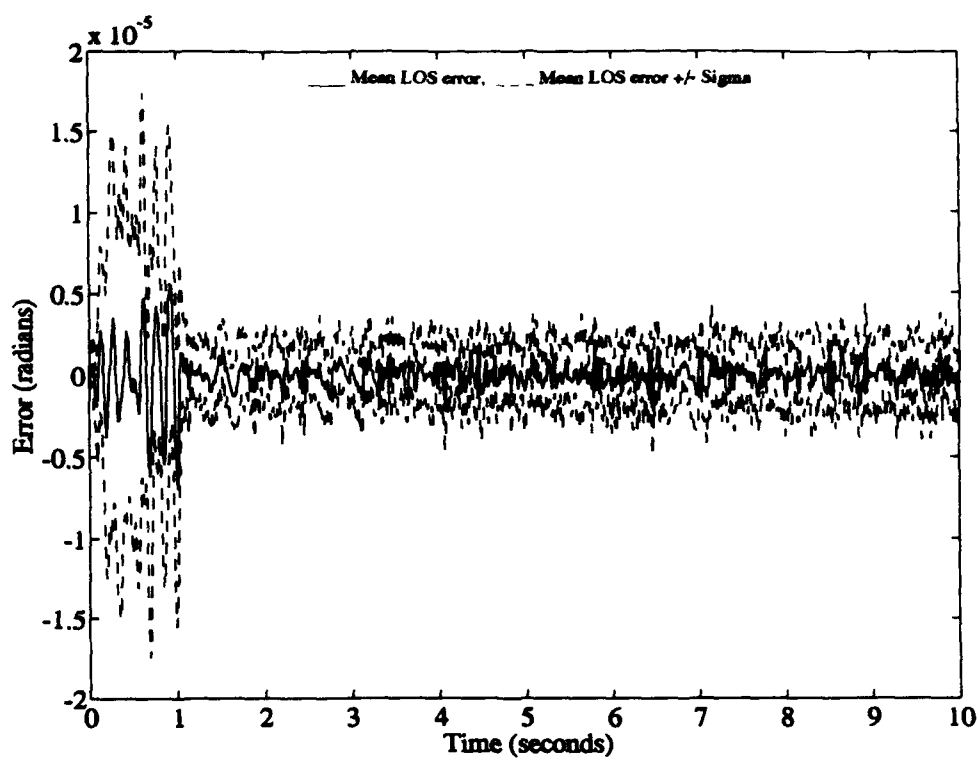


Figure F-21. 10-Modal-Cost Model Controller X-Axis LOS Error - W/ Control Applied

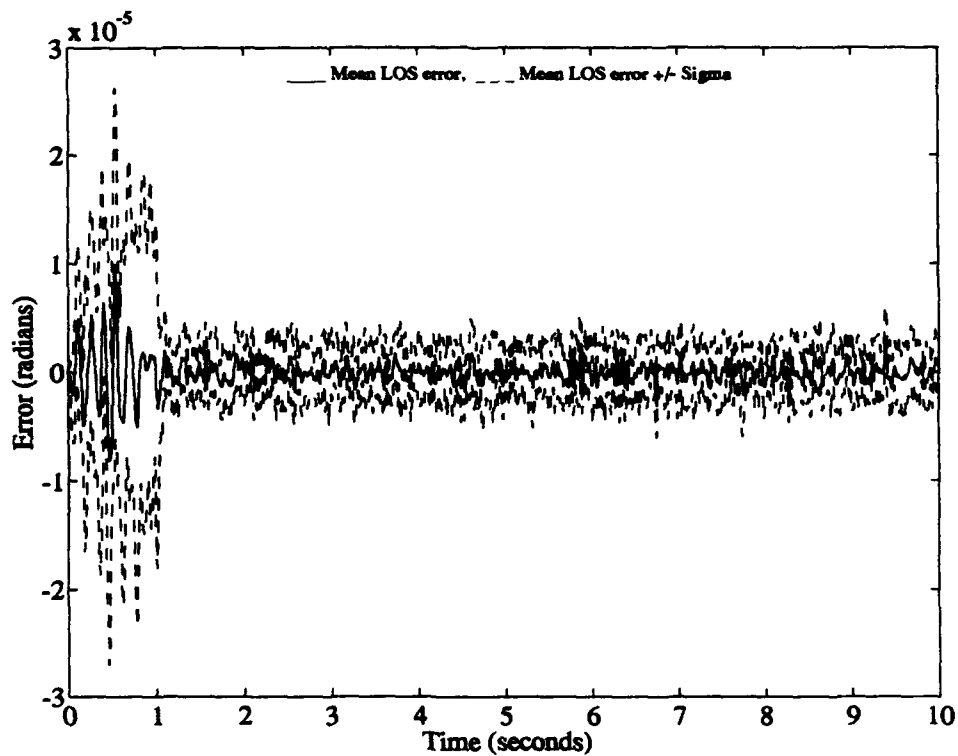


Figure F-22. 10-Modal-Cost Model Controller Y-Axis LOS Error - W/ Control Applied

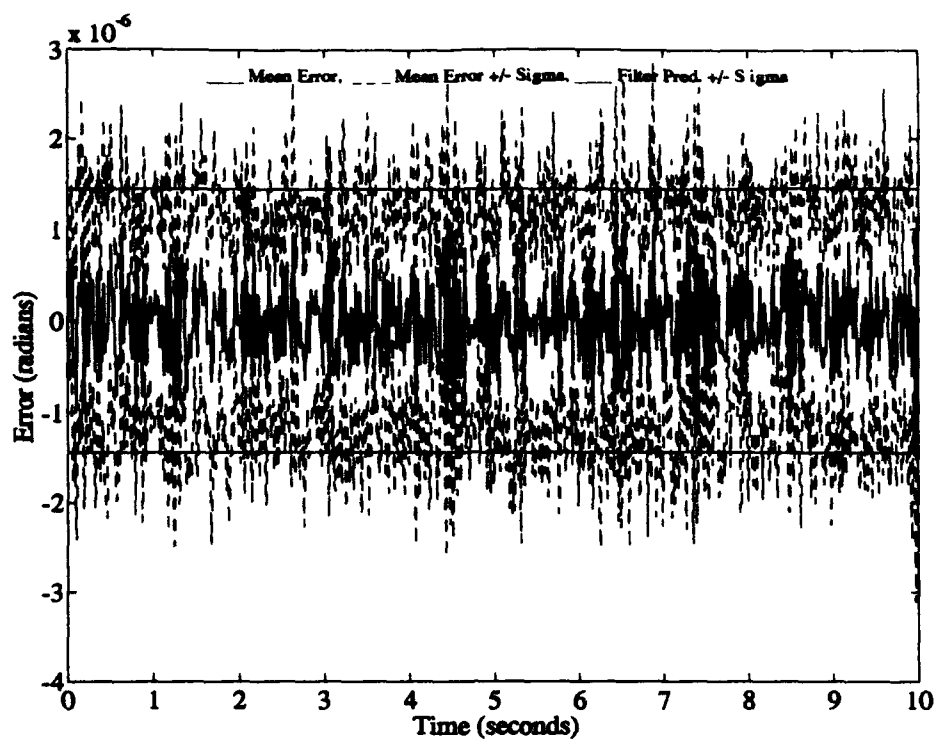


Figure F-23. 15-Modal-Cost Model Filter X-Axis Estimation Error

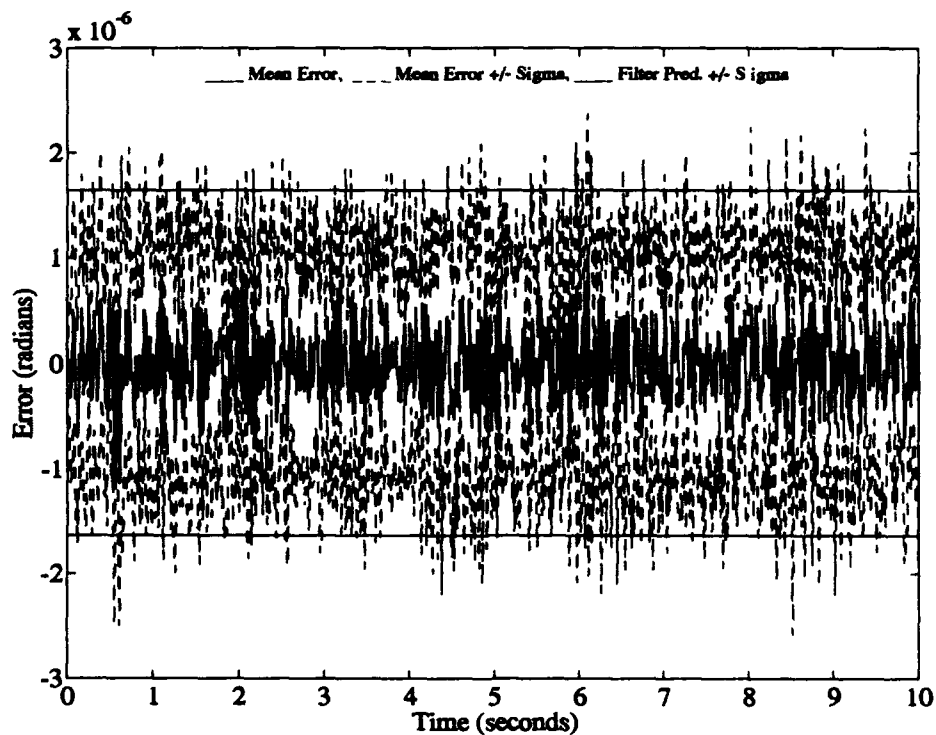


Figure F-24. 15-Modal-Cost Model Filter Y-Axis Estimation Error

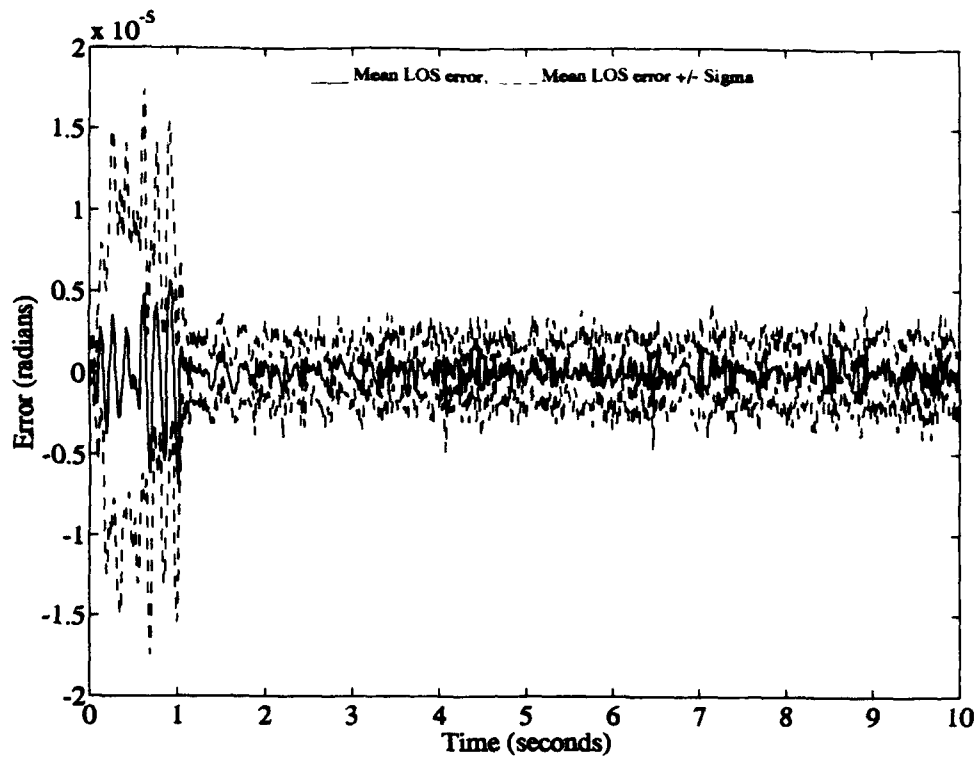


Figure F-25. 15-Modal-Cost Model Controller X-Axis LOS Error - W/ Control Applied

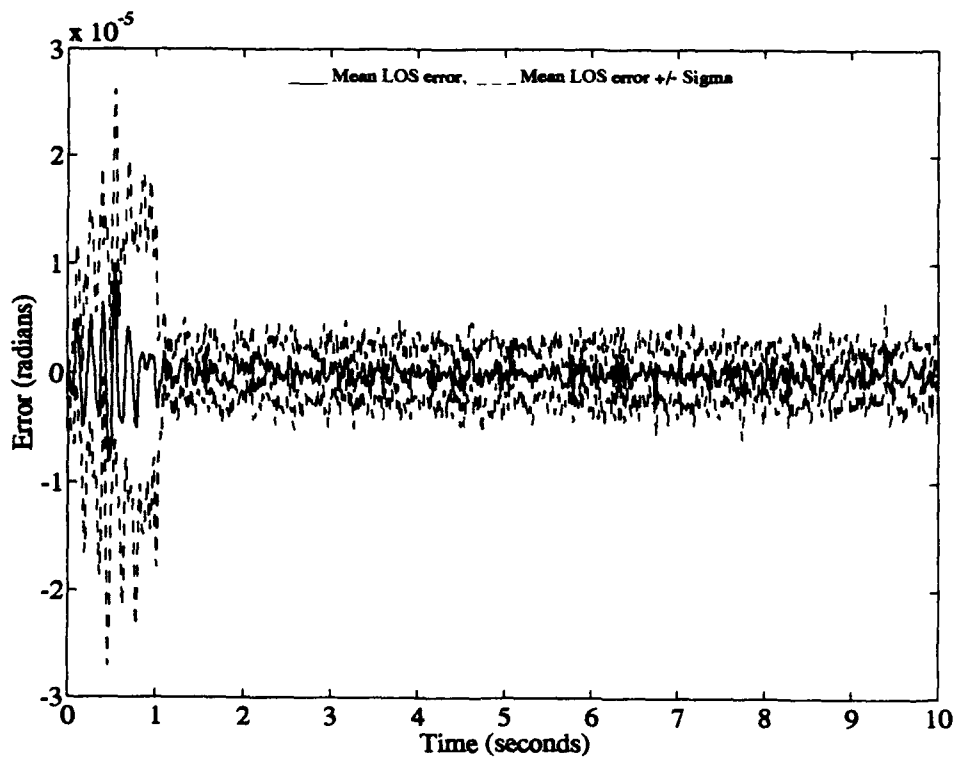


Figure F-26. 15-Modal-Cost Model Controller Y-Axis LOS Error - W/ Control Applied

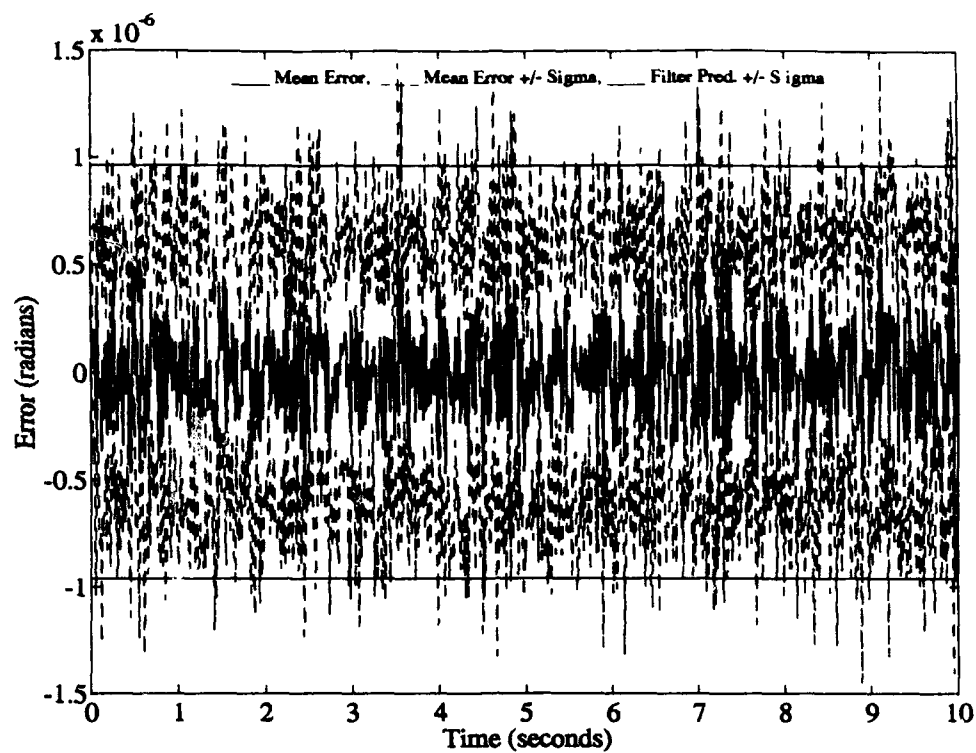


Figure F-27. 20-Modal-Cost Model Filter X-Axis Estimation Error

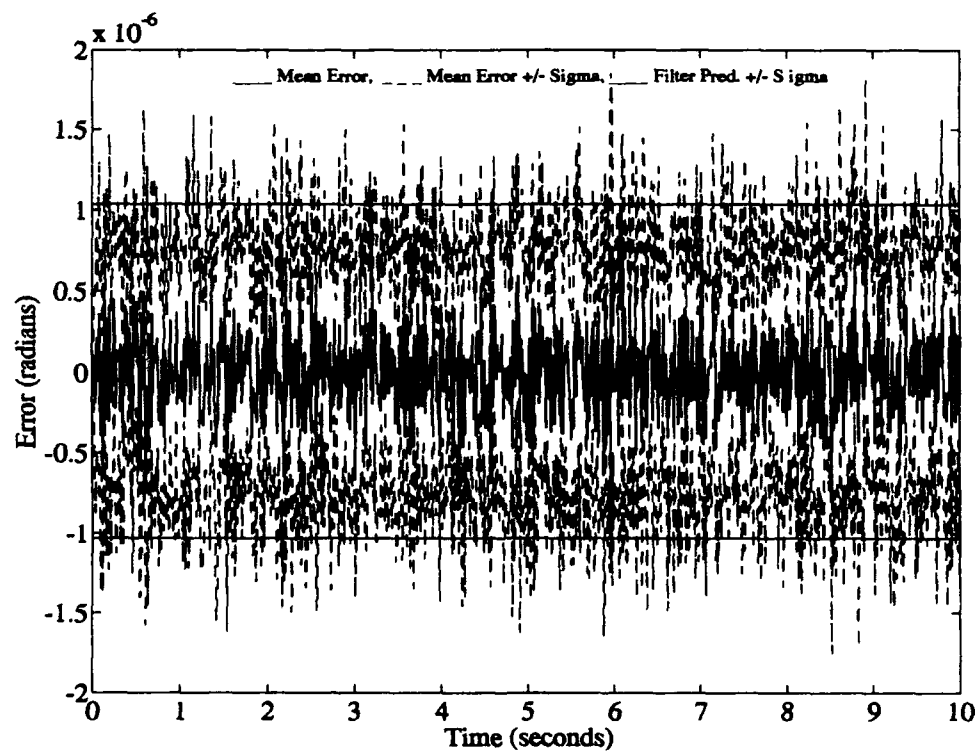


Figure F-28. 20-Modal-Cost Model Filter Y-Axis Estimation Error

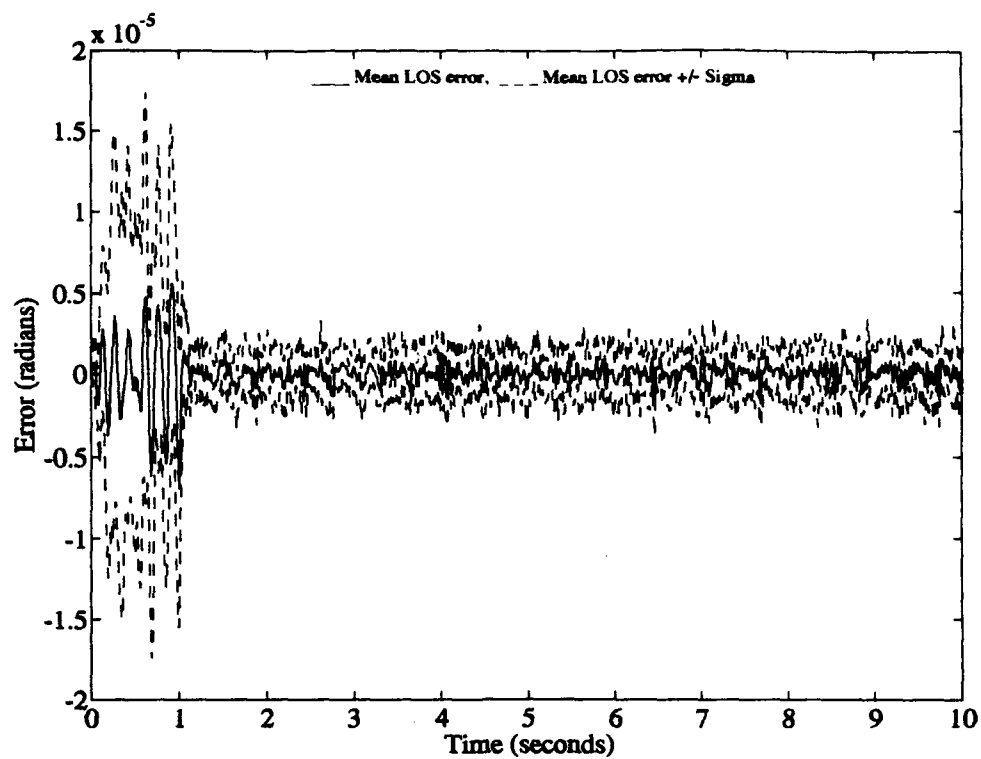


Figure F-29. 20-Modal-Cost Model Controller X-Axis LOS Error - W/ Control Applied

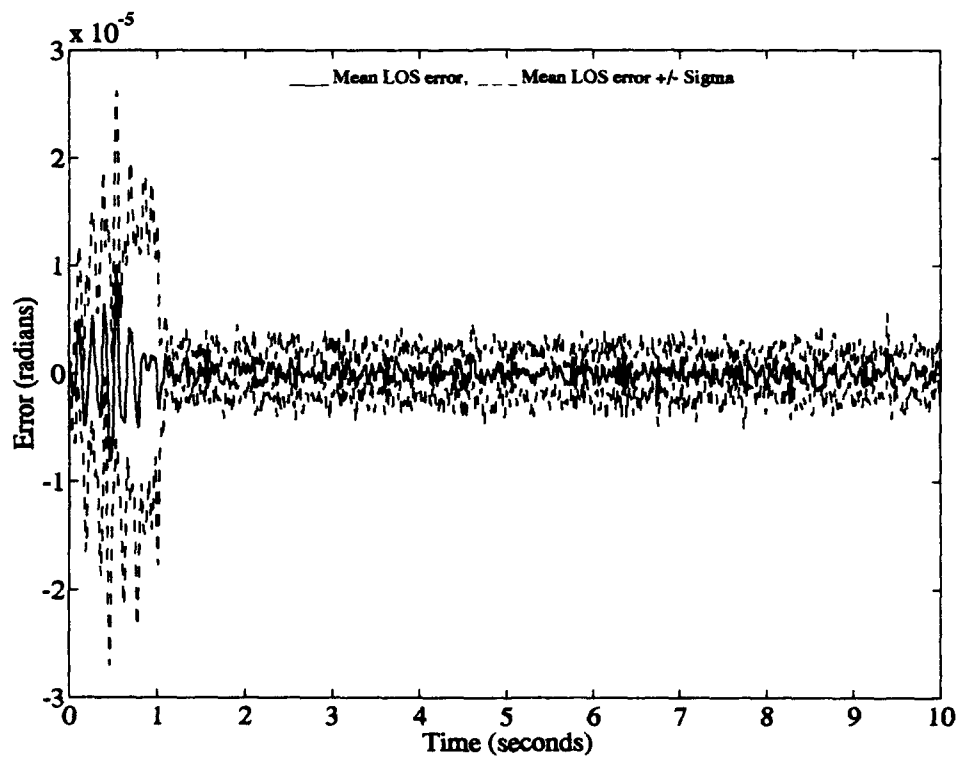


Figure F-30. 20-Modal-Cost Model Controller Y-Axis LOS Error - W/ Control Applied



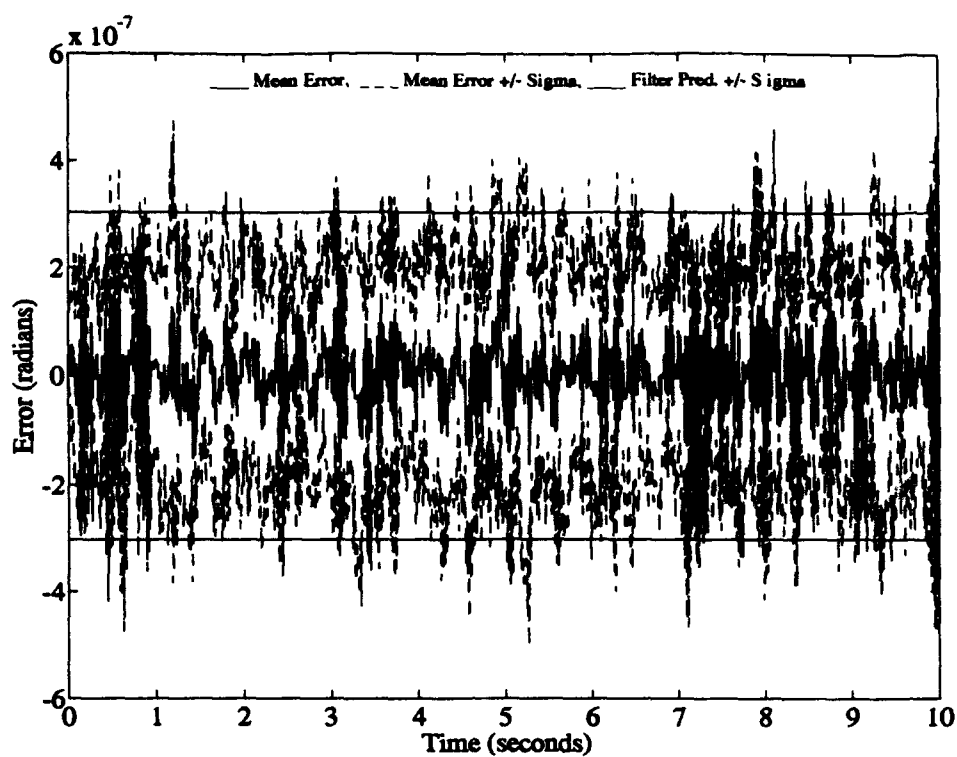


Figure F-31. 26-Modal-Cost Model Filter X-Axis Estimation Error

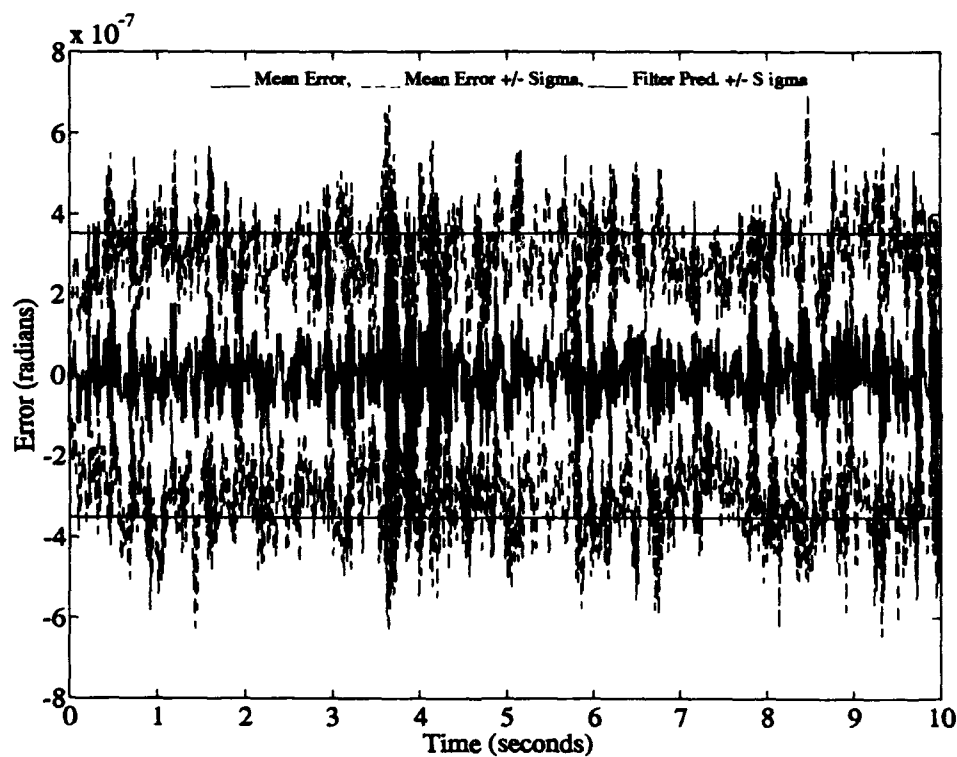


Figure F-32. 26-Modal-Cost Model Filter Y-Axis Estimation Error

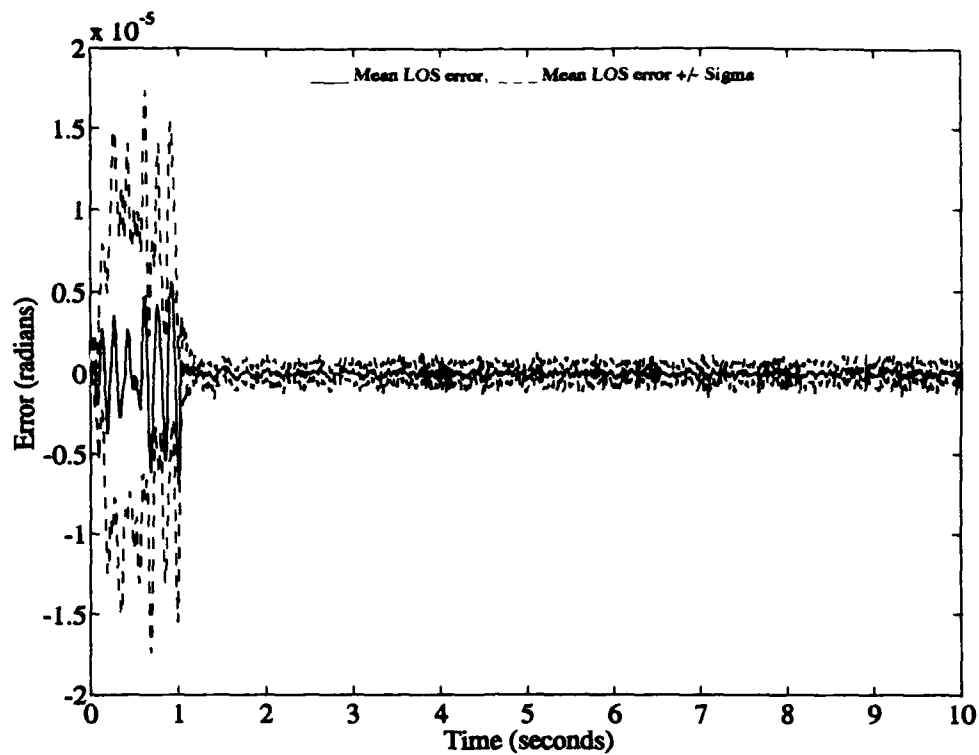


Figure F-33. 26-Modal-Cost Model Controller X-Axis LOS Error - W/ Control Applied

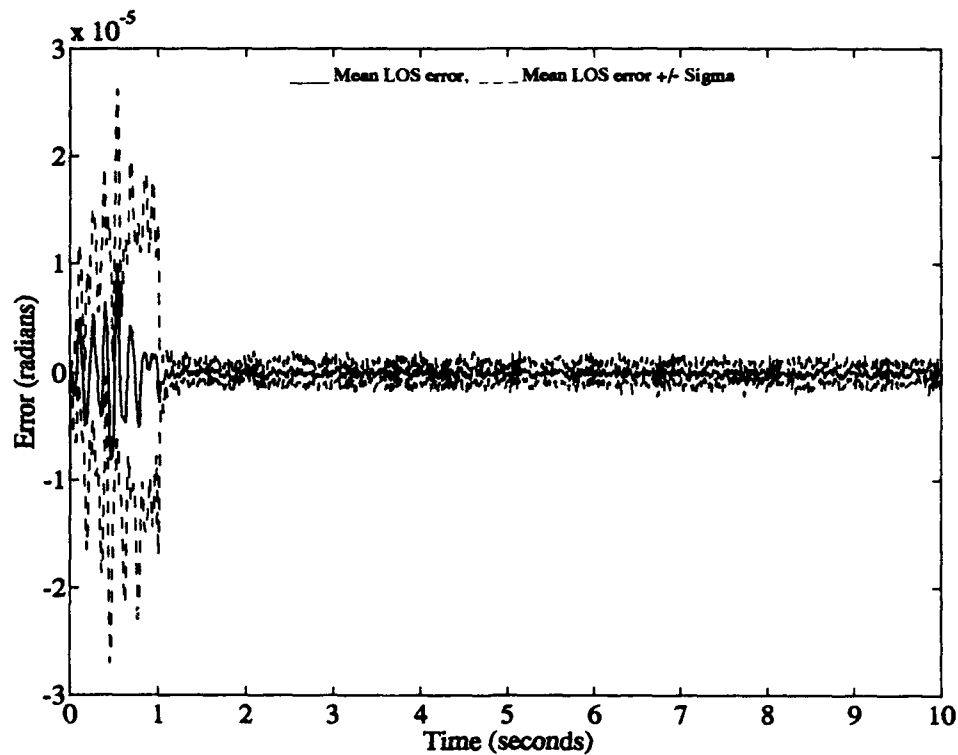


Figure F-34. 26-Modal-Cost Model Controller Y-Axis LOS Error - W/ Control Applied

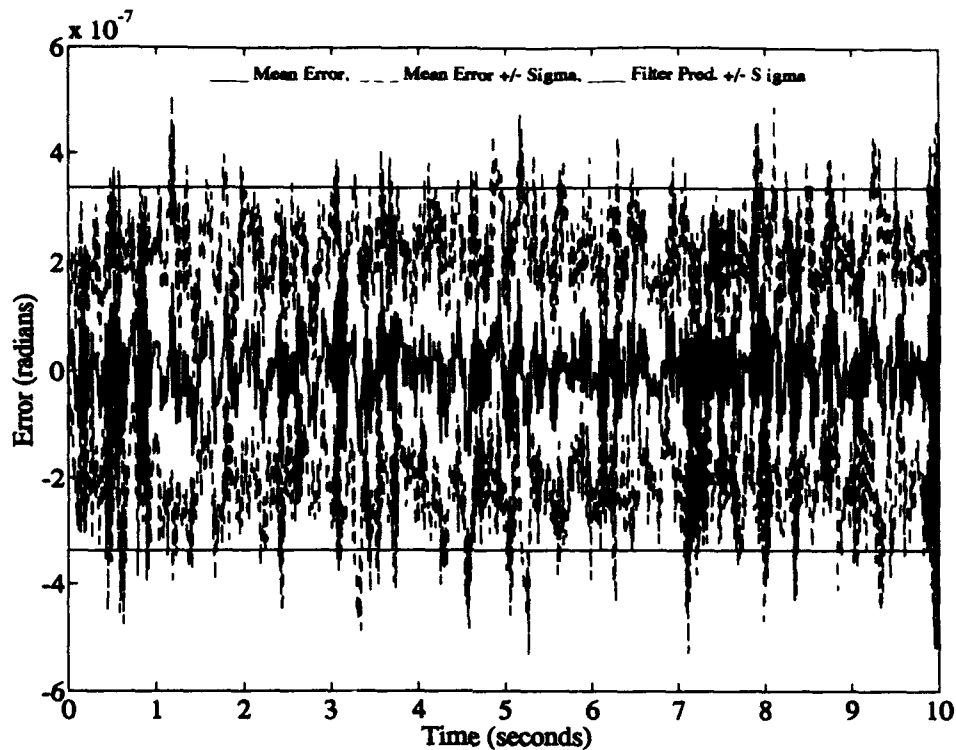


Figure F-35. 26-Truncated-Modal Model Filter X-Axis Estimation Error

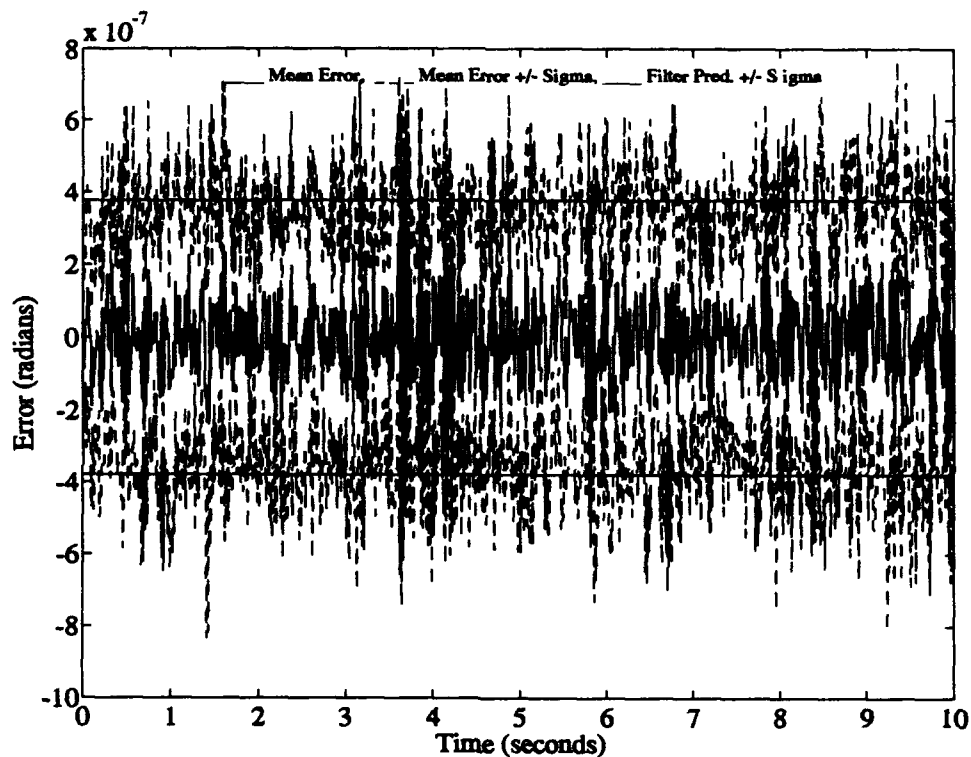


Figure F-36. 26-Truncated-Modal Model Filter Y-Axis Estimation Error

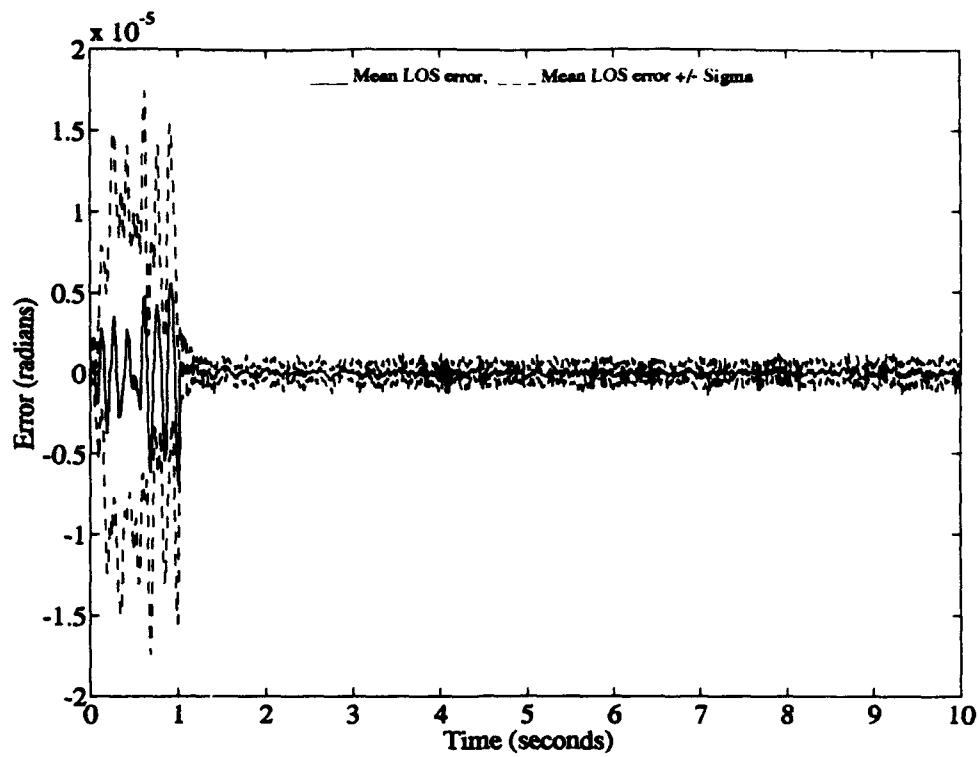


Figure F-37. 26-Trunc.-Modal Model Contr. X-Axis LOS Error - W/ Control Applied

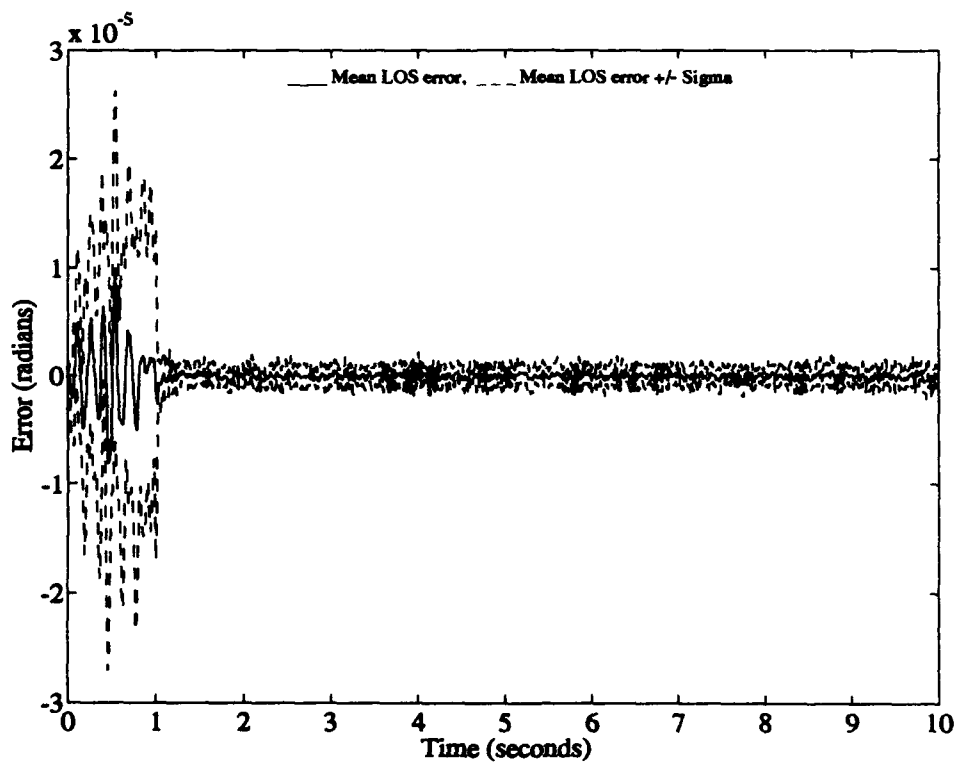


Figure F-38. 26-Trunc.-Modal Model Contr. Y-Axis LOS Error - W/ Control Applied

## **Appendix G: MMAE Design Performance Results**

This appendix presents all the plot results for the MMAE analysis in Section 5.5. The plots in this appendix represent a very good representative sample of all the actual simulations conducted for this section. Although there is no legend associated with each of the parameter identification plots, it should be fairly evident that the true parameter is indicated by the straight lines and the parameter estimate (mean value obtained from a ten-run Monte Carlo analysis) is indicated by the wavering lines. (It was decided not to include mean  $\pm 1\sigma$  plots because the  $1\sigma$  values were very small for all but the short transient period following a true parameter move and the addition of the extra lines would cause undue clutter to the plots.) In each of the plots, the Bayesian form is assumed, except where noted (Figures G-3 through G-8). *Parameter match* refers to the situation in which the true parameter is held stationary at  $\omega_5$  and the filter bank is initially centered at the same location. *Parameter offset up* refers to the situation in which the true parameter is held stationary at  $\omega_{17}$ , and the filter bank center is initially positioned at  $\omega_5$ . *Parameter offset down* refers to the situation in which the true parameter is held stationary at  $\omega_5$ , and the filter bank center is initially positioned at  $\omega_{17}$ . *Parameter jump up* refers to the situation in which the true parameter and filter bank center are initially positioned at  $\omega_5$ , then the true parameter makes a discrete jump to  $\omega_{17}$  at the five second mark. *Parameter jump down* refers to the situation in which the true parameter and filter bank center are initially positioned at  $\omega_{17}$ , then the true parameter makes a discrete jump to  $\omega_5$  at the five second mark. *Parameter move up* refers to the situation in which the true parameter and the filter bank center are initially positioned at  $\omega_2$ , then the true parameter is moved up in discrete jumps of 2 every two seconds for 30 seconds. *Parameter move down* refers to the situation in which the true parameter and the filter bank center are initially positioned at  $\omega_{18}$ , then the true parameter is moved down in discrete jumps of 2 every two seconds for 30 seconds.

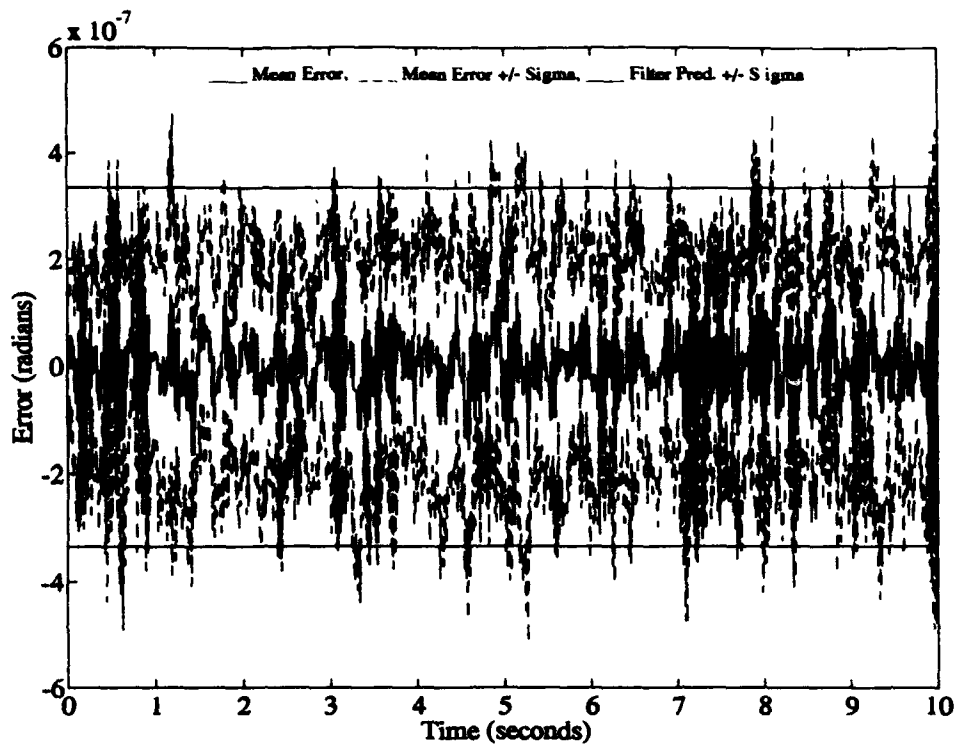


Figure G-1. MMAE X-axis Estimation Error

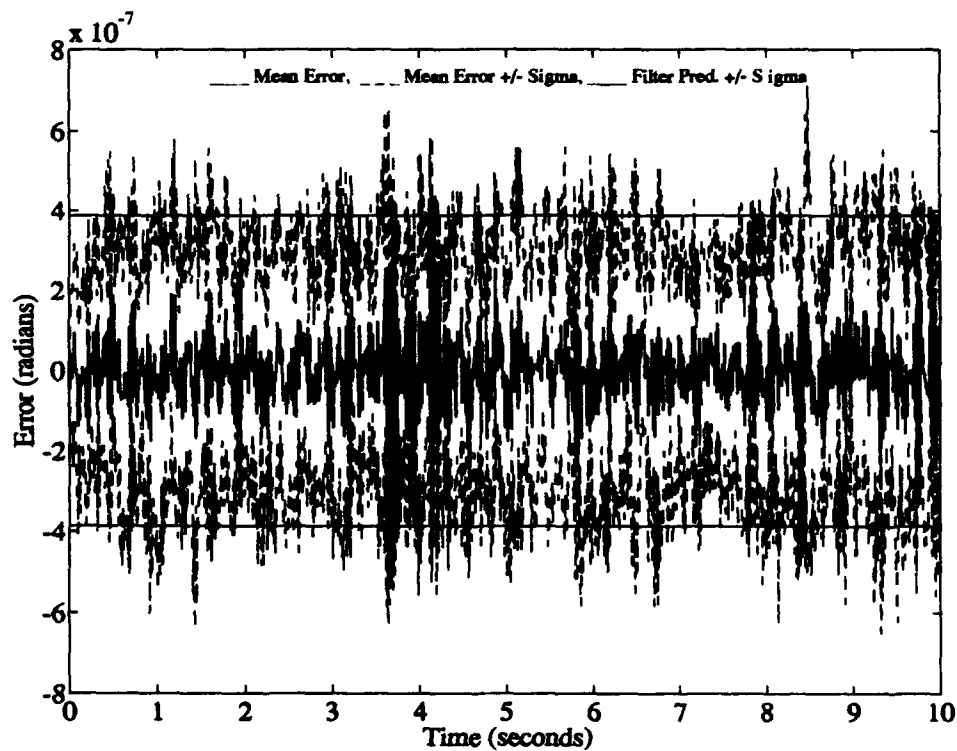


Figure G-2. MMAE Y-axis Estimation Error

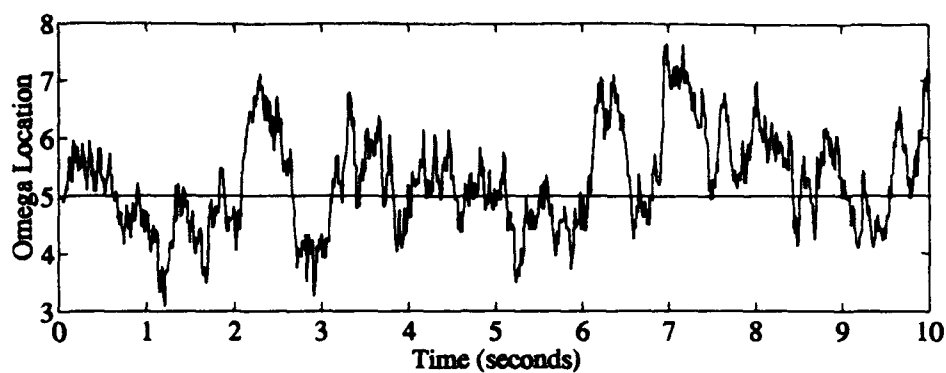


Figure G-3. Parameter Position Monitoring with Parameter Match (ME/I)

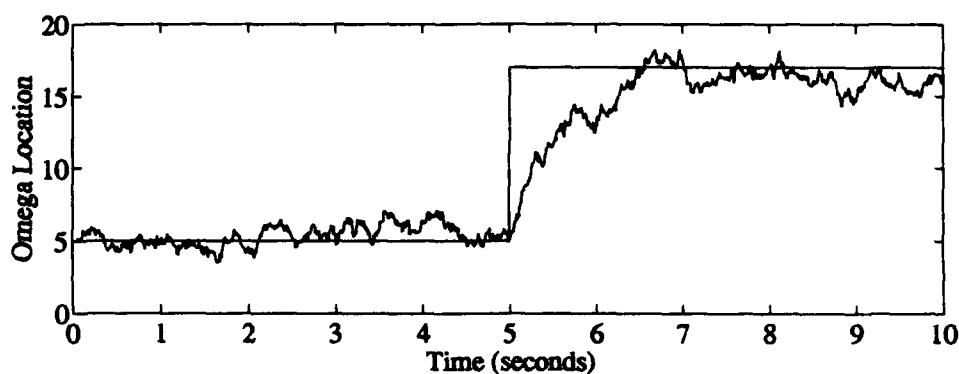


Figure G-4. Parameter Position Monitoring with Parameter Jump Up (ME/I)

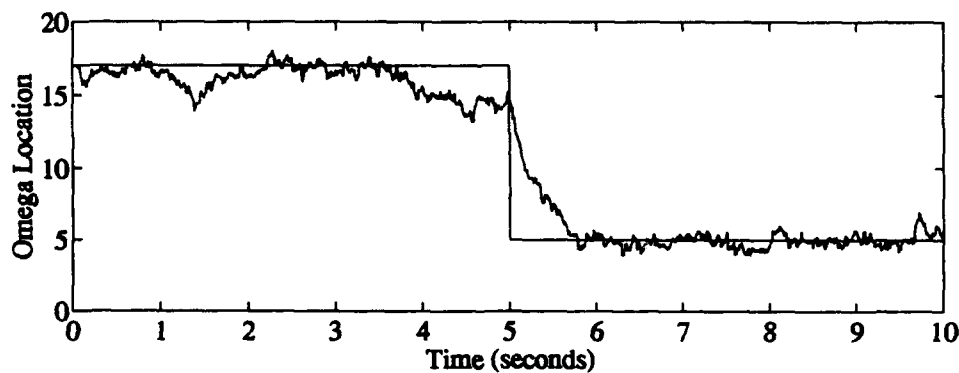


Figure G-5. Parameter Position Monitoring with Parameter Jump Down (ME/I)

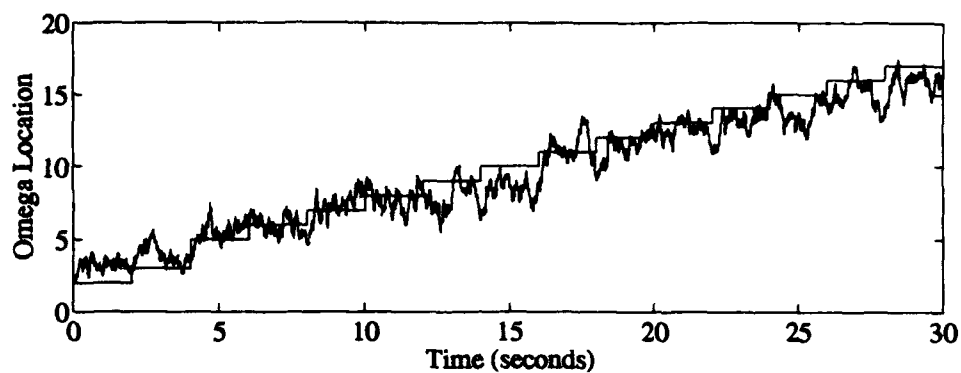


Figure G-6. Parameter Position Monitoring with Parameter Move Up (ME/I)

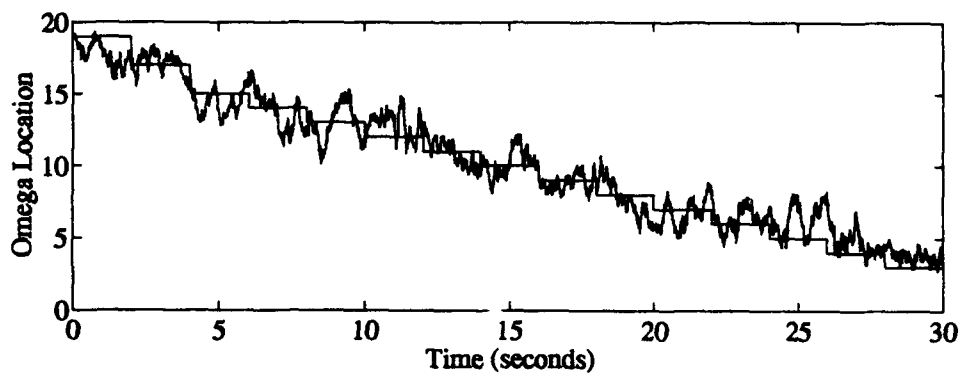


Figure G-7. Parameter Position Monitoring with Parameter Move Down (ME/I)



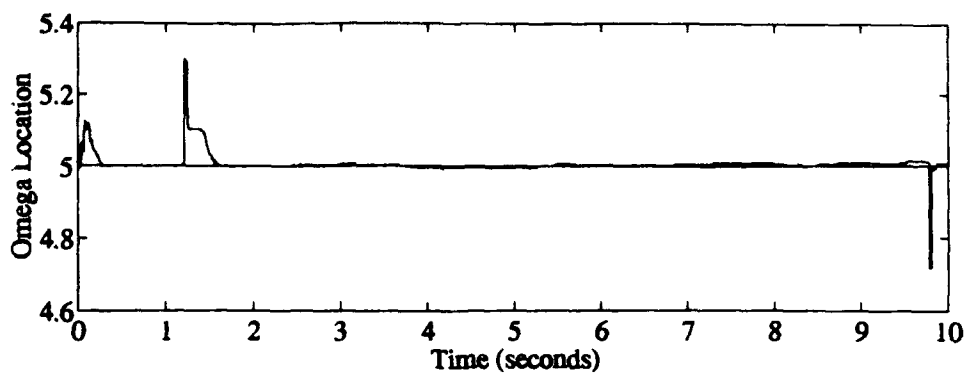


Figure G-8. Residual Monitoring with Parameter Match

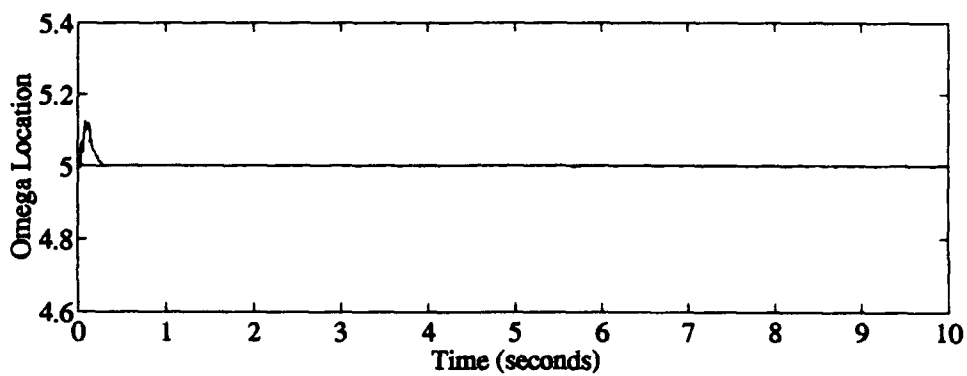


Figure G-9. Probability Monitoring with Parameter Match

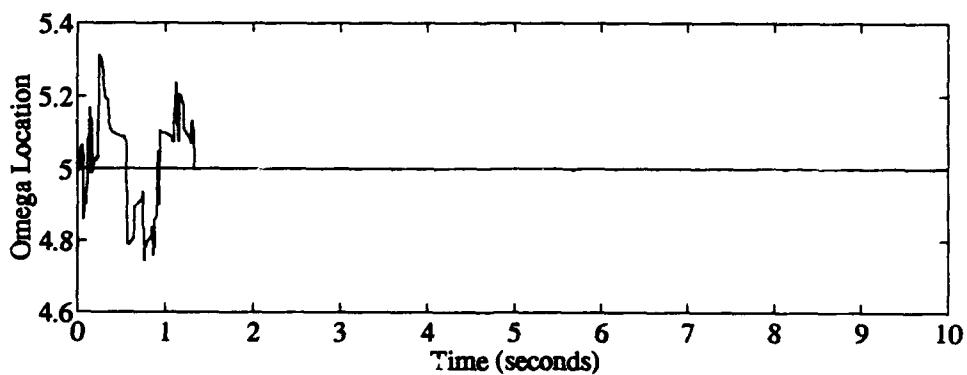


Figure G-10. Parameter Position Monitoring with Parameter Match

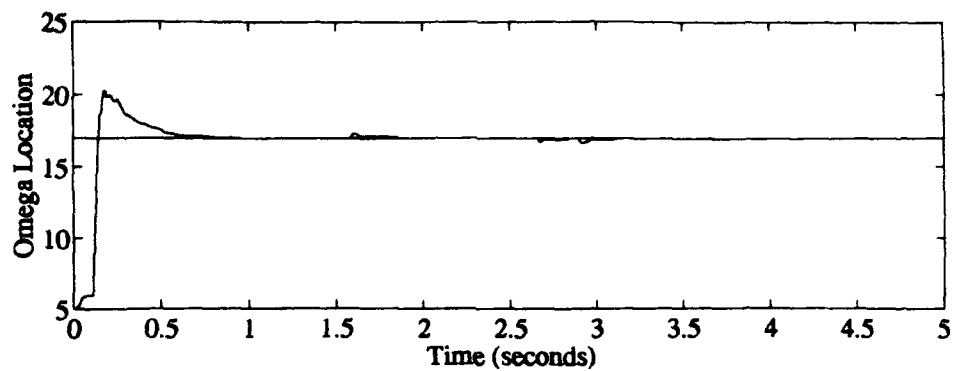


Figure G-11. Residual Monitoring with Parameter Offset Up

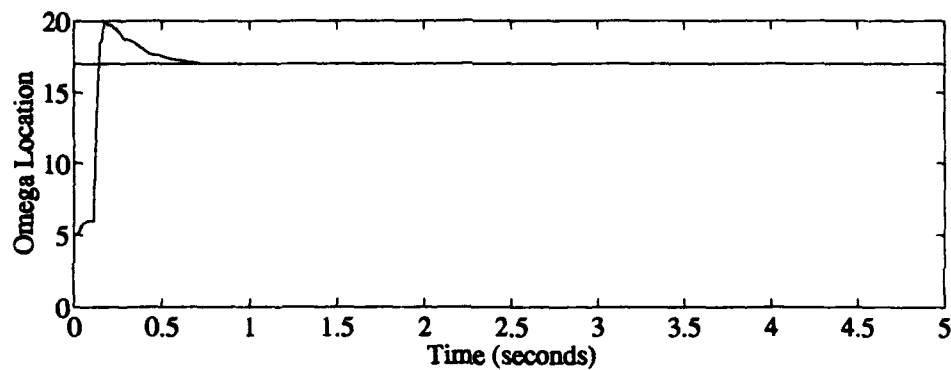


Figure G-12. Probability Monitoring with Parameter Offset Up

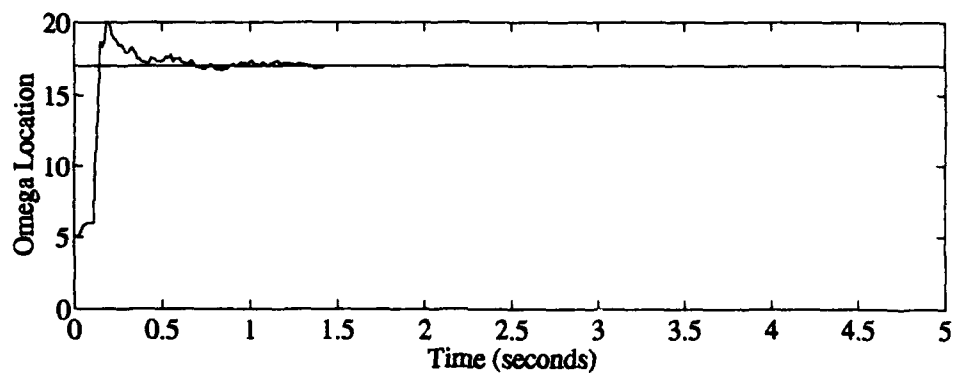


Figure G-13. Parameter Position Monitoring with Parameter Offset Up

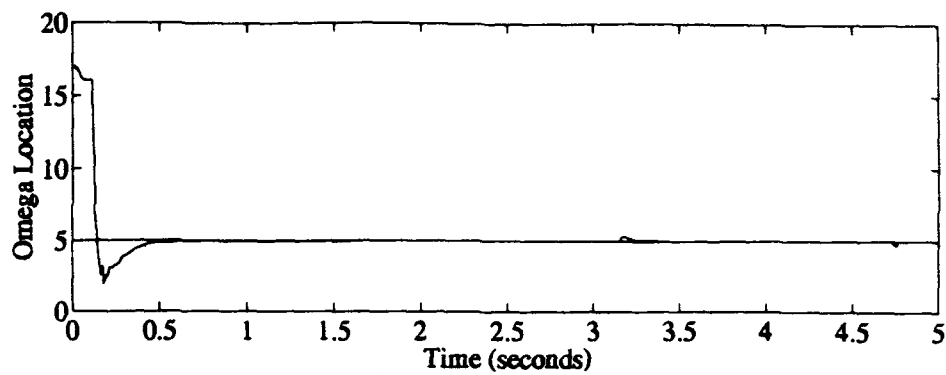


Figure G-14. Residual Monitoring with Parameter Offset Down

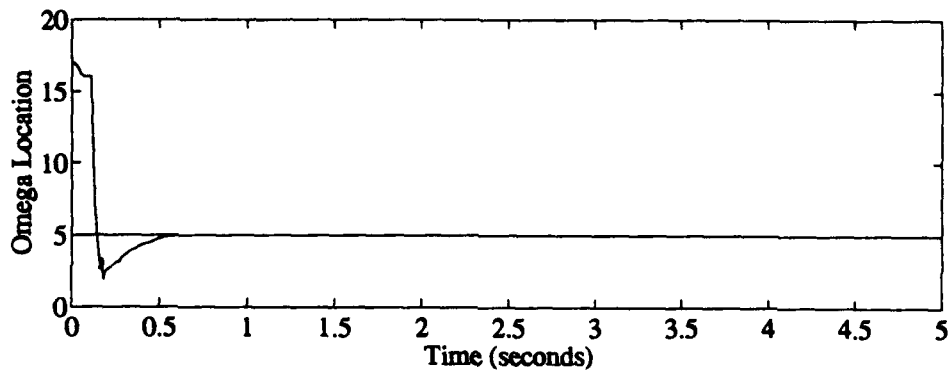


Figure G-15. Probability Monitoring with Parameter Offset Down

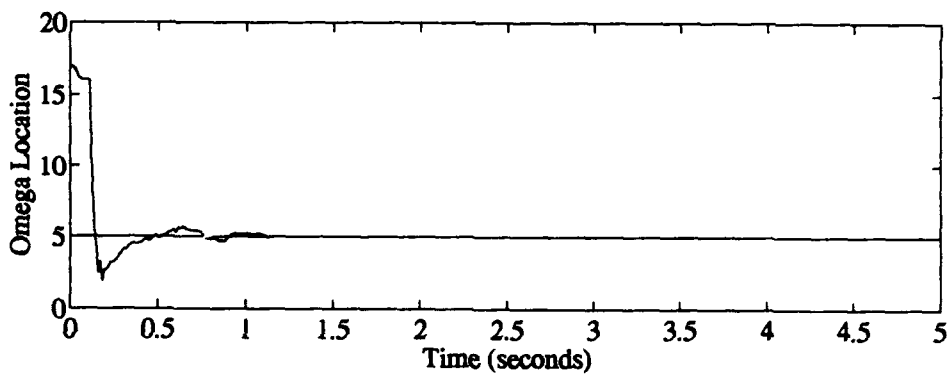


Figure G-16. Parameter Position Monitoring with Parameter Offset Down

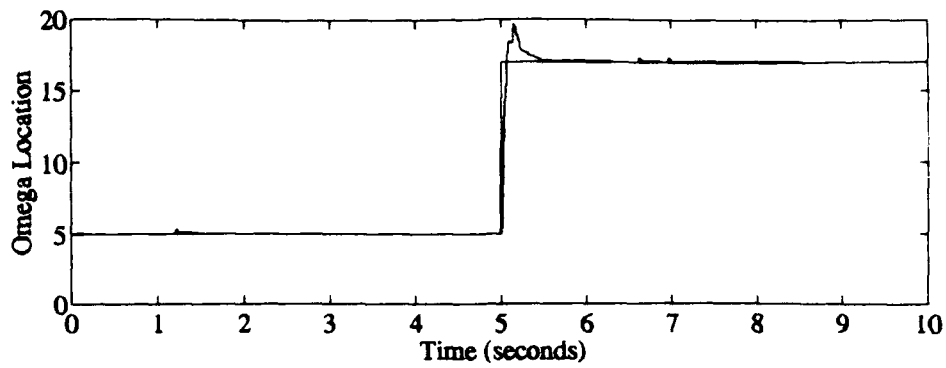


Figure G-17. Residual Monitoring with Parameter Jump Up

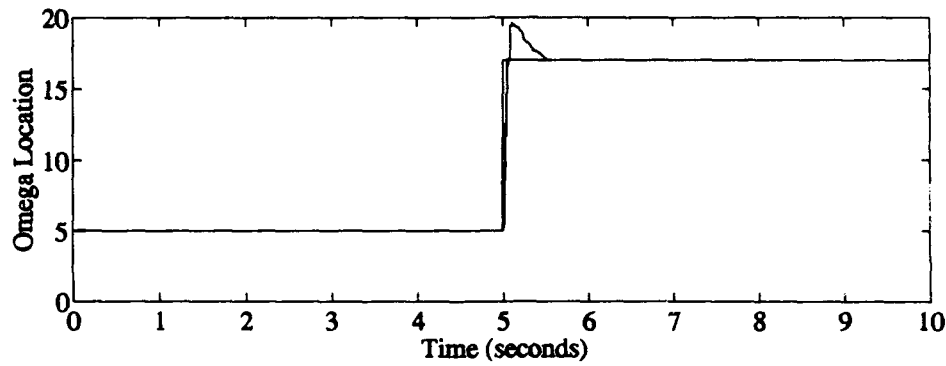


Figure G-18. Probability Monitoring with Parameter Jump Up

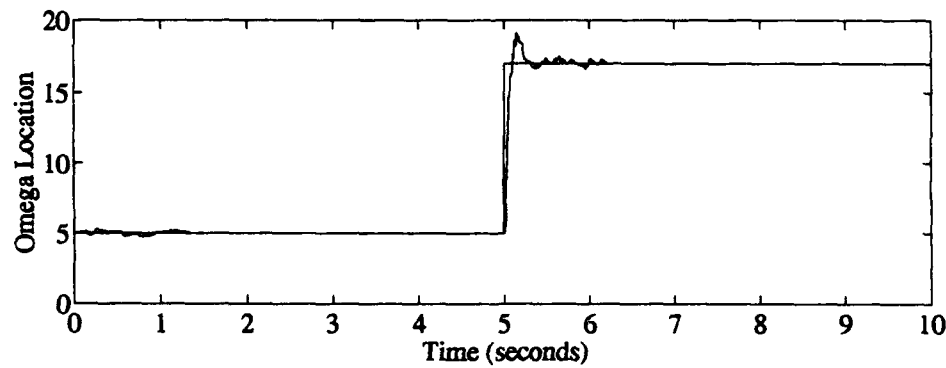


Figure G-19. Parameter Position Monitoring with Parameter Jump Up

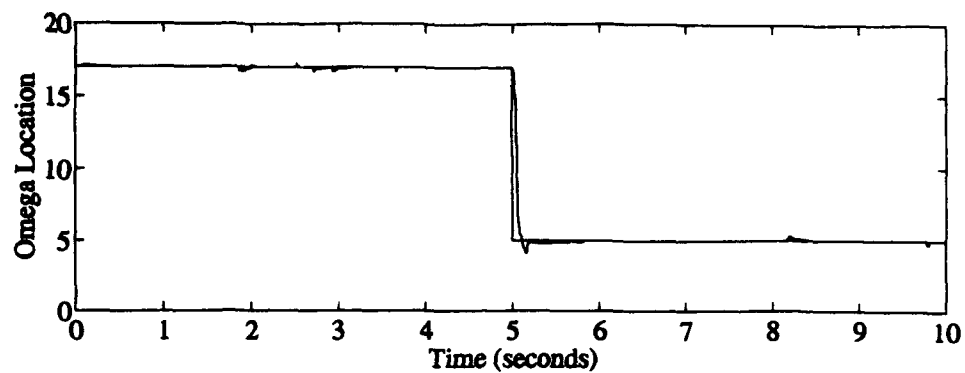


Figure G-20. Residual Monitoring with Parameter Jump Down

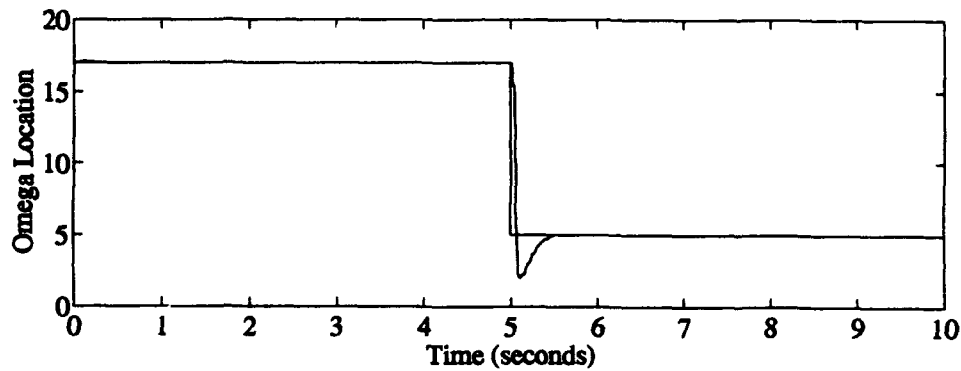


Figure G-21. Probability Monitoring with Parameter Jump Down

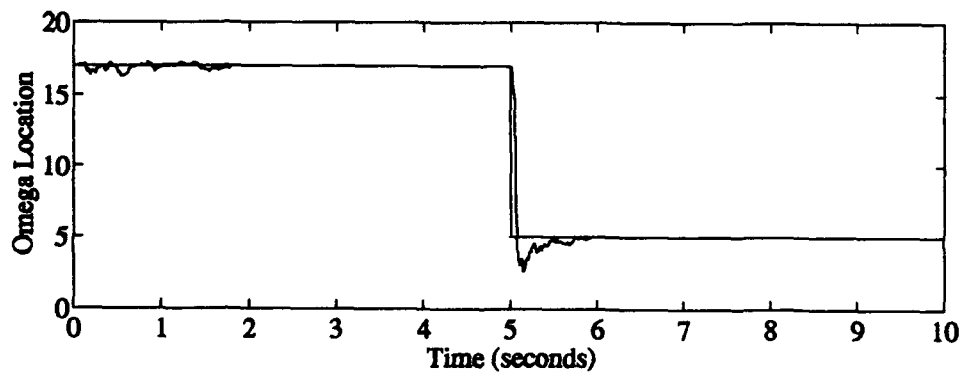


Figure G-22. Parameter Position Monitoring with Parameter Jump Down

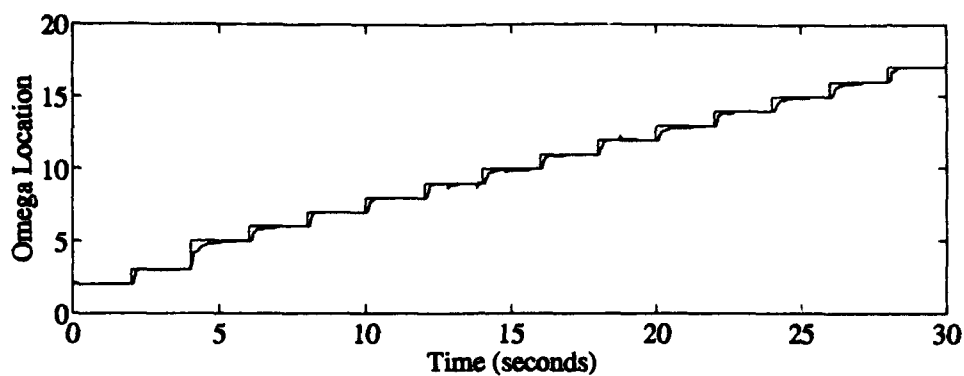


Figure G-23. Residual Monitoring with Parameter Move Up

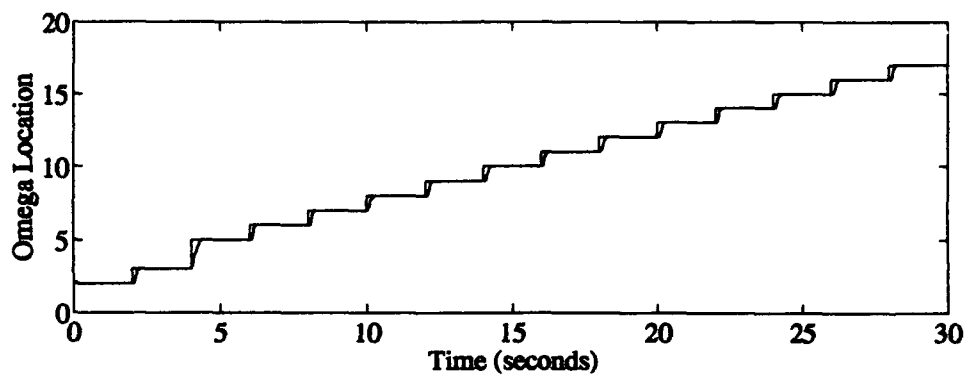


Figure G-24. Probability Monitoring with Parameter Move Up

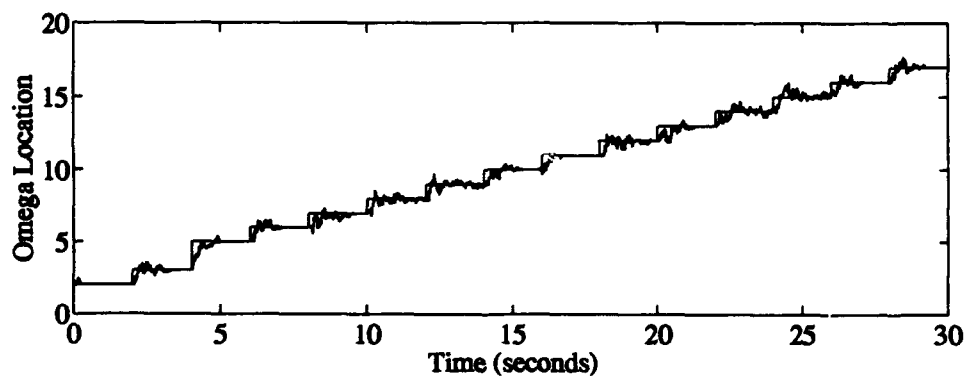


Figure G-25. Parameter Position Monitoring with Parameter Move Up

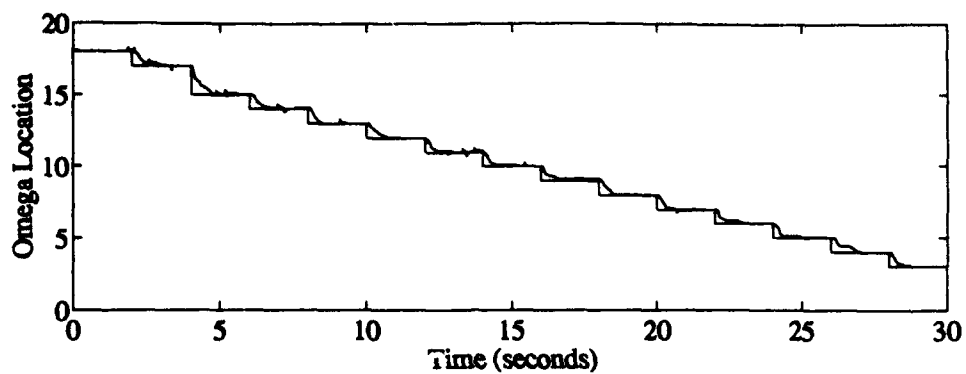


Figure G-26. Residual Monitoring with Parameter Move Down

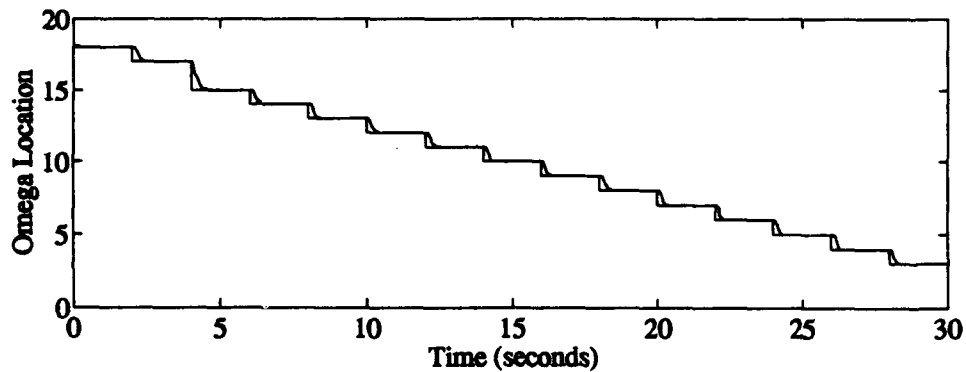


Figure G-27. Probability Monitoring with Parameter Move Down

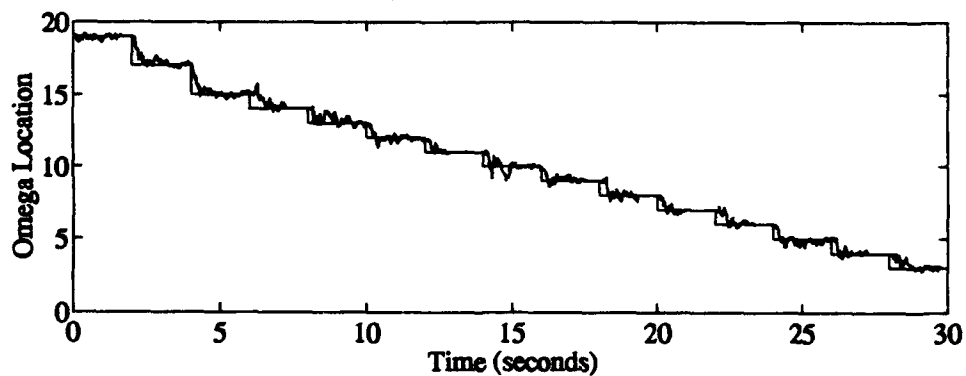


Figure G-28. Parameter Position Monitoring with Parameter Move Down

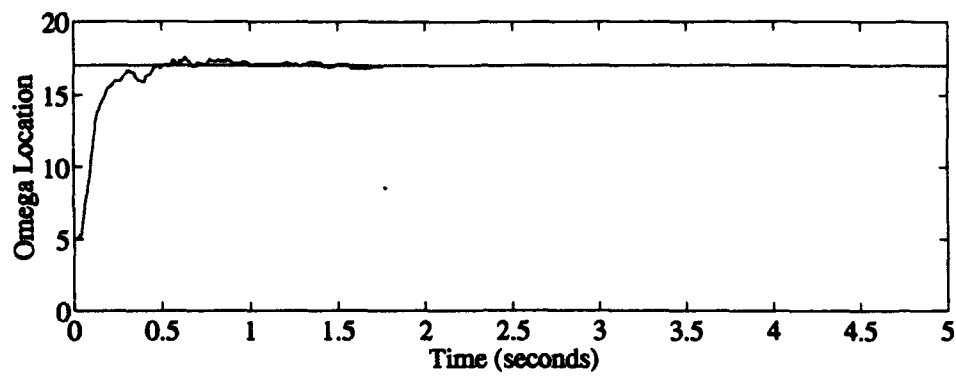


Figure G-29. Parameter Position Mon. with Parameter Offset Up (Move Logic Only)

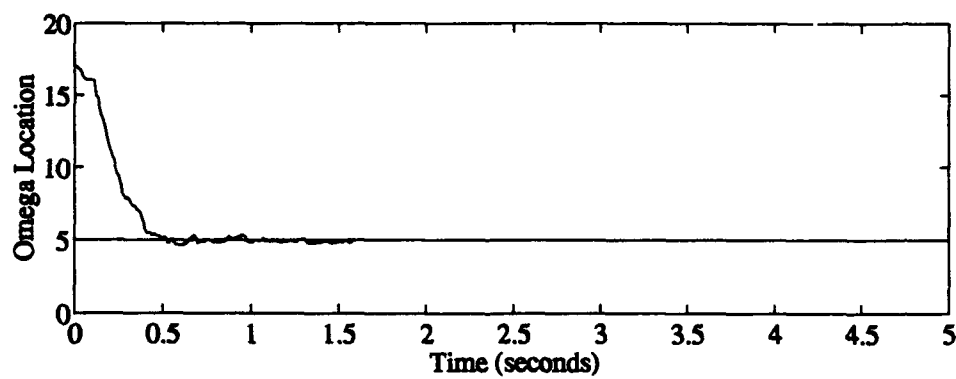


Figure G-30. Parameter Position Mon. with Parameter Offset Down (Move Logic Only)



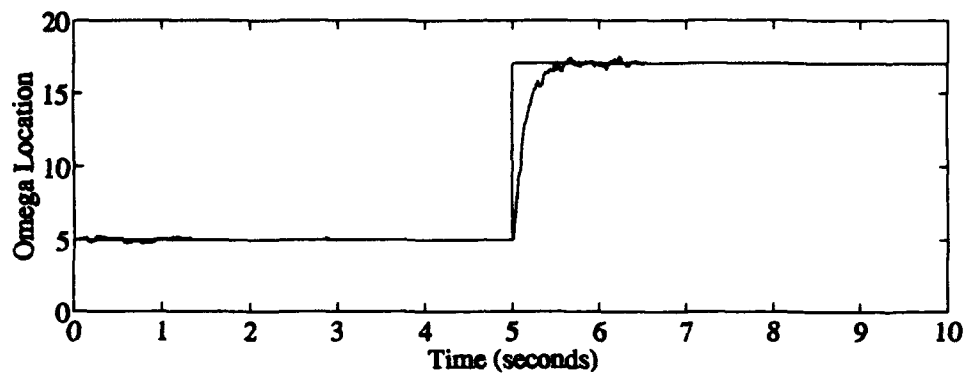


Figure G-31. Parameter Position Mon. with Parameter Jump Up (Move Logic Only)

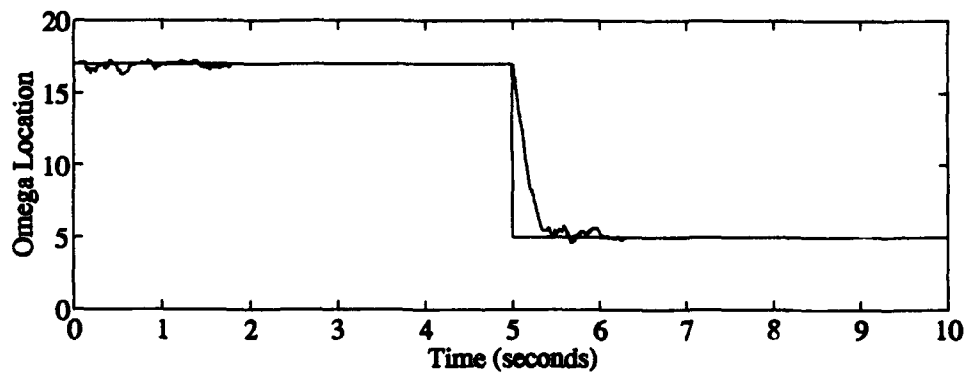


Figure G-32. Parameter Position Mon. with Parameter Jump Down (Move Logic Only)

## **Appendix H: MMAC Design Performance Results**

This appendix presents all the plot results for the MMAC analysis in Section 5.6. The plots in this appendix represent a very good representative sample of all the actual simulations conducted for this section. Although there is no legend associated with each of the parameter identification plots, it should be fairly evident that the true parameter is indicated by the straight lines and the parameter estimate (mean value obtained from a ten run Monte Carlo analysis) is indicated by the wavering lines. (It was decided not to include mean  $\pm 1\sigma$  plots because the  $1\sigma$  values were very small for all but the short transient period following a true parameter move and the addition of the extra lines would cause undue clutter to the plots.) *Parameter match* refers to the situation in which the true parameter is held stationary at  $\omega_5$  and the filter bank is initially centered at the same location. *Parameter jump* refers to the situation in which the true parameter and filter bank center are initially positioned at  $\omega_5$ , then the true parameter makes a discrete jump to  $\omega_{17}$  at the five second mark. *Parameter move* refers to the situation in which the true parameter and the filter bank center are initially positioned at  $\omega_2$ , then the true parameter is moved up in discrete jumps of 2 every two seconds for 30 seconds. Each of the four control methods investigated are represented in this appendix. The MMAC utilizes the unconditional "blending" of the control inputs from each of the active filter/controllers. Modified MMAC institutes a lower bound of 0.25 on the probability of each filter/controller before computing the probability-weighted average as the MMAC control output, which precludes the blending of those under this threshold. The MAP method declares the filter/controller with the highest probability as the one to provide the final control input. The Modified MAP method declares the filter/controller based on the parameter value closest to the parameter estimate as the one to provide the final control input.

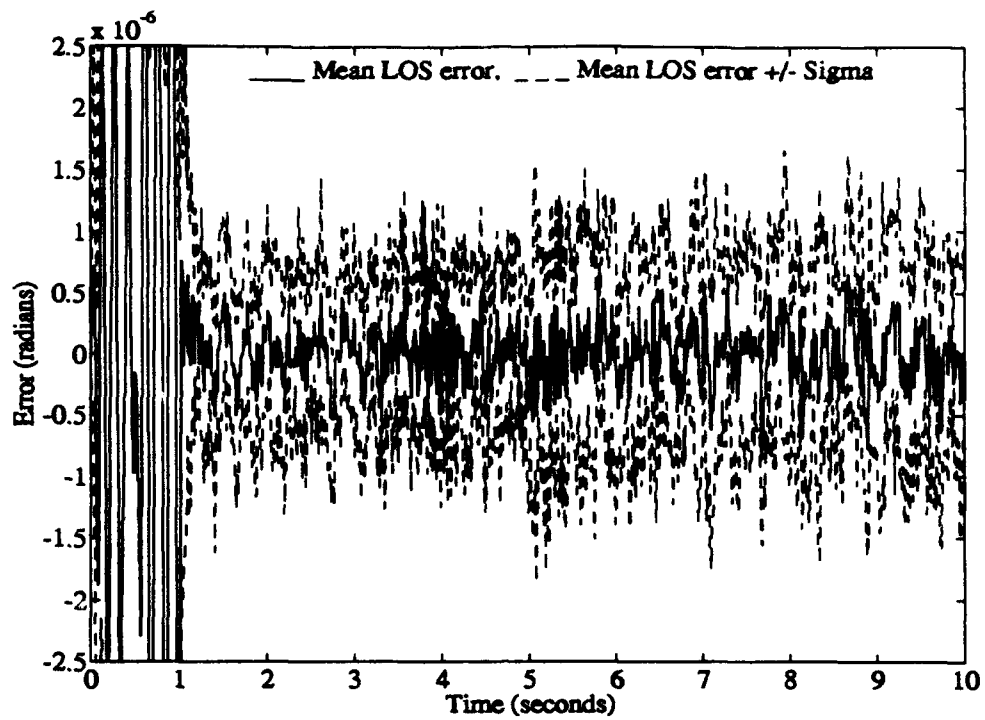


Figure H-1. MMAC X-axis LOS Error

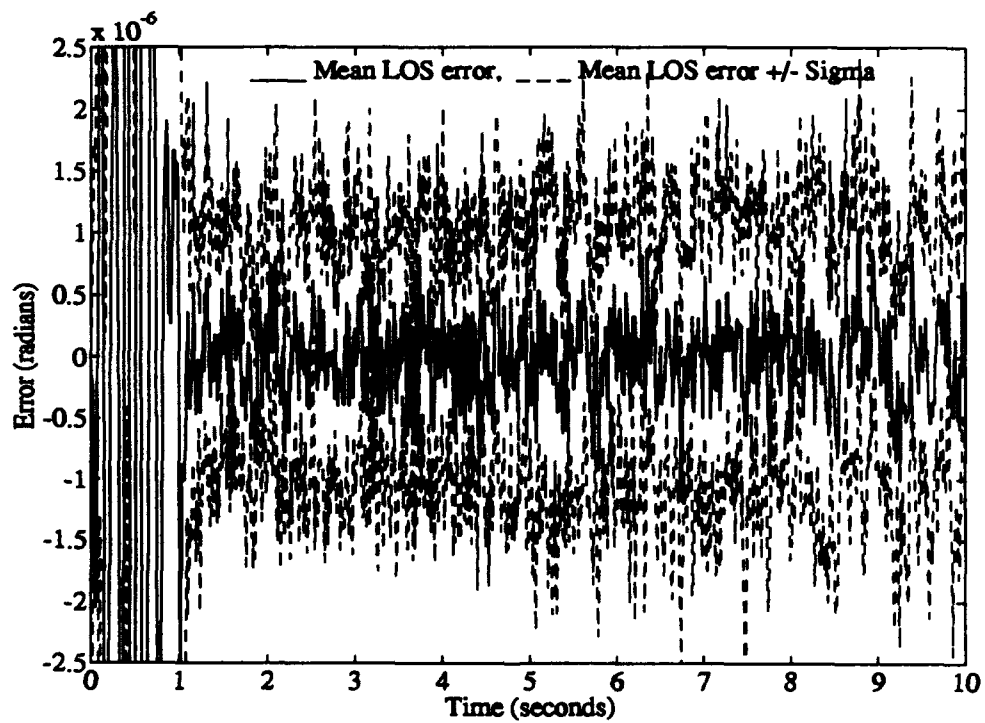


Figure H-2. MMAC Y-axis LOS Error

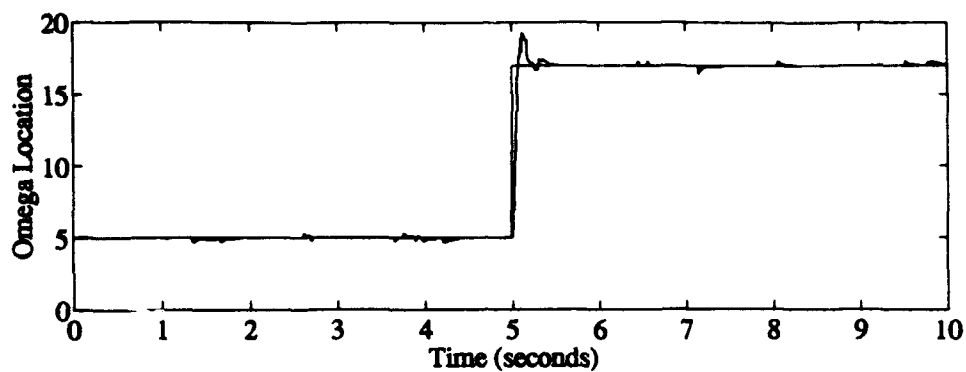


Figure H-3. Residual Monitoring w/MMAC and Parameter Jump

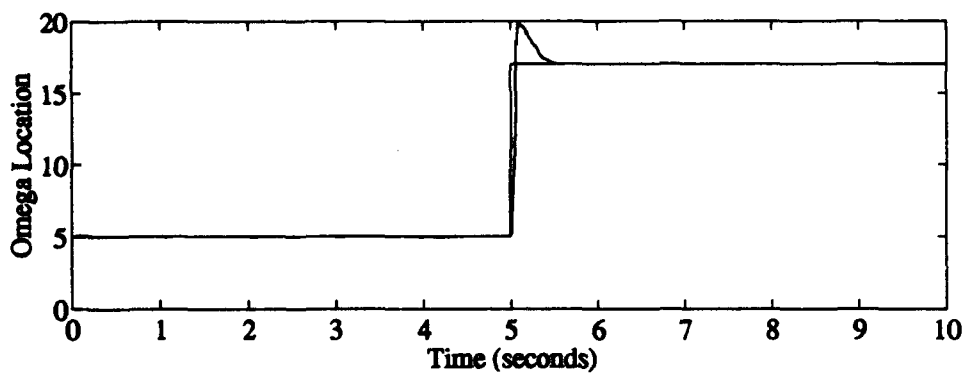


Figure H-4. Probability Monitoring w/MMAC and Parameter Jump

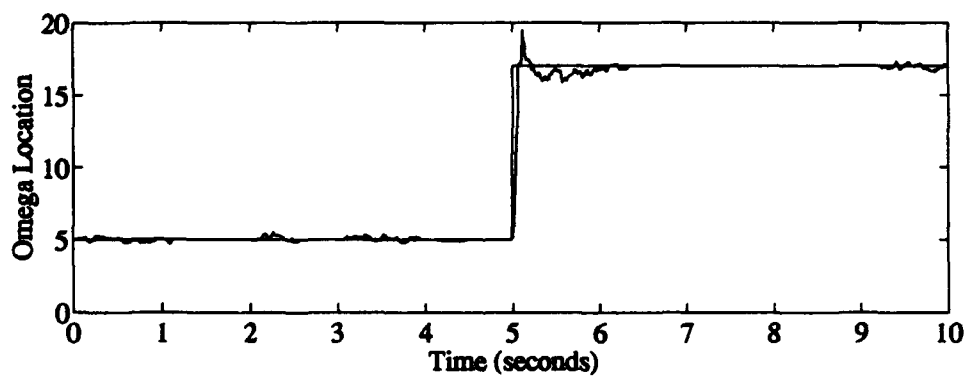


Figure H-5. Parameter Position Monitoring w/MMAC and Parameter Jump

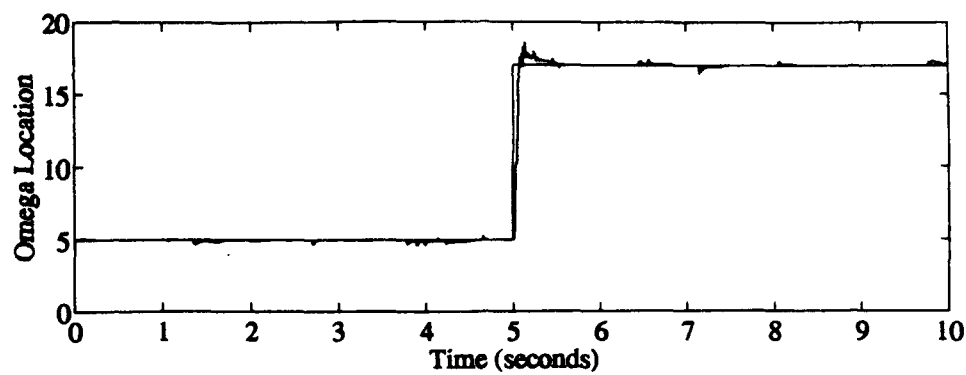


Figure H-6. Residual Monitoring w/Mod MMAC and Parameter Jump

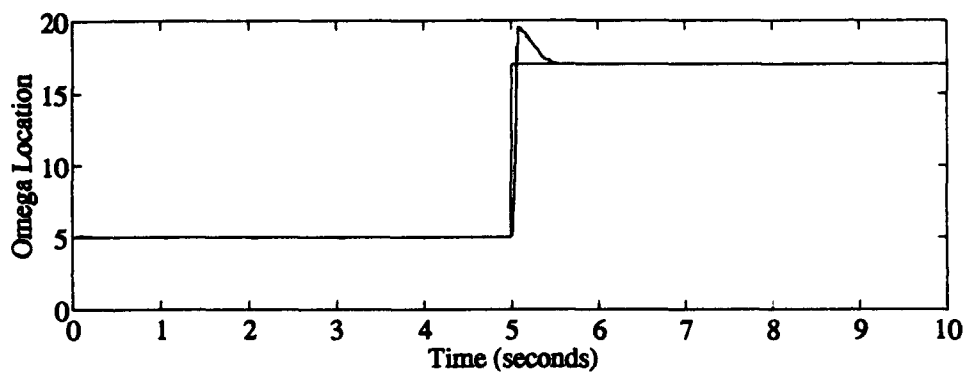


Figure H-7. Probability Monitoring w/Mod MMAC and Parameter Jump

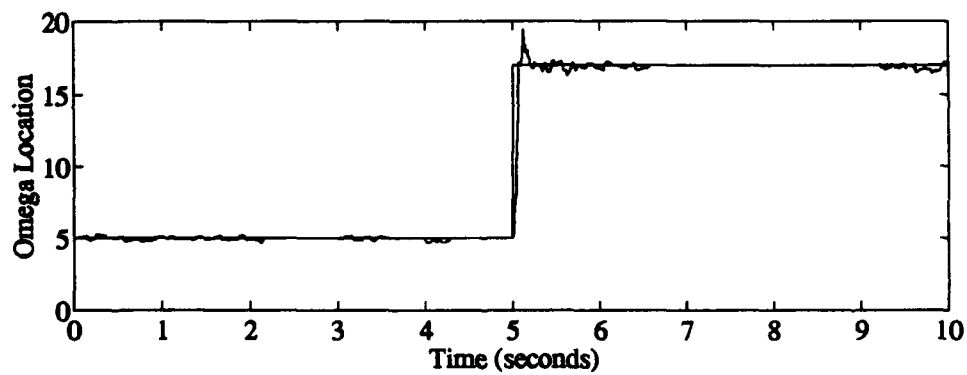


Figure H-8. Parameter Position Monitoring w/Mod MMAC and Parameter Jump

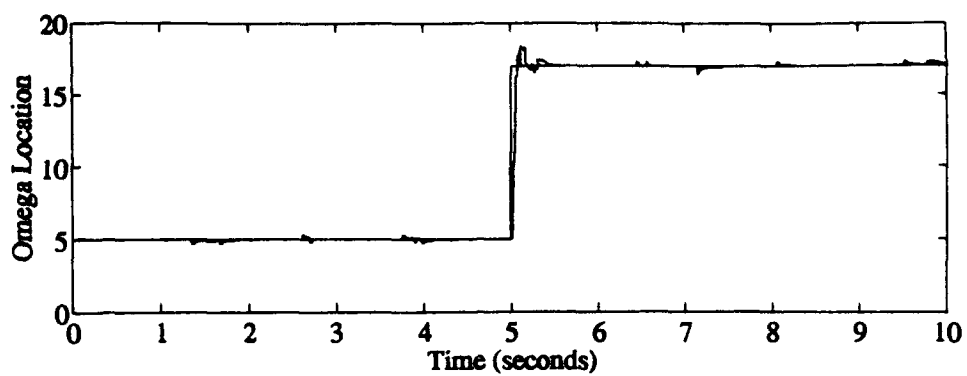


Figure H-9. Residual Monitoring w/MAP and Parameter Jump

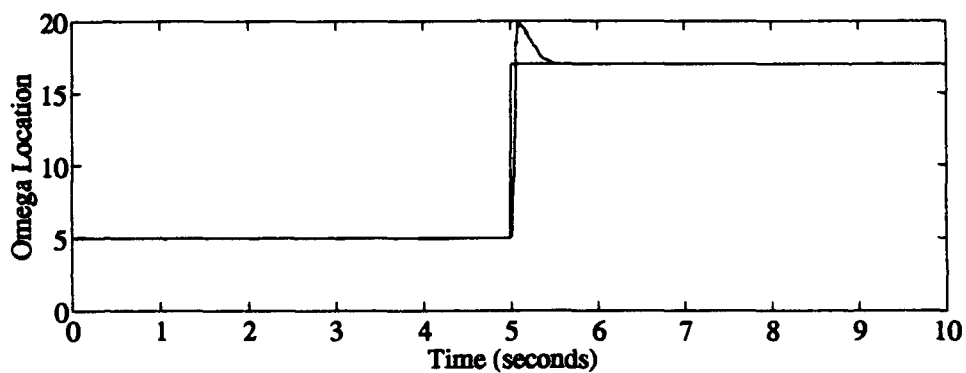


Figure H-10. Probability Monitoring w/MAP and Parameter Jump

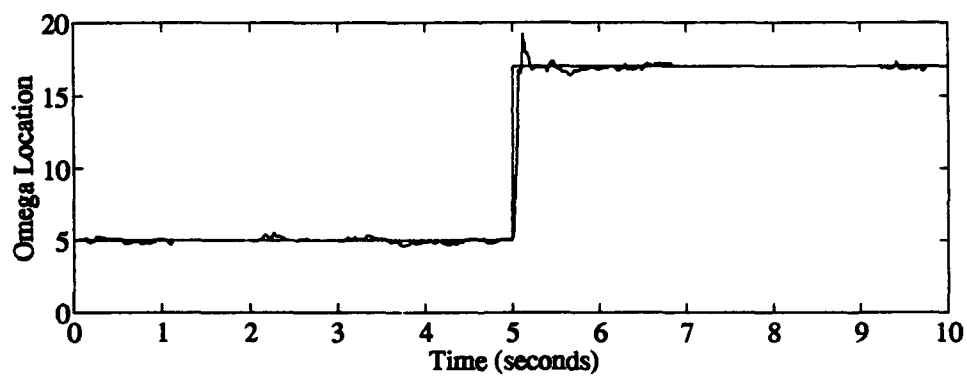


Figure H-11. Parameter Position Monitoring w/MAP and Parameter Jump

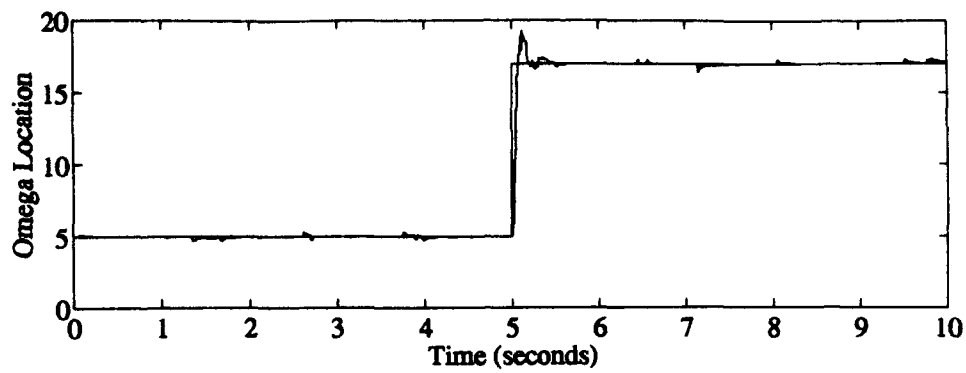


Figure H-12. Residual Monitoring w/Modified MAP and Parameter Jump

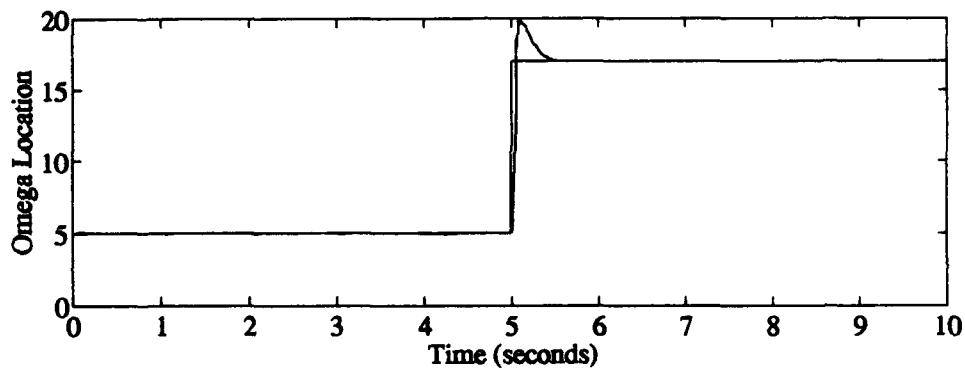


Figure H-13. Probability Monitoring w/Modified MAP and Parameter Jump

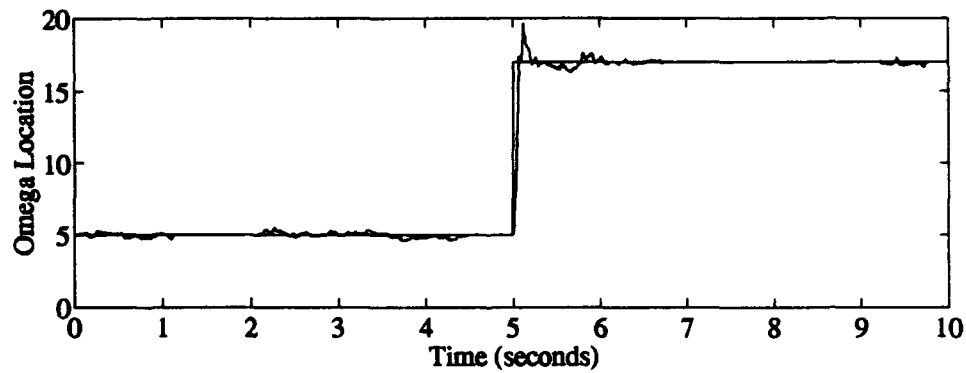


Figure H-14. Parameter Position Monitoring w/Modified MAP and Parameter Jump

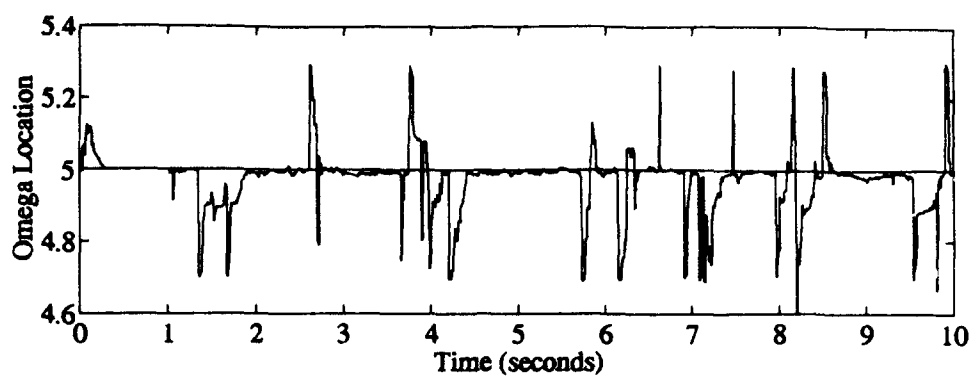


Figure H-15. Residual Monitoring w/MMAC and Parameter Match

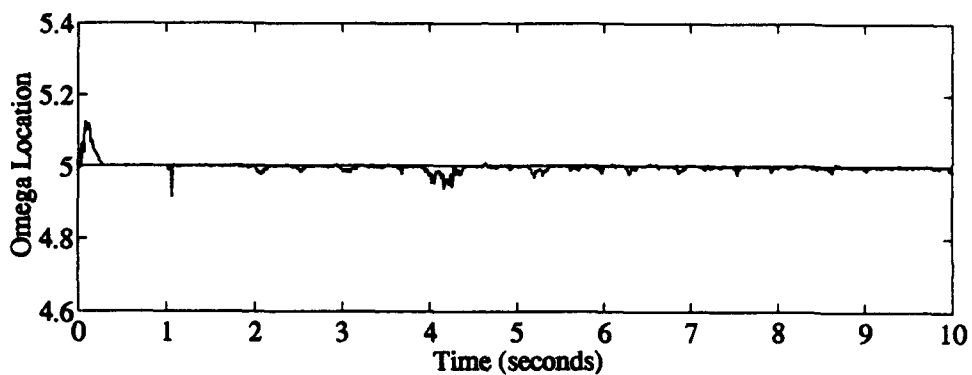


Figure H-16. Probability Monitoring w/MMAC and Parameter Match

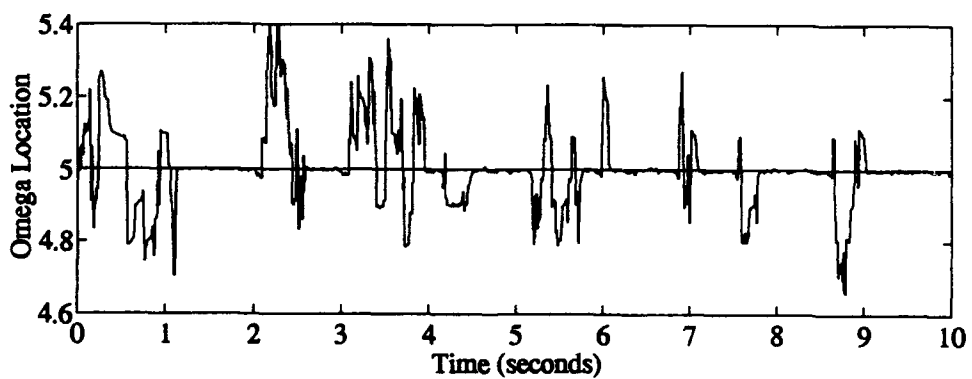


Figure H-17. Parameter Position Monitoring w/MMAC and Parameter Match



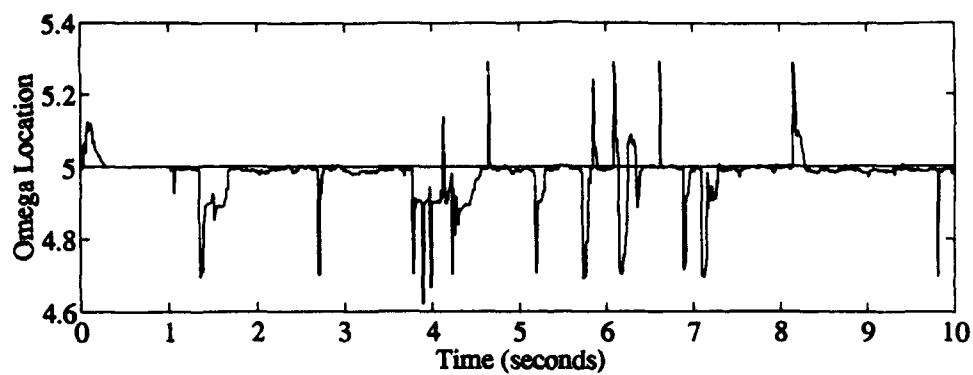


Figure H-18. Residual Monitoring w/Mod MMAC and Parameter Match

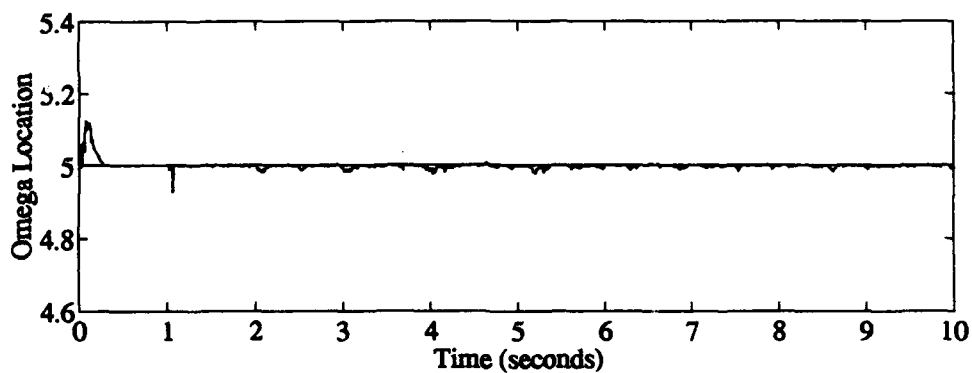


Figure H-19. Probability Monitoring w/Mod MMAC and Parameter Match

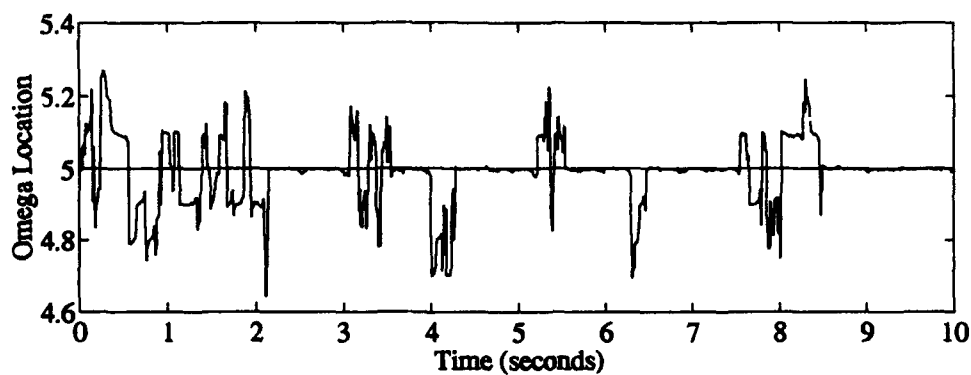


Figure H-20. Parameter Position Monitoring w/Mod MMAC and Parameter Match

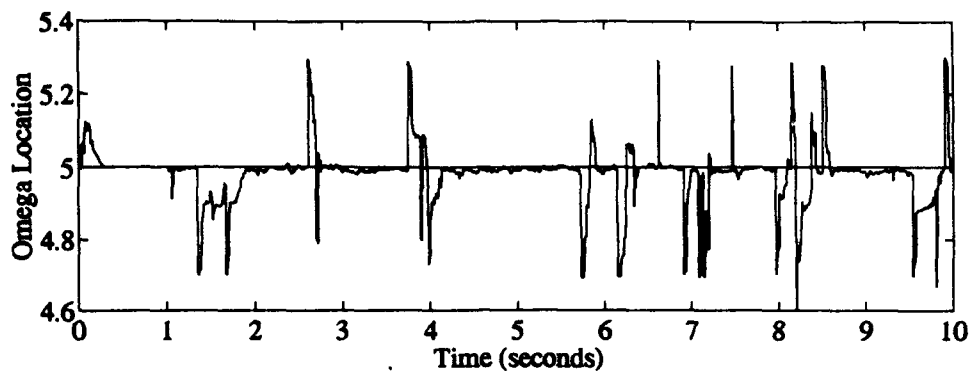


Figure H-21. Residual Monitoring w/MAP and Parameter Match

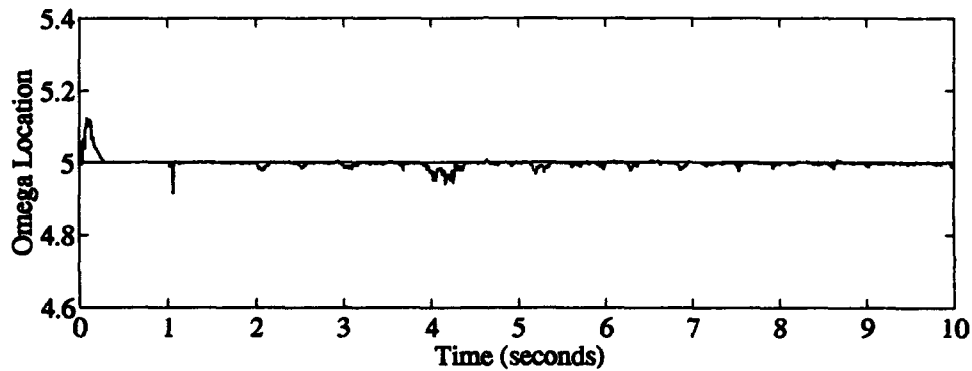


Figure H-22. Probability Monitoring w/MAP and Parameter Match

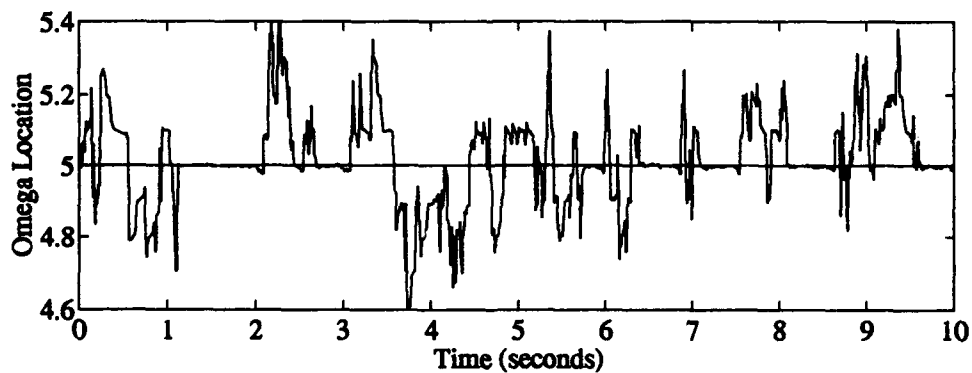


Figure H-23. Parameter Position Monitoring w/MAP and Parameter Match

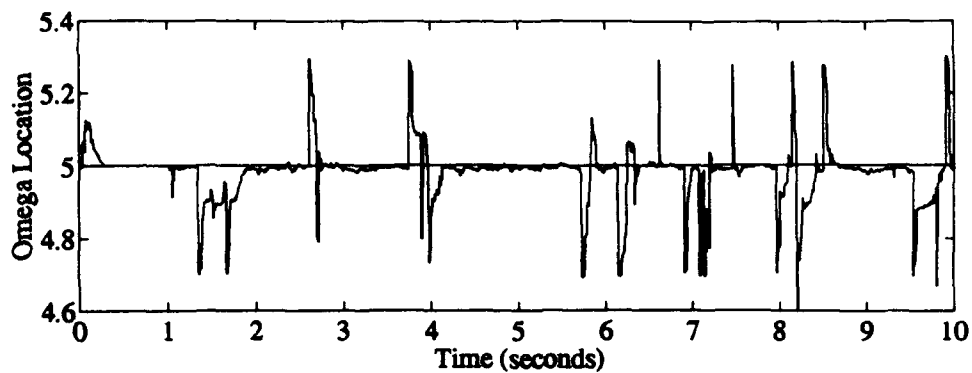


Figure H-24. Residual Monitoring w/Modified MAP and Parameter Match

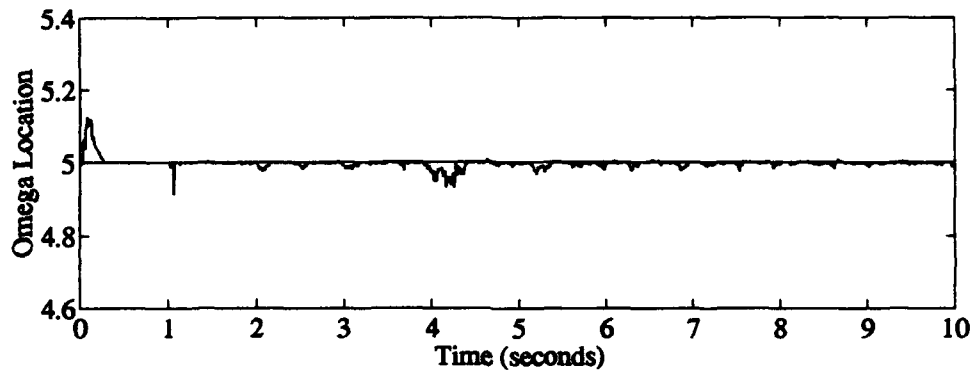


Figure H-25. Probability Monitoring w/Modified MAP and Parameter Match

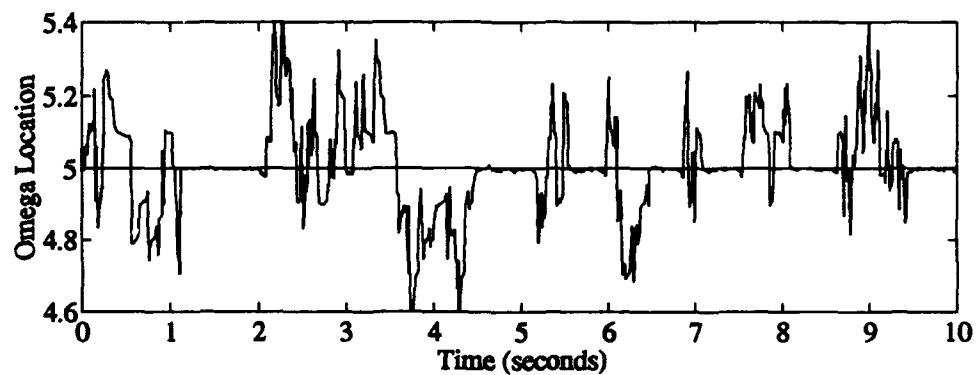


Figure H-26. Parameter Position Monitoring w/Modified MAP and Parameter Match

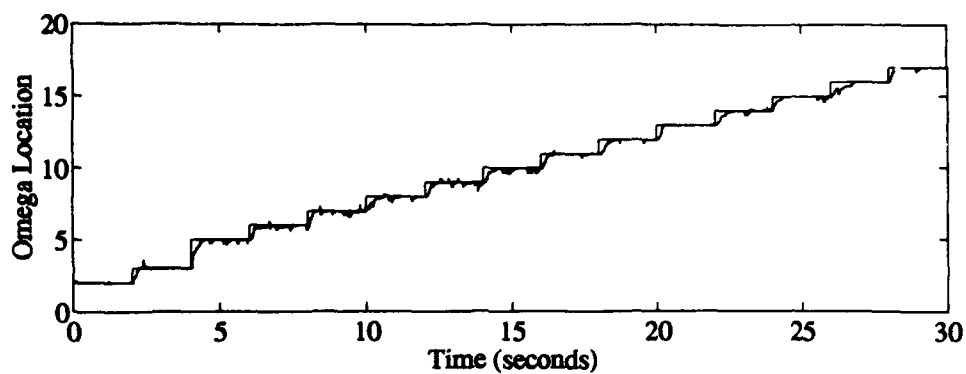


Figure H-27. Residual Monitoring w/MMAC and Parameter Move

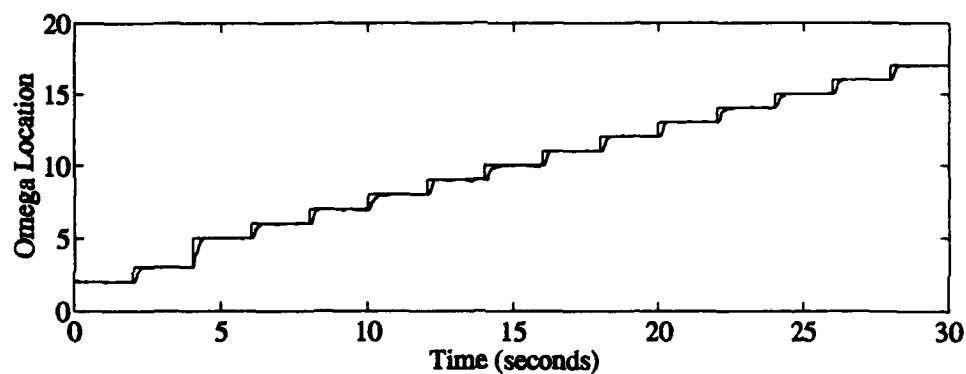


Figure H-28. Probability Monitoring w/MMAC and Parameter Move

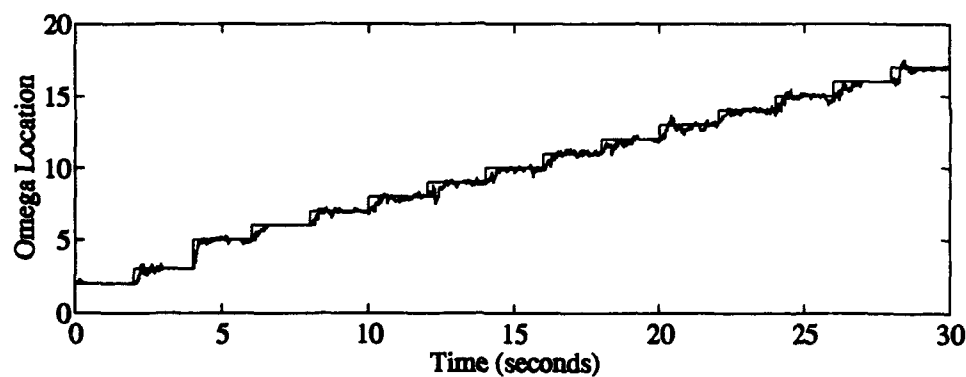


Figure H-29. Parameter Position Monitoring w/MMAC and Parameter Move

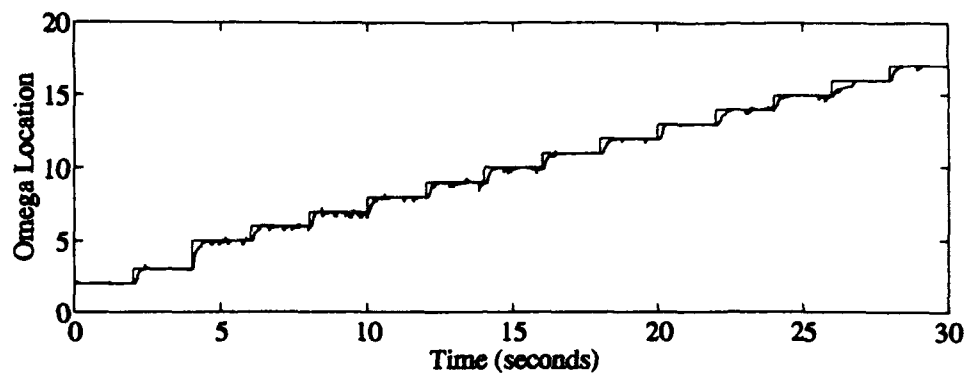


Figure H-29. Residual Monitoring w/Mod MMAC and Parameter Move

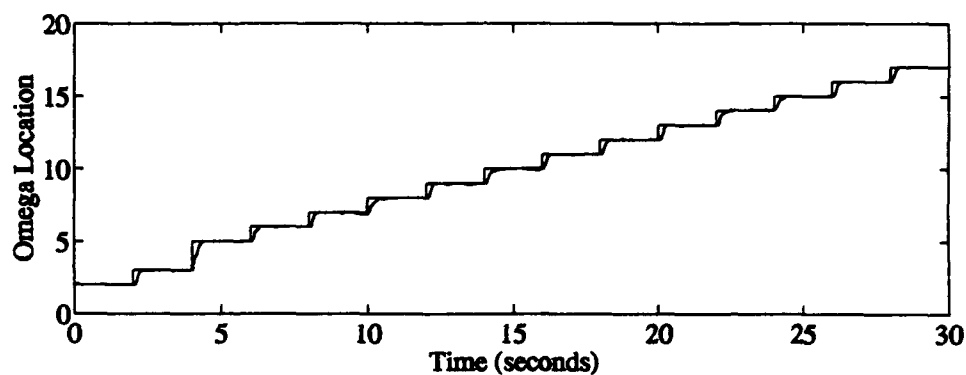


Figure H-30. Probability Monitoring w/Mod MMAC and Parameter Move

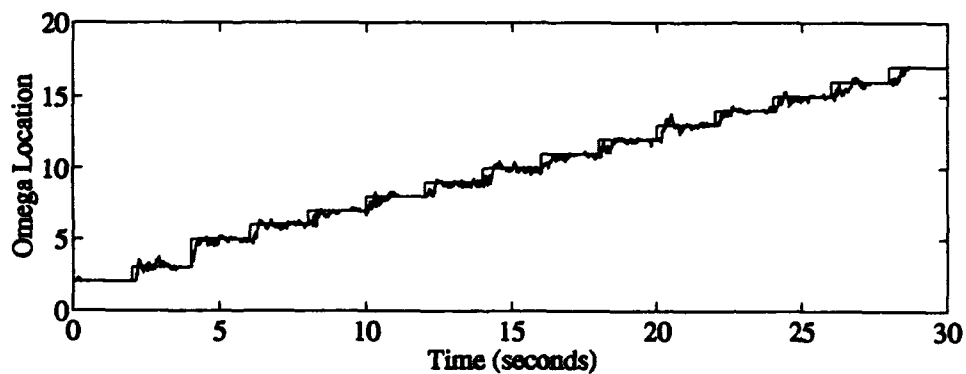


Figure H-31. Parameter Position Monitoring w/Mod MMAC and Parameter Move

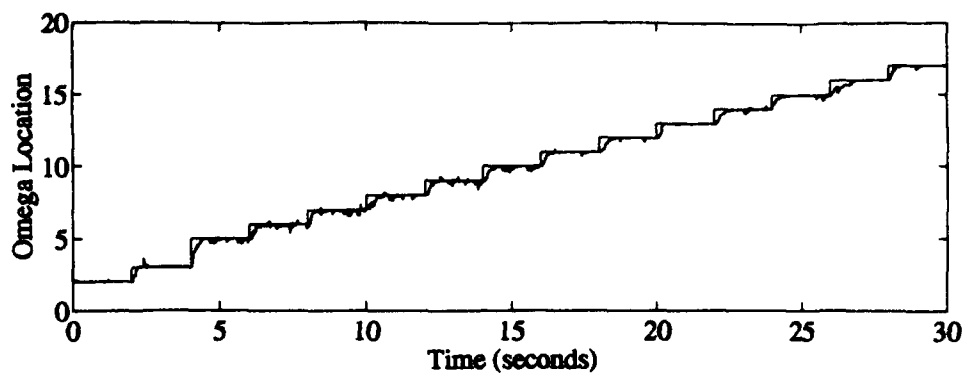


Figure H-32. Residual Monitoring w/MAP and Parameter Move

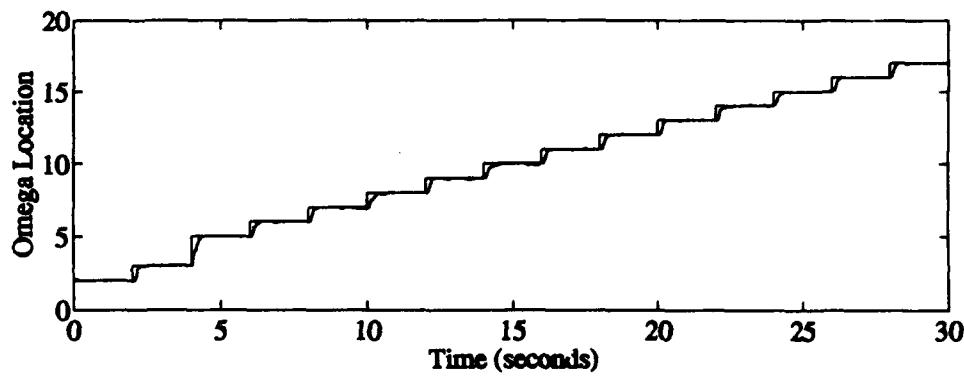


Figure H-33. Probability Monitoring w/MAP and Parameter Move

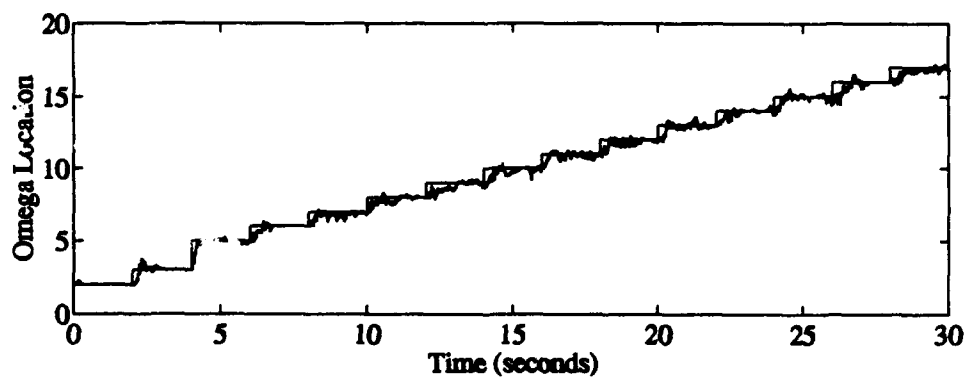


Figure H-35. Parameter Position Monitoring w/MAP and Parameter Move

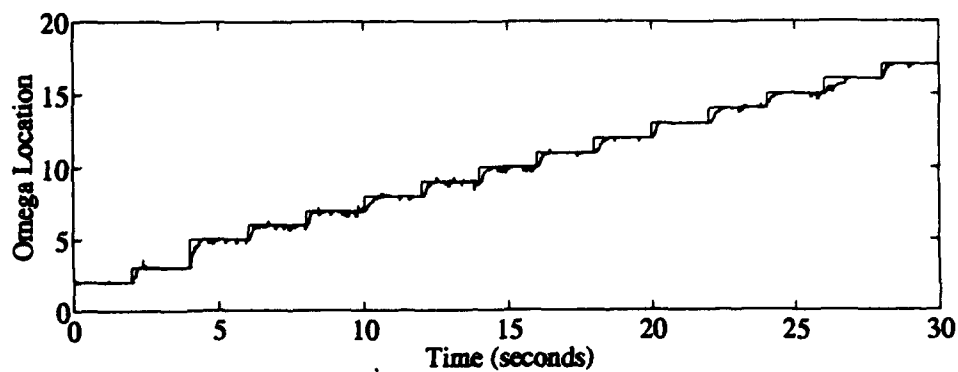


Figure H-34. Residual Monitoring w/Modified MAP and Parameter Move

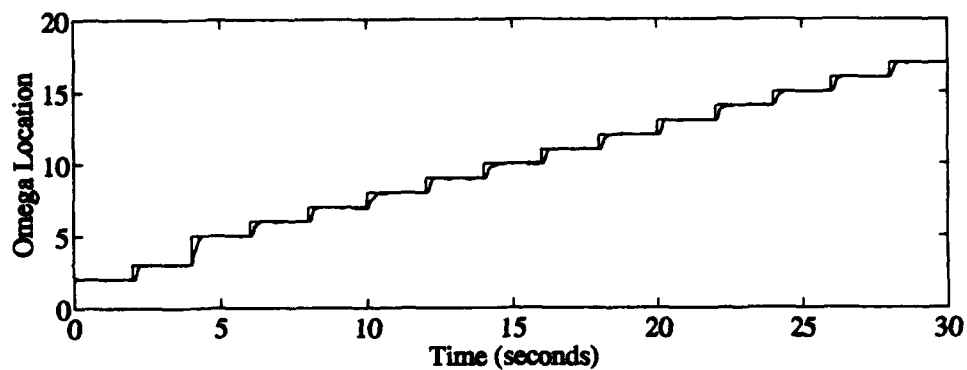


Figure H-35. Probability Monitoring w/Modified MAP and Parameter Move

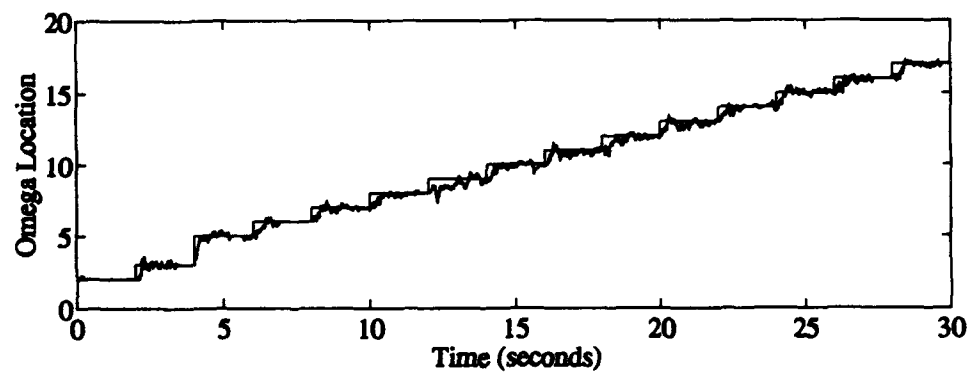


Figure H-36. Parameter Position Monitoring w/Modified MAP and Parameter Move

### *Vita*

Captain Gregory J. Schiller was born on 27 November 1962 in Omro, Wisconsin. He graduated from Eldorado High School in Las Vegas, Nevada in 1981 and attended the Air Force Academy in Colorado Springs, Colorado. Upon graduation in 1985 with a Bachelor of Science in Astronautical Engineering, he received a regular commission as a second lieutenant in the United States Air Force. His first assignment was at Onizuka AFB, California, where he was trained as Planner/Analyst (PA) for the NATO Communications Satellite Program. His responsibilities included analyzing satellite telemetry, planning routine and emergency command and control procedures, and investigating all problems with the constellation. His second assignment was at Falcon AFB, Colorado, where he was trained as a PA for the Fleet Satellite Communications (FLTSATCOM) Program. He held positions as the FLTSATCOM Current Operations Lead and finally as the FLTSATCOM Program Lead Engineer. As the lead engineer, his responsibilities included managing and controlling all engineering aspects of 5 operational satellites, and directing all activities to resolve grave satellite malfunctions, including troubleshooting, corrective action, and failure mode analysis. In May 1992, he entered the Graduate School of Engineering, Air force Institute of Technology.

Permanent address: 60 N. Clayton  
Las Vegas, Nevada 89110



## ***Bibliography***

1. Baldwin, Rick, and Ross Blankenship, Telephone Interviews. Lockheed, Albuquerque NM, 15 Feb through 15 Aug 1993.
2. Baram, Y., and N. R. Sandell, Jr. "An Information Theoretic Approach to Dynamic System Modeling and Identification," *IEEE Transactions on Automatic Control*, AC-23 (1): 61-66, 1978.
3. Chow, James, Telephone Interviews. Honeywell, Phoenix Az, 15 Feb through 15 Aug 1993.
4. Clark, S. Y. *Control System Performance and Stability Sensitivity Studies for the SPICE Precision Pointing Experiment*. Contract 87-A/K-03-18-164. Albuquerque, NM: R & D Associates Systems Technology Operation. 7 Aug 1991.
5. Dailey, R. L. Lecture notes distributed at workshop on  $H^\infty$  and  $\mu$  Methods for Robust Control. School of Engineering, 1990 American Control Conference, San Diego, CA, Jan 1991.
6. Enns, Dale. *Model Reduction for Control System Design*. PhD Dissertation. Department of Aeronautics and Astronautics, Stanford University, Palo Alto, CA, June 1984.
7. Filios, Capt Paul G. *Moving-Bank Multiple Model Adaptive Algorithms Applied to Spacecraft Control*. MS Thesis AFTT/GE/ENG/85D-14. School of Engineering, Air Force Institute of Technology (AU), Wright-Patterson AFB, OH, Dec 1985 (AD-A164 016).
8. Fitch, Capt James. *Moving-Bank Multiple Model Adaptive Control of a Large Flexible Space Structure with Purposeful Dither for Enhanced Identifiability*. MS Thesis AFTT/GA/ENG/93D-01. School of Engineering, Air Force Institute of Technology (AU), Wright-Patterson AFB, OH, Dec 1993.
9. Fitch, Capt James. Personal interviews. School of Engineering, Air Force Institute of Technology (AU), Wright-Patterson AFB, OH, Feb through Nov 1993.
10. FORTRAN 77: IMSL Math/library: Fortran Subroutines for Mathematical Applications. IMSL, Inc., Houston, Texas, January 1989.

11. Gustafson, Capt John A. *Control of a Large Flexible Space Structure Using Multiple Model Adaptive Algorithms*. MS Thesis AFIT/GE/ENG/91D-22. School of Engineering, Air Force Institute of Technology (AU), Wright-Patterson AFB, OH, Dec 1991. (AD-A243 759).
12. Gustafson, Capt John A., and P. S. Maybeck. "Control of a Large Flexible Space Structure Using Multiple Model Adaptive Algorithms," *Proceedings of the IEEE Conference on Decision and Control*: 1273-1278. Tucson, AZ, Dec 1992.
13. Gustafson, Capt John A. Personal interviews. Wright Laboratories, Wright-Patterson AFB, OH, Feb through Nov 1993.
14. Hentz, 1Lt Karl P. *Feasibility Analysis of Moving Bank Multiple Model Adaptive Estimation and Control Algorithms*. MS Thesis AFIT/GE/ENG/84D-32. School of Engineering, Air Force Institute of Technology (AU), Wright-Patterson AFB, OH, Dec 1984 (AD-A152 015).
15. Karnick, 2Lt Drew A. *Moving Bank Multiple Model Adaptive Estimation Applied to Flexible Spacestructure Control*. MS Thesis AFIT/GE/ENG/86D-41. School of Engineering, Air Force Institute of Technology (AU), Wright-Patterson AFB, OH, Dec 1986 (AD-A178 870).
16. Karnick, Drew A., and Peter S. Maybeck. "Moving Bank Multiple Model Adaptive Estimation Applied to Flexible Spacestructure Control," *Proceedings of the 26th IEEE Conference on Decision and Control*: 1249-1257. Los Angeles, CA, Dec 1987.
17. Kokotovic, P.V., R.E. O'Malley, Jr., and P. Sannuti. "Singular Perturbations and Order Reduction in Control Theory -- An Overview," *Automatica*, 12: 123-132, 1976.
18. Lashlee, Capt Robert W. *Moving Bank Multiple Model Adaptive Estimation Applied to Flexible Spacestructure Control*. MS Thesis AFIT/GE/ENG/87D-36. School of Engineering, Air Force Institute of Technology (AU), Wright-Patterson AFB, OH, Dec 1987.
19. Lashlee, Robert W., and Peter S. Maybeck. "Spacestructure Control Using Moving Bank Multiple Model Adaptive Estimation," *Proceedings of the 27th IEEE Conference on Decision and Control*: 712-717. Austin, TX, Dec 1988.
20. Lockheed et al. "Preliminary Design Review: Space Integrated Controls Experiment". Subtask 02-03. 21-22 Feb 1991.

21. Lynch, P.J., and Siva S. Banda. "Active Control for Vibration Damping," *Damping: 1986 Proceedings*, Technical Report. Flight Dynamics Laboratory, Air Force Wright Aeronautical Laboratory, Wright-Patterson AFB, OH, 1986 (AFWAL-TR-86-3509).
22. MATRIXx: ANALYSIS AND DESIGN MANUAL. "A CAD/CAE Program." Integrated Systems Inc., Santa Clara, CA, April 1990.
23. MATLAB: Pro-MATLAB For Sun Workstations. The MathWork, Inc., South Natick, MA, January 1990.
24. Maybeck, Peter S. *Stochastic Models, Estimation, and Control, Volume 1*. NY: Academic Press, 1979.
25. Maybeck, Peter S. *Stochastic Models, Estimation, and Control, Volume 2*. NY: Academic Press, 1982.
26. Maybeck, Peter S. *Stochastic Models, Estimation, and Control, Volume 3*. NY: Academic Press, 1982.
27. Maybeck, Peter S. "Moving-Bank Multiple Model Adaptive Estimation and Control Algorithms: An Evaluation," *Control and Dynamic Systems: Advances in Aerospace System Dynamics and Control Systems*, Edited by C. T. Leondes, 31: 1-31. Academic Press, San Diego CA. 1989.
28. Maybeck, Peter S. Class handout distributed in MMAE special study session. School of Engineering, Air Force Institute of Technology (AU), Wright-Patterson AFB, OH, Dec 1992.
29. Maybeck, Peter S. Professor. Personal interviews. School of Engineering, Air Force Institute of Technology (AU), Wright-Patterson AFB, OH, Feb through Nov 1993.
30. Maybeck, Peter S., and Capt Karl P. Hentz. "Investigation of Moving-Bank Multiple Model Adaptive Algorithms," *AIAA Journal of Guidance, Control, and Dynamics*, Vol. 10, No. 1: 90-96, Jan/Feb 1987.
31. Maybeck, Peter S., and Michael R. Schore. "Reduced-Order Multiple Model Adaptive Controller for Flexible Spacestructure," *IEEE Transactions on Aerospace and Electronics Systems*, Vol. AES-28, No. 3: 756-767, July 1992.
32. Maybeck, Peter S., and Richard D. Stevens. "Reconfigurable Flight Control Via Multiple Model Adaptive Control Methods," *IEEE Transactions on Aerospace and Electronic Systems*, Vol. AES-27, No. 3: 470-480, May 1991.

33. Moyle, Capt Robert B. *Moving-Bank Multiple Model Adaptive Estimation and Control to a Large Space Structure*. MS Thesis AFIT/GE/ENG/90D-45. School of Engineering, Air Force Institute of Technology (AU), Wright-Patterson AFB, OH, Dec 1990.
34. Nash, Capt Anthony. *Modeling of a Large Undamped Space Structure Using Time Domain Techniques*. MS Thesis AFIT/GA/ENY/93D-03. School of Engineering, Air Force Institute of Technology (AU), Wright-Patterson AFB, OH, Dec 1993.
35. Ninnerman, Rory, Telephone interviews. PL/VTSA, Kirtland AFB, NM, Feb through Nov 1993.
36. Muravez, Randall Joseph. *Multiple Model Adaptive Estimation and Prediction with the Harmonically Balanced Kalman Filter Bank*. PhD dissertation. Cal-State Poly Technic University, Pamon, CA, 1989.
37. Schore, Capt Michael Roger. *Robustness of a Moving-Bank Multiple Model Adaptive Controller for a Large Space Structure*. MS Thesis AFIT/GE/ENG/89D-46. School of Engineering, Air Force Institute of Technology (AU), Wright-Patterson AFB, OH, Dec 1989.
38. Sheldon, Stuart N. *An Optimizing Design Strategy for Multiple Model Adaptive Estimation and Control*. PhD dissertation. School of Engineering, Air Force Institute of Technology (AU), Wright-Patterson AFB, OH, Dec 1989.
39. Sheldon, Stuart N., and Peter S. Maybeck. "An Optimizing Design Strategy for Multiple Model Adaptive Estimation and Control." *IEEE Transactions on Automatic Control*. Vol. 38, No. 4, 651-654, April 1993.
40. Skelton, Robert E, and Ajmal Yousuff. "Component Cost Analysis of Large Scale Systems" *International Journal of Control*, 37: 285-304, 1983.
41. Stevens, Richard D. *Characterization of a Reconfigurable Multiple Model Controller Using a STOL F-15 Model*. MS Thesis AFIT/GE/ENG/89D-52. School of Engineering, Air Force Institute of Technology (AU), Wright-Patterson AFB, OH, Dec 1989 (AD-B139 226).
42. Van Der Werken, Capt Daniel F., Jr. *A Robustness Analysis of Moving-Bank Multiple Model Adaptive Estimation and Control of a Large Flexible Space Structure*. MS Thesis AFIT/GE/ENG/88D-59. School of Engineering, Air Force Institute of Technology (AU), Wright-Patterson AFB, OH, Dec 1988.
43. Venkayya, Vipperla B., and Victoria A. Tischler. "Frequency Control and Its Effect on the Dynamic Response of Flexible Structures," *AIAA Journal*, 23: 1768-1774, Nov 1985.

44. Venkayya, Vipperla B. 'Analyze' -- Analysis of Aerospace Structures with Membrane Elements}. Technical Report. Analysis and Optimization Branch, Structural Mechanics Division, Air Force Flight Dynamics Laboratory, Air Force Wright Aeronautical Laboratories, Wright-Patterson AFB, OH, Dec 1978 (AFFDL-TR-78-170).
45. Venkayya, Vipperla B. Personal interviews. Air Force Flight Dynamics Laboratory, Air Force Wright Aeronautical Laboratories, Wright-Patterson AFB, OH, Sept 1993.

# REPORT DOCUMENTATION PAGE

1. AGENCY USE ONLY (Leave blank)

December 1993

Master's Thesis

4. TITLE AND SUBTITLE

## Control of a Large Flexible Space Structure Using Multiple Model Adaptive Estimation and Control Techniques

6. AUTHOR

Gregory John Schiller, Captain, USAF

7. PERFORMING ORGANIZATION NAME(S)

Air Force Institute of Technology, Wright-Patterson AFB,  
OH, 45433-6583

AFIT/GA/ENG/93D-02

9. SPONSORING / MONITORING AGENCY NAME(S)

Phillips Laboratory/VTSA Kirtland AFB, NM 87117

11. SUPPLEMENTARY NOTES

12a. DISTRIBUTION STATEMENT (If applicable)

Approved for public release; distribution unlimited

13. ABSTRACT

The purpose of this thesis is to apply moving-bank multiple model adaptive estimation and control (MMAE/MMAC) algorithms to an actual space structure (SPICE) being examined at Phillips Laboratory at Kirtland AFB, NM. The structure consists of a large platform and a smaller platform connected by three legs in a tripod fashion. Kalman filtering and LQG control techniques are utilized as the primary design tool. Implementing a bank of filters increases the robustness of the LQG controller when uncertainties exist in the system model, whereas the moving bank is utilized to reduce the computational load. Several reduced-order models are developed from the truth model using modal analysis and modal cost analysis. The MMAE/MMAC design with a dramatically reduced-order filter model provides an excellent method to estimate a wide range of parameter variations and to quell oscillations in the structure.

14. SUBJECT TERMS

Multiple Model Adaptive Estimation, Multiple Model Adaptive Control, LQG Control, Flexible Space Structure, Parameter Identification

358

17. SECURITY CLASSIFICATION OF REPORT

Unclassified

18. SECURITY CLASSIFICATION OF ABSTRACT

Unclassified

19. SECURITY CLASSIFICATION OF ABSTRACT

Unclassified

UL